Title
Proceedings of the Exotic Nuclei Symposium

Permalink
https://escholarship.org/uc/item/4nk2c3qq

Author
Moltz, D.M.

Publication Date
1996-04-15

LBNL-39750
CONF-9604189
UC-413

ERNEST ORLANDO LAWRENCE
BERKELEY NATIONAL LABORATORY

Proceedings of the Exotic Nuclei Symposium

D. Moltz, Editor
Nuclear Science Division

April 1996
Presented at the
Exotic Nuclei Symposium,
Bodega Bay, CA,
April 14–15, 1996,
and to be published in
the Proceedings

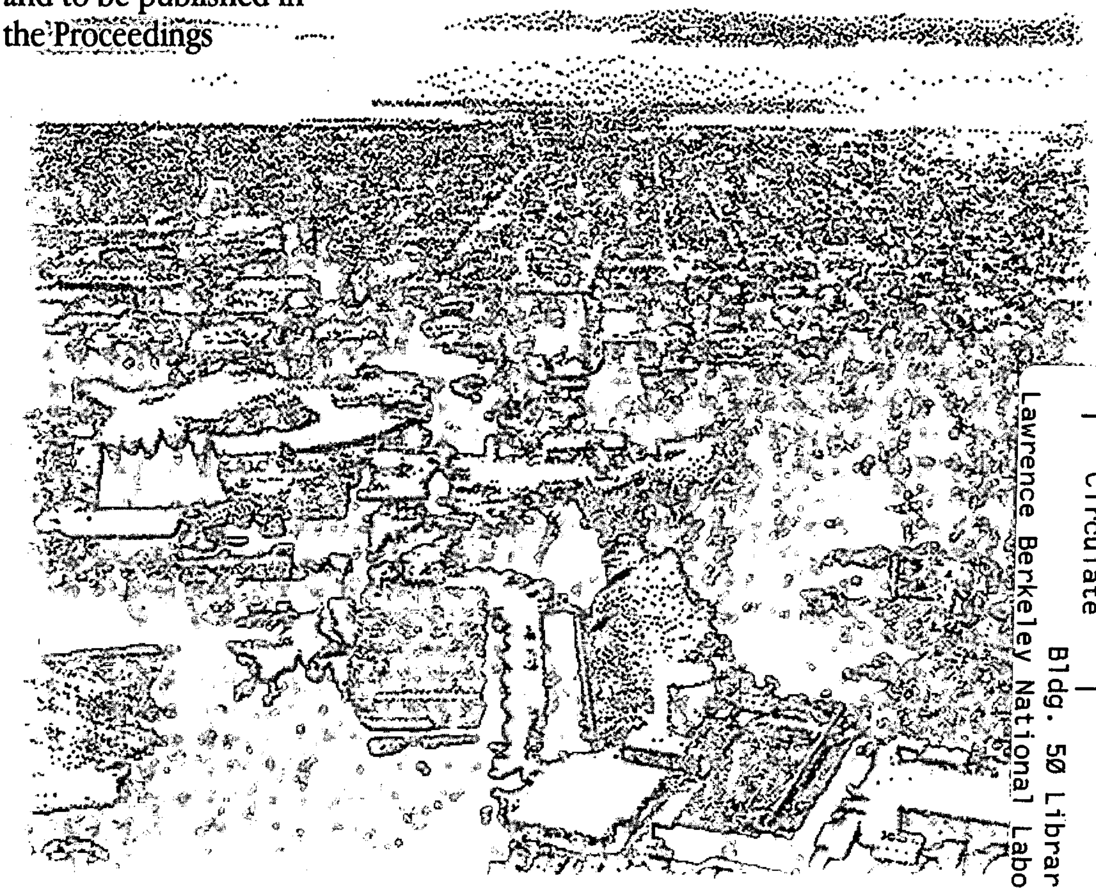

LBNL-39750
CONF-9604189
UC-413

Proceedings of the Exotic Nuclei Symposium

D. Moltz, Editor

Nuclear Science Division
Ernest Orlando Lawrence Berkeley National Laboratory
University of California
Berkeley, California 94720

April 1996

This work was supported by the Director, Office of Energy Research, Office of High Energy and Nuclear Physics, Division of Nuclear Physics, of the U.S. Department of Energy under Contract No. DE-AC03-76SF00098.

Exotic Nuclei Symposium

Bodega Bay, Ca.

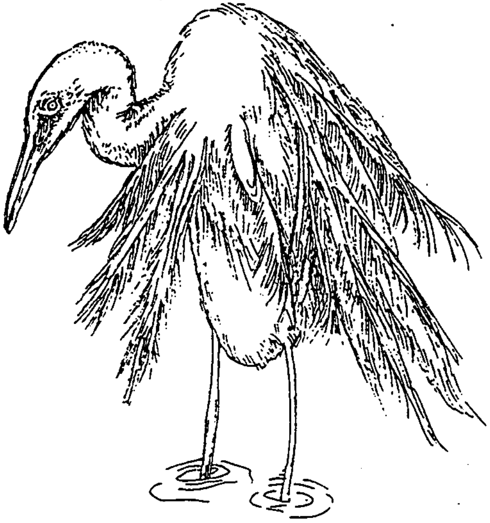

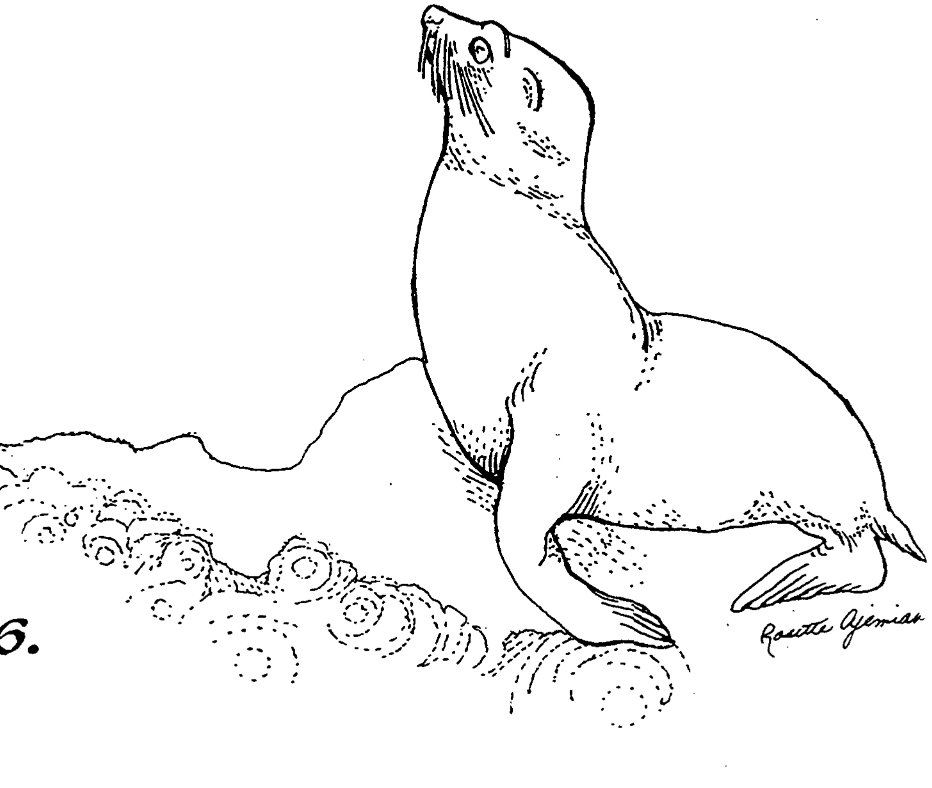

April 14-16, 1996.

Foreword

This document constitutes the proceedings of the Exotic Nuclei Symposium held in Bodega Bay, California from April 14-16, 1996. All of the speakers were invited and were past associates either as visitors, postdocs or graduate students of Joseph Cerny. The timing of this symposium was such that it coincided closely with Joe's 60th birthday. Although a university professor can measure his own research productivity in a rather straightforward manner, probably the best overall measure is the research accomplishments of those who were directly influenced either as postdocs or graduate students. Almost all of those associated with Joe over the years are still active in research in one form or another. Furthermore, the majority of these individuals are still in nuclear physics and chemistry. The breadth of just the work presented herein is indicative of this point.

Many individuals either planned to attend and cancelled at the last minute or the April timing conflicted with other meetings or teaching duties. Since a couple of hundred people were invited including all of Joe's past associates (to the best of my knowledge), I obviously have a rather complete list of the whereabouts of these individuals. Since I have had numerous requests for this information, I have appended both regular mail and electronic mail addresses to the end of this document.

The banquet was particularly memorable because of the many humorous presentations by both volunteers and conscripts. I am grateful to all who participated. I wish to thank all those who responded so promptly to my initial queries and all of those who were able to attend. I am particularly thankful to everyone for keeping the entire affair as a surprise to Joe. In this light, I am especially grateful to Susan Cerny for arranging for Joe's presence. I also want to thank Linda Lopez for creating a credible work schedule for April 15 and 16. I wish to thank the Bodega Bay Lodge for making the organization rather trivial from my perspective. Finally, I would like to thank my wife Rosette for designing the cover page art. I believe everyone had a good time, while still managing to learn a bit.

Dennis M. Moltz

EXOTIC NUCLEI SYMPOSIUM SCHEDULE

April 14 - 19:30 Registration and Welcome Reception

April 15, 1996

9:00 - 9:05 Introduction

9:05 - 10:20 Session I Peter Haustein, Chairman

9:05 - 9:30	Robert Weisenmiller MRW Assoc.	*Exotic Energy Policy*
9:30 - 9:55	Rainer Jahn U. Bonn, Germany	*Recent Results from COSY*
9:55 - 10:20	Jon Batchelder LSU	*Study of Alpha-Emitters near* $Z = 82$

Break 10:20 - 10:45

10:45 - 12:30 Session II John Hardy, Chairman

10:45 - 11:10	JamesPowell LBNL	*Measurement of the* $^{7}Be(p, \gamma)$ *Cross Section at Low Energies*
11:10 - 11:35	Mike Zisman LBNL	*Building a Factory for B's*
11:35 - 12:00	Gordon Ball CRL, Canada	*Pionic Fusion of Heavy Ions*
12:00 - 12:25	Joseph Cerny LBNL	*A Small Scale RNB Facility at Berkeley*

Lunch 12:30 - 14:00

14:00 - 15:40 Session III Gordon Wozniak, Chairman

14:00 - 14:25	Alan Shotter U. Edinburgh, U.K.	*Radioactive Beam Research at Louvain la Neuve*
14:25 - 14:50	Rick Gough LBNL	*Selected Accelerator Applications*
14:50 - 15:15	Ted Ognibene LBNL	*Low-Energy Proton Decays in* $^{27,28}P$ *and* $^{31,32}Cl$
15:15 - 15:40	David Vieira LANL	*Mass and Decay Measurements of Exotic Nuclei Using the TOFI Spectometer*

Break 15:40 - 16:05

16:05 - 17:20 Session IV Rainer Jahn, Chairman

16:05 - 16:30	John Hardy CRL, Canada	*Superallowed beta-decay: a Nuclear Probe of the Standard Model*
16:30 - 16:55	Juha Äystö, U. of Jyväskylä,Finland	*Beta-Delayed Neutron Emission*
16:55 - 17:20	Gordon Wozniak LBNL	*From Exotic Reactions to Multifragmentation*

Banquet 19:30

EXOTIC NUCLEI SYMPOSIUM SCHEDULE

Day 2

April 16, 1996

9:00 - 9:05 Introduction

9:05 - 10:20 Session V David Vieira, Chairman

9:05 - 9:30	Mike Rowe LBNL	*Beta-Delayed Particle Decays of Light Nuclei*
9:30 - 9:55	Dennis Moltz LBNL	*Dark Matter Axions*
9:55 - 10:20	Claude Detraz IN2P3, France	*Nuclear and Particle Physics in Europe; A View from the Skipper*

Break 10:20 - 10:45

10:45 - 12:30 Session VI Juha Äystö, Chairman

10:45 - 11:10	Creve Maples Musetech	*A New Dimension in Human-Computer Interaction*
11:10 - 11:35	Mike Cable LLNL	*Nuclear Measurement Techniques for Inertial Confinement Fusion*
11:35 - 12:00	Peter Haustein BNL	*Nuclear Stimulated Desorption from Surfaces and Thin Films*
12:00 - 12:15	Joseph Cerny	*The Final Word*

Conference Photograph

First Row- Gordon Ball, Lee Schroeder, Dennis Moltz, Joe Cerny, Susan Cerny

Second Row- John Hardy, Bernard Harvey, Norman Glendenning, Peter Haustein, Ruth-Mary Larimer, Janis Dairiki, Rick Gough, Alan Shotter

Third Row- Mike Zisman, Jorgen Randrup, Juha Äystö, Eric Norman, Bob McGrath, Claude Detraz, Rainer Jahn, Bob Weisenmiller

Fourth Row- Creve Maples, Peter Jackson, David Vieira, James Powell, Mike Cable, Jon Batchelder, Ted Ognibene, Mike Rowe, Gordon Wozniak

Registered Conference Attendees not making Presentations

Bernard Harvey, LBNL
Lee Schroeder, LBNL
Norman Glendenning, LBNL
Ruth-Mary Larimer, LBNL
Janis Dairiki, LBNL
Ned Dairiki, LLNL
Jorgen Randrup, LBNL
Eric Norman, LBNL
James Symons, LBNL
John Rasmussen, LBNL and UCBerkeley
Gabor Somorjai, LBNL and UCBerkeley
Sam Markowitz, LBNL and UCBerkeley
Ian Carmichael, UCBerkeley
Carol Christ, UCBerkeley
Dan Mote, UCBerkeley
Bob McGrath, SUNY Stony Brook
Peter Jackson, TRIUMF

Robert Weisenmiller

MRW & Associates
Oakland, CA

EXOTIC ENERGY POLICY

How I Spent from 1977-96

by

Dr. Robert B. Weisenmiller

Morse, Richard, Weisenmiller
& Associates, Inc.
April 12, 1996

MRW & ASSOCIATES

OVERVIEW

- 1977 - PhD in Chemistry
- 1977 - M.S. in Energy & Resources
- 1977 - California Energy Commission
- 1982 - Independent Power Corporation
- 1986 - Morse, Richard, Weisenmiller, & Associates, Inc..

California Energy Commission

- Established in 1975 by the Warren-Alquist Act (signed by Governor Reagen)
- Act Implemented by Commissioners Appointed by Governor Jerry Brown
- Roughly 500 person staff with about $50 million budget
- Located in Sacramento

California Energy Commission Responsibilities

- Forecasting future electricity and energy needs
- Licensing energy facilities to meet these needs
- Promoting energy efficiency
- Developing alternate energy technologies
- Planning for energy emergencies

Energy Context in 1975

- It was assumed energy requirements rose in lock step with economic growth
- It was assumed that over the next twenty years, California would require about 20 1000 MW coal or nuclear power plants
- These plants could be either located along the California coast with seismic issues or inland with water issues

Energy Context (cont'd)

- Nuclear plants were perceived to have safety and waste disposal issues
- Coal plants had obvious air quality concerns
- Electric utilities were monopolies from power plant to meter
- Natural gas prices were regulated and low, so regulation rationed supply. Shortages were common.

Energy Context (cont'd)

- Nuclear plants were perceived to have safety and waste disposal issues
- Coal plants had obvious air quality concerns
- Electric utilities were monopolies from power plant to meter
- Natural gas prices were regulated and low, so regulation rationed supply. Shortages were common.

Energy Context (cont'd)

- Natural gas service was also generally provided by monopolies, aside from production
- Domestic oil supplies were also price controlled, while foreign oil supplies were controlled by OPEC
- California's energy needs would require the sacrifice of its environmental quality

California Energy Commission

- 1977 -- Advisor to Commissioner Ron Doctor
- 1978-79 -- Office Manager of the Special Project Office (Overall RDD Policy, Cogeneration, Small Power, Power Pooling)
- 1980-82 -- Director of the Office of Policy and Program Evaluation

CEC Accomplishments

- Developed Comprehensive Energy Policy Package for Brown in 1978, which included legislation and administrative actions
- Blocked utility commitments to coal plants
- Developed energy services concept which lead to utility conservation programs
- Developed avoided cost concept which lead to cogeneration and renewable industry

State of California
GOVERNOR'S OFFICE
SACRAMENTO 95814

EDMUND G. BROWN JR.
GOVERNOR

November 10, 1982

Dr. Robert B. Weisenmiller
Director,
Policy and Programs
California Energy Commission
Sacramento, CA 95825

Dear Dr. Weisenmiller:

On the occasion of your departure from the California Energy Commission, I want to congratulate you for your accomplishments in the energy field and wish you success in the future.

I understand your efforts have left a mark of excellence at the Commission and been a critical component of California's progressive energy policy.

Thank you for your service to the people of California.

Sincerely,

Edmund G. Brown, Jr.
Governor

Consulting Career

- Co-founded and managed two nationally known energy consulting firms
- Testified as an expert witness in about 100 proceedings
- Representing Dow, Arco, Chevron, Simpson Paper, Proctor & Gamble, etc.. established framework for cogeneration industry in California

Consulting Career (cont'd)

- Established bankable reputation with the financial community for their investments in energy projects
- Lead witness for the City of San Diego to block SCE/SDG&E merger
- Lead witness for El Paso, Mojave, and Kern River pipelines in pipeline rates and expansion cases

Current Energy Realities

- California's (and U.S.) economic growth has occurred with little energy growth
- Beyond their earlier commitments California utilities have built limited resources since 1977 (i.e., Palo Verde)
- Conservation limited need for additional utility power plants.

Current Energy Realities (cont'd)

- Cogeneration dissolved utility monopoly on generation services.
- California gets between 20 and 30% of its power from cogeneration
- California has surplus power situation
- Natural gas is cheap and plentiful

Current Energy Realities (cont'd)

- Gas and power markets on a national and international level are being restructured by competitive forces
- Higher oil prices depressed demand, increased alternatives, and broke OPEC stranglehold at least in the near-term

Rainer Jahn

University of Bonn
Bonn, Germany

Two - Meson - Production

at

COSY

Basics + Exotics

Rainer Jahn

Bodega Bay Meeting

IV/96

$$\boxed{\begin{array}{ll} p + d \longrightarrow {}^{3}He + \pi^{+}\pi^{-} & T_{thr} = 432\ MeV \\ p + d \longrightarrow {}^{3}He + K^{+}K^{-} & T_{thr} = 1.73\ GeV \end{array}}$$

MOMO

COSY

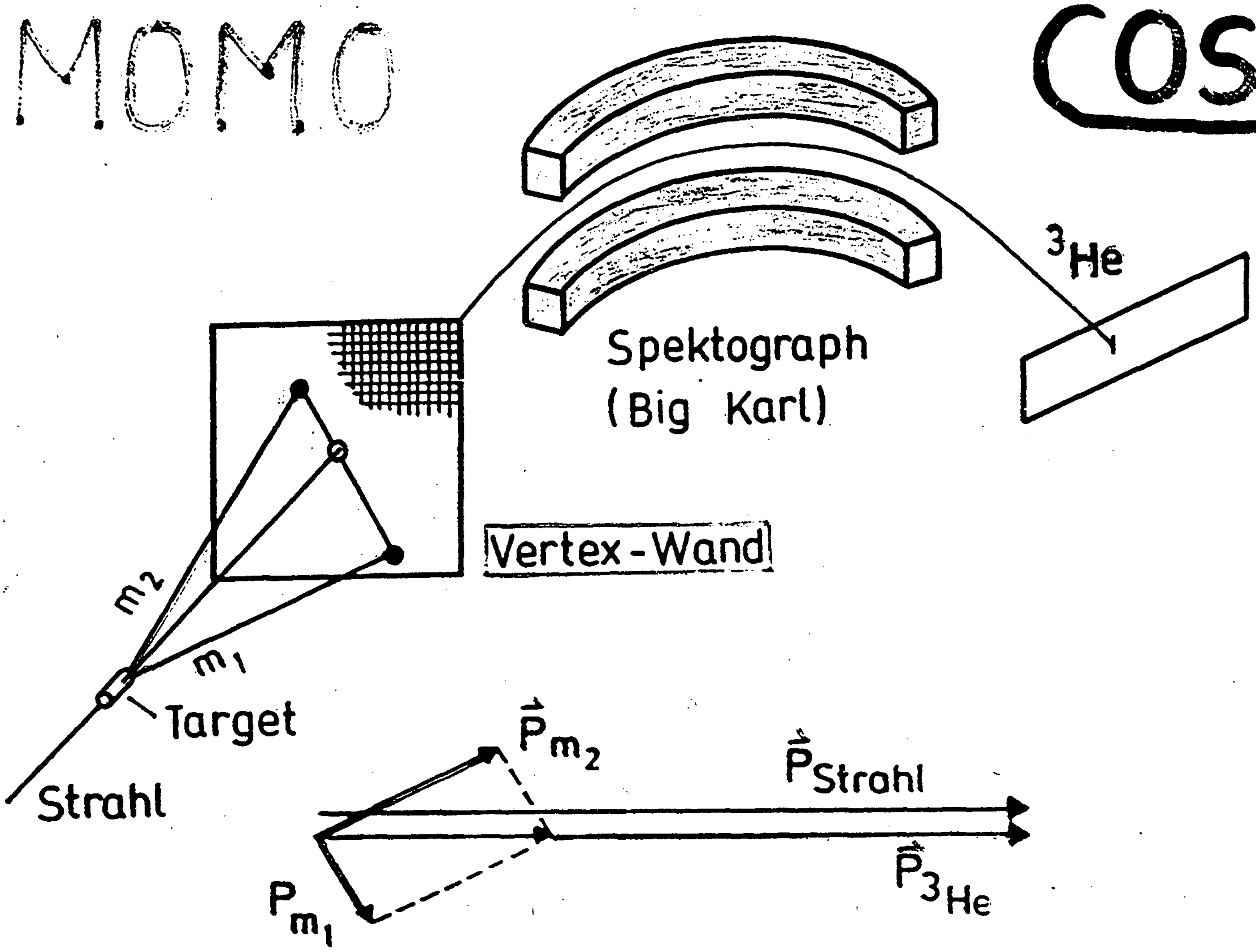

detected: $\vec{P}_{^3He}$, $T_{^3He}$

$\vec{P}_{m_1} \rightarrow T_{m_1}$

$\vec{P}_{m_2} \rightarrow T_{m_2}$

Energy conservation $\rightarrow m_1 + m_2$

→ kinematically complete

Physics with MOMO

- low energy $\pi^+\pi^-$ and K^+K^- interaction
- KK molecules
- meson nucleon Resonances
  d'?

in near threshold two meson production

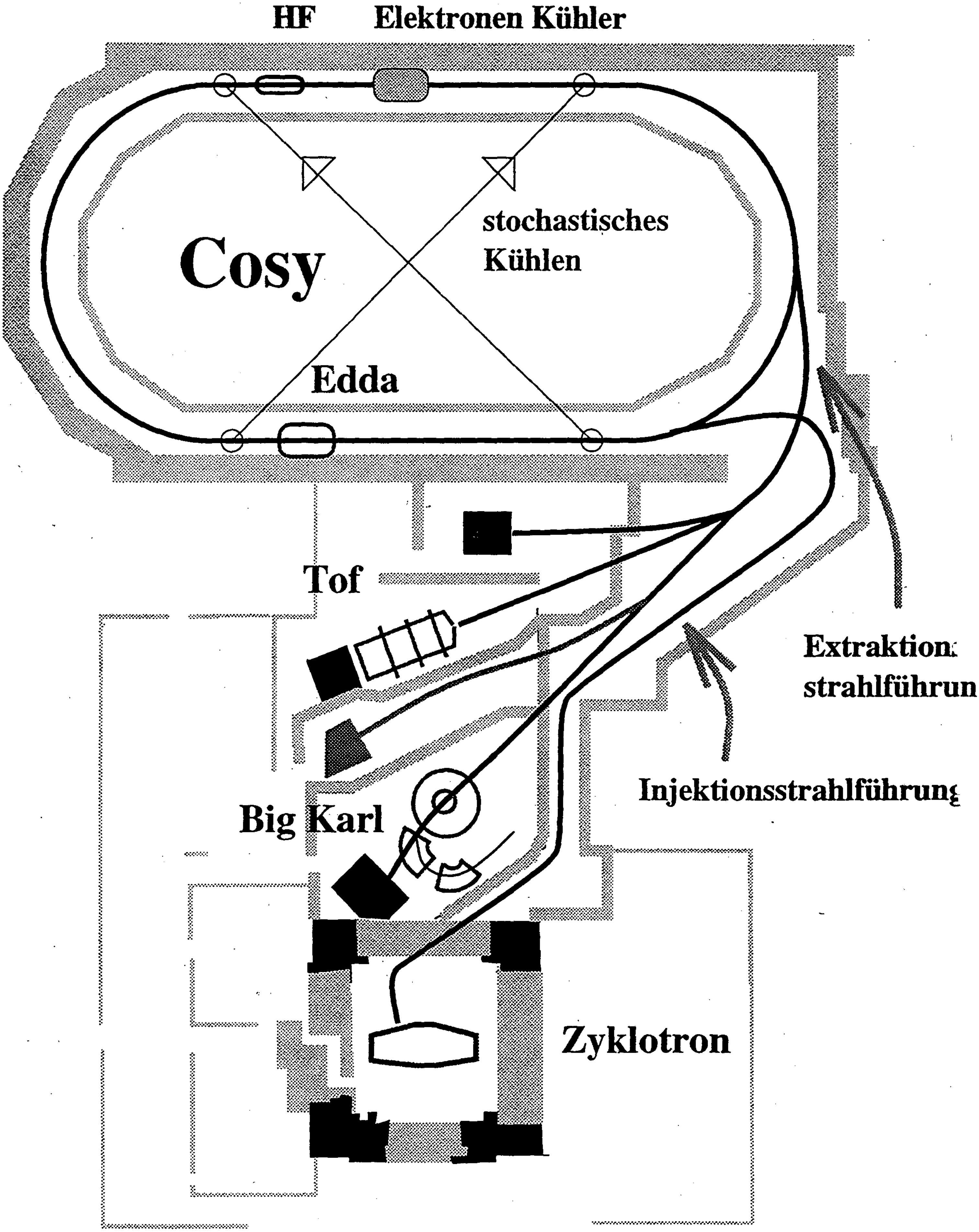
HF
Elektronen Kühler
Cosy
stochastisches
Kühlen
Edda
Tof
Extraktion
strahlführun
Injektionsstrahlführung
Big Karl
Zyklotron

Strahlplatz BIG KARL

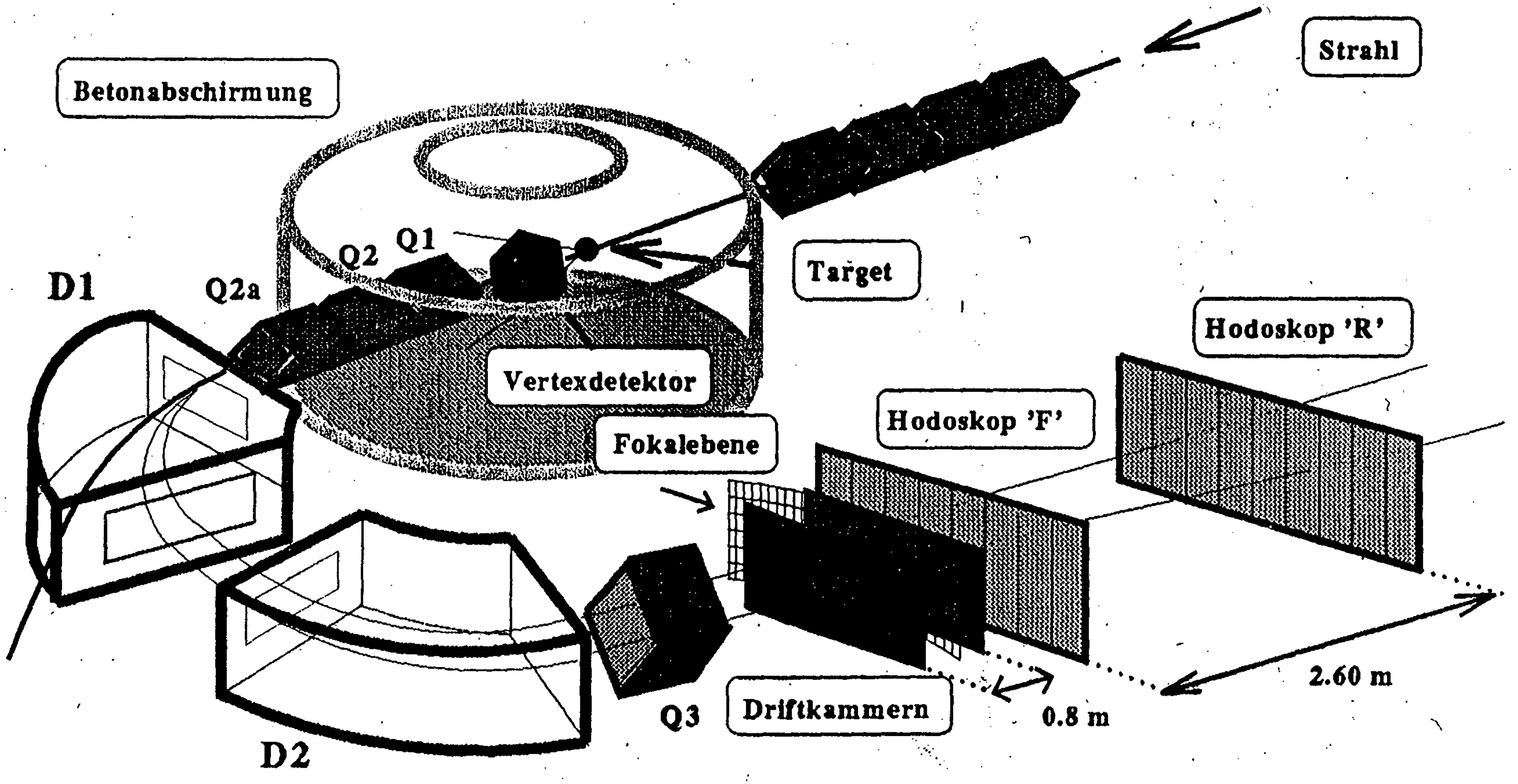

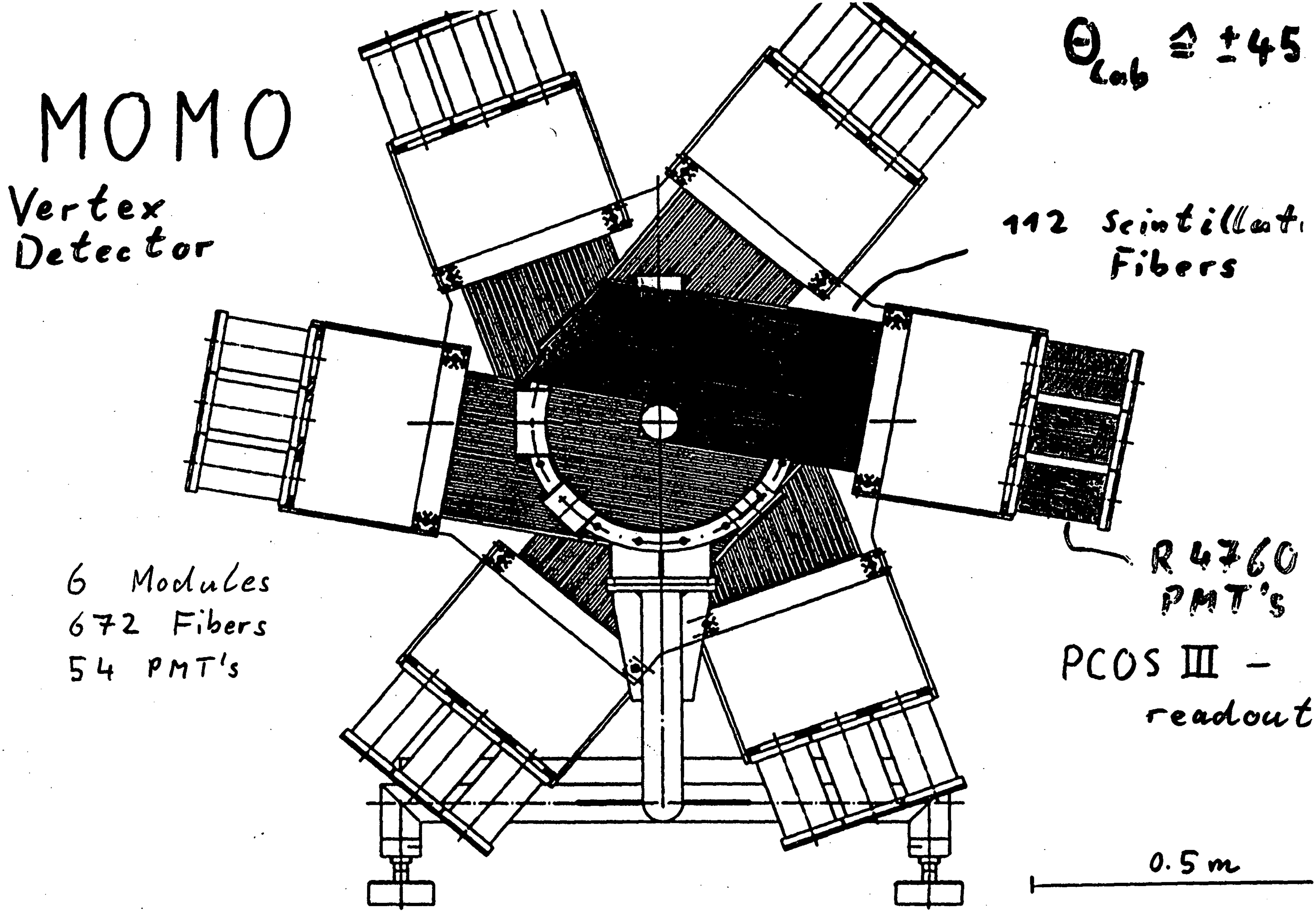
MOMO
Vertex Detector
$\Theta_{Lab} \triangleq \pm 45$
112 Scintillati
Fibers
R 4760 PMT's
PCOS III - readout
6 Modules
672 Fibers
54 PMT's
0.5 m

F[redacted]e [redacted]po[redacted]t[redacted]ng

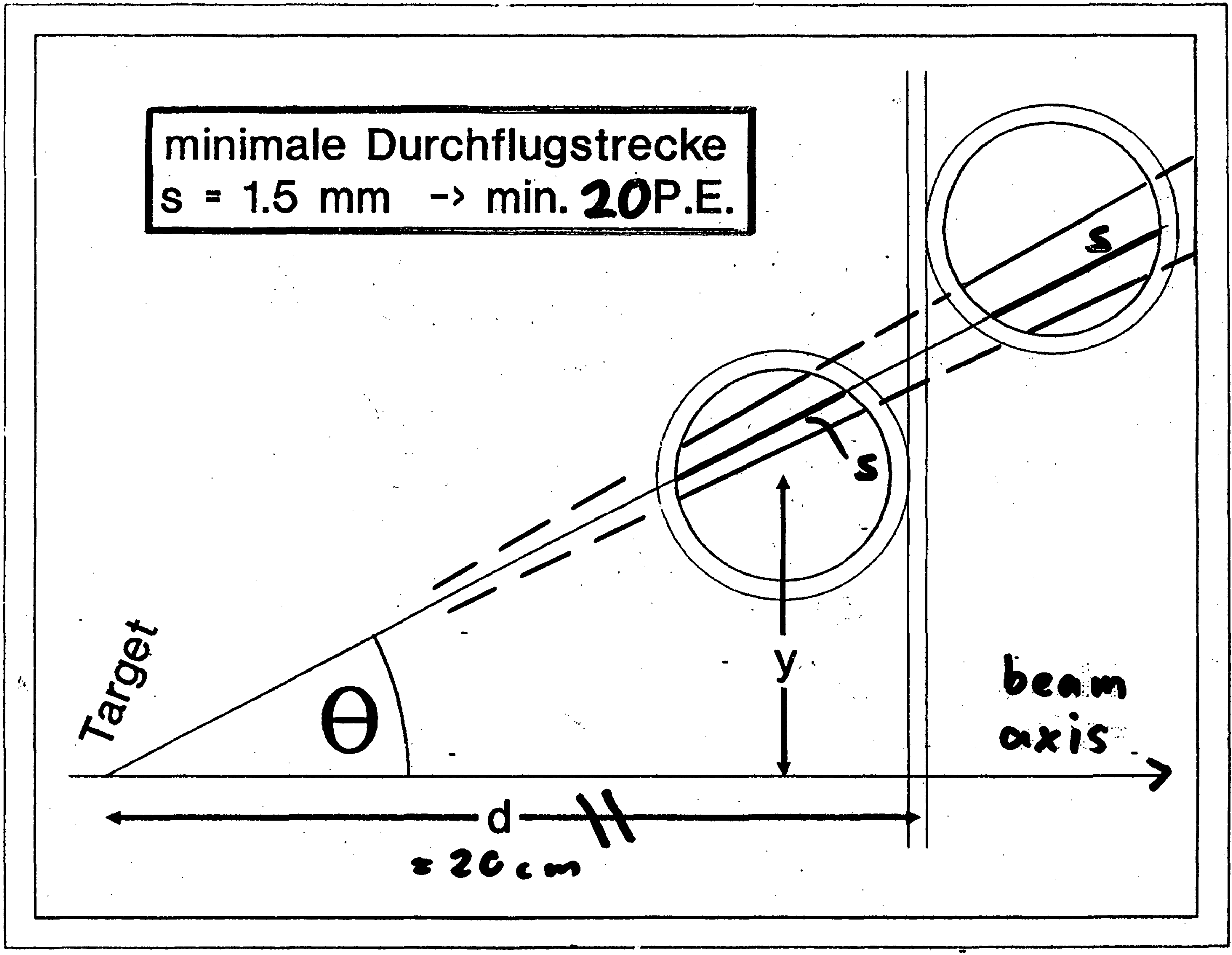

minimale Durchflugstrecke
s = 1.5 mm -> min. **20**P.E.

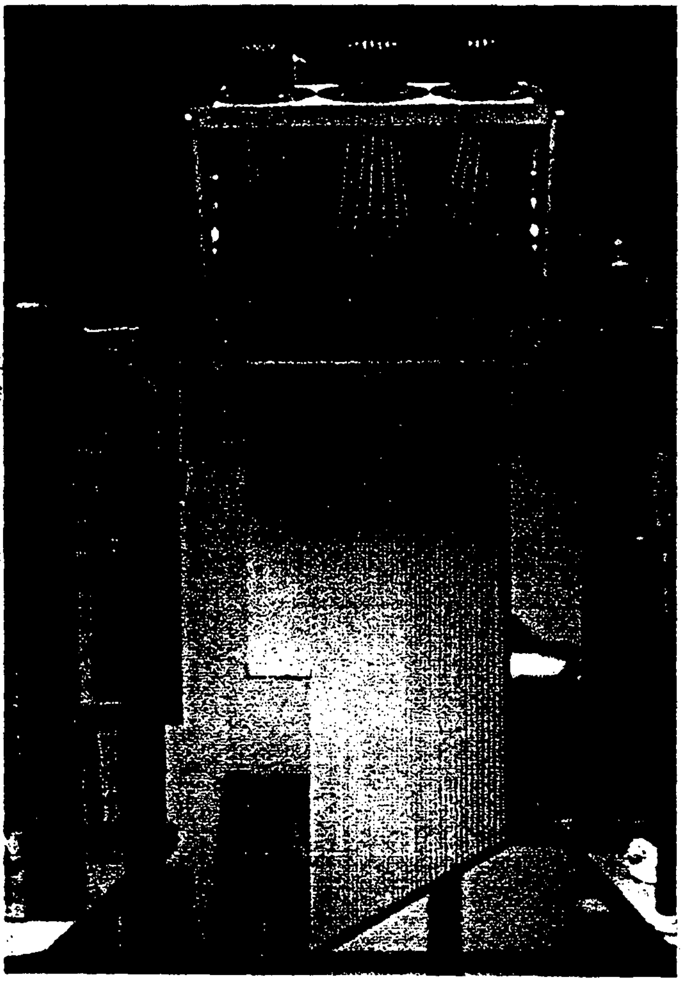

Vertexrekonstruktion

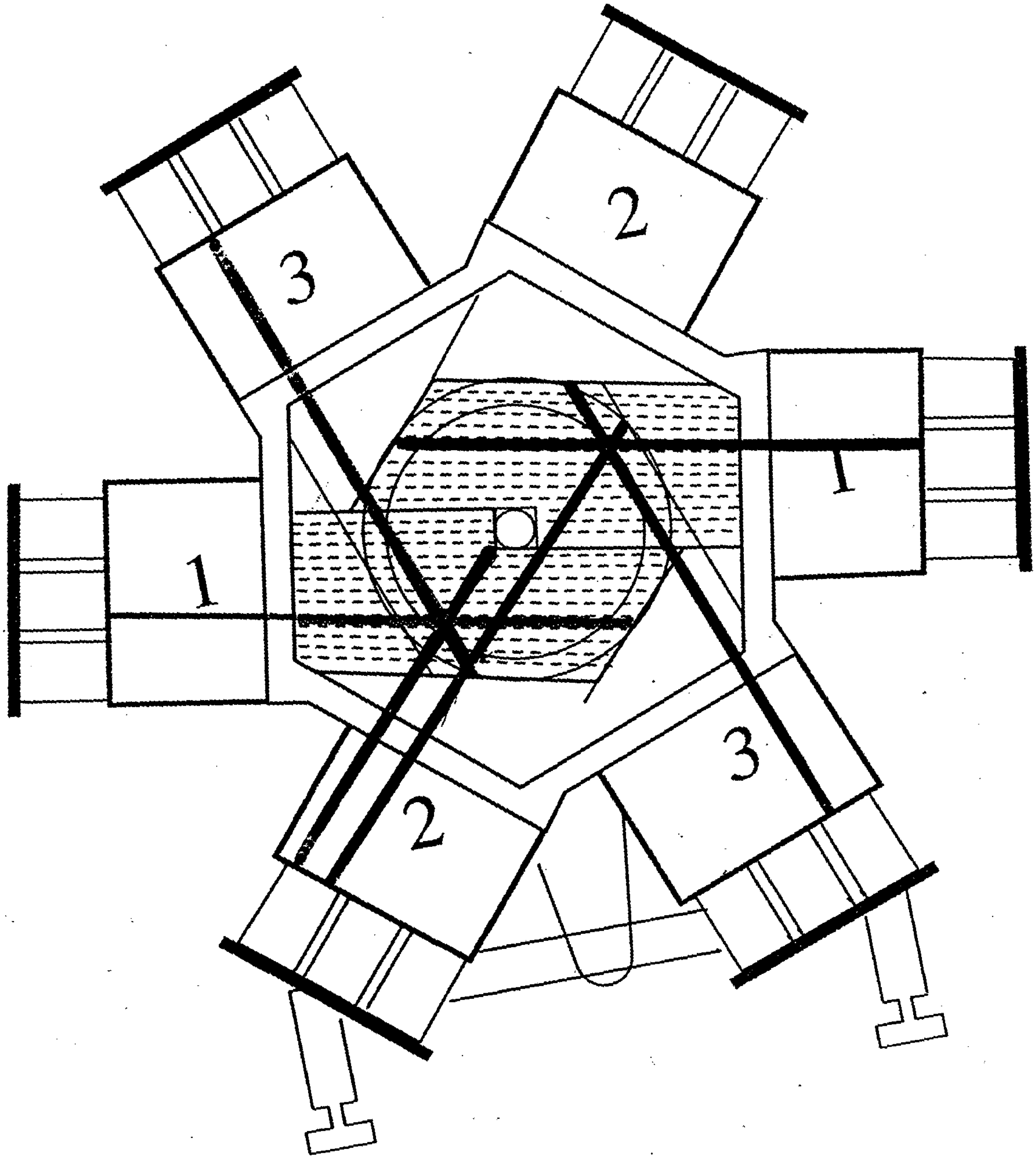

Beam Halo

The vertex wall is used as monitor

triggered on all events, not only ^{3}H

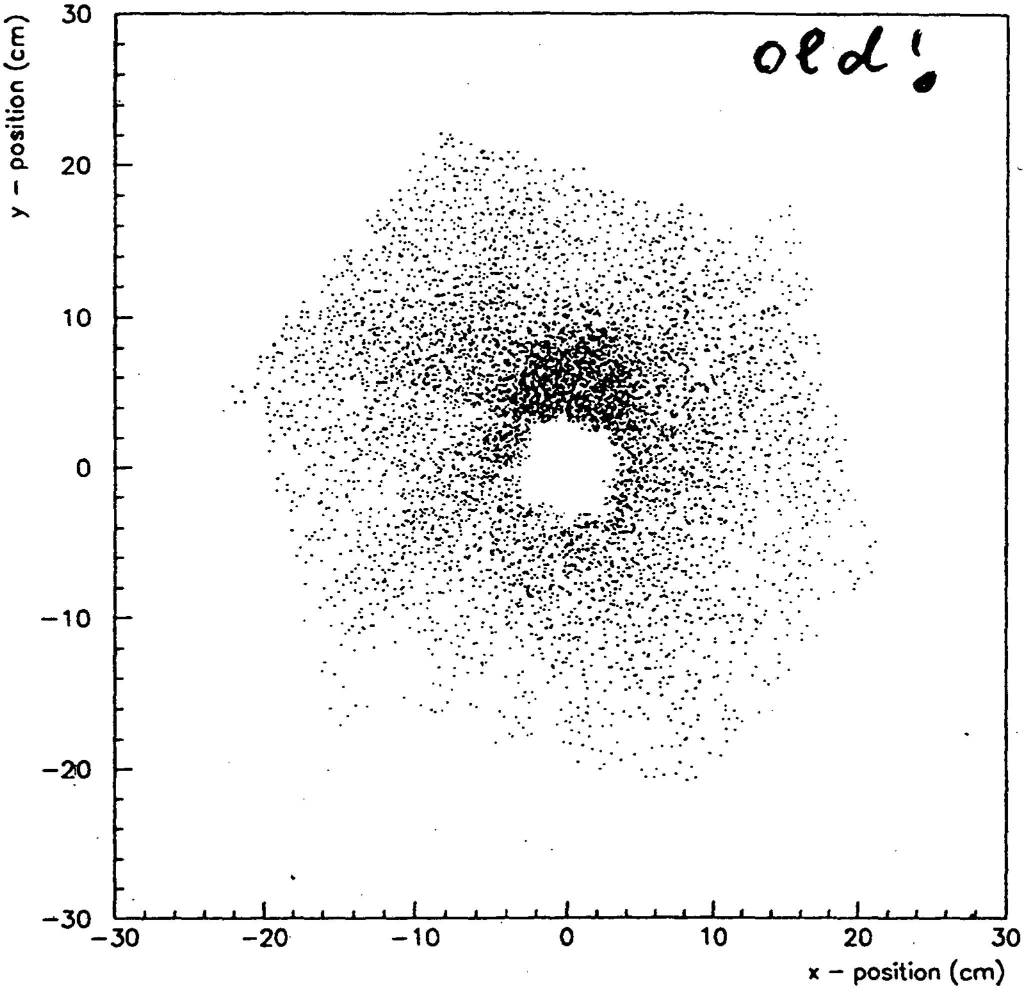

old!

all hits

1150 MeV/c

$\sim 10^{7}$ p/

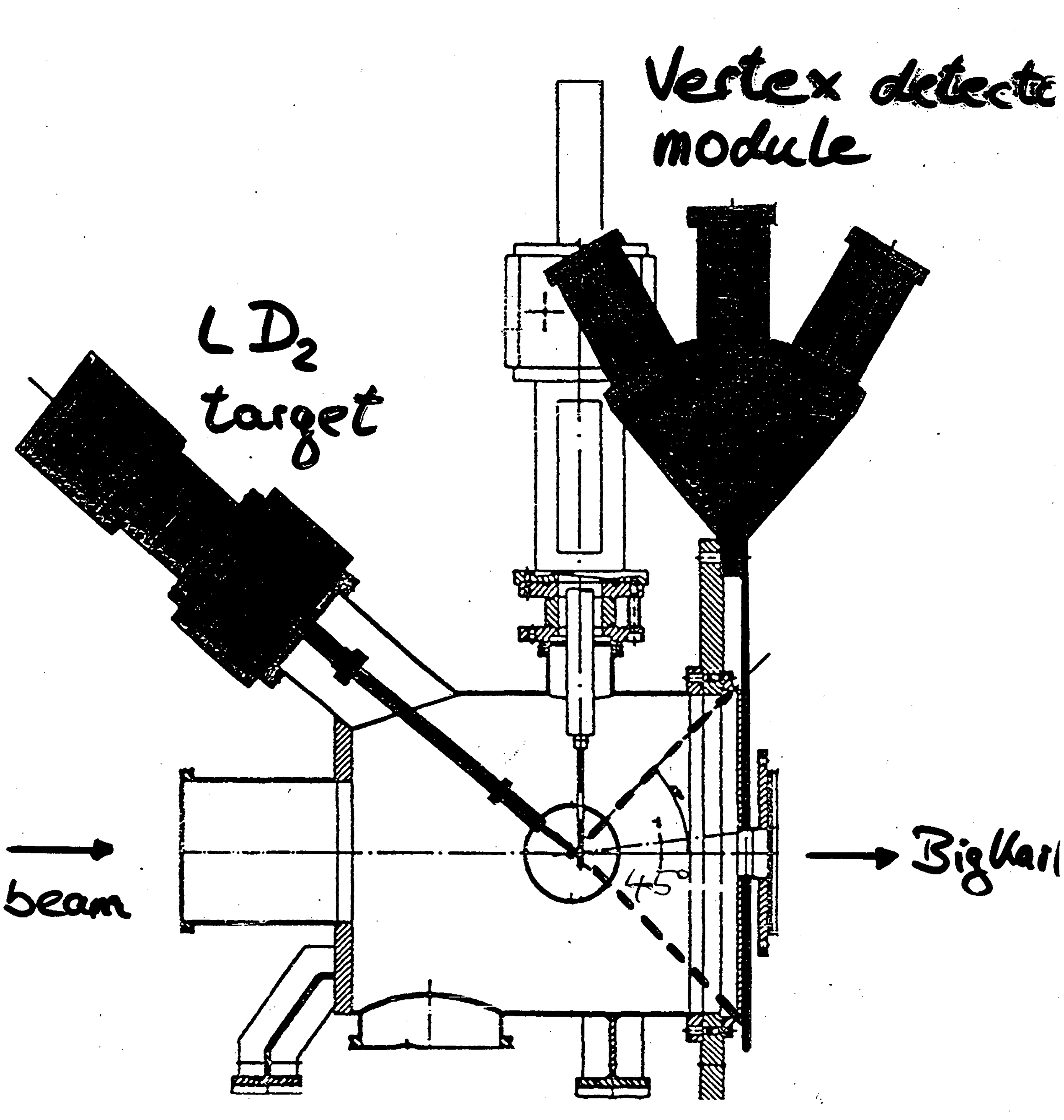

MOMO Target area

MOMO

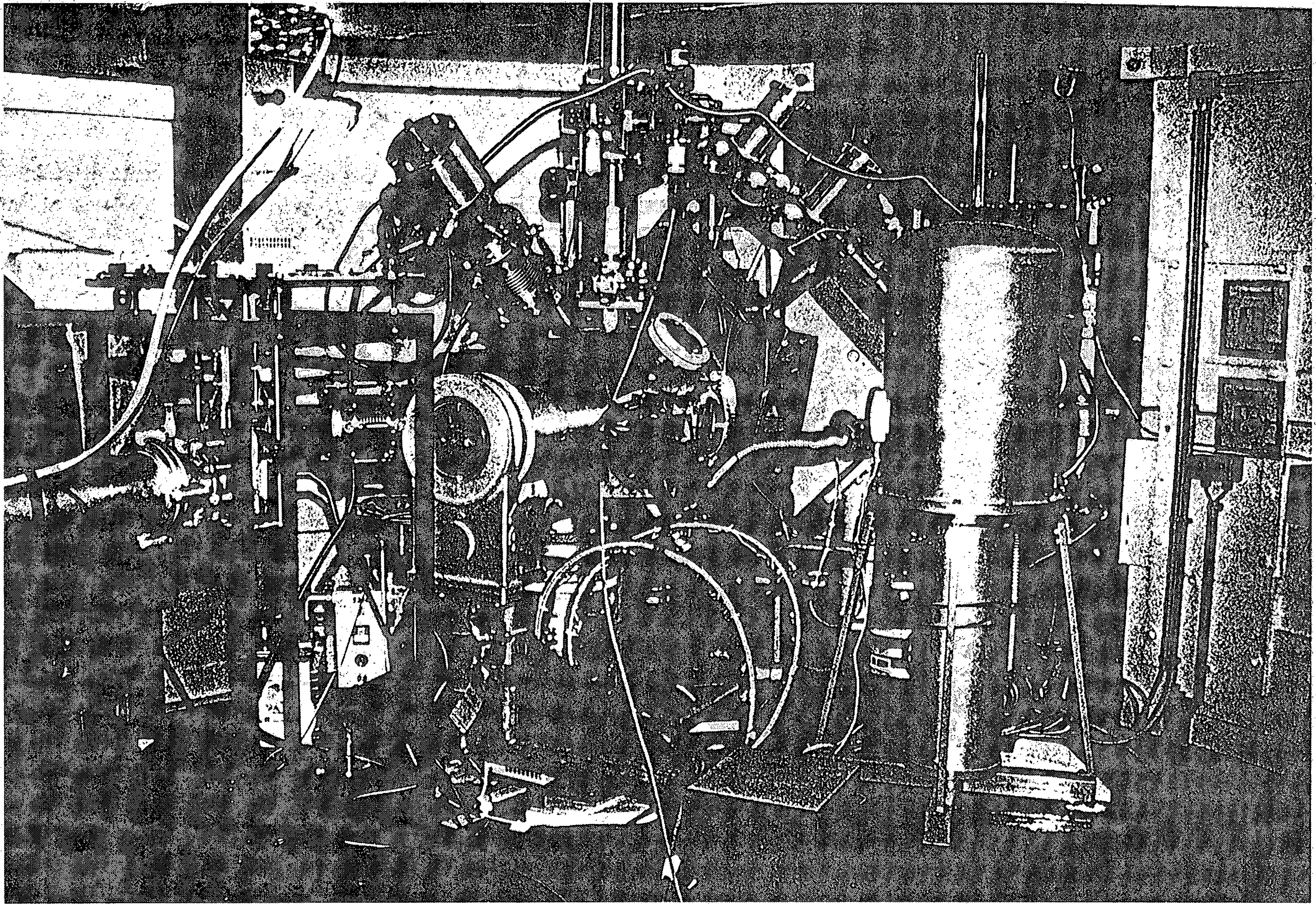

BIG KARL DRIFT CHAMBER

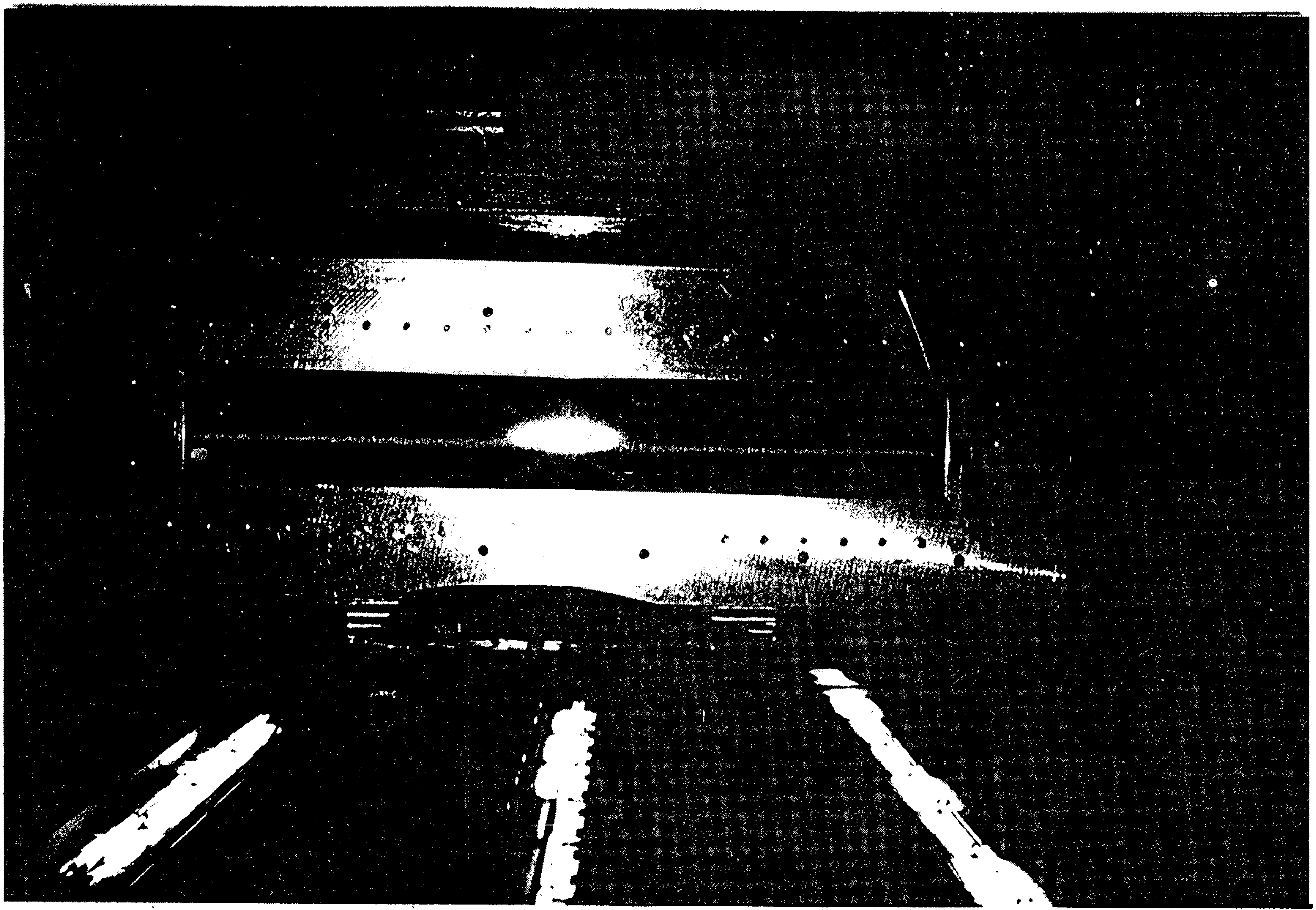

KRAKOW - JÜLICH - BONN

Abbildungseigenschaften
von Big Karl

vertikale Abbildung : vertikaler Winkel -> y Position in der Fokalkebene

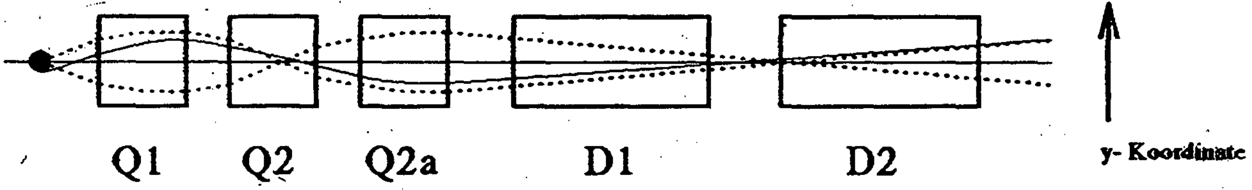

horizontale Abbildung :

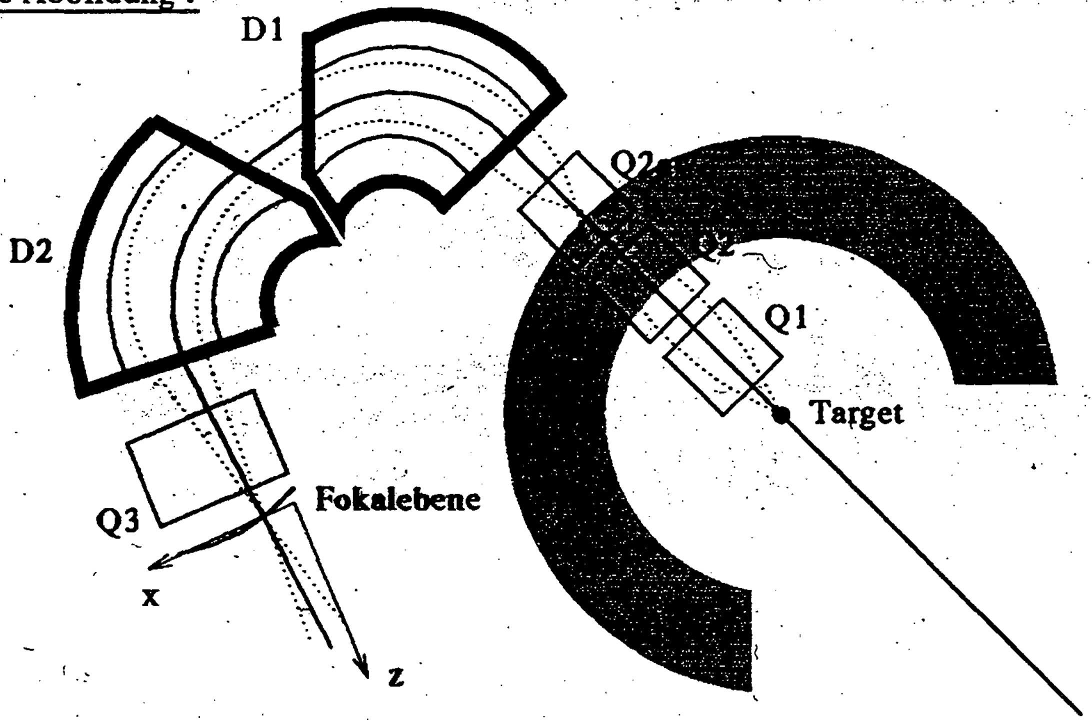

Gesamtimpuls -> x Position in der Fokalebene

horizontaler Winkel -> horizontalen Winkel in der Fokalebene

$p + d \rightarrow X$

1150 MeV/c

Teilchenidentifikation

Energieverlust im ersten Szintillatorhodoskop gegen Flugzeit zwischen den beiden Hodoskoplagen

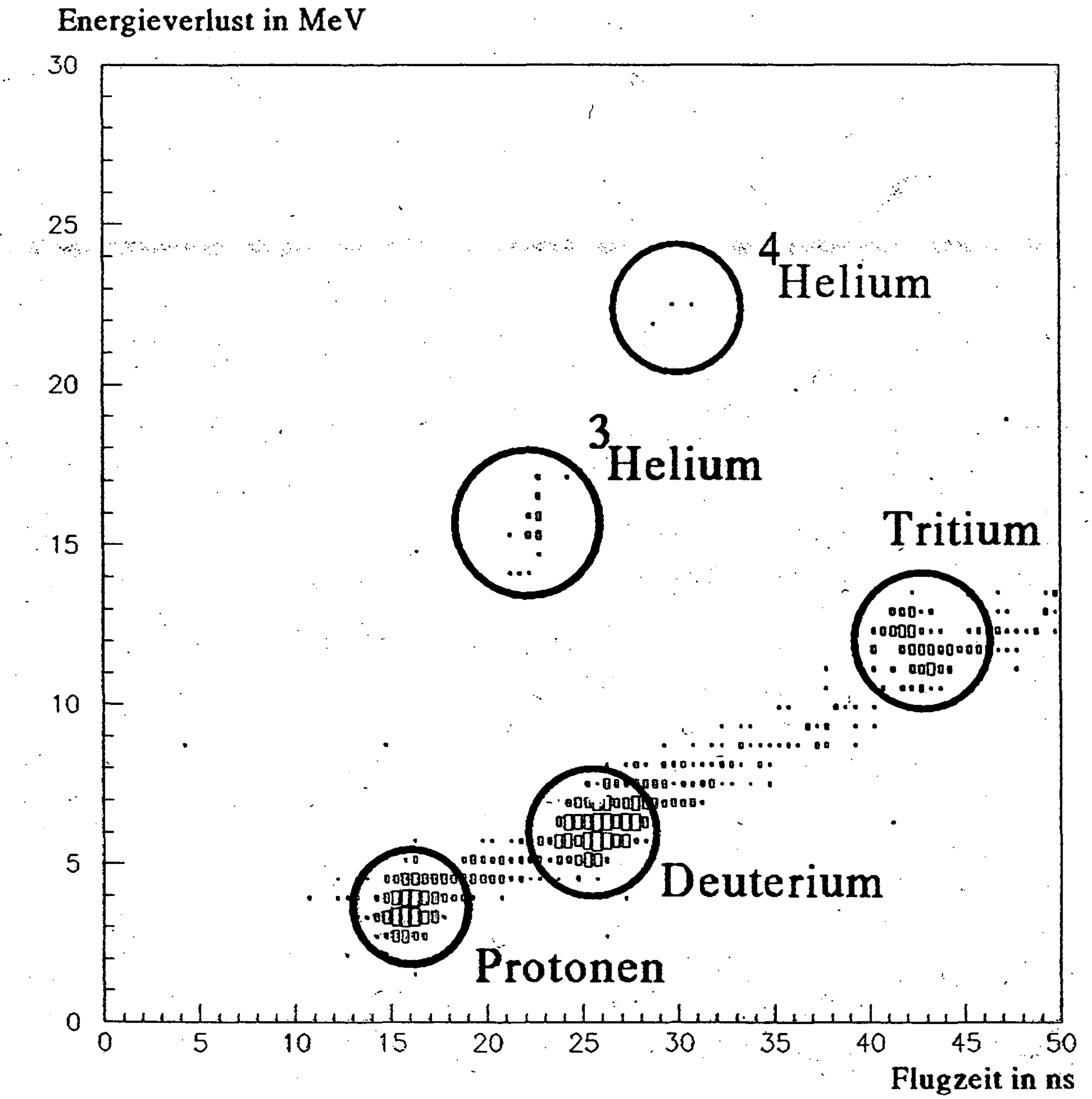

Fokalebenenspektren

BIG KAR

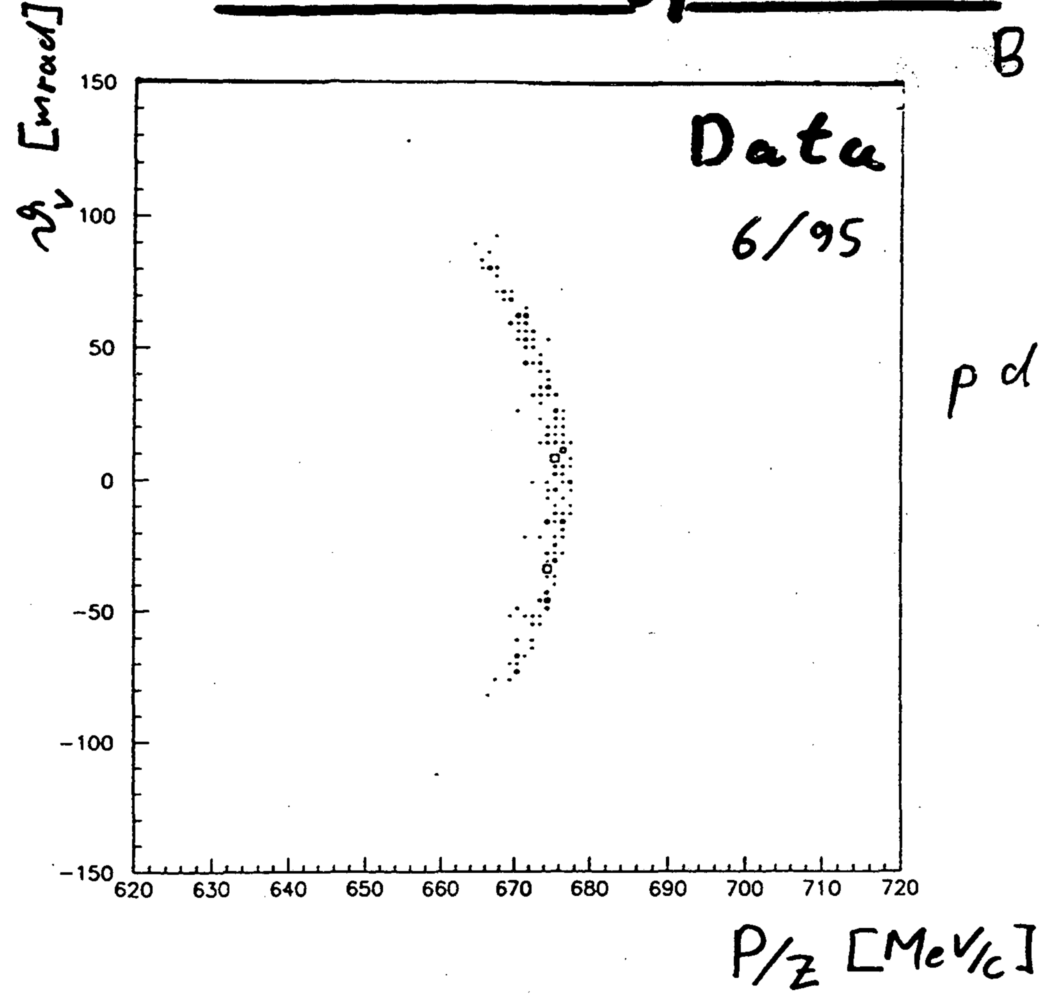

$p d \rightarrow {}^{3}He\pi$

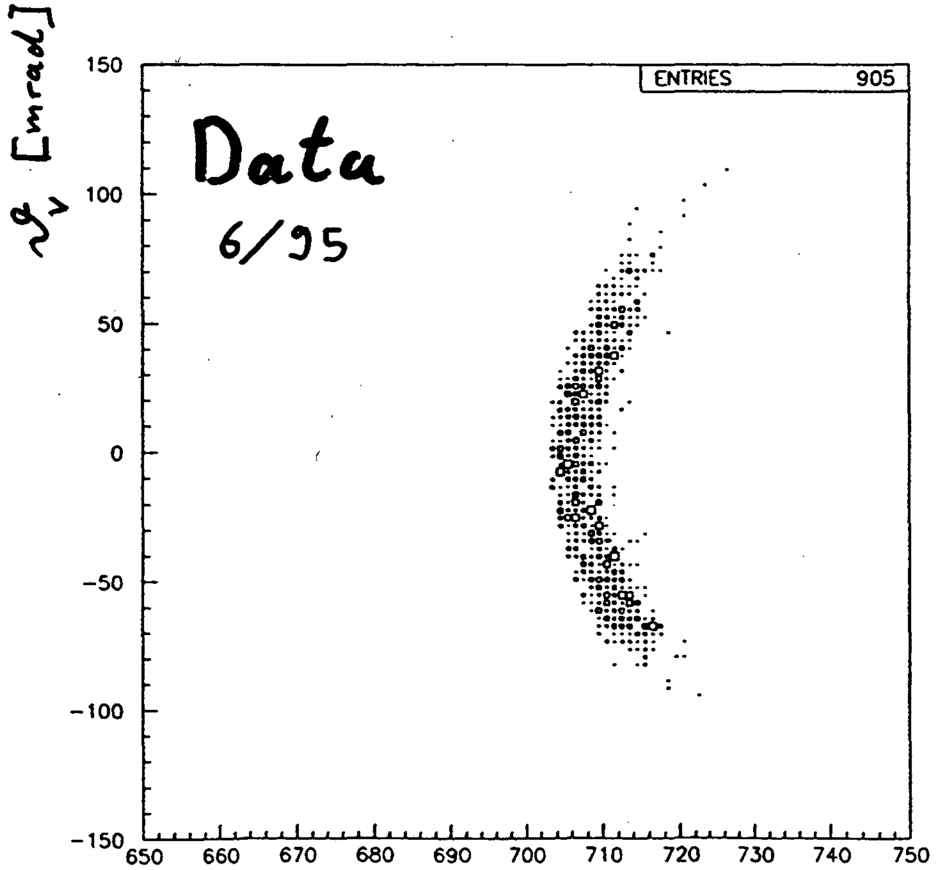

$p d \rightarrow {}^{3}H \pi^{+}$

missing m ss

5/95

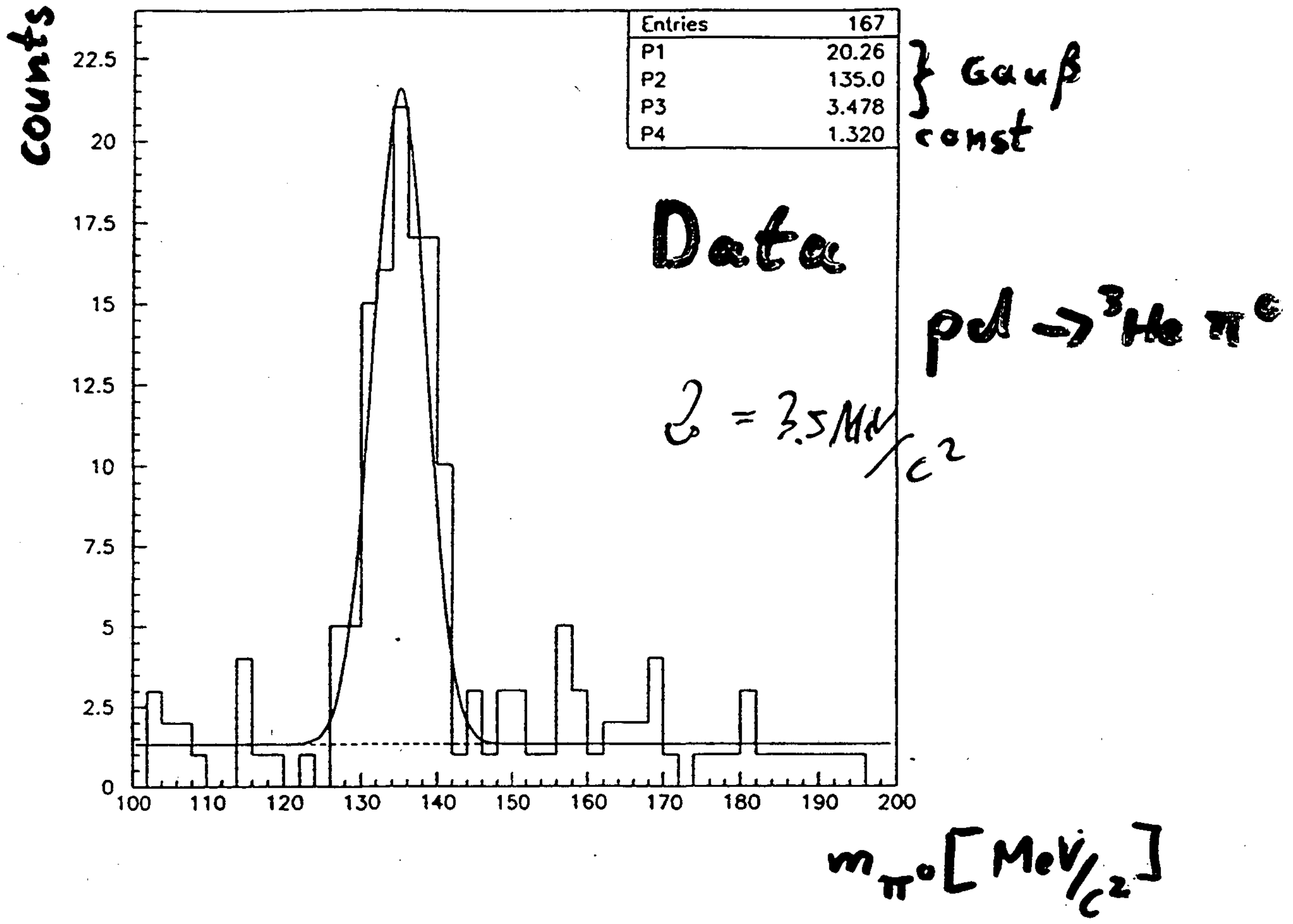

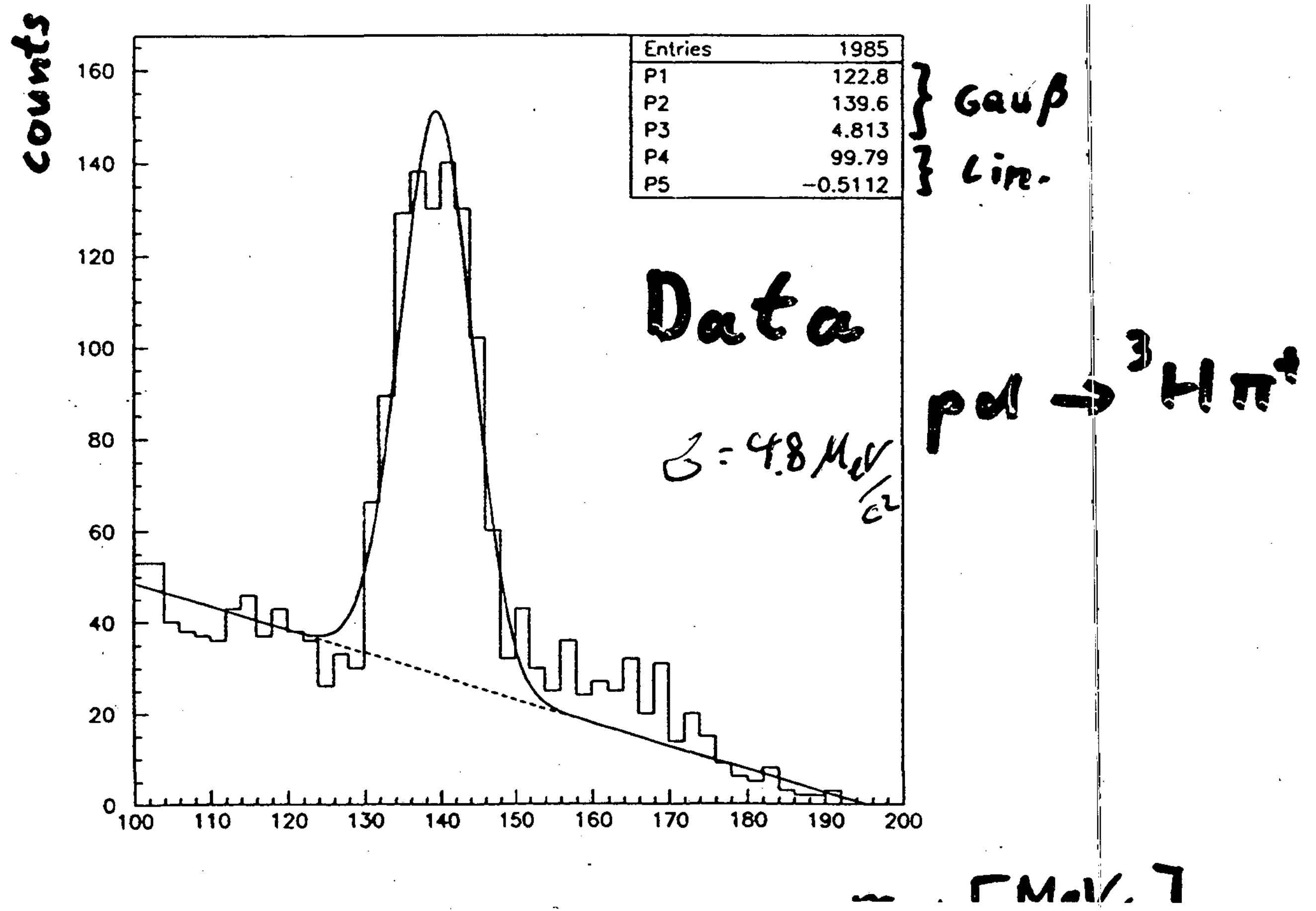

Two Pion Hits

V/96

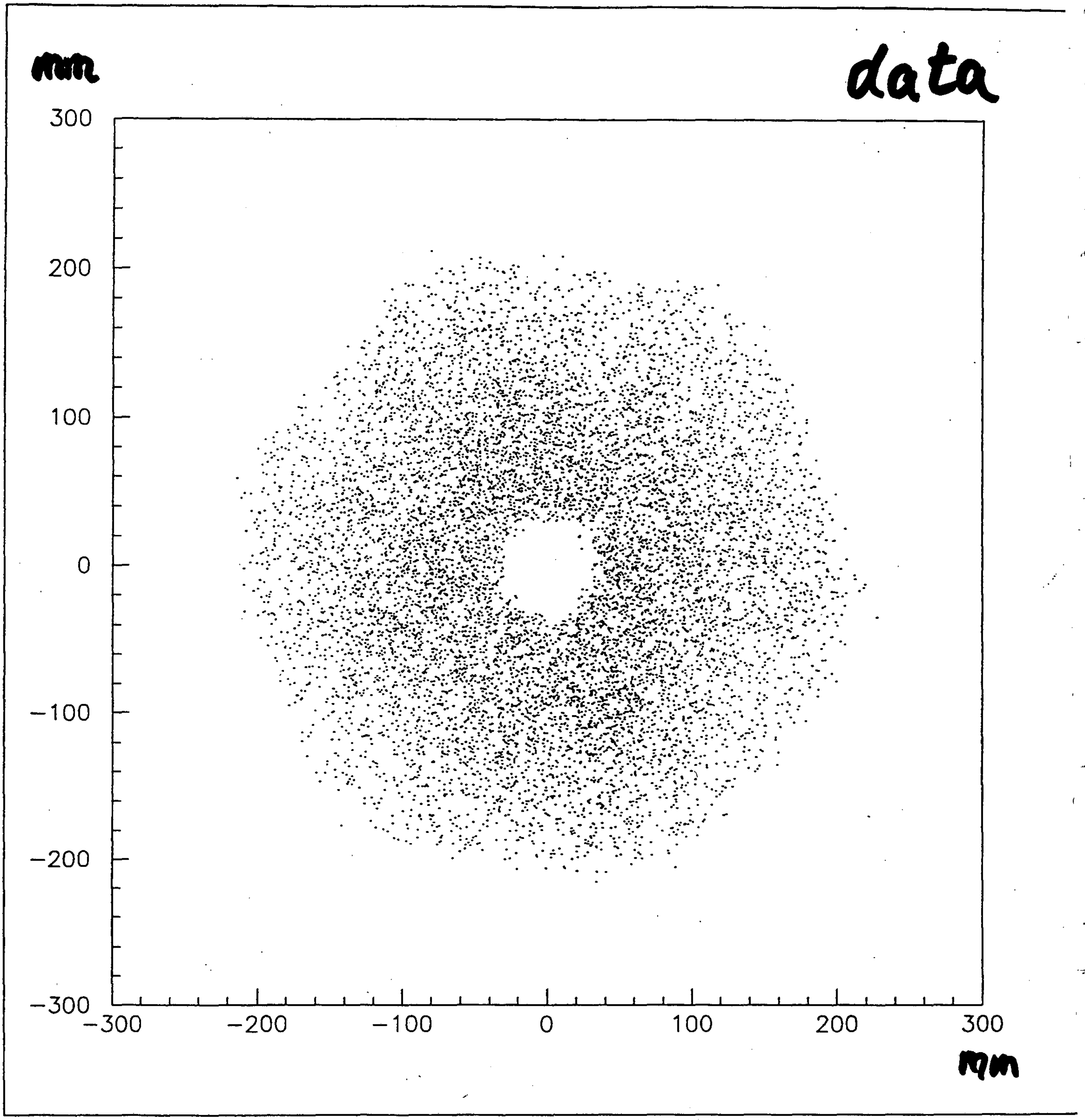

$pd \rightarrow {}^3He\,\pi^+\pi^-$

$p_p = 1150$ MeV/c

Koplanaritätstest

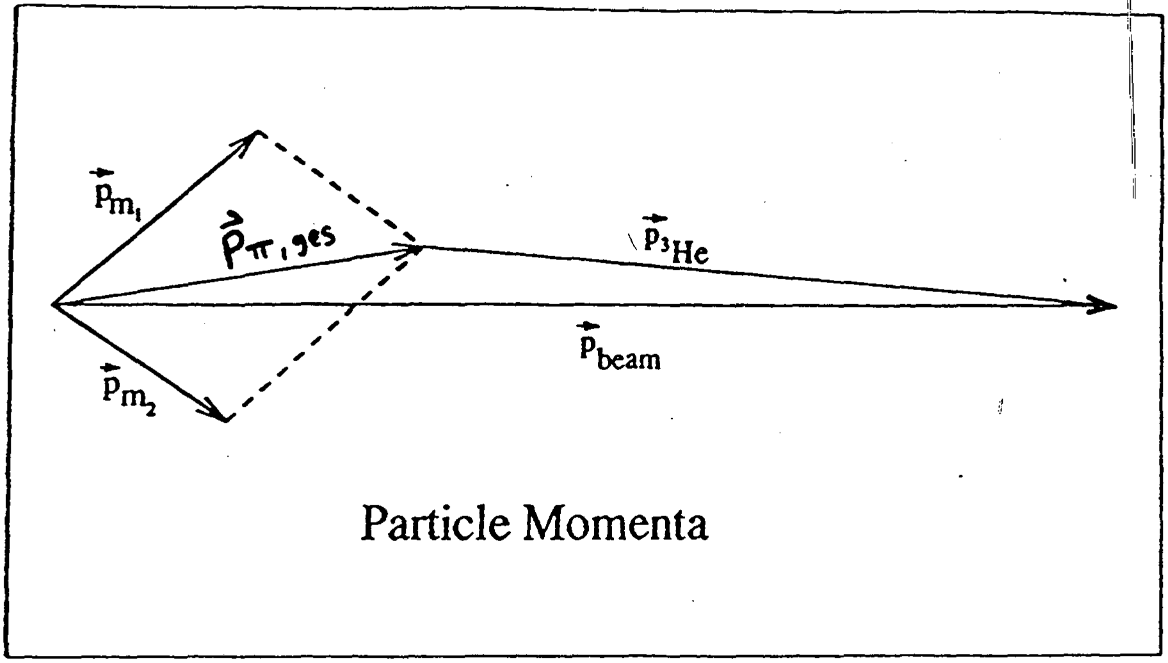

Particle Momenta

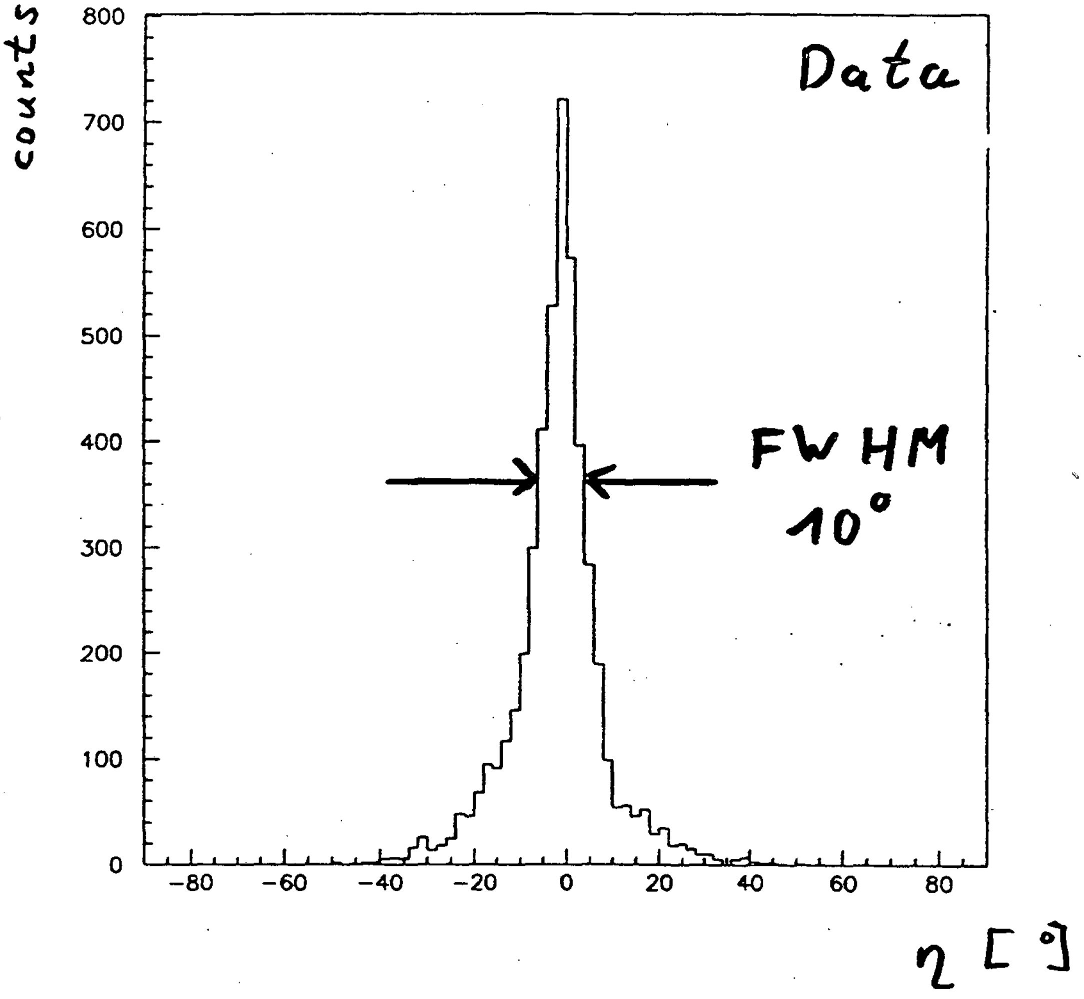

DALITZPLOT

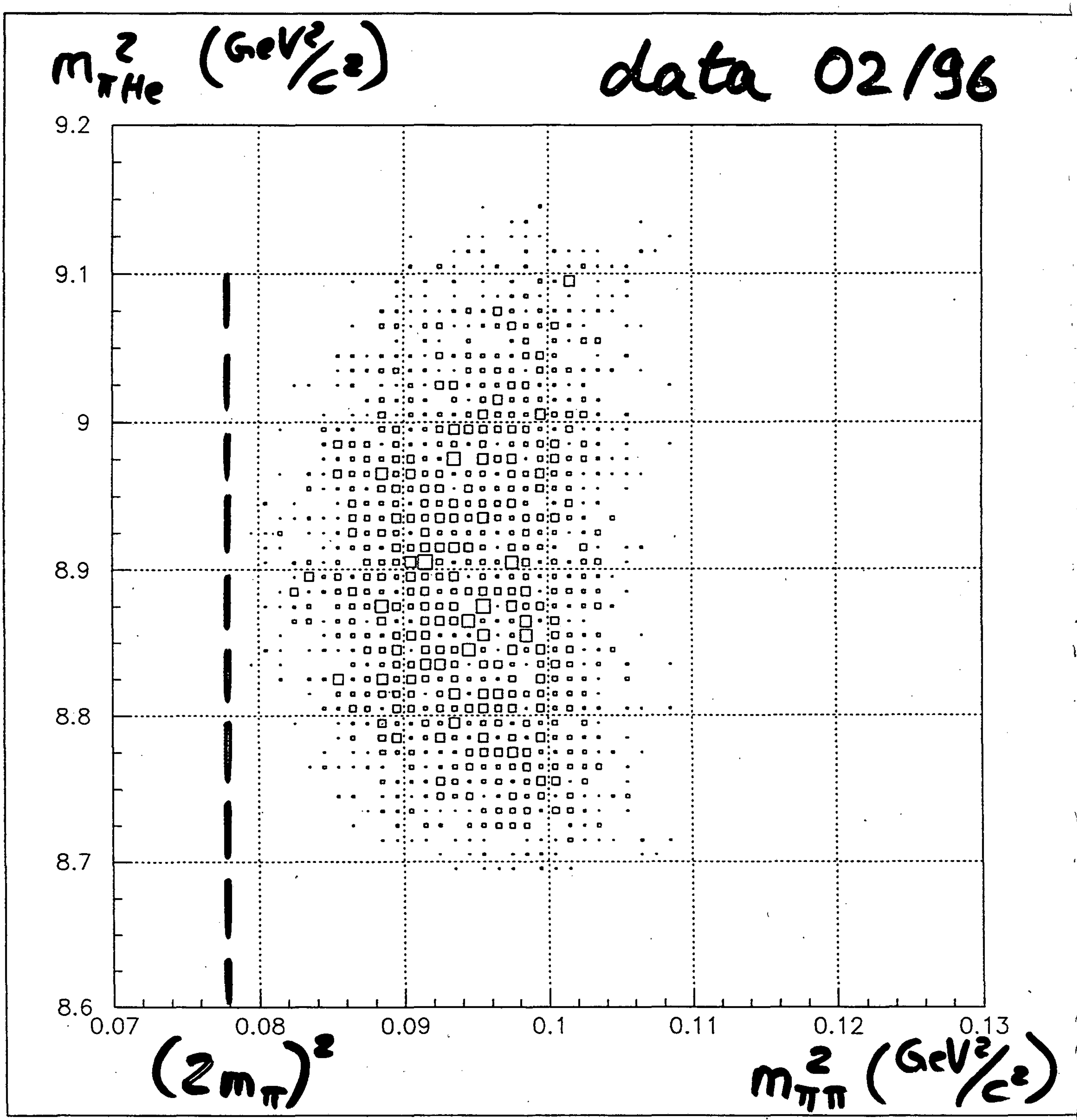
$m^2_{\pi He}$ (GeV²/c²)
data 02/96
9.2
9.1
9
8.9
8.8
8.7
8.6
0.07
0.08
0.09
0.1
0.11
0.12
0.13
$(2m_\pi)^2$
$m^2_{\pi\pi}$ (GeV²/c²)

II/96

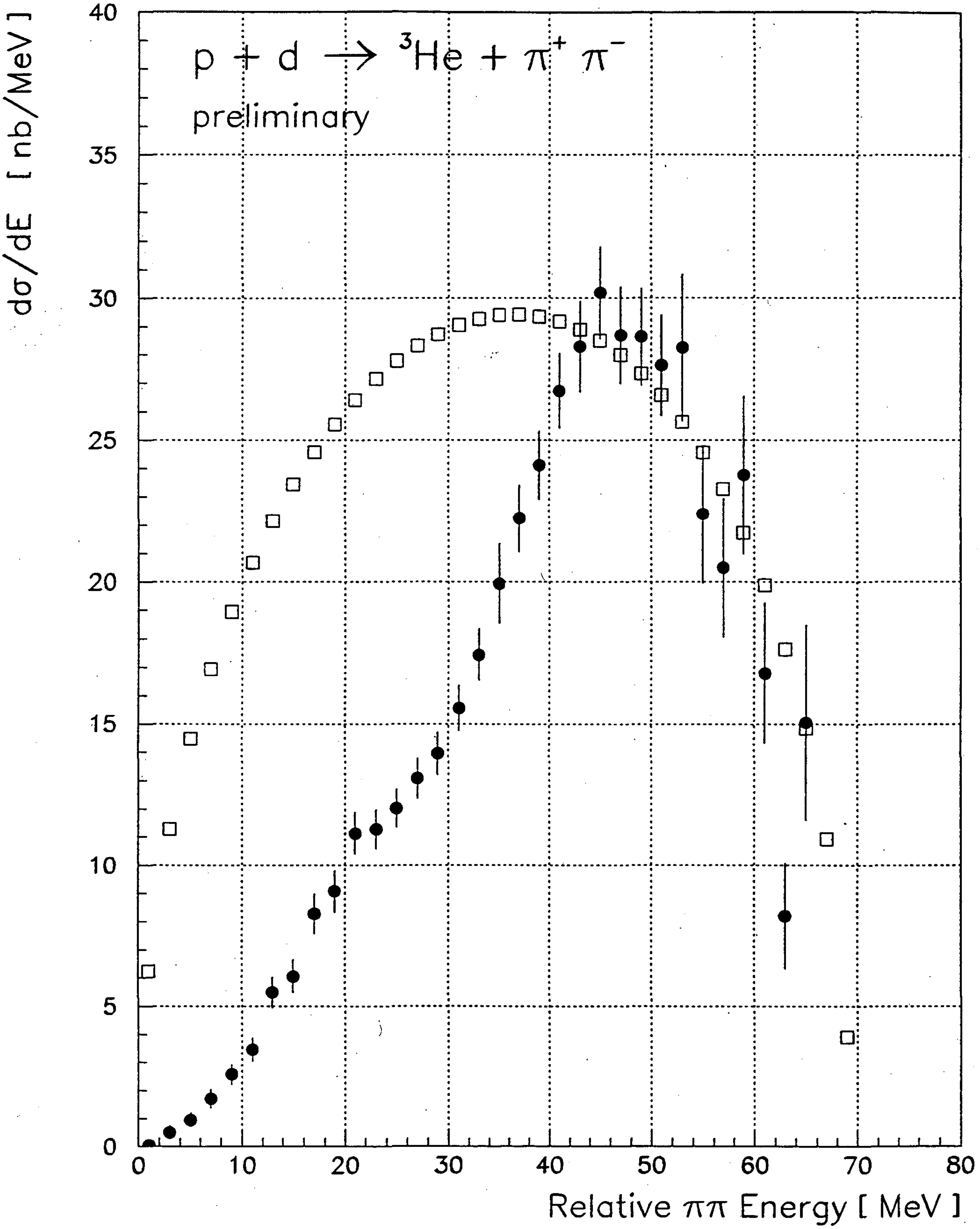

differential cross section

'Exotics'
at
MOMO

e.g. $\pi - {}^3He$ resonances

d' Hypothesis

$d' \hat{=} \pi NN$ resonance

$M = 2.06\ GeV/c^2$

$\Gamma = 0.5\ MeV$

d' in the reaction

$$p + d \rightarrow d'n + \pi^+$$

$$\hookrightarrow {}^3He\,\pi^-$$

as a ${}^3He\,\pi^-$ resonance

$p + d \rightarrow {}^3He + \pi^+\pi^-$

$+ 1\%\ d'n$

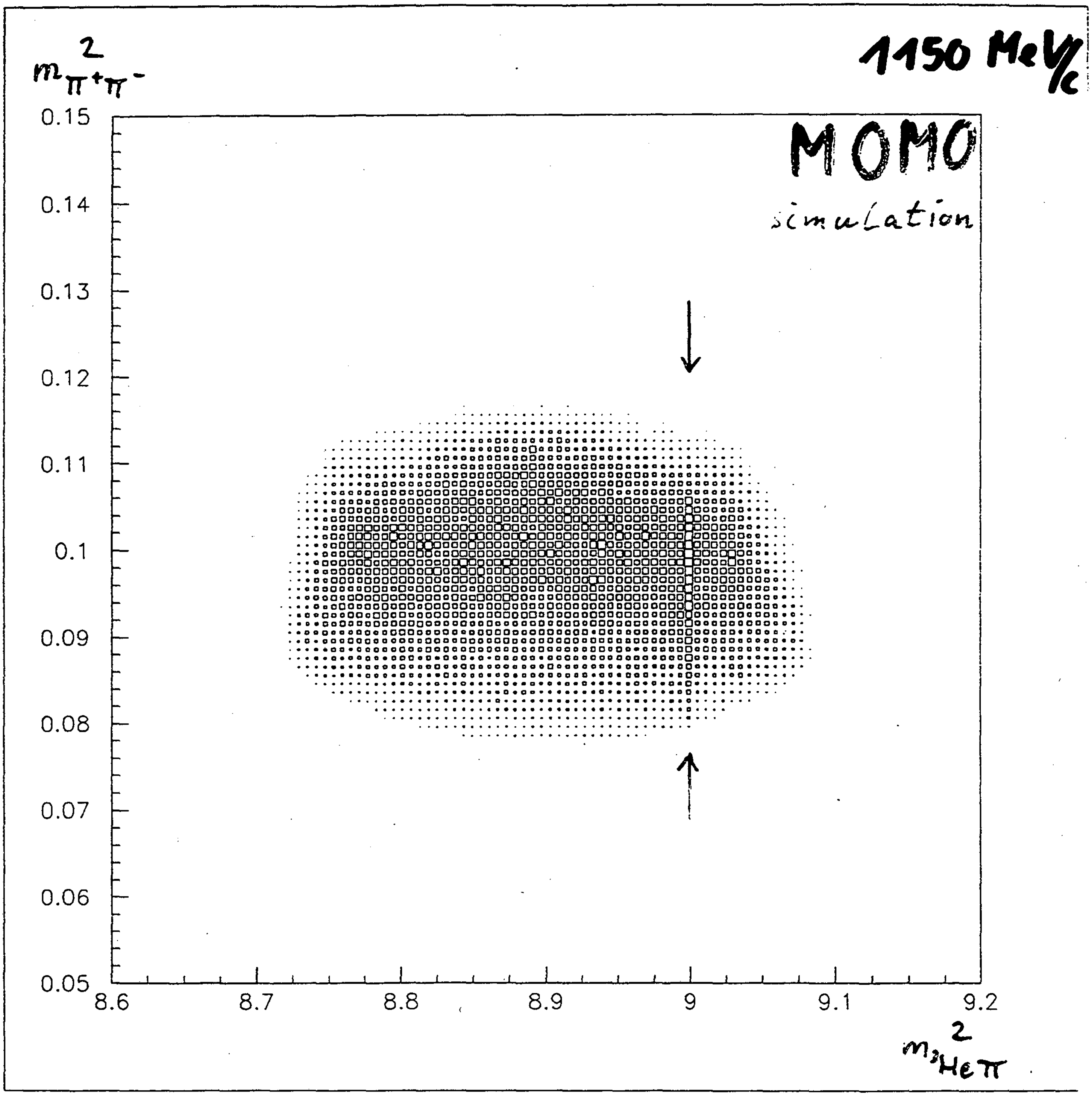

GISMO

$p + d \longrightarrow {}^3He + \pi^+\pi^-$

+ 1% $d'n$

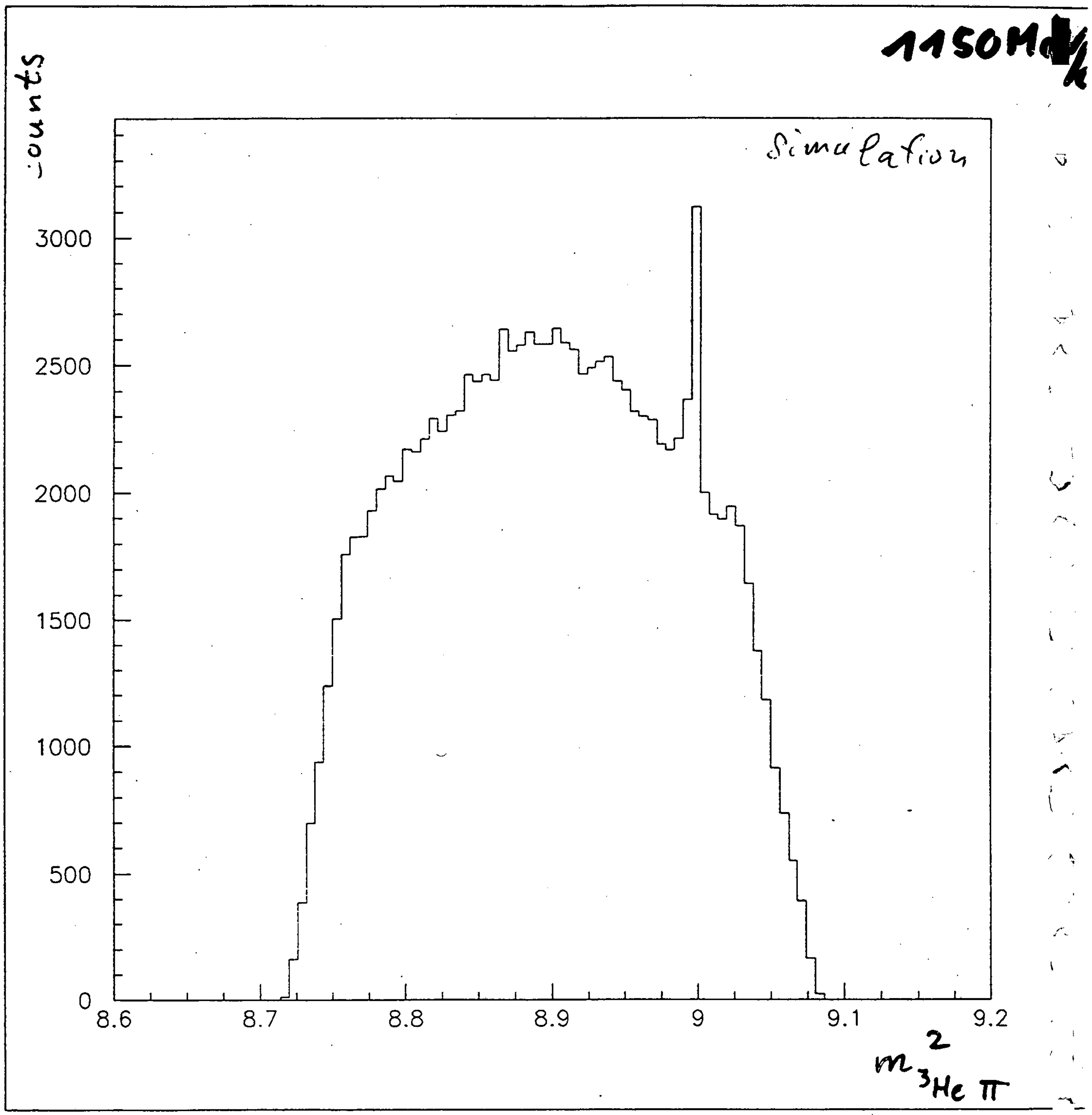

GISMO

II/96
data

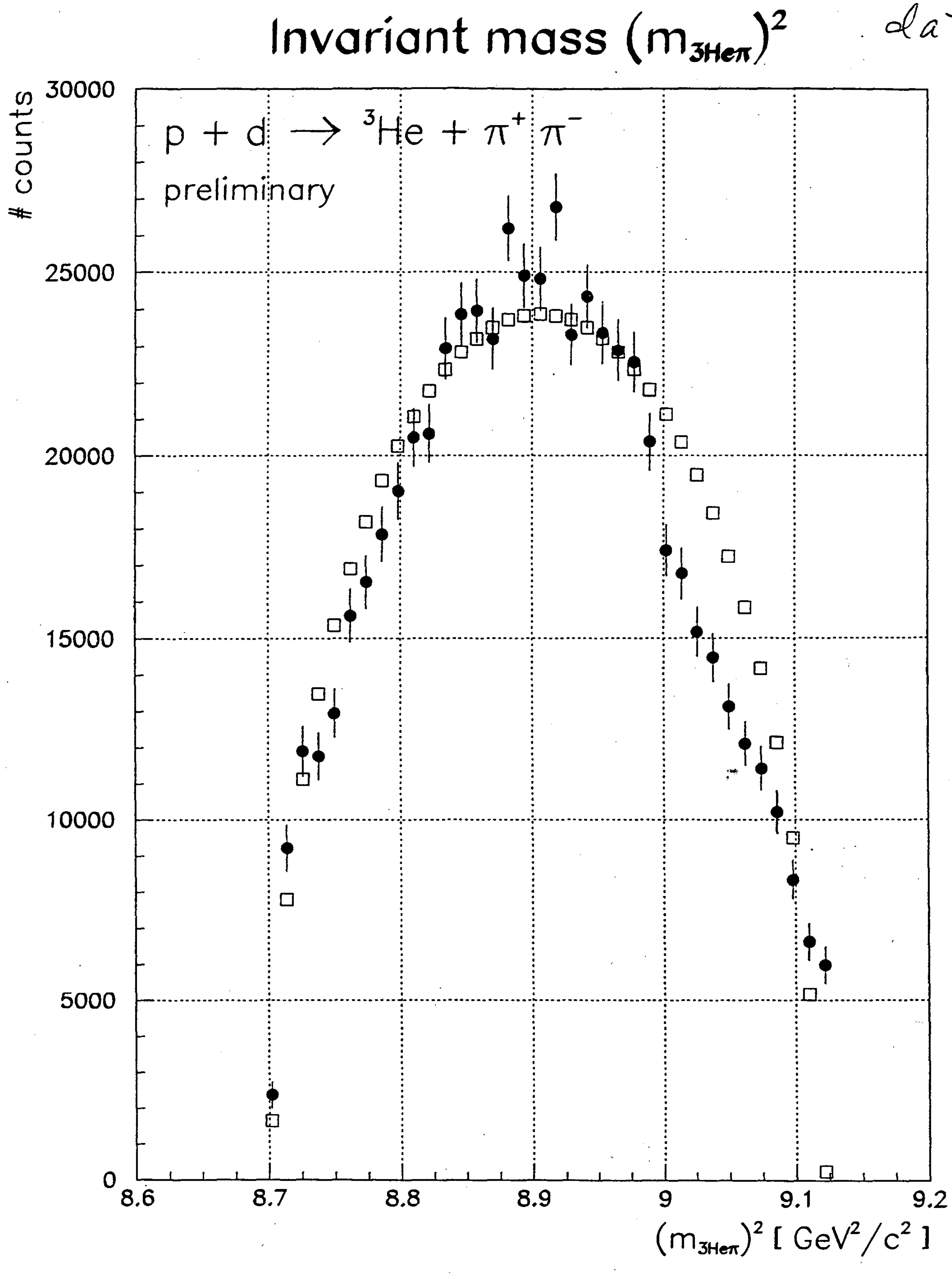
Invariant mass $(m_{3He\pi})^2$
$p + d \rightarrow {}^3He + \pi^+ \pi^-$
preliminary
counts
30000
25000
20000
15000
10000
5000
0
8.6
8.7
8.8
8.9
9
9.1
9.2
$(m_{3He\pi})^2$ [GeV^2/c^2]

Many

Online

Mesons

On time

Die MOMO - Kollaboration

F. Bellemann[1], A. Berg[1], J. Bisplinghoff[1], G. Bohlscheid[1], J. Ernst[1], R. Frascaria[6], C. Henrich[1], F. Hinterberger[1], R. Ibald[1], R. Jahn[1], L. Jarczyk[2], R. Joosten[1], A. Kozela[2], U. Kuhn[1], H. Machner[3], R. Maschuw[1], T. Mayer-Kuckuk[1], G. Mertler[1], B. Metsch[4], J. Munkel[1], P. v. Neumann-Cosel[5], T. v. Oepen[1], H. R. Petry[4], D. Rosendaal[1], P. v. Rossen[3], K. Scho[1], F. Schwandt[1], R. Siebert[6], J. Smyrski[2], A. Strzalkowski[2], R. Tölle[3], W. Wiedmann[1], R. Wurzinger[1], R. Ziegler[1]

[1] Institut für Strahlen- und Kernphysik, Universität Bonn
[2] Institute for Physics, Jagellonian University Krakow, Poland
[3] Institut für Kernphysik, Forschungszentrum Jülich
[4] Institut für theoretische Kernphysik, Universität Bonn
[5] Institut für Kernphysik, Technische Hochschule Darmstadt
[6] IPN Orsay, France

Jon Batchelder

Louisiana State University
Baton Rouge, LA

The study of Intruder States Near Z = 82 via Alpha Emission: The Decays of ^{187,189}Bi

J. C. Batchelder
Louisiana State University

presented at the Exotic Nuclei Symposium,
Bodega Bay, Ca, April 14-16, 1996

Argonne National Laboratory

C. N. Davids, D.J. Blumenthal, D.J. Henderson, D. Seweryniak

University of Edinburgh

P. J. Woods, R. J. Irvine

Louisiana State University

J. C. Batchelder, E. F. Zganjar

University of Tennessee

C. R. Bingham, B. E. Zimmerman, J. Wauters

Oak Ridge National Laboratory

K. S. Toth

University of Maryland

W. B. Walters, L. F. Conticchio

Vanderbilt University

L. T. Brown

University of California, Berkely

D. M. Moltz, T. J. Ognibene, J. Powell, M. W. Rowe, R. J. Tighe

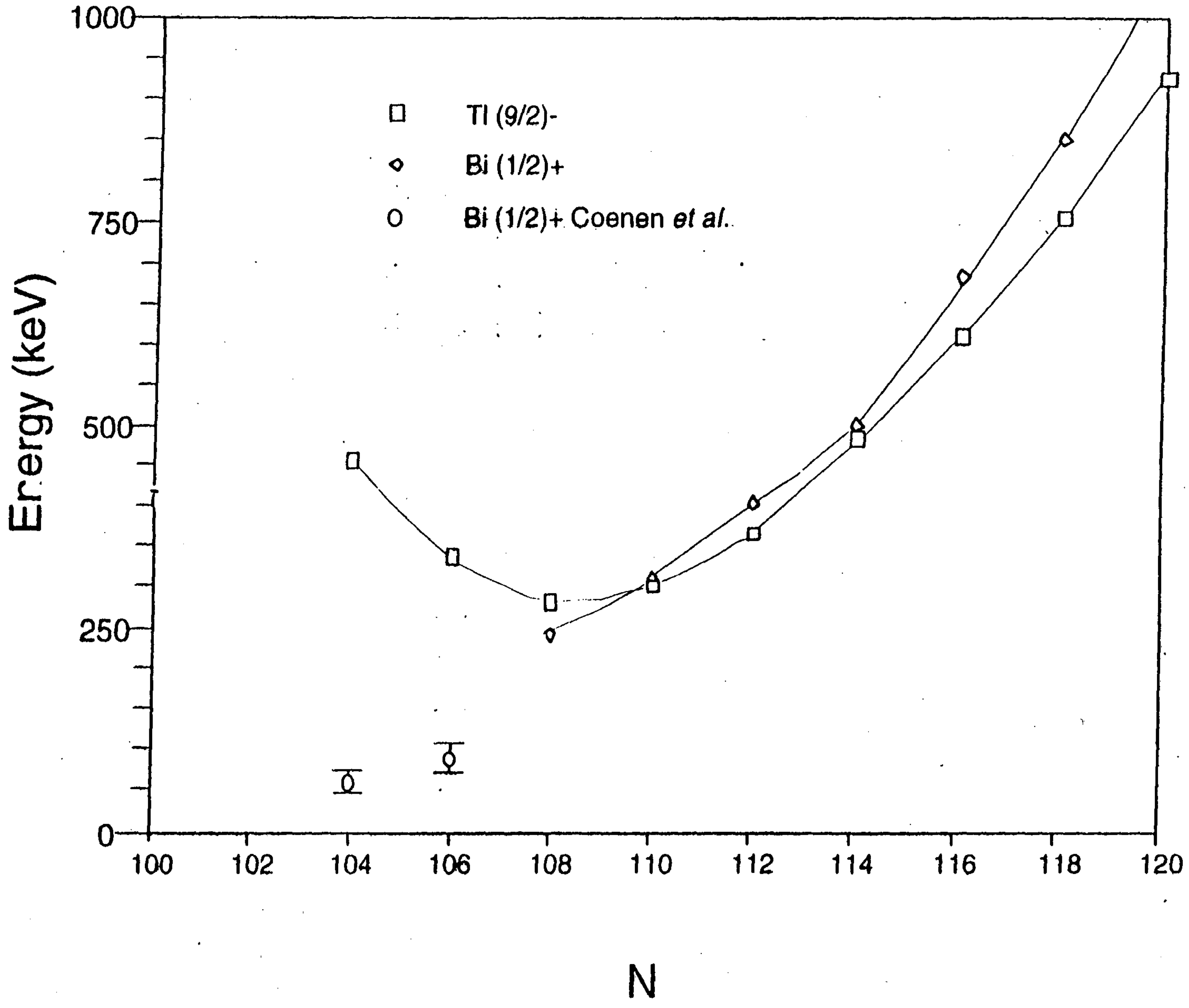

Plot of the intruder state excitation energies versus N for odd-mass Tl ($\pi h_{9/2}$) and Bi ($\pi s_{1/2}$) isotopes.

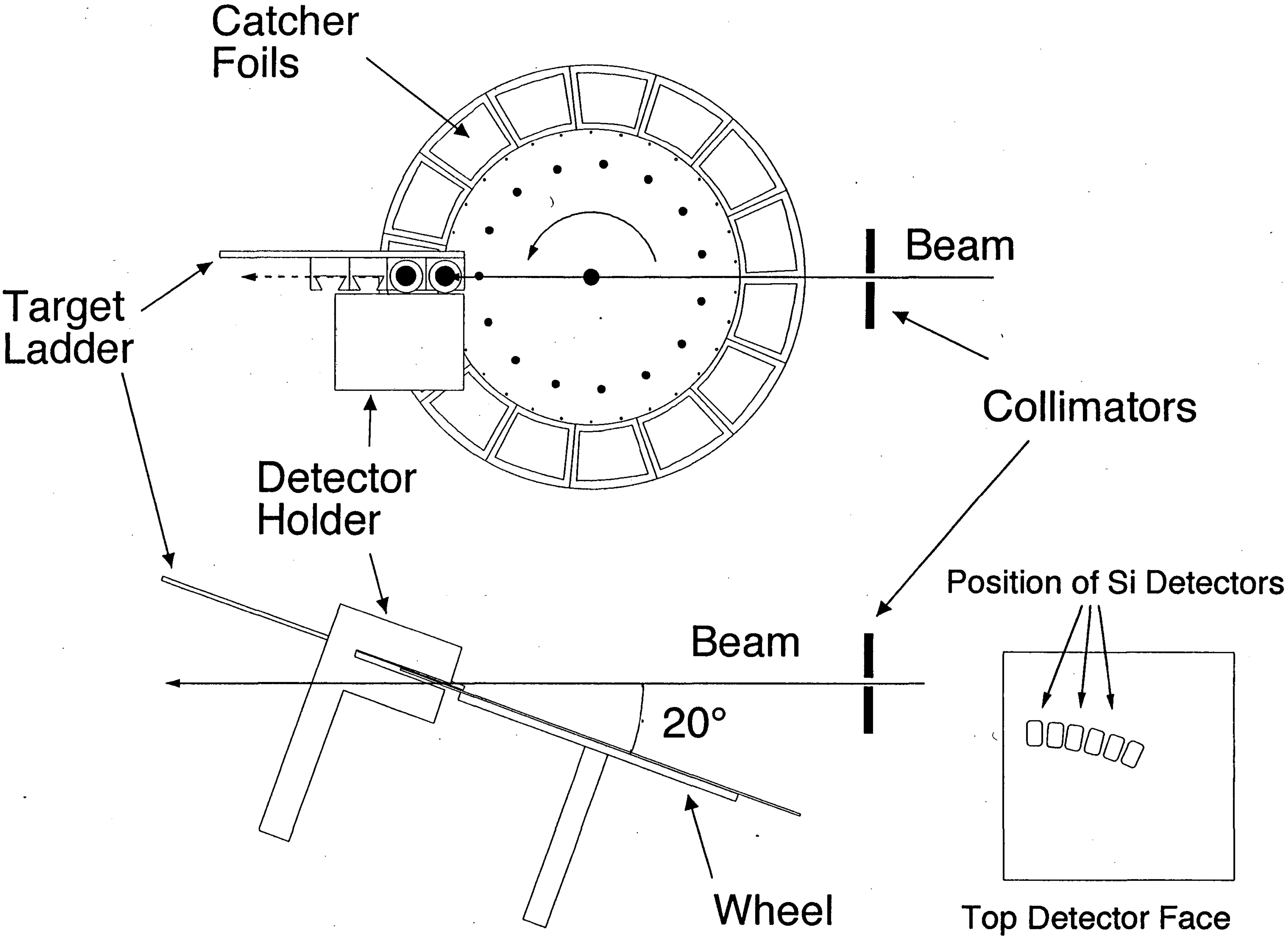
Catcher Foils
Beam
Target Ladder
Collimators
Detector Holder
Position of Si Detectors
Beam
20°
Wheel
Top Detector Face

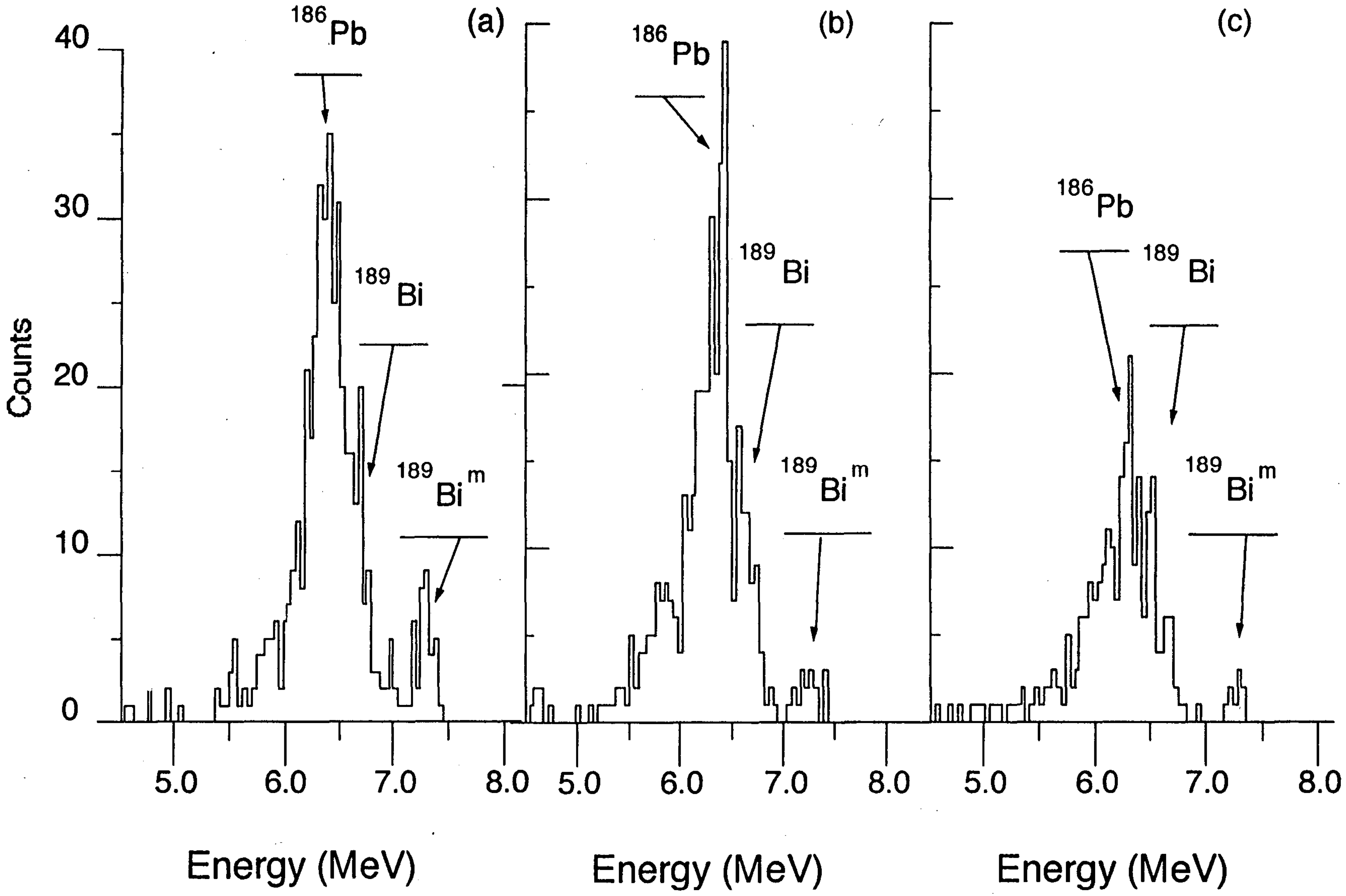
(a)
(b)
(c)
186Pb
189Bi
189Bim
Counts
0
10
20
30
40
5.0
6.0
7.0
8.0
Energy (MeV)

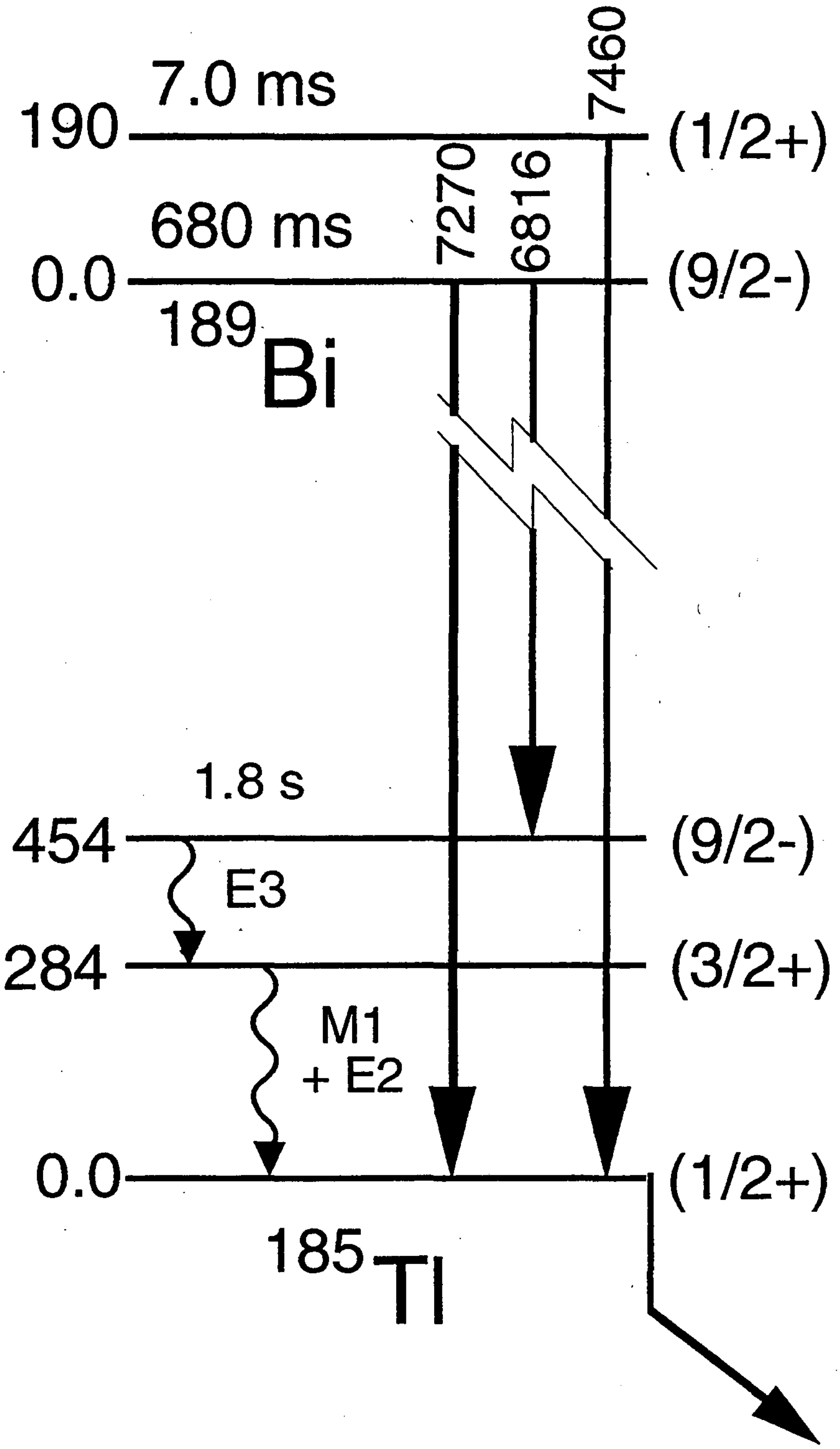
7.0 ms
190
7460
(1/2+)
7270
6816
680 ms
0.0
(9/2-)
189Bi
1.8 s
454
(9/2-)
E3
284
(3/2+)
M1
+ E2
0.0
(1/2+)
185Tl

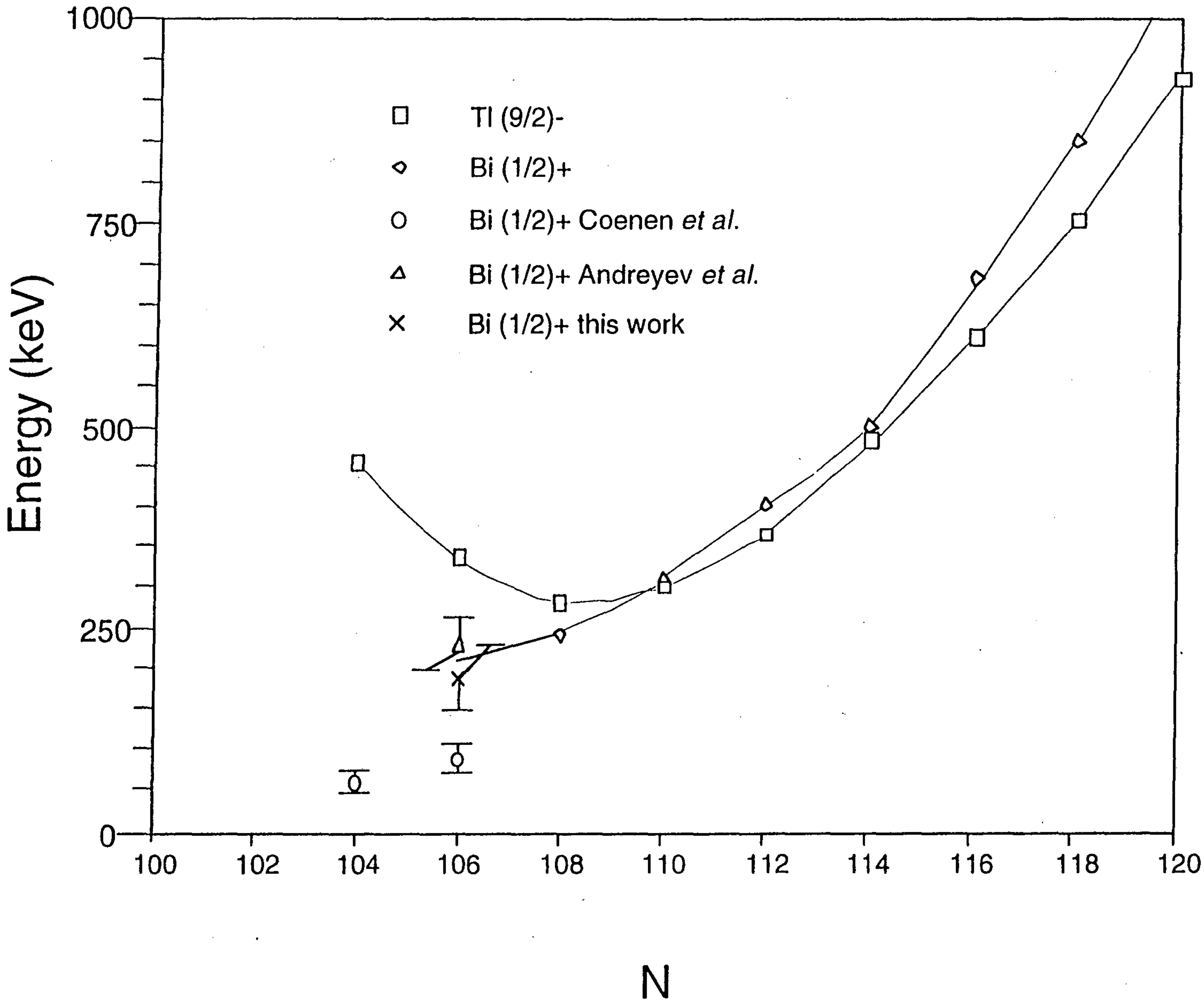

Plot of the intruder state excitation energies versus N for odd-mass Tl ($\pi h_{9/2}$) and Bi ($\pi s_{1/2}$) isotopes.

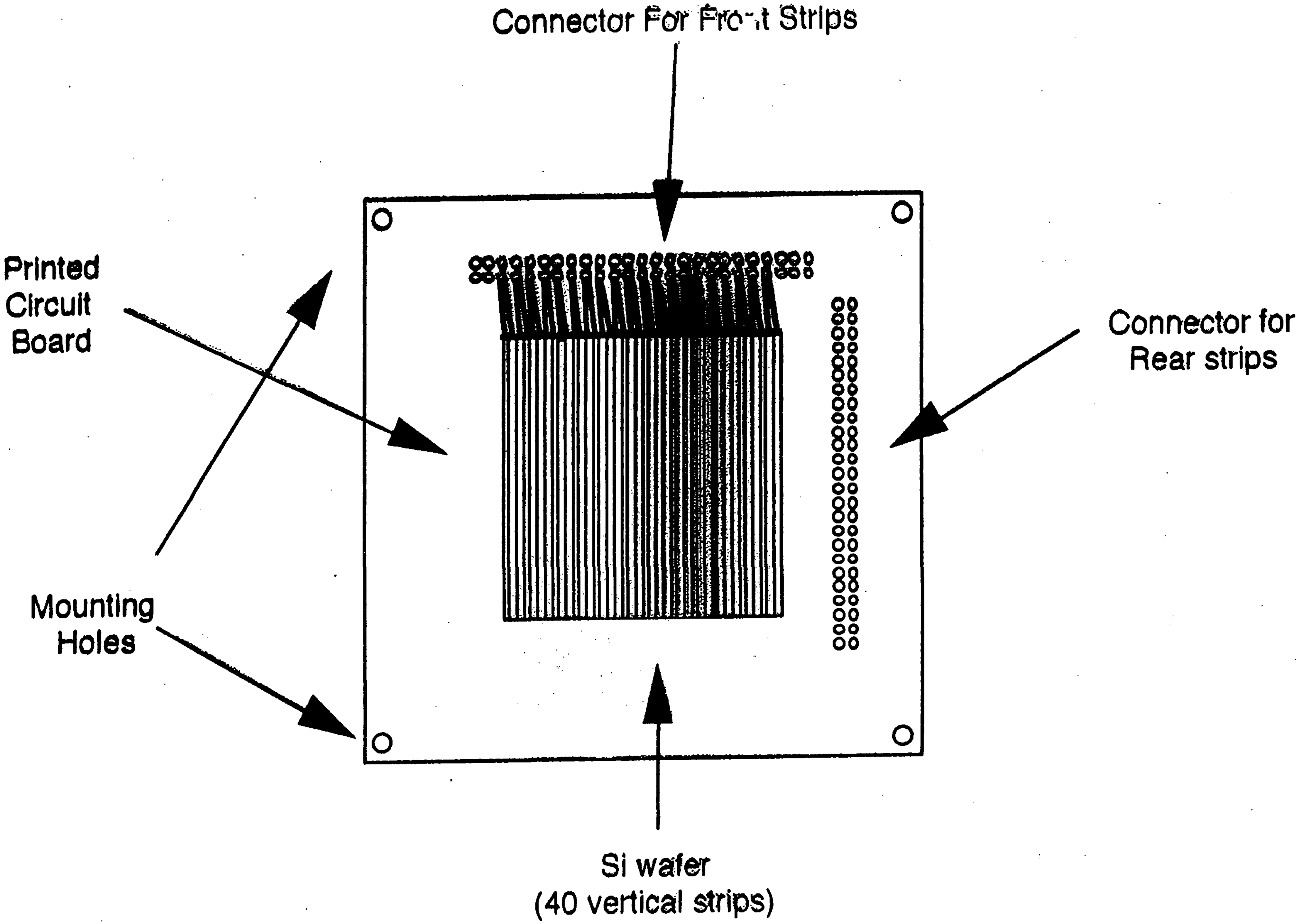
Connector For Front Strips
Printed Circuit Board
Connector for Rear strips
Mounting Holes
Si wafer (40 vertical strips)

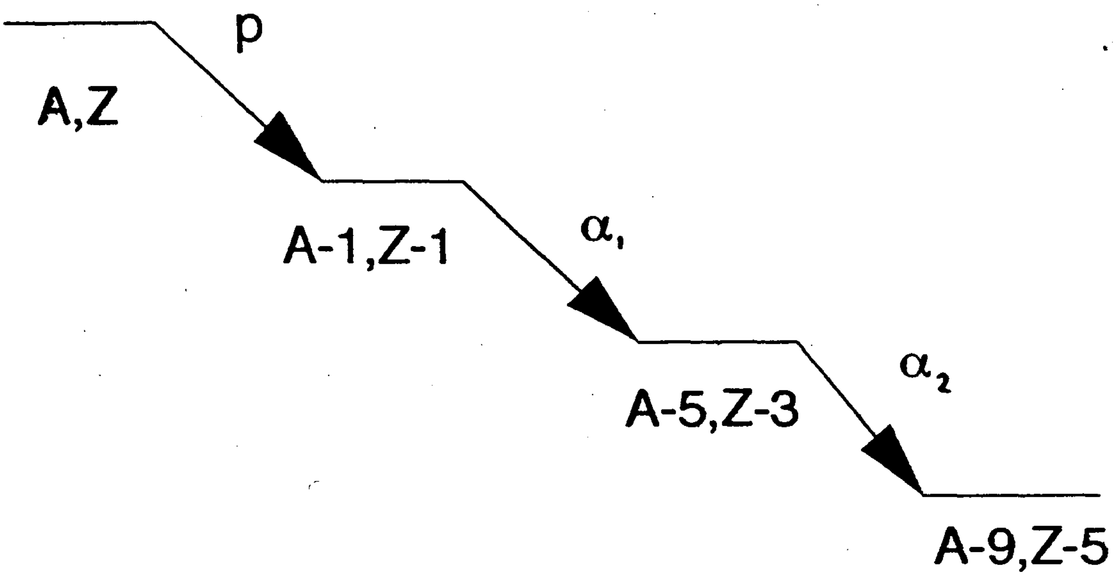
p
A,Z
α₁
A-1,Z-1
α₂
A-5,Z-3
A-9,Z-5

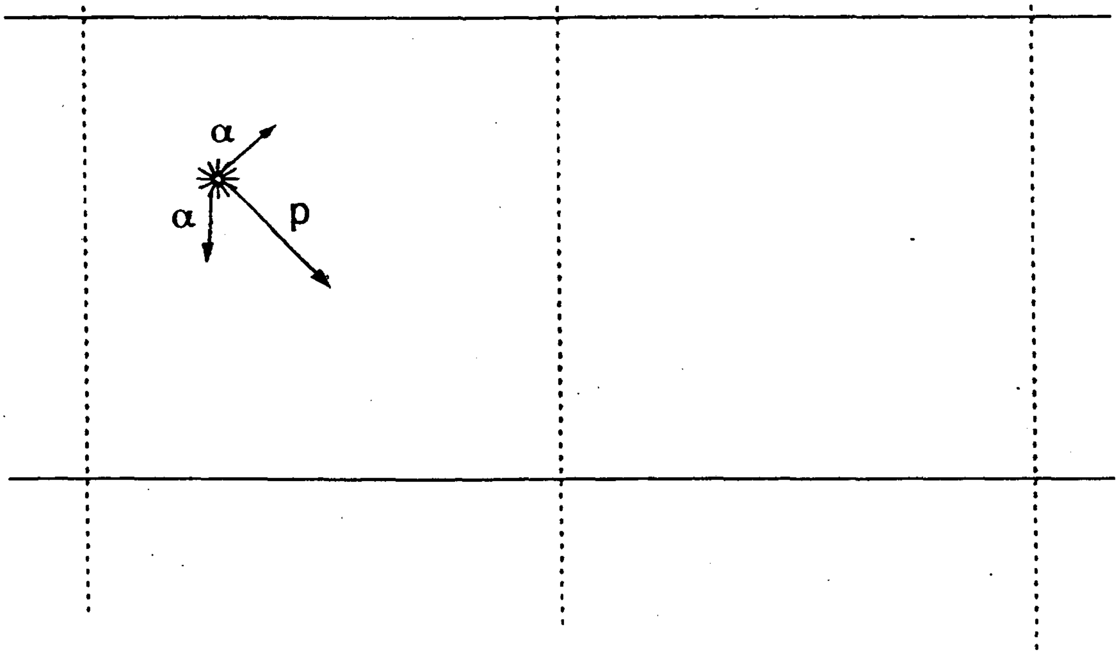
α
α
p

Advantages over a standard ΔE-E Si telescope

1). Virtually invisible to beta particles (i.e. betas are unlikely to leave much energy in such a small area.

2). Excellent resolution (~ 30 keV for alpha particles).

3). When particles are implanted, the solid angle is nearly 50%.

4). Small pixelation effectively results in many independent detectors

  a). Timing correlations between recoil and decay

  b). Parent-daughter correlations (both energy and timing information).

5). Combining with PSAC allows determination of the previous recoil's mass.

Limitations

1). Low energy threshold ~ 600 keV for protons.

2). No event by event particle identification

3). Half-life measurement threshold limited to ~ 10μs.

4). Low beam rates.

58NI+54FE AT 240 MEV; FMA: M=109,Q=25,E=102.8 MEV
00:36 25-Mar-96 Run 14

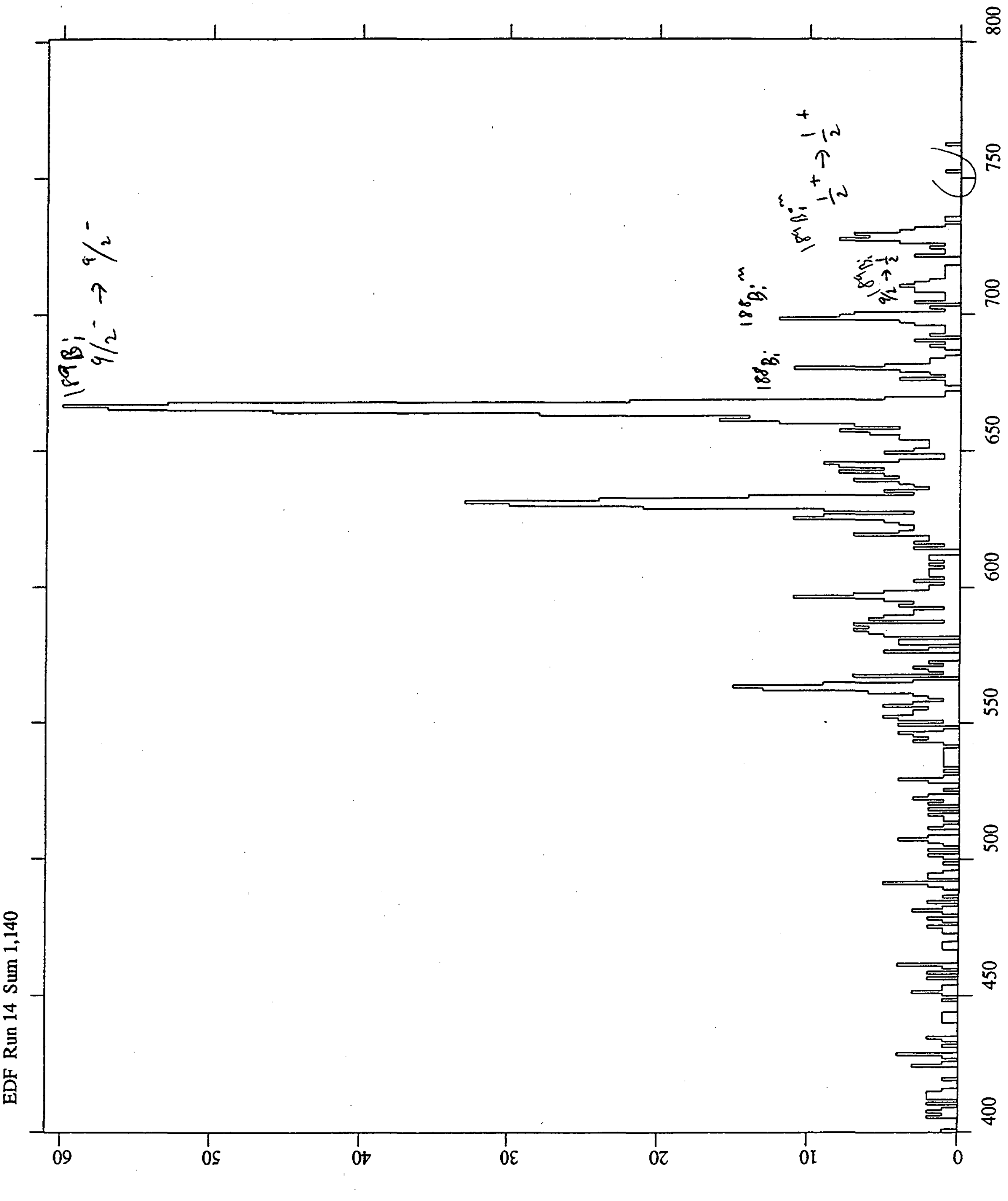

~~P4 Sum 6,353~~

20:50 10-Apr-96

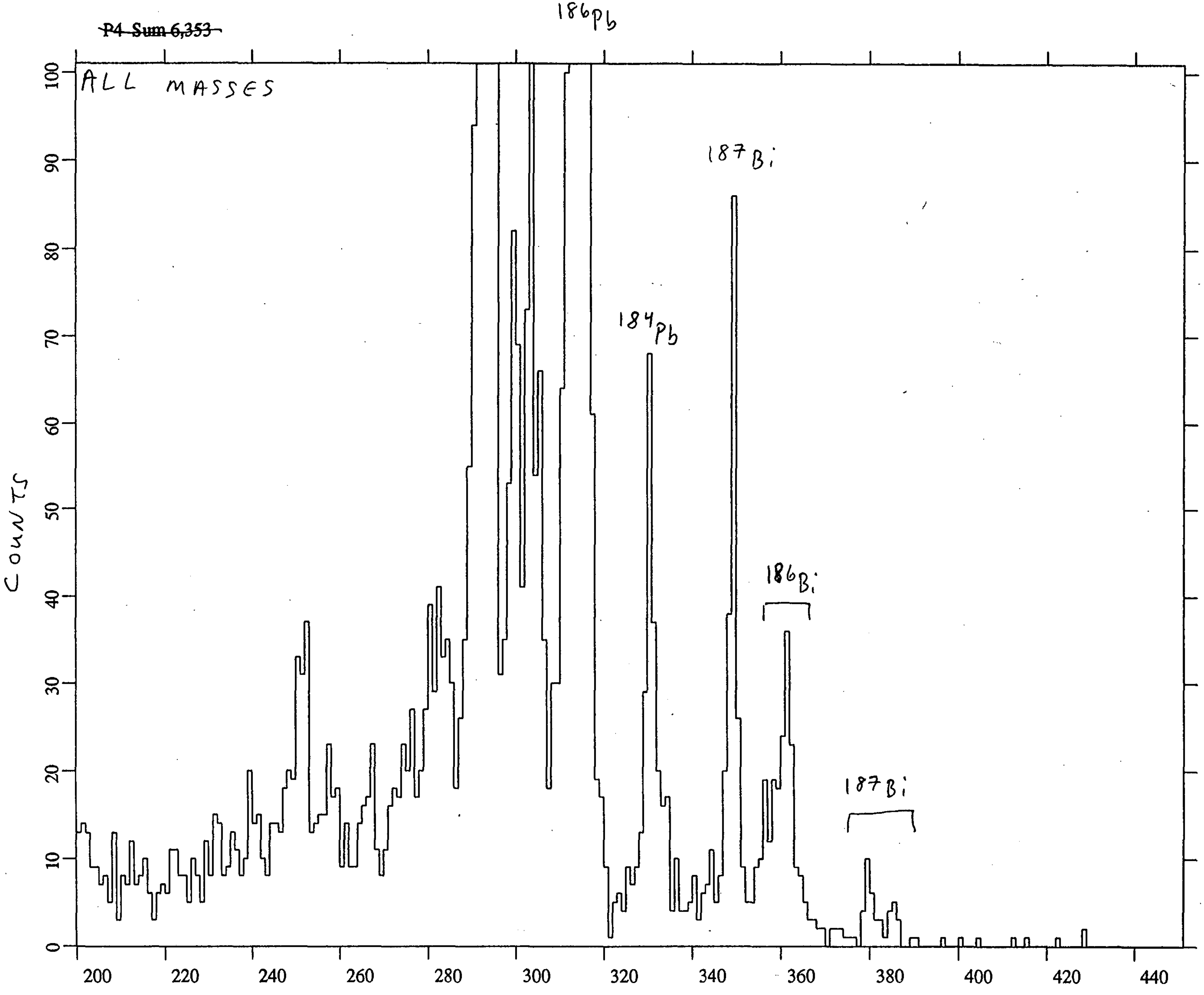

20:52 10-Apr-96

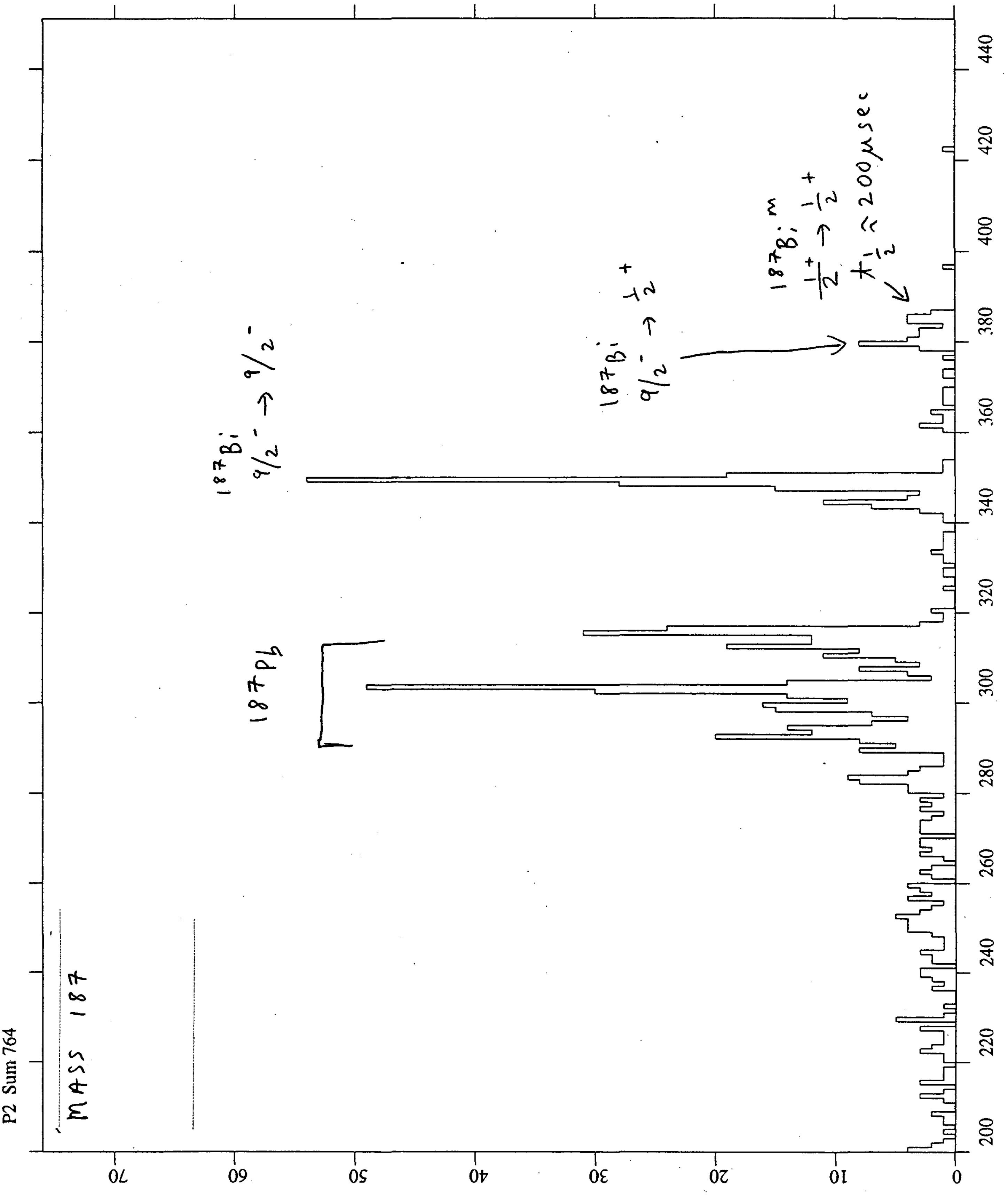

22:40 11-Apr-96

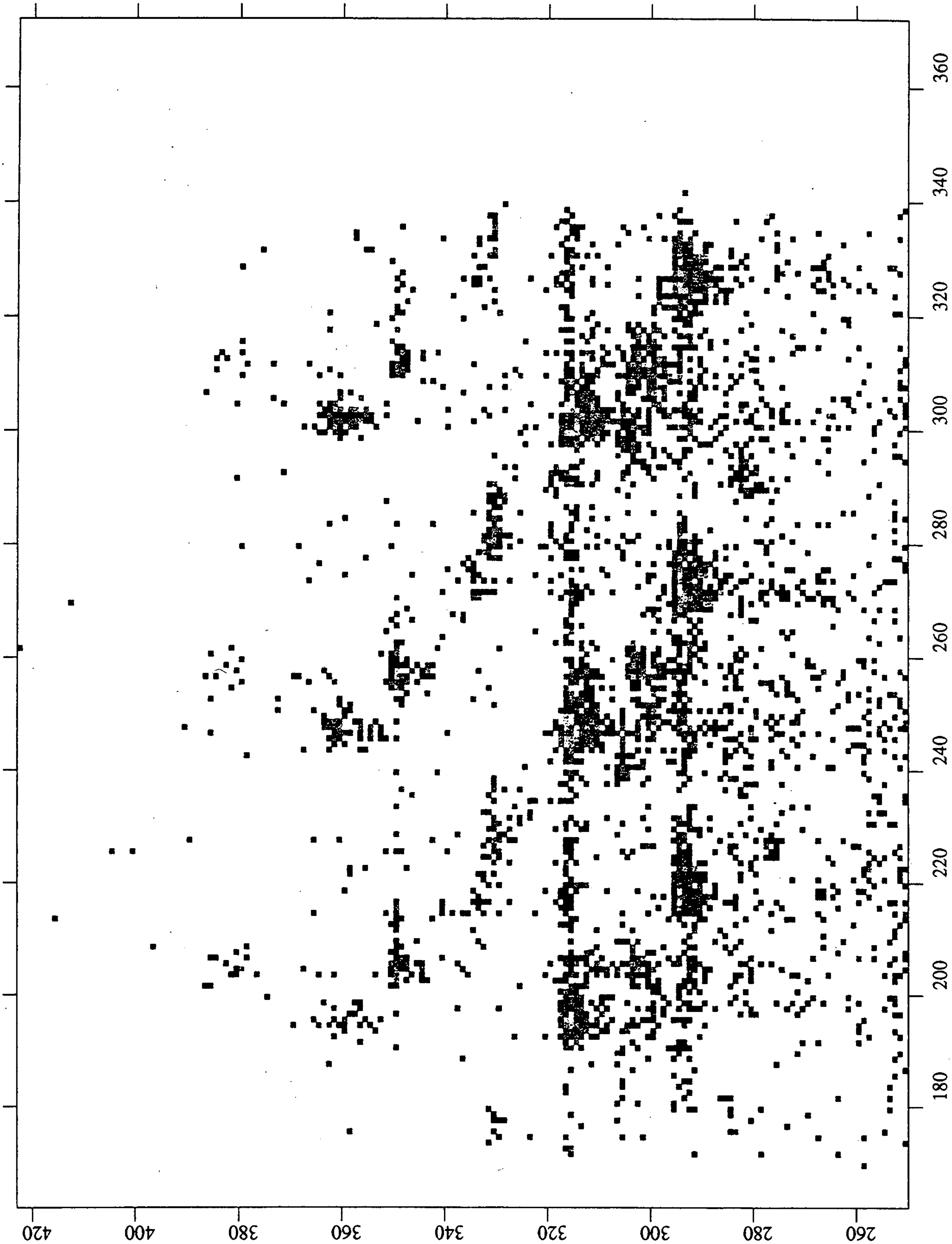

XE1 Sum 5,838 Peak 55 Scale Log Run 14

E1E2 Sum 452 Peak 22 Scale Log Run 14

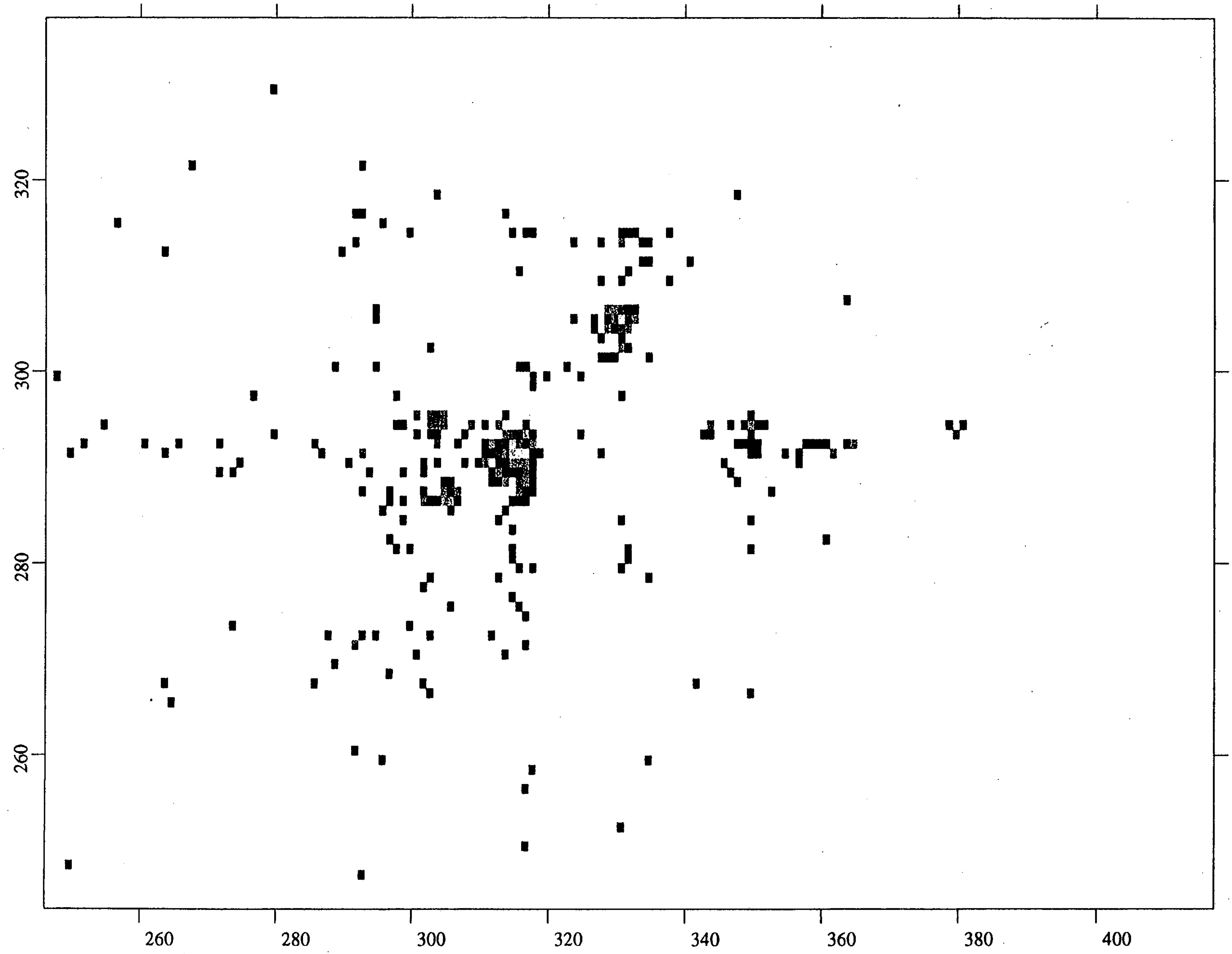

23:11 10-Apr-96

23:10 10-Apr-96

E1T1C_1 Sum 1,060 Peak 26 Scale Log Run 14

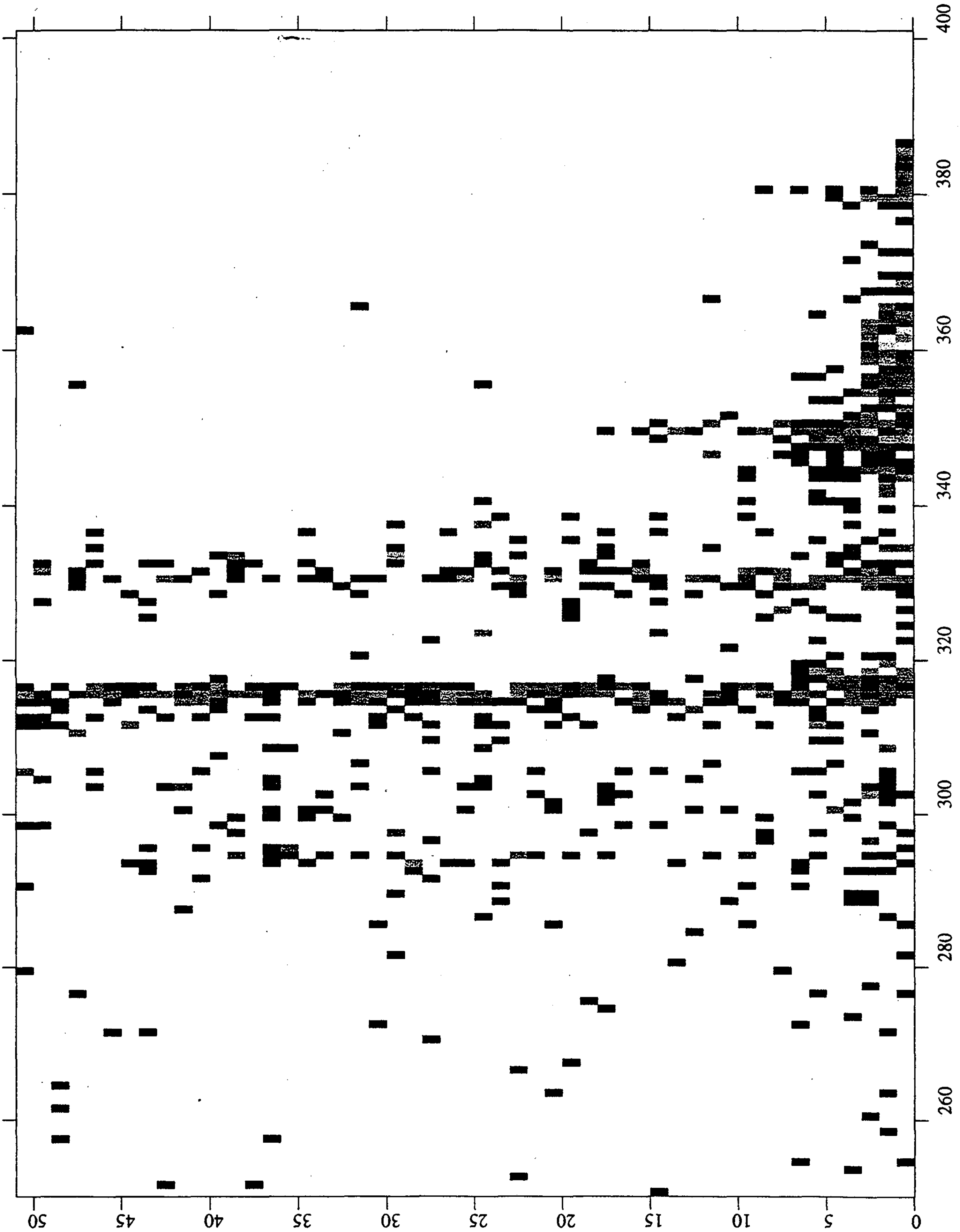

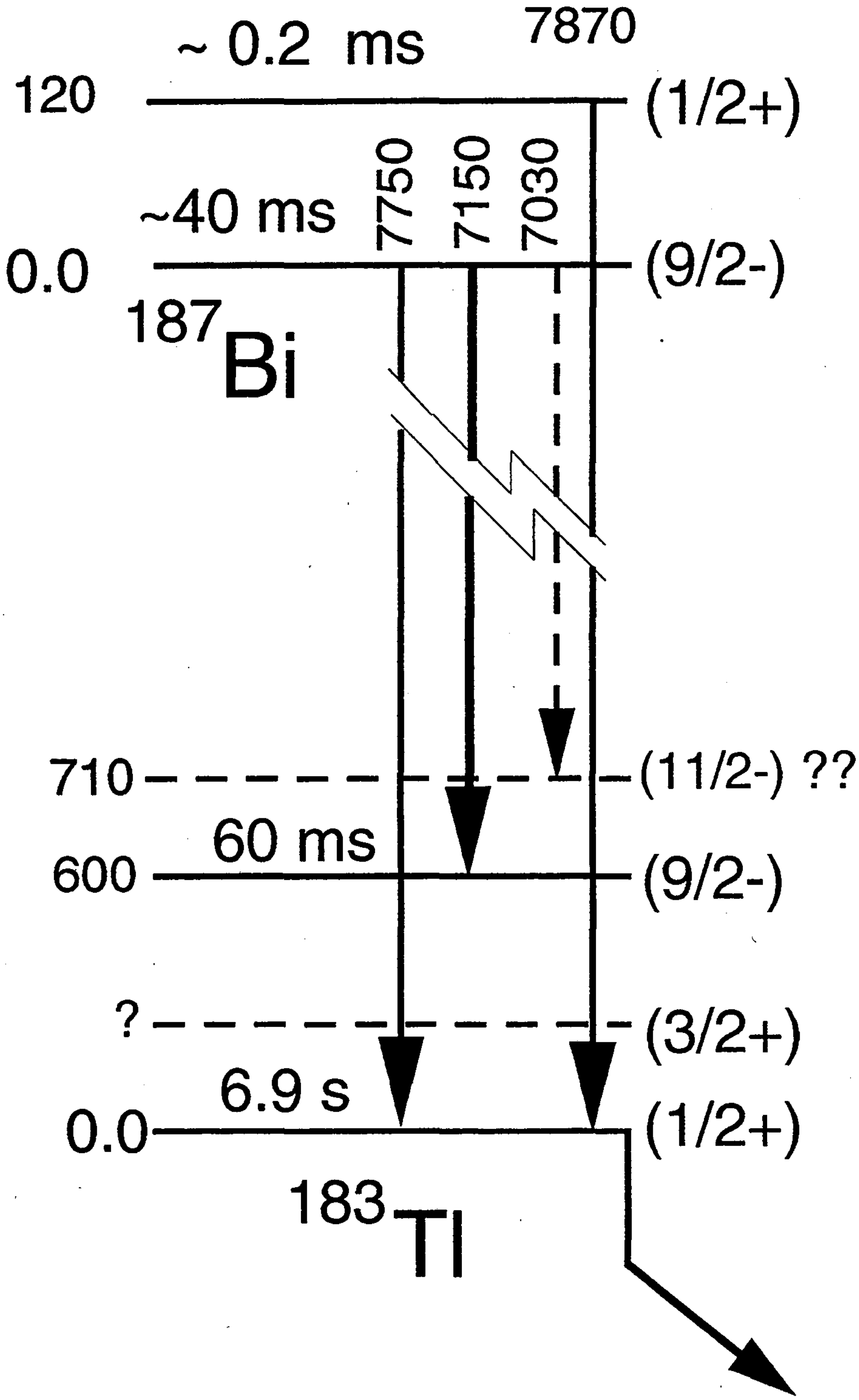
~ 0.2 ms
7870
120
(1/2+)
7750
7150
7030
~40 ms
0.0
(9/2-)
^{187}Bi
710
(11/2-) ??
60 ms
600
(9/2-)
?
(3/2+)
6.9 s
0.0
(1/2+)
^{183}Tl

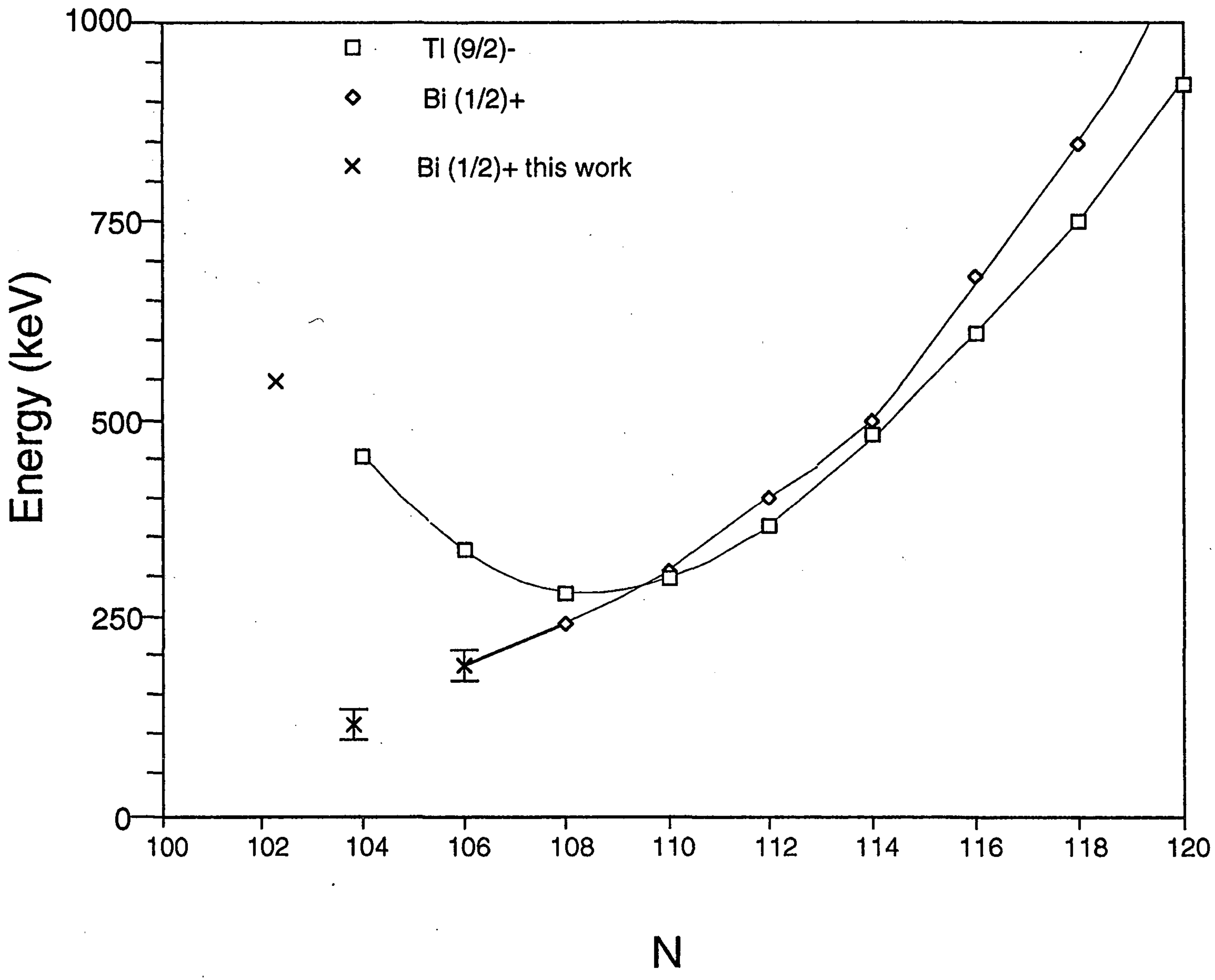
□ Tl (9/2)-
◇ Bi (1/2)+
× Bi (1/2)+ this work
Energy (keV)
1000
750
500
250
0
100
102
104
106
108
110
112
114
116
118
120
N

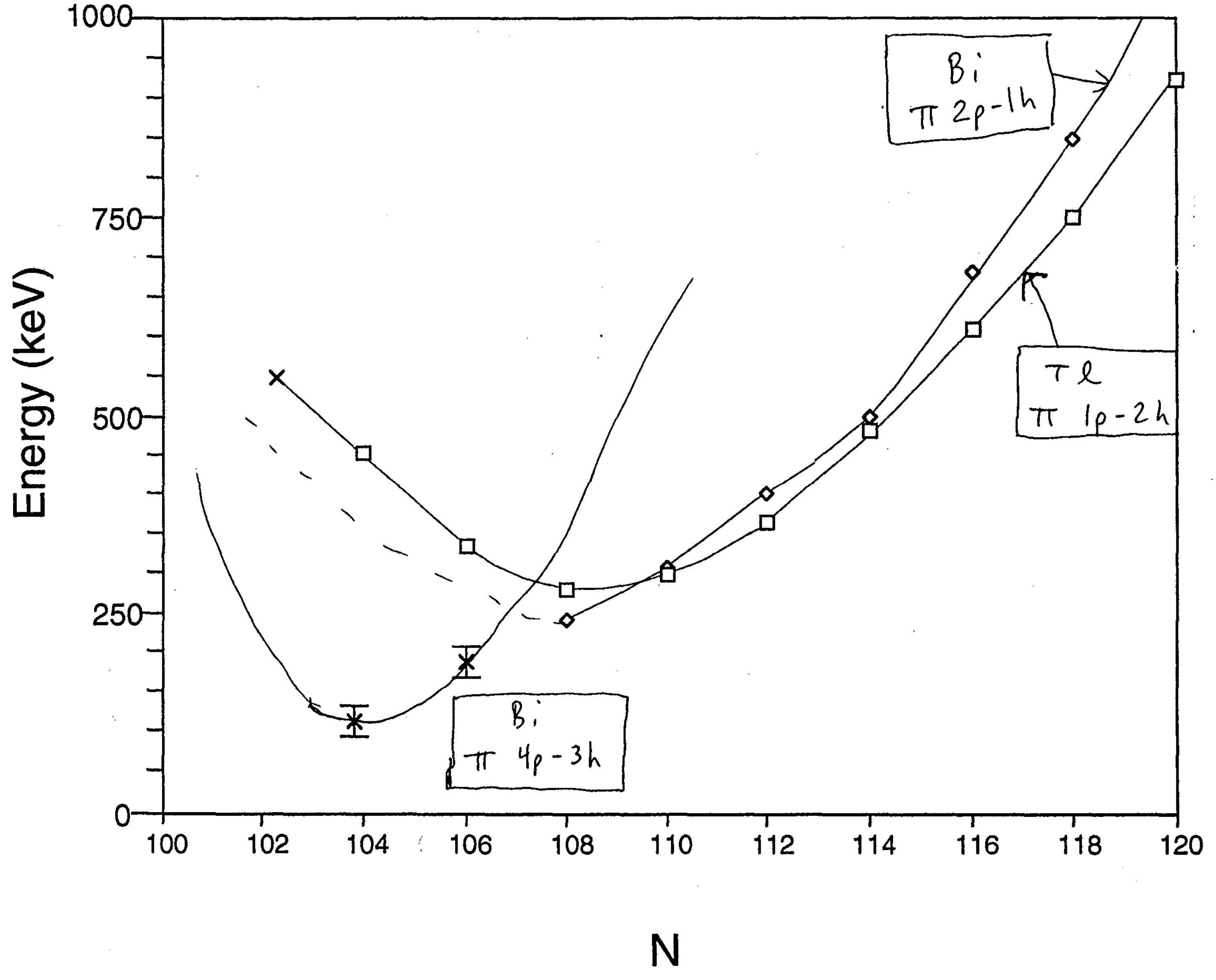
Energy (keV)
1000
750
500
250
0
100
102
104
106
108
110
112
114
116
118
120
N
Bi
π 2p-1h
Tl
π 1p-2h
Bi
π 4p-3h

James Powell

Lawrence Berkeley National Laboratory
Berkeley, CA

A New Measurement of ^{7}Be(p,γ) and the Solar Neutrino Problem

J. Powell, D.M. Moltz, A. Rice
M. W. Rowe and J. Cerny
LBNL

A. Champagne, J. Guillemette
V. Hansper and H. Weller
TUNL

M. Hofstee
Colorado School of Mines

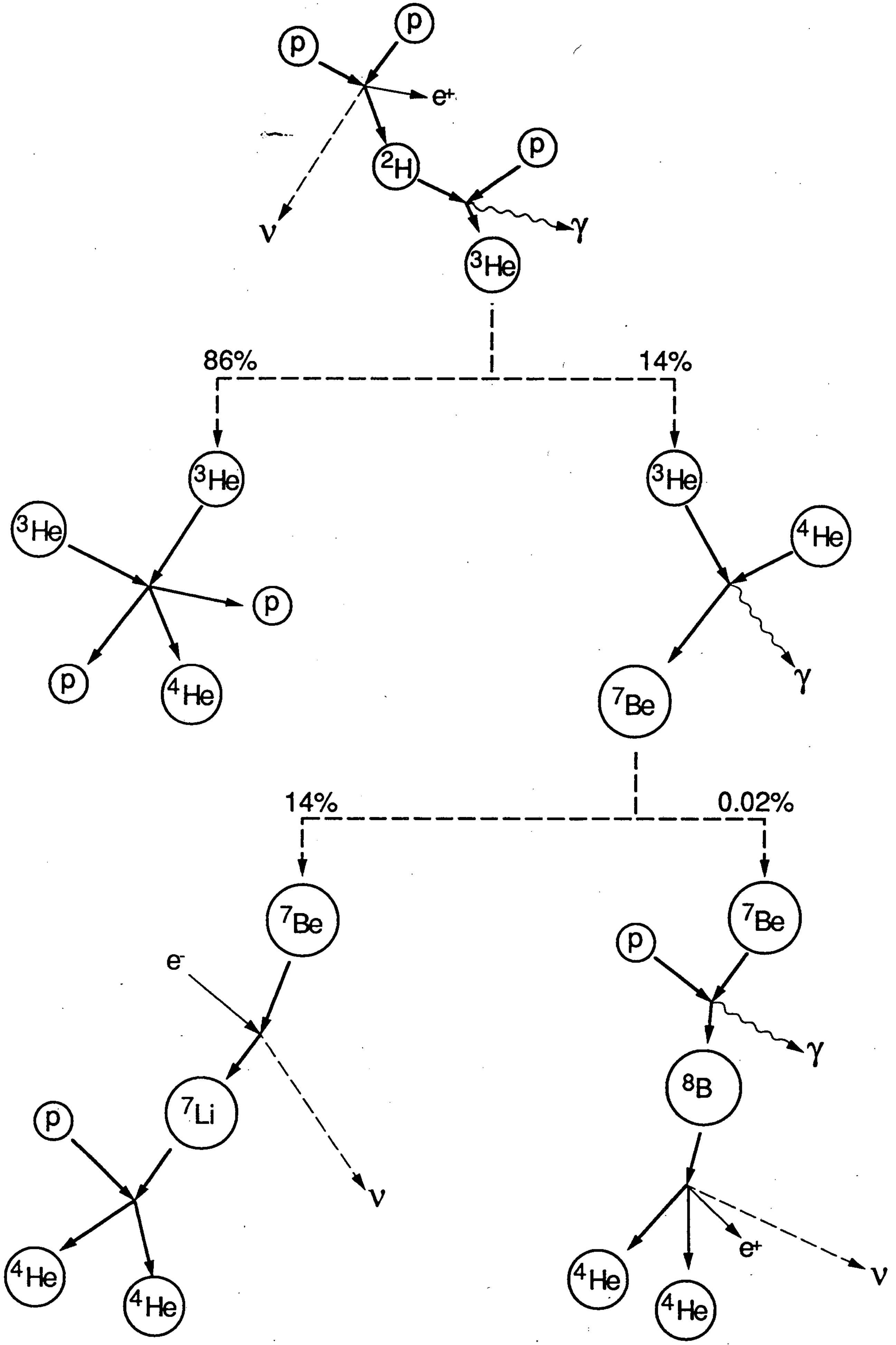
p
p
e+
ν
2H
p
γ
3He
86%
14%
3He
3He
p
p
4He
3He
4He
γ
7Be
14%
0.02%
7Be
e-
7Li
ν
p
4He
4He
7Be
p
γ
8B
e+
ν
4He
4He

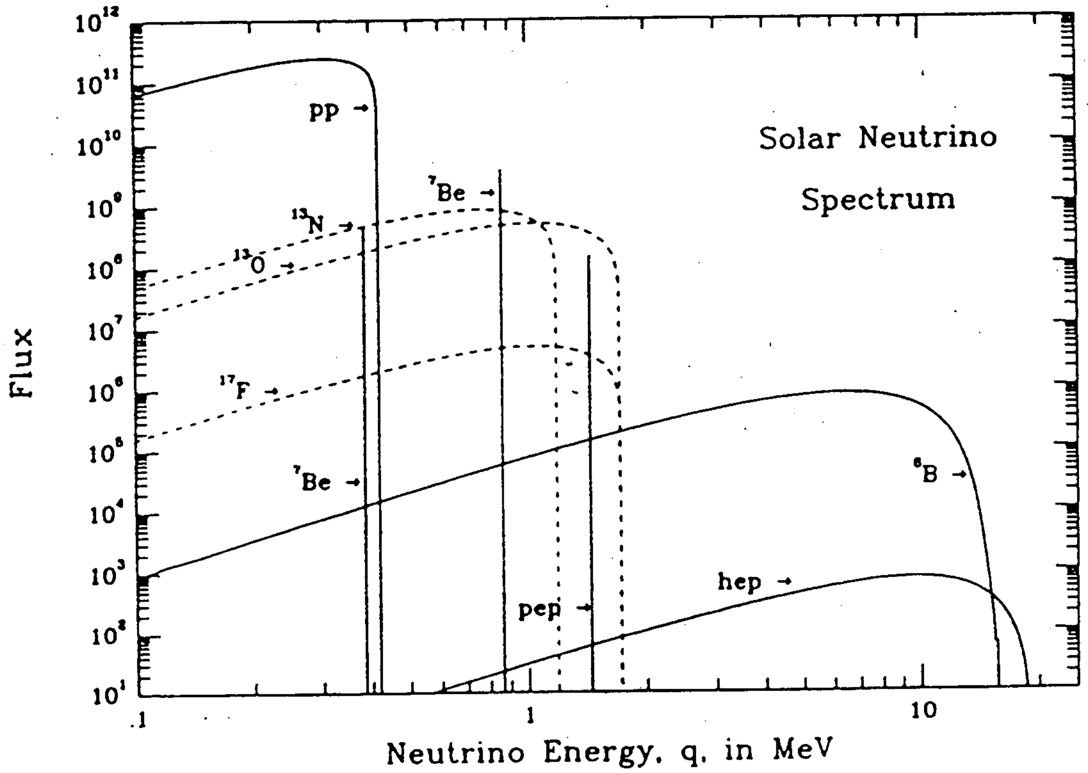

Neutrino Detectors:

Homestake Mine

$^{37}Cl + \nu \rightarrow {}^{37}Ar + e^-$

- Expected rate due to ν's from ^8B (77%), ^7Be (14%) and other sources (9%)

--> Observe only $^1/_4$ to $^1/_3$ of rate calculated from the standard solar models

Kamiokande

water Cherenkov experiment

- Sensitive to high-energy neutrinos, mostly ^8B

--> Observe only about $^1/_2$ of the ^8B flux expected

SAGE and GALLEX

$^{71}Ga + \nu \rightarrow {}^{71}Ge + e^-$

- Expected rate due to ν's from p-p (54%), ^7Be (26%), ^8B (11%) and other sources (10%)

--> Observe about $^1/_2$ of calculated rate

"Solar Neutrino Problem"

Several other detector facilities being constructed (SNO, Super-Kamiokanda) or developed (BOREXINO, etc.).

Solutions to the Solar Neutrino Problem?

1) Neutrino Oscillations $\nu_e <-> \nu_x$

   -- vacuum oscillations
   -- MSW effect

2) Inaccuracies in some of the Input Quantities

   -- stellar reaction rates
   -- neutrino capture rates
   -- details of the solar models

$^7Be(p,\gamma)^8B$

-- rate directly affects the high energy ^8B neutrino flux that is the dominant component seen by many types of neutrino detectors

-- one of the most significant uncertainties remaining in the solar models

Measuring $^7Be(p,\gamma)^8B$ Directly:

^7Be Target:

{^7Be electron captures to ^7Li: $t_{1/2} = 53$ days}

-- produced through $^7Li(p,n)^7Be$

-- chemically separated and formed into a thin target

-- 11% of decays emit 478 keV γ rays

Observe 8B produced:

{^8B β decays to $^8Be \rightarrow 2\alpha$: $t_{1/2} = 0.77$ s}

-- detect either the β or α particles in a suitable detector

Trace reaction over a range of higher energies, where the cross section is large enough to measure, and extrapolate down to the energy most relevant for solar hydrogen burning (about 20 keV)

Filippone et al, Phys. Rev. C **28** (1983) 2222

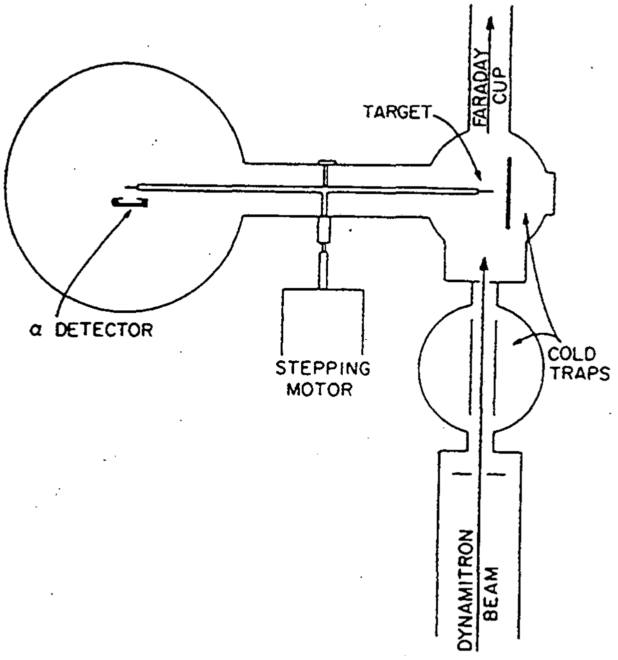

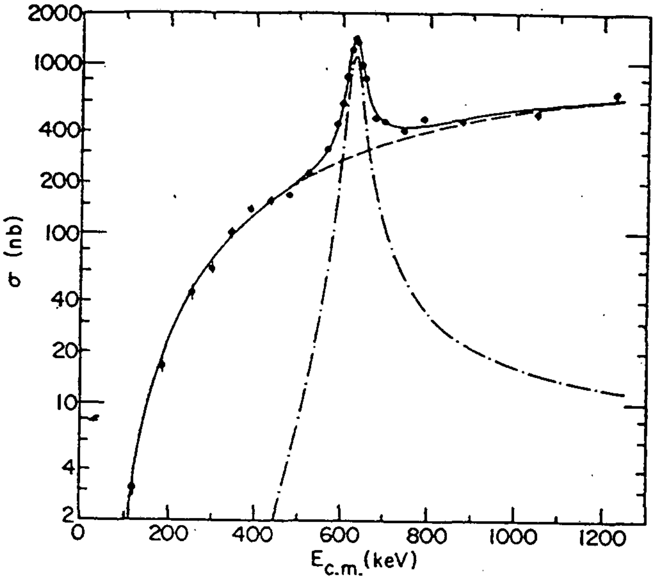

Total $^7Be(p,\gamma)^8B$ cross section

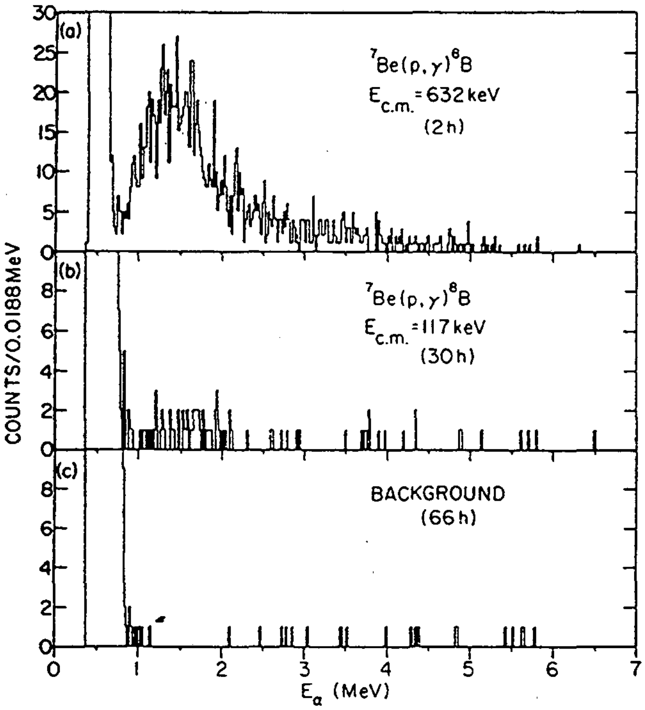

α-particle spectra

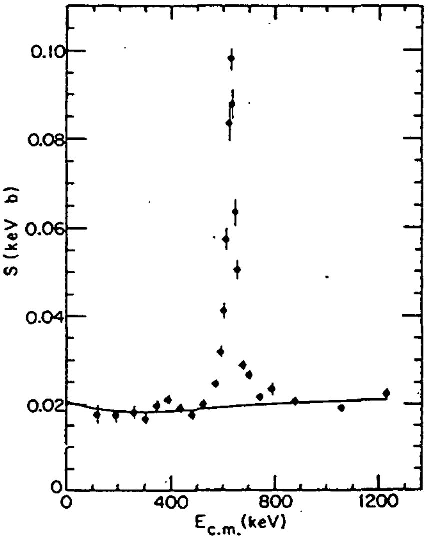

S factor for $^7Be(p,\gamma)^8B$
{ $S(E)=\sigma(E)\,E\exp(2\pi\eta)$ }

^{7}Be(p, γ)^{8}B CROSS SECTION

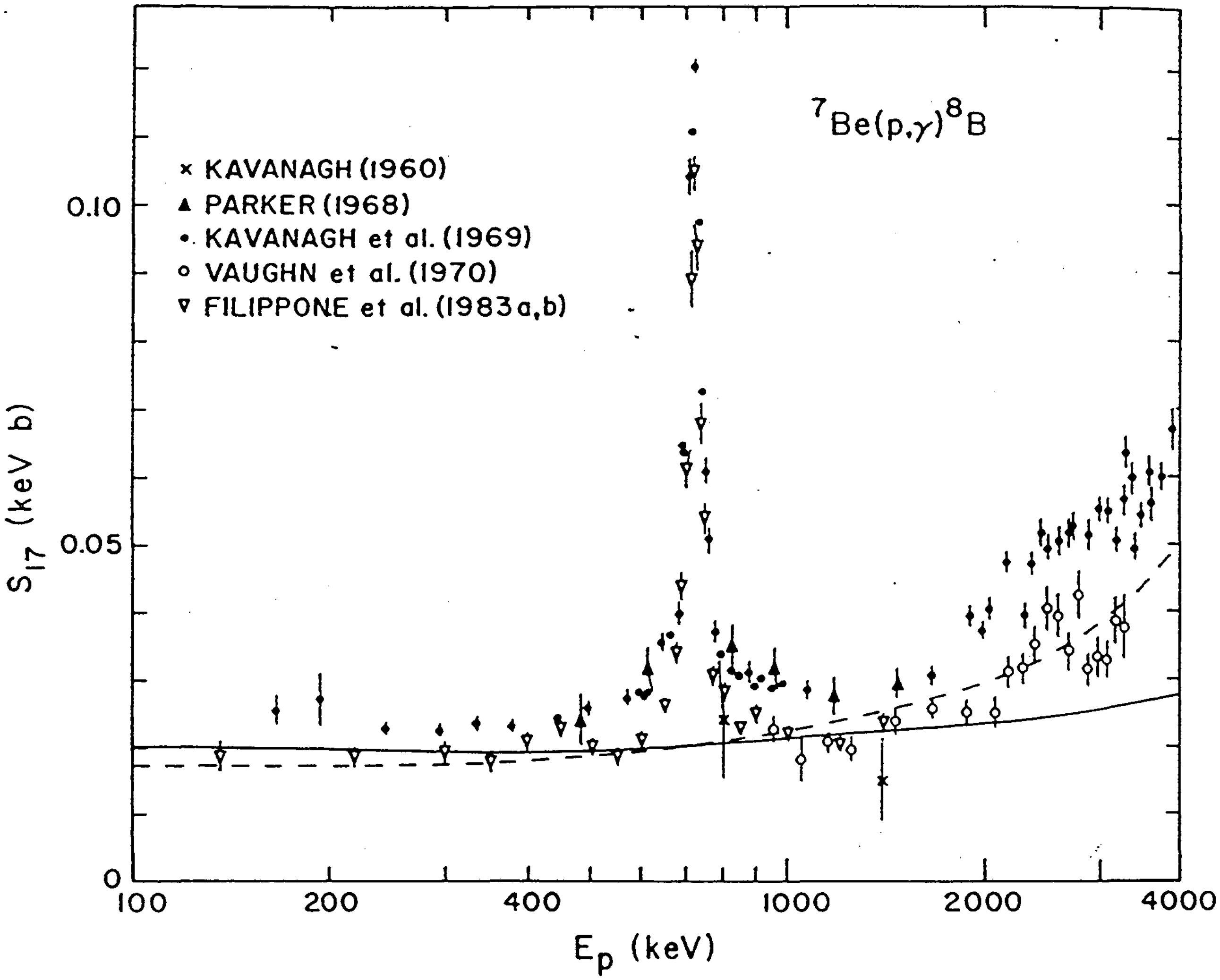

Recent Calculations:

Johnson *et al.*: ApJ 392(1992)320 — $S_{17}(0) = 20.2 \pm 2.3$ eVb (Filippone *et al.* data)
$= 25.2 \pm 2.4$ eVb (Kavanagh *et al.* data)
adopted $S_{17}(0) = 22.4 \pm 2.1$ eVb

Barker, NP A588(1995)693: $S_{17}(0) = 17 \pm 3$ eVb

Xu *et al.*, PRL 73 (1994)2027: $S_{17}(0) = 17.6$ eVb estimated

Descouvemont and Baye, NP A567(1994)341: $S_{17}(0) \geq 24$ eVb

Kim *et al.*, PRC 35(1987)363: $S_{17}(0) = 24$ eVb

Ongoing Experimental Work:

1) Coulomb Dissociation, ^{8}B (Pb) -> ^{7}Be + p

RIKEN
Motobayashi et al., PRL 73(1994)2680

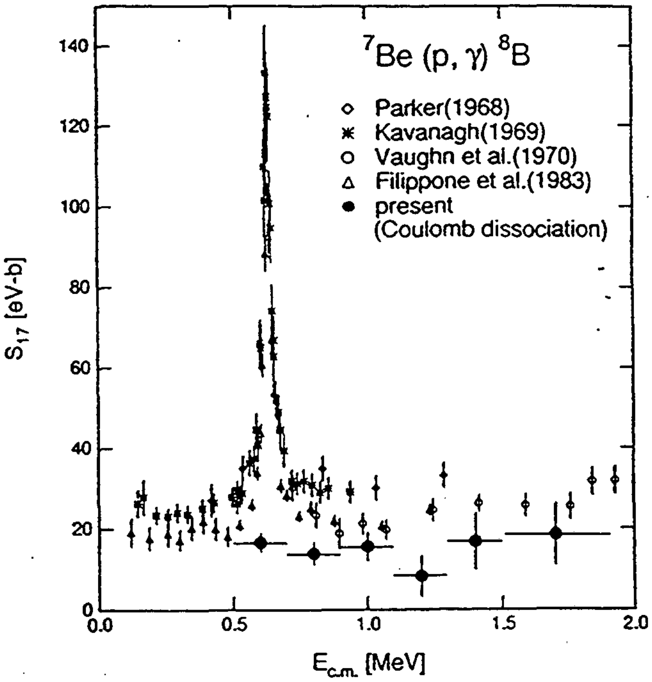

2) p + ^{7}Be

TRIUMF and U. of Washington (1997?)

TRIUMF (inverse reaction, ^{7}Be+p, 2000?)

LBNL and TUNL (1996)

Bochum and Karlsruhe (?)

3) ^{10}B(^{7}Be,^{8}B)^{9}Be

Texas A&M

4) Possible large p-wave component suggested by 7Li(p,γ) being explored at TUNL and CalTech

The LBNL + TUNL Experiment:

--> produce ^{7}Be via the ^{7}Li(p,n)^{7}Be reaction
at the new medical cyclotron at LBNL (10 MeV)

--> separate ^{7}Be chemically and electroplate onto a
platinum backing (5 mm diam. spot)

--> use acceleraters at TUNL
-- Tandem
-- ion implanter (high currents at the lowest energies)

--> use a large area version of the low-energy
charged-particle detector telescopes pioneered by
the Cerny group at LBNL.

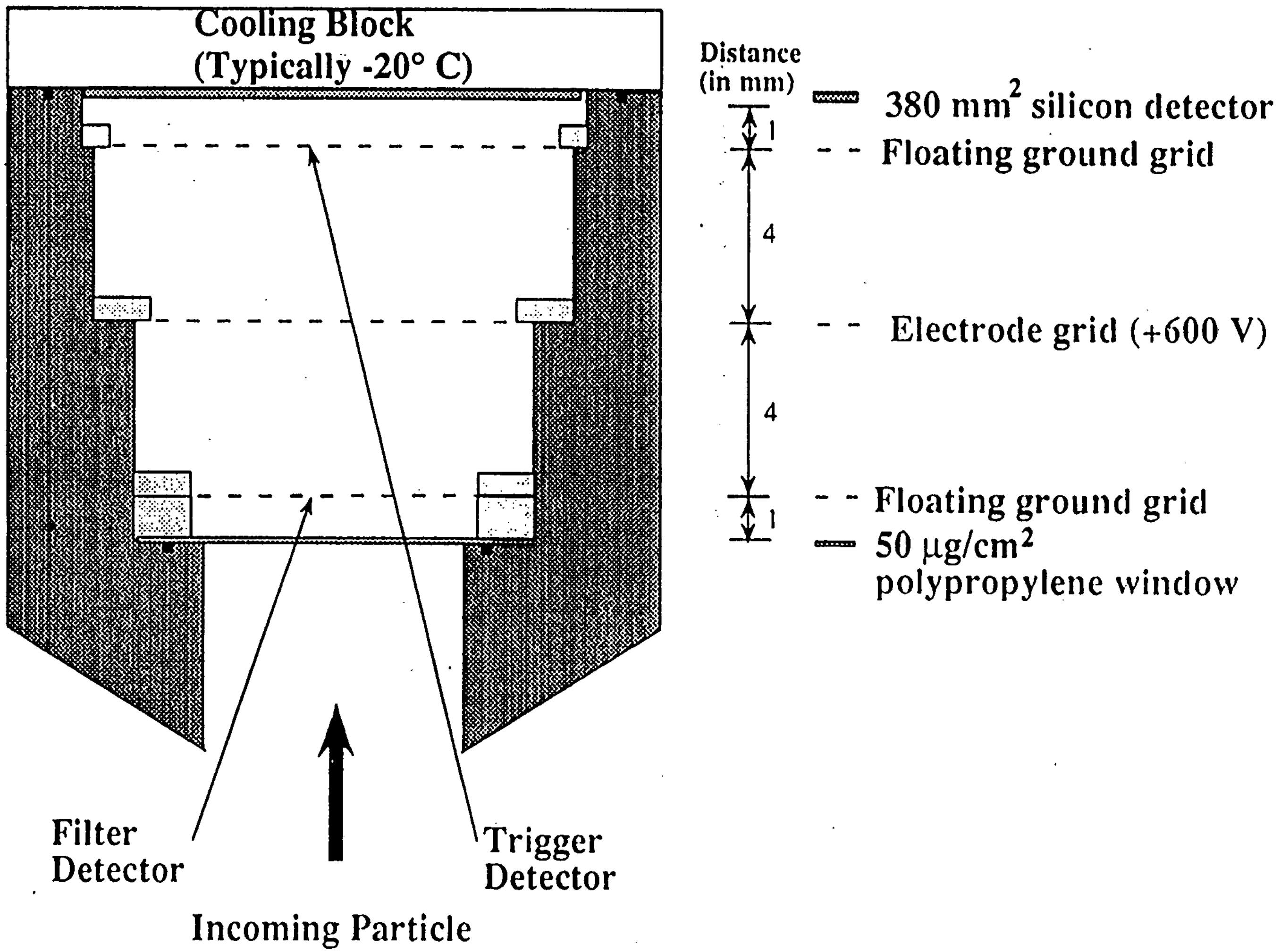
Cooling Block
(Typically -20° C)
Distance
(in mm)
380 mm² silicon detector
Floating ground grid
1
4
Electrode grid (+600 V)
4
Floating ground grid
1
50 µg/cm²
polypropylene window
Filter
Detector
Trigger
Detector
Incoming Particle

Improvements Over Previous Experiments:

--> 10 times more ^{7}Be in the target
  -- 1 full Curie as compared to the 0.08 Ci used by Filippone et al.

--> low-energy detector telescopes
  -- precise identification of α particles with reduced background

--> an improved energy calibration
  -- accurate to about 1 keV compared to 3 keV

Together, the above improvements will allow the measurement of much smaller cross sections leading to an extension of the ^{7}Be(p,γ) measurement down to lower energies (60 keV as compared to $\geq$ 117 keV)
  -- improves the extrapolation down to solar energies
  -- tests the predicted energy dependence

Timeline:

Ongoing:

--> detector station design	LBNL, TUNL
--> detector design and purchase	LBNL
--> electroplating developement and tests with stable ^{9}Be	LBNL
--> develope scheme for energy calibration and current integration of proton beam	TUNL

August, 1996:

--> prduce and perform test run on weaker ^{7}Be target (~0.1 Ci)
--> do higher energy measurements
--> investigate systematic errors

Early 1997:

--> Full experiment on hot target (1 Ci)

Mike Zisman

Lawrence Berkeley National Laboratory
Berkeley, CA

Building a Factory

for B's:

The

PEP-II

Project

Michael S. Zisman
LER System Manager
PEP-II *B* Factory Project
Accelerator & Fusion Research Division
Ernest Orlando Lawrence
Berkeley National Laboratory

Cerny Symposium
April 15, 1996

Outline

- Introduction
- PEP-II history
- Typical parameters
- Design challenges
- Project overview
- Project status
- Cost and schedule
- Summary

Introduction

- Strong interest (worldwide) in past few years in design of high-$\mathcal{L}$ e^+e^- collider for a "*B* factory"
  - — primary motivation: study origin of *CP* violation
    - o effect expected to be large in $B\overline{B}$ system
- Experiment will probe the origins of the universe
  - — why do we live in a matter dominated world?
- At Big Bang, equal amounts of matter and anti-matter
  - — slight asymmetry in reaction rates caused matter to dominate
    - o this is thought to be related to *CP* violation
    - o we know it happens, but not why
- Machine to answer this question requires several novel features compared with existing colliders

- *CP*-violation studies benefit from moving $B\overline{B}$ c.m.

  $\Rightarrow$ "asymmetric" collider, $E_1 \neq E_2$

  — permits spatial resolution of B and $\overline{B}$ decays

  - energy asymmetry has broad optimum

$$\frac{7}{4} \leq \frac{E_1}{E_2} \leq \frac{12}{2.3}$$

- Statistics for decay channels of interest, require high collision rate ("luminosity" in collider parlance)

  — $R = \mathcal{L}\sigma$

- Need $\mathcal{L} = 3 \text{ x } 10^{33}$ cm^{-2} s^{-1} for *CP* violation study

- Actual figure of merit is <u>integrated</u> $\mathcal{L}$

  — must produce abundant sample of $B\overline{B}$ pairs

  - meaning (and challenge) of "factory"

  — aim for $\int_{\text{year}} \mathcal{L} \cdot dt = 3 \times 10^{40}\ \text{cm}^{-2} = 30\ \text{fb}^{-1}$

  - based on canonical "year" of 10^7 seconds

PEP-II History

- Concept for asymmetric e^-e^+ collider to serve as *B* factory due to Oddone (1987)
  - — initial accelerator design studies at LBNL led by Chattopadhyay (1988–1989)
  - — SLAC-LBNL-LLNL design study done in 1990
- Original CDR for project completed February '91
  - — to avoid stigma of new machine, ours was an "upgrade," whence PEP-II
- Design extensively reviewed over 3-year period
  - — Cornell put forth competing proposal "CESR-B"
- Ultimate hurdle was Joint DOE/NSF *B* Factory Review in 1993
- After Joint Review, President Clinton announced SLAC as site for U.S. *B* factory
- Japan is building an equivalent machine: "KEKB"

  ⇒ we have a race on our hands!

Typical Parameters

- **Luminosity is**

$$\mathcal{L} = \frac{N_+ N_- f_c}{4\pi\sigma_x^*\sigma_y^*}$$

- **For machine design purposes write $\mathcal{L}$ as**

$$\mathcal{L} = 2.17\times 10^{34}\,\xi(1+r)\left(\frac{I\cdot E}{\beta_y^*}\right)_{+,-} \quad [\mathrm{cm}^{-2}\mathrm{s}^{-1}]$$

where

I = **total current [A]**

β_y^* = **vertical beta function at IP [cm]**

r = **aspect ratio (σ_y/σ_x) (detector constraint)**

E = **beam energy [GeV] (physics constraint)**

ξ = $\Delta\nu_{\mathrm{bb,max}}$ **(accelerator physics constraint)**

- **Justification for writing $\mathcal{L}$ as above is empirical limit on ξ**

- Must improve luminosity by a factor of 15
  - — need higher I and smaller beam sizes at IP!
    - o both are challenging
- Typical parameters for $\mathscr{L} = 3 \times 10^{33}$ cm^{-2} s^{-1} are:

$I_b \approx$ 1 – 5 mA

$\varepsilon_x \approx$ 100 nm·rad

$\sigma_\ell \approx$ 1 cm

$I \approx$ 1 – 3 A

$k_B \approx$ 100 – 2000

Design Challenges

- Design of high-$\mathcal{L}$ asymmetric *B* factory gives both physics and technology challenges
  - design choices are interrelated
    - proper optimization is the "art"
- BF parameter regime forces two-ring collider
  - different energies, high currents, many bunches
- Two-ring collider gives physics challenges in
  - collider design
    - beam separation and common focusing of unequal energy beams; keeping beams in collision
- Multibunch instabilities severe for *B* factory
  - wakefields induced by displaced bunches (mainly in RF cavity HOMs) can cause other bunches to be displaced
    - for certain bunch patterns, get exponential growth of amplitude, leading to beam loss
  - growth rates scale with <u>total</u> current, which we require to be very high

- Physics issues just discussed make certain implicit assumptions about *B* factory hardware

- Technology challenges can be summarized as:

  Don't make a liar out of the accelerator physicists!

- Examples:

  — lifetime estimates assume low *P* in rings despite copious photodesorption

  — $\mathcal{L}$ estimates assume that high beam currents can be supported without melting anything

  — coupled-bunch instability estimates assume RF cavities with heavily damped HOMs

  — performance estimates assume components are sufficiently reliable that the machine does not "spend all its time in the shop"

- For any BF design, main technological challenges lie in the following areas:

  — vacuum system

  — RF system

  — feedback system

    ○ even with heavily damped cavity modes, must combat growth times ≈1 ms

Project Overview

- High-energy ring (HER)
  - 9 GeV e^- in PEP (C = 2200 m)
    - reuses all magnets; new RF & vacuum system
      - some new magnets required
- Low-energy ring (LER)
  - 3.1 GeV e^+ in new ring ($C = C_{PEP}$)
    - located above PEP ring in same tunnel
- Injection system based on present SLC injector
  - world's most powerful positron source
  - run in "top-off" mode to maintain high average luminosity
    - time to top-off operating collider is 3 minutes; time to fill from zero is 6 minutes
- LBNL is lead lab for design, construction, commissioning of LER
  - I serve as LER System Manager

PEP-II

Main Collider Parameters

	LER	HER
Energy, E [GeV]	3.1	9
Circumference, C [m]	2199.32	2199.32
$\varepsilon_y/\varepsilon_x$ [nm·rad]	2.0/66	1.5/49
β_y^*/β_x^* [cm]	1.5/50.0	2.0/66.7
$\xi_{ox,oy}$	0.03	0.03
f_{RF} [MHz]	476	476
V_{RF} [MV]	5.1	14.0
Bunch length, σ_ℓ [mm]	10	11.5
Number of bunches, k_B	1658†	1658†
Bunch separation, s_B	1.26	1.26
Damping time, τ_E/τ_x [ms]	30.0/62.5	18.3/37.0
Total current, I [A]	2.16	1.00
U_0 [MeV/turn]	0.75	3.59
Luminosity, $\mathscr{L}$ [$cm^{-2}s^{-1}$]	3×10^{33}	

†includes gap of ≈5% for ion clearing

PEP-II *B*-Factory

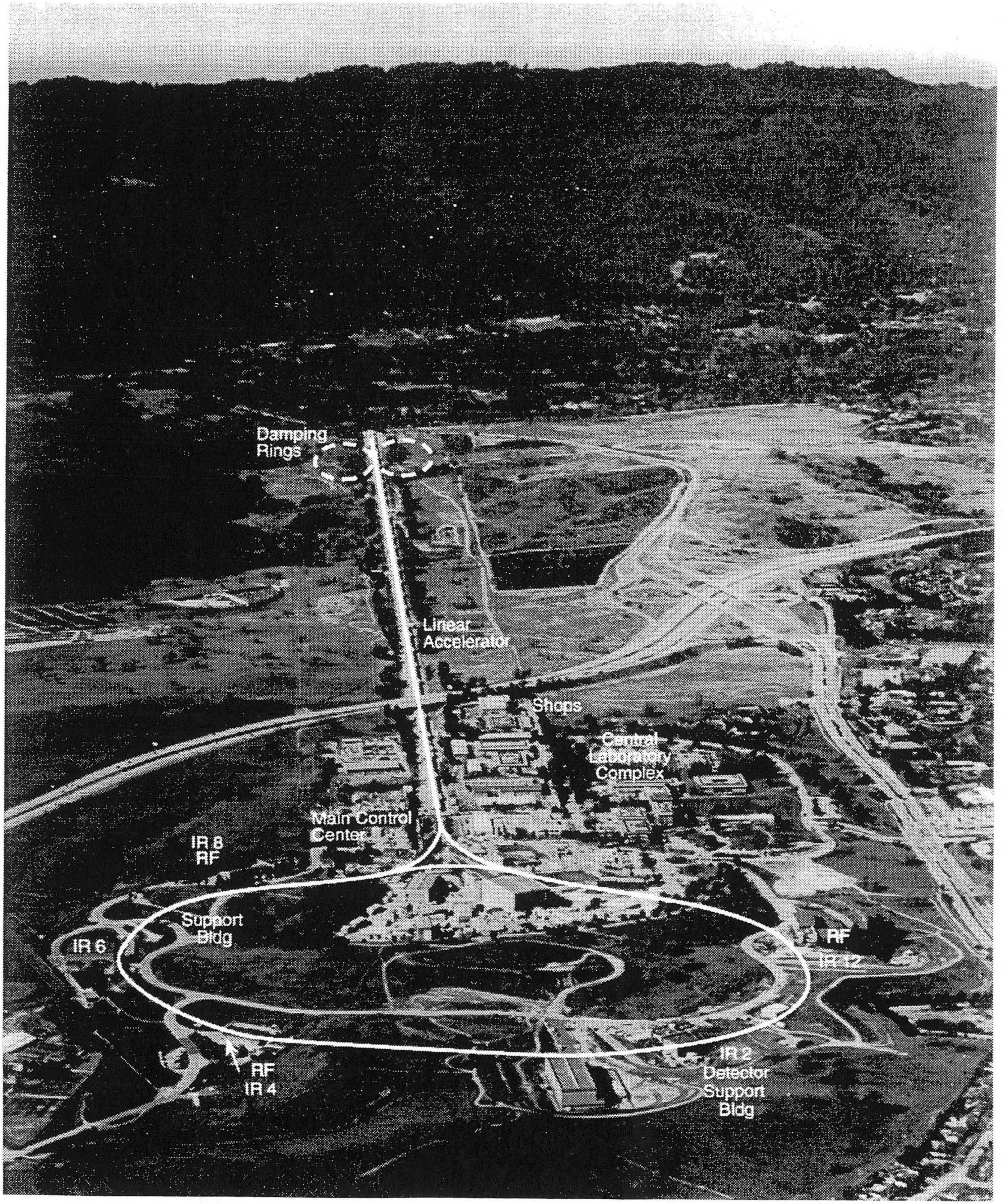

Project Status

- Injection
  - — electron extraction and both bypass lines installed
    - o electron line being commissioned
  - — components for positron extraction line being fabricated for installation in Summer ’96
- HER
  - — magnet refurbishment and remeasurement completed
    - o arc dipoles reinstalled
    - o quadrupole rafts being installed
    - o vacuum chamber production under way
      - – arcs use in-house e-beam welder

PEP-II *B*-Factory

Installation of the e^+ and e^- Bypass Lines in LINAC Housing

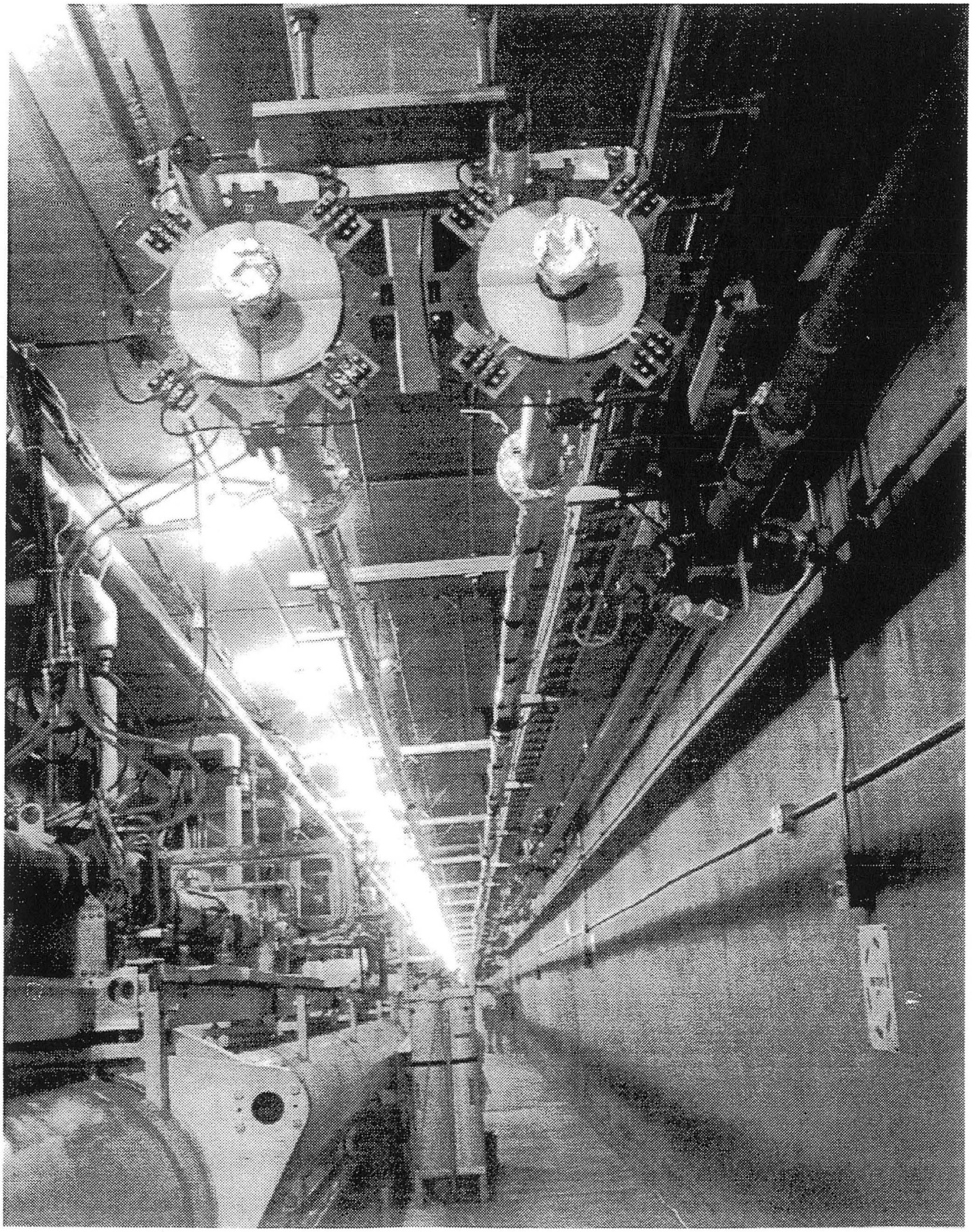

High Energy Ring ARC Section History

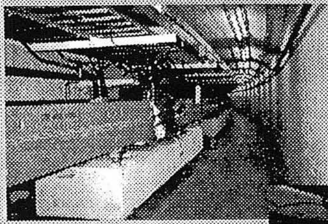

Jan. 94

Jul. 94

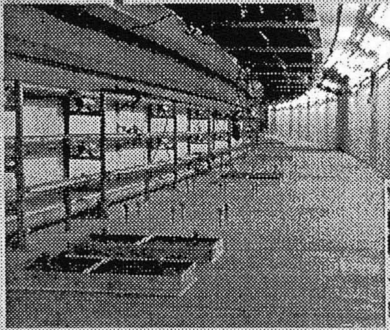

Feb. 95

Apr. 95

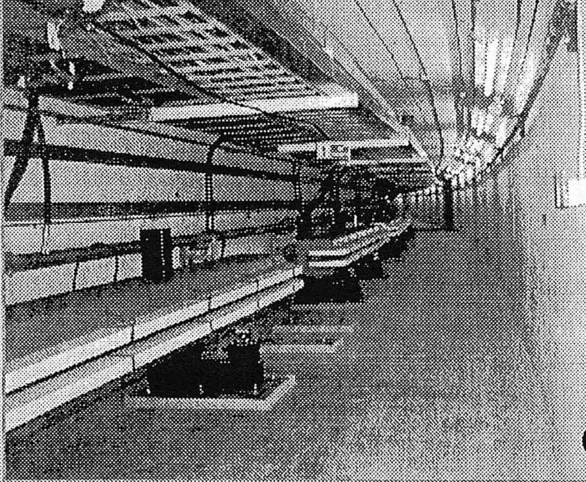

Oct. 95

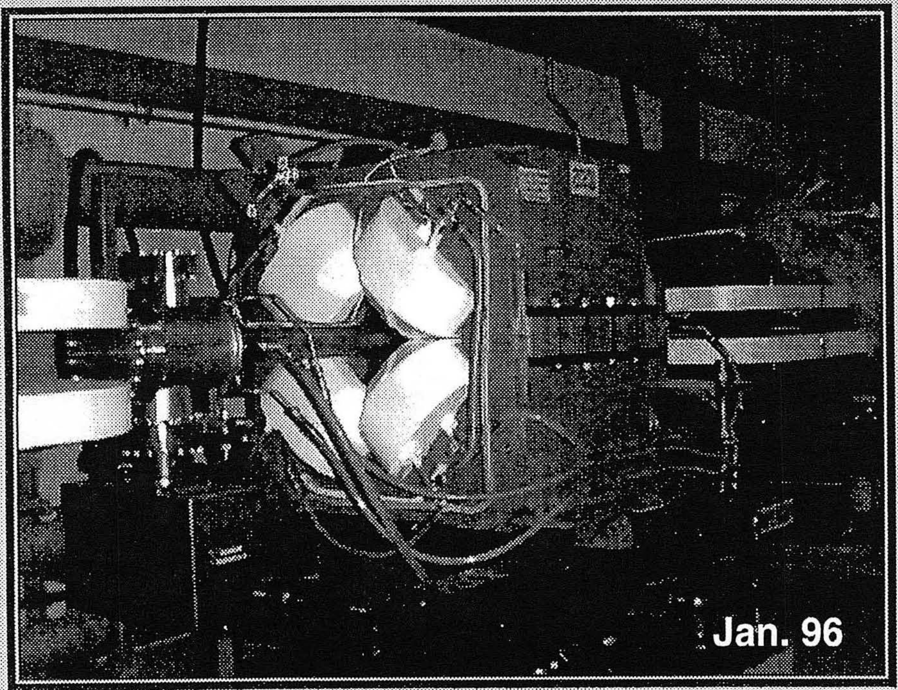

Jan. 96

HER First Arc Dipole Installation

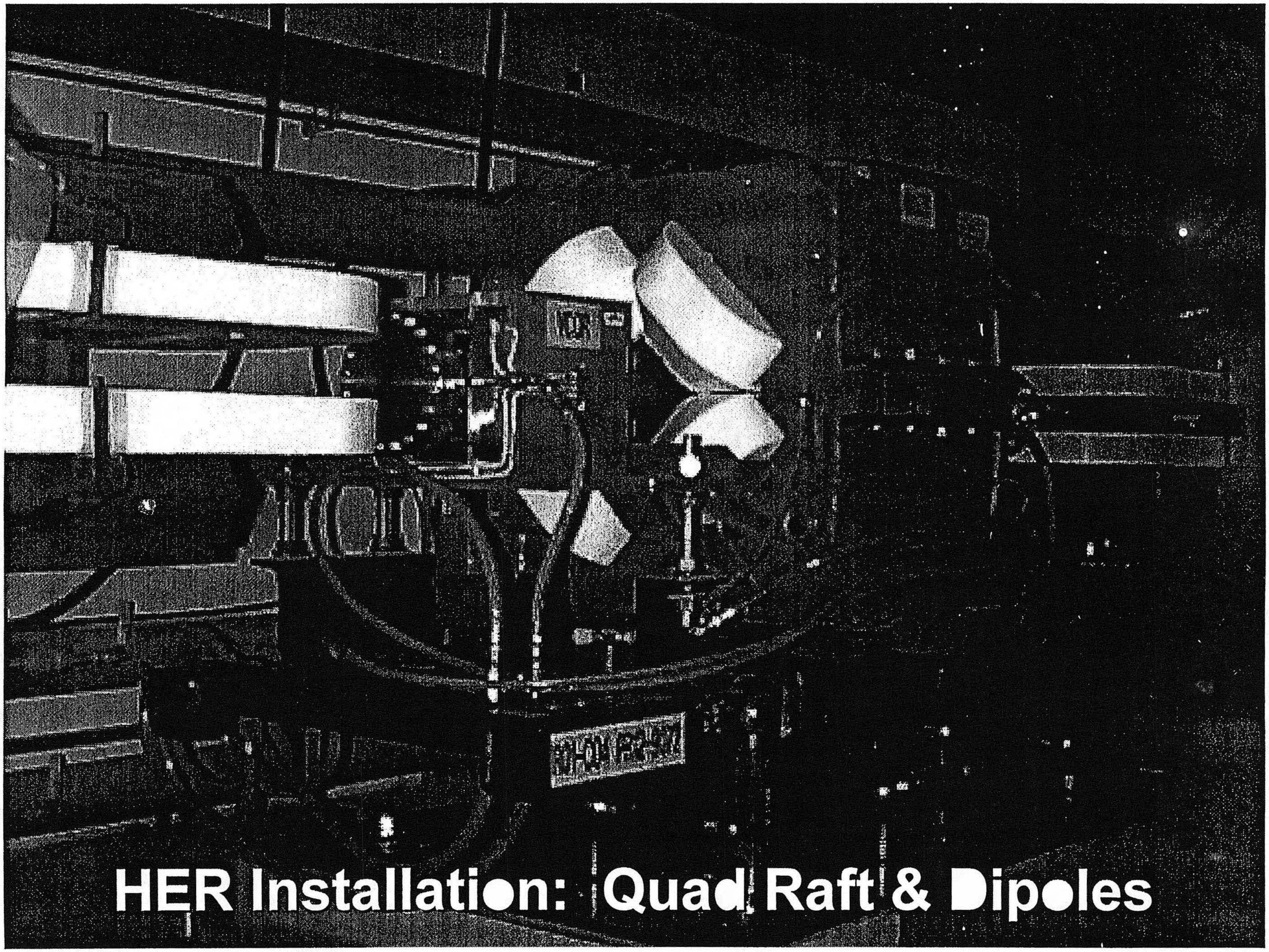

HER Installation: Quad Raft & Dipoles

High Energy Ring Vacuum Chamber

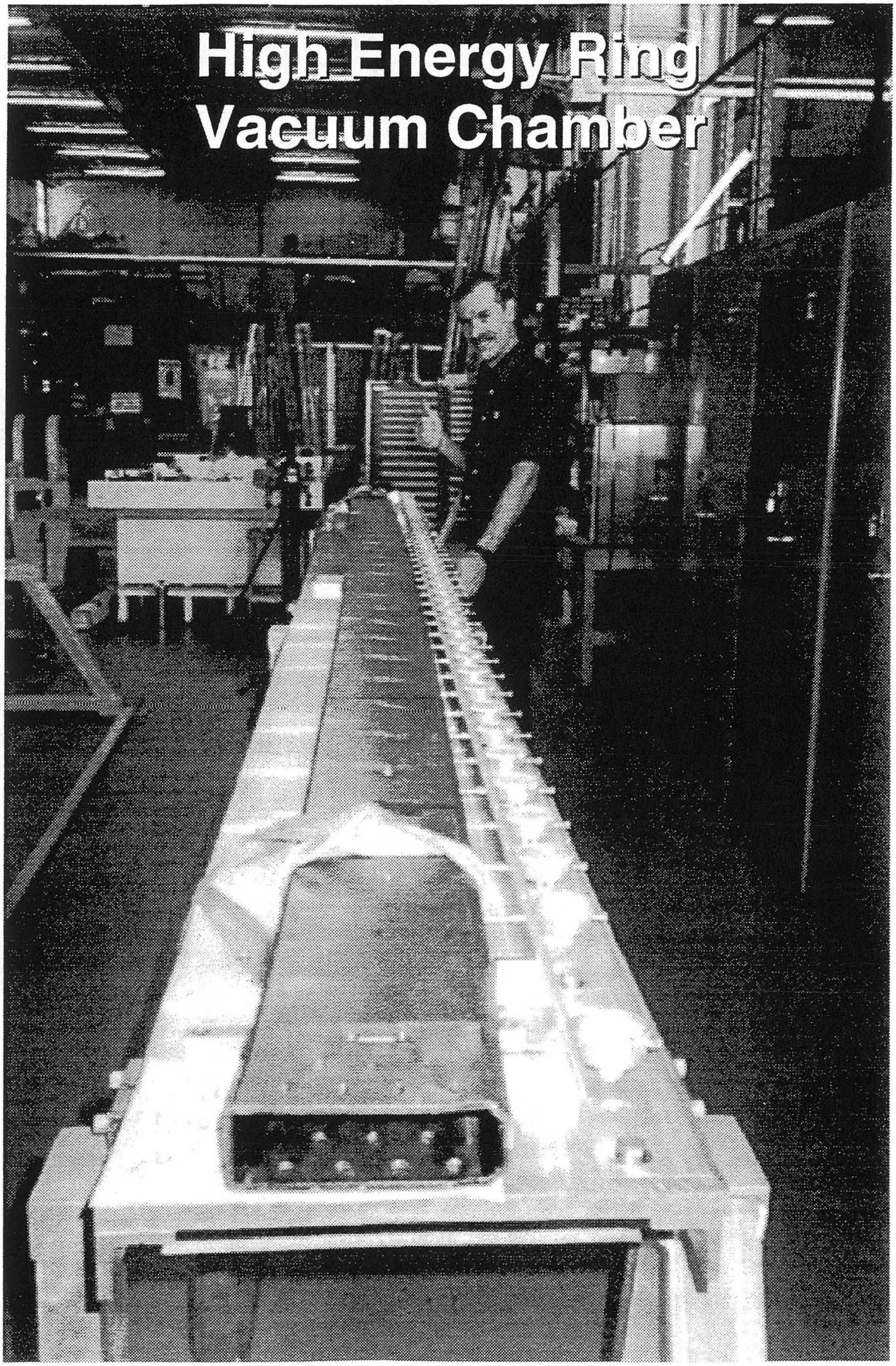

HER Quad Chamber in the E-Beam Welder

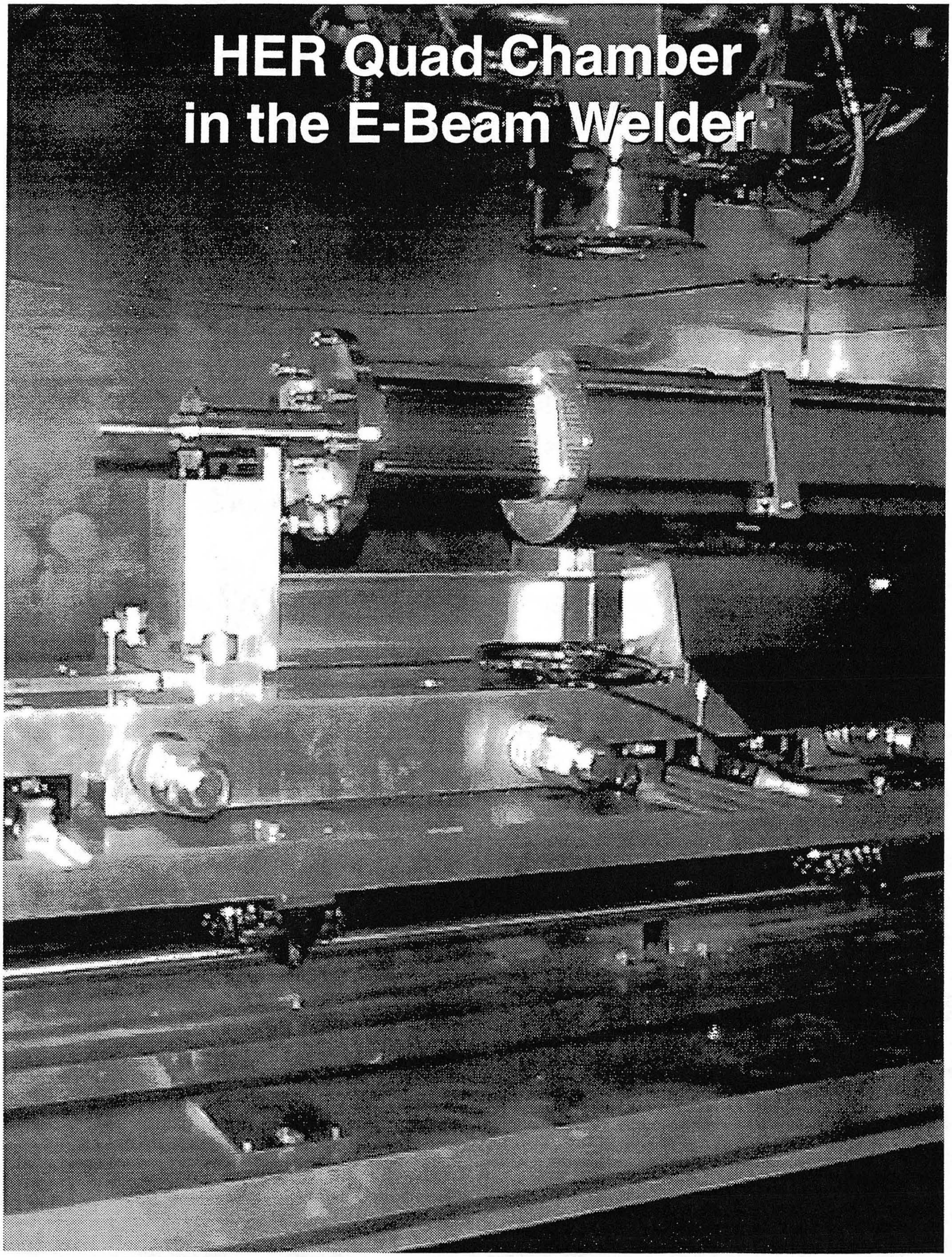

- LER
  - quad and dipole production under way in collaboration with IHEP (Beijing)
    - quad quality exceeds design specs
    - prototype dipole approved for production
  - corrector magnets being constructed in industry
  - sextupoles being refurbished from PEP (new coils)
  - prototype arc and straight section rafts completed
  - arc vacuum chamber extrusions in hand
- IR
  - intricate region to design and build
  - prototype of Q1 being developed
  - design of supports under way

LER Quads Awaiting Measurement at IHEP

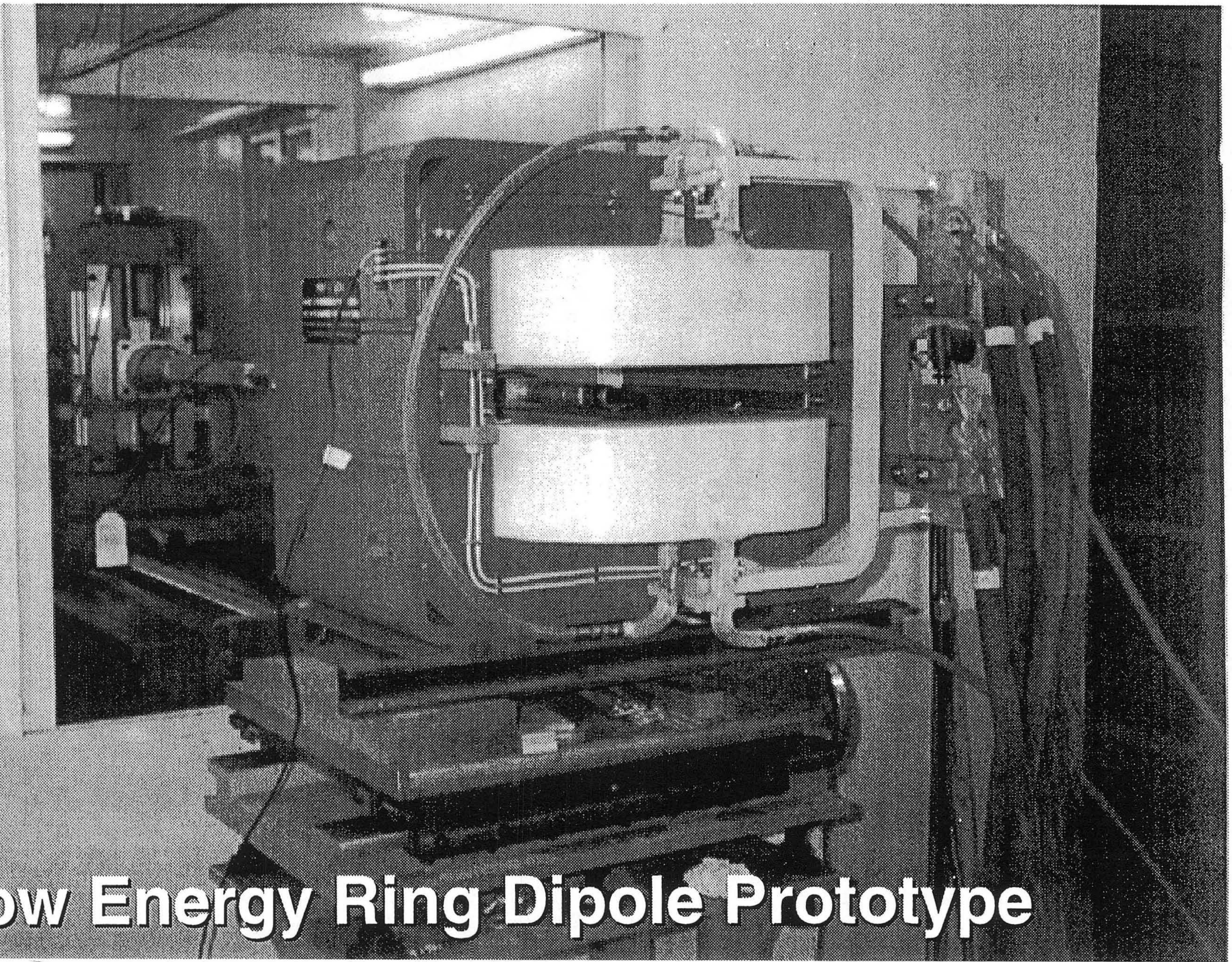

Low Energy Ring Dipole Prototype

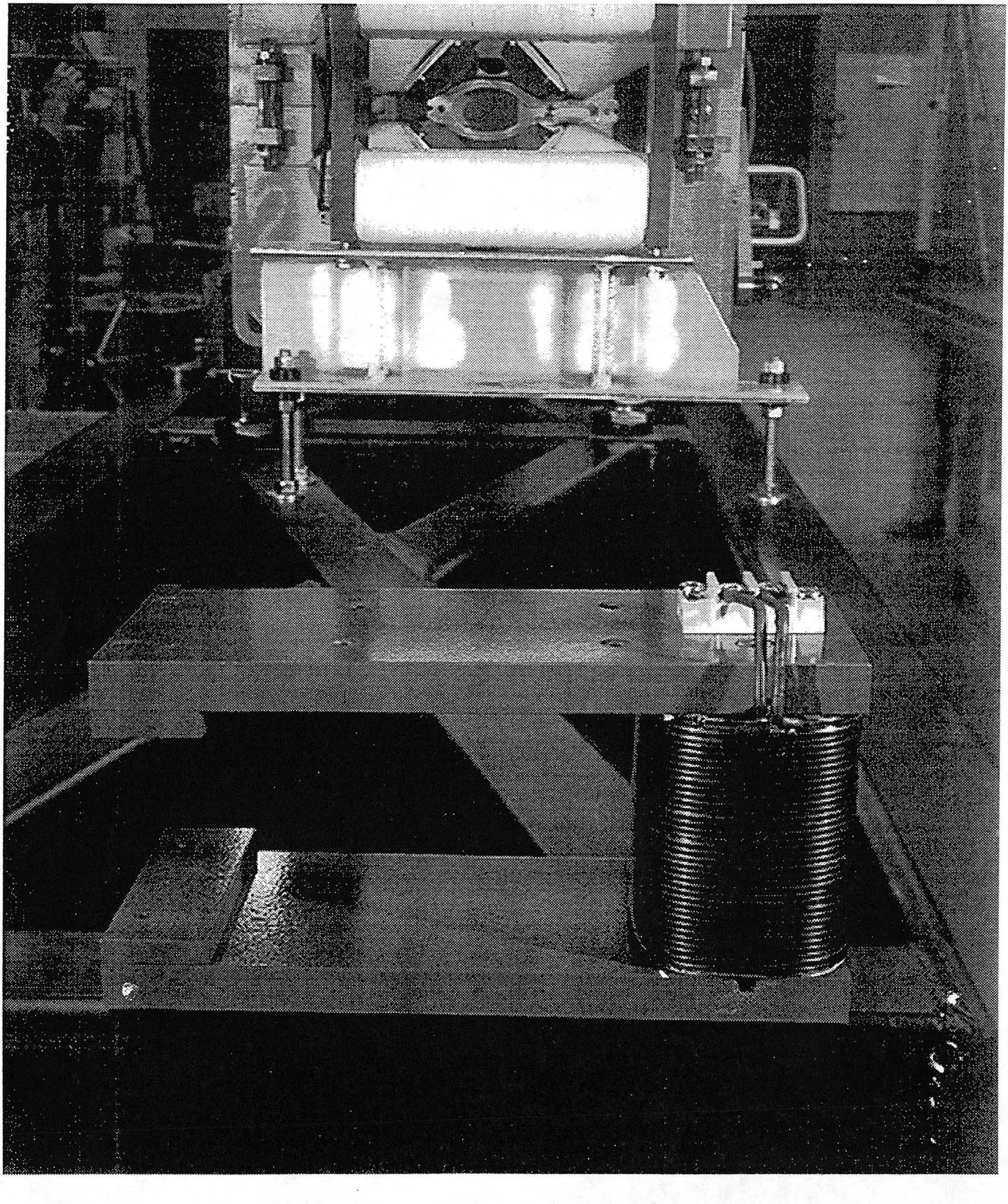

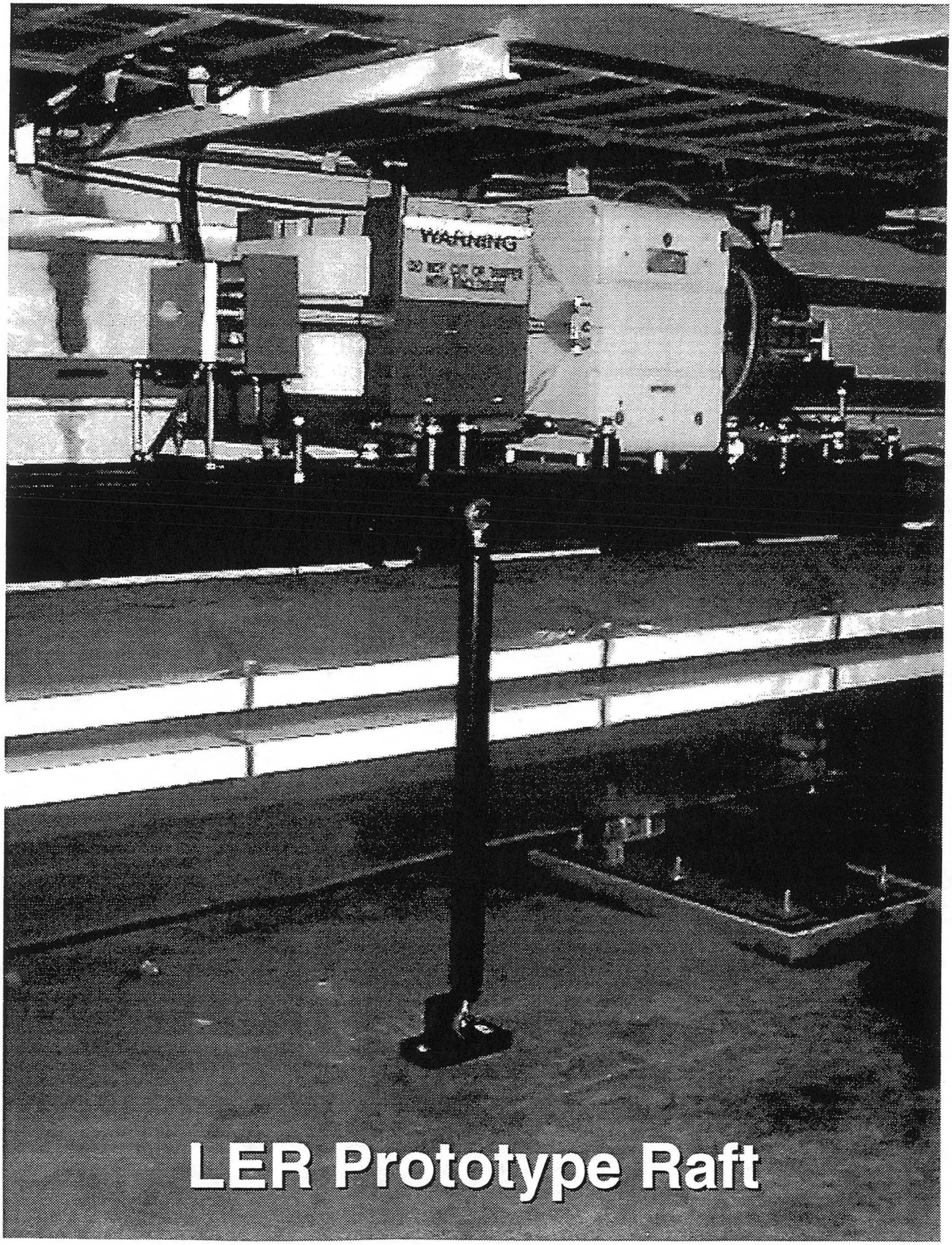

LER Prototype Raft

PEP-II *B*-Factory

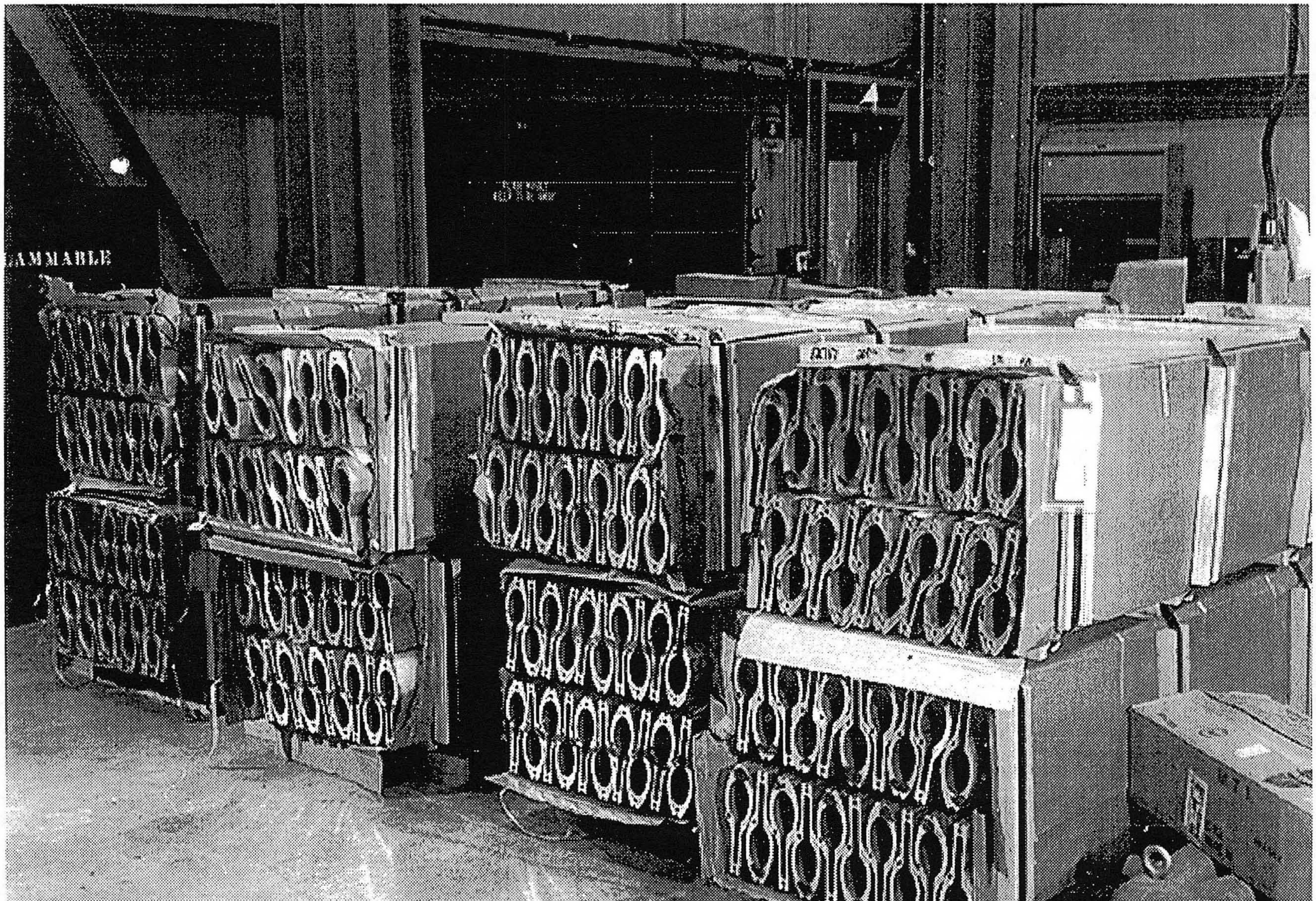

PEP-II *B*-Factory

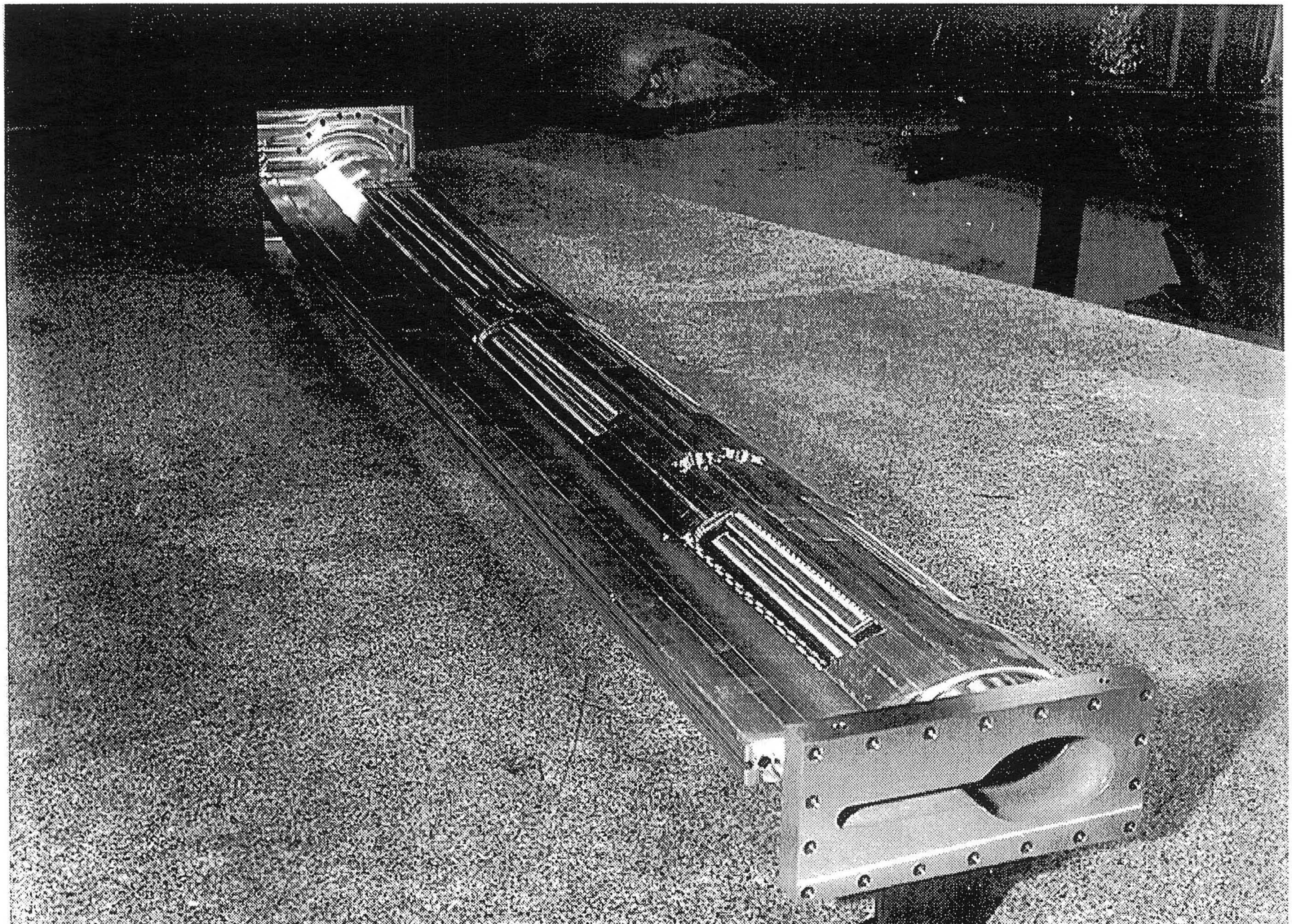

PEP-II *B*-Factory

Magnet Design

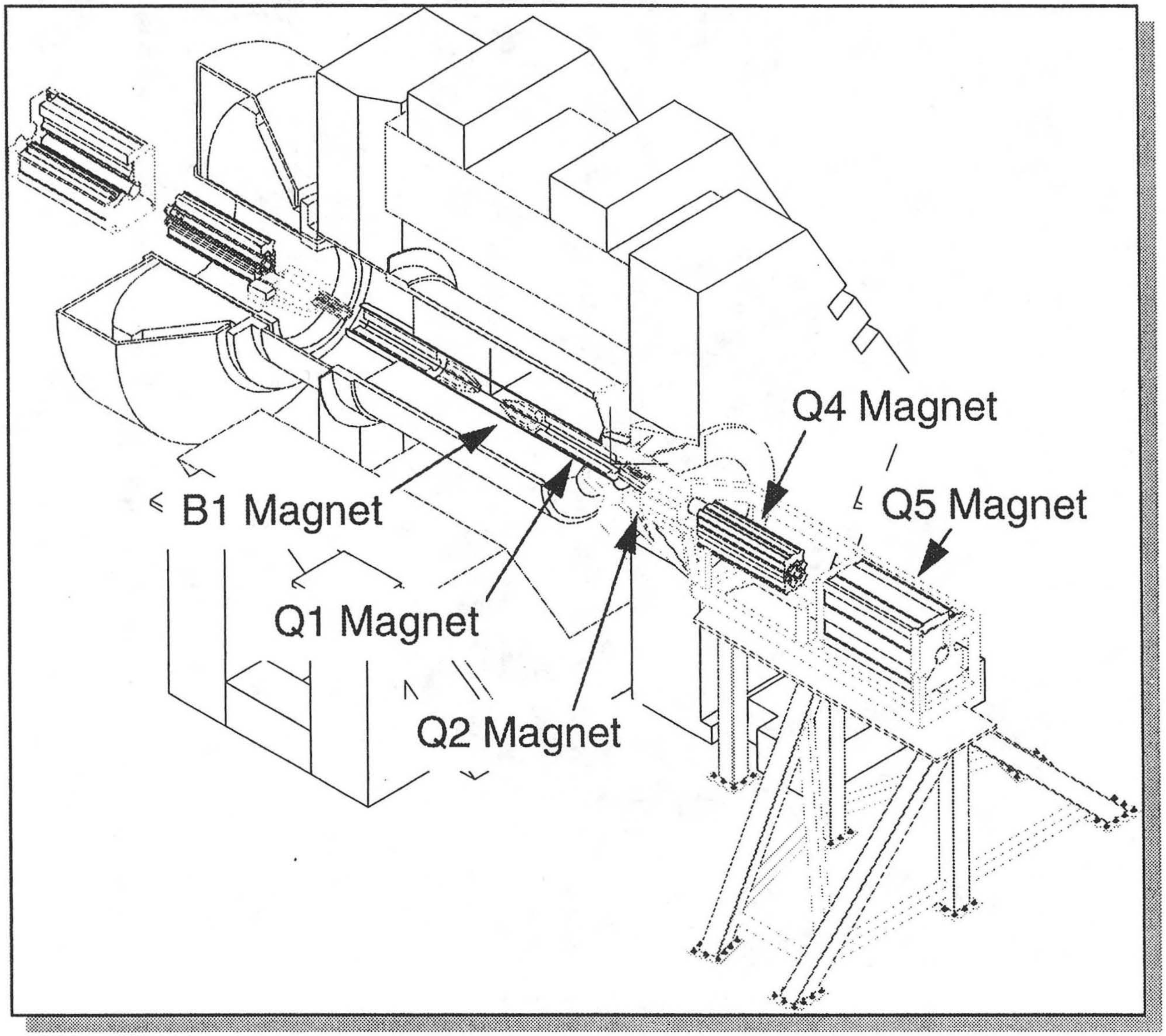

Support Tube Design

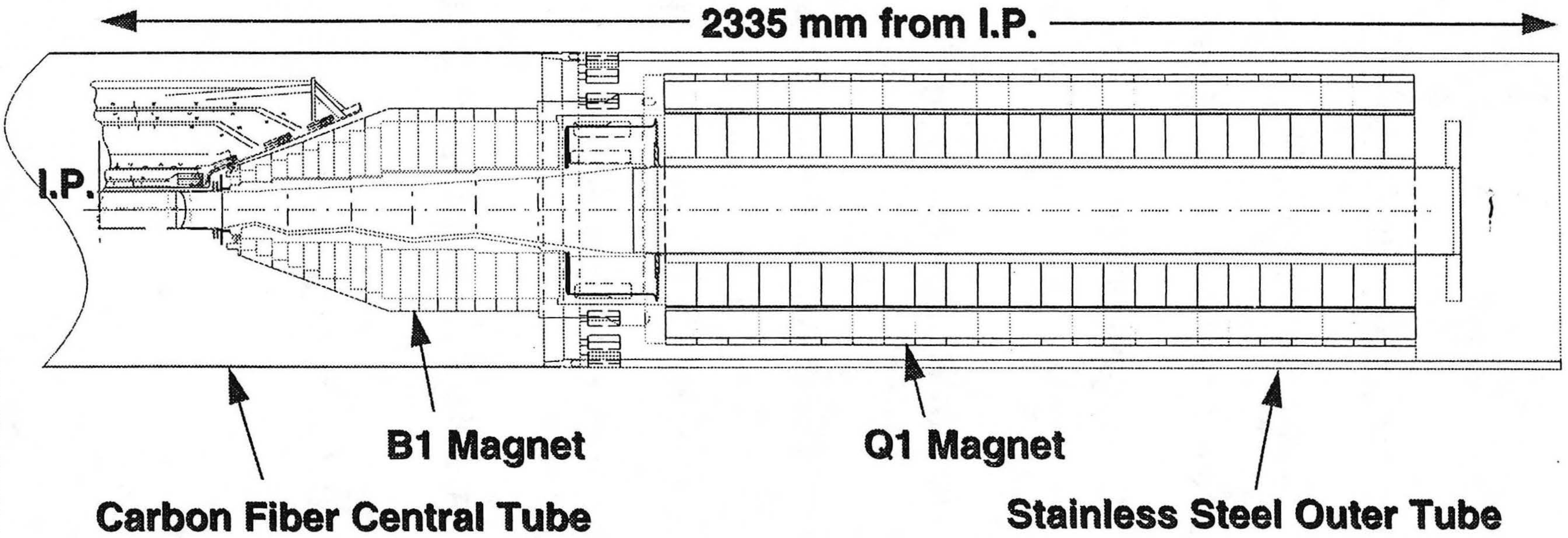

Plan View of Near IR Components in Support Tube

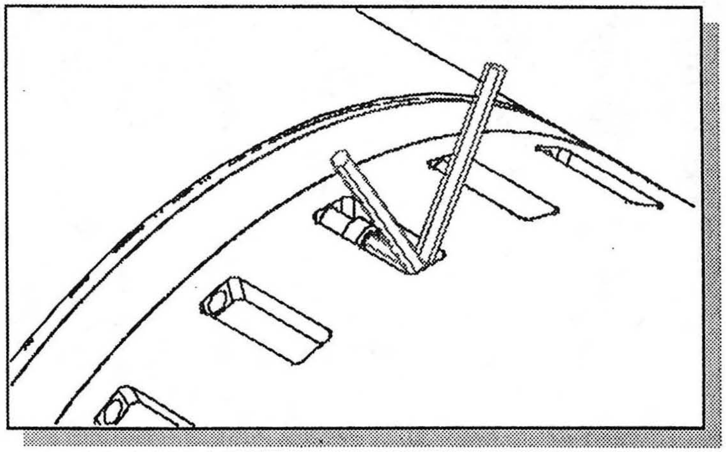

**Detail of C.F.C.
Bolted Joint**

- RF system
  - — test cavity demonstrated wall power of 120 kW
  - — RF window demonstrated 500 kW power
  - — first-article klystron produced required 1.2 MW
  - — damping loads undergoing tests at 714 MHz
- Feedback systems
  - — preferred approach is bunch-by-bunch feedback in time domain
    - o detect bunch displacement, kick it back where it belongs
  - — considerable design verification done at ALS
    - o both longitudinal and transverse systems work as expected
      - – ALS requirements are comparable to PEP-II needs
        - ⇒ doing realistic “battlefield” testing

RF Cavity Assembly

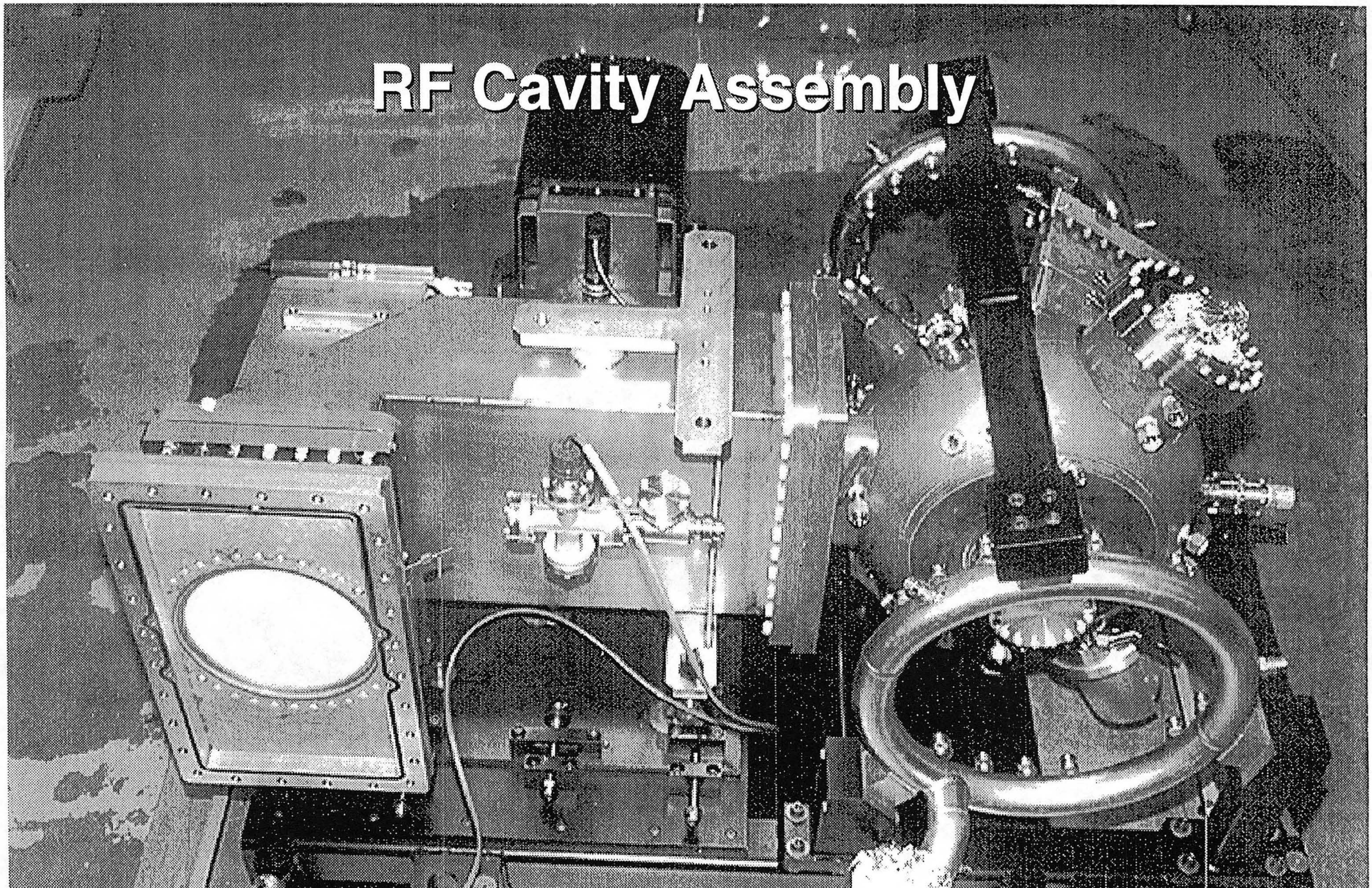

YK 1360 - Tube #1

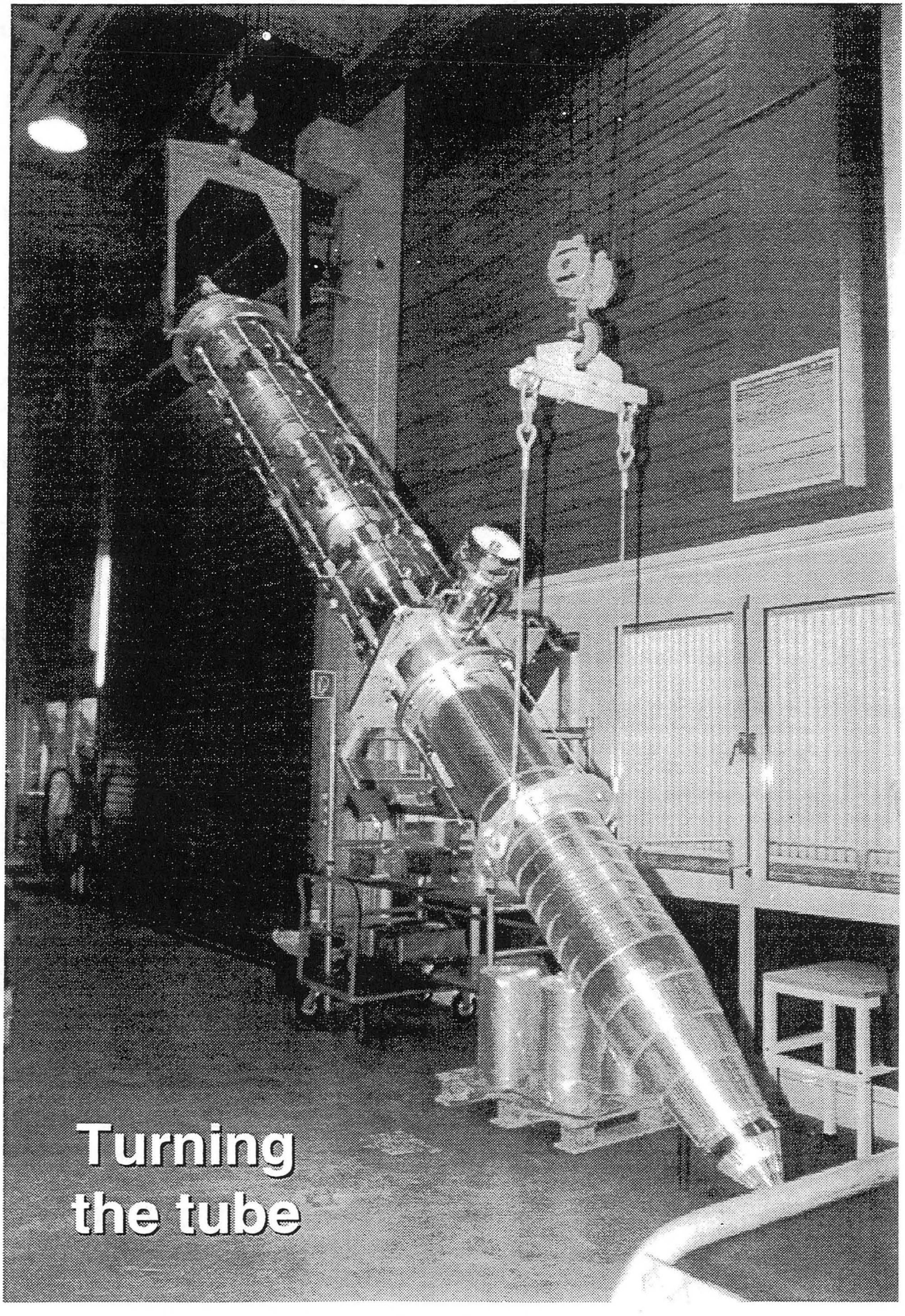

Turning the tube

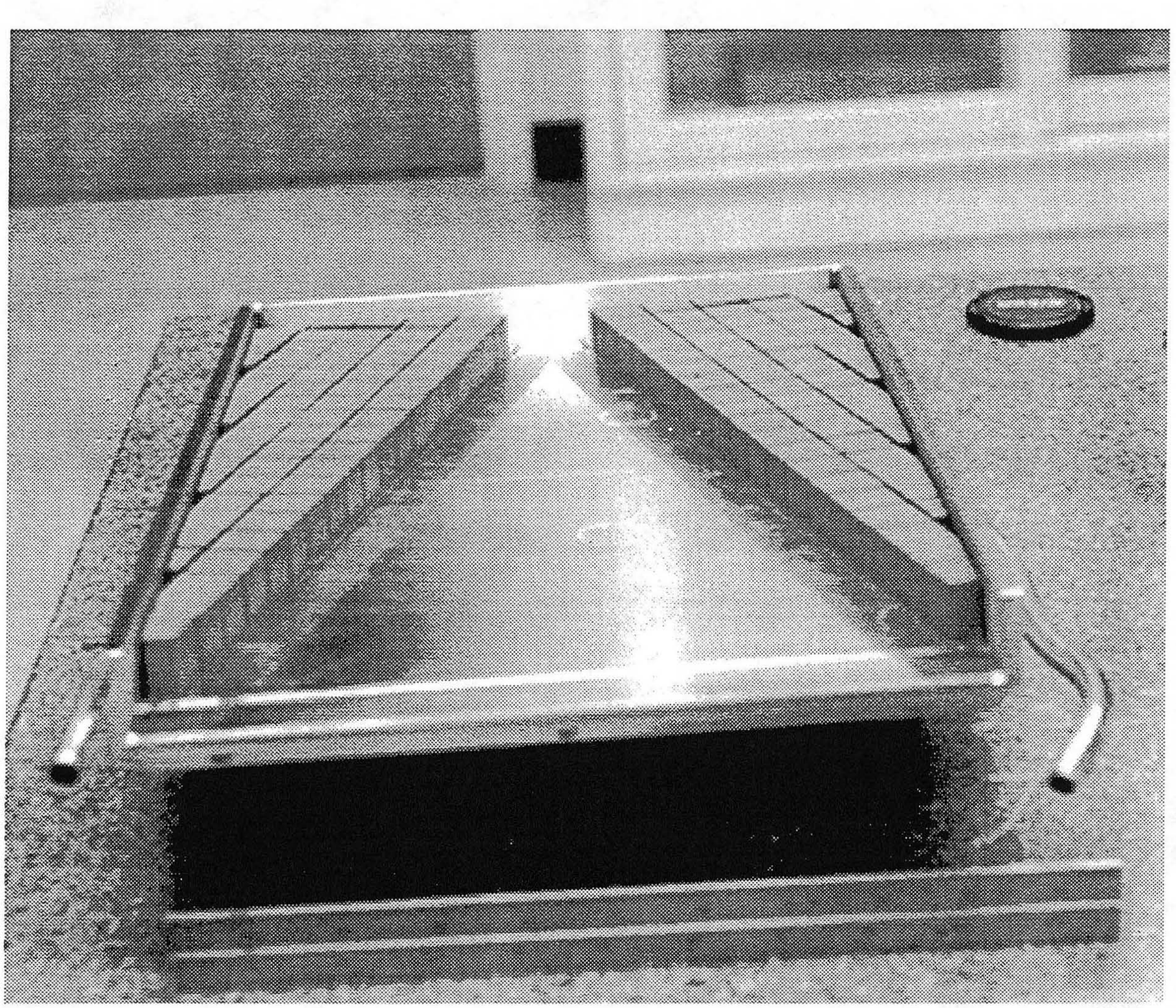

HOM Load High-Power Prototype

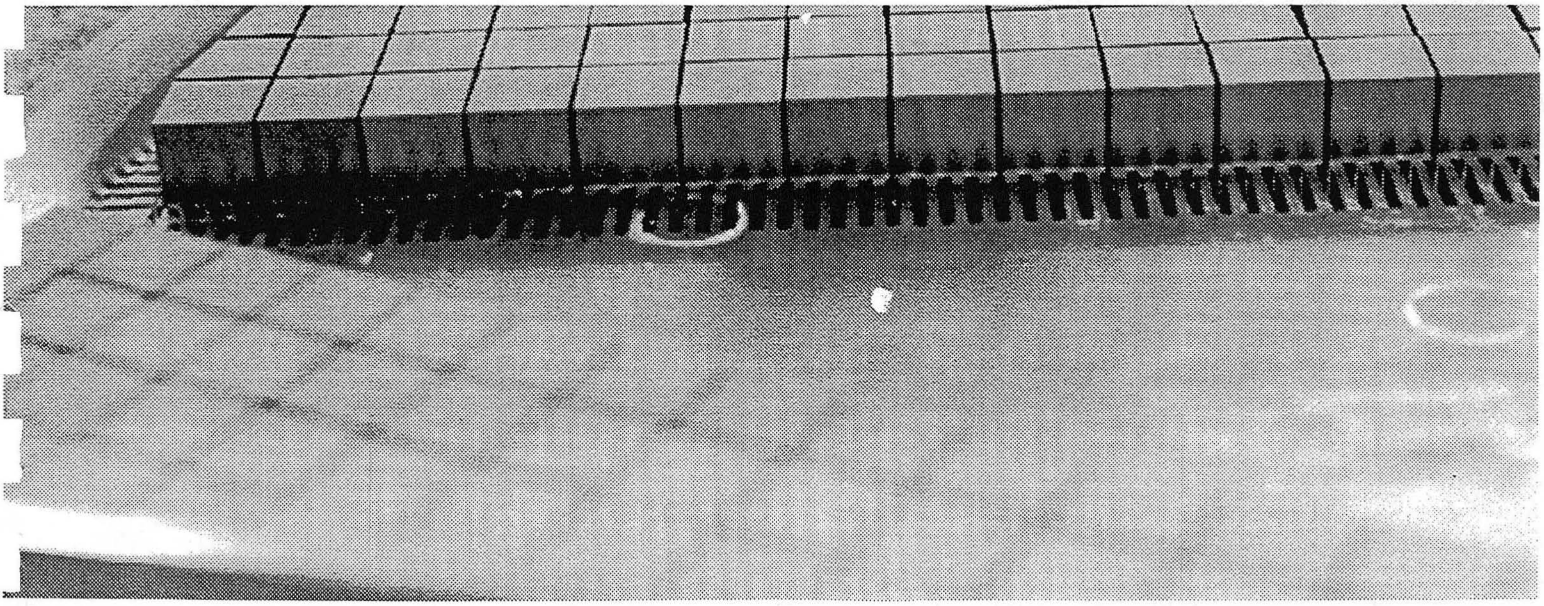

Longitudinal Feedback Kicker

ALS Longitudinal Feedback System

Diagnostic beamline images

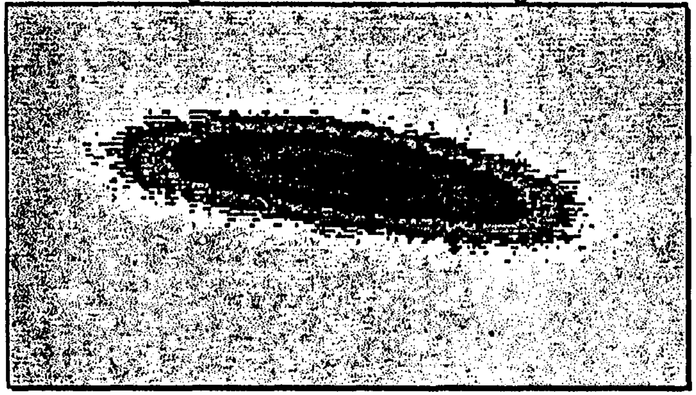

LONGITUDINAL FEEDBACK OFF
Vertical and Horizontal feedback on
Horizontal blow-up & tilt due to dispersion

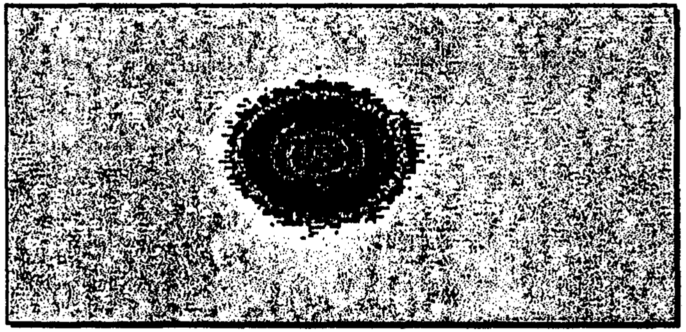

175 mA in 40 bunches

LONGITUDINAL FEEDBACK ON
Vertical and Horizontal feedback on

Feedback system time domain data

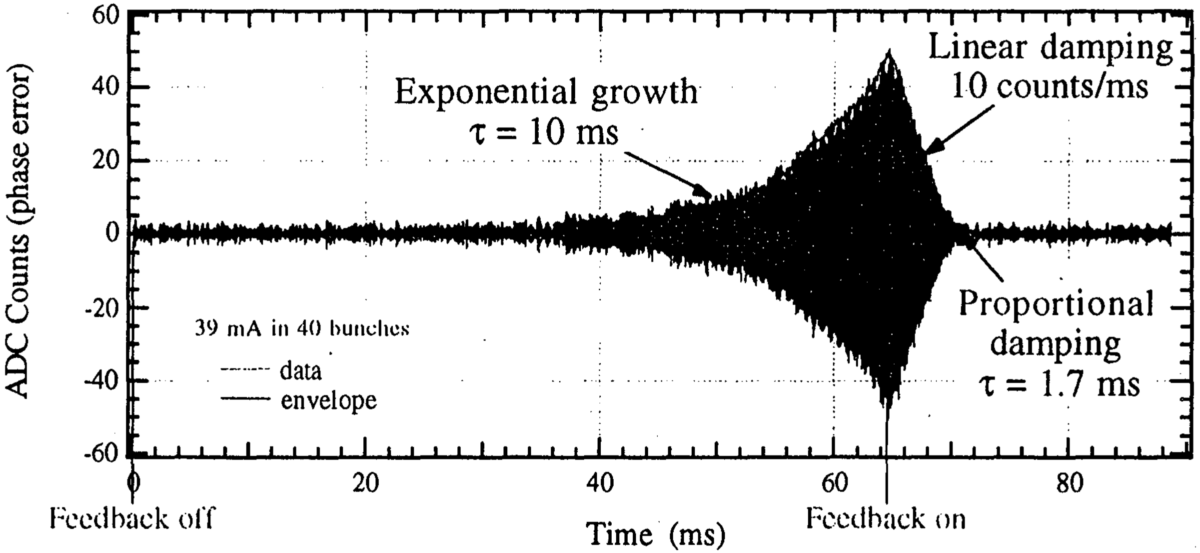

Cost and Schedule

- Cost estimate is \$177M
  - — activities split among SLAC, LBNL, and LLNL
- DOE plan calls for 5-year construction schedule

PEP-II Funding Profile

	FY94 (\$M)	FY95 (\$M)	FY96 (\$M)	FY97 (\$M)	FY98 (\$M)
Budget authority	36	44	52	45	--
Budget outlay	27	42	50	47	11

- Strategy
  - — complete HER first
    - o study injection and high-current multibunch operation
  - — then finish LER
    - o study beam-beam collision issues

Summary

- After 5 years of R&D, PEP-II project funded beginning FY94
- Project addresses a fundamental outstanding problem in HEP
- Considerable progress made
  - — injection system mostly installed
  - — HER components being installed
  - — LER components in production
  - — IR components in final design and prototyping
- PEP-II team is looking forward to continuing our phased commissioning process with HER in about one year!

Gordon Ball

Chalk River Laboratories
Chalk River, Ontario, Canada

"PIONIC FUSION OF HEAVY IONS"

G.C. BALL

Presented At

Exotic Nuclei Symposium

Honoring The 60th Birthday Of Joseph Cerny

April 14-16, 1996

1. Introduction

a) Subthreshold pion production in heavy ion collisions.

$E_{cm} \leq 135A$ MeV

b) Coherent mechanisms at low E_{cm}

2. Experiment—Pionic Fusion

$$^{12}C + {}^{12}C \rightarrow {}^{24}X + \text{pion}$$

3. Results

4. Summary

Collaborators:

Chalk River		University Laval
G.C. Ball	A.C. Hayes	L. Beaulieu
D.R. Bowman	D. Horn	Y. Larochelle
W.G. Davies	G. Savard	C. St. Pierre
D. Fox		

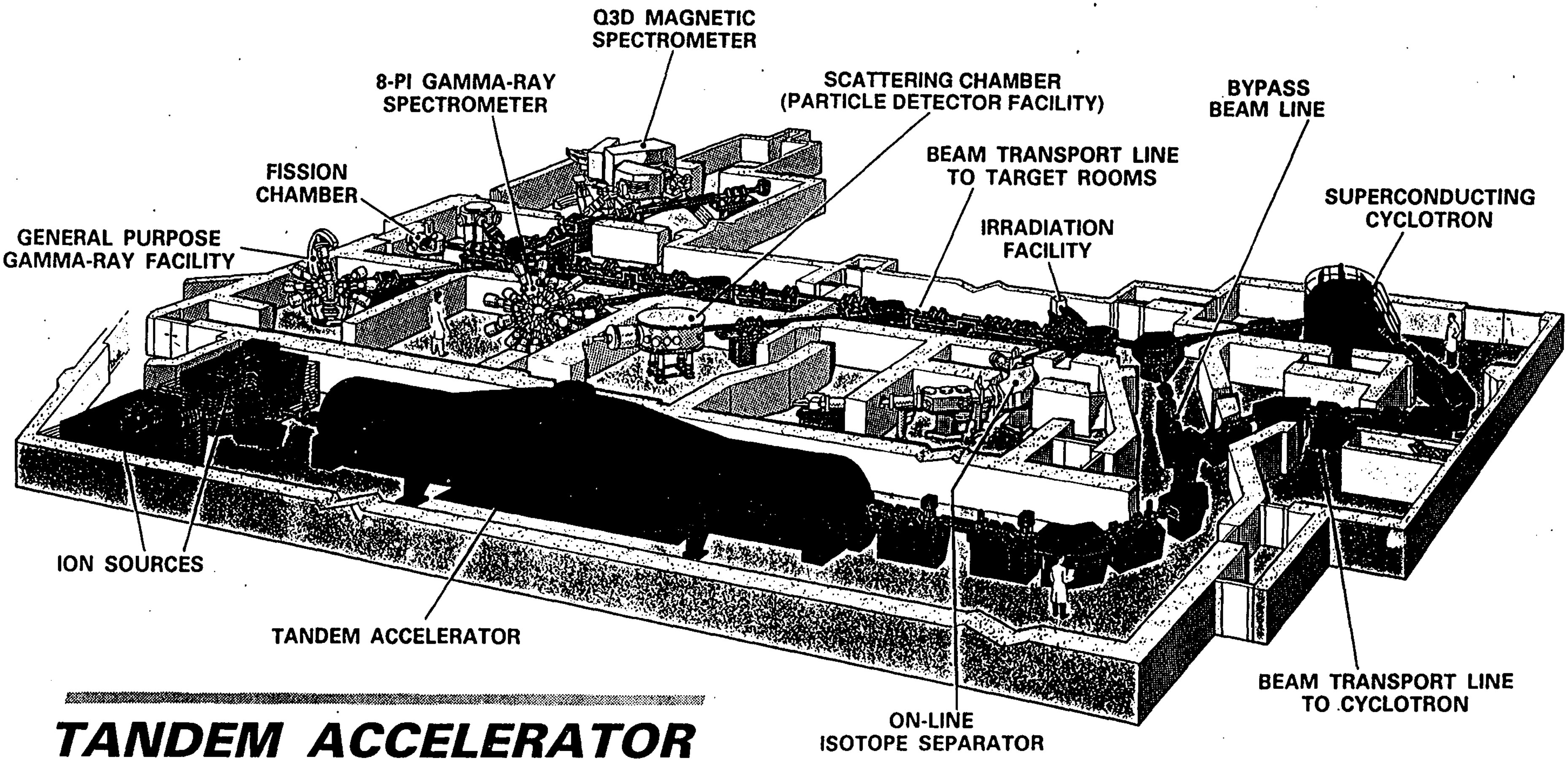

TANDEM ACCELERATOR SUPERCONDUCTING CYCLOTRON (TASCC)

Chalk River, Canada

Pion Production in Heavy-ion Reactions

ENTRANCE CHANNEL:

MECHANISM:

FINAL STATE:

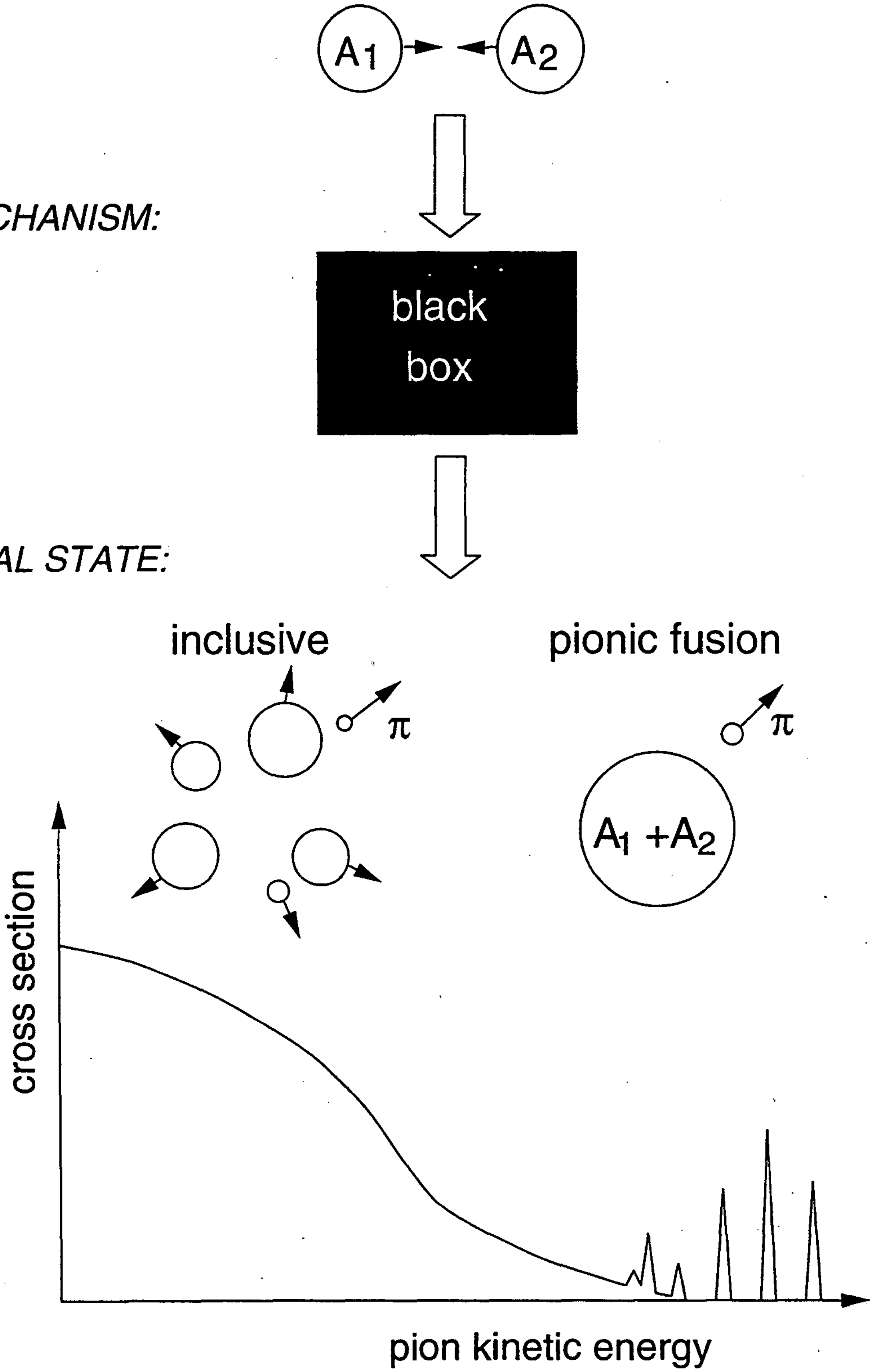

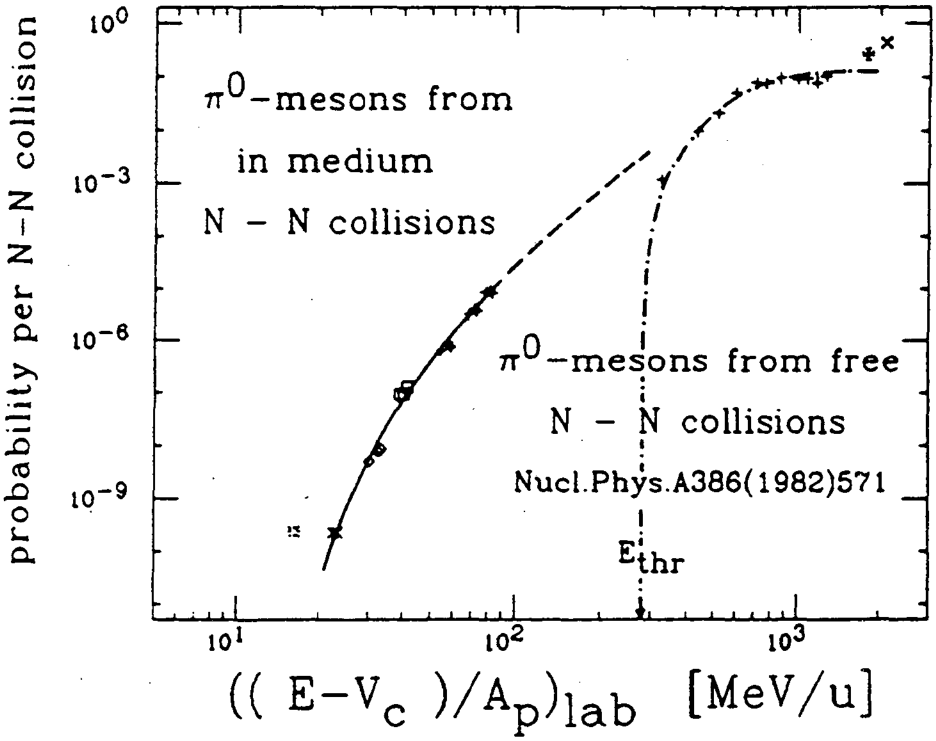
probability per N–N collision
10^0
10^{-3}
10^{-6}
10^{-9}
π^0–mesons from
in medium
N – N collisions
π^0–mesons from free
N – N collisions
Nucl.Phys.A386(1982)571
E_{thr}
10^1
10^2
10^3
$((E-V_c)/A_p)_{lab}$ [MeV/u]

"SUBTHRESHOLD PION PRODUCTION IN HEAVY-ION COLLISIONS"

- Incoherent summation of nucleon-nucleon collisions

- "Coherent" models

    1. Pionic bremsstrahlung model

    2. Statistical or compound nucleus models

       (—model of reaction dynamics to define source)

    3. Microscopic models

"SUBTHRESHOLD" PION PRODUCTION MECHANISMS

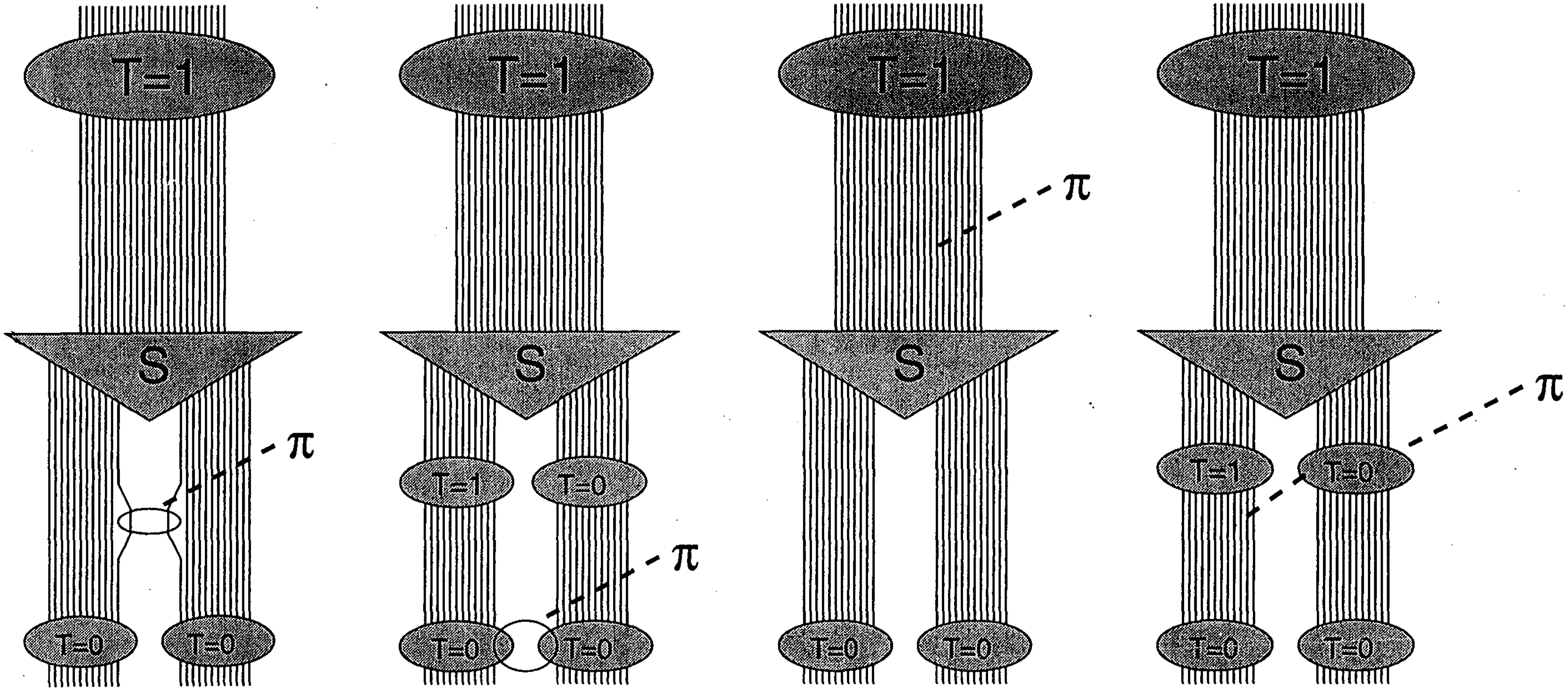

nucleon-nucleon	pionic brems-strahlung	compound nucleus	2-nucleon coherent
Cassing et al. Bertsch	Vasak et al.	Aichelin-Bertsch Prakash et al. Potvin et al.	Huber et al. Gibbs-Hayes

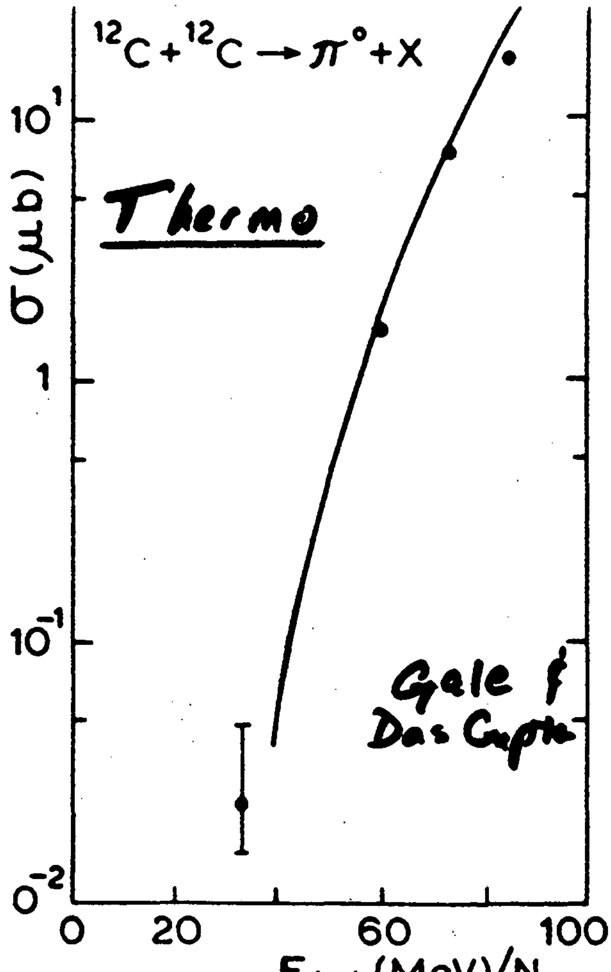

IG. 1. Total inclusive π^0 cross section. The curve is our ther-
dynamic calculation. The parameters of the calculation are given
he text. The data are from Ref. 1.

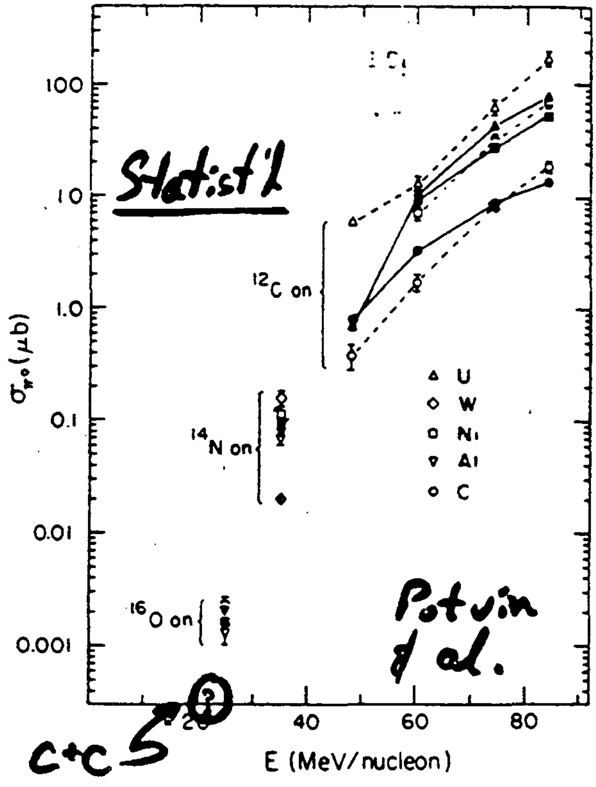

FIG. 1. Experimental and calculated σ_{π^0} total cross sections of ^{12}C, ^{14}N, and ^{16}O beams on different targets as a function of energy. The open symbols are used for the experimental data (Refs. 1 and 3) and the calculated yields are shown by solid symbols. In the case of ^{12}C beams, the values are linked by lines to guide the eye.

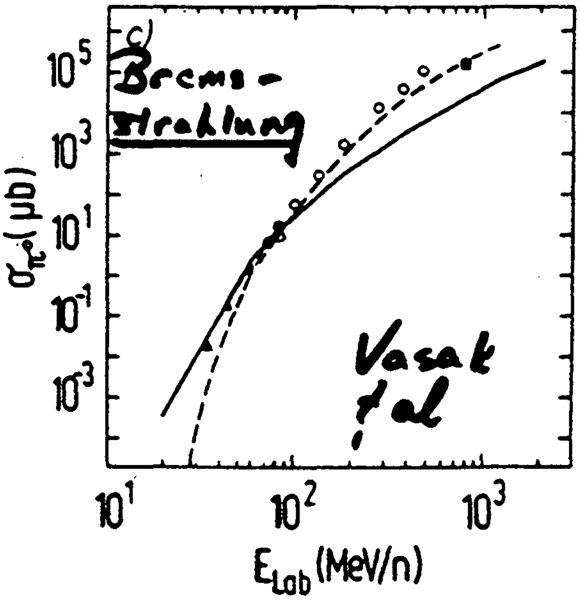

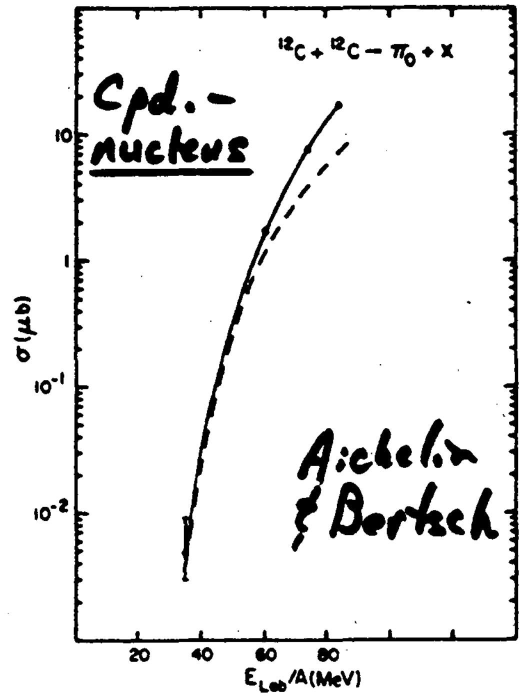

Fig. 1. Calculated total π_0 cross section and the data of ref. [1]. The point at 35 MeV/*N* is extracted from the reaction $^{14}N + ^{27}Al \rightarrow \pi_0 + X$ as explained in the text. The cross section for forming the compound system in the reaction $^{12}C + ^{12}C$, which finally emits a pion, is taken as σ_0 = 160 mb. The dotted line shows the cross section of pions emitted in the first step, the full line represents the sum over all steps.

Pionic Fusion

- ***E_{cm} near absolute threshold limit***

- ***Previous data***

  ^{3}He (^{3}He, π+)^6 Li — Le Bornec *et al.* (1981)

  ^{12}C (^{3}He, ^{15}N)π+ — Homolka *et al.* (1988)

- ***Present experiment***

  $^{12}C + {}^{12}C \rightarrow {}^{24}X$ + pion

  E_{cm} ~137 MeV

  σ (expected) ~.01 - 1.0 nb

  detect A=24 residues

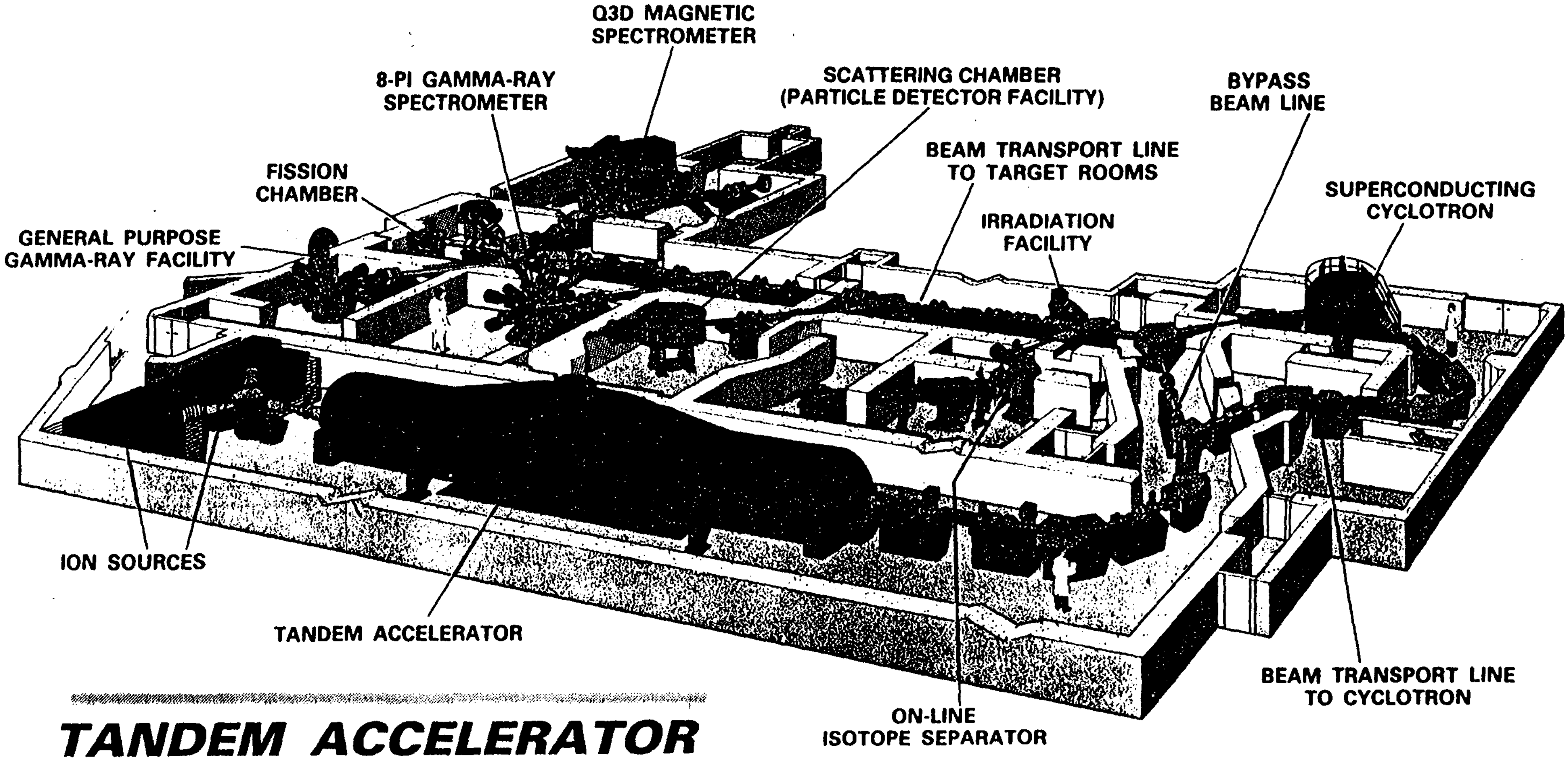

TANDEM ACCELERATOR SUPERCONDUCTING CYCLOTRON (TASCC)

Chalk River, Canada

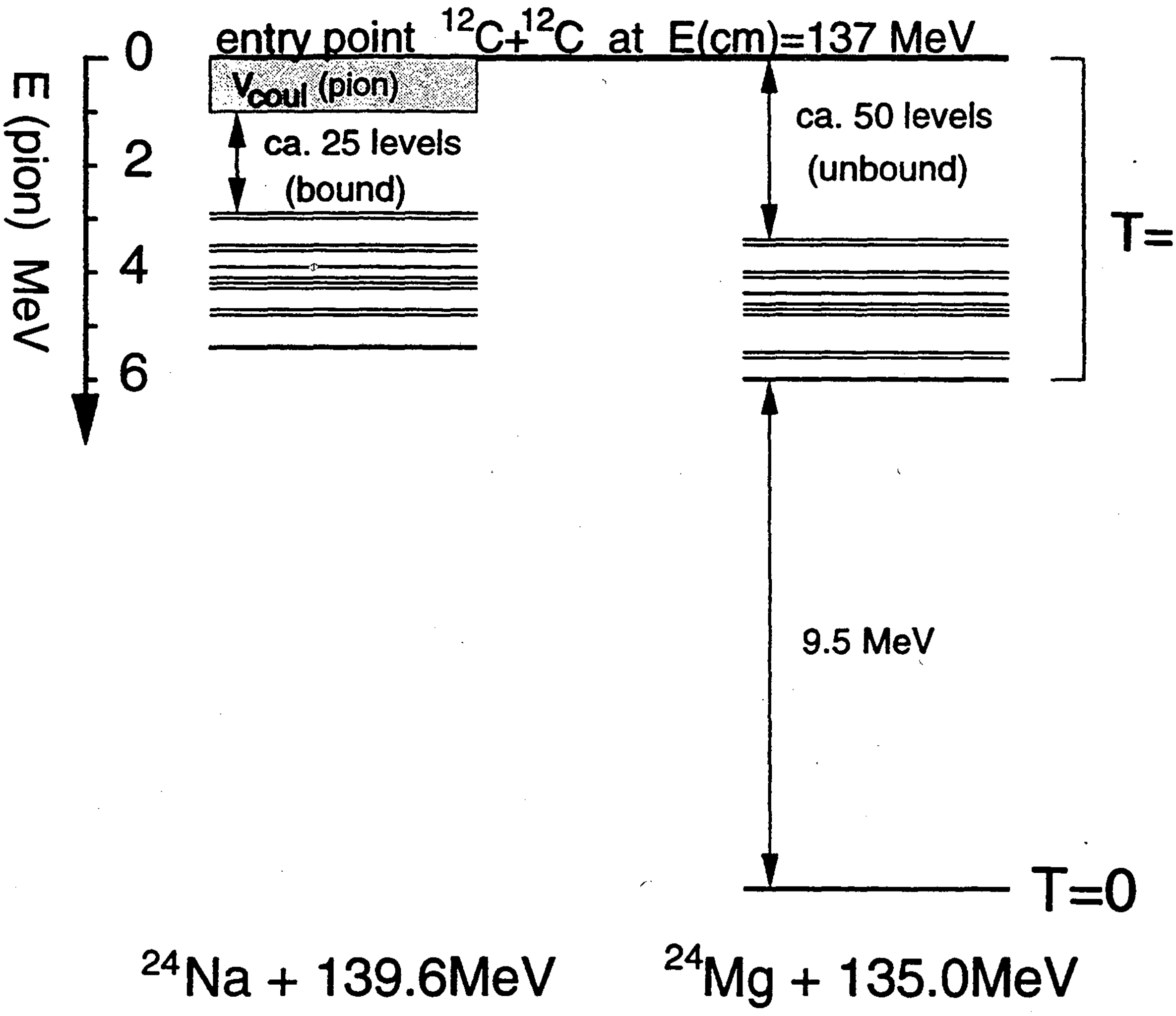
entry point $^{12}C+^{12}C$ at E(cm)=137 MeV
E (pion) MeV
0
2
4
6
V_{coul} (pion)
ca. 25 levels
(bound)
ca. 50 levels
(unbound)
T=1
9.5 MeV
T=0
^{24}Na + 139.6MeV
^{24}Mg + 135.0MeV

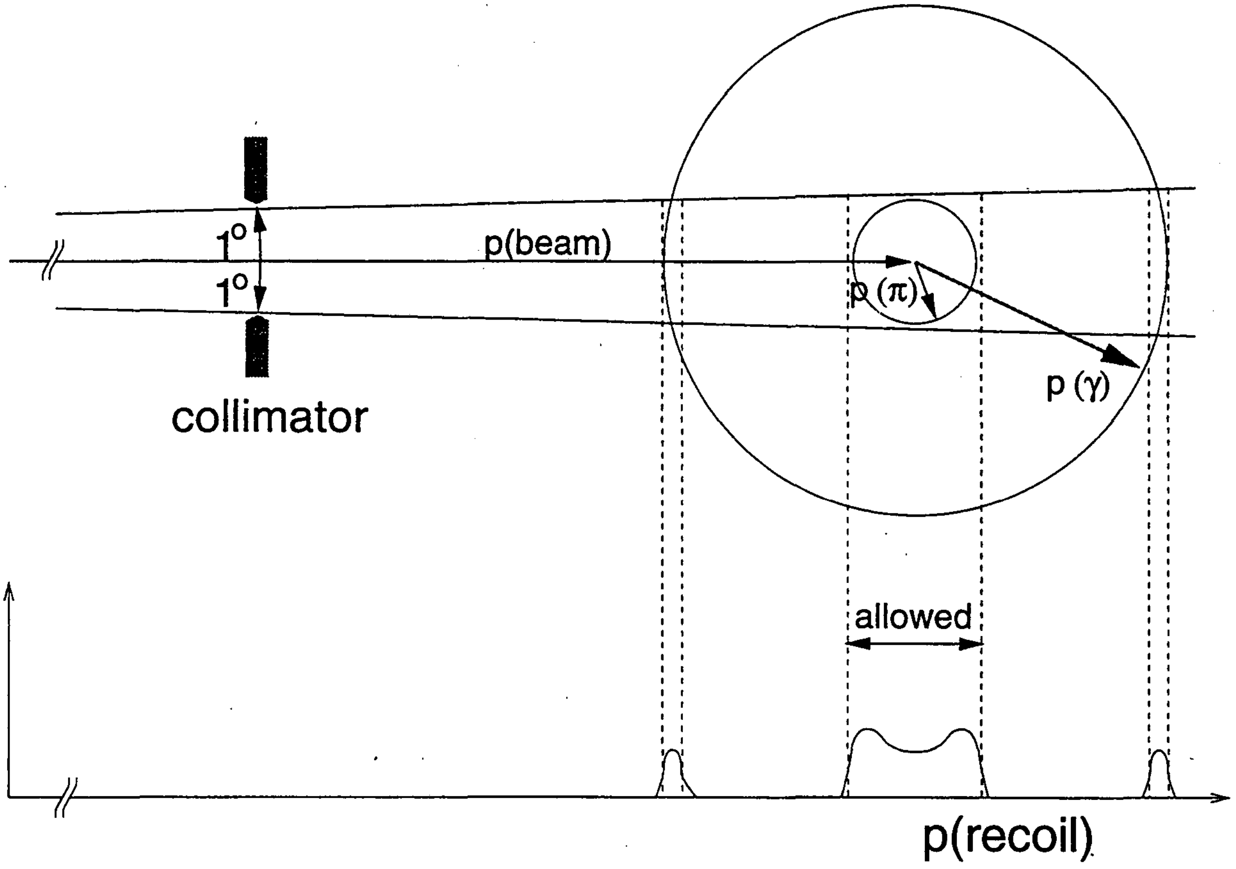

RECOIL KINEMATICS

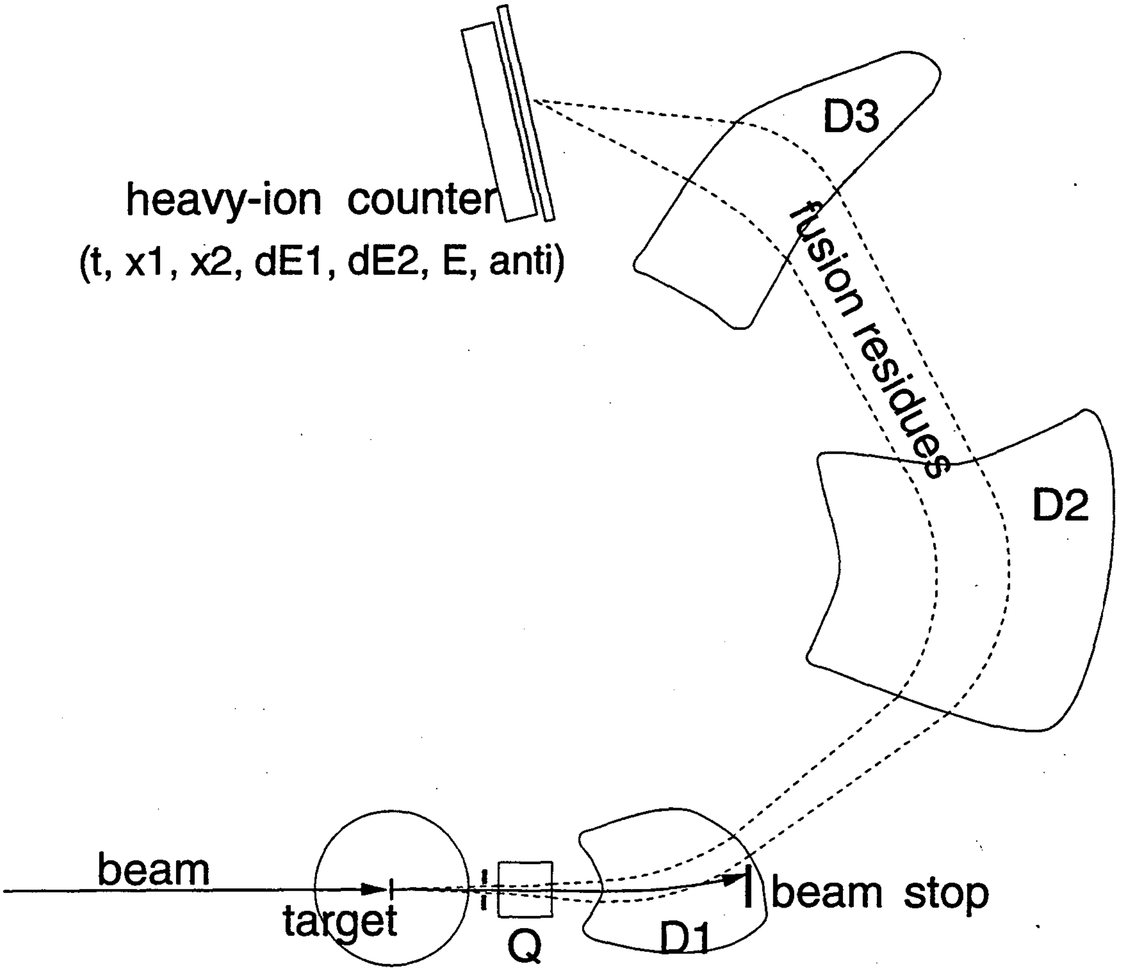

QDDD SPECTROMETER

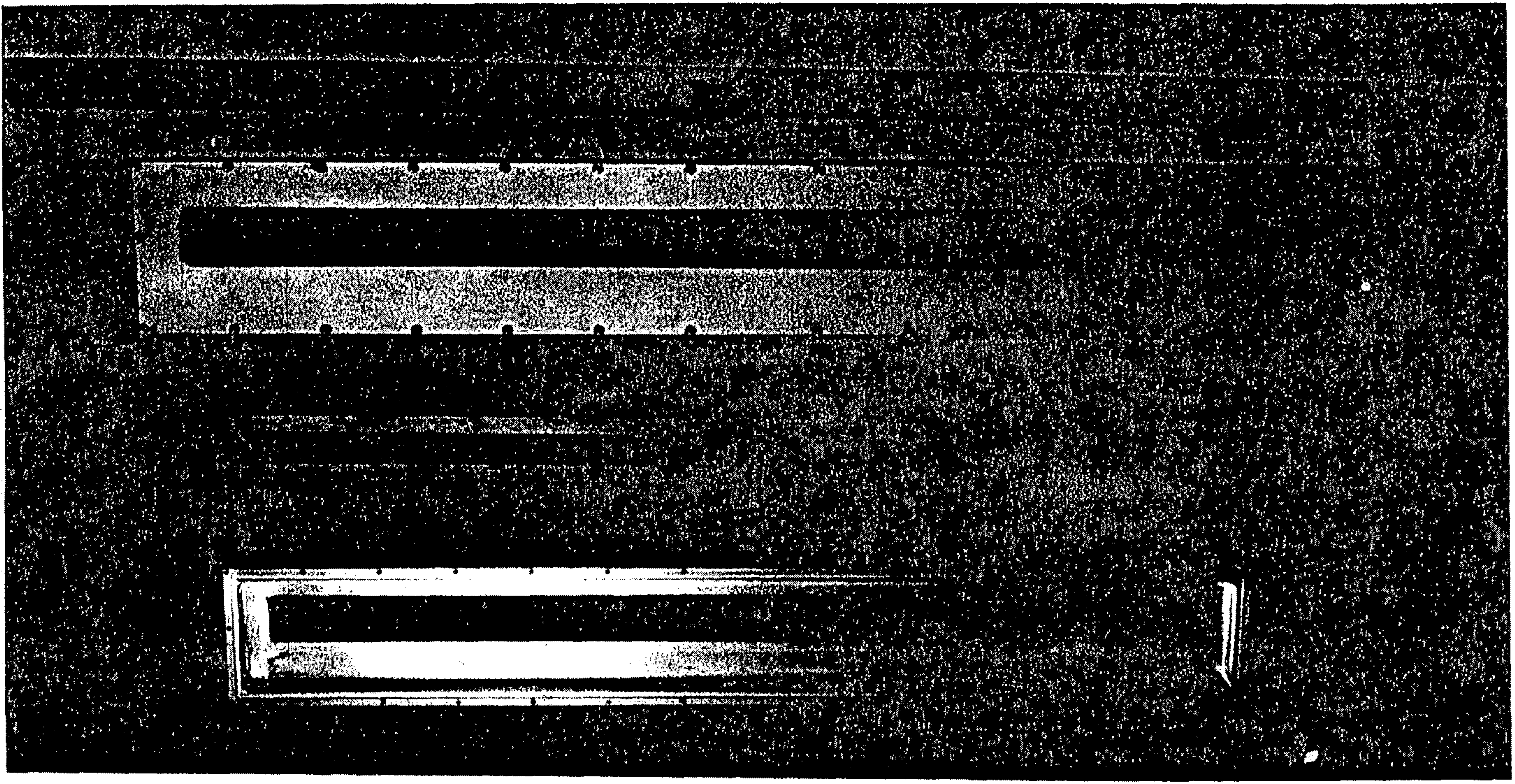

21921-7

[redacted] [illegible] [redacted] [illegible] [redacted]

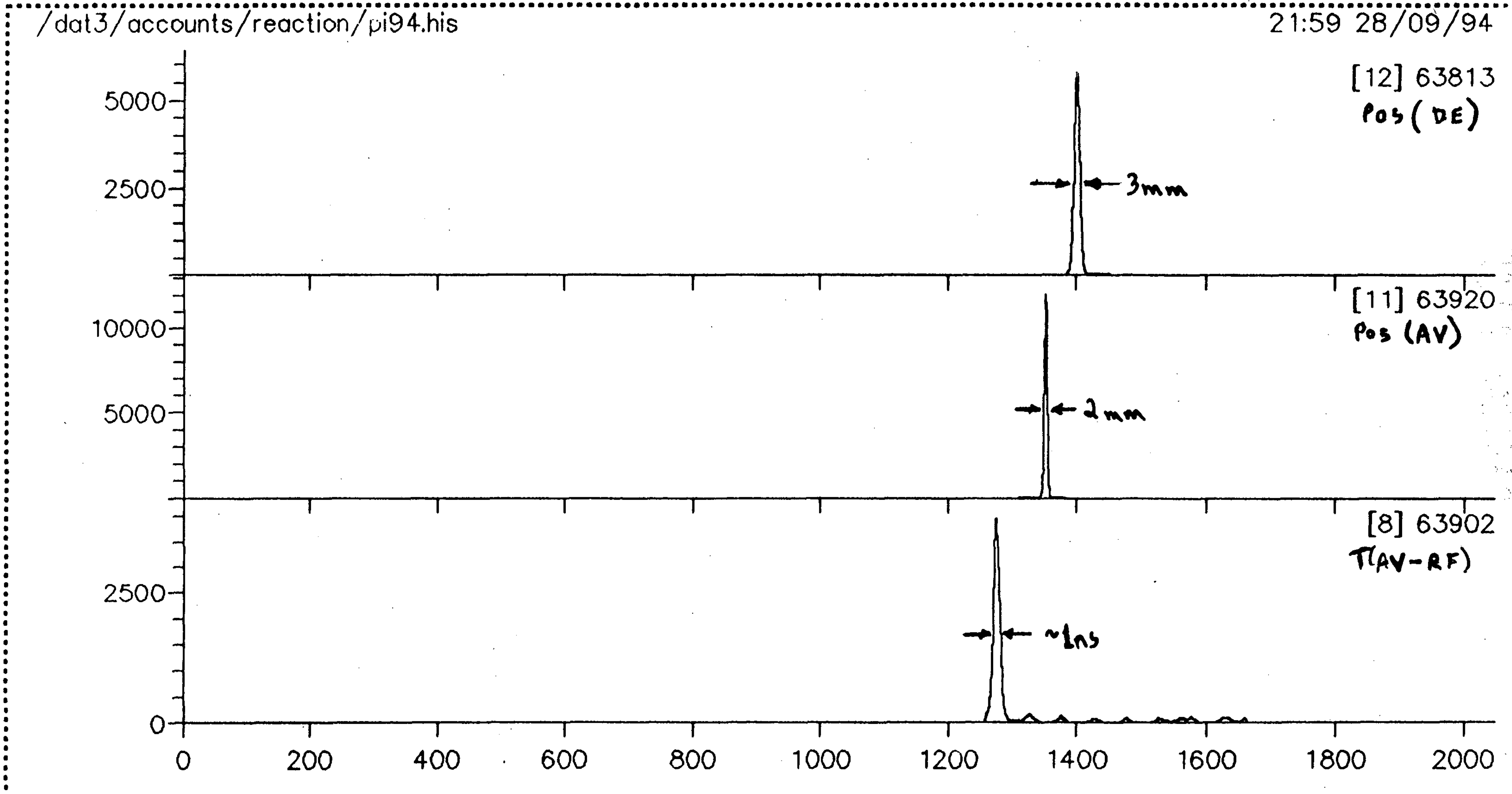

```
/dat3/accounts/reaction/pi94.his                                    21:59 28/09/94
```

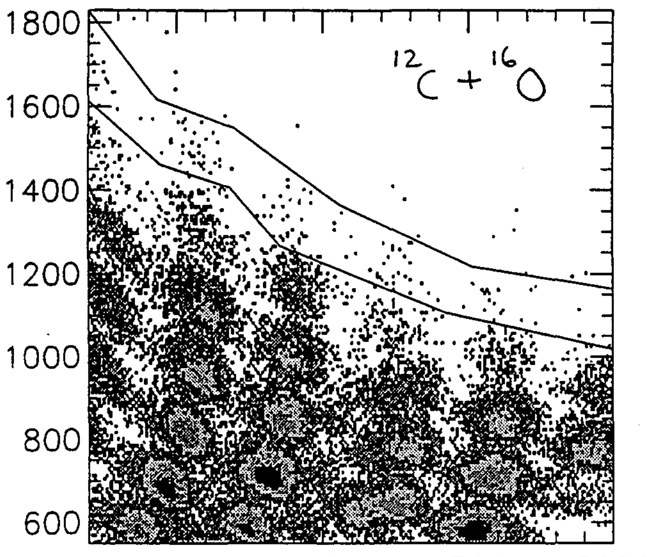

ΔE_2 vs E

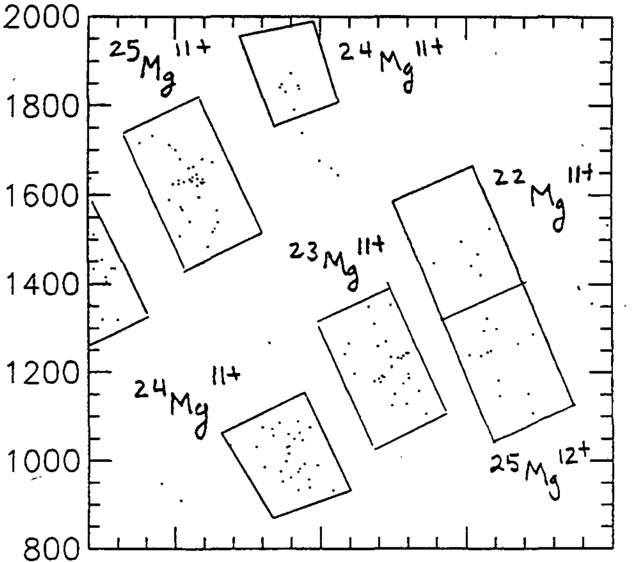

RFAV VS E

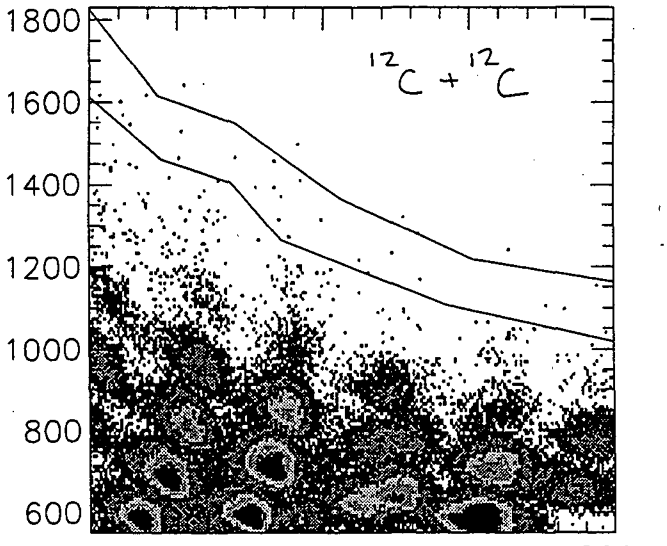

ΔE_2 vs E

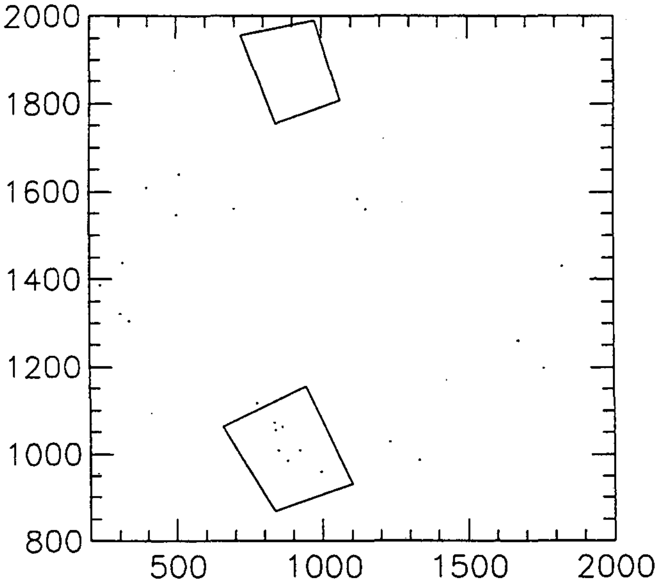

RFAV VS E

Experimental Difficulties

challenge	**solution**
low cross section	$I_{beam} \geq 200$nA (charge)
target E loss	0.5mg/cm^2 ^{12}C
Bρ calibration	^{24}Mg tandem beam
charge state fractions unknown	measure 62% 12$^+$; 33% 11$^+$
$\Delta p/p > 4.7\%$ (ctr limit)	measure at 4 field settings
scattered beam particles	tune; slits after 90° magnet; anti p/t
high-energy gamma decay	collimate to 1°
target impurities	isotopic target; vacuum oven; Ar transfer
knowing impurities	oxide run; assay target
pileup	fast multiple hit reject; TOF
ion ID	TOF

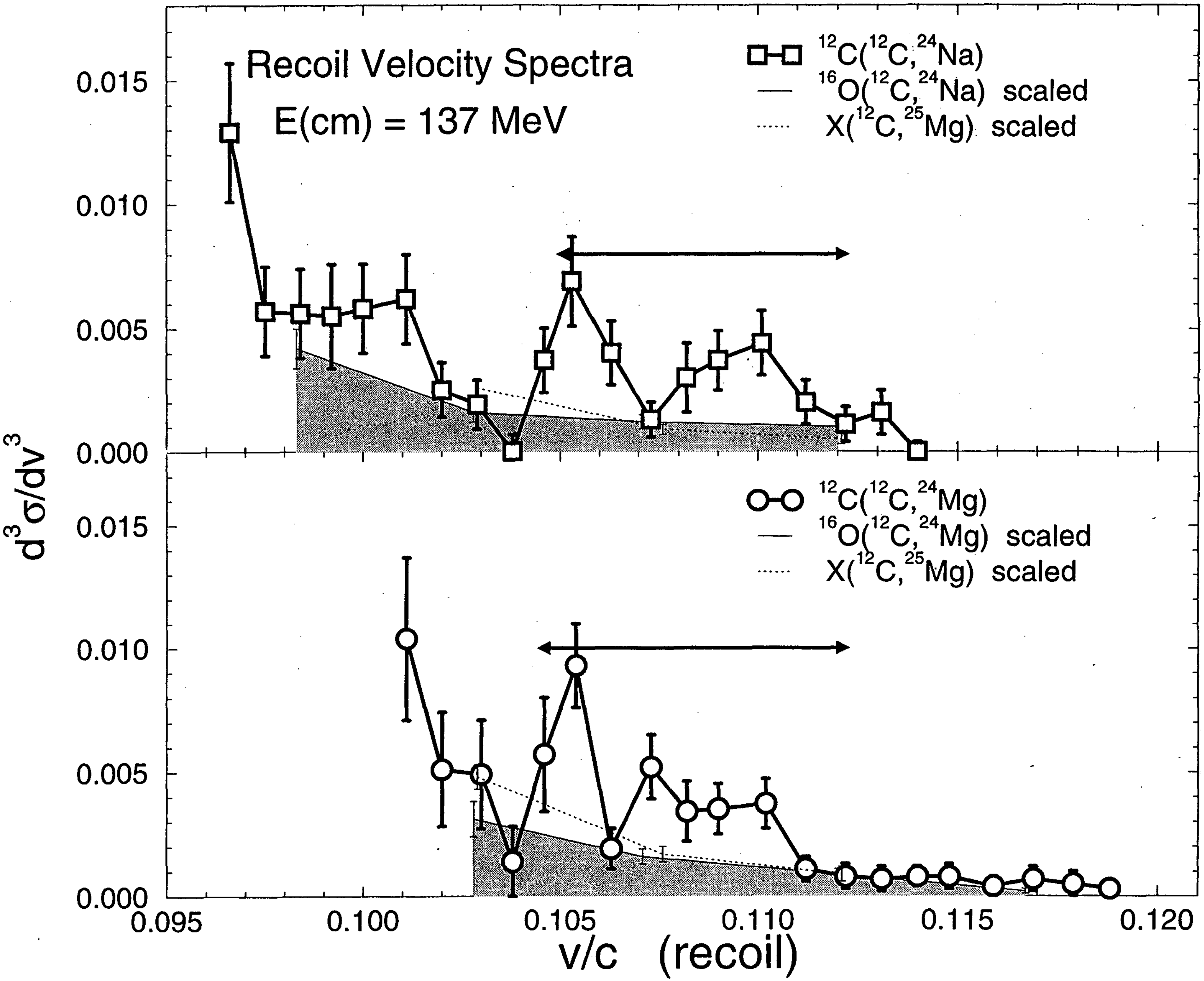
Recoil Velocity Spectra
E(cm) = 137 MeV
$^{12}C(^{12}C,^{24}Na)$
$^{16}O(^{12}C,^{24}Na)$ scaled
$X(^{12}C,^{25}Mg)$ scaled
$^{12}C(^{12}C,^{24}Mg)$
$^{16}O(^{12}C,^{24}Mg)$ scaled
$X(^{12}C,^{25}Mg)$ scaled
$d^3\sigma/dv^3$
0.000
0.005
0.010
0.015
0.095
0.100
0.105
0.110
0.115
0.120
v/c (recoil)

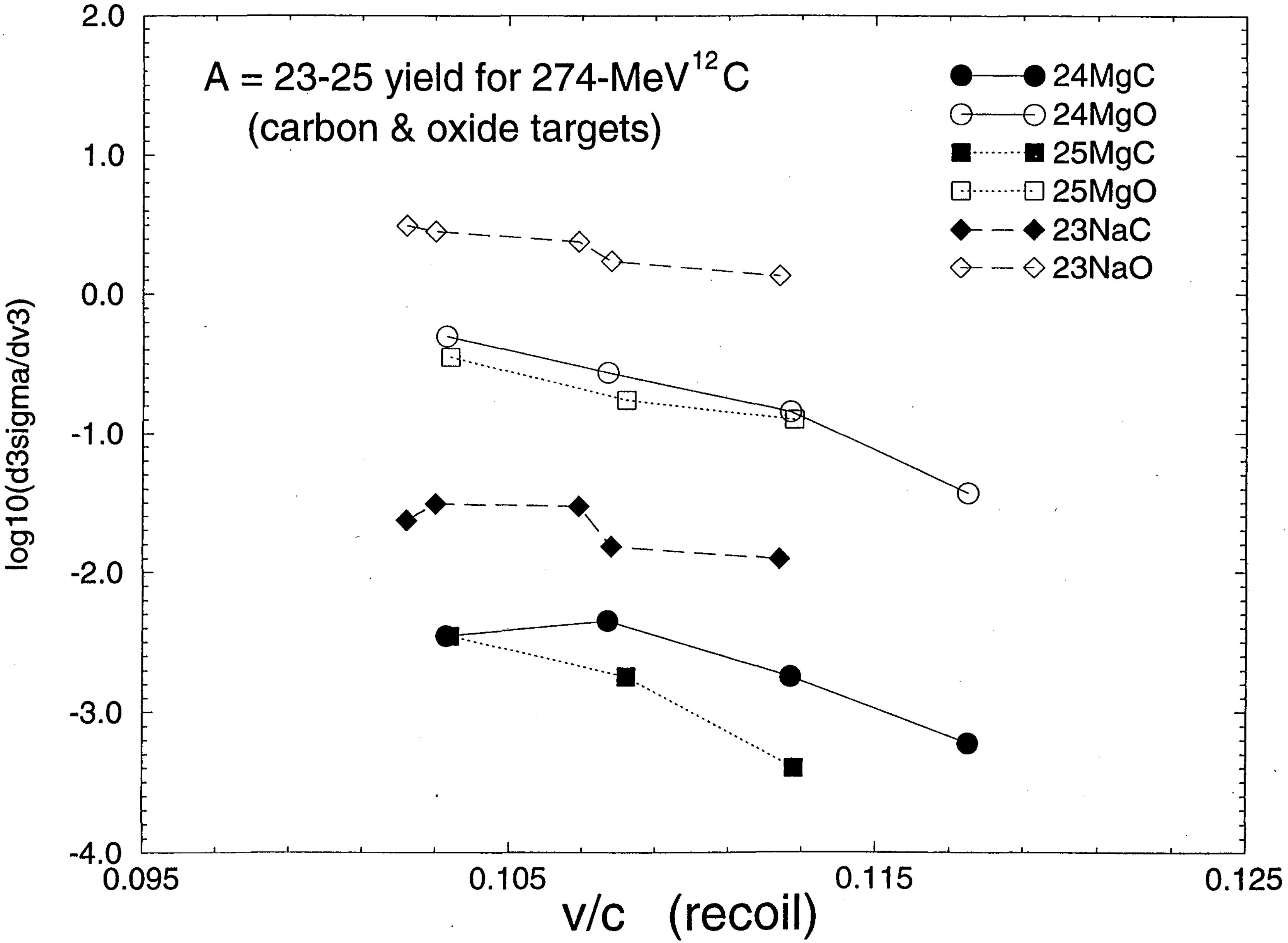
A = 23-25 yield for 274-MeV ^{12}C
(carbon & oxide targets)
24MgC
24MgO
25MgC
25MgO
23NaC
23NaO
log10(d3sigma/dv3)
2.0
1.0
0.0
-1.0
-2.0
-3.0
-4.0
0.095
0.105
0.115
0.125
v/c (recoil)

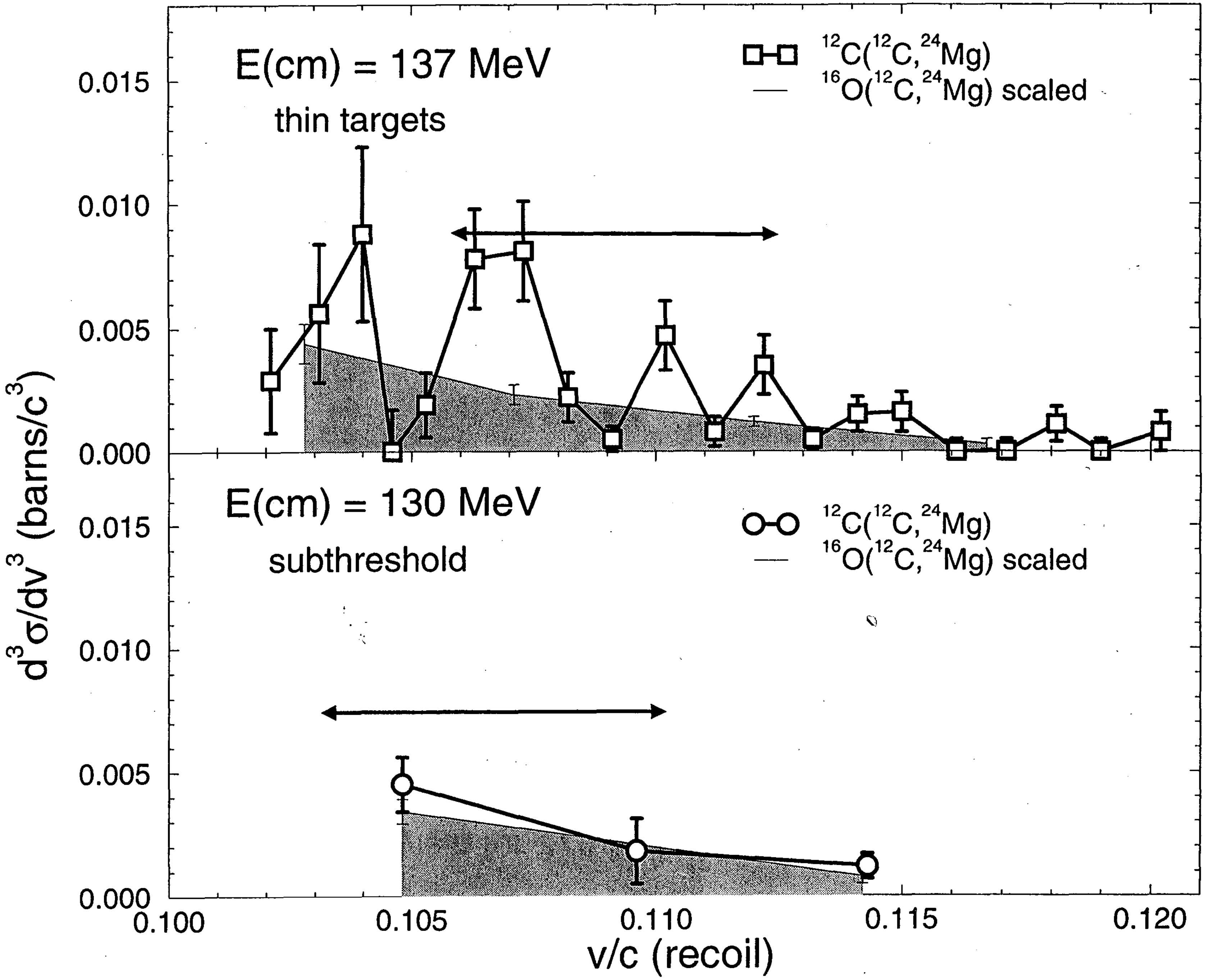
E(cm) = 137 MeV
thin targets
$^{12}C(^{12}C,^{24}Mg)$
$^{16}O(^{12}C,^{24}Mg)$ scaled
E(cm) = 130 MeV
subthreshold
$^{12}C(^{12}C,^{24}Mg)$
$^{16}O(^{12}C,^{24}Mg)$ scaled
$d^3\sigma/dv^3$ (barns/c^3)
0.000
0.005
0.010
0.015
0.100
0.105
0.110
0.115
0.120
v/c (recoil)

Measurement	Counts	σ_{gross} (pb)	σ_{bkgd} (pb)	σ_{net} (pb)
^{24}Mg (thick)	98	397(40)	166(25)	231(47)
^{24}Na (thick)	68	353(43)	126(22)	227(48)
^{24}Mg (thin)	58	329(43)	163(46)	166(63)
^{24}Mg (subthresh)	14	279(90)	220(62)	59(109)

Theory

- $\sigma(^{24}\text{Mg} + \pi^{\circ})/\sigma(^{24}\text{Na} + \pi+) = 2.0$
- Estimate that ≈ half the ^{24}Mg yield goes to unbound levels

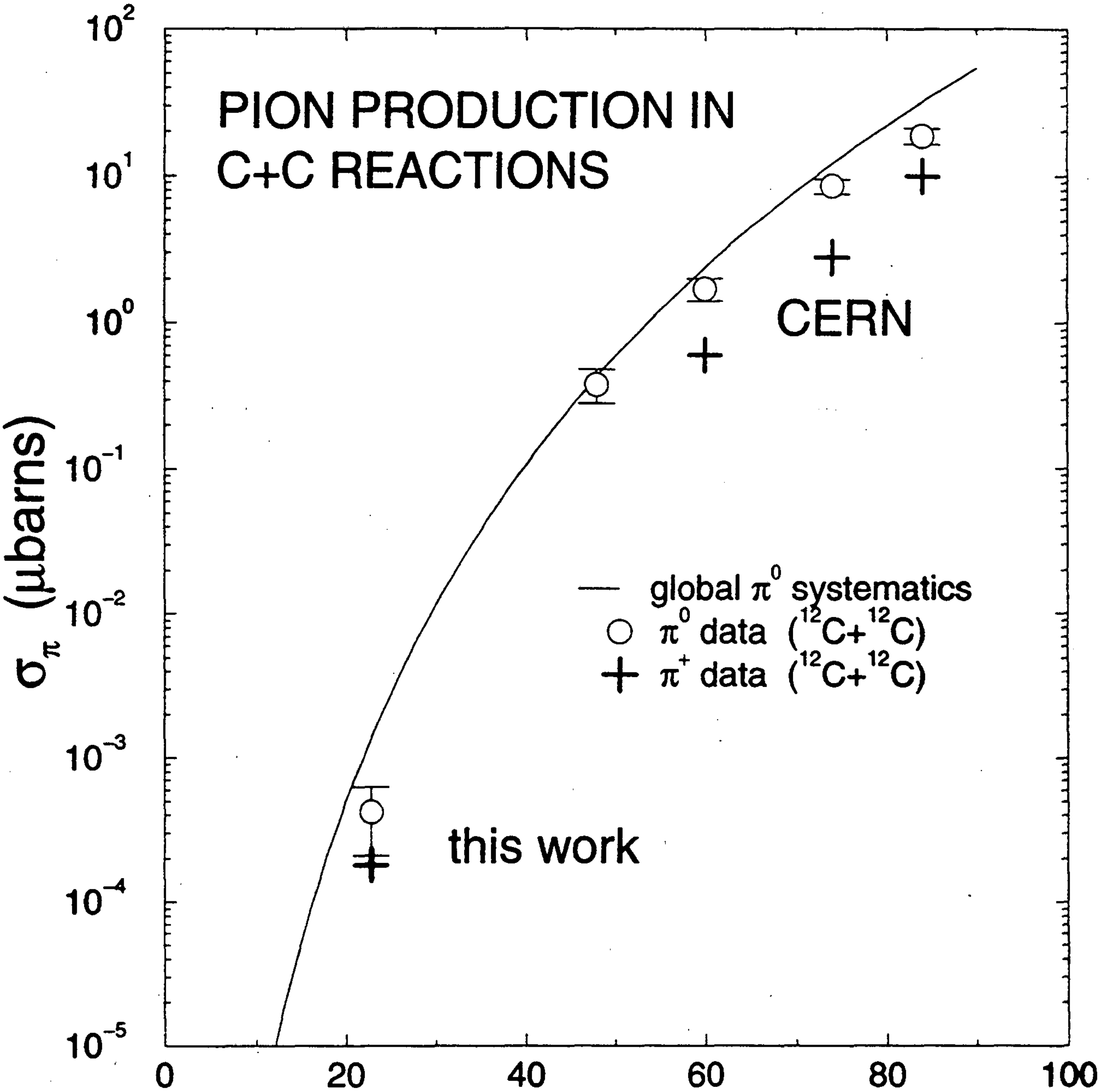
PION PRODUCTION IN C+C REACTIONS
CERN
this work
— global π⁰ systematics
○ π⁰ data (¹²C+¹²C)
+ π⁺ data (¹²C+¹²C)
σπ (μbarns)
10^2
10^1
10^0
10^-1
10^-2
10^-3
10^-4
10^-5
0
20
40
60
80
100
(E_lab–V_c)/A_p (MeV/nucleon)

Summary of Pionic Fusion Results

- We have measured the ^{12}C(^{12}C,^{24}Mg)π^0 and ^{12}C(^{12}C,^{24}Na)π^+ reactions at $E_{cm} = 137$ MeV.
- The ^{24}Na velocity spectrum in the "allowed" region displays the double-lobed structure characteristic of a forward-backward emission pattern.
- Backgrounds interpolated from "forbidden" velocity regions and from explicit background measurements account for approximately one-half the observed A=24 yield.
- The net ^{24}Mg yield, representing part of the total π^0 production cross section was 208 ± 38 picobarns.
- The net ^{24}Na yield, representing all of the π^+ production cross section was 182 ± 84 picobarns.
- Observation of pion production so near threshold places constraints on the mechanisms, requiring that they incorporate the kinetic energy of the entire 24-nucleon system as well as the binding energy gained in fusion.

Joseph Cerny

University of California
and
Lawrence Berkeley National Laboratory
Berkeley, CA

? The Very Poor Man's Bevalac ?

- Develop <u>some</u> radioactive beams at the 88" by producing radioactive nuclides at Budinger's medical isotope cyclotron.

Where: Bevatron floor

What type of cyclotron: 10-11 MeV H^-, 20-40 μA

Focus: Light, short-lived gaseous isotopes

Transfer! By a long capillary to the 88"
(trap unwanted activity at the cyclotron area)

Examples!

	$T_{1/2}$	Reaction	Q-value
^{11}C	20 min	$^{11}B(p,n)$	-2.8 MeV
^{13}N	10 min	$^{13}C(p,n)$	-3.0 MeV
^{18}F	1.8 hours	(they make this now)	

and there are more!

Nuclear Astrophysics

$({}^{14}O + {}^{4}He \rightarrow {}^{17}F + p)$

E. Norman, T. Wang

Reactions and Structure of Mirror Nuclei

$({}^{11}C + {}^{11}B$ and ${}^{13}N + {}^{13}C)$

J. Cerny, D. Moltz

Nuclear Physics at the Proton Drip Line

(e.g., studies of ${}^{11}N$, ${}^{15}F$)

F. Ajzenberg-Selove, H. Weller

Isospin Mixing in the GDR

$({}^{16}O + {}^{12}C, {}^{15}O + {}^{13}C)$

K. Snover

Spectroscopy of Proton-rich 1f-2p Nuclei

(e.g., ${}^{14}O + {}^{40}Ca \rightarrow$)

J. Becker, P. Haustein, F. Stephens

Subbarrier Fusion and Transfer

$({}^{15,16}O + {}^{143,144}Nd)$

D. Di Gregorio, Y. Chan, R. Stokstad

Mass Measurements of Nuclei Five Neutrons from Stability

(e.g., the (${}^{10}C$, ${}^{15}C$) Reaction)

J. Cerny, D. Moltz

Charge Exchange in Elastic Scatt. of Mirror Nuclei
(Inelastic)

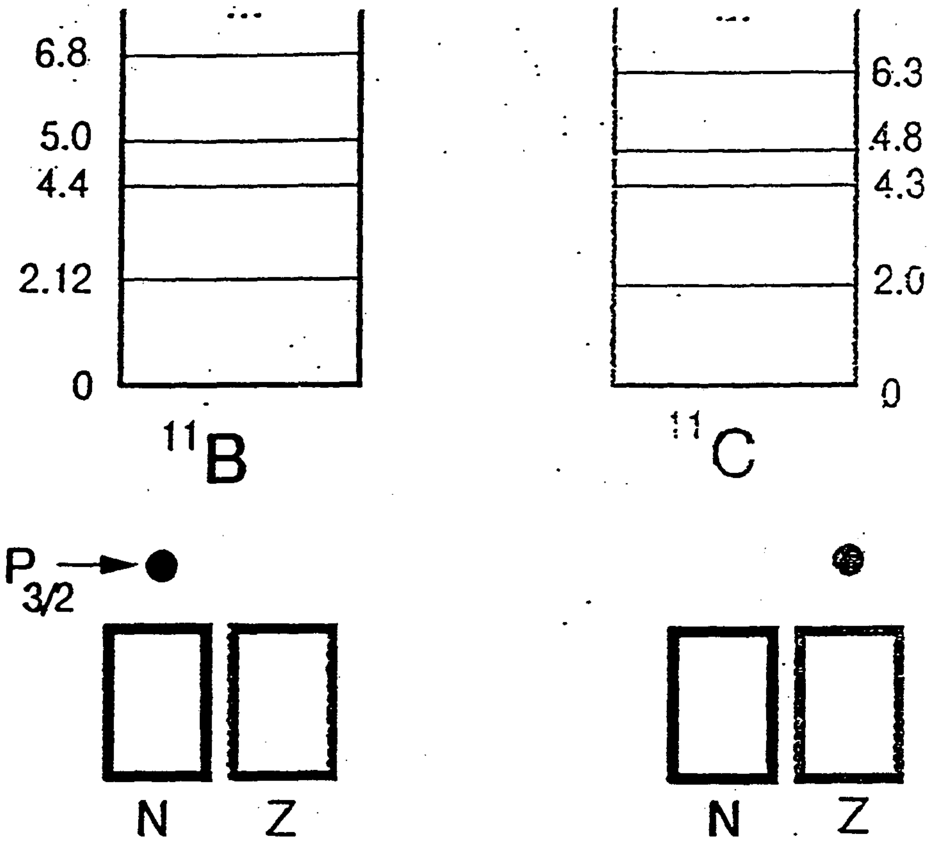

Resonant Charge Exchange Effects between Mirror Nuclei
M.A. Nagarajan and J.P. Vary (1984)

{ Mean Field / Direct } and Charge Exchange Amplitudes both contribute to elastic scattering

Q=0 cross sections large near Coulomb Barrier

Cores (^{10}B) are identical, so calculation is simple(r)

{ Coupled Channel formalism
Microscopic Wave Functions } are in hand
·Optical potentials

Goal : new knowledge of g.s. wave functions

From EB-88   1990 Review

Figure xx. Low-lying level structure of the A =11,13 $T_z = \pm 1/2$ mirror nuclei.

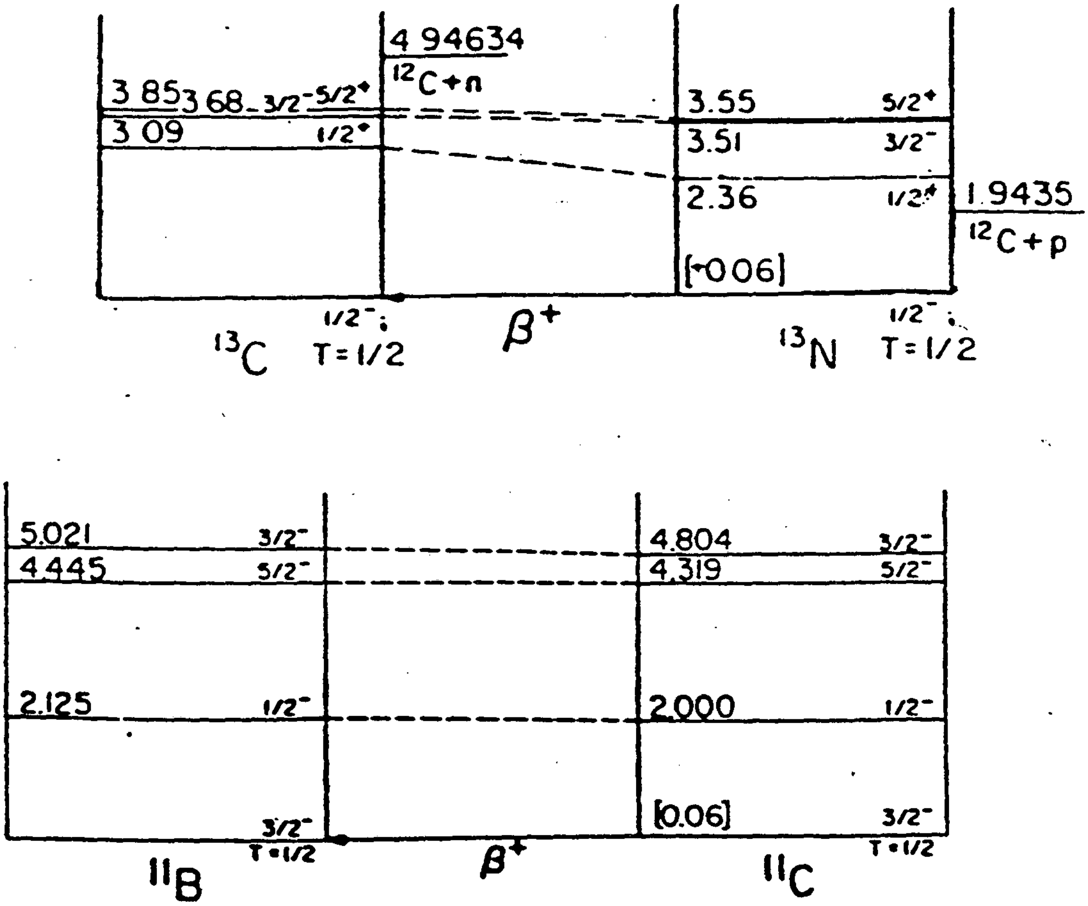

^{11}C Production Yields	**Helium Jet Targets** 20 x 220 µg/ cm^2
Production	1.4×10^9 sec^{-1}
Target Efficiency	50 %
Initial Rate	7×10^8 sec^{-1}
Transit Time (200 m)	~ 30 sec
Yield for 20 min Activity	7×10^8 sec^{-1}
Skimmer Efficiency	50 %
Yield into ECR	3.5×10^8 sec^{-1}
Yield out of ECR (~ 1 %)	3.5×10^6 sec^{-1}
Cyclotron Efficiency (~ 30 %)	1.2×10^6 sec^{-1}
Optics (80 %)	1×10^6 sec^{-1}

Outlook

- Beam intensities of $10^6 - 10^8/s$ are adequate for many experiments.

Selective exciting experiments in nuclear astrophysics.

A wide-open field in Nuclear Reactions and Spectroscopy

with

highly exothermic Q-values (at least relatively)

and

transfers of unusual spin and isospin

Situation at ORNL

Beams: (Alleged) ^{74}As, ^{72}As, ^{70}As

possibly ^{17}F

possibly ^{33}Cl, ^{34}Cl

They received 34 Letters of Intent

7 Reaction Studies

9 Nuclear Astrophysics

18 Nuclear Structure

Measured Yields- 25 m capillary

10 MeV p + ^{14}N, 10 small capillaries

^{11}C	^{14}O
1.9×10^8 /sec/μA	6.35×10^9 /sec/μA

Alan Shotter

University of Edinburgh
Edinburgh, UK

Radioactive Beam Research at Louvain la Neuve

a) Brief word about facility

b) General experimental problems with intense radioactive beams

c) Examples of Nuclear Astrophysics experiments

d) List of Nuclear physics experiments

e) Instrumentation

Collaboration: Brussels-Budapest-Edinburgh-Leuven -LLN-Notre Dame

LOUVAIN

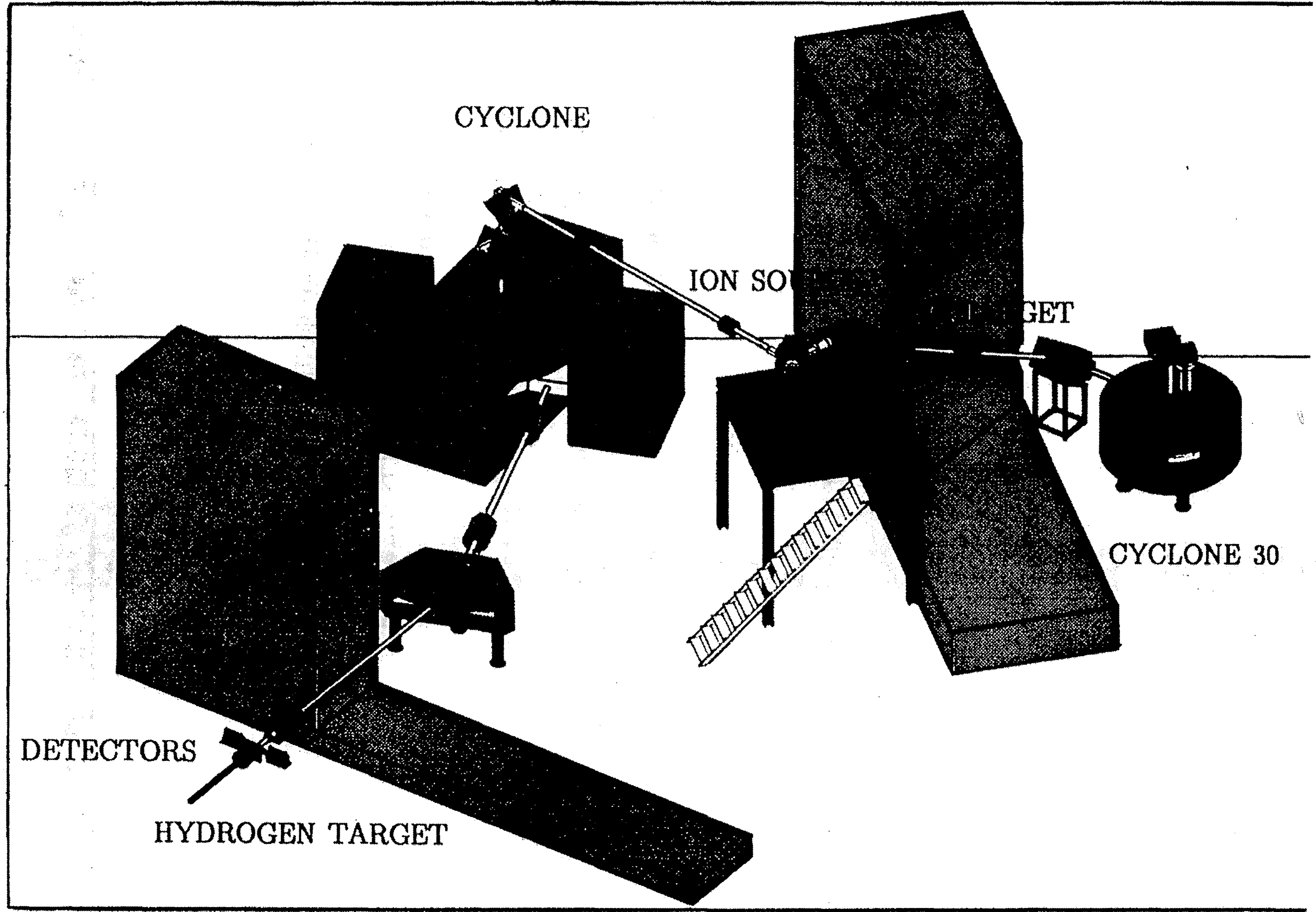

P.A.I. – 08–02–91 – HG

Beams available:

Element	$T_{1/2}$	Q	Intensity (pps)	Maximum energy (MeV)
^{6}He	0.8 s	1^+	1.2×10^6	18
^{11}C	20 min	1^+	1.0×10^7	10
^{13}N	10 min	1^+	4.0×10^8	8.5
		2^+	3.0×10^8	34
		3^+	3.0×10^7	70
^{18}Ne	1.7 s	3^+	4.2×10^5	55
^{19}Ne	17 s	2^+	1.9×10^9	23
		3^+	1.5×10^9	50
		4^+	5.0×10^8	93
^{35}Ar	1.8 s	5^+	10^5	79
^{18}F	110 min	2^+	1×10^6	24

Experimental problems

1) Radioactive beam intensity << stable beams

2) Radioactive beams produce more background radiation

To overcome 1) --- use high efficiency detector systems

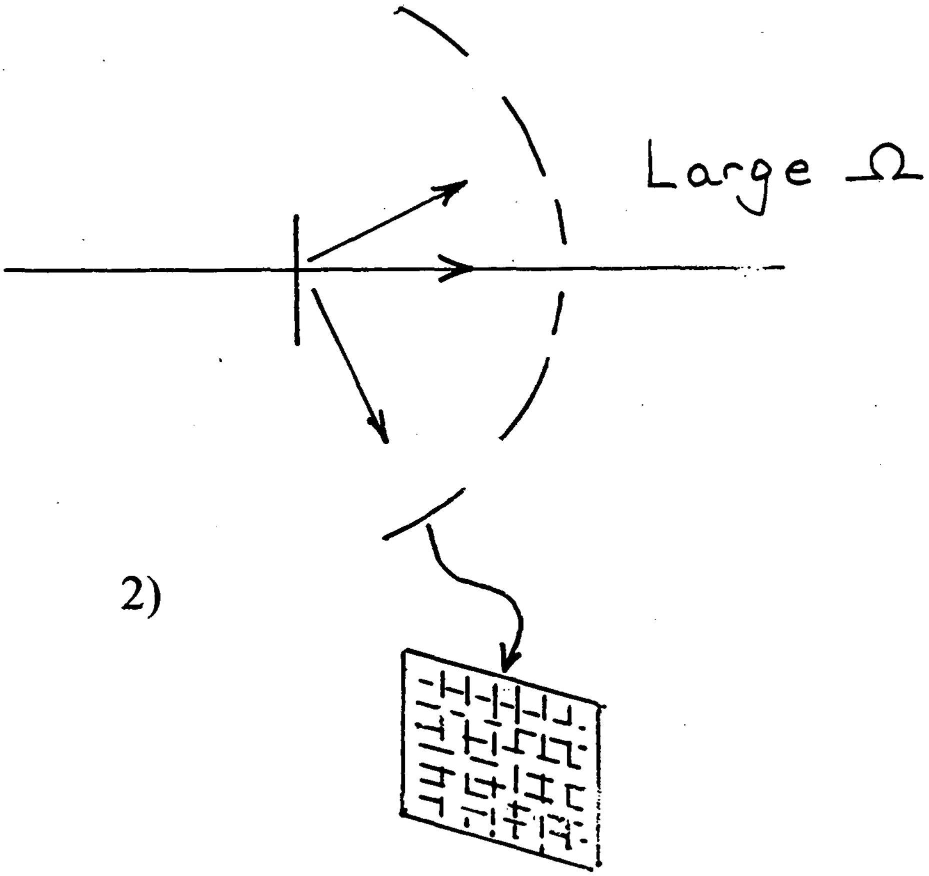

2)

segmented detector

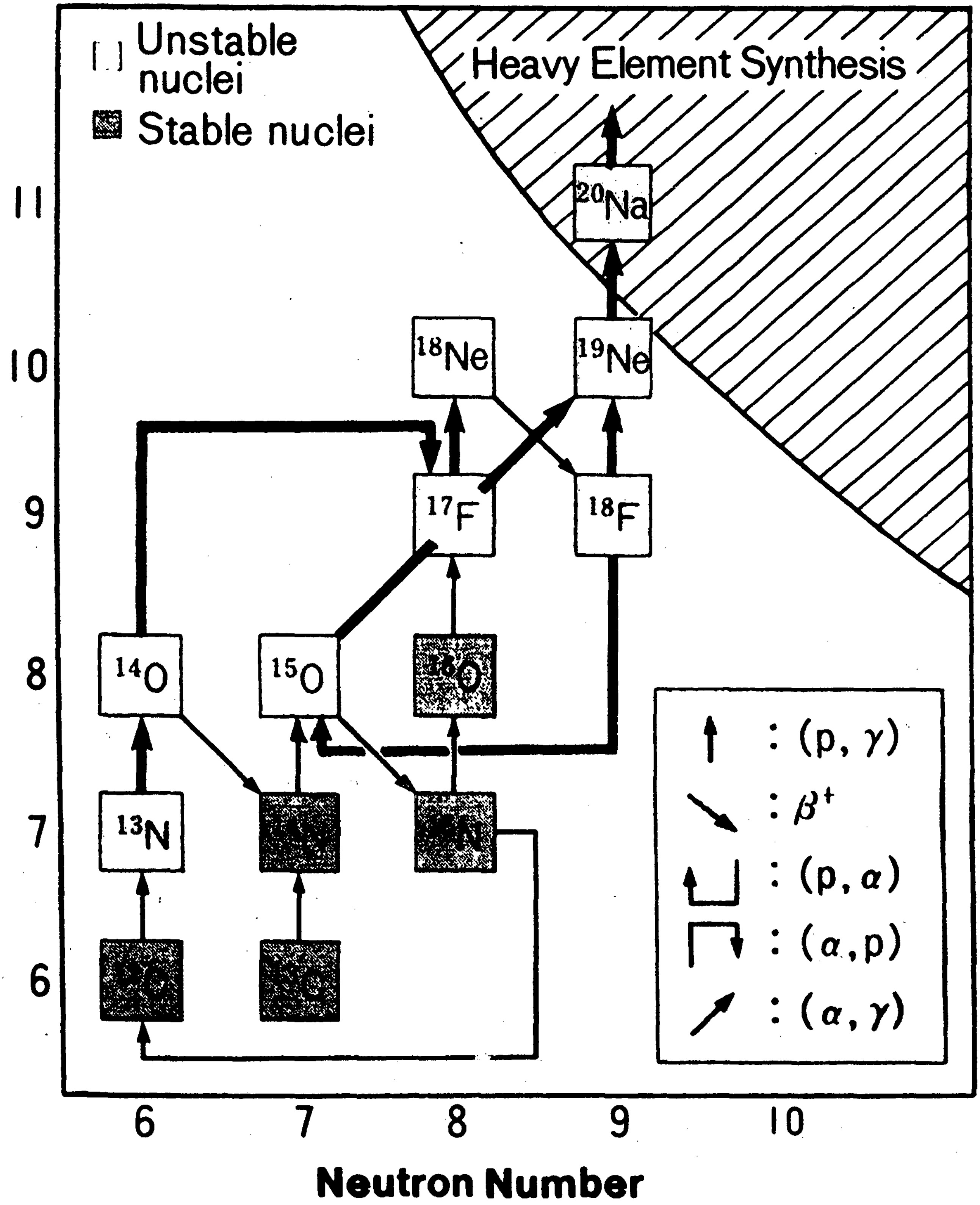
Unstable nuclei
Stable nuclei
Heavy Element Synthesis
11
10
9
8
7
6
^{20}Na
^{18}Ne
^{19}Ne
^{17}F
^{18}F
^{14}O
^{15}O
^{16}O
^{13}N
^{14}N
^{15}N
^{12}C
^{13}C
: (p, γ)
: β⁺
: (p, α)
: (α, p)
: (α, γ)
6
7
8
9
10
Neutron Number

$^{18}F(p,\alpha)^{15}O \Rightarrow \Omega$

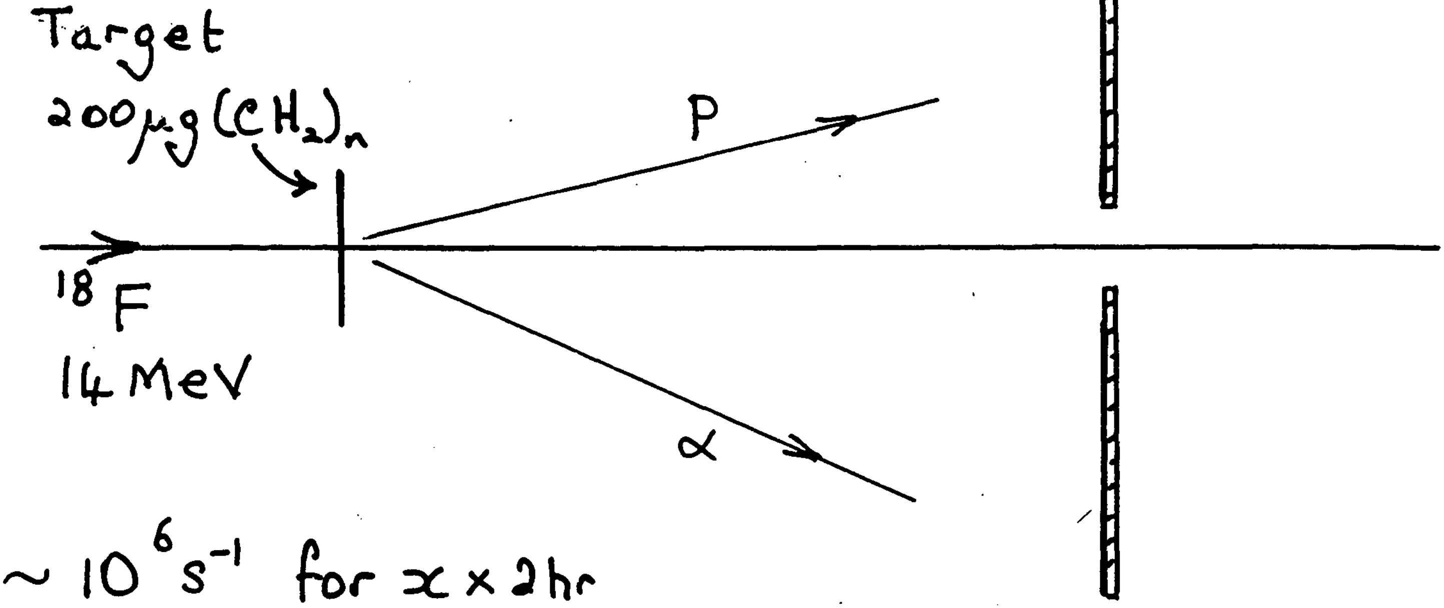

$\sim 10^6 s^{-1}$ for $x \times 2hr$

L.E.D.A.

(Louvain - Edinburgh - Detector - Array)

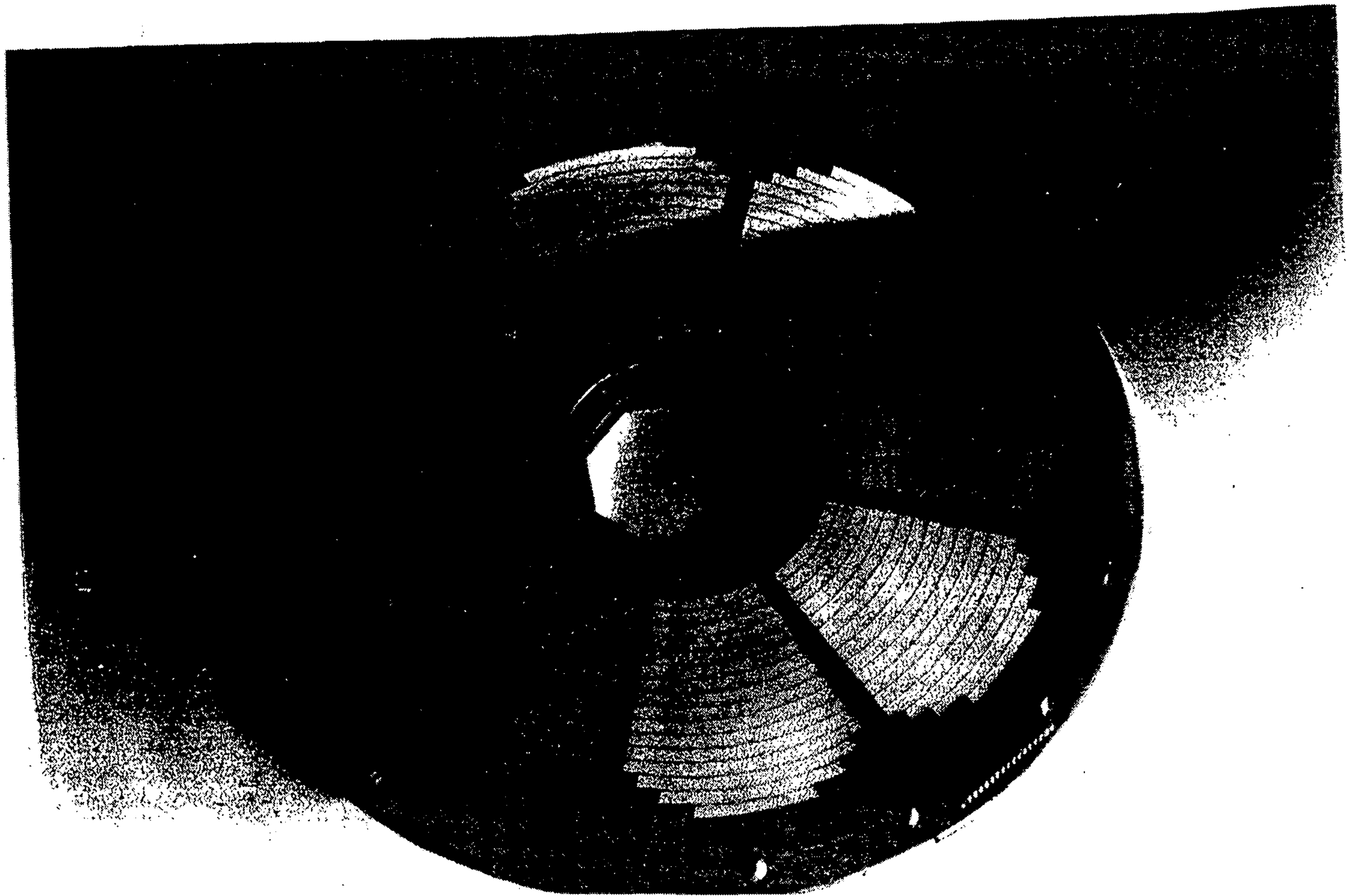

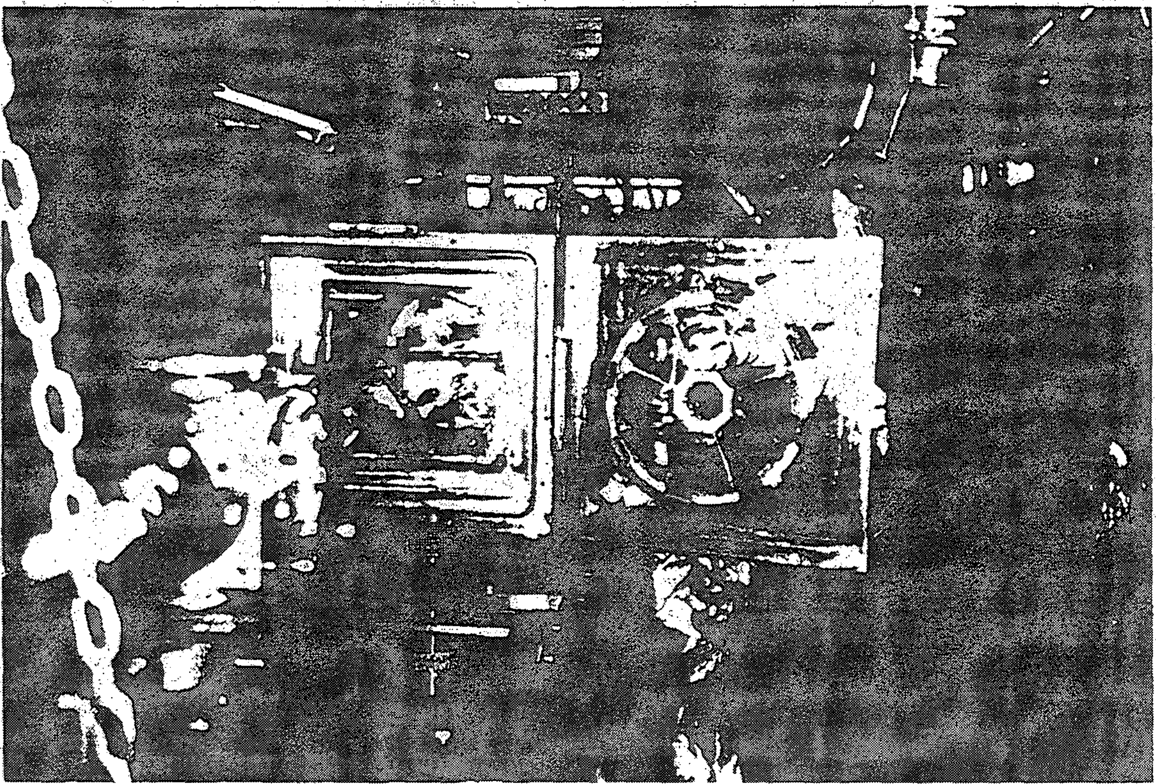

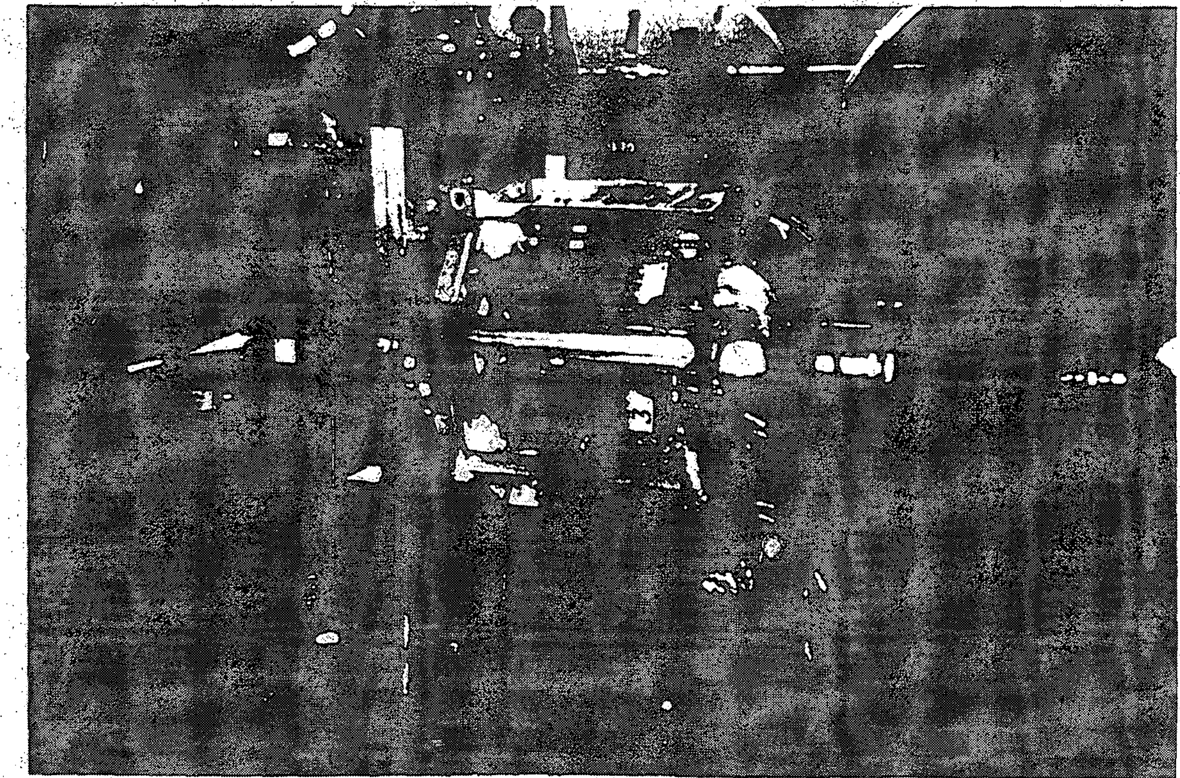

$^{18}F(p,\alpha)$

thick target scan 550 - 740 keV
above threshold

$^{3}F \sim 10^{6}\,s^{-1}$
for 4 hours

P.L. 353 (199[illegible])
184

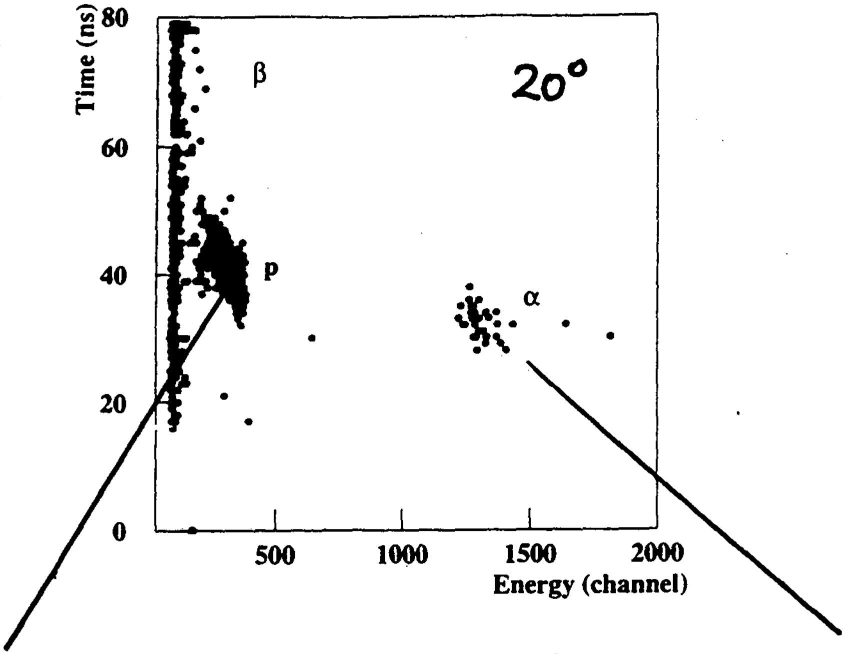

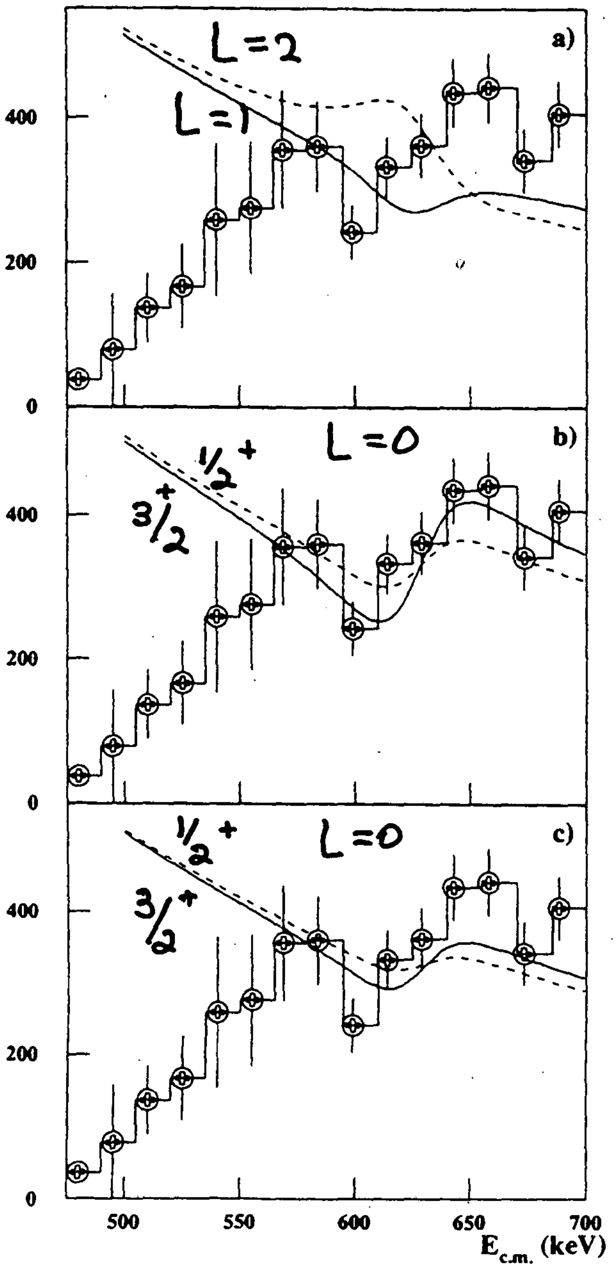

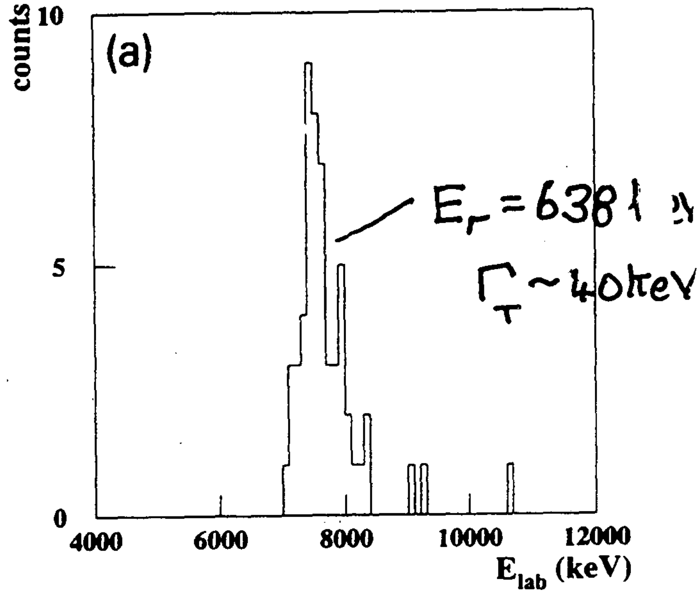

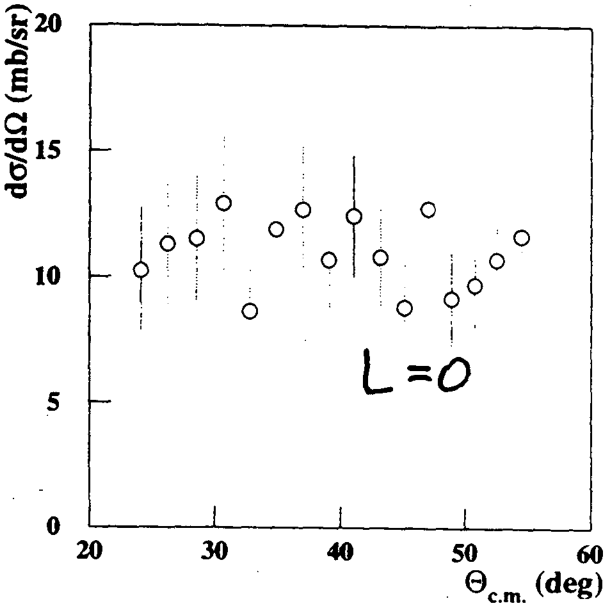

$\omega\gamma = (\Gamma$

$^{19}Ne(p,\gamma)^{20}Na$ (large B.G. $\Downarrow$ segmentation)

$E_p \sim 450$ keV

Decay of ^{20}Na

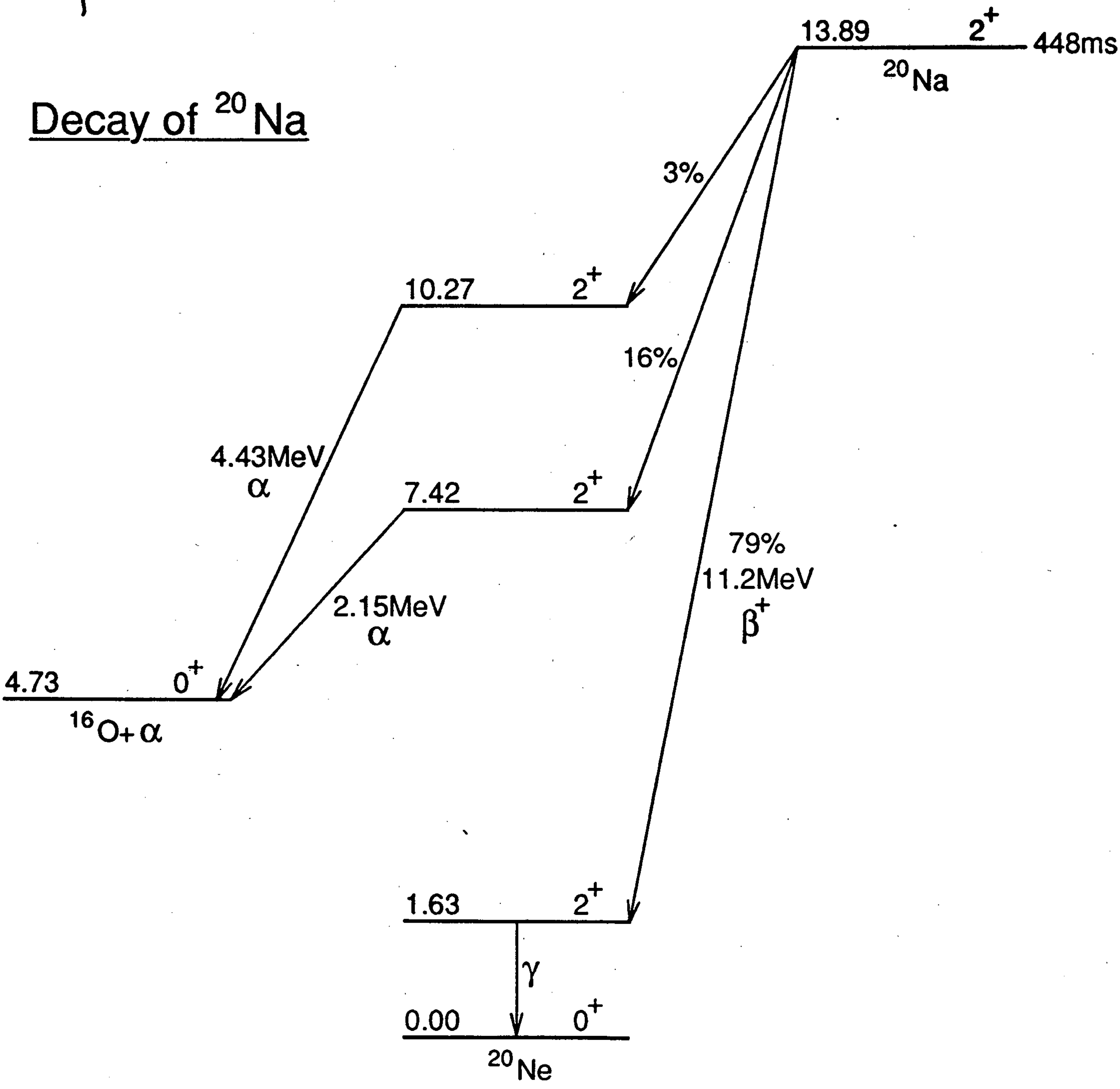

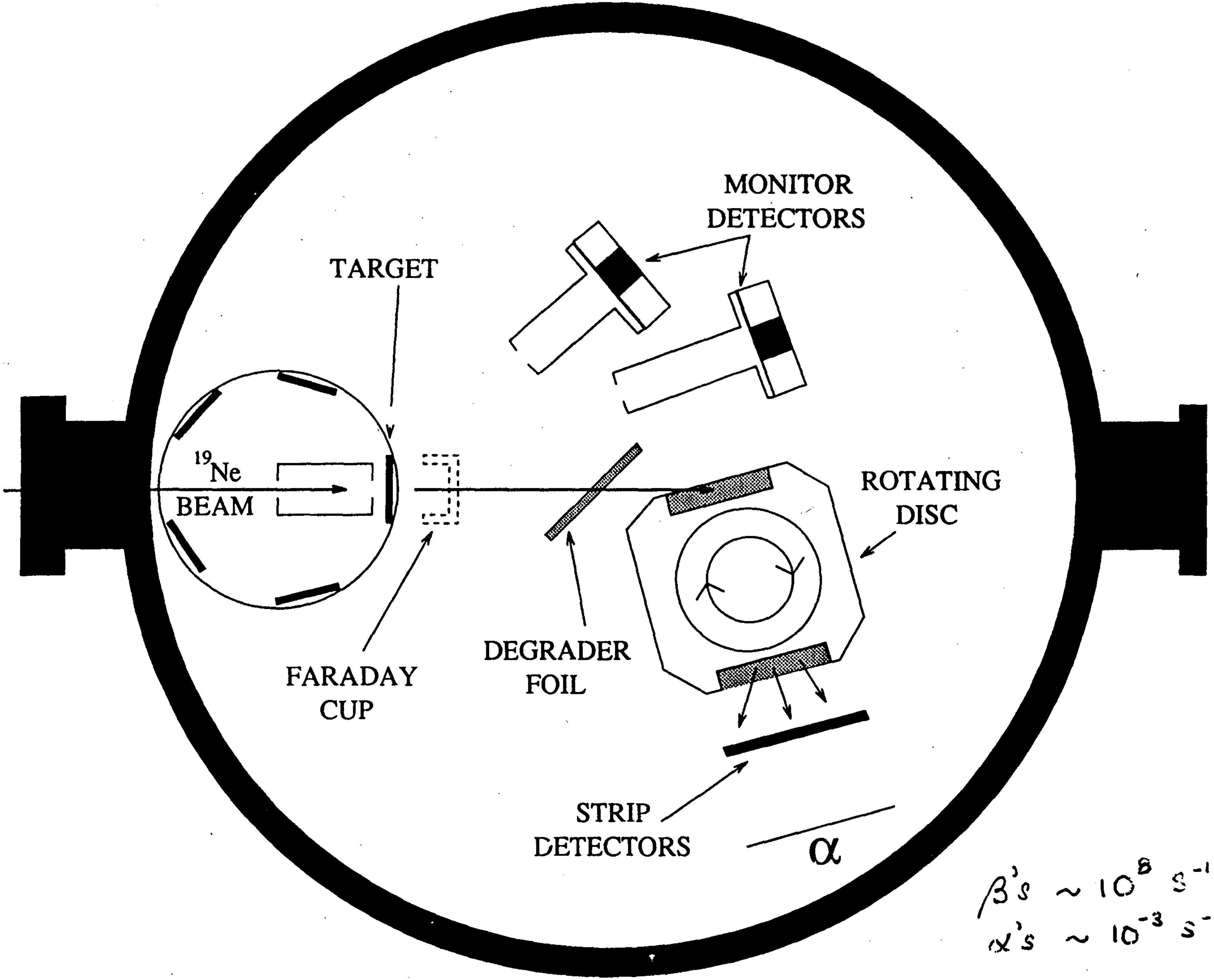

β's ~ 10^{8} s^{-1}
α's ~ 10^{-3} s^{-1}

Rejection of β's

1) Use thin detectors

2) Use DSSSD

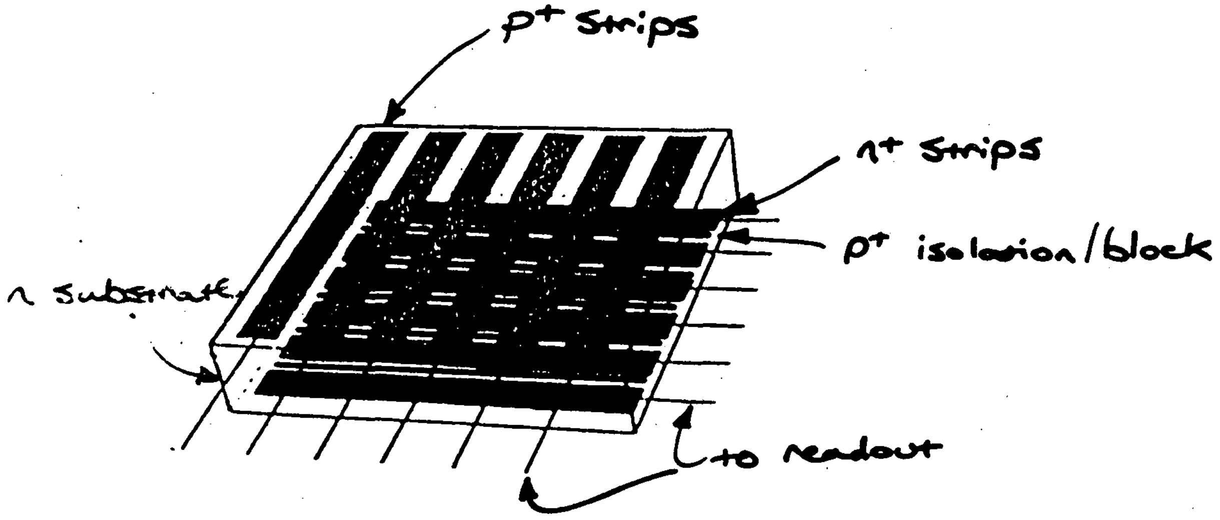

DOUBLE SIDED SILICON STRIP DETECTOR

(DSSSD)

A)

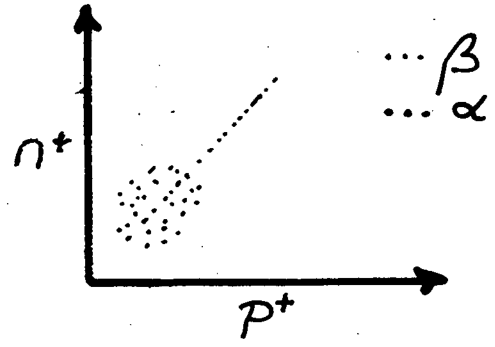

B) Demand multiplicity .1. n^+, p^+

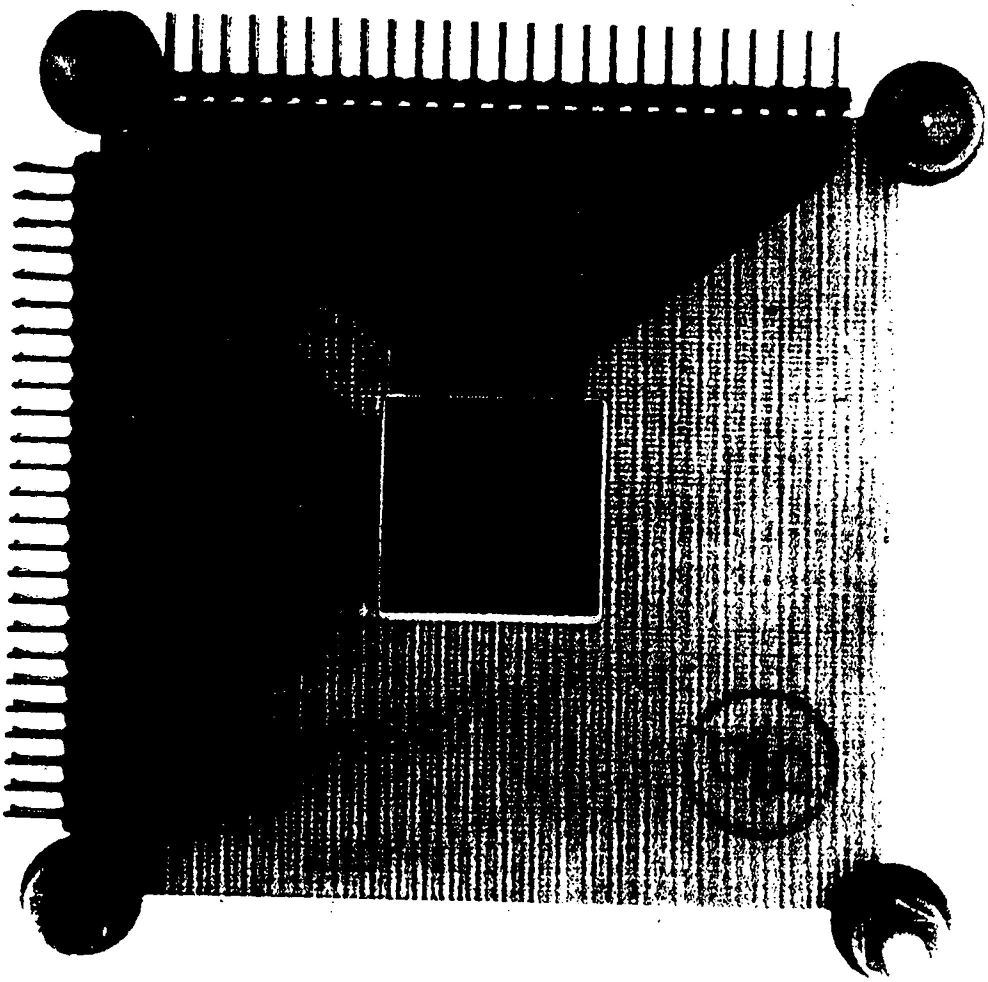

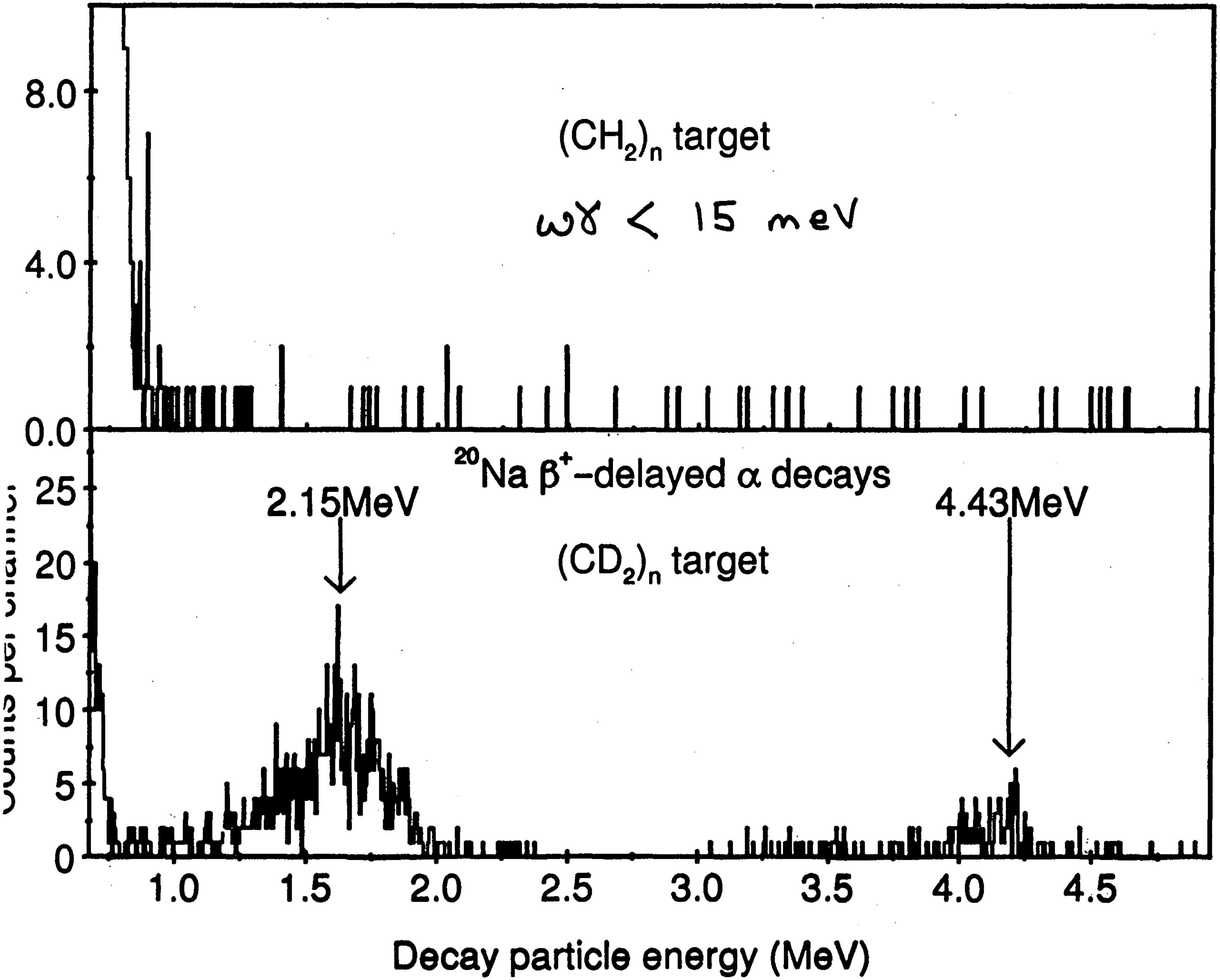

PRL 73(1994)
3066

In general for radioactive beam experiments

⇓

Low beam intensities / High backgrounds

⇓

Use Large segmented detectors

⇓

Need many hundreds channels of electronics

↳ problems: Space / Cost

⇓

LEDA microelectronics overcomes these problems

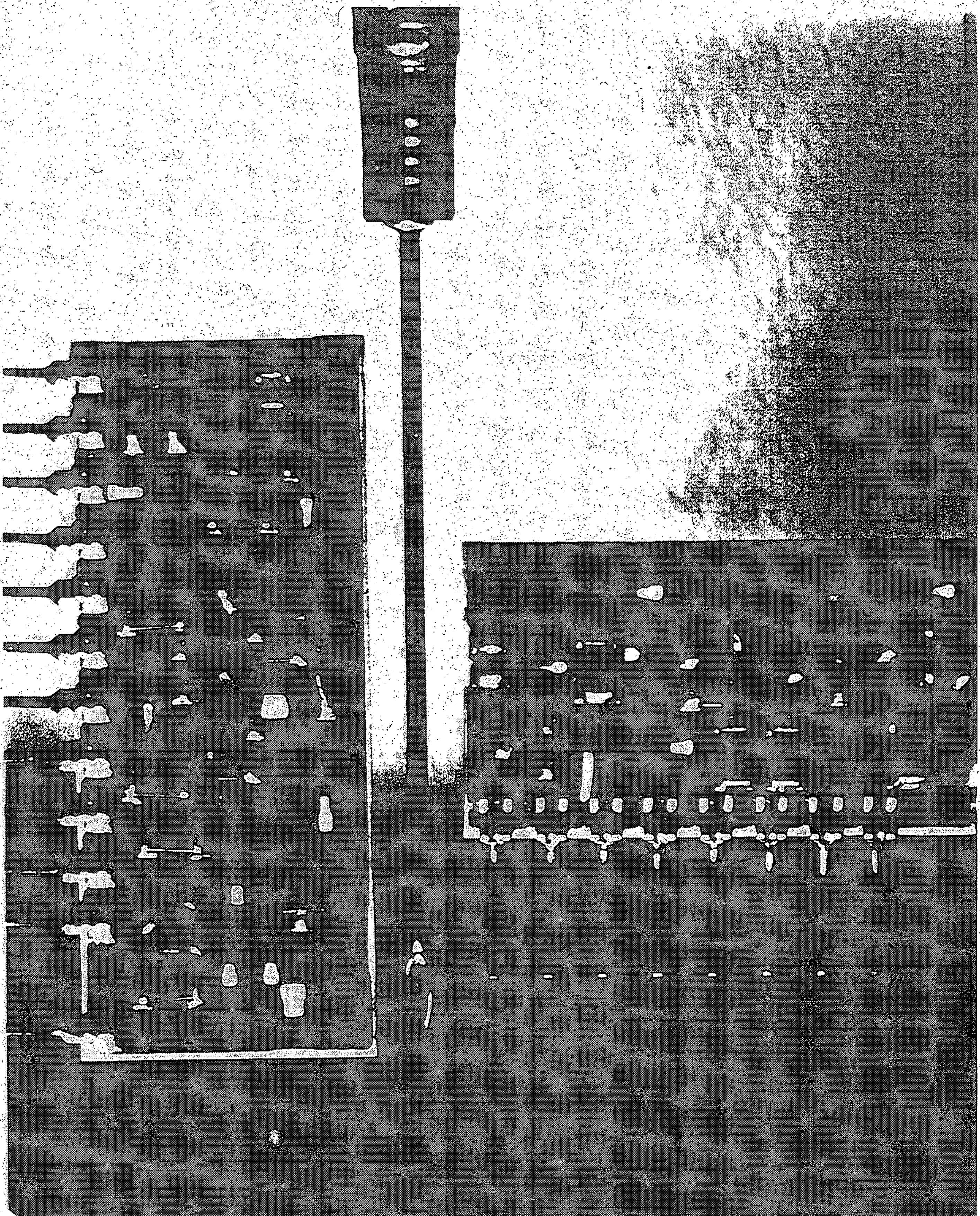

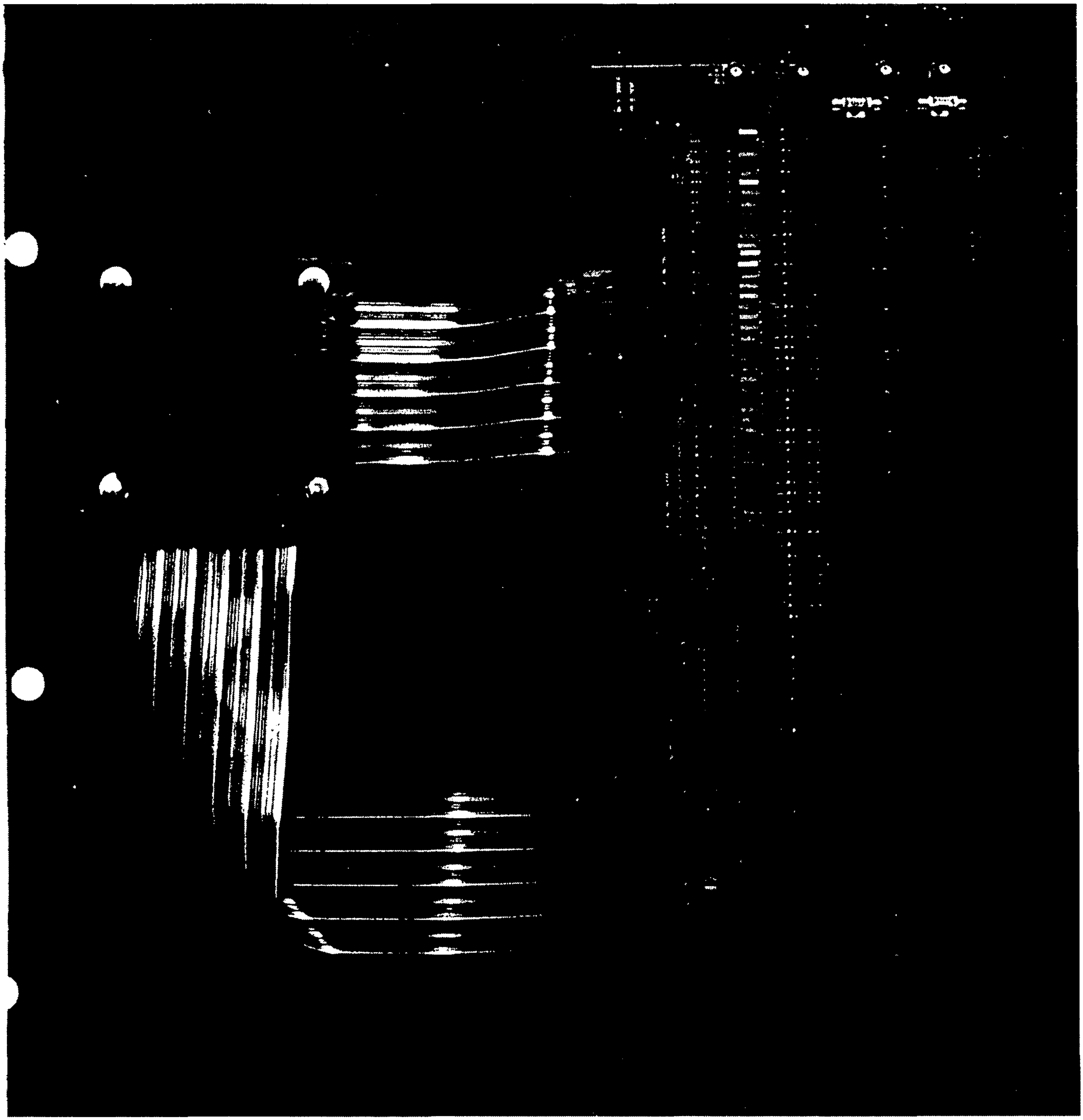

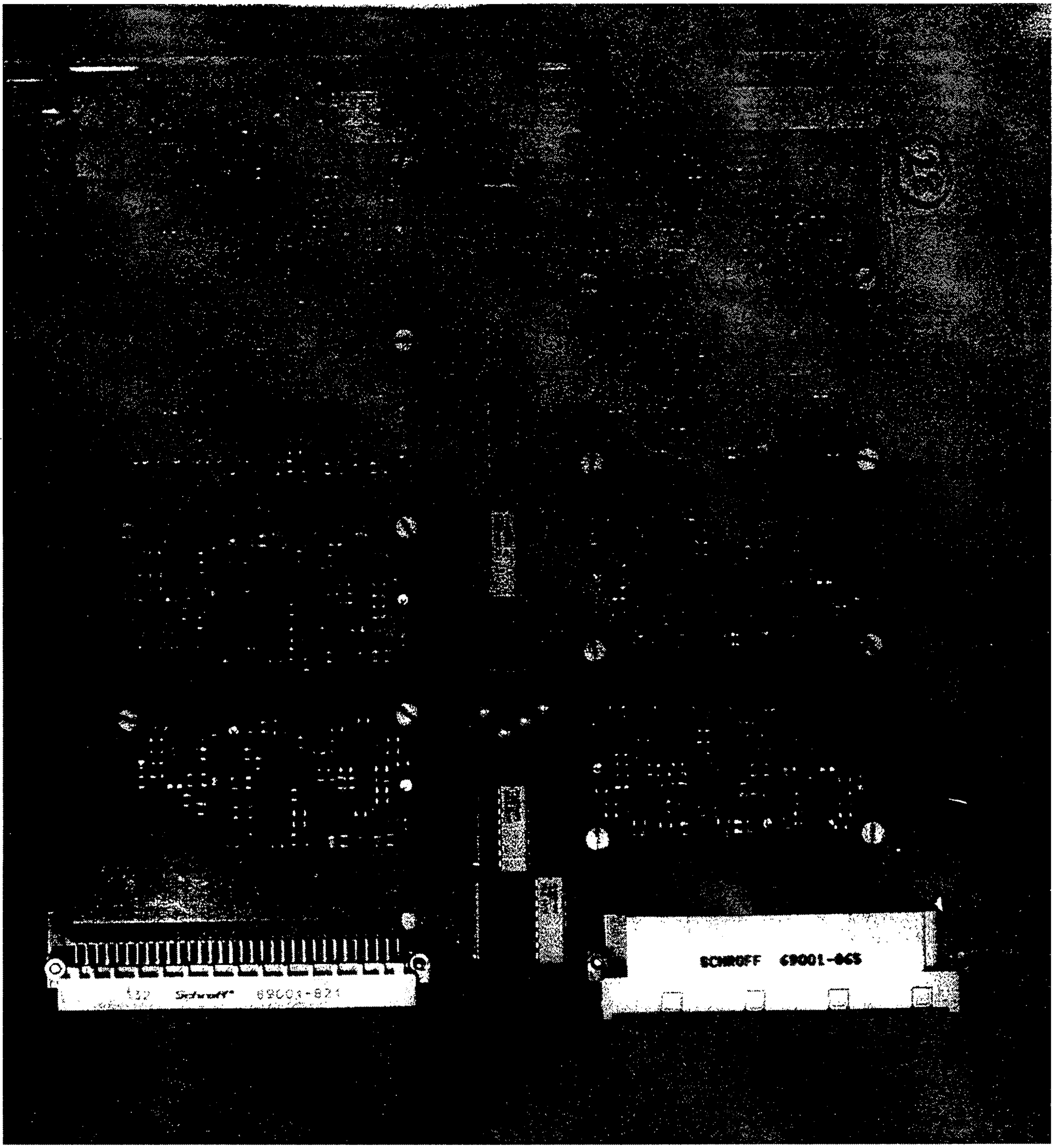
Schroff 69001-821
SCHROFF 69001-065

e.g.

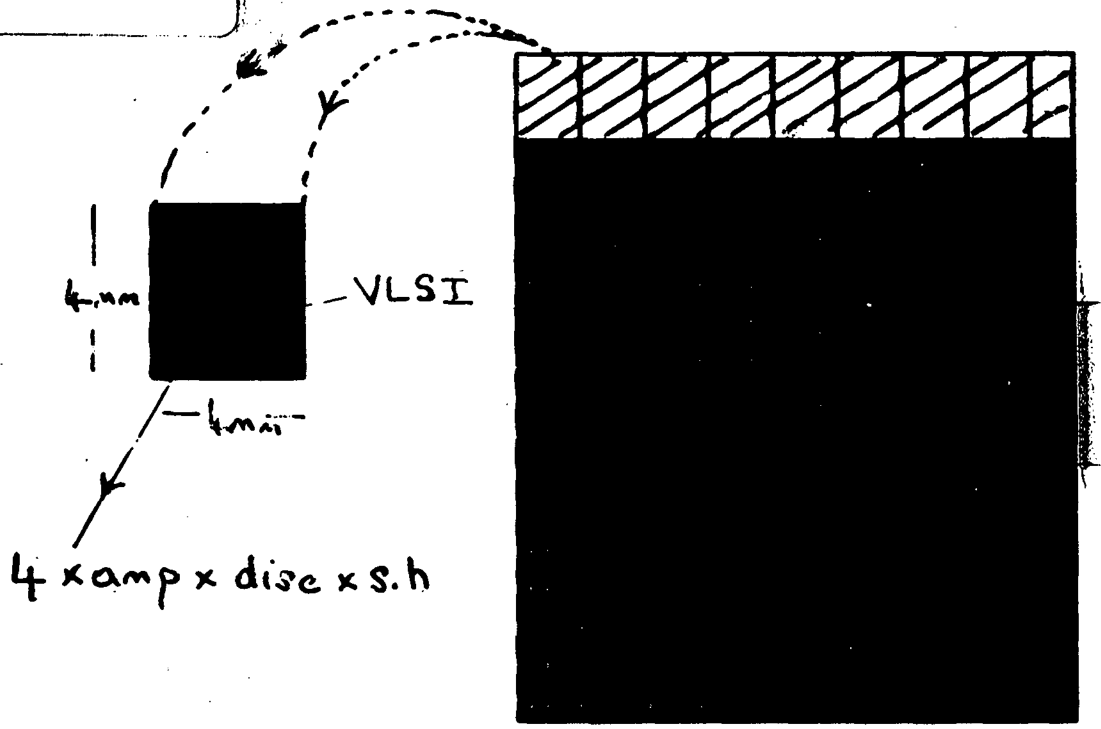

Some Nuclear Physics experiments with LEDA

1) ${}^{13}N + {}^{11}B \; \text{-->} \; {}^{12}C^* + {}^{12}C^*$

Tranfer :
${}^{13}N$ Proton wavefunction

2) ${}^{13}N + p \; \text{-->} \; {}^{14}O$

$\hookrightarrow p + p + {}^{12}C$

2 p decay mechanism

3) ${}^{13}N + {}^{11}B \; \text{-->} \; {}^{24}Mg + \gamma$

${}^{19}Ne + {}^{9}Be \; \text{-->} \; {}^{28}Si + \gamma$

$\hookrightarrow p, \alpha + \gamma$

Fusion :
T dependence of GDR

4) ${}^{6}He + {}^{4}He \; \text{-->} \; {}^{6}He + {}^{4}He$

${}^{13}N + {}^{12}C \; \text{-->} \; {}^{13}N + {}^{12}C$

Exchange scattering

5) ${}^{6}He + p \; \text{-->} \; \alpha + t$

2 n structure of ${}^{6}He$

Reaction studies experimental configuration.

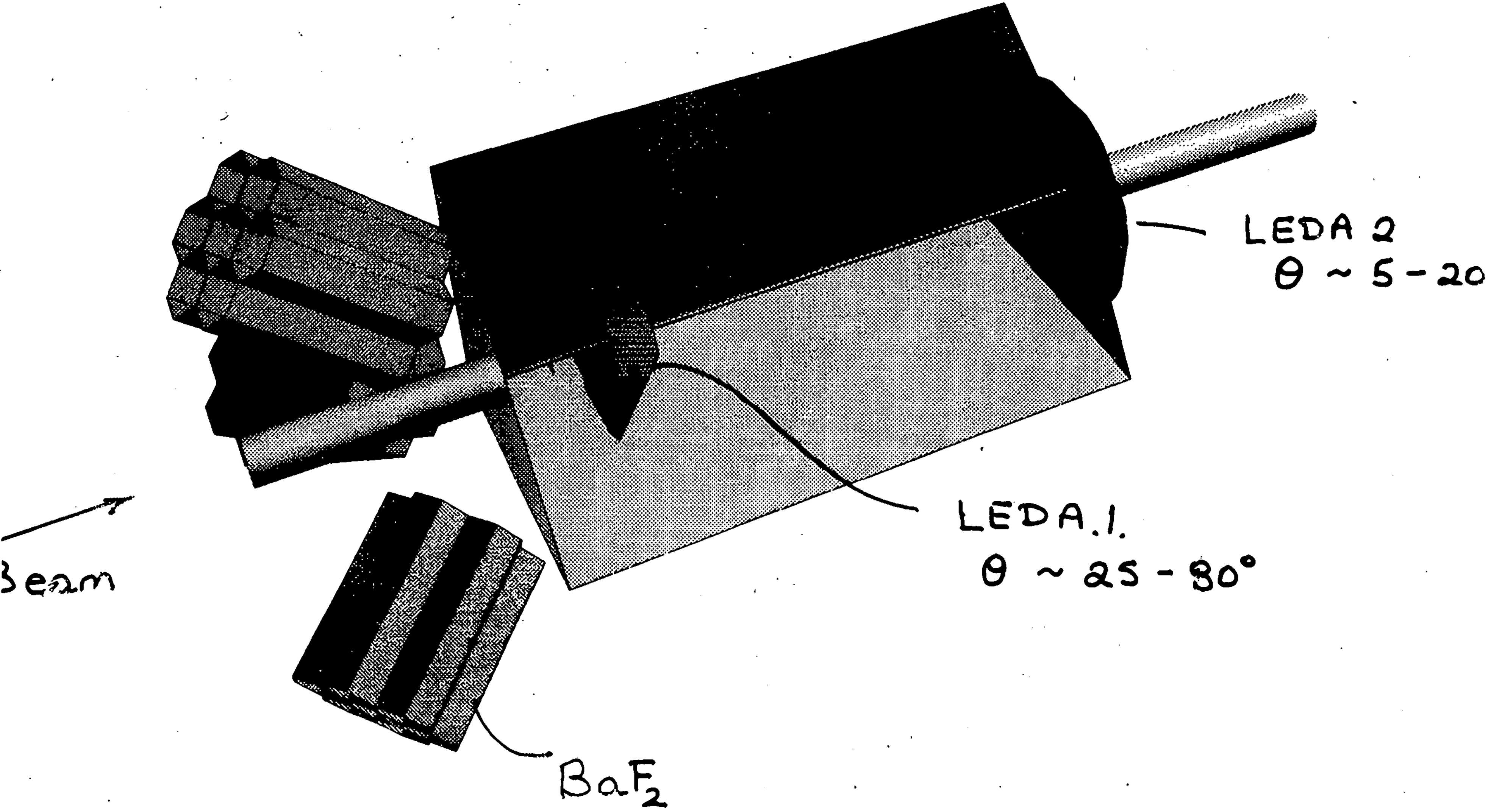

High resolution γ-ray experiments

$$^{19}\text{Ne} + {}^{40}\text{Ca} \longrightarrow {}^{59}\text{Zn}^{*} \begin{cases} {}^{55}\text{Co} \\ {}^{55}\text{Ni} \end{cases}$$

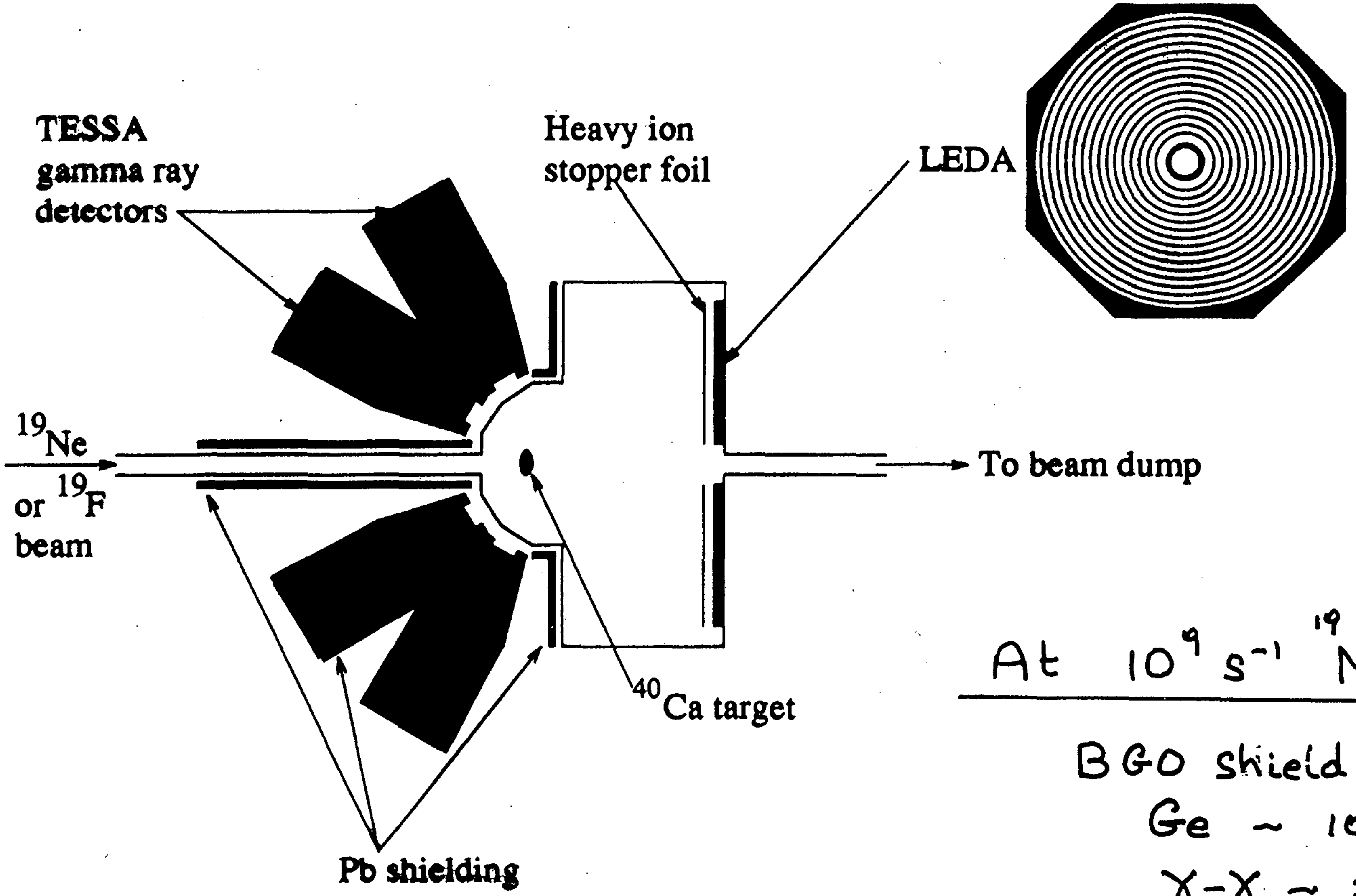

At 10^{9} s^{-1} ^{19}Ne

BGO shield ~ 50k s^{-1}

Ge ~ 1000 s^{-1}

γ-γ ~ 20 s^{-1}

γ-LEDA ~ 800 s^{-1}

Figure 10: Comparison of the background subtracted gamma-ray singles spectra for (a) the ^{19}Ne beam, and (b) the ^{19}F beam data. Data from all 90° Ge detectors.

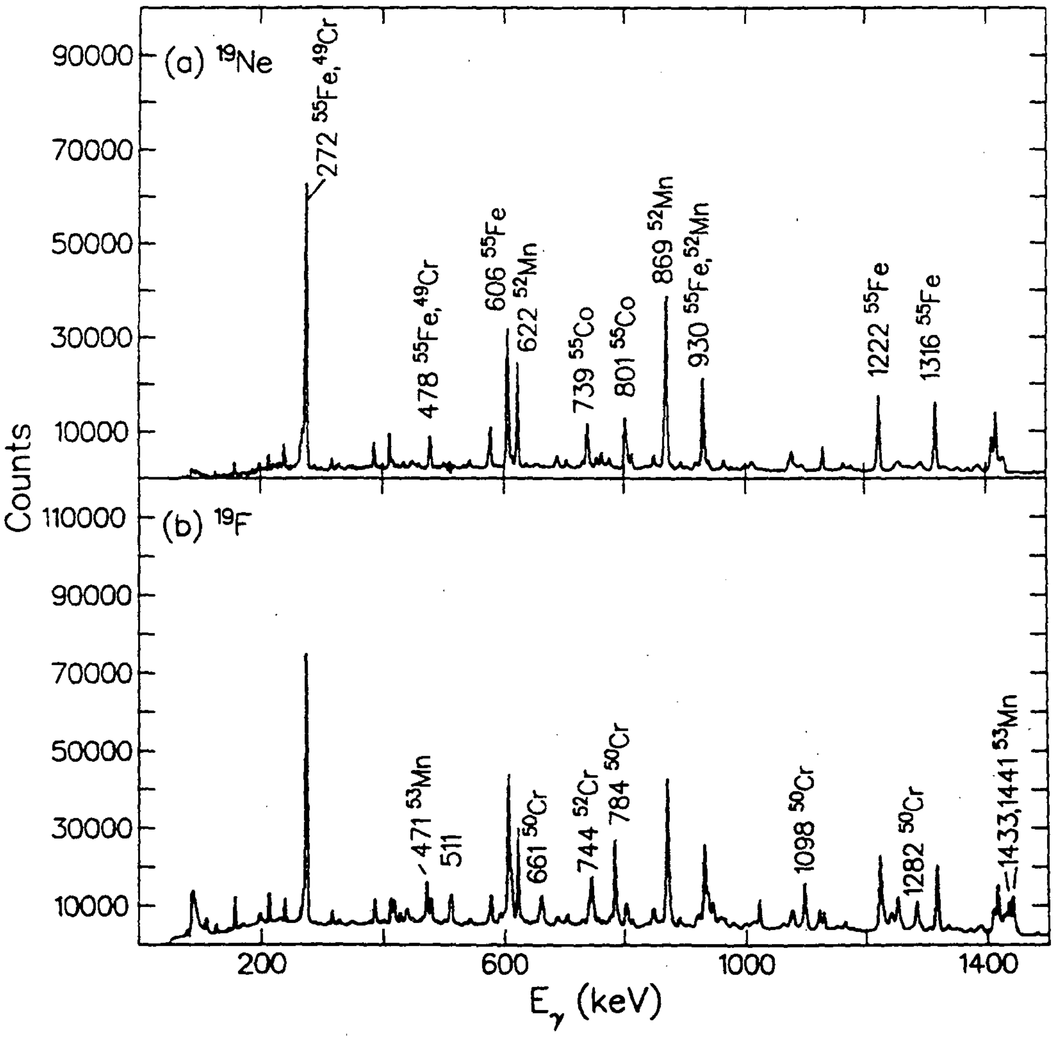

Summary

* At LLN several beams are available :

^{6}He ^{11}C ^{13}N ^{18}F ^{18}Ne ^{19}Ne ^{35}Ar

(^{10}C ^{7}Be ^{15}O ^{34}Ar under consideration)

* Beams used for a variety of nuclear and nuclear astrophysics experiments

experience shows a lot of innovation is needed both for production and exploitation

* New cyclotron will increase intensity by×10

1978 -1980 $(^{4}\text{He},2p)$

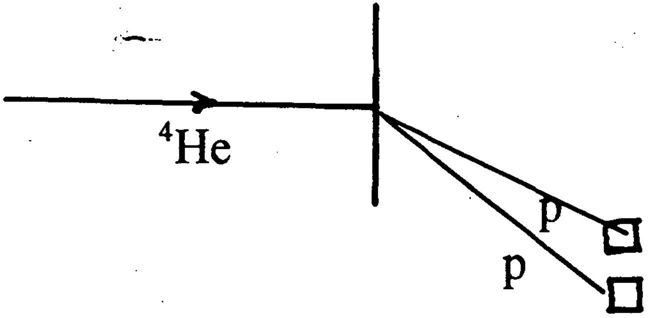

Used apparatus for : $(^{12}\text{C},{}^{8}\text{Be}+\alpha)$

$(^{7}\text{Li},\alpha+t)$ -------------> Direct Breakup

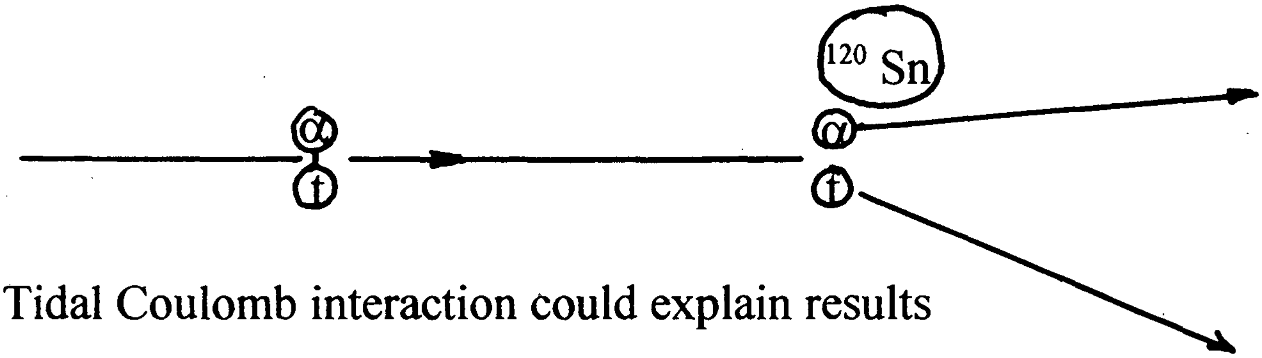

* Tidal Coulomb interaction could explain results

* Relates $\left\{\begin{array}{l} ^{7}\text{Li}+\gamma \text{ ---->} \alpha+t \\ \alpha+t \text{ ----->} {}^{7}\text{Li}+\gamma \end{array}\right.$ Breakup σ_b Capture σ_c

Larger detectors

Ideal for Radioactive beam experiments

Deduce σ_c from σ_b

e.g. $^{14}\text{O} \text{ -->} {}^{13}\text{N}+p$

Rick Gough

Lawrence Berkeley National Laboratory
Berkeley, CA

Selected Accelerator Applications

Richard A. Gough

Exotic Nuclei Symposium
Bodega Bay, California
April 15-16, 1996

BERKELEY LAB
Ernest Orlando Lawrence
Berkeley National Laboratory

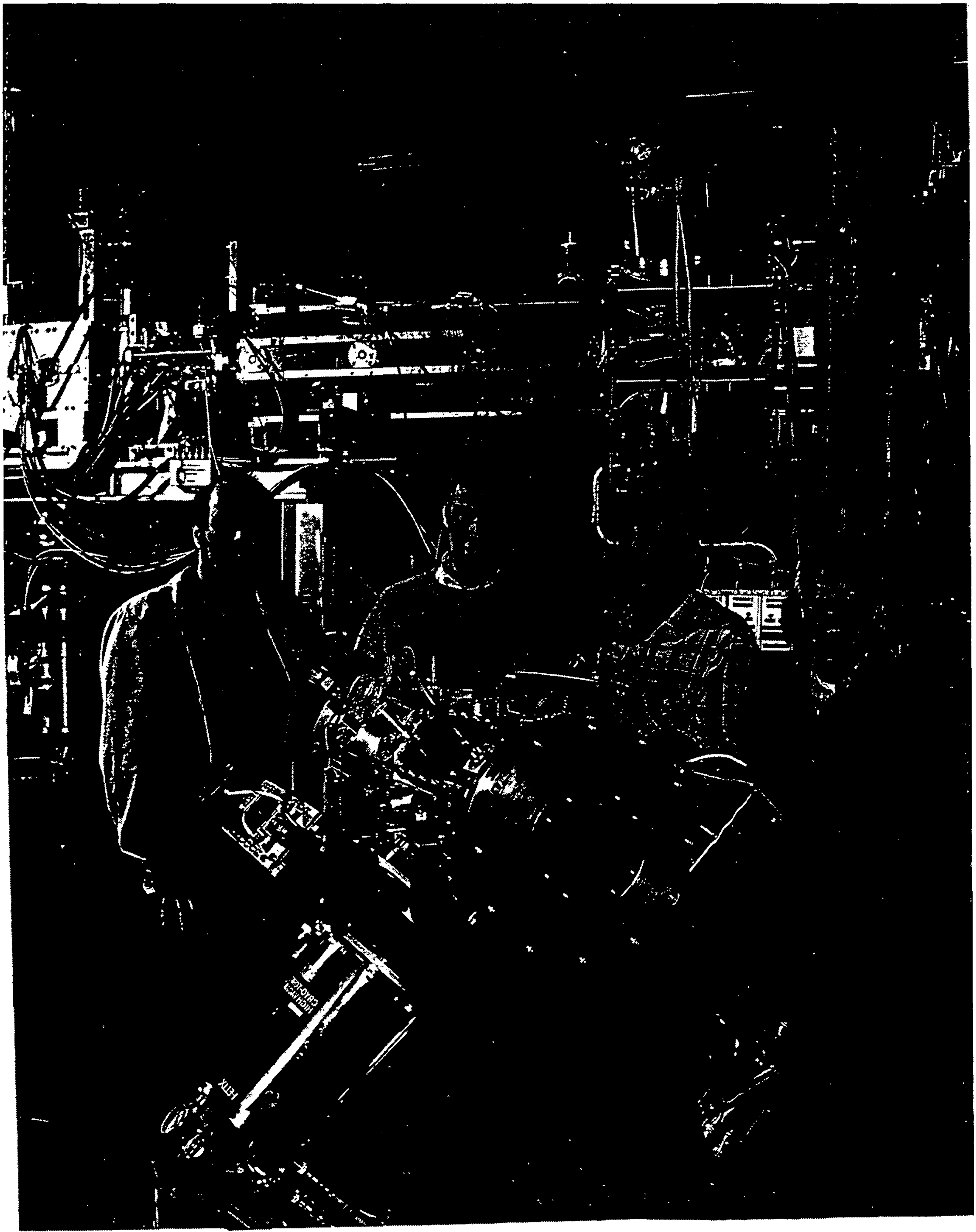

BBC855-4195

Ion Beam Technologies

Technology for the DOE

- ion source development
- advanced accelerator structures
- heavy ion beam cooling

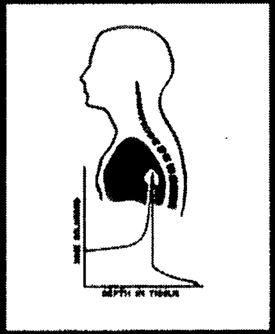

Medical Applications

- radiotherapy
- radioisotope production
- instrumentation

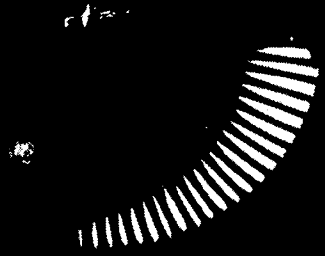

Materials Applications

- ion implantation
- surface modification
- ion beam lithography

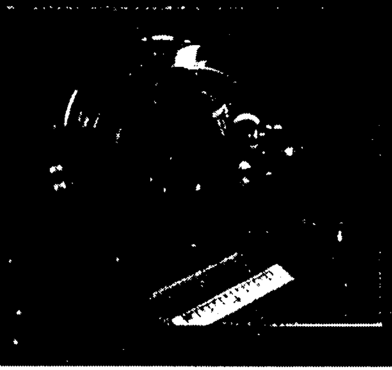

IBT Scientific Staff

Alonso, Jose
Anders, Andre
Anders, Simone
Brown, Ian
Chu, Bill
Gough, Rick
Hernandez, Jacob
Lee, Yung-Hee
Leung, Ka-Ngo
Liu, Fenghua
Ludewigt, Bernhard
Monterio, Othon
Olgetree, Marie-Paule
Perkins, Luke
Pickard, Dan
Rutkowski, Henry
Staples, John
Sun, Lee
Vilaithong, Rummiya
Wang, Zhi
Wengrow, Adam
Wutte, Daniela

R&D Topics in the Ion Beam Technology Program

- Ion Source Development
- RFQ Linac Development

Integrated Ion Source / RFQ Testing

- Stochastic Cooling (with CBP)
- Beam Optics
- **Pulsed Spallation Neutron Source**
- **Boron Neutron Capture Therapy**
- Proton Therapy

- Surface Modification Studies
- Biocompatible Materials
- Neutron Logging
- MeV Implantation
- Ion Beam Lithography
- Ion Doping
- Flat Panel Display Technology
- Diamond Coatings
- MutiLayers

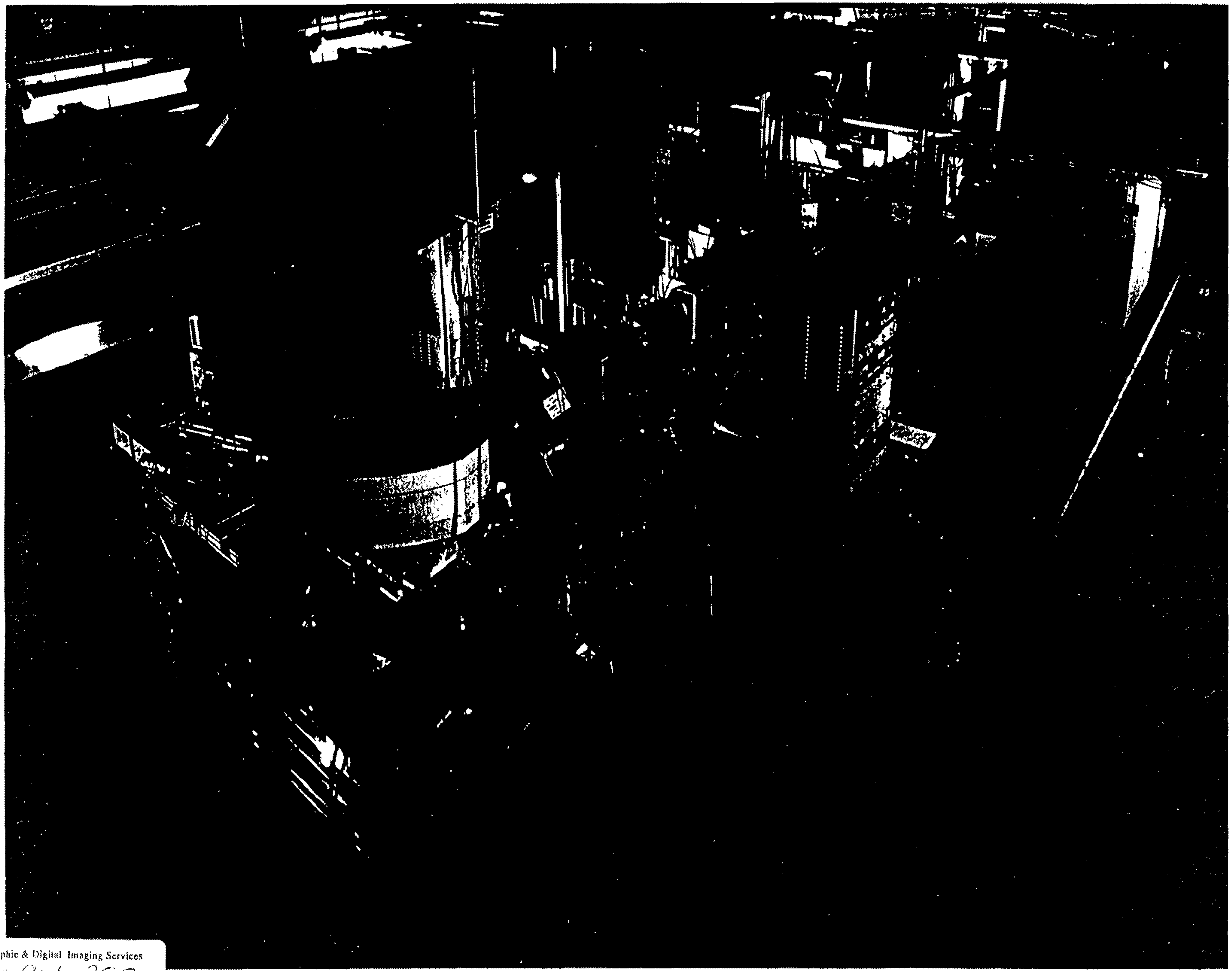

hotographic & Digital Imaging Services
KSC 961-797

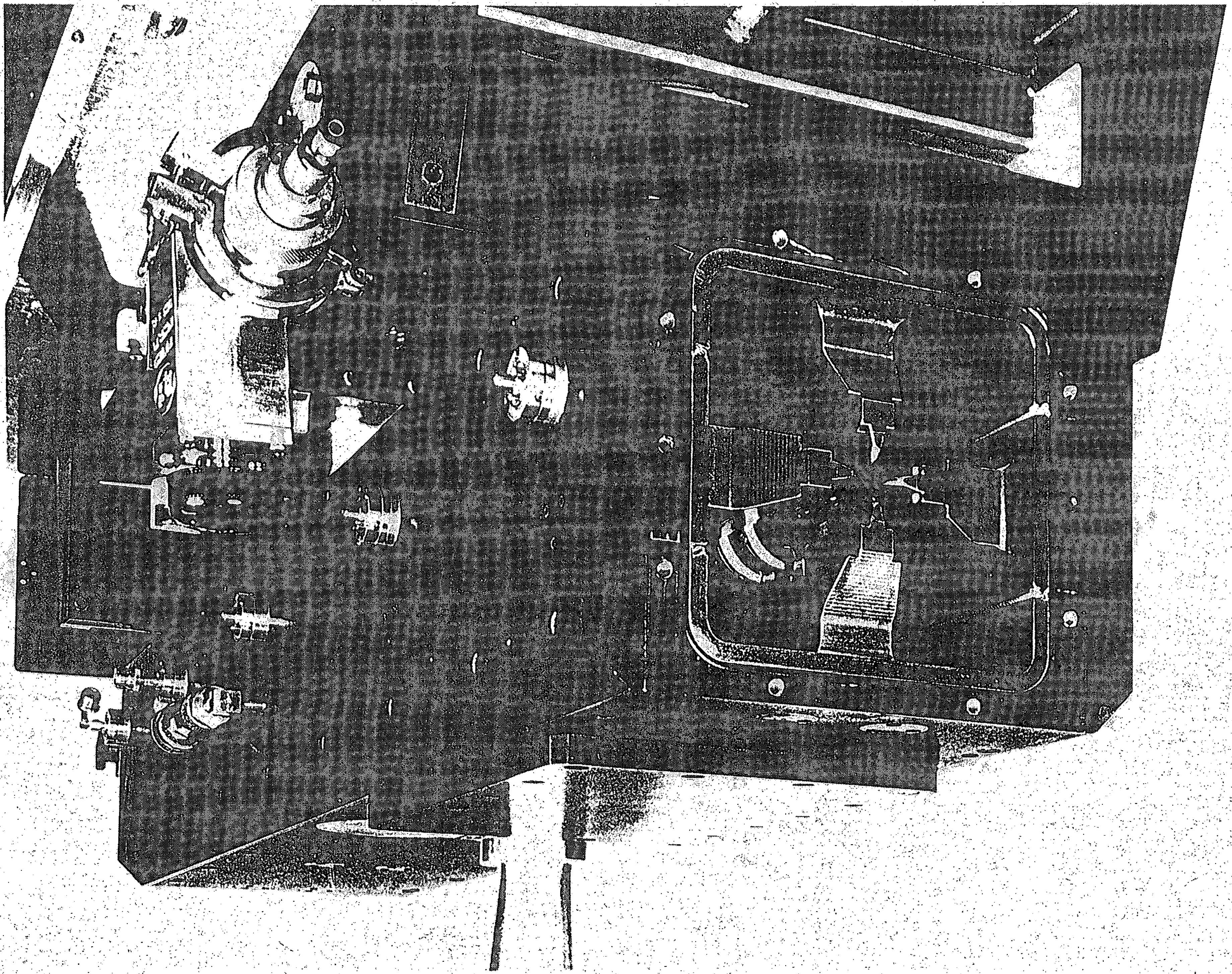
E

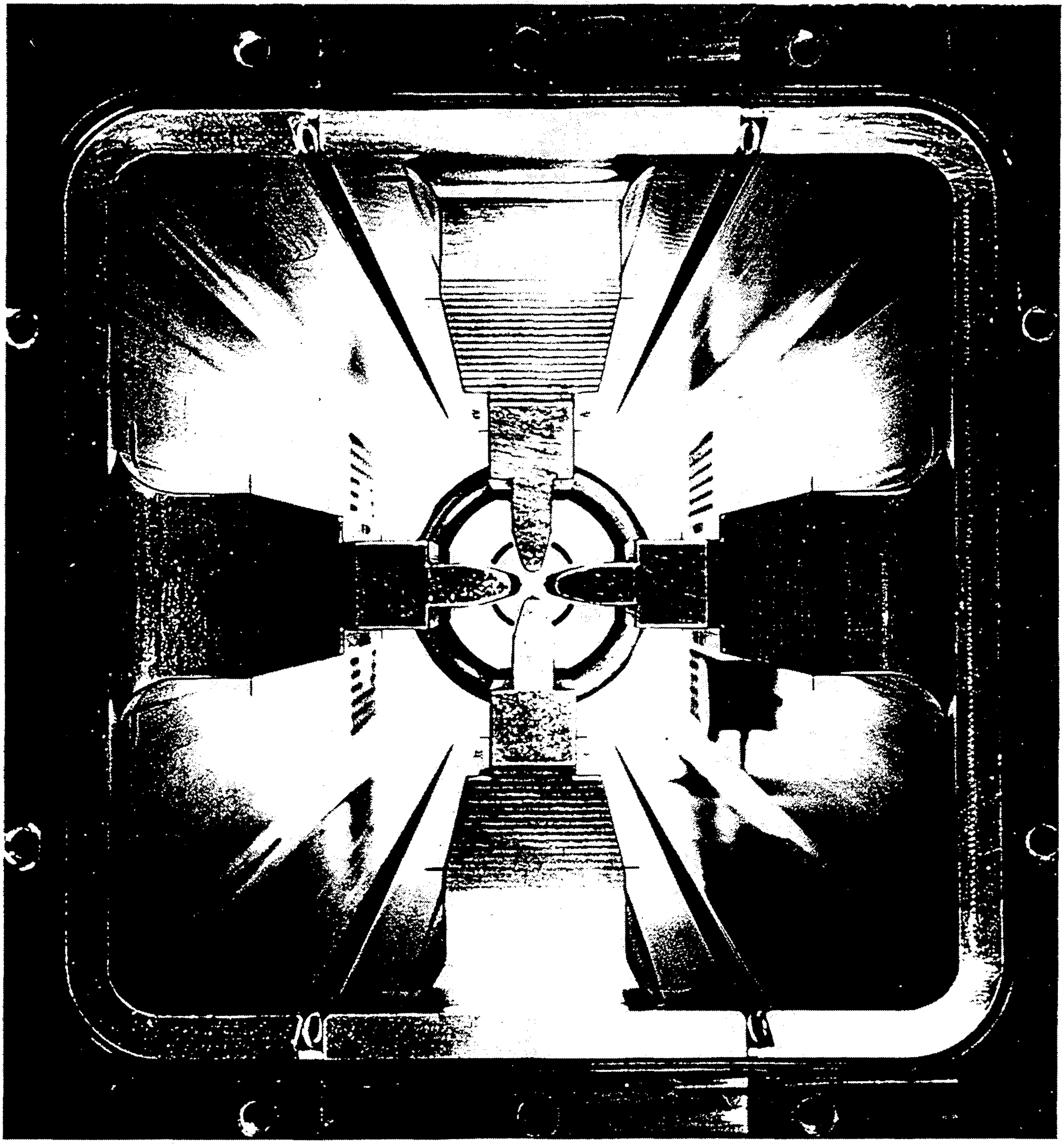

Integrated
Source – LEBT – RFQ
Experiment with 30 mA
Proton Beam

cm

0 10

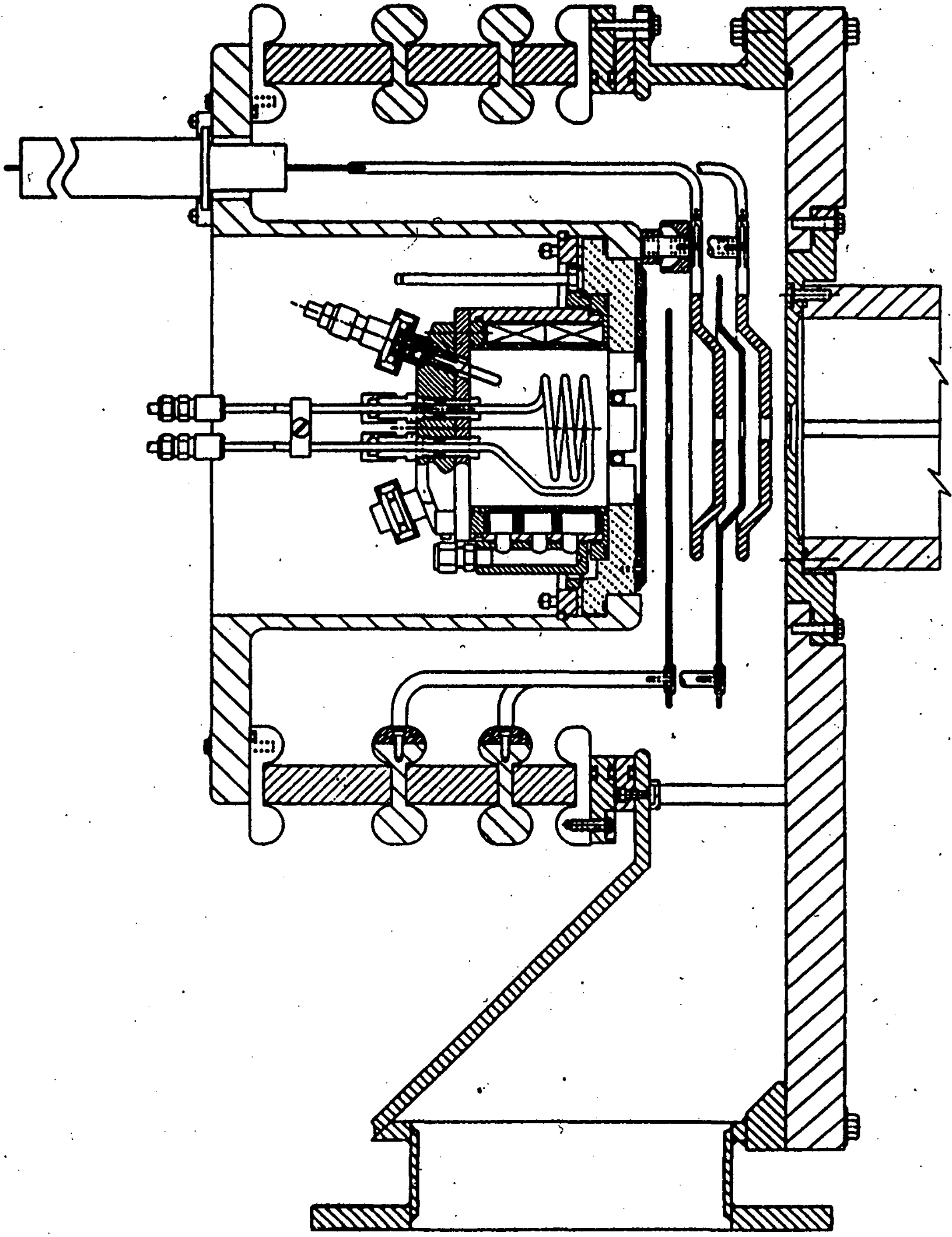

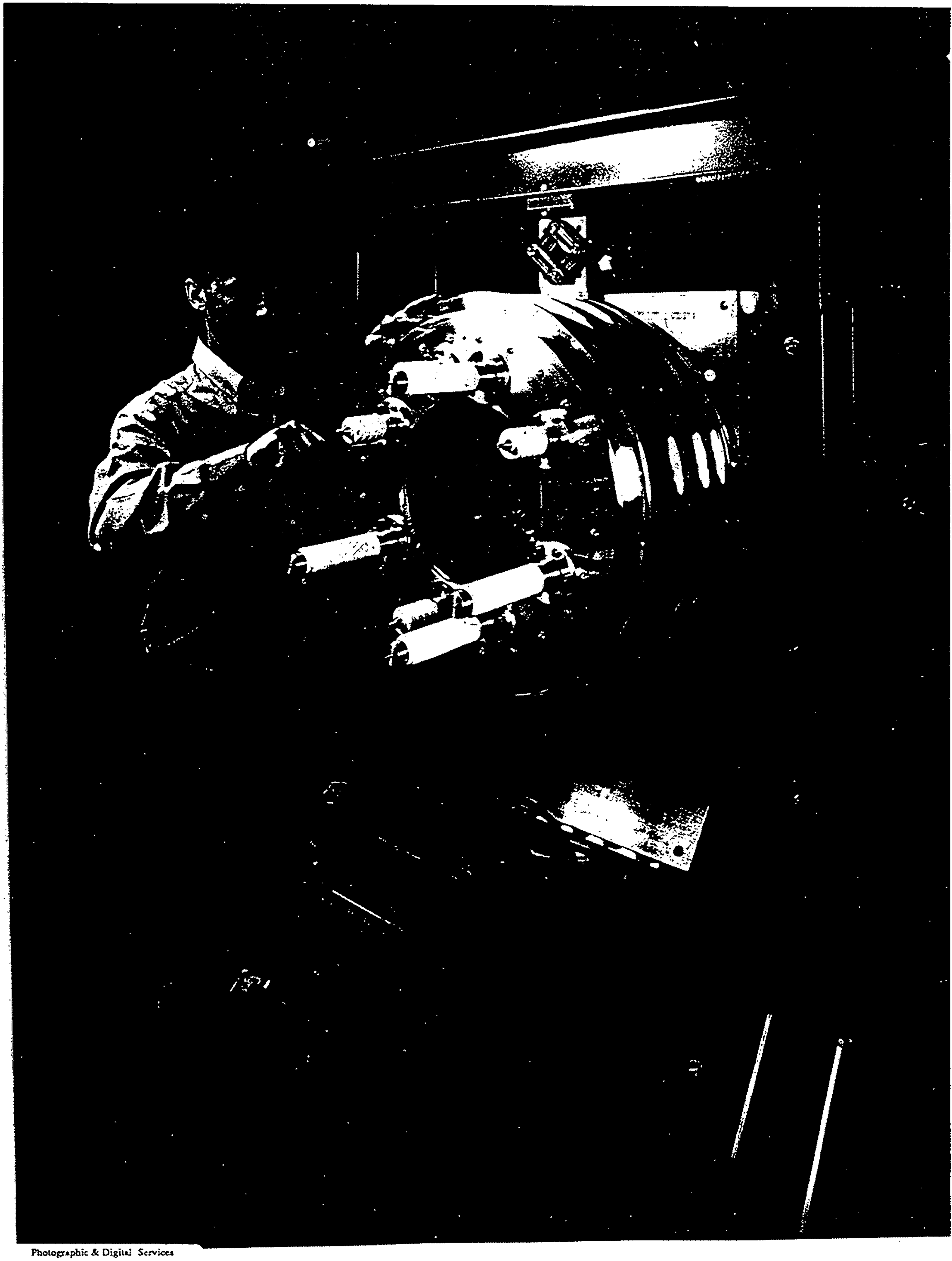

Photographic & Digital Services

XBC957-3444

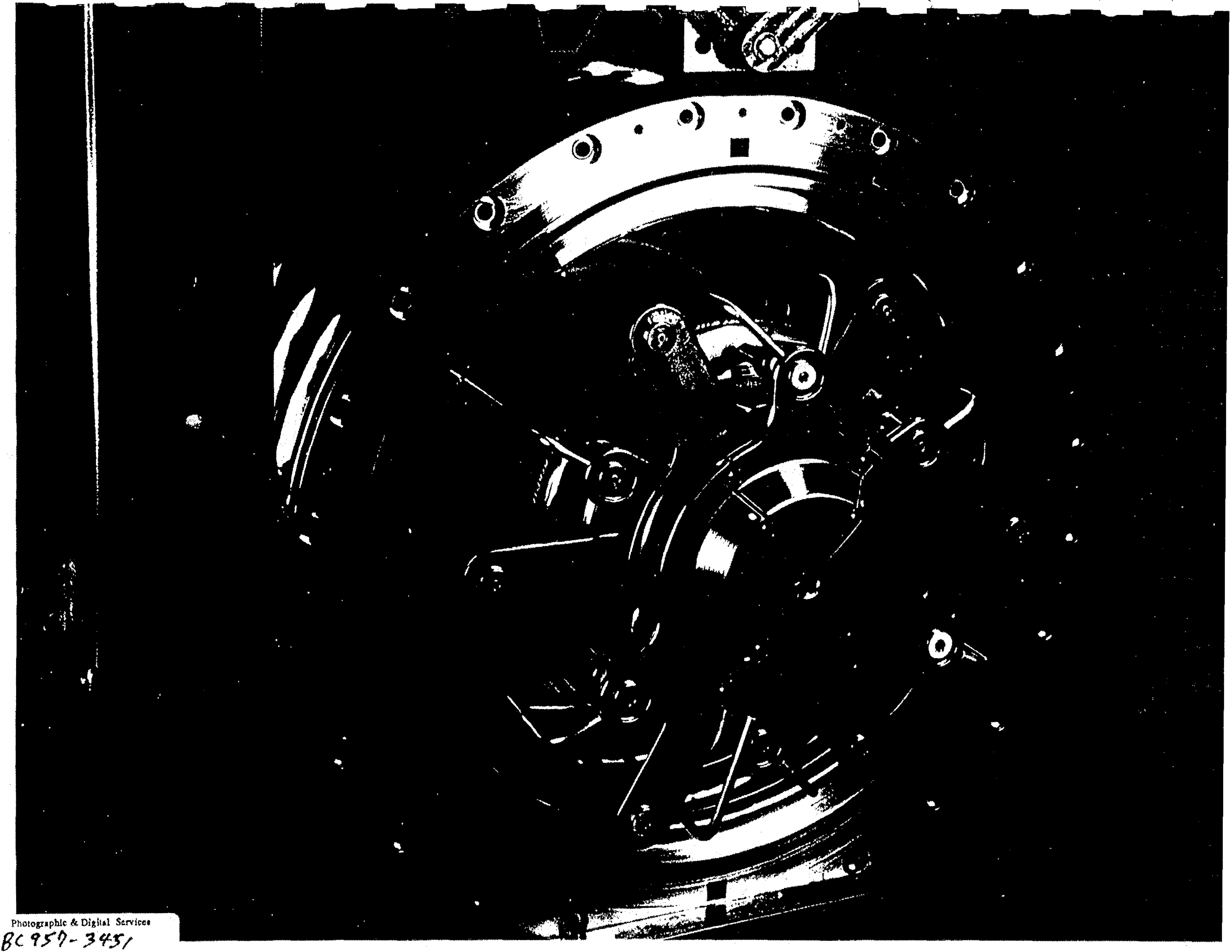

Photographic & Digital Services
XBC957-3451

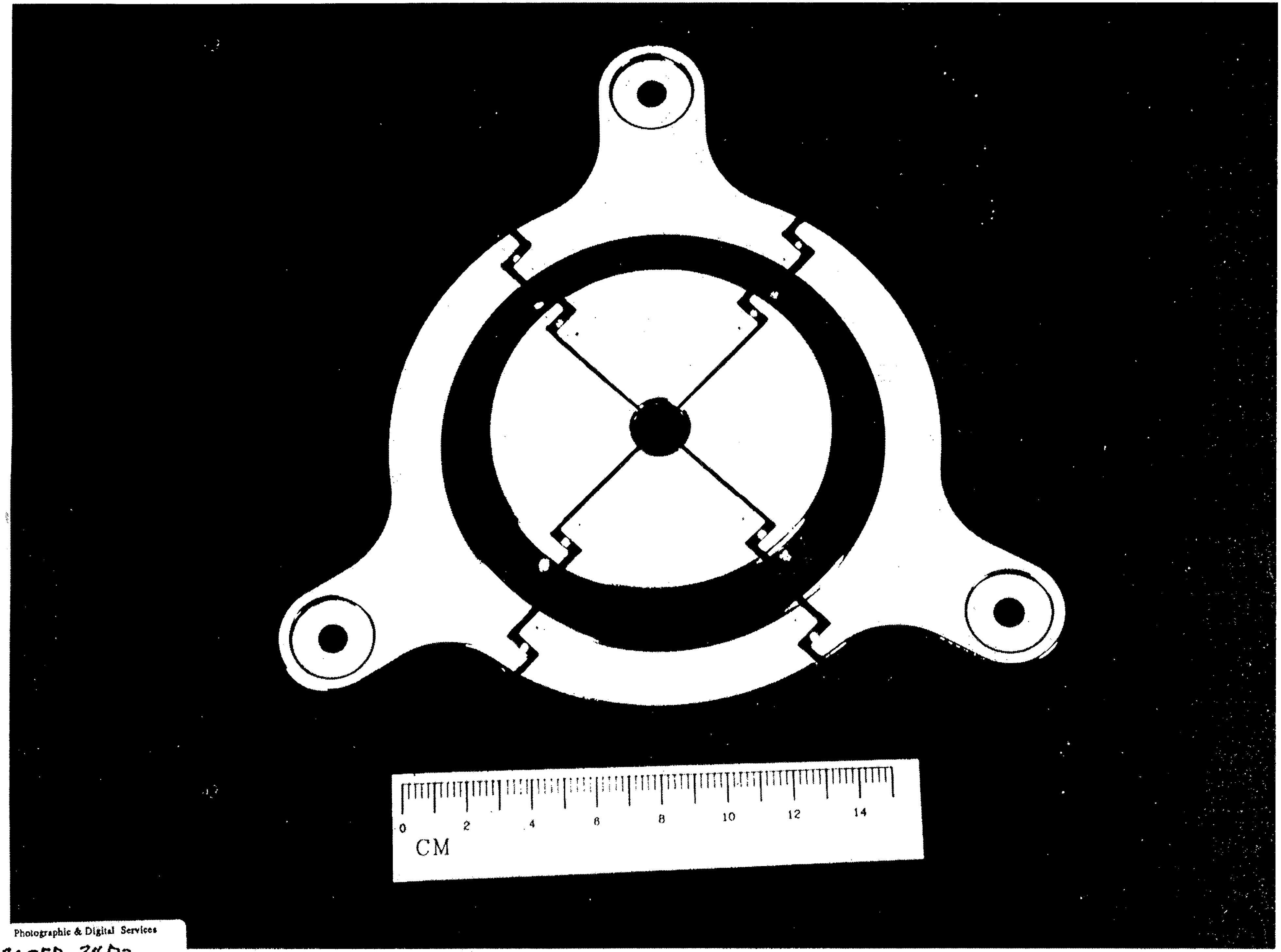

Photographic & Digital Services

BC957-3472

Phase Space Plot Format

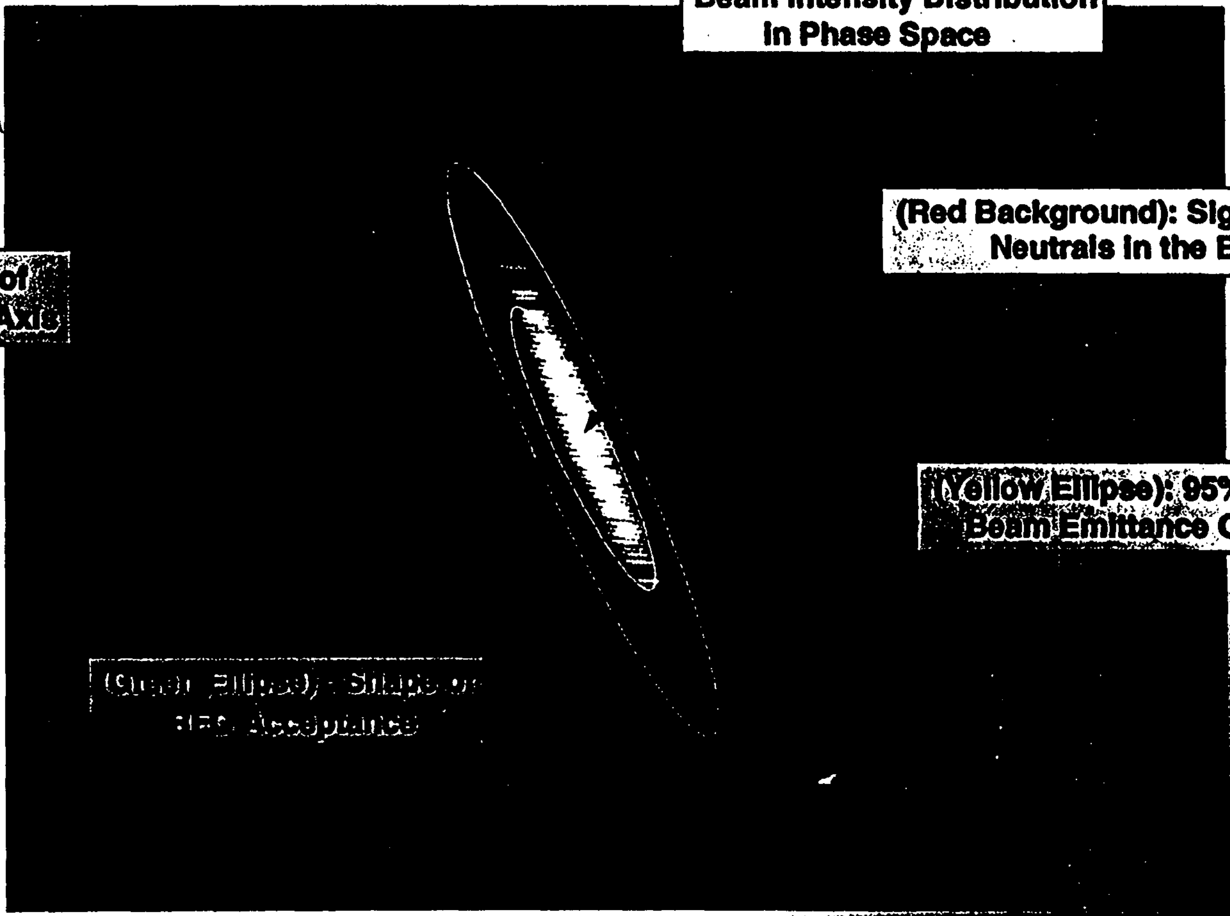

Phase Space Plot
x vs. x'

Beam Intensity Distribution in Phase Space

(Red Background): Signature of Neutrals in the Beam

Origin of Scanner Axis

(Yellow Ellipse): 95% and 50% Beam Emittance Contours

(Green Ellipse) - Shape of RFQ Acceptance

Steering at Second Einzel Lens as a function of % Steering Strength

Notice the 95% emittance contour (yellow) moving with respect to the stationary neutrals background (red).

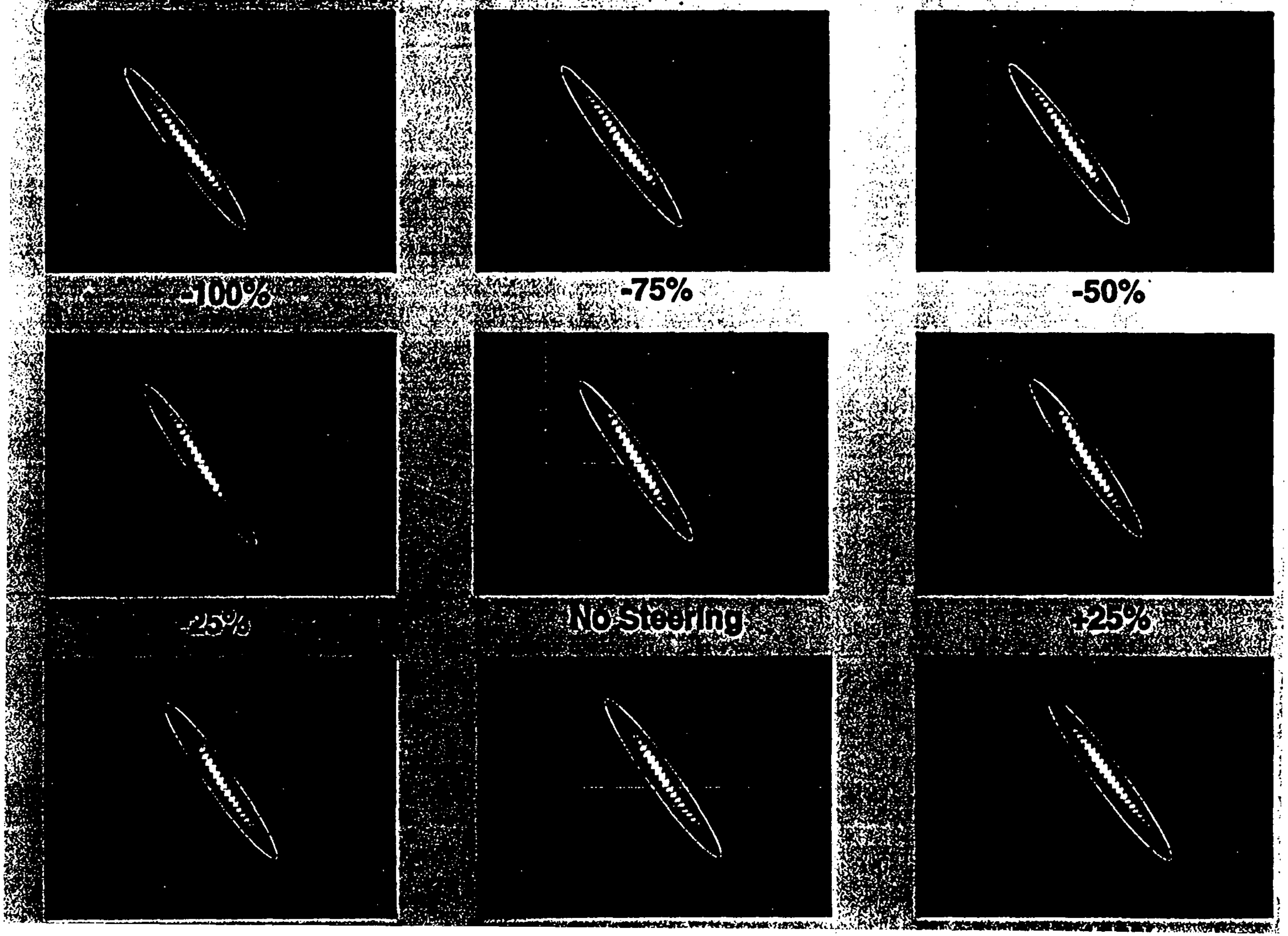

The Oak Ridge Spallation Neutron Source

– a Multi - Laboratory Partnership –

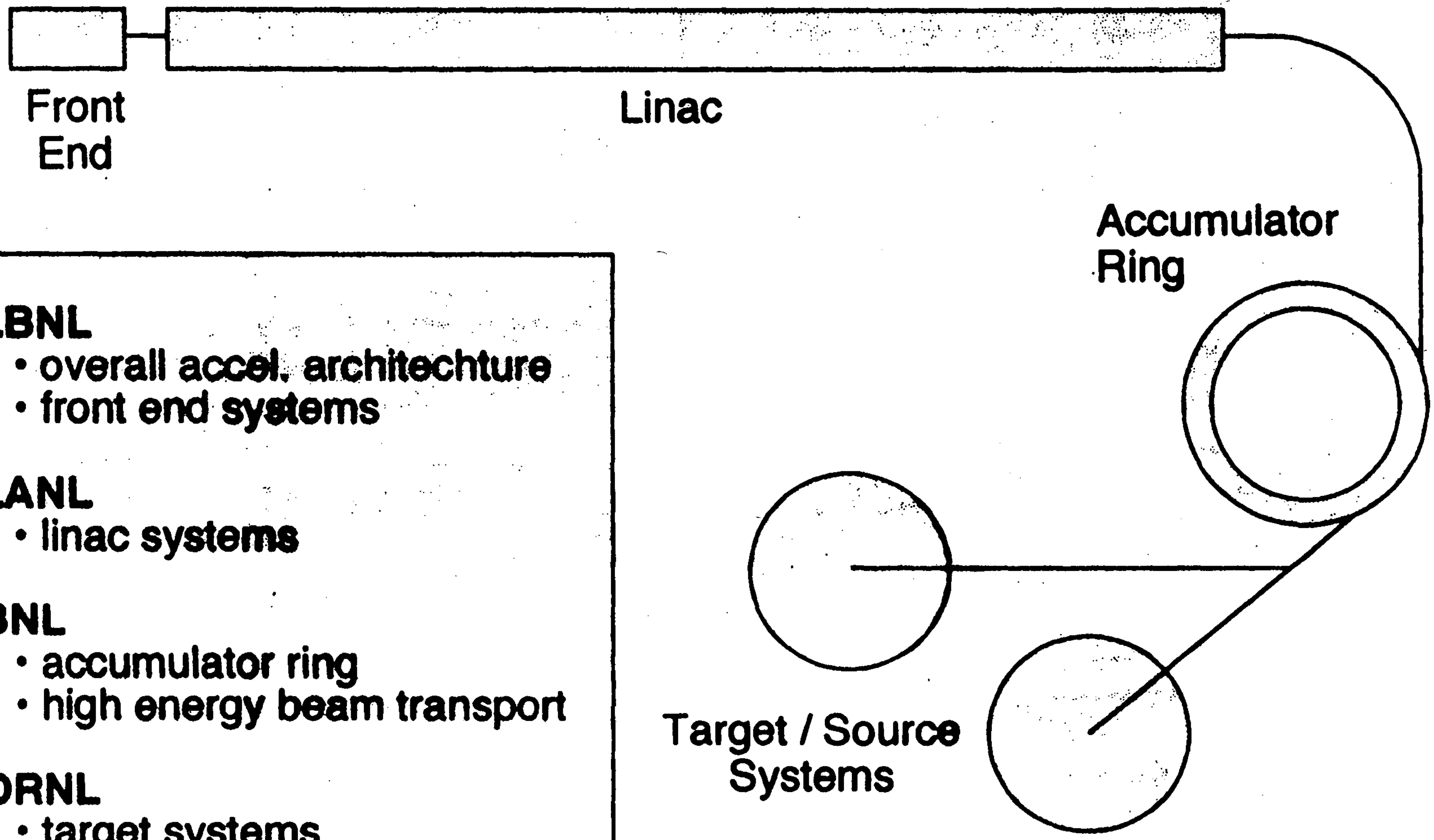

Front End

Linac

Accumulator Ring

Target / Source Systems

LBNL
- overall accel. architechture
- front end systems

LANL
- linac systems

BNL
- accumulator ring
- high energy beam transport

ORNL
- target systems
- balance of plant

rg.sns.3/3/96

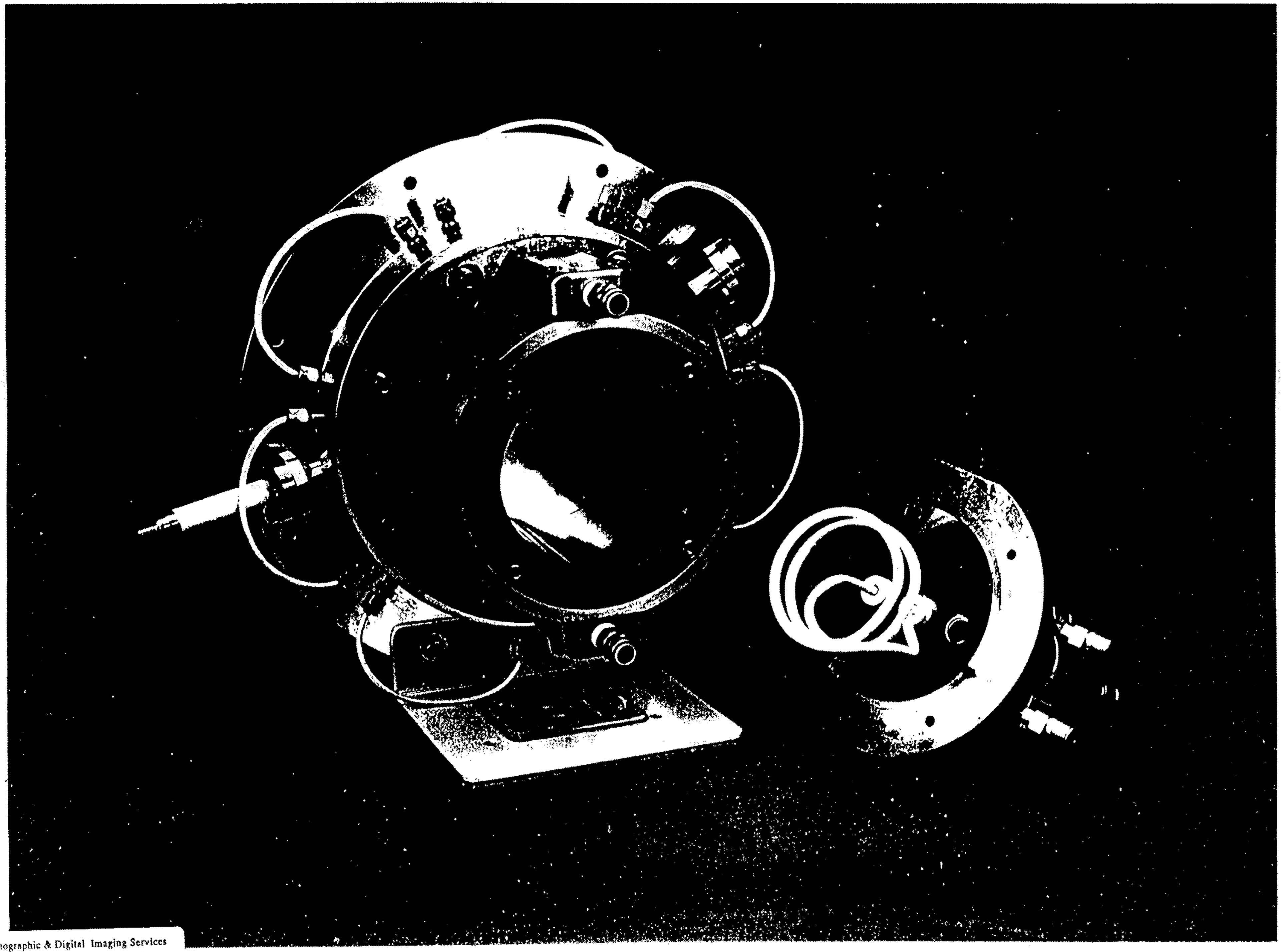

Photographic & Digital Imaging Services

BBC 959-5264

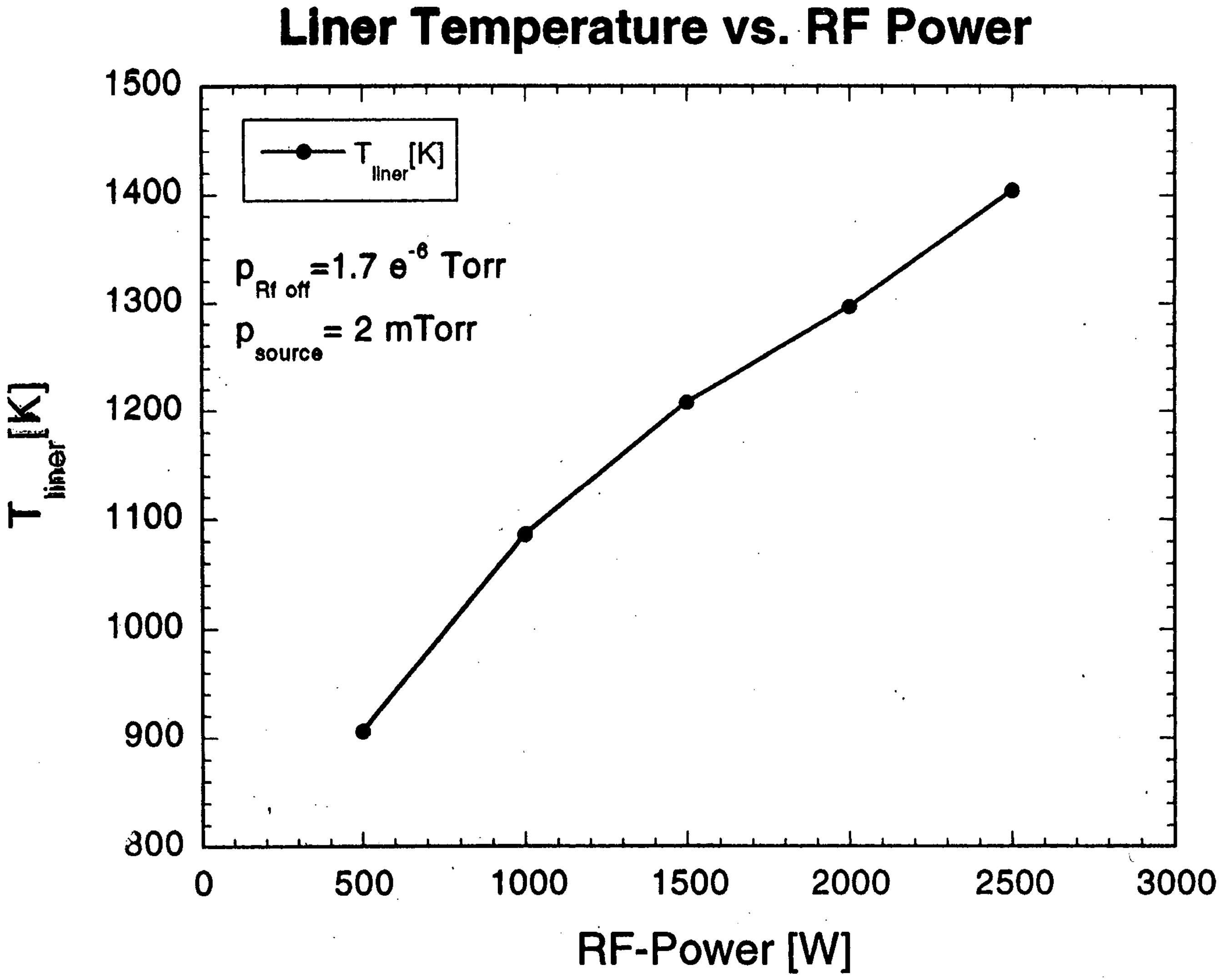
Liner Temperature vs. RF Power
T_{liner}[K]
$p_{Rf\ off}$=1.7 e^{-6} Torr
p_{source}= 2 mTorr
1500
1400
1300
1200
1100
1000
900
800
0
500
1000
1500
2000
2500
3000
RF-Power [W]
T_{liner}[K]

gas efficiency Argon
vs.
RF Power

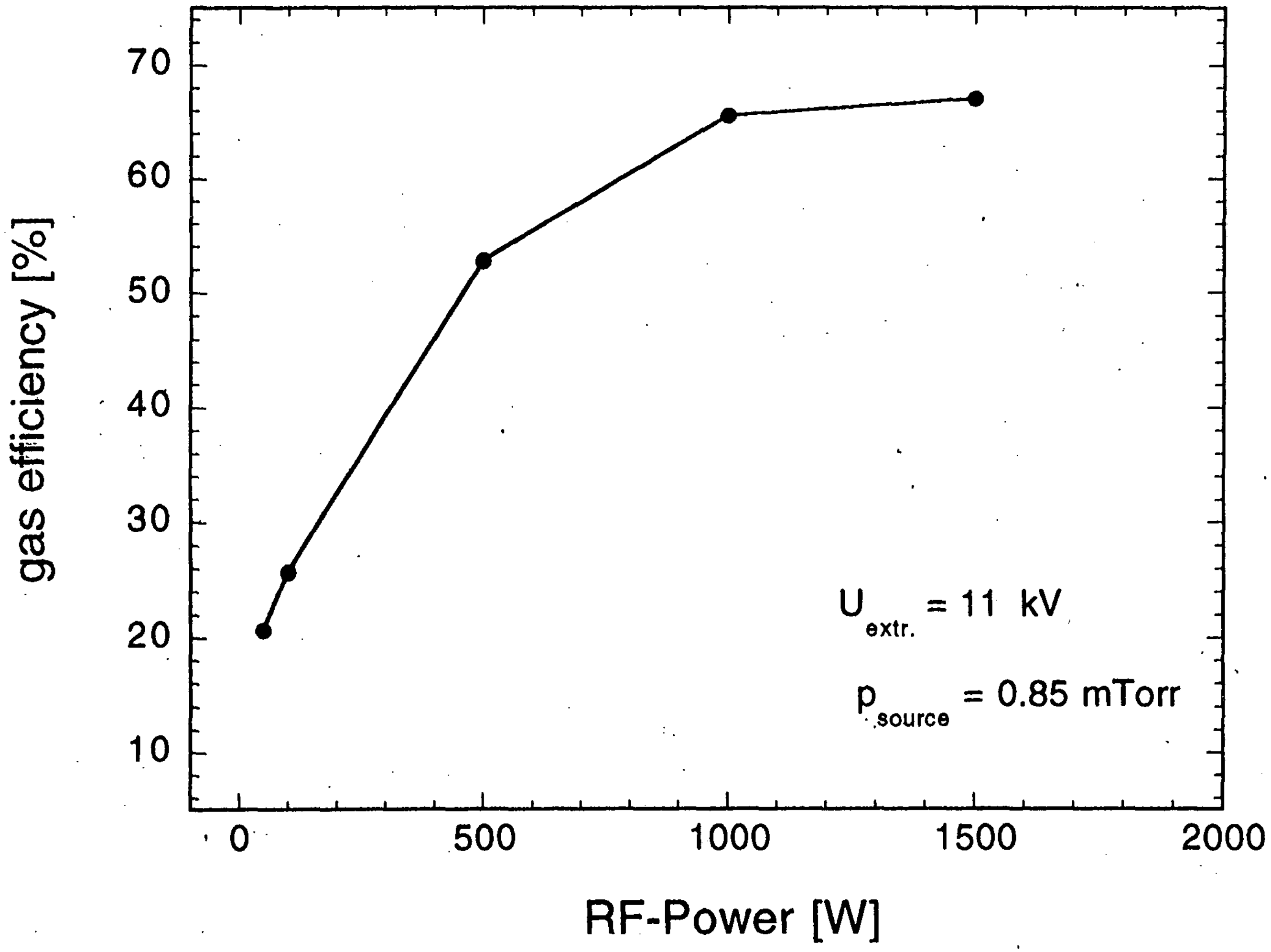

Extracted ion current
vs.
RF Power

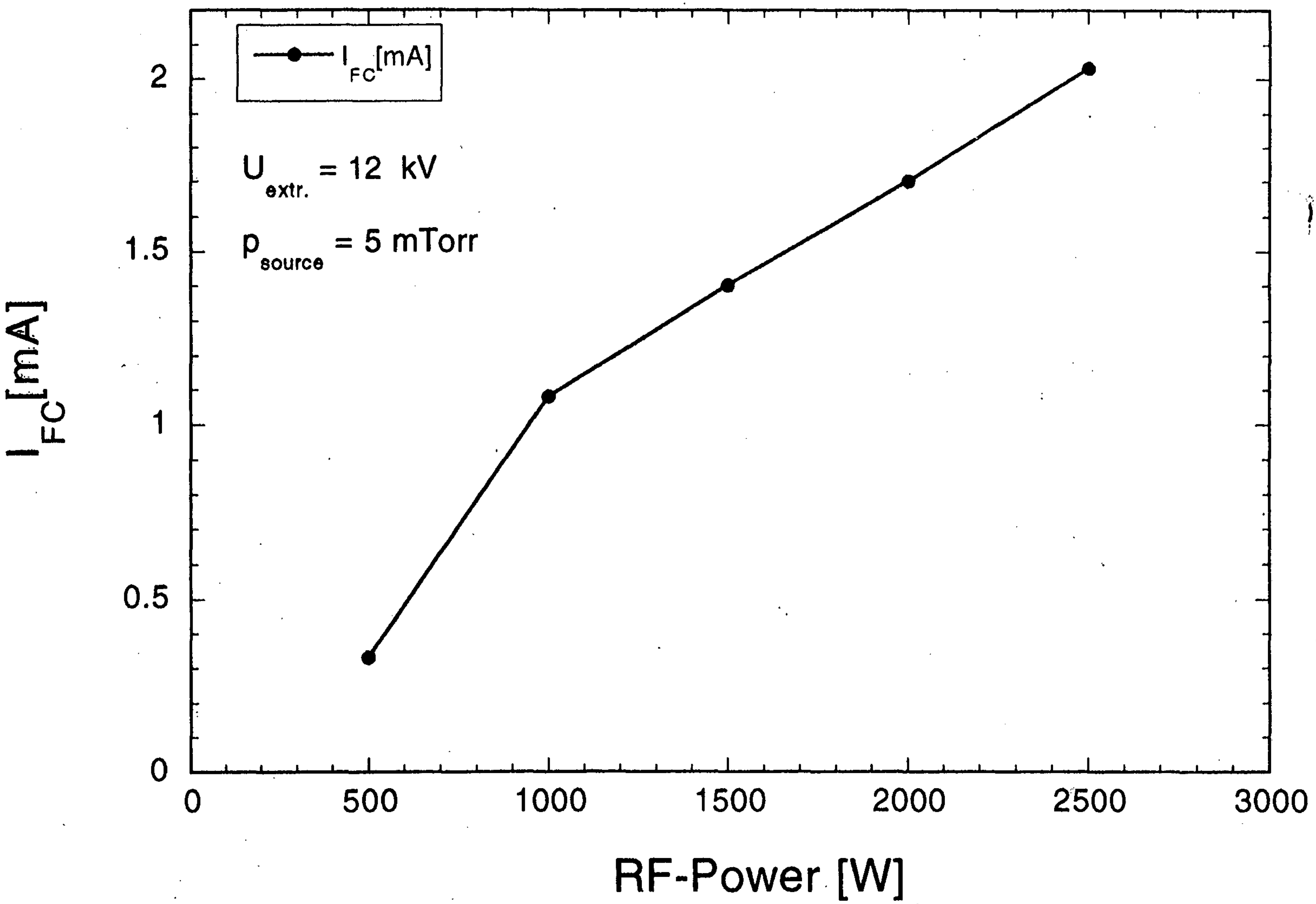

TRIUMF SOURCE

(FOR RADIOACTIVE ION BEAM PRODUCTION)

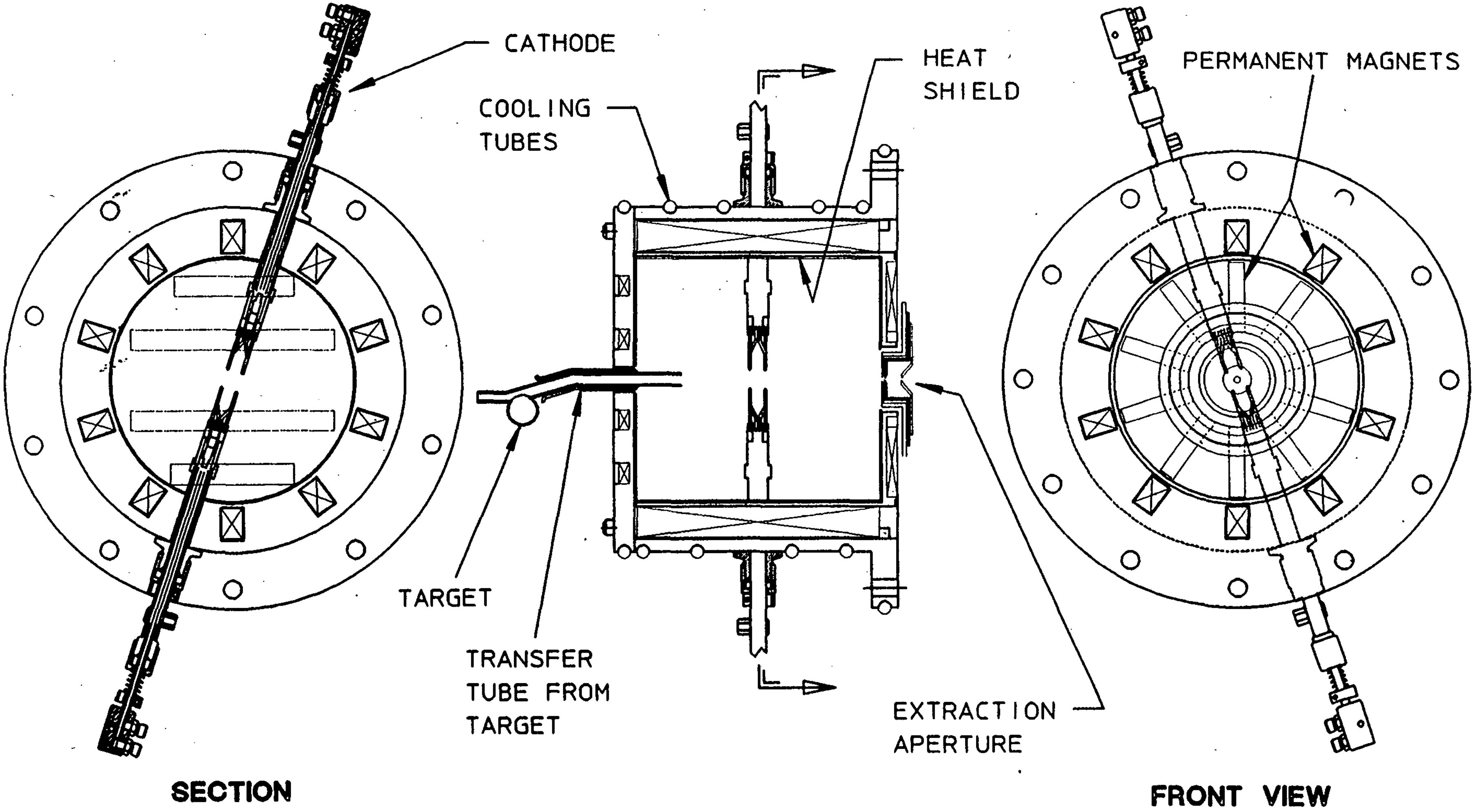

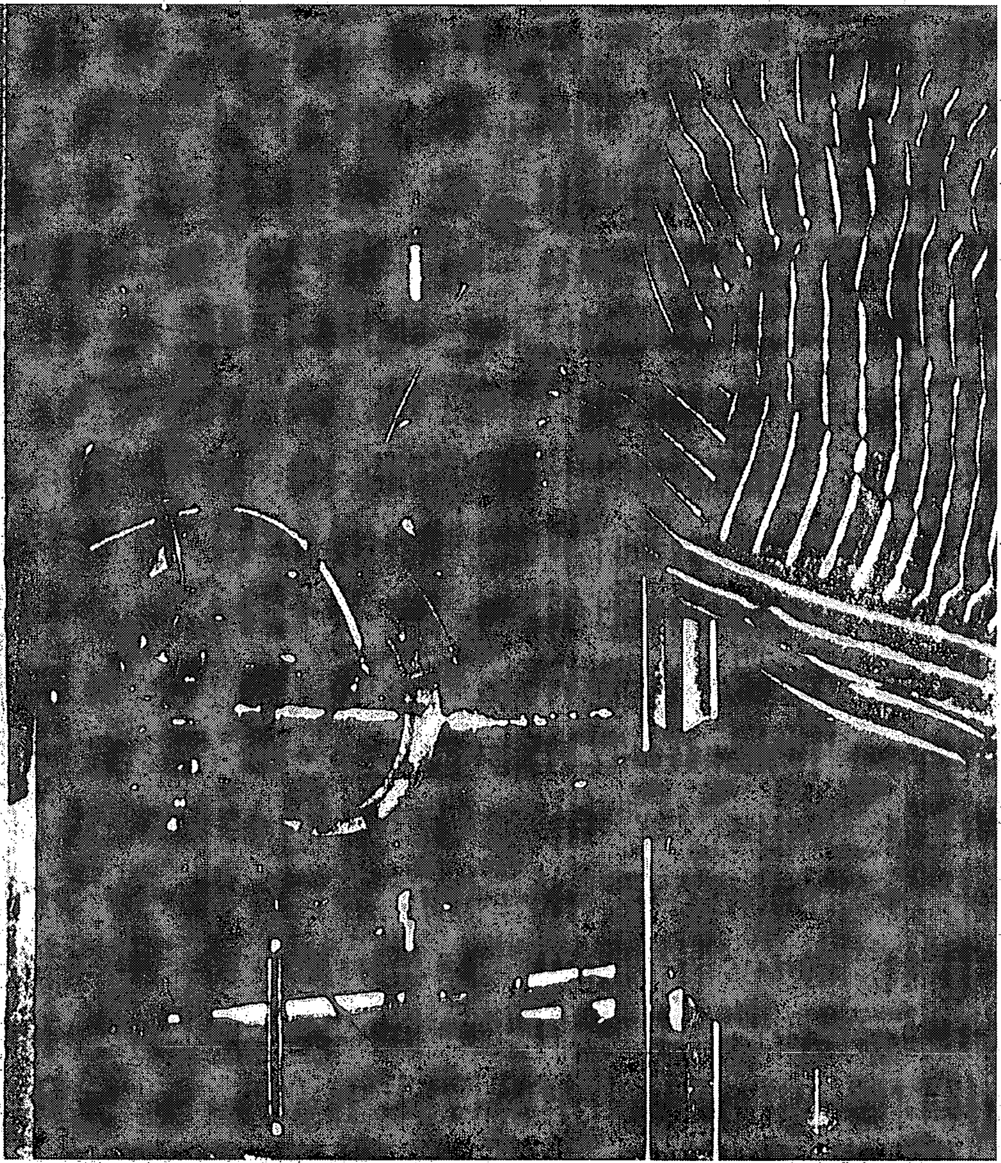

Alpha – 5x Ion Projection Exposure

Ion Microfabrication Systems (IMS)

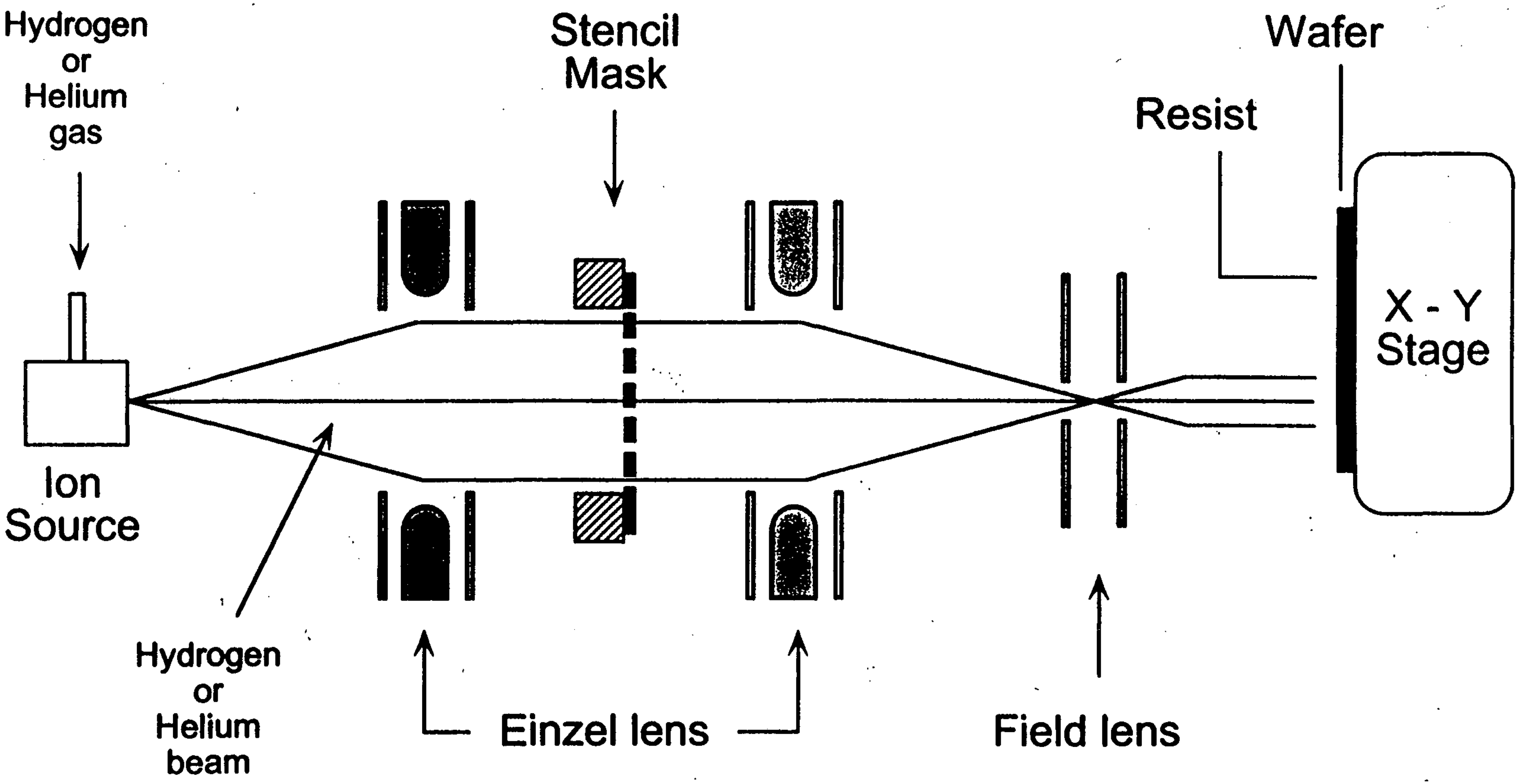

ENERGY ANALYZER SCHEMATIC

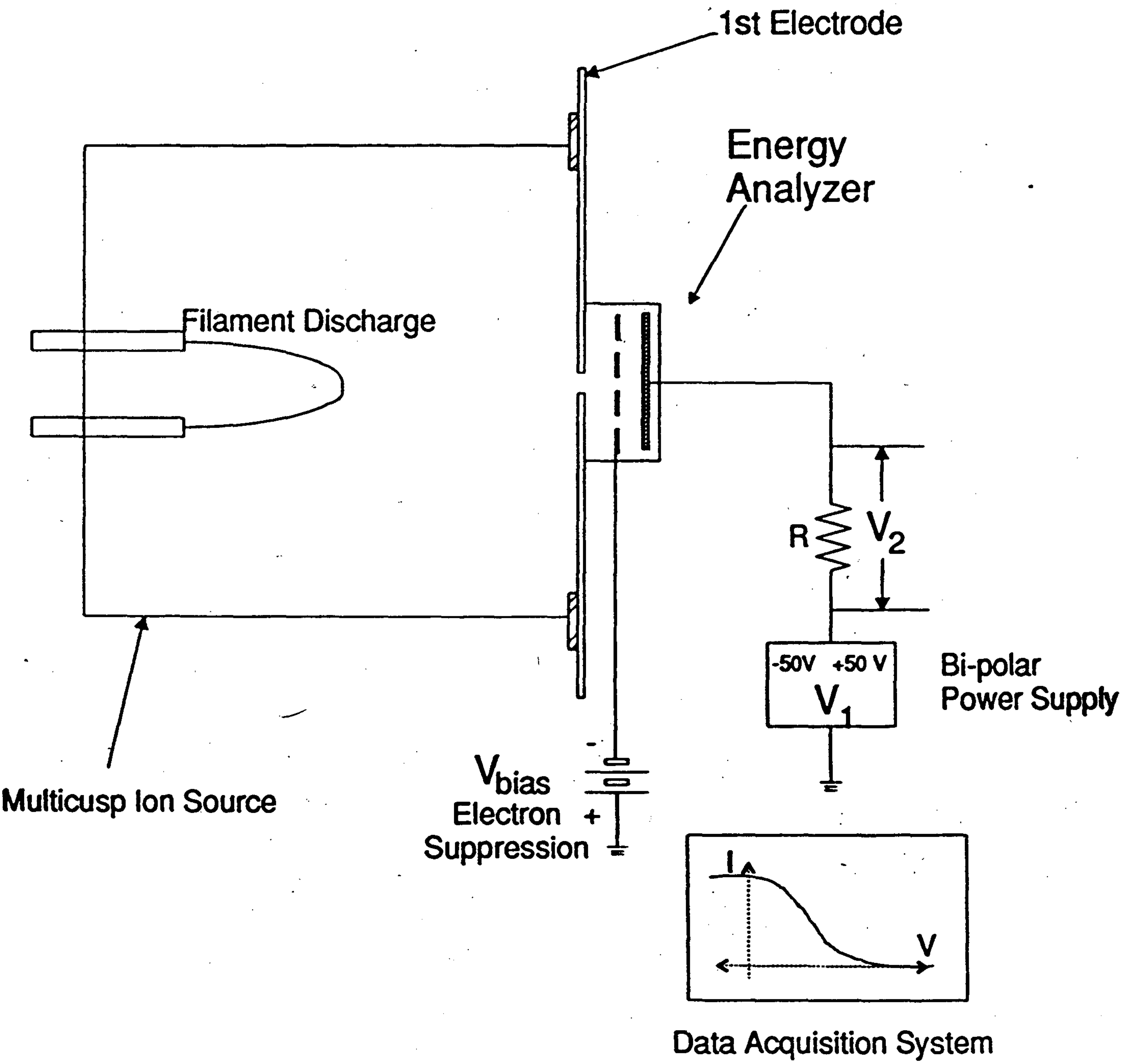

$$V = V_1 + V_2 ; I = \frac{V_2}{R}$$

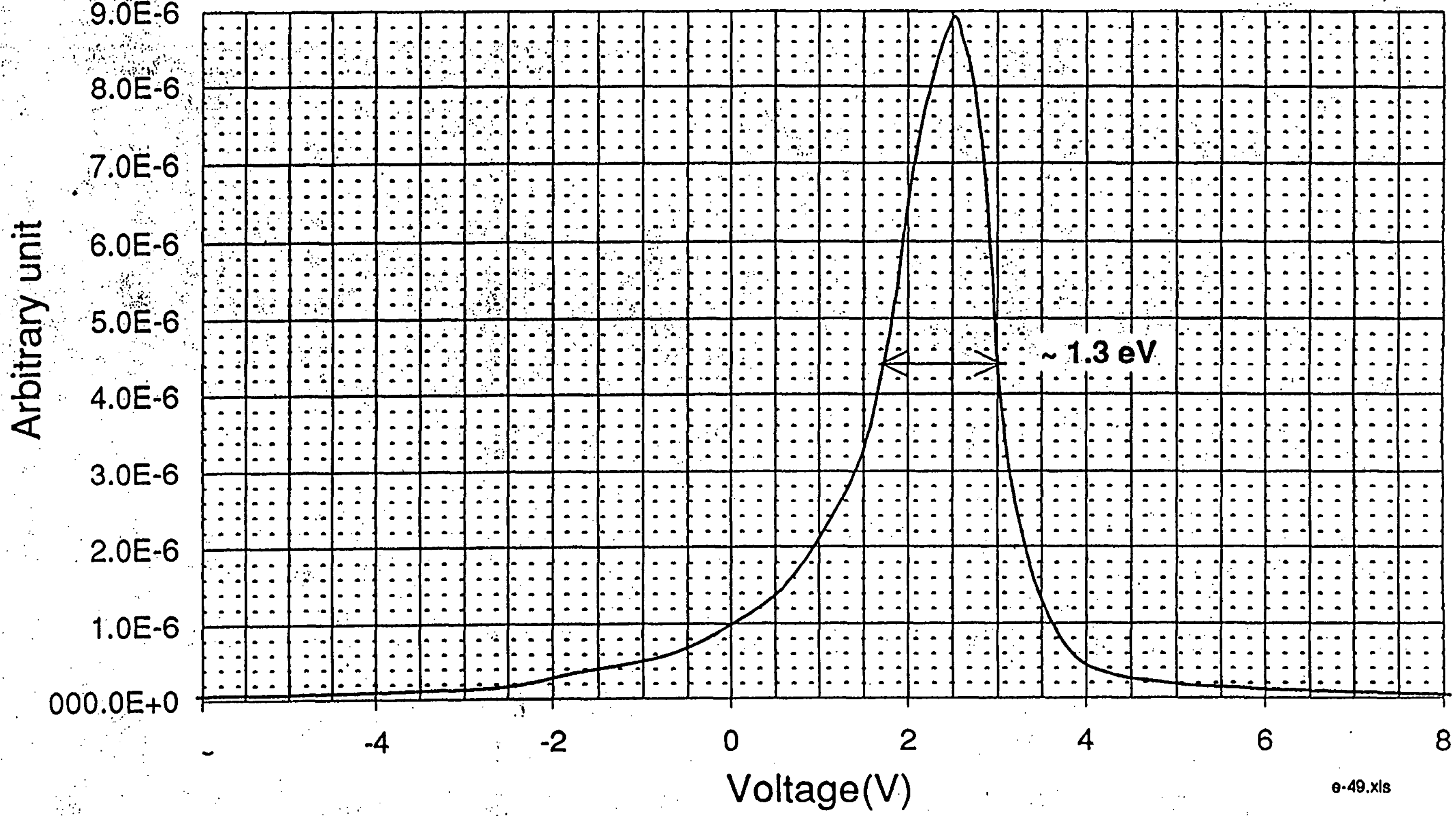

10 cm ALG Source, Filament Operation
With filters, first electrode floating

Mevva ion sources

- Vacuum-arc-based ion sources havevirtue of producing ion beams that are

    high current
    metal

- Important applications are

    ion implantation
    accelerator injection
    tool for fundamental vacuum arc physics

- It is feasible to make a giant ion beam device (implanter)

- A new ion source looking for new applications

Accelerator Injection Applications

For synchrotron injection

- Bevalac, LBL – Limited tests
- Unilac & SIS, GSI – Program is ongoing
- ITEP, Moscow – Limited tests

For heavy ion fusion

- ITEP, Moscow – In development

Problem: Transport of high current beams

Source & beam characteristics

Extraction voltage	10 – 100 kV
Beam current	10 mA – 20 A
" diameter	0.1 – 50 cm
" divergence	≥ 2°
" emittance	≥ 0.05 π cm.mrad.
" length	10 μs – dc
Ion species	Li, C, Mg, Al, Si, Ca, Sc, Ti, V, Cr, Mn, Fe, Co, Ni, Cu, Zn, Ge, Sr, Y, Zr, Nb, Mo, Pd, Ag, Cd, In, Sn, Sb, Ba, La, Ce, Pr, Nd, Sm, Gd, Dy, Ho, Er, Tm, Yb, Hf, Ta, W, Ir, Pt, Au, Pb, Bi, Th, U
Ion charge state	1 – 6
Ion energy	10 - 600 keV

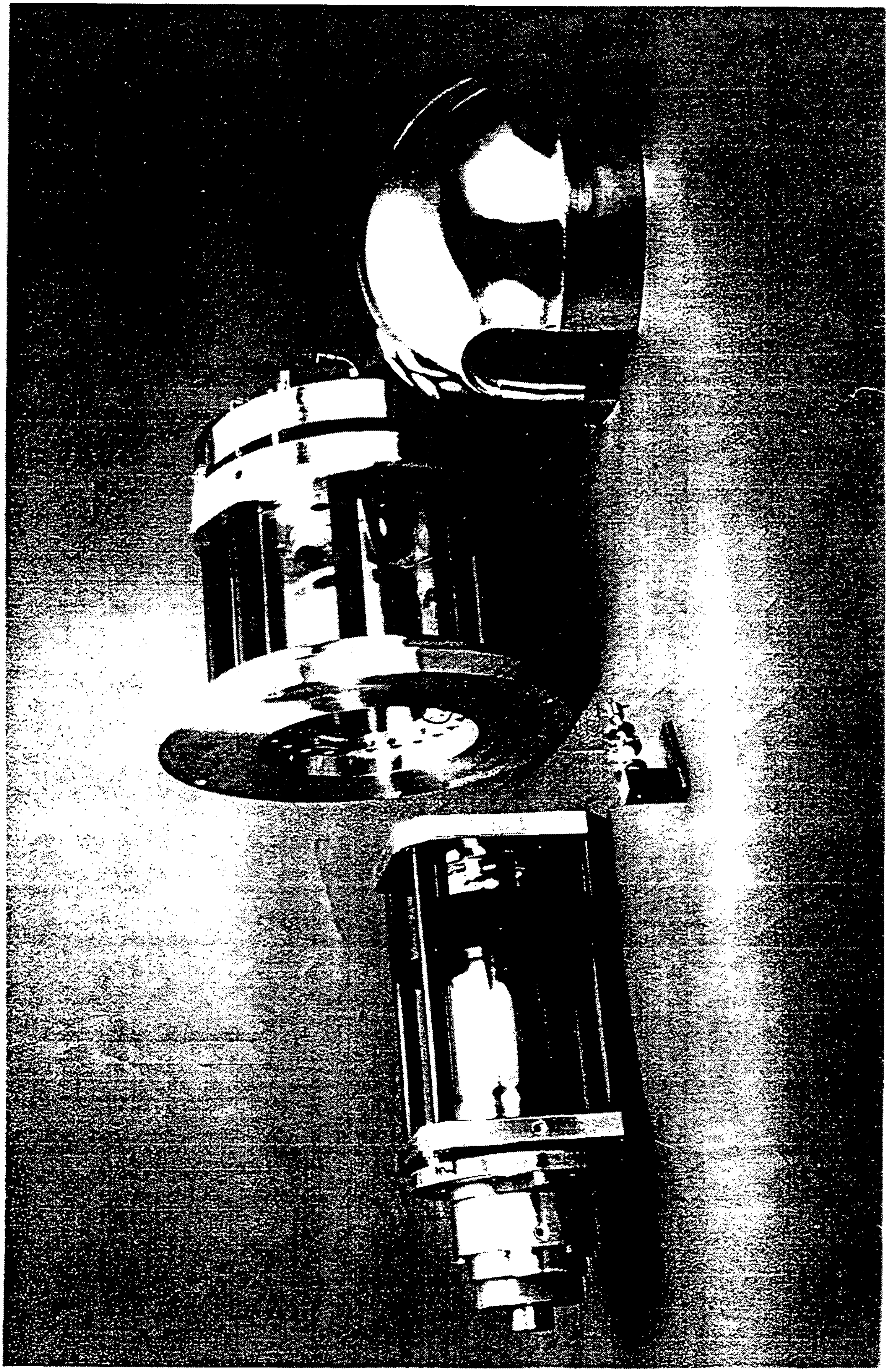

Photographic & Digital Services

XBD 9508-04558.BL4

[illegible] NATIONAL LABORATORY

ELEMENT	Z	Q=1+	2+	3+	4+	5+	6+	$\overline{Q}_p$
Li	3	100						1.0
C	6	100						1.0
Mg	12	46	54					1.5
Al	13	38	51	11				1.7
Si	14	63	35	2				1.4
Ca	20	8	91	1				1.9
Sc	21	27	67	6				1.8
Ti	22	11	75	14				2.1
V	23	8	71	20	1			2.1
Cr	24	10	68	21	1			2.1
Mn	25	49	50	1				1.5
Fe	26	25	68	7				1.8
Co	27	34	59	7				1.7
Ni	28	30	64	6				1.8
Cu	29	16	63	20	1			2.0
Zn	30	80	20					1.2
Ge	32	60	40	*				1.4
Sr	38	2	98					2.0
Y	39	5	62	33				2.3
Zr	40	1	47	45	7			2.6
Nb	41	1	24	51	22	2		3.0
Mo	42	2	21	49	25	3		3.1
Pd	46	23	67	9	1			1.9
Ag	47	13	61	25	1			2.1
Cd	48	68	32					1.3
In	49	66	34	*				1.4
Sn	50	47	53					1.5
Ba	56		100					2.0
La	57	1	76	23				2.2
Ce	58	3	83	14				2.1
Pr	59	3	28	69				2.7
Nd	60		83	17				2.2
Sm	62	2	83	15				2.1
Gd	64	2	76	22				2.2
Dy	66	2	66	32				2.3
Ho	67	2	66	32	*			2.3
Er	68	1	63	35	1			2.4
Yb	70	3	88	8				2.1
Hf	72	3	24	51	21	1		2.9
Ta	73	2	33	38	24	3		2.9
W	74	2	23	43	26	5	1	3.1
Ir	77	5	37	46	11	1		2.7
Pt	78	12	69	18	1			2.1
Au	79	14	75	11				2.0
Pb	82	36	64					1.6
Bi	83	83	17					1.2
Th	90		24	64	12			2.9
U	92		12	58	30			3.2

C

Ion implantation research applications

Some examples of research projects done:

- High temperature oxidation inhibition
- Corrosion resistance
- Hardening of ceramics
- Buried conducting layers in Si ($IrSi_3$)
- Buried strained layers in Si ($Si_{1-x}Ge_x$)
- Hi-T_c film compositional "tuning": Y, Cu into YBaCuO
- Fundamental study of implantation ranges in C
- Effect of implantation on diamond nucleation
- ....

PHYSICS AND BIOLOGY OF BNCT

WHAT IS BNCT

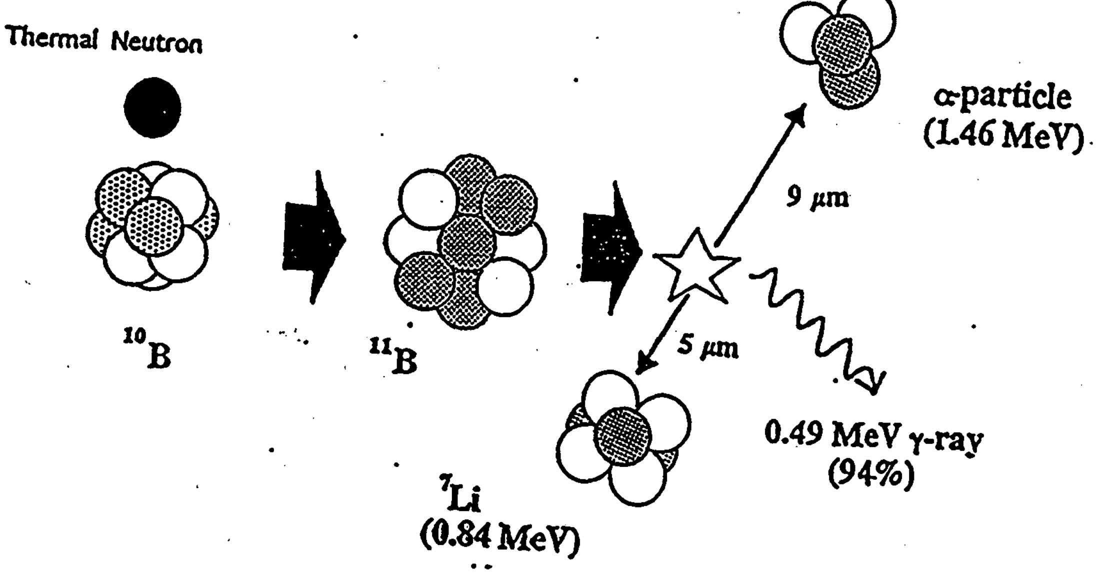

$$^{10}B + {}^{1}n_{th} \rightarrow [^{11}B] \begin{array}{l} \nearrow {}^{4}He + {}^{7}Li + 2.79\ MeV\ (6\%) \\ \searrow {}^{4}He + {}^{7}Li + 0.48\ MeV\ \gamma + 2.31\ MeV\ (94\%) \end{array}$$

AUG 2,1995

BORON NEUTRON CAPTURE THERAPY
(BNCT)

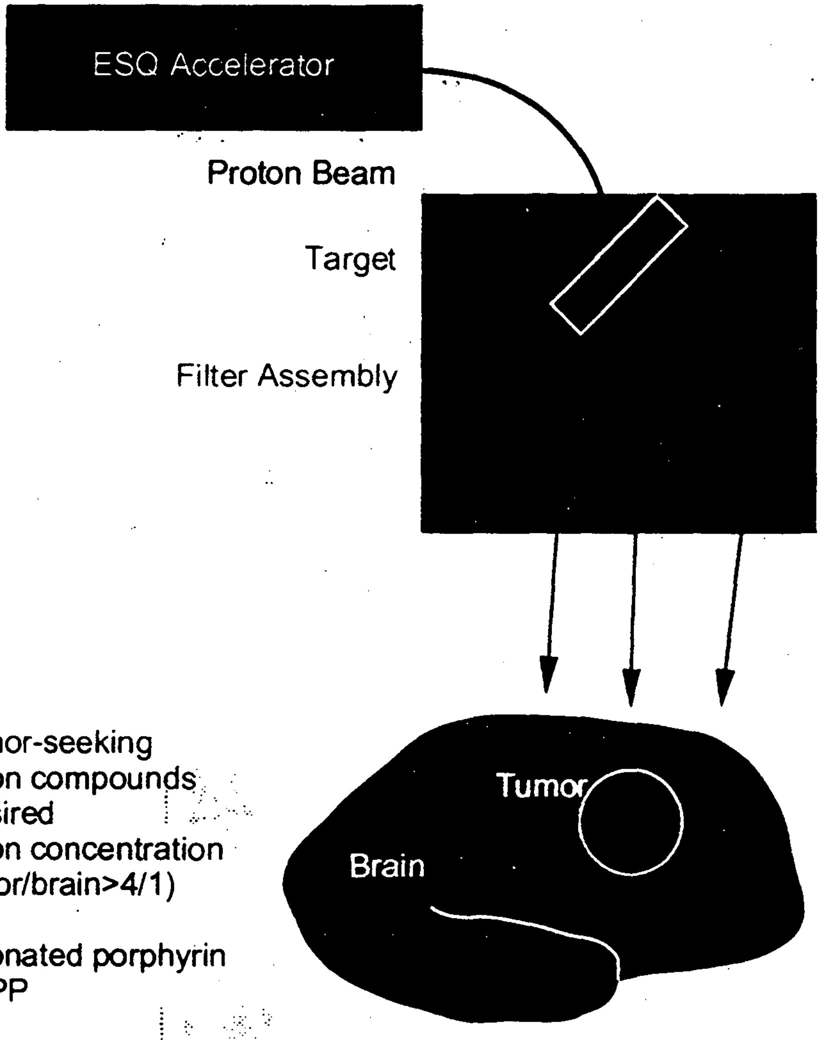

Proton Beam

Target

Filter Assembly

Tumor-seeking
boron compounds
(desired
boron concentration
tumor/brain>4/1)

boronated porphyrin
BOPP

2.5 MeV, 10-20 mA protons

25 kW beam power

$^{7}\mathrm{Li(p.n)}^{7}\mathrm{Be}$
E_n<800 keV

10-cm diameter beam
320W/cm^2

Moderating
Reflecting
Thermal neutron absorbtion
photon attenuation

Epithermal neutrons
(~1 eV-10 keV)

Thermal neutrons
(~0.025 ev)

Desired reaction
$^{10}\mathrm{B}(\mathrm{n}, \alpha)^{7}\mathrm{Li}$

Background radiation
$^{1}\mathrm{H}(\mathrm{n}, \mathrm{n})\mathrm{p}$
$^{14}\mathrm{N}(\mathrm{n}, \mathrm{p})^{14}\mathrm{C}$
$^{1}\mathrm{H}(\mathrm{n}, \gamma)^{2}\mathrm{H}$
γ from target

STUDIES FOR BNCT RADIOBIOLOGY

BOPP Boronated protoporphyrin

- 30% boron by weight
- highly water soluble
- 10 boron atoms / cage
- 40 boron atoms / molecule
- tumor/normal tissue ratio in mice: 400/1

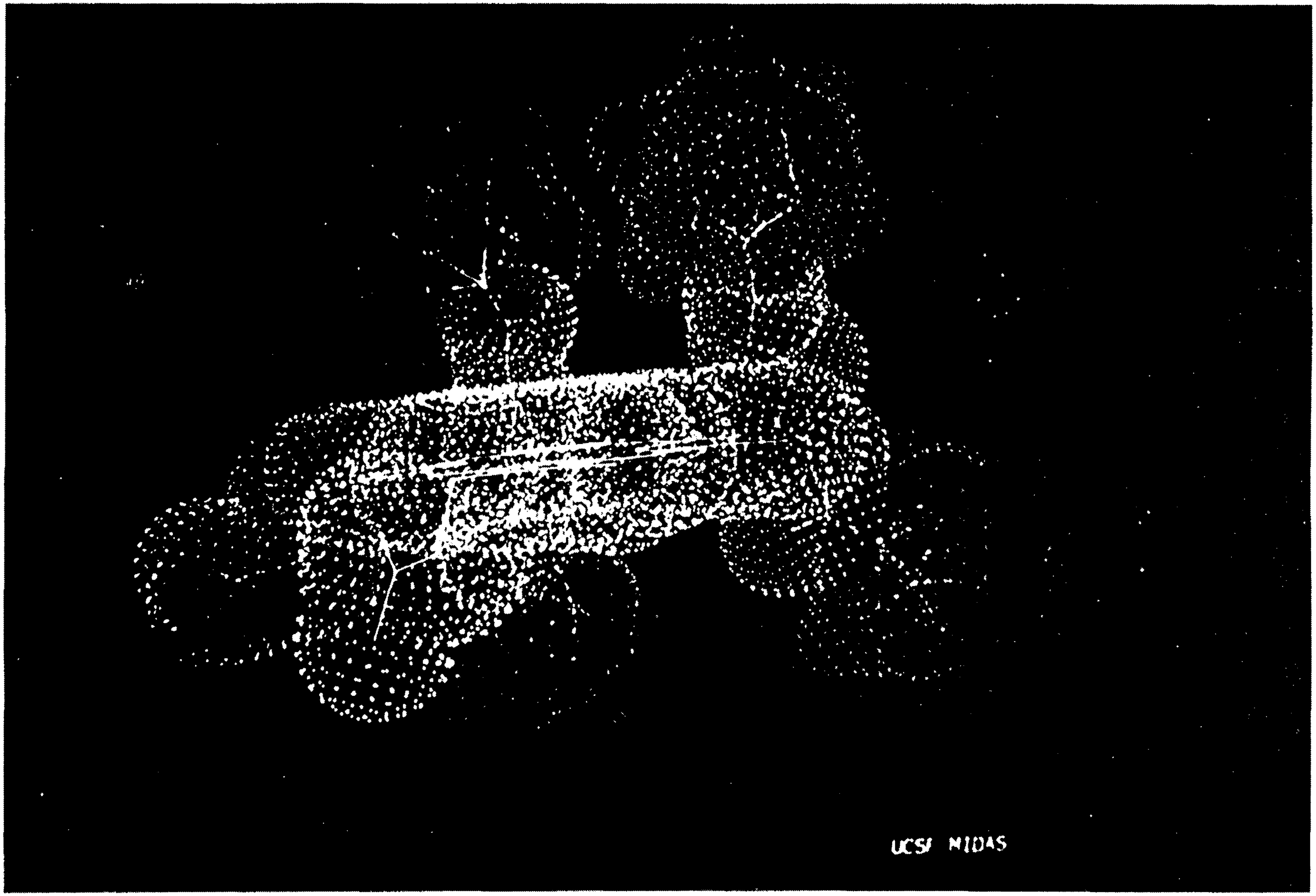
UCSF MIDAS

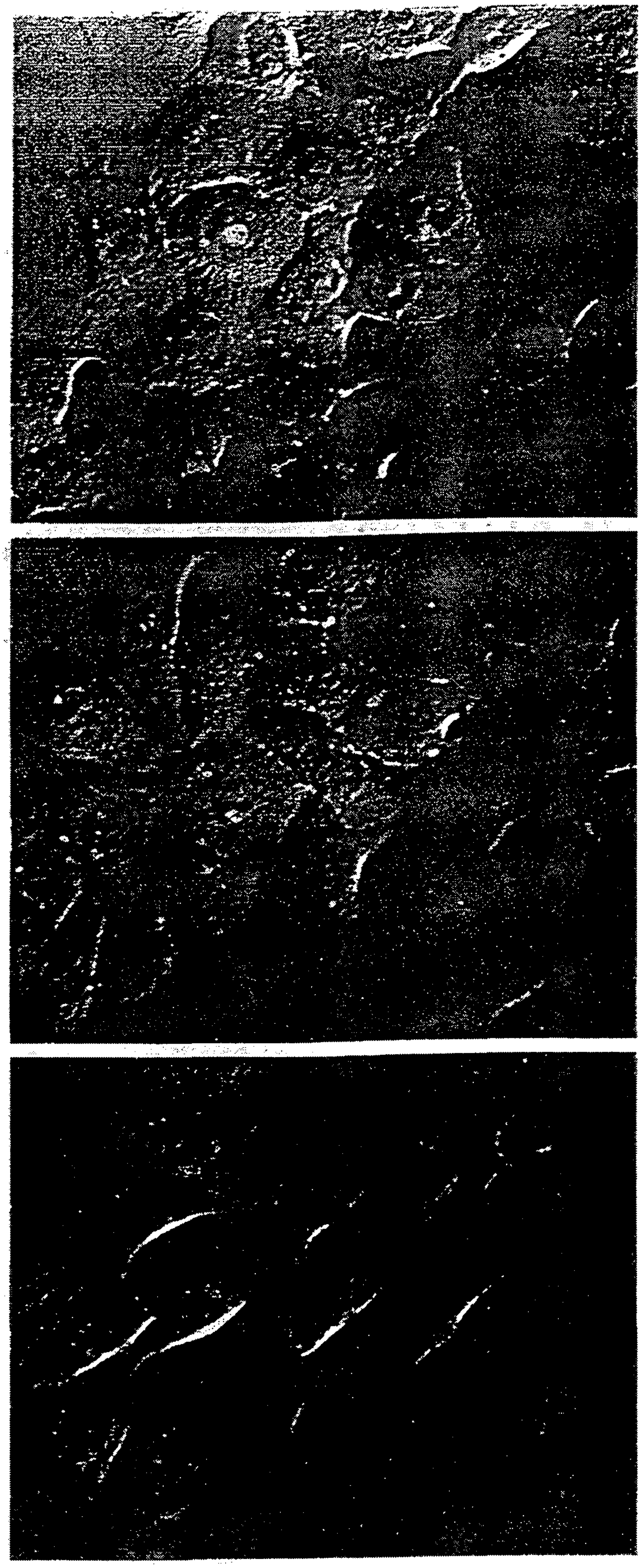

POTENTIAL TUMORS FOR BNCT TREATMENT

INITIAL TARGETS

- GLIOBLASTOMA MULTIFORME
- ANAPLASTIC ASTROCYTOMAS
- SQUAMOUS CELL CANCER OF THE HEAD AND NECK
- MELANOMA
- PANCREATIC CANCER

Purpose:

- Prepare an ESQ-based BNCT facility *at Berkeley Lab.*
- Perform multi-faceted *science-based* Phase I/II BNCT clinical trials starting in 1999.
- Advanced accelerator studies leading to the design of *hospital-based* BNCT facilities.
- Technology transfer of BNCT to medical centers for Phase III clinical trials.

Ted Ognibene

Lawrence Berkeley National Laboratory
Berkeley, CA

Beta-Delayed Proton Decays of ^{27}P and ^{31}Cl

T. J. Ognibene, J. Powell, D. M. Moltz,
M. W. Rowe and Joseph Cerny

88-Inch Cyclotron

Department of Chemistry,
Lawrence Berkeley National Laboratory,
University of California, Berkeley

Outline

- Introduction
- Experimental Techniques
- Results
    - ^{27}P
    - ^{31}Cl
- Conclusions

$$T_Z = \frac{N-Z}{2}$$

April 1996

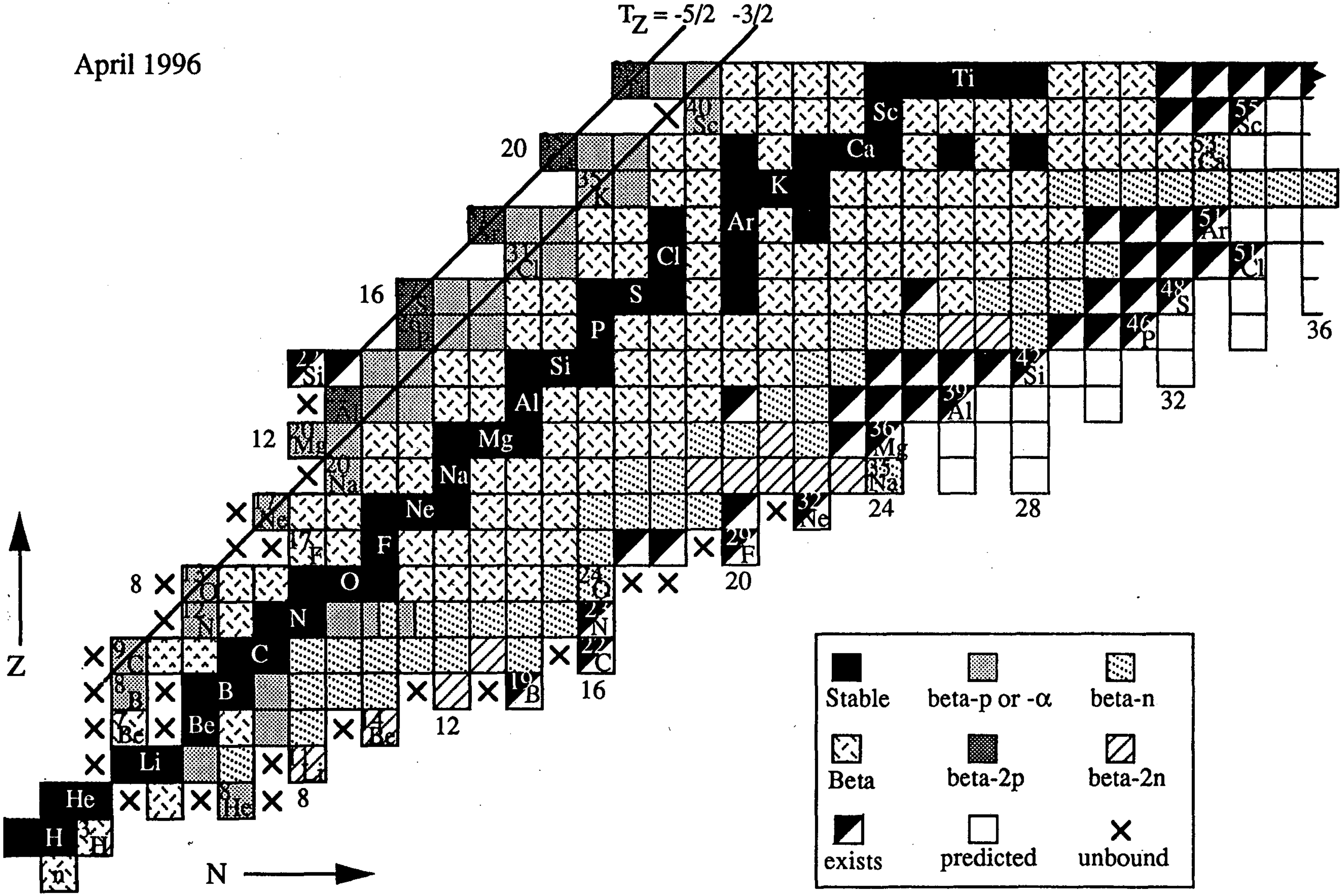

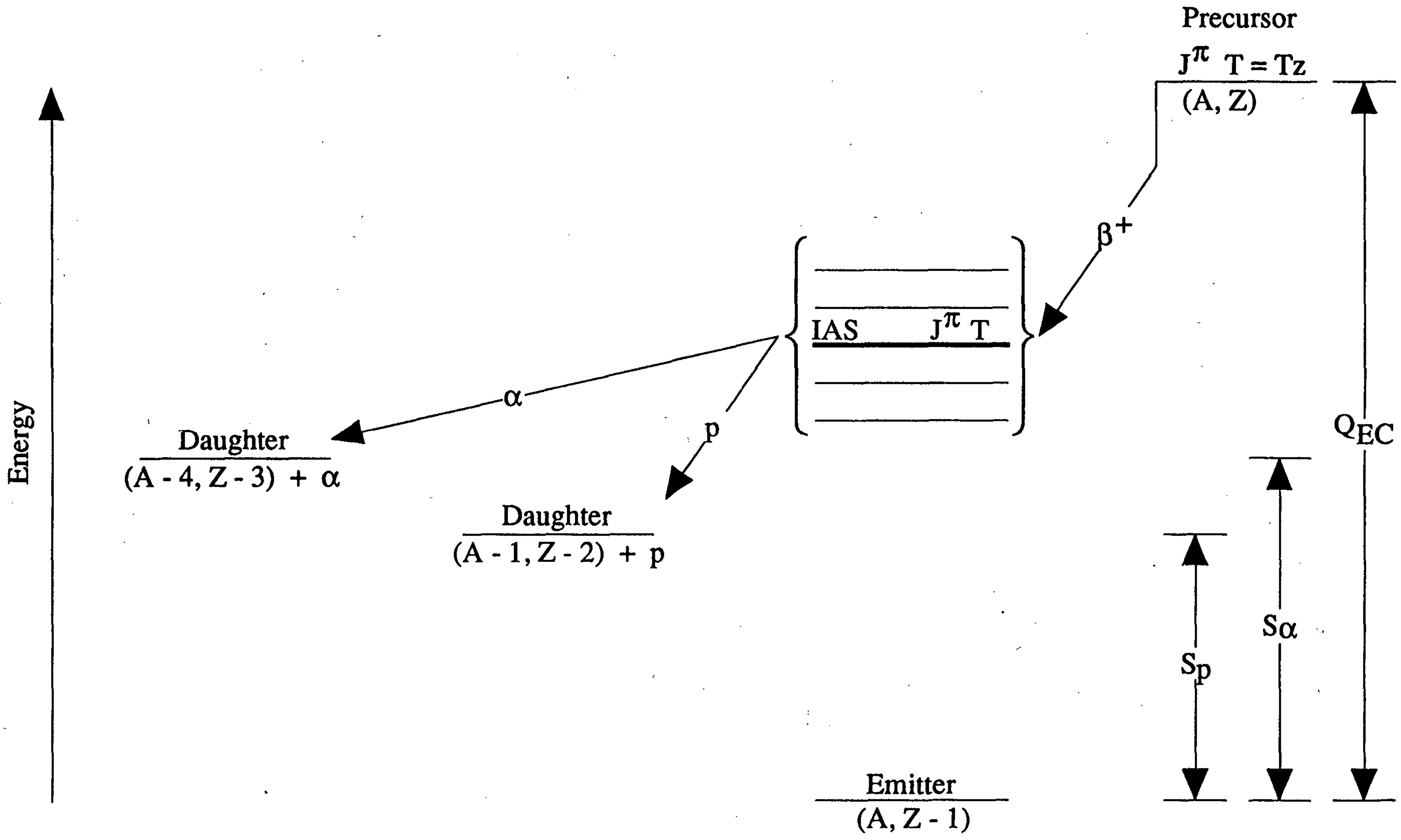
Precursor
J^{π} T = Tz
(A, Z)
β^+
IAS J^{π} T
α
p
Daughter
(A - 4, Z - 3) + α
Daughter
(A - 1, Z - 2) + p
Emitter
(A, Z - 1)
Q_{EC}
Sα
Sp
Energy

Goals

- Shell Model Tests

$$ft = \frac{K}{g_v^2 <1>^2 + g_a^2 <\sigma\tau>^2}$$

- Mass Models

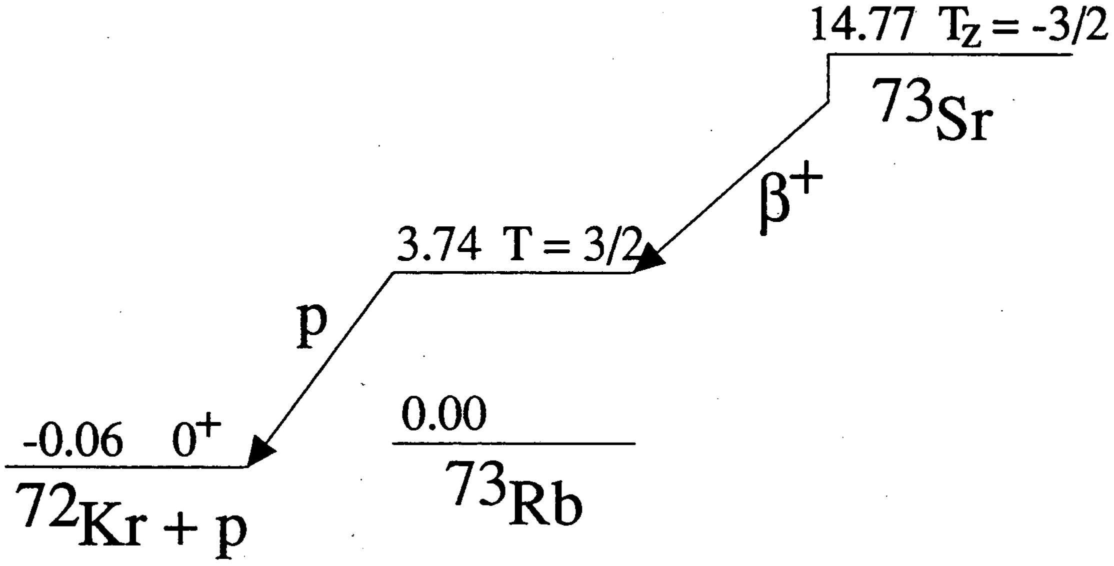

- Nuclear Astrophysics

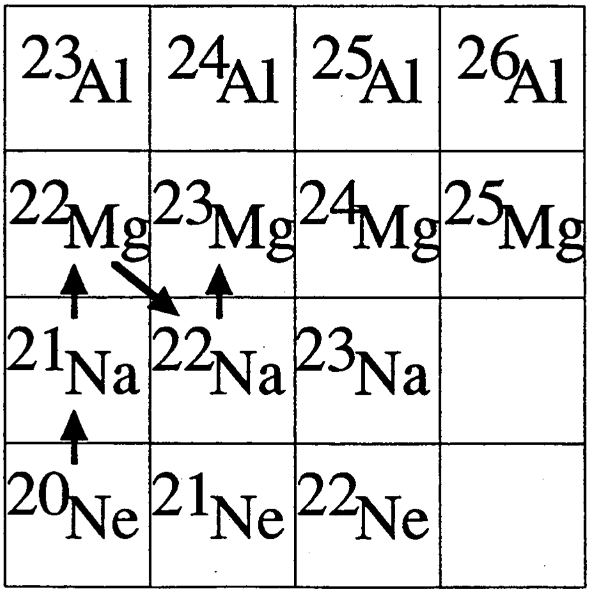

^{23}Al	^{24}Al	^{25}Al	^{26}Al
^{22}Mg	^{23}Mg	^{24}Mg	^{25}Mg
^{21}Na	^{22}Na	^{23}Na	
^{20}Ne	^{21}Ne	^{22}Ne	

The Beta-Delayed Proton Emission of ^{27}P and ^{31}Cl

$$^{27}\mathrm{P} \xrightarrow{\beta^{+}\nu} {}^{27}\mathrm{Si}^{*} \rightarrow {}^{26}\mathrm{Al} + \mathrm{p}$$

$$^{27}\mathrm{P(QEC)} = 11.6\ \mathrm{MeV}$$

$$^{31}\mathrm{Cl} \xrightarrow{\beta^{+}\nu} {}^{31}\mathrm{S}^{*} \rightarrow {}^{30}\mathrm{P} + \mathrm{p}$$

$$^{31}\mathrm{Cl(QEC)} = 12.0\ \mathrm{MeV}$$

$$ft = \frac{6170\ \mathrm{sec}}{B(F) + B(GT)}$$

$$B(F) = (T - T_Z)(T + T_Z + 1) \text{ for } \Delta T = \Delta J = 0$$
$$= 0 \text{ for } T_i \neq T_f,\ J_i \neq J_f$$

$$B(GT) = \frac{g_a^2}{g_V^2}\langle\sigma\tau\rangle^2 \text{ for } \Delta J = 0, \pm 1$$

$$f = \int_{1}^{W_0} F(Z,W)W(W^2-1)^{1/2}(W_0-W)^2\,dW$$

W = positron energy in units of $m_e c^2$

$$F(Z,W) = \frac{2\pi Ze^2}{\hbar v\left(1-\exp\left(\frac{2\pi Ze^2}{\hbar v}\right)\right)}$$

SETUP FOR THE PHOSPHORUS AND CHLORINE βp EXPERIMENTS

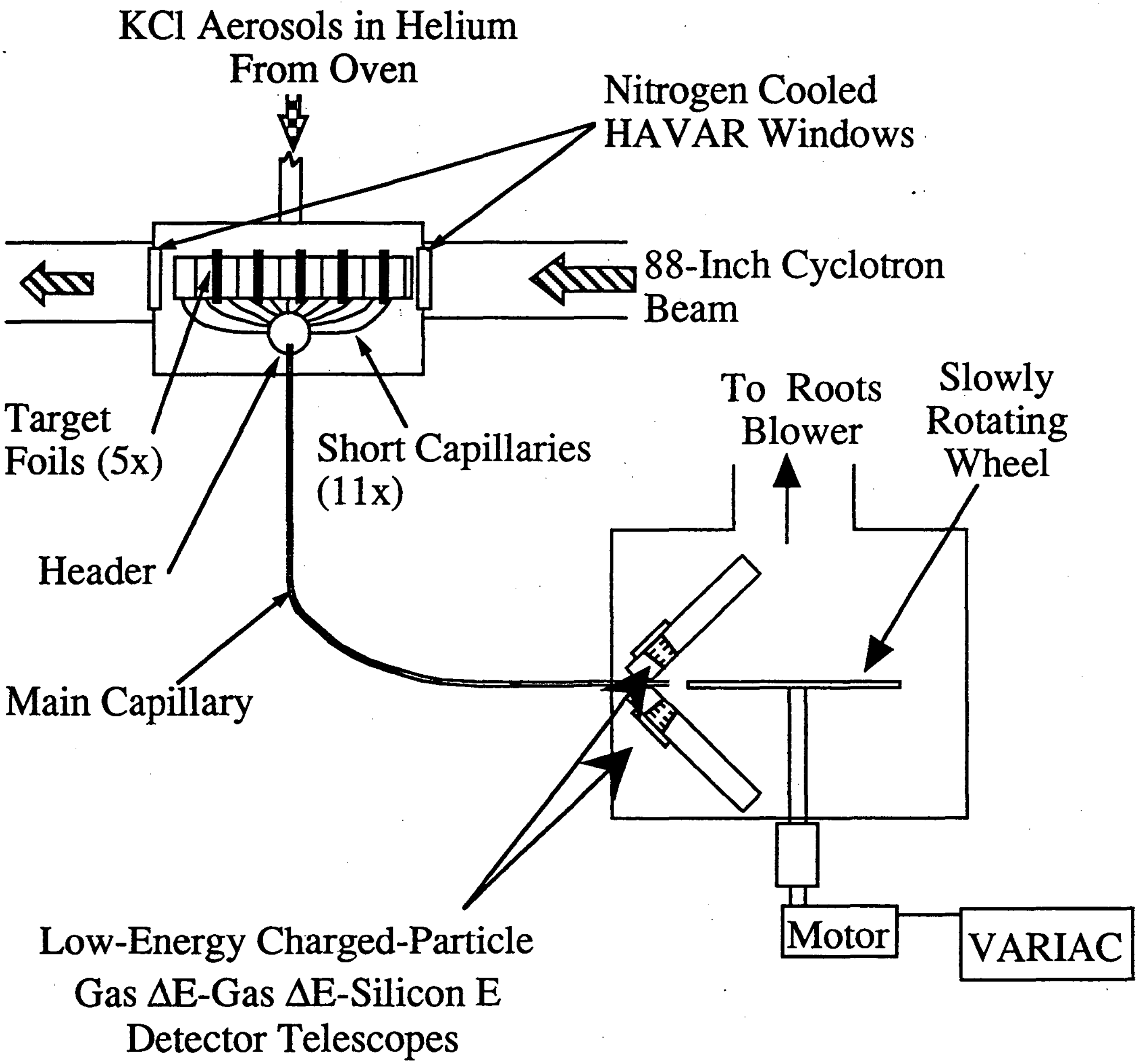

Cross Section
Low-Energy Charged-Particle
Gas ΔE-Gas ΔE-Silicon E Detector Telescope

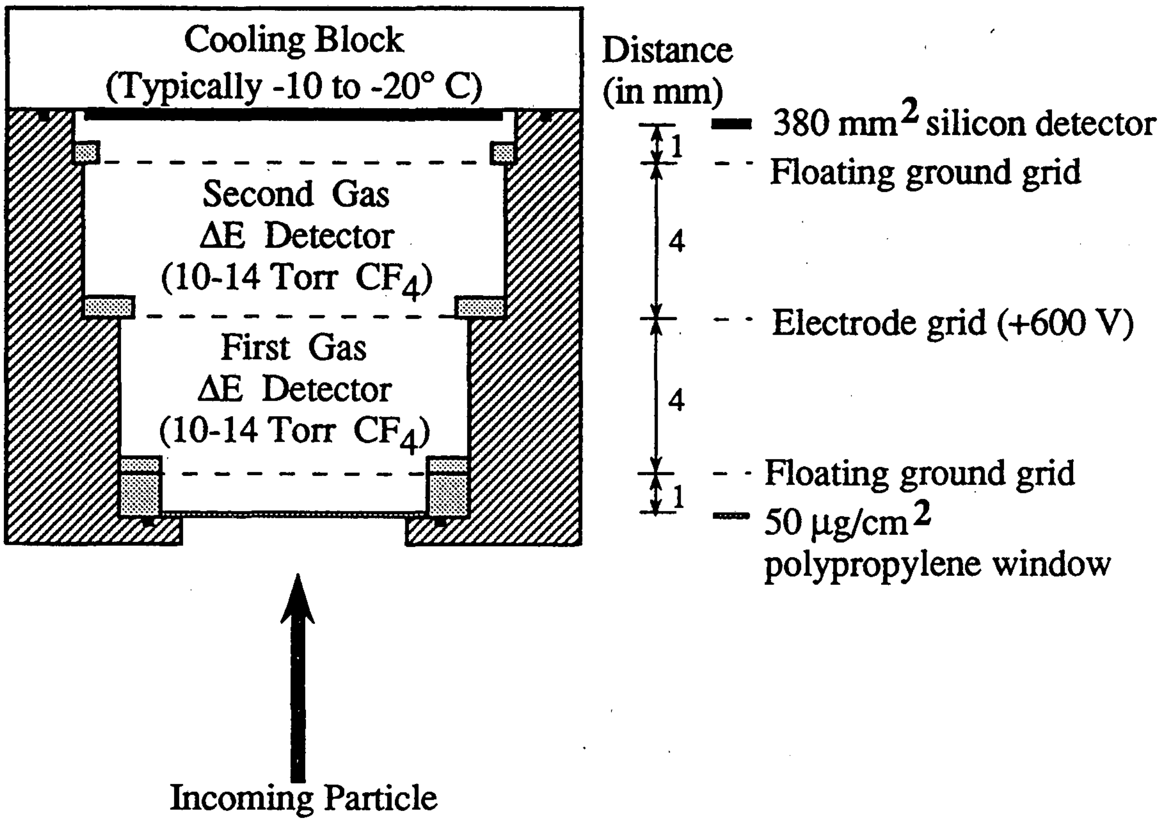

Features

- Low Energy Threshold
- Particle Identification In High Beta Backgrounds

Triple Coincidence Gating

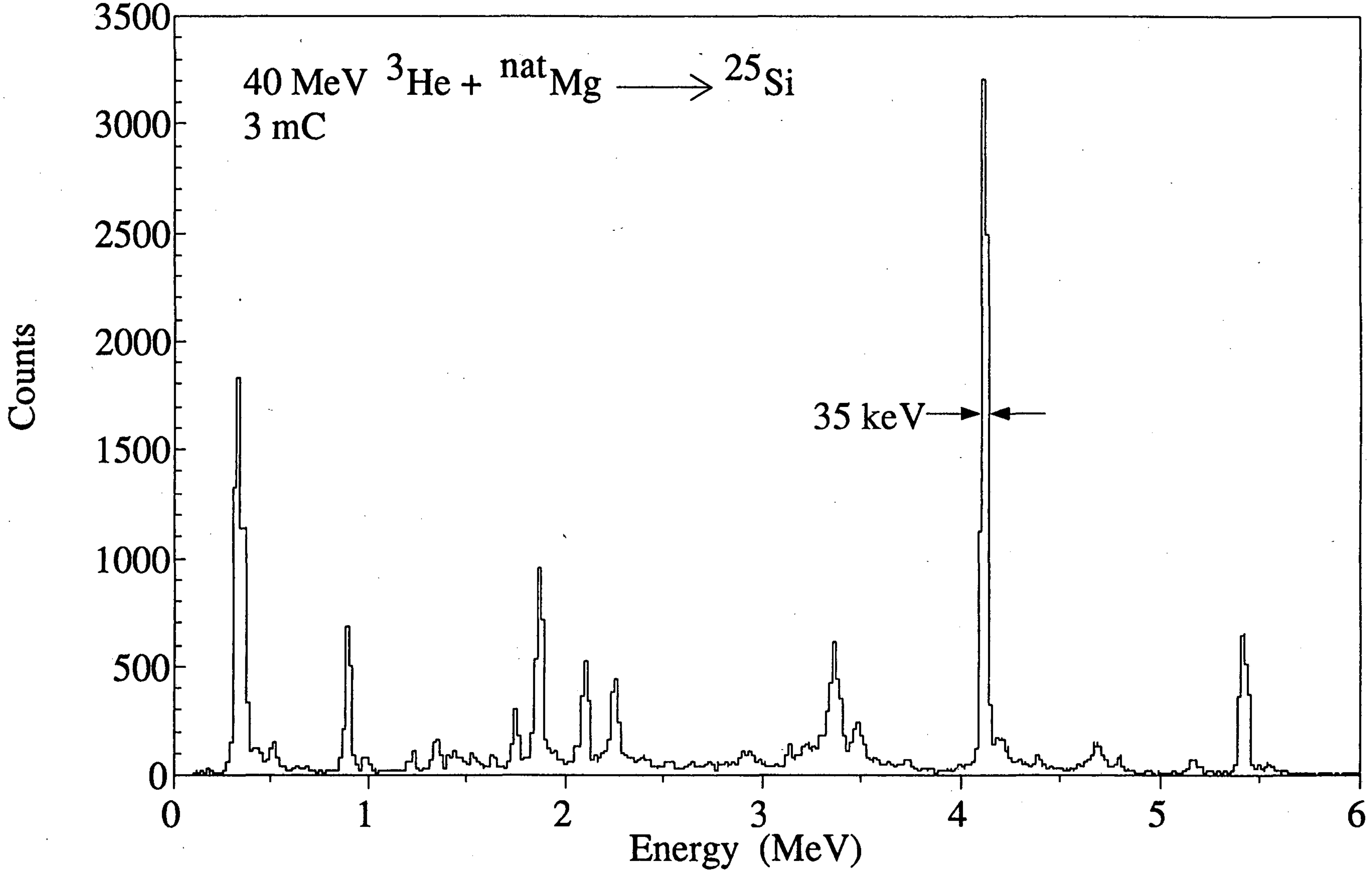
40 MeV ^{3}He + ^{nat}Mg ⟶ ^{25}Si
3 mC
35 keV
Counts
Energy (MeV)
0
500
1000
1500
2000
2500
3000
3500
0
1
2
3
4
5
6

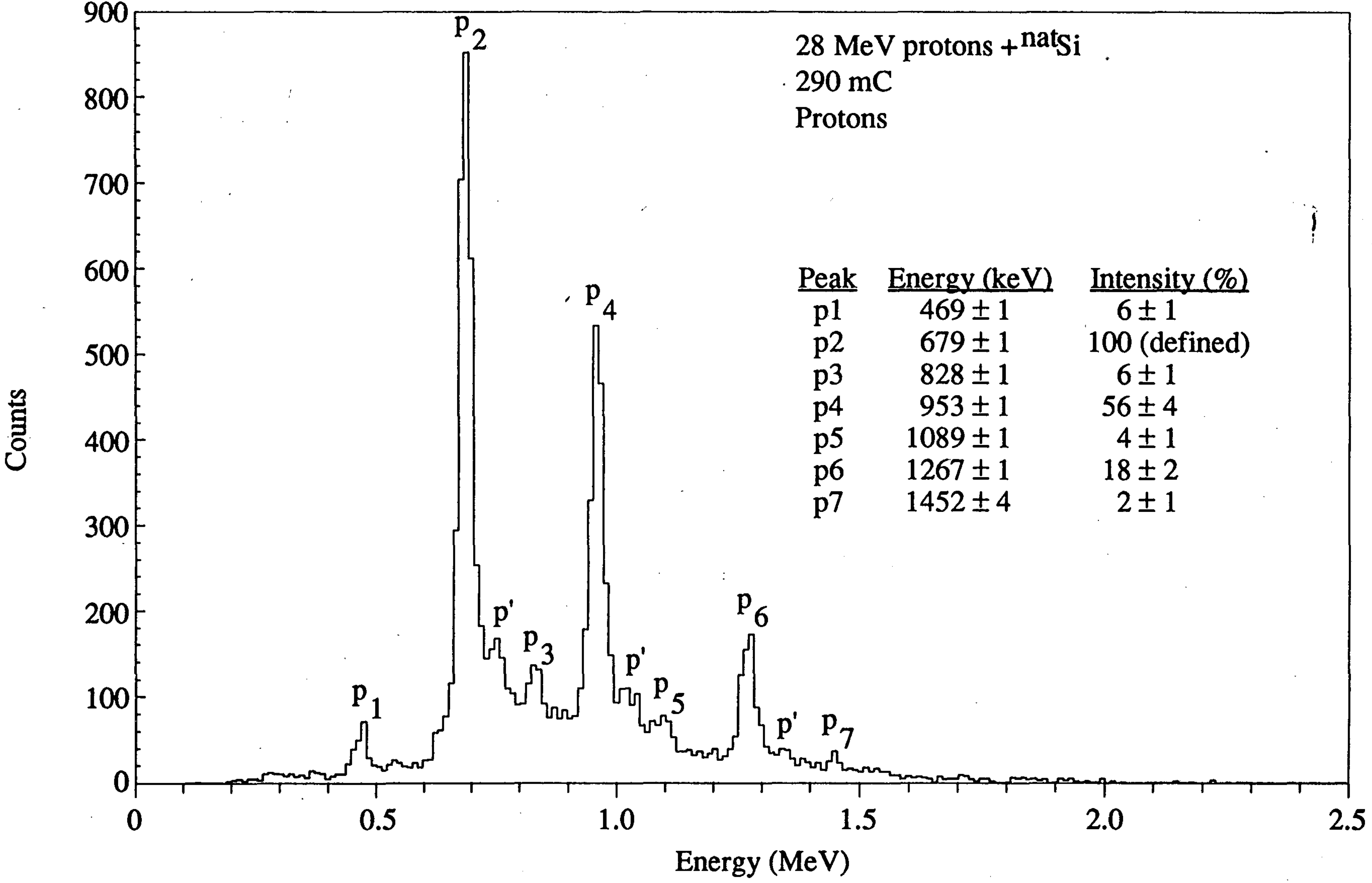

Peak	Energy (keV)	Intensity (%)
p1	469 ± 1	6 ± 1
p2	679 ± 1	100 (defined)
p3	828 ± 1	6 ± 1
p4	953 ± 1	56 ± 4
p5	1089 ± 1	4 ± 1
p6	1267 ± 1	18 ± 2
p7	1452 ± 4	2 ± 1

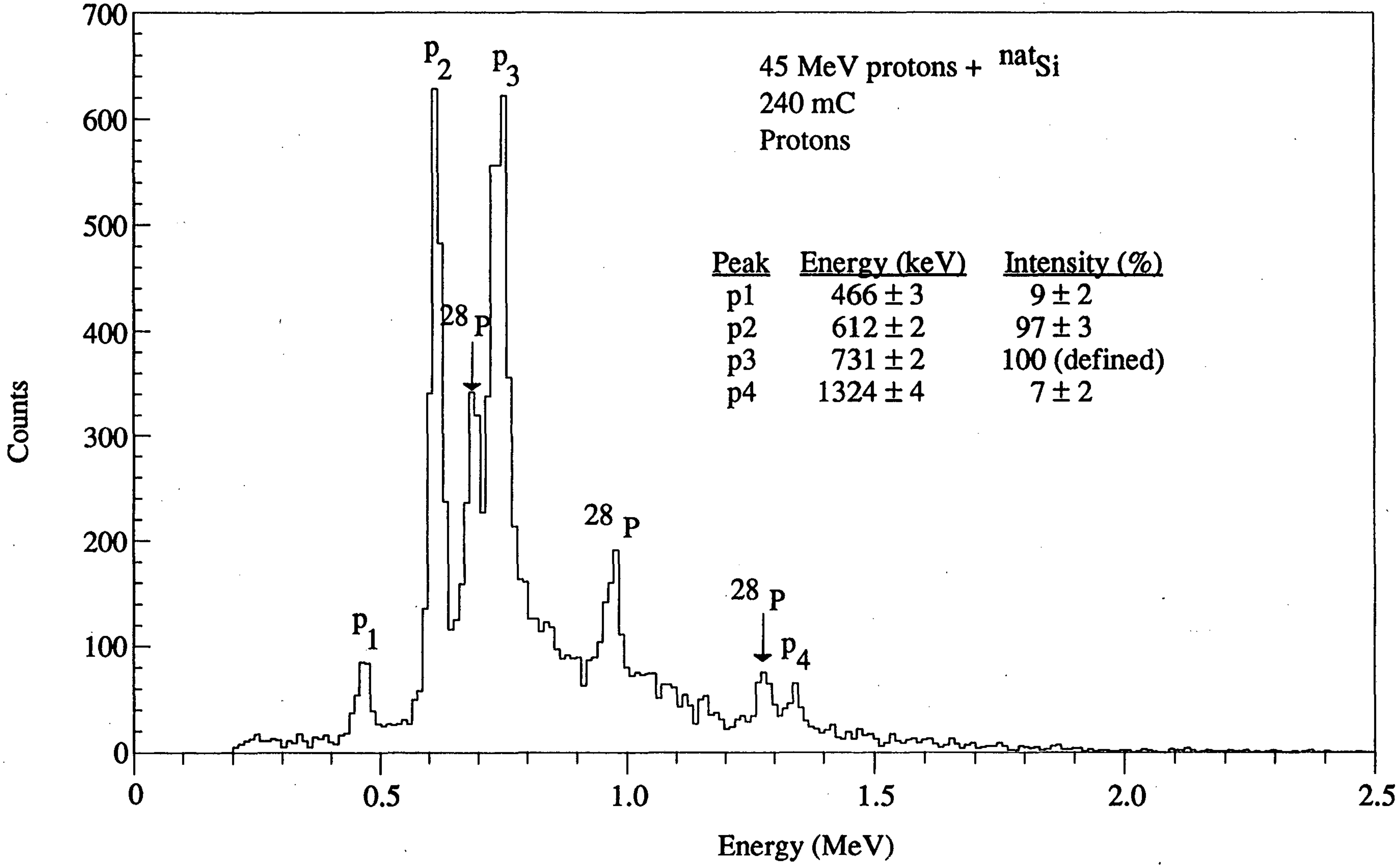

Peak	Energy (keV)	Intensity (%)
p1	466 ± 3	9 ± 2
p2	612 ± 2	97 ± 3
p3	731 ± 2	100 (defined)
p4	1324 ± 4	7 ± 2

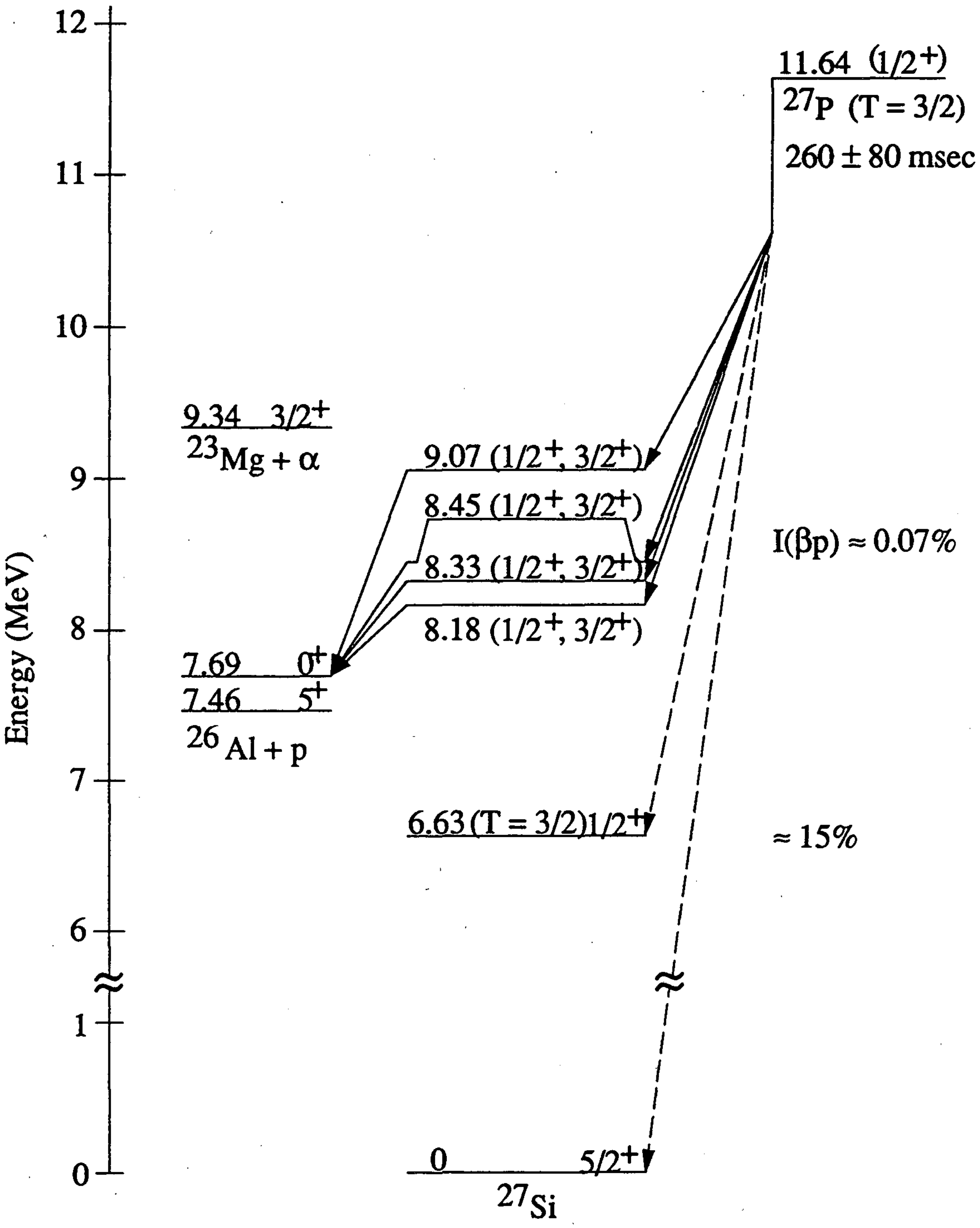

Peak	Energy (keV)	Intensity (%)	E*(27Si)
p1	466 ± 3	9 ± 2	8176 ± 3
p2	612 ± 2	97 ± 3	8328 ± 2
p3	731 ± 2	100 (defined)	8451 ± 2
p4	1324 ± 4	7 ± 2	9067 ± 4

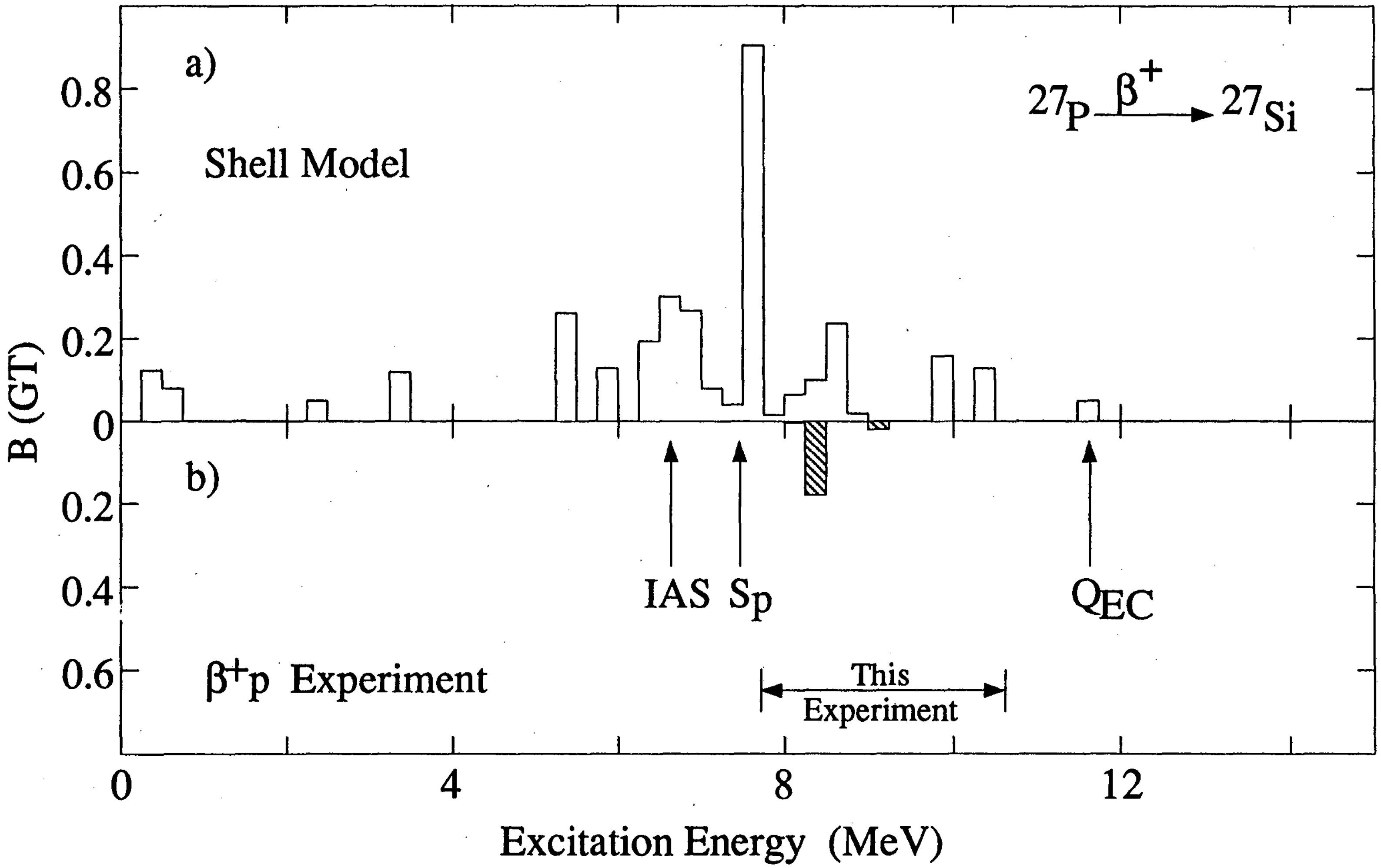
a)
Shell Model
$^{27}P \xrightarrow{\beta^+} {^{27}Si}$
b)
IAS
Sp
Q_{EC}
β^+p Experiment
This Experiment
B (GT)
0.8
0.6
0.4
0.2
0
0.2
0.4
0.6
0
4
8
12
Excitation Energy (MeV)

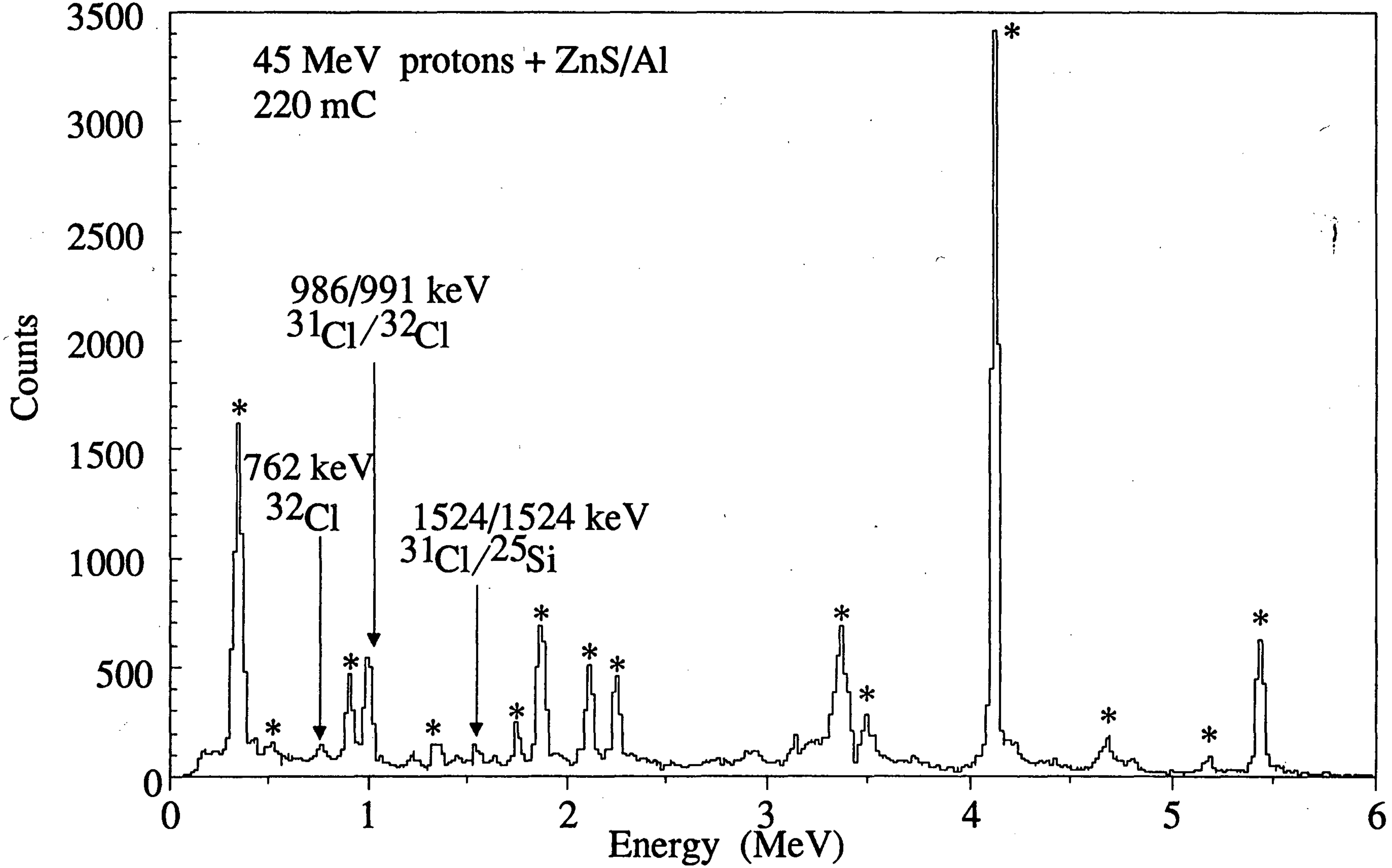
45 MeV protons + ZnS/Al
220 mC
986/991 keV
^{31}Cl/^{32}Cl
762 keV
^{32}Cl
1524/1524 keV
^{31}Cl/^{25}Si
*
Counts
Energy (MeV)
0
500
1000
1500
2000
2500
3000
3500
0
1
2
3
4
5
6

^{31}Cl Beta-Delayed Proton Groups.

	Relative Proton Intensity	
Ep[a)]	This Work	Äystö *et al.*
845 ± 30	b)	3 ± 2
986 ± 10	100[c)]	100 ± 2[c)]
1173 ± 30	b)	3 ± 2
1520 ± 15	11 ± 5	23 ± 6
1695 ± 20	≤ 1	10 ± 3
1827 ± 20	≤ 1	13 ± 4
2113 ± 30	≤ 1	7 ± 3
2204 ± 30	≤ 1	6 ± 3

a) Energies are reported in keV in the laboratory system and are from Äystö *et al.*

b) These proton groups could not be positively identified because of the significant levels of contamination of ^{25}Si beta-delayed protons.

c) Defined.

- Conclusions

  New proton groups in $^{27,28}P$

  Shell Model Tests

  βp groups in ^{31}Cl

- Future Work

  ^{27}P and ^{31}Cl βγ decay studies

  Targets for ^{31}Cl

David Vieira

Los Alamos National Laboratory
Los Alamos, NM

Bodega Bay

Joe's 60th

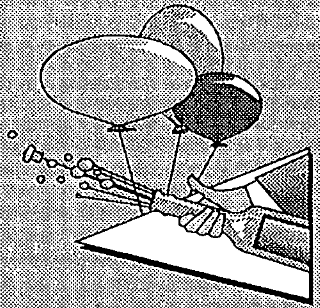

Dave Vieira
April 15, 1996

UCB/LBL graduate student days

Cerny's group: '73 - '77
- post-docs: Rick Gough, Mike Zisman, Nick Jelley, Gary Kekelis, Rainer Jahn, Hugh Evans (visitor from Queen's Univ.)
- grad. students: Rich Sextro, Gordon Wozniak, John McDonald, Ken Wilcox, Bob Weisenmiller, DJV, Dieter Stahel, Dennis Moltz, Jan Wouters, Alden Bice, Mike Cable

Good times / set the stage for a career
- stimulating environment
- working with others
- designing, fabricating & doing experiments
  Ray Burton, Jack Walton & the 88" shop
- developed the taste for small, but very challenging exps.
  "ones which you can get your hands around"

Outline (25 min.):
1. TOFI spectrometer - mass & decay properties of exotics
2. High-intensity, He-jet thin-target tests - radioactive beams
3. Trapping radioactive atoms - electroweak interaction exps.

Los Alamos

TOFI
TIME-OF-FLIGHT
ISOCHRONOUS
SPECTROMETER FOR
MASS MEASUREMENTS
OF EXOTIC NUCLEI

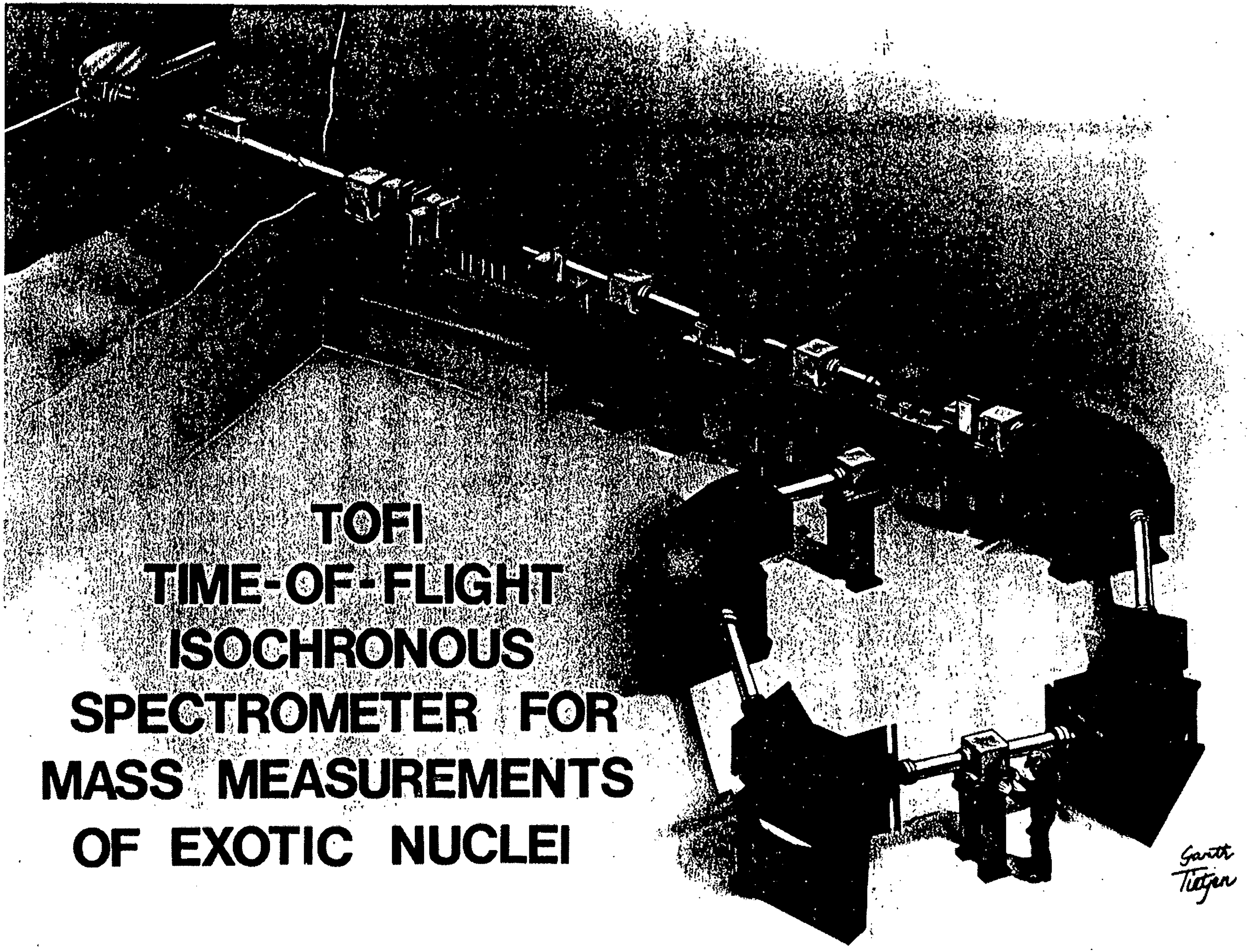

TOFI

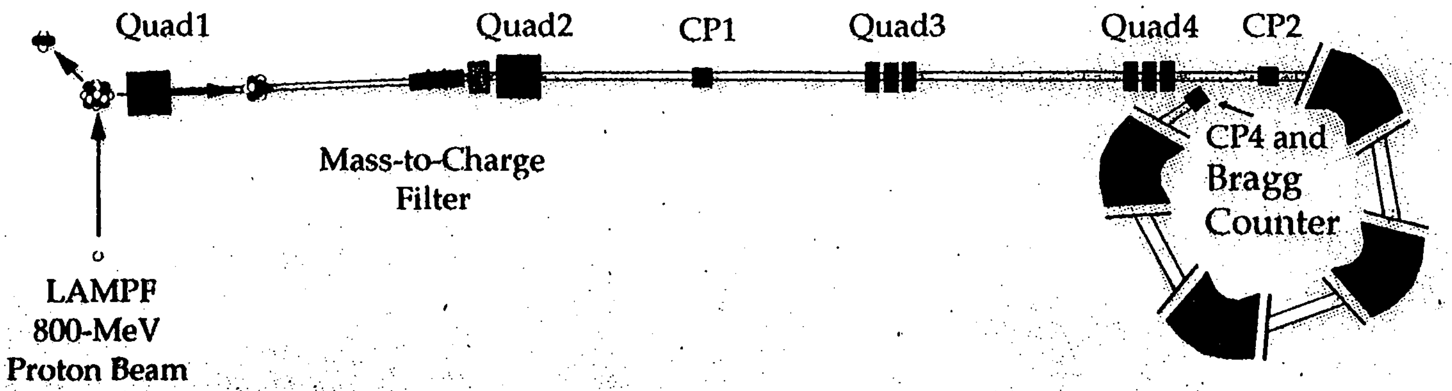

Experimental Setup

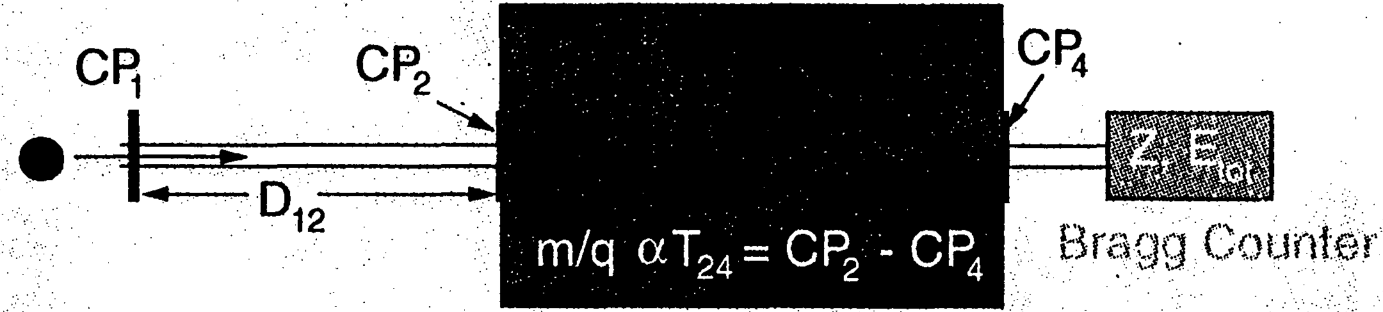

$$\left.\begin{aligned} T_{12} &= CP_1 - CP_2 \\ Vel &= D_{12} / T_{12} \\ m_{low} &= 2 \times E_{tot} / Vel^2 \end{aligned}\right\} \quad q = m_{low} / (m/q)$$

Los Alamos

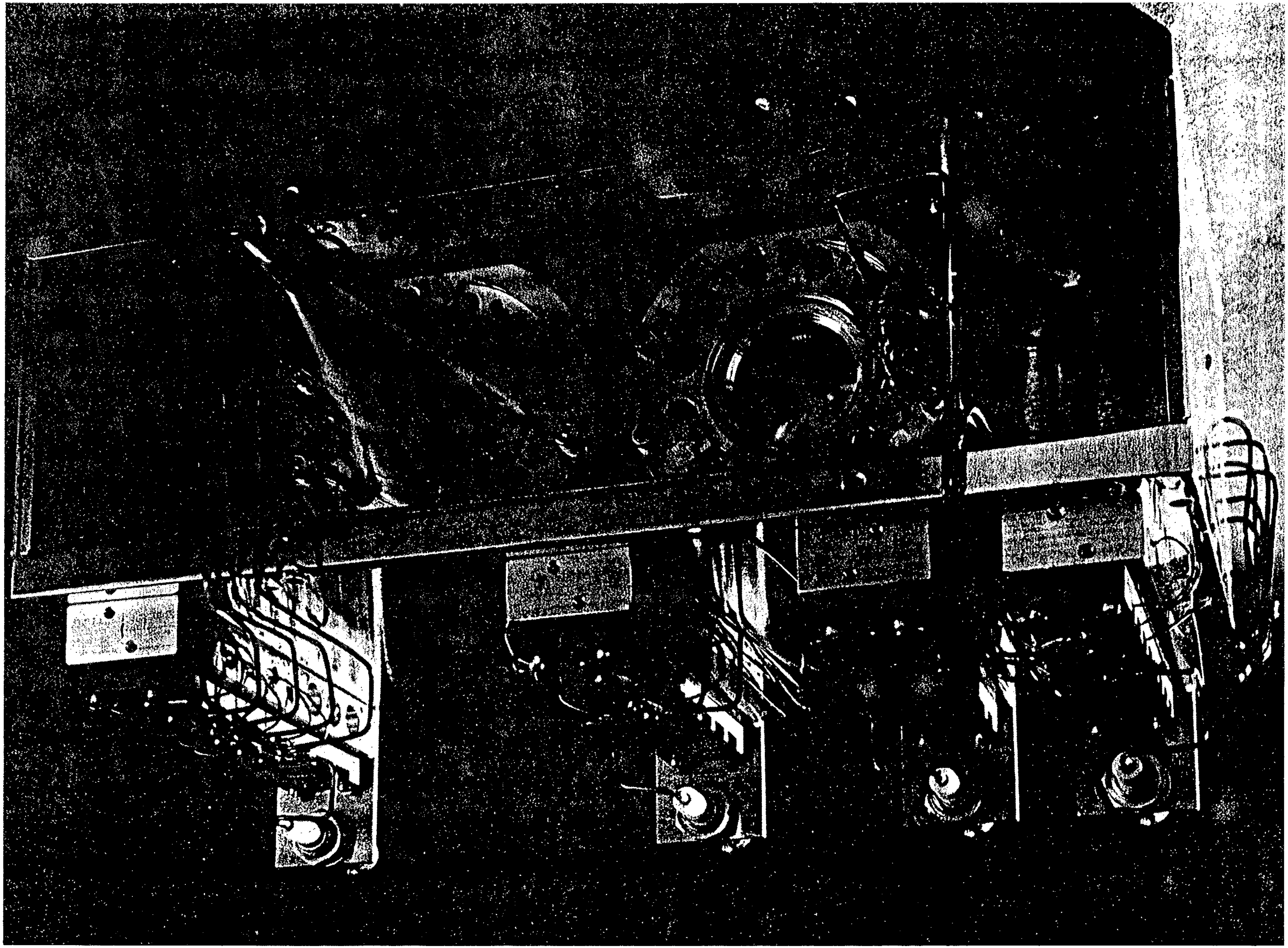

TOFI

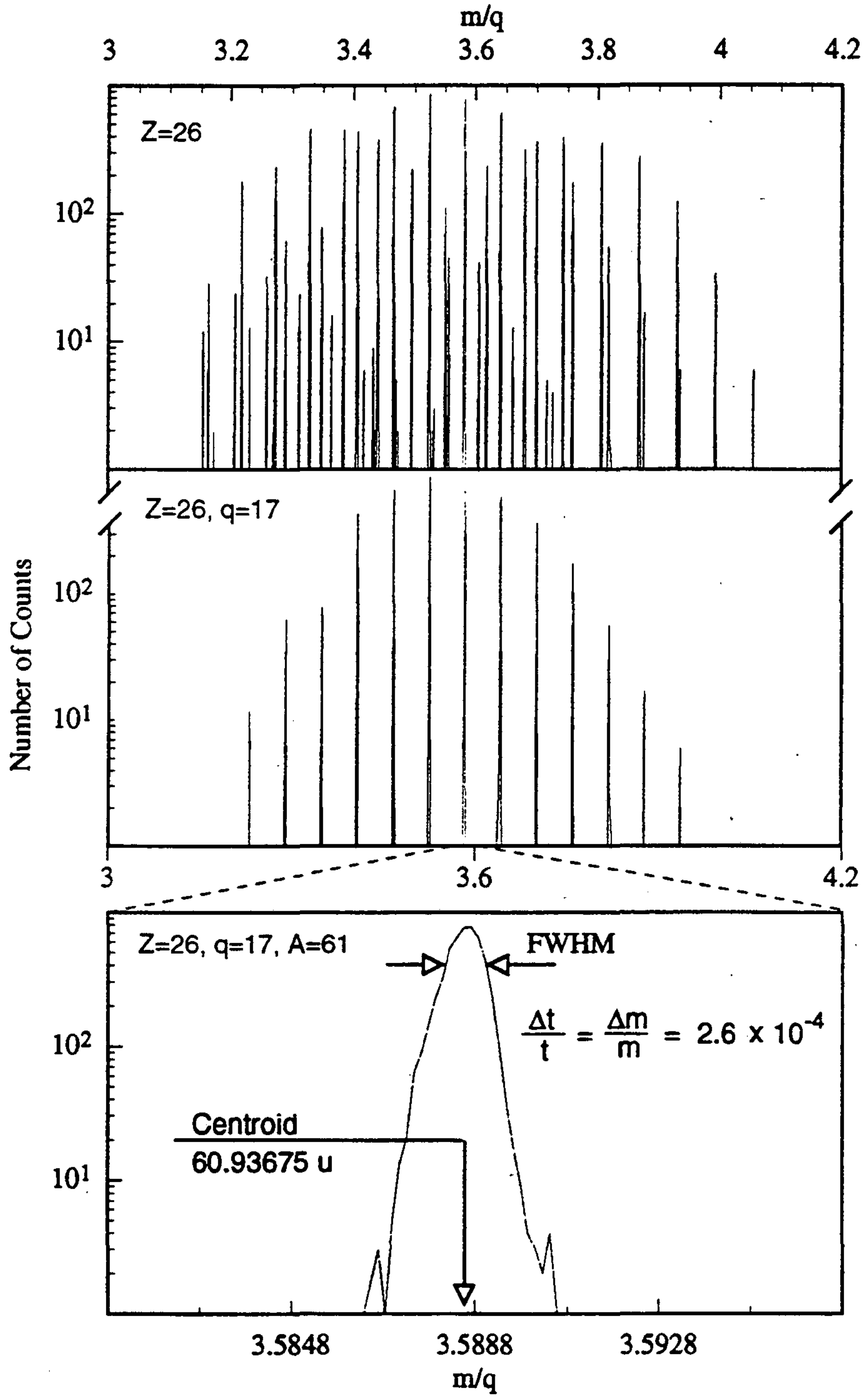
m/q
3
3.2
3.4
3.6
3.8
4
4.2
Z=26
10^2
10^1
Z=26, q=17
Number of Counts
10^2
10^1
3
3.6
4.2
Z=26, q=17, A=61
FWHM
$\frac{\Delta t}{t} = \frac{\Delta m}{m} = 2.6 \times 10^{-4}$
10^2
Centroid
60.93675 u
10^1
3.5848
3.5888
3.5928
m/q

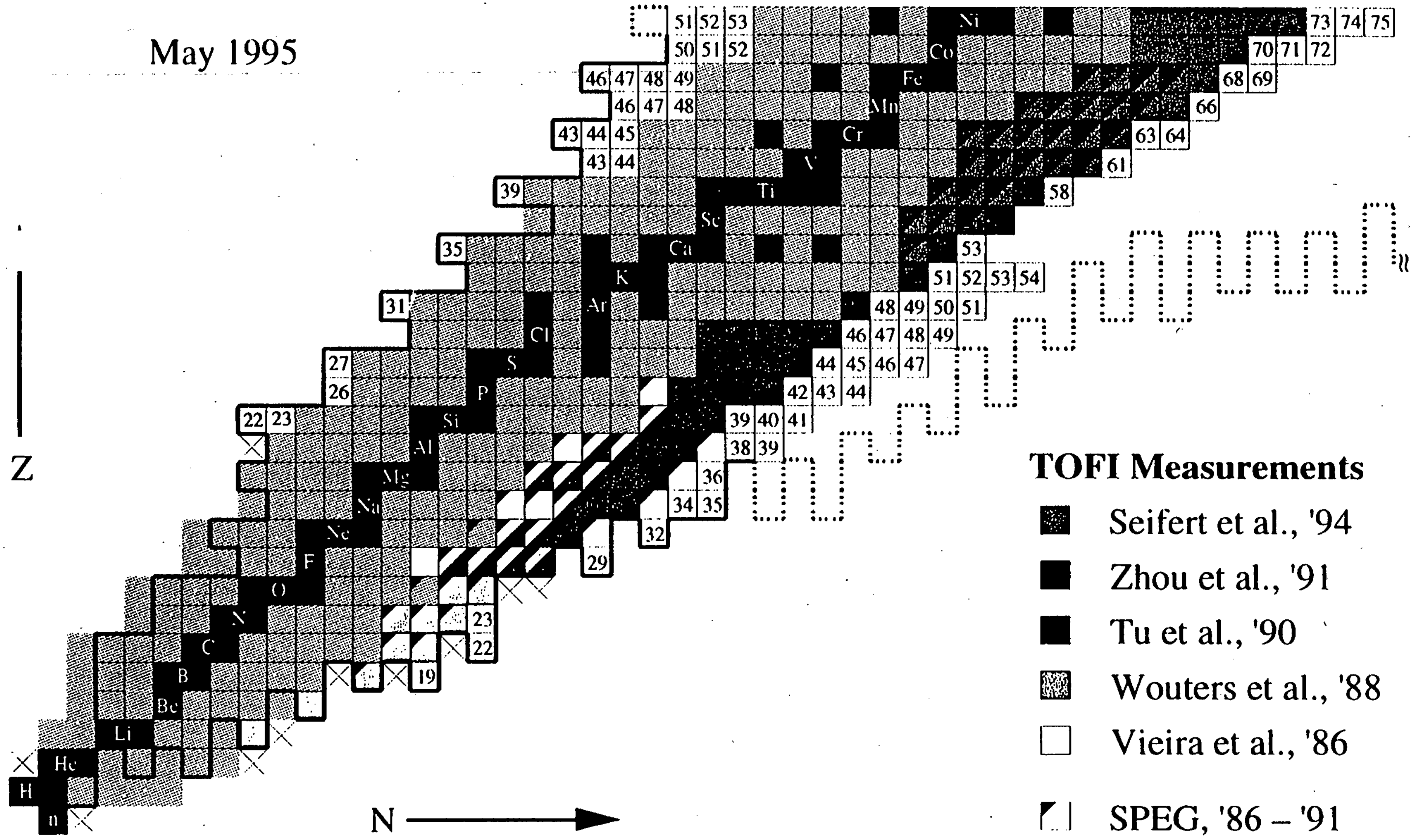
May 1995
Z
N
n
H
He
Li
Be
B
C
N
O
F
Ne
Na
Mg
Al
Si
P
S
Cl
Ar
K
Ca
Sc
Ti
V
Cr
Mn
Fe
Co
Ni
51 52 53 73 74 75
50 51 52 70 71 72
46 47 48 49 68 69
46 47 48 66
43 44 45 63 64
43 44 61
39 58
35 53
51 52 53 54
31 48 49 50 51
46 47 48 49
27 44 45 46 47
26 42 43 44
22 23 39 40 41
38 39
36
34 35
32
29
23
22
19
TOFI Measurements
Seifert et al., '94
Zhou et al., '91
Tu et al., '90
Wouters et al., '88
Vieira et al., '86
SPEG, '86 – '91

TOFI COLLABORATION

Los Alamos
Gil Butler
Larry Ulibarri
Dave Vieira
Jan Wouters

Utah State Univ.
Gordon Lind
**Xiao-Lin Tu*
**Xiao-Gong Zhou*

Battelle Northwest
Walt Hensley
Paul Reeder
Ray Warner

Visitors
**Hardy Seifert*
Tong-Yuan Zhou

INC DIVISION
Los Alamos

Recoil Tagging - β-n - Delayed Coin. Exp.

Detector Geometry

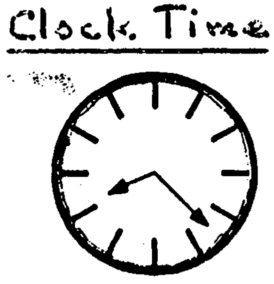

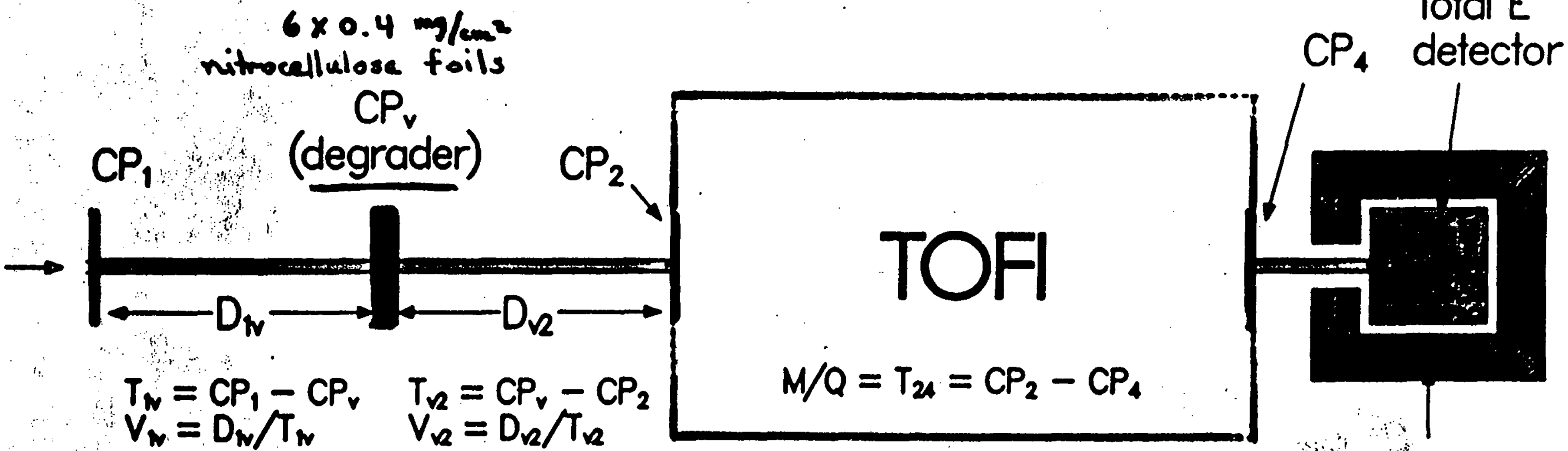

$T_{1v} = CP_1 - CP_v$
$V_{1v} = D_{1v}/T_{1v}$

$T_{v2} = CP_v - CP_2$
$V_{v2} = D_{v2}/T_{v2}$

$M/Q = T_{24} = CP_2 - CP_4$

CP: Channel–plate timing detector

Neutron detector

40 moderated ^{3}He prop. ctrs.

Charge:

$$M_{low} = 2 \times E_{tot}/V_{v2}^2$$
$$Q = M_{low} \,/\, (M/Q)$$

Z:

$$\Delta E = M \times (V_{1v}^2 - V_{v2}^2)/2$$
$$Z = f(\overline{V}, \Delta E)$$

Passive Degrader - ΔV^2 Techni ue

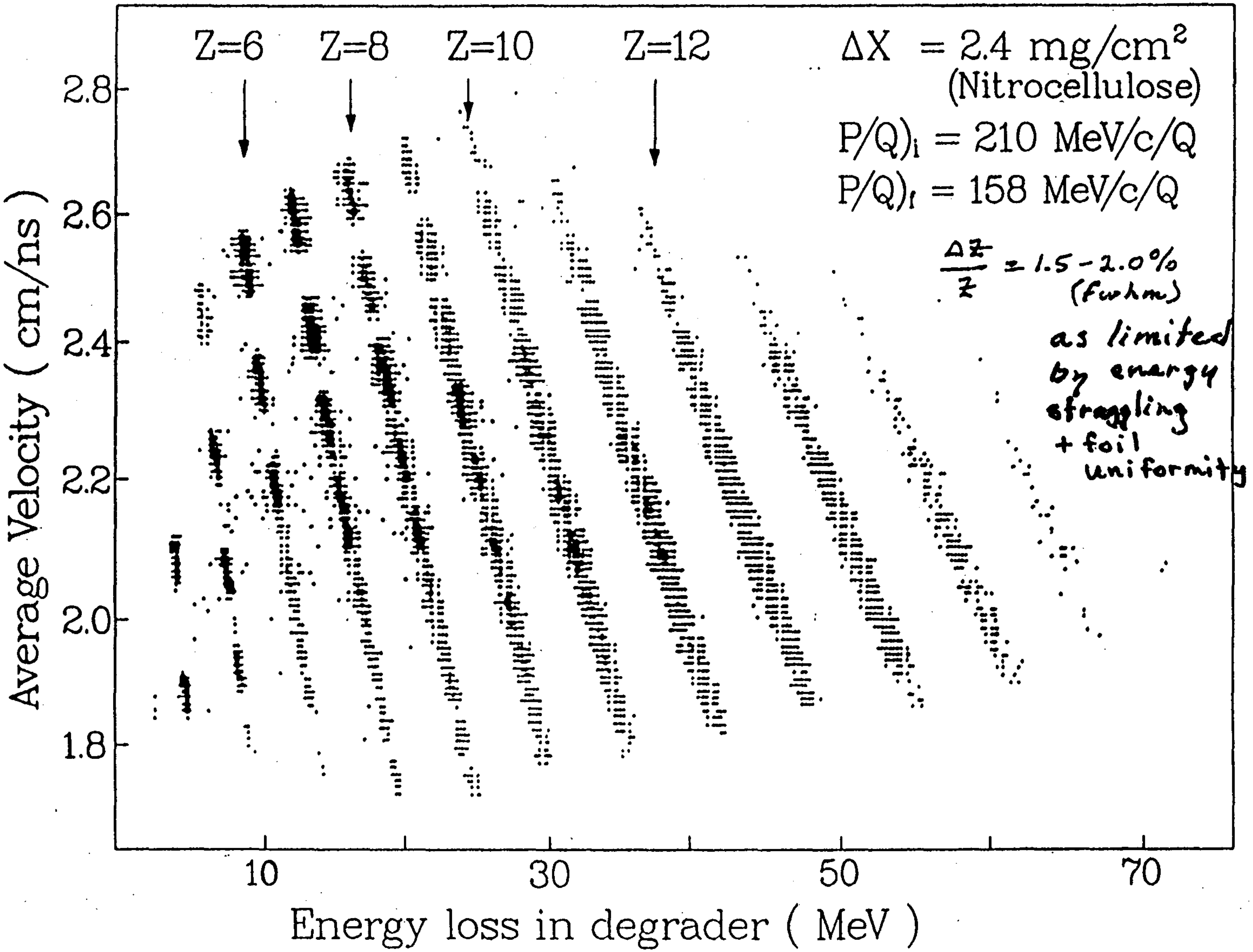

$\frac{\Delta Z}{Z} = 1.5 - 2.0\%$ (fwhm)

as limited by energy straggling + foil uniformity

M.S. thesis - Y.-K. Kim

(Utah State, 1989)

Delayed ion - neutron counting technique

11Li Beta-Neutron Coinc. Decay Curve

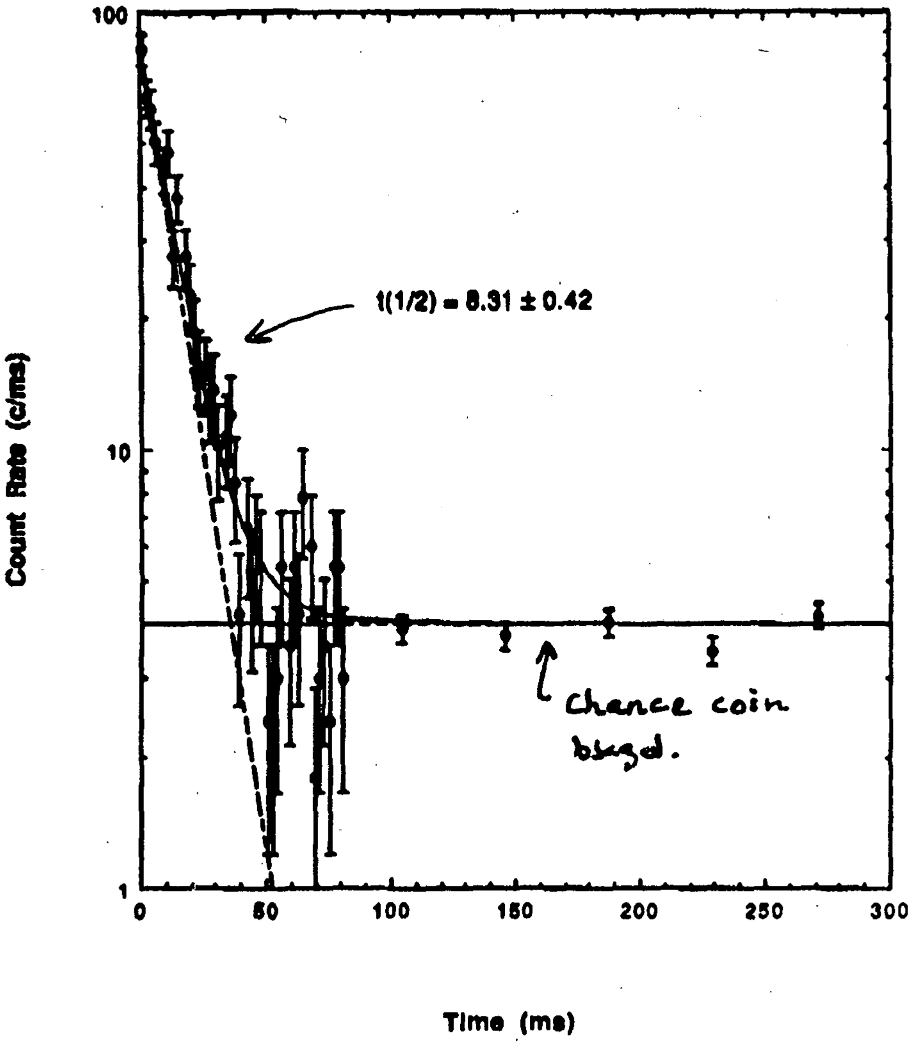

14Be Beta-Neutron Coinc. Decay Curve

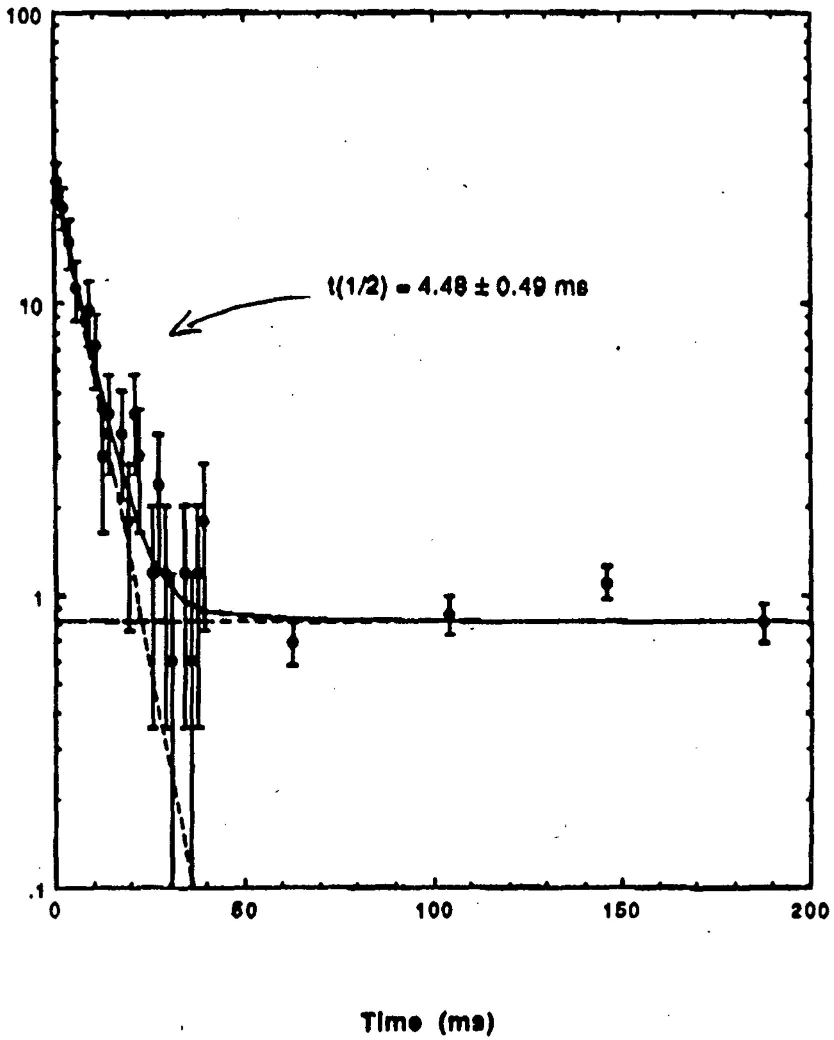

P. Reeder, etal. - 1992 data

Radioactive Beams at LAMPF

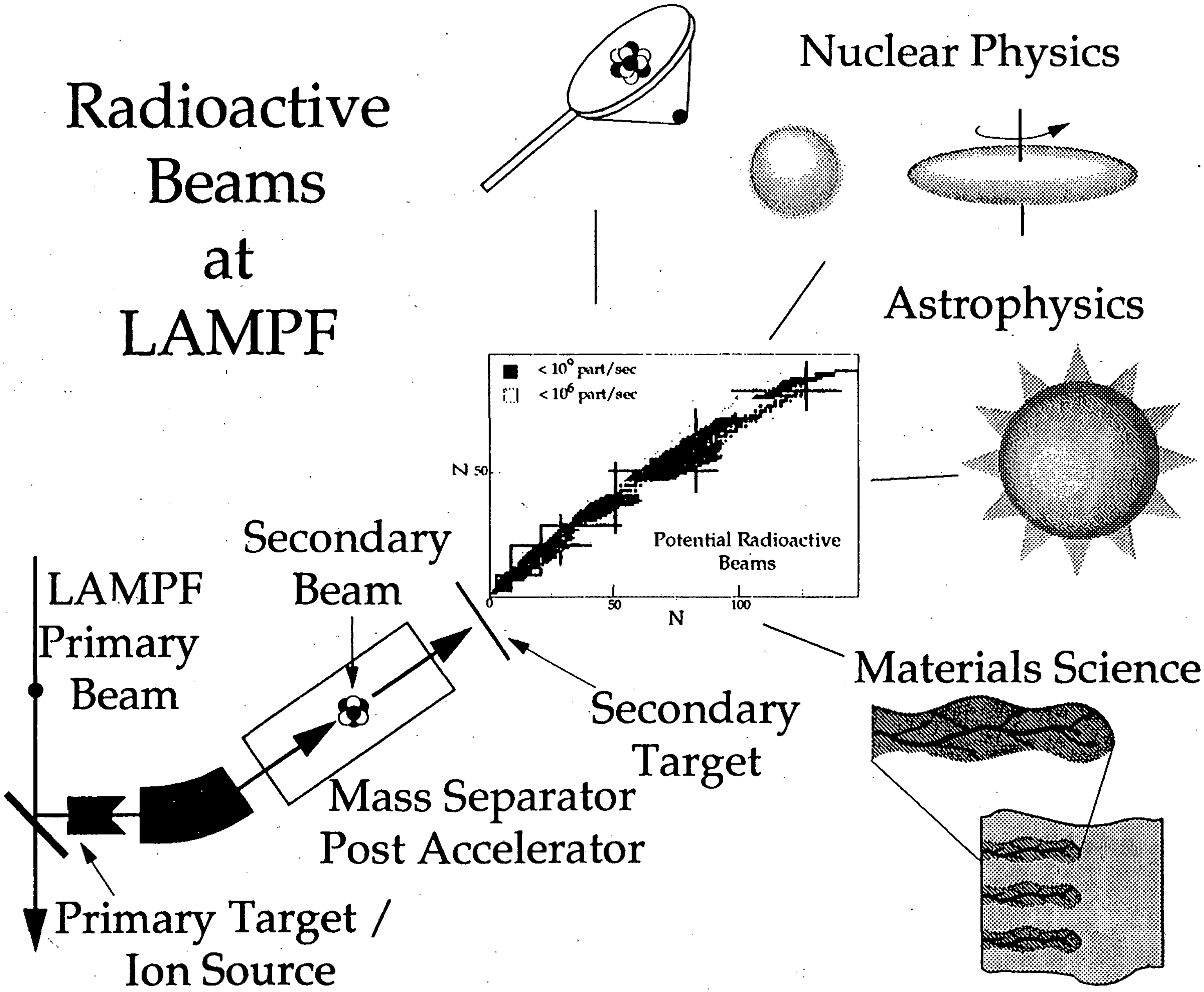

Nuclear Physics

Astrophysics

Materials Science

LAMPF Primary Beam

Secondary Beam

Secondary Target

Mass Separator Post Accelerator

Primary Target / Ion Source

He-jet Test Experiment

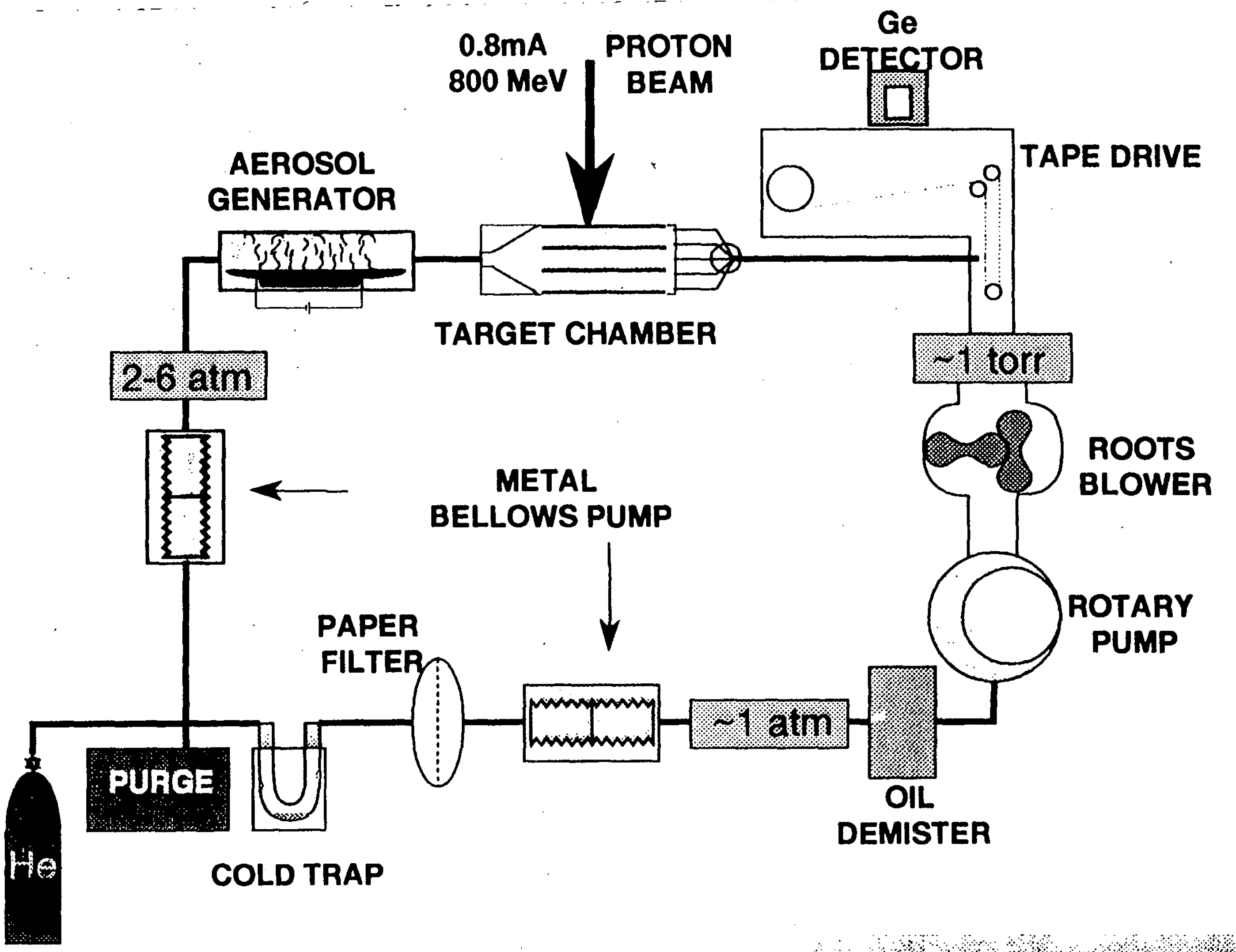

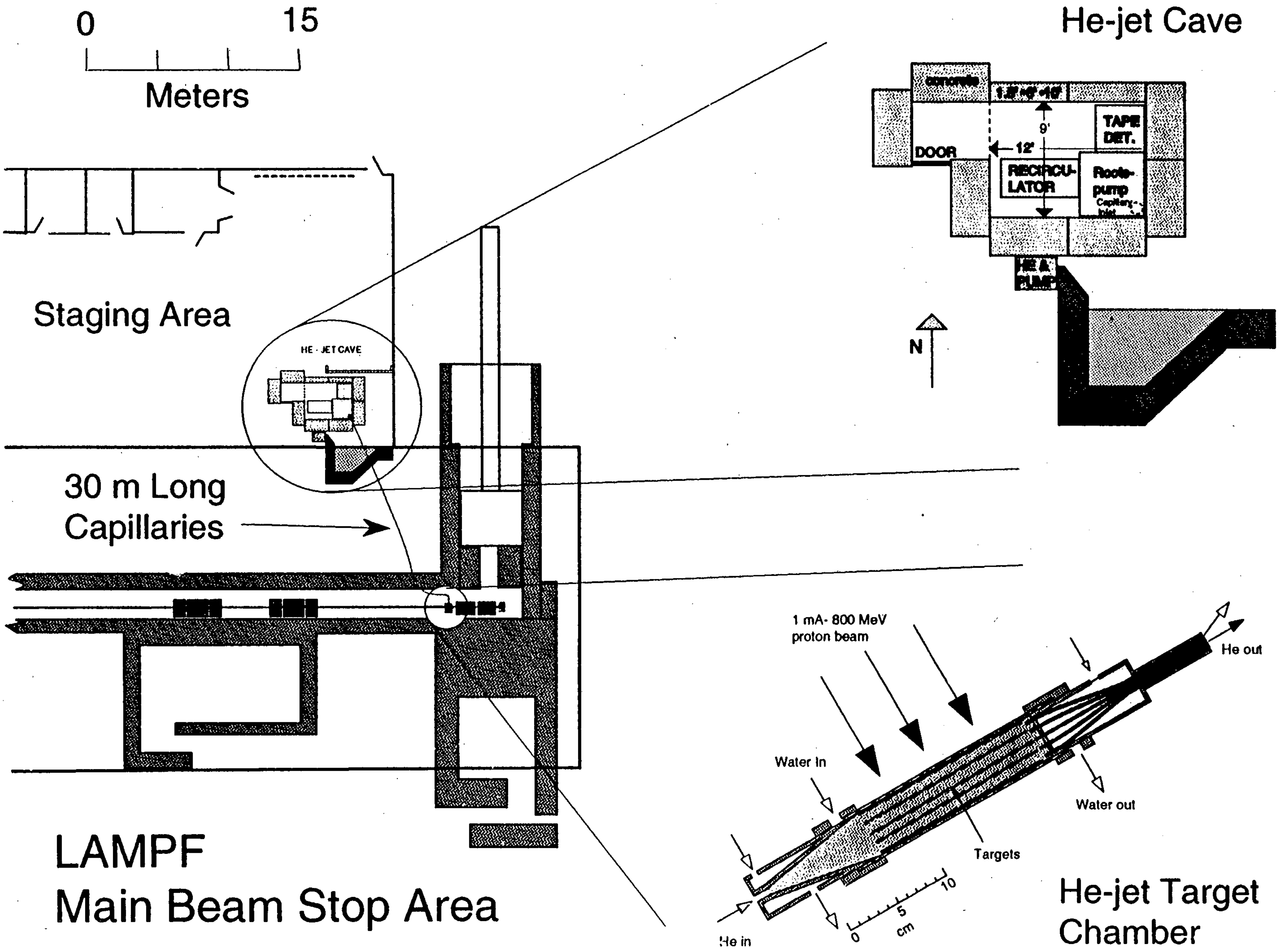0
15
Meters
Staging Area
HE - JET CAVE
30 m Long Capillaries
LAMPF
Main Beam Stop Area
He-jet Cave
concrete
1.5' x6' x16'
TAPE DET.
9'
DOOR
12'
RECIRCU-LATOR
Roots-pump
Capillary inlet
HE & PUMP
N
1 mA- 800 MeV proton beam
He out
Water in
Water out
Targets
He in
0
5
10
cm
He-jet Target Chamber

High-Intensity He-jet Tests at Los Alamos

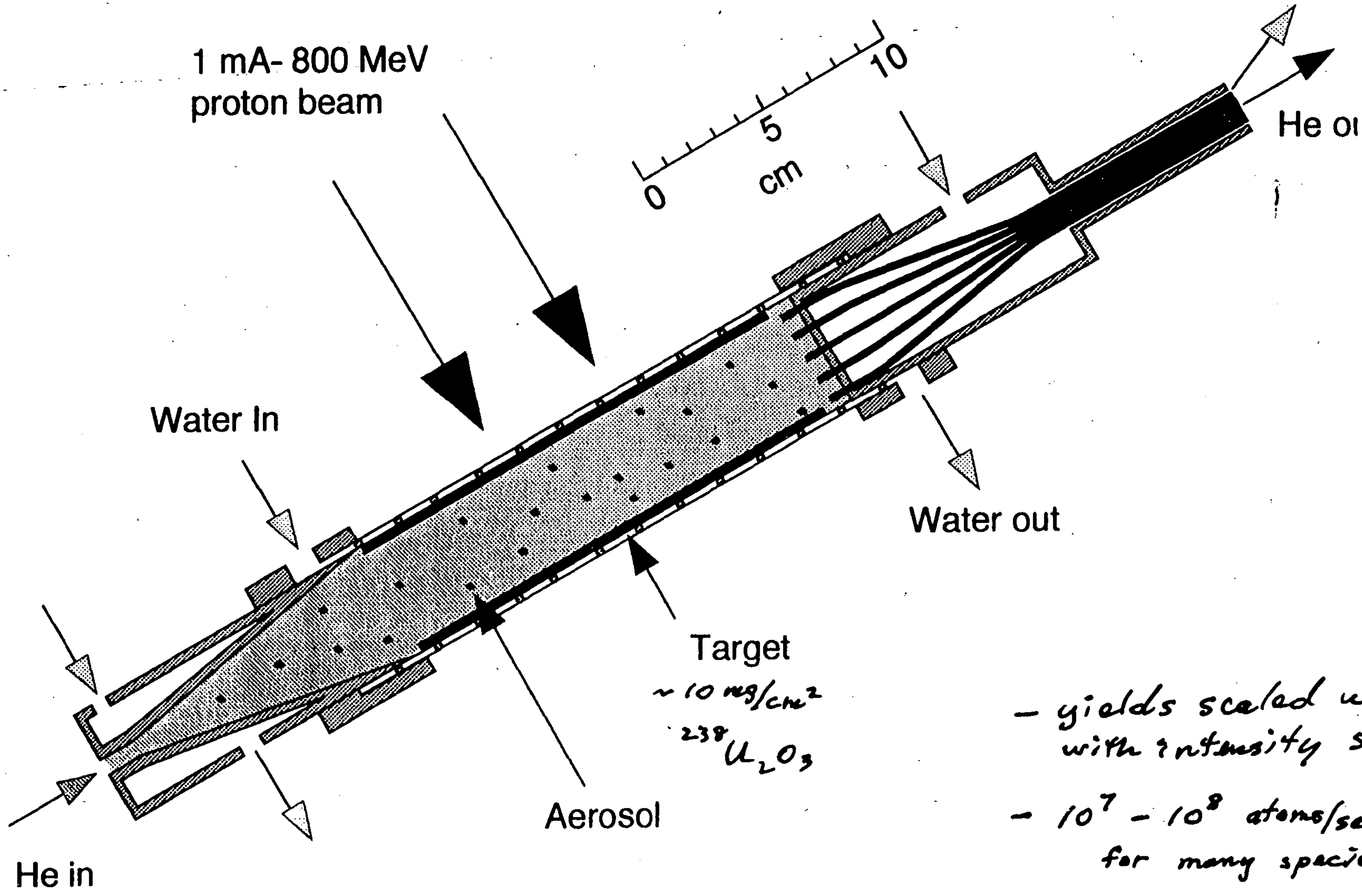

- yields scaled up with intensity 5 → 700μ
- $10^7 - 10^8$ atoms/sec/isotope for many species
- He-jet eff. of 15-20%

Overview of the multi-isotope Cs - PNC experiment

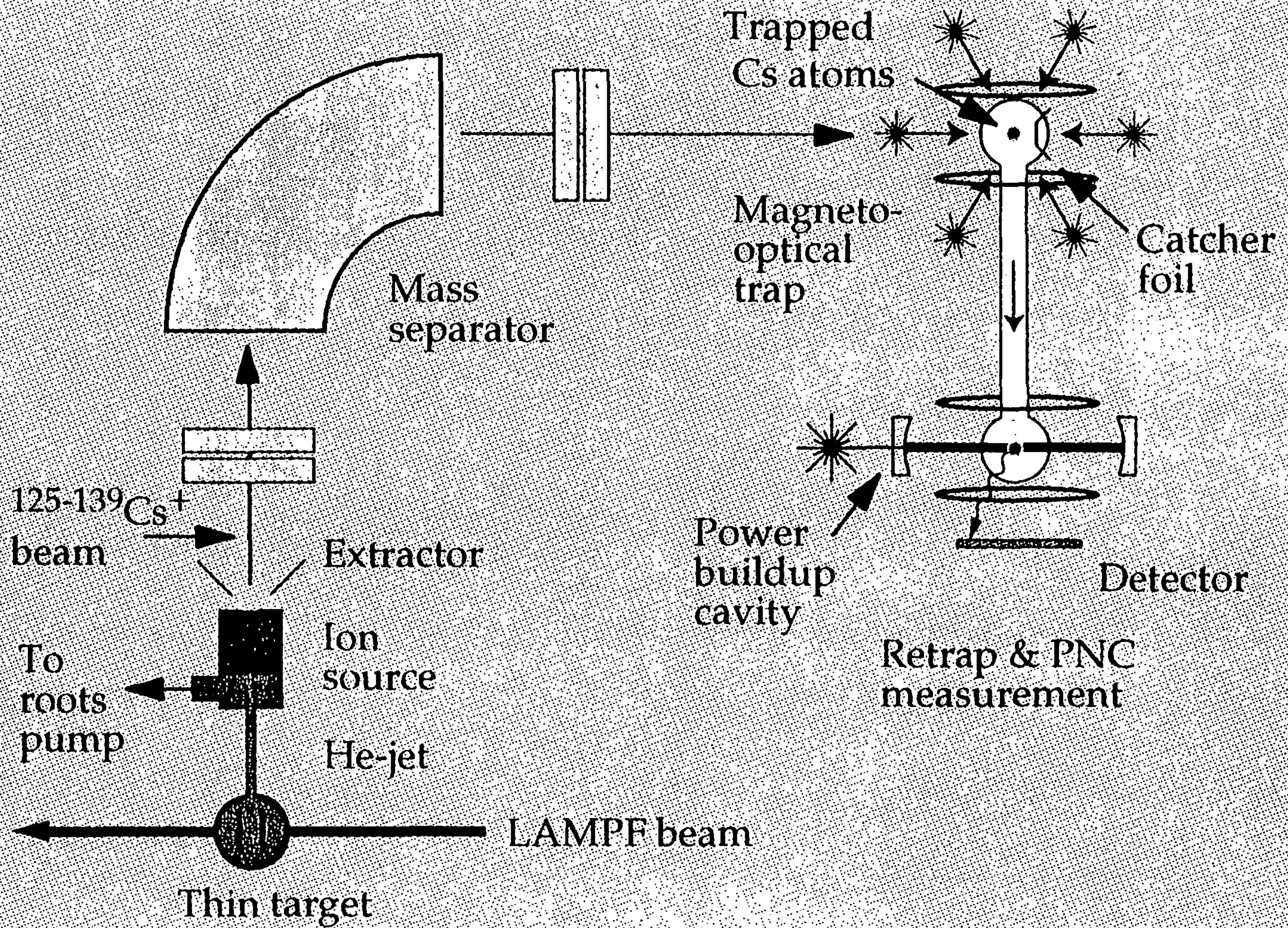

U. Colo. & Los Alamos

Magneto-Optical Trap (MOT)

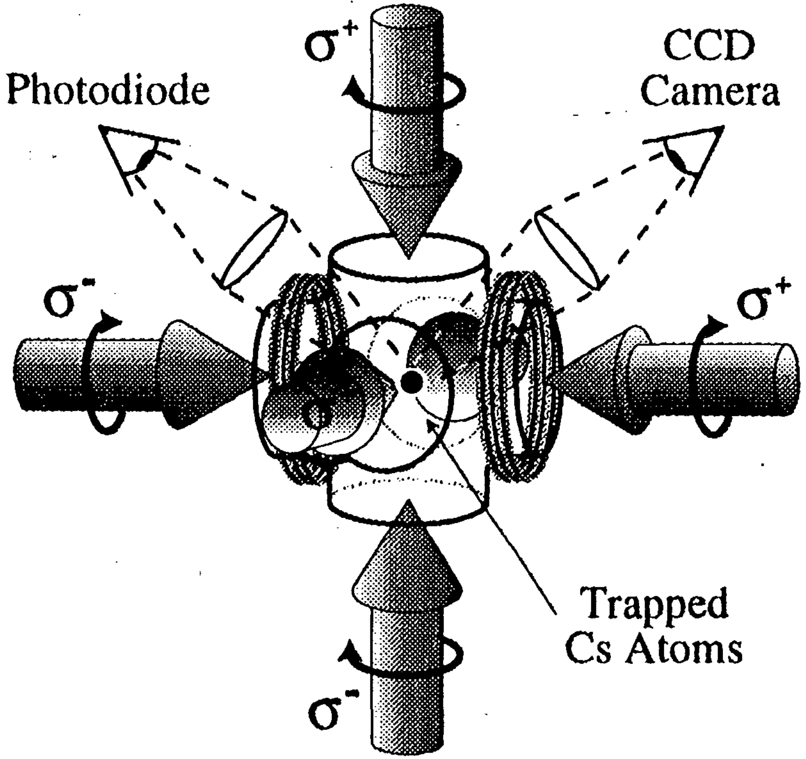

- Highly-concentrated, point-like source (10^8 atoms / 2 mm ϕ)
- Long trapping times (1-100 sec)
- Cold sample (< 1 mK)
- UHV environment (10^{-8} - 10^{-9} torr)
- Atoms/nuclei can be easily polarized & manipulated

Atomic PNC Experiment in Cs (Fr): A Low-Energy Test of the Standard Model

Neutral current e-q coupling leads to parity mixing of atomic states.

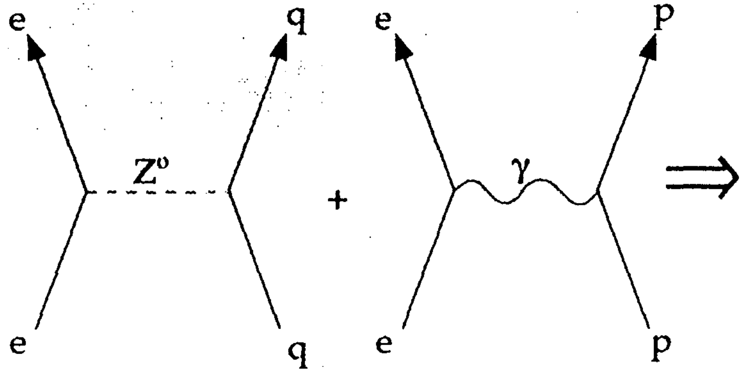

Weak neutral current
(parity violating)

Coulomb interaction
(parity conserving)

W.-S.-G. Electroweak theory
Standard Model

predicts mixing of S + P states

$$|S'\rangle = |S\rangle + \delta_{PNC}|P\rangle$$

$$\delta_{PNC} \propto Q_w \gamma_5$$

weak charge

atomic matrix element ∝ Z^3

$$Q_w = -2[(2Z+N)C_{1u} + (Z+2N)C_{1d}]$$

+ % rad. corr.

with $C_{1u} = -1/2 + 4/3\sin^2\theta_w$

$C_{1d} = 1/2 - 2/3\sin^2\theta_w$

$$= -N + Z(1-4\sin^2\theta_w)$$

(0.076 from Z^0)

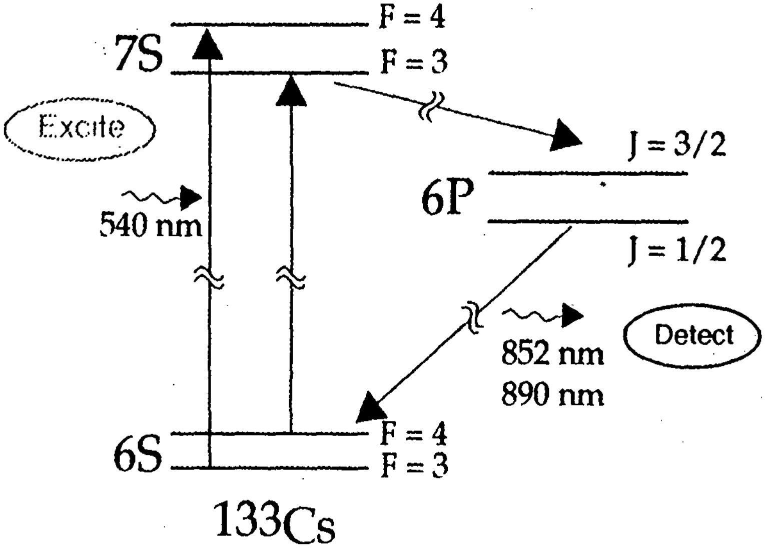

U. Colo. & LANL

John Hardy

Chalk River Laboratories
Chalk River, Ontario, Canada

SUPERALLOWED BETA–DECAY:

A Nuclear Probe of the Electroweak Standard Model

J.C. Hardy
E. Hagberg
V. Koslowsky
G. Savard
I.S.Towner

Chalk River Laboratories

ALLOWED NUCLEAR BETA DECAY

EXPERIMENT

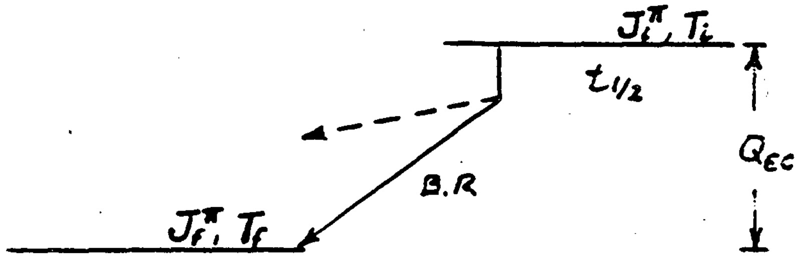

WEAK DECAY EQUATION

$$\boxed{ft = \frac{K}{G_V^2\langle 1\rangle^2 + G_A^2\langle \sigma\tau\rangle^2}}$$

$f = f(Z, Q_{EC})$
$t = f(t_{1/2}, BR)$
$G_{V,A}$ = coupling constants
$\langle\ \rangle$ = matrix elements

SELECTION RULES

	$\langle 1\rangle$	$\langle \sigma\tau\rangle$
ΔJ	0	0,1 (not 0→0)
ΔT	0	0,1
$\Delta\pi$	no	no

PURE VECTOR DECAY

$$\boxed{0^+ \longrightarrow 0^+, \ \Delta T = 0}$$

SUPERALLOWED $0^+ \rightarrow 0^+$ BETA DECAY

EXPERIMENT

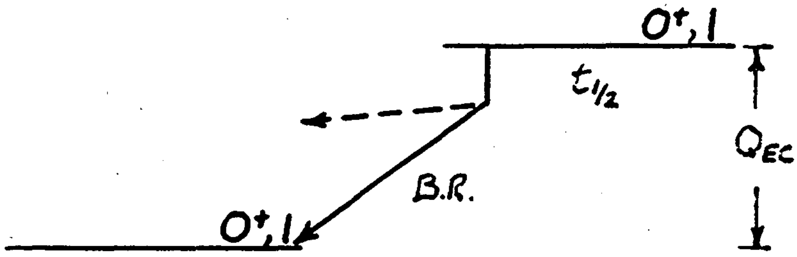

WEAK DECAY EQUATION

$$\boxed{ft = \frac{K}{G_V^2 \langle 1 \rangle^2}}$$

RADIATIVE CORRECTIONS

$$\boxed{\begin{array}{l} t \longrightarrow t(1+\delta_R) \\ G_V^2 \longrightarrow G_V^2(1+\Delta_R) \end{array}}$$

$\delta_R = f(Z, Q_{EC}, \text{nuclear structure})$

$\Delta_R = f(\text{interaction})$

CHARGE CORRECTIONS

$$\boxed{\langle 1 \rangle^2 \longrightarrow 2(1-\delta_c)}$$

$\delta_c = f(\text{nuclear structure})$

CVC TEST

$$\boxed{\mathcal{F}t \equiv ft(1+\delta_R)(1-\delta_c) = \frac{K}{2G_V^2(1+\Delta_R)}}$$

CONSTANT

UNITARITY TEST

CABIBBO - KOBAYASHI - MASKAWA QUARK-MIXING MATRIX

$$\begin{pmatrix} d' \\ s' \\ b' \end{pmatrix} = \begin{pmatrix} V_{ud} & V_{us} & V_{ub} \\ V_{cd} & V_{cs} & V_{cb} \\ V_{td} & V_{ts} & V_{tb} \end{pmatrix} \begin{pmatrix} d \\ s \\ b \end{pmatrix}$$

THREE-GENERATION UNITARITY

$$\boxed{V_{ud}^2 + V_{us}^2 + V_{ub}^2 = 1}$$

$V_{ud} \sim 0.97$

$V_{us} \sim 0.22$

$V_{ub} \sim 0.003$

NUCLEAR CONTRIBUTION

$$\boxed{\begin{aligned} |V_{ud}| &= G_V / G_\mu \\ &= \left(\frac{K}{2(1+\Delta_R)\mathcal{F}t} \right)^{1/2} G_\mu^{-1} \end{aligned}}$$

$\mathcal{F}t$ = AVERAGE $0^+ \to 0^+$ NUCLEAR RESULT

G_μ = MUON COUPLING CONSTANT

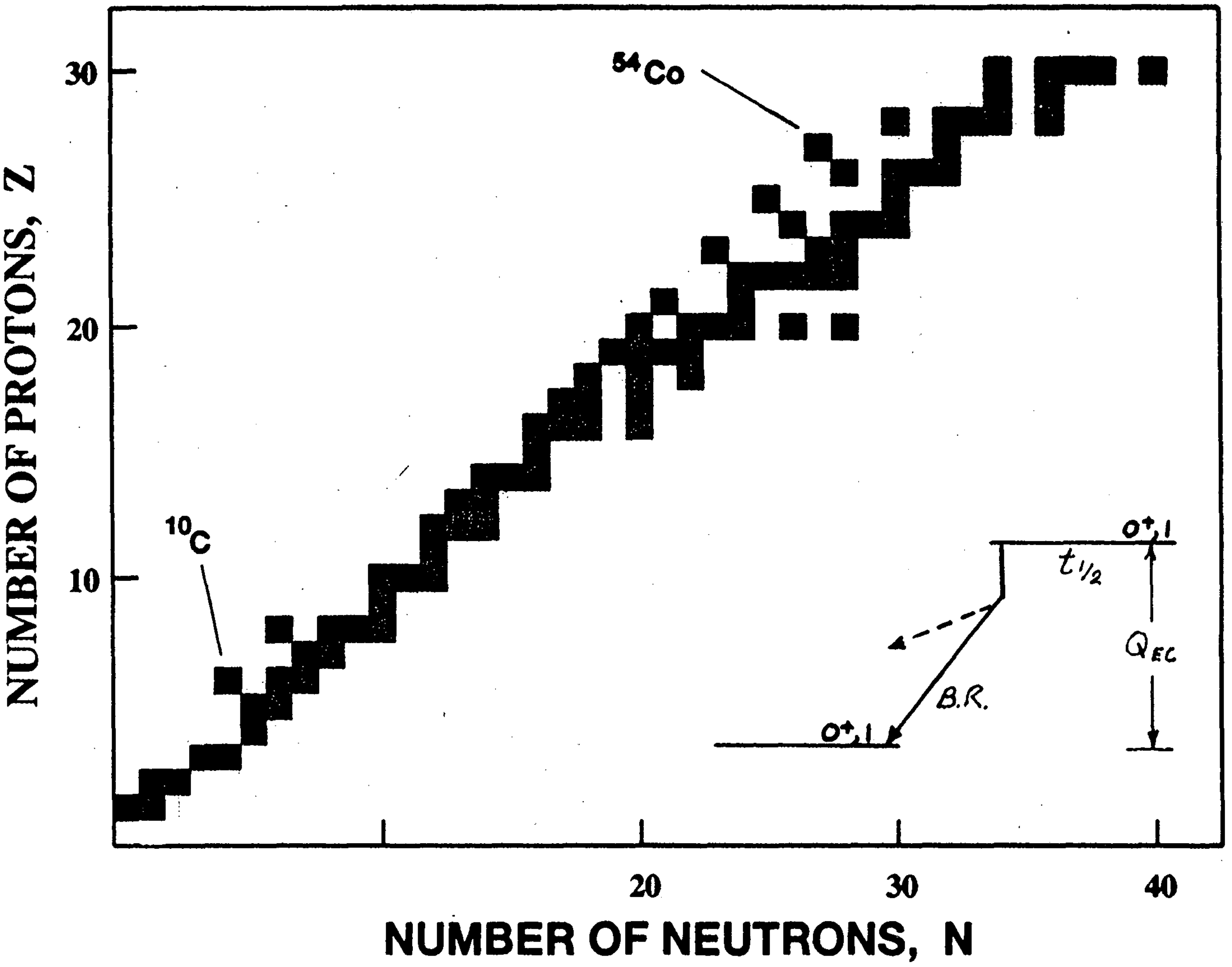

NUMBER OF PROTONS, Z
30
20
10
NUMBER OF NEUTRONS, N
20
30
40
^{54}Co
^{10}C
0⁺,1
0⁺,1
$t_{1/2}$
B.R.
Q_{EC}

EXPERIMENTAL RESULTS

1. Q_{EC} VALUE

precision $\gtrsim$ 100 eV

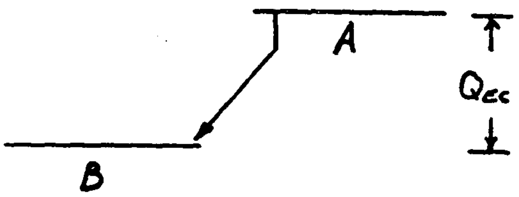

- $B(p,n)A$ threshold (Aukland)
- $C(p,\gamma)A$ & $C(n,\gamma)B$ Q values (Oak Ridge/Utrecht,
- $B(^3He,t)A$ & $B'(^3He,t)A'$ Q-value doublet (Chalk River)

2. LIFETIME

precision $\gtrsim$ 0.03%

- Isotope-seperated samples (Chalk River)

3. BRANCHING RATIO

- ^{10}C, direct measurement with γ-ray spectrometer (Chalk River, LBL)
- All others indirect : $BR > 99\%$ (Chalk River)

BRANCHING-RATIO MEASUREMENTS

1. DIRECT MEASUREMENT OF SUPERALLOWED BRANCH

- ^{10}C branching ratio = 1.46%

2. MEASUREMENT OF OTHER WEAK BRANCHES

- All other cases, superallowed branching ratio > 99%
- $0^+ \rightarrow 1^+$ Axial-vector decay branches
  - affects superallowed branching ratio
  - sensitivity required ≈ 500ppm
- $0^+ \rightarrow 0^+$ Non-analogue vector-decay branches
  - tests charge corrections
  - locates relevant 0^+ states
  - sensitivity required ~1ppm

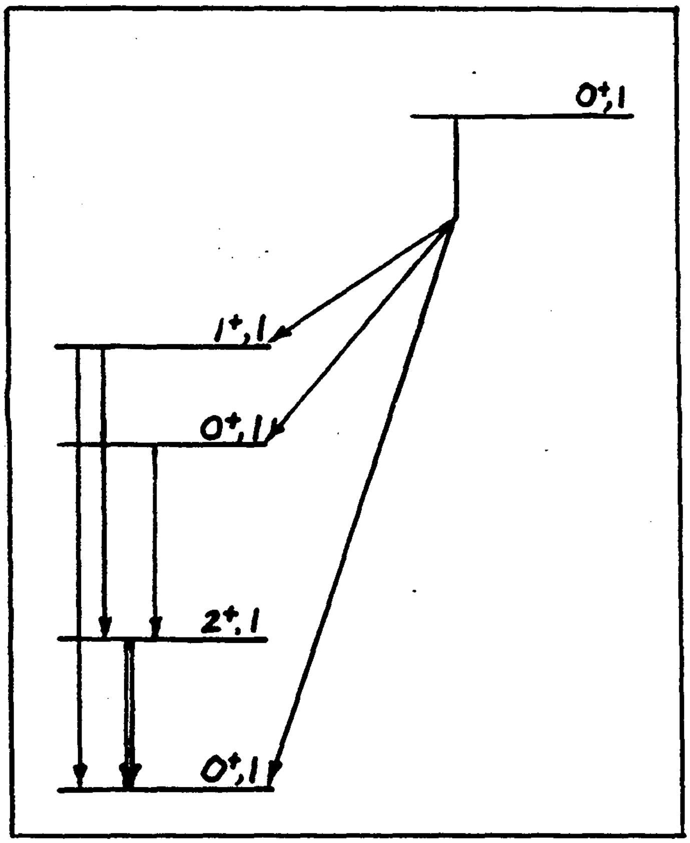

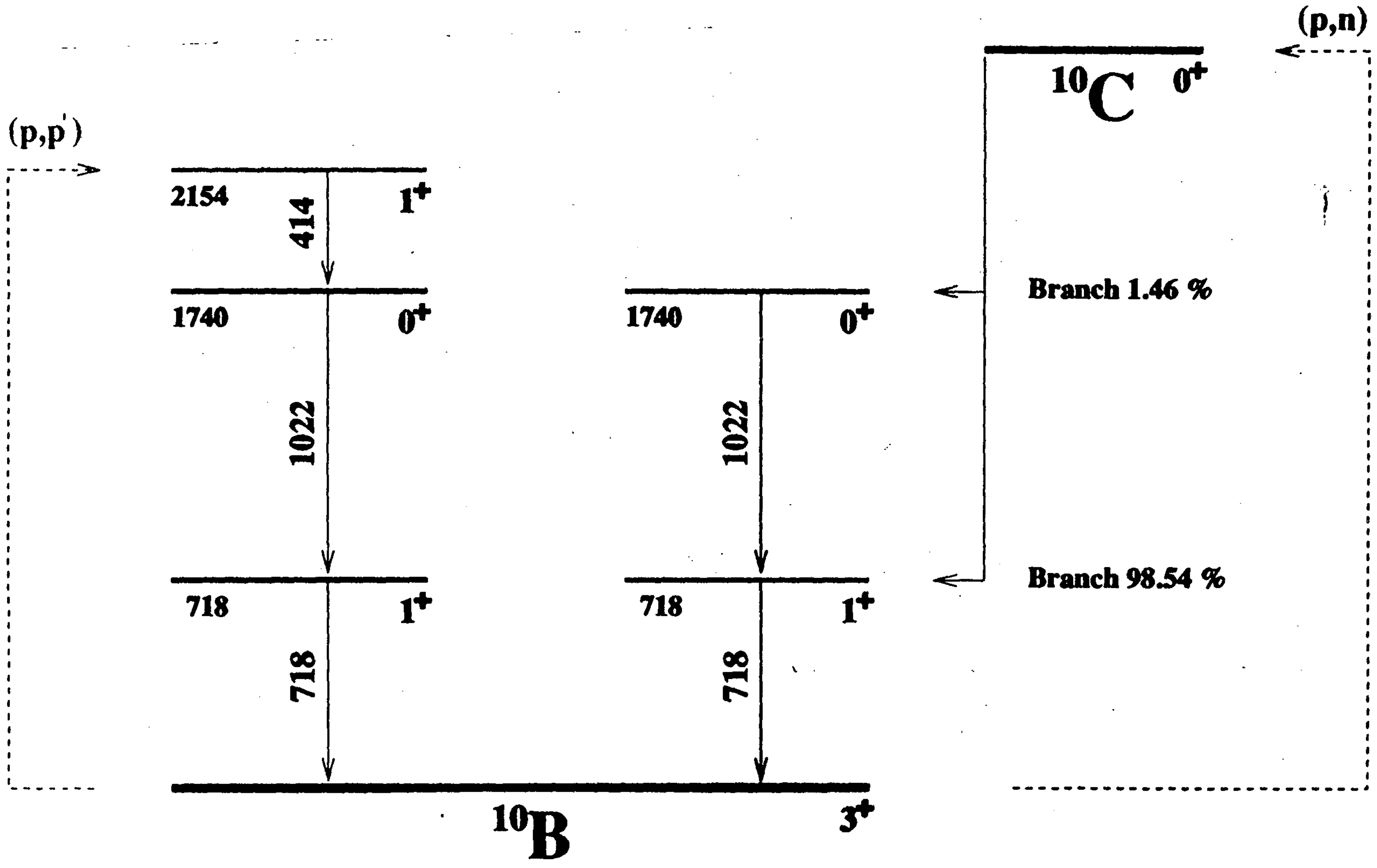

$BR = 1.4625 \pm \underset{(stat)}{0.0020} \pm \underset{(syst)}{0.0015}$ %

CHARGE CORRECTION

$$\delta_C \quad = \quad \delta_{CM} \quad + \quad \delta_{RO}$$

δ_{CM}:

- Difference in configuration mixing between parent and daughter.
- Shell-model calculation fitted to 0^+ states, IMME & non-analogue branch.
- ~0.1%

δ_{RO}:

- Mismatch in radial wave function between parent and daughter
- Woods-Saxon wave functi matched to experimental binding energy and shell-model parentage
- ~0.4%

EXPERIMENTAL TEST

(Hagberg et al, P.R.L. 73 (1994) 396)

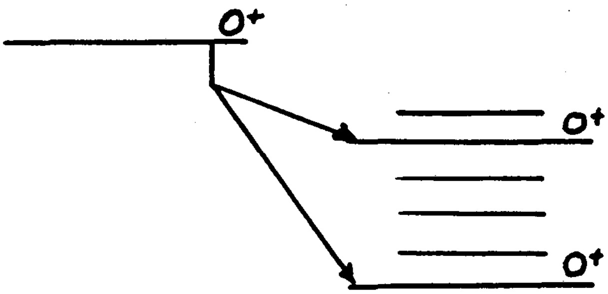

$$\langle M_1 \rangle^2 = 2\,\delta^1_{CM}\,(1-\delta_{RO})$$

$$\langle M_0 \rangle^2 = 2\,(1-\delta_{CM})(1-\delta_{RO})$$

BRANCHING RATIOS TO NON-ANALOGUE 0+ STATES

PARENT	EXPERIMENTAL RESULTS (ppm)	CALCULATION (ppm)
^{38m}K	<19	6±1
^{46}V	39±4	34±4
^{50}Mn	<3	10±4
^{54}Co	45±6	48±10

CVC TEST - WORLD DATA, 1995

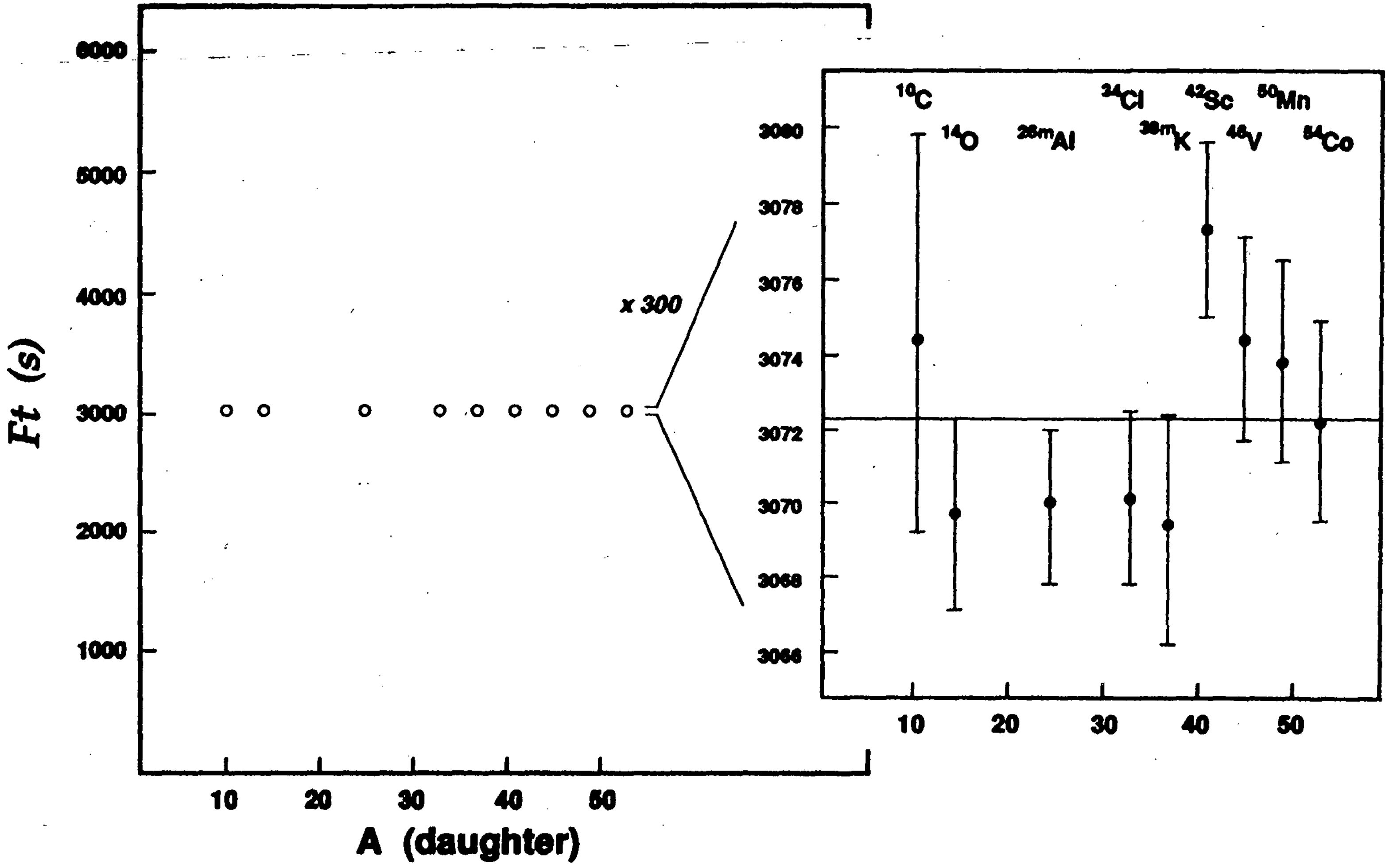

$$\boxed{\overline{\mathcal{F}t} = 3072.3 \pm 1.0 s}$$

- "STATISTICAL" UNCERTAINTY ON δ_c
- $\chi^2/N = 1.20$

UNITARITY TEST - WORLD DATA, '94

- NUCLEAR $0^+ \rightarrow 0^+$ DECAYS

$$\mathcal{F}t = (3072.3 \pm 1.0 \pm 1.0)\ s$$

- MUON LIFETIME

$$G_\mu/(\hbar c)^3 = (1.16639 \pm 0.00002) \times 10^{-5}\,GeV^{-2}$$

- RADIATIVE CORRECTION (Z MASS,...)

$$\Delta_R = (2.46 \pm 0.09)\%$$

$$\boxed{\begin{aligned} V_{ud} &= \left(\frac{K}{2(1+\Delta_R)\mathcal{F}t}\right)^{1/2} G_\mu^{-1} \\ &= 0.9740 \pm 0.0005 \end{aligned}}$$

± 0.0002 experimental

- K_{e3} & HYPERON DECAYS

$$V_{us} = 0.2205 \pm 0.0018$$

- B-MESON DECAY

$$V_{ub} = 0.0032 \pm 0.0009$$

$$\boxed{V_{ud}^2 + V_{us}^2 + V_{ub}^2 = 0.9972 \pm 0.0013}$$

EXPLANATIONS OF "NON-UNITARITY"

TRIVIAL

- INADEQUATE CHARGE CORRECTIONS TO NUCLEAR $0^+ \rightarrow 0^+$ DECAYS : RESIDUAL Z-DEPENDENCE IN $\mathcal{F}t$ VALUES.

$$\Sigma = 0.9985 \pm 0.0015$$

- REANALYSIS OF HYPERON DECAYS (V_{us})

$$\Sigma = 0.9987 \pm 0.0013$$

NON-TRIVIAL

- RIGHT-HAND CURRENTS
- ADDITIONAL NEUTRAL GAUGE BOSONS
-
-

Juha Äystö

University of Jyväskylä
Jyväskylä, Finland

Beta-delayed neutron emission in the A $\sim$ 100 region

Juha Äystö

University of Jyväskylä
Finland

PHYSICS AT IGISOL in 1996-97

- * Light ion fusion
- * Heavy —"—
- * Fission

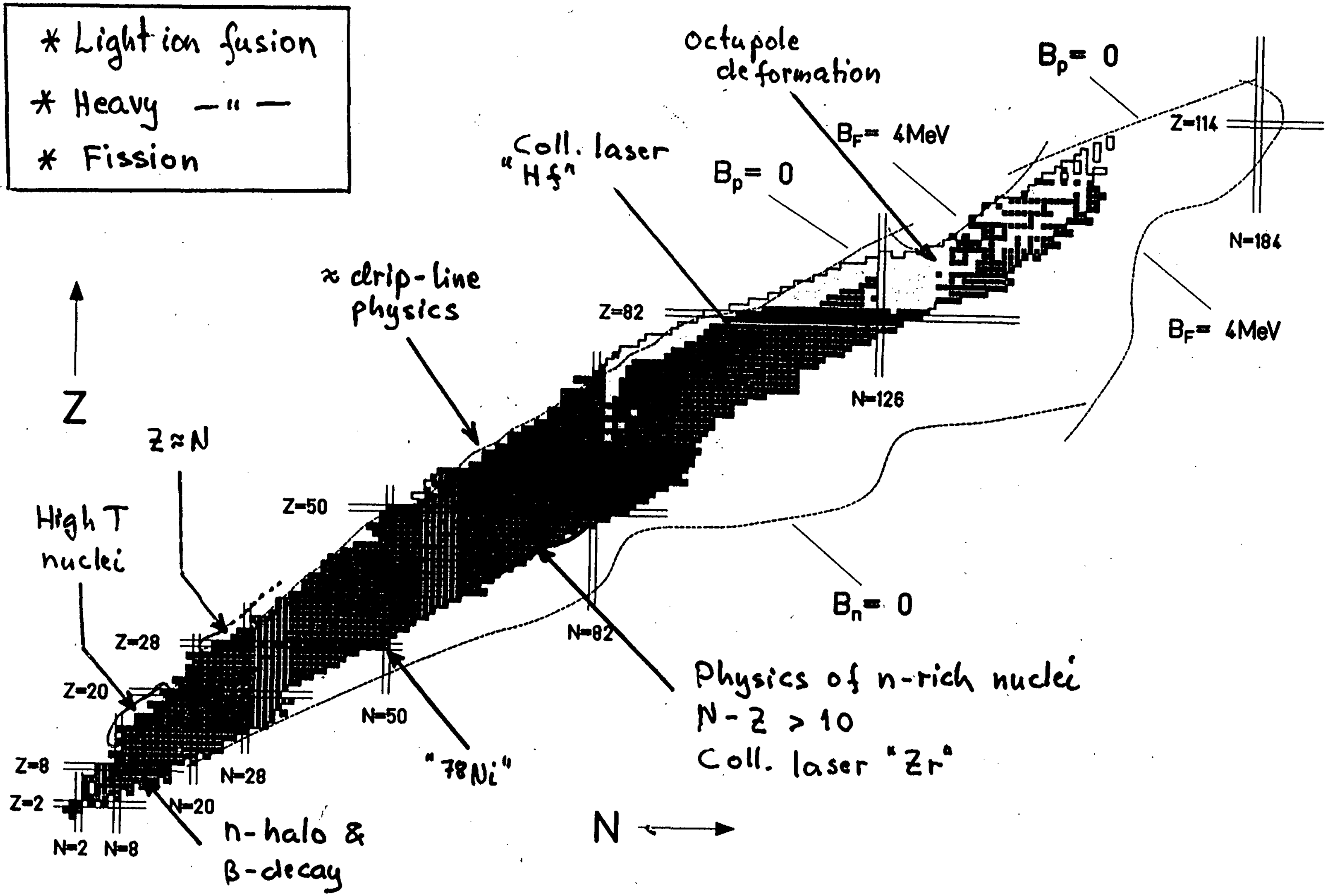

BETA-DELAYED NEUTRON EMISSION

(probe ~~for~~ new n-rich nuclei)

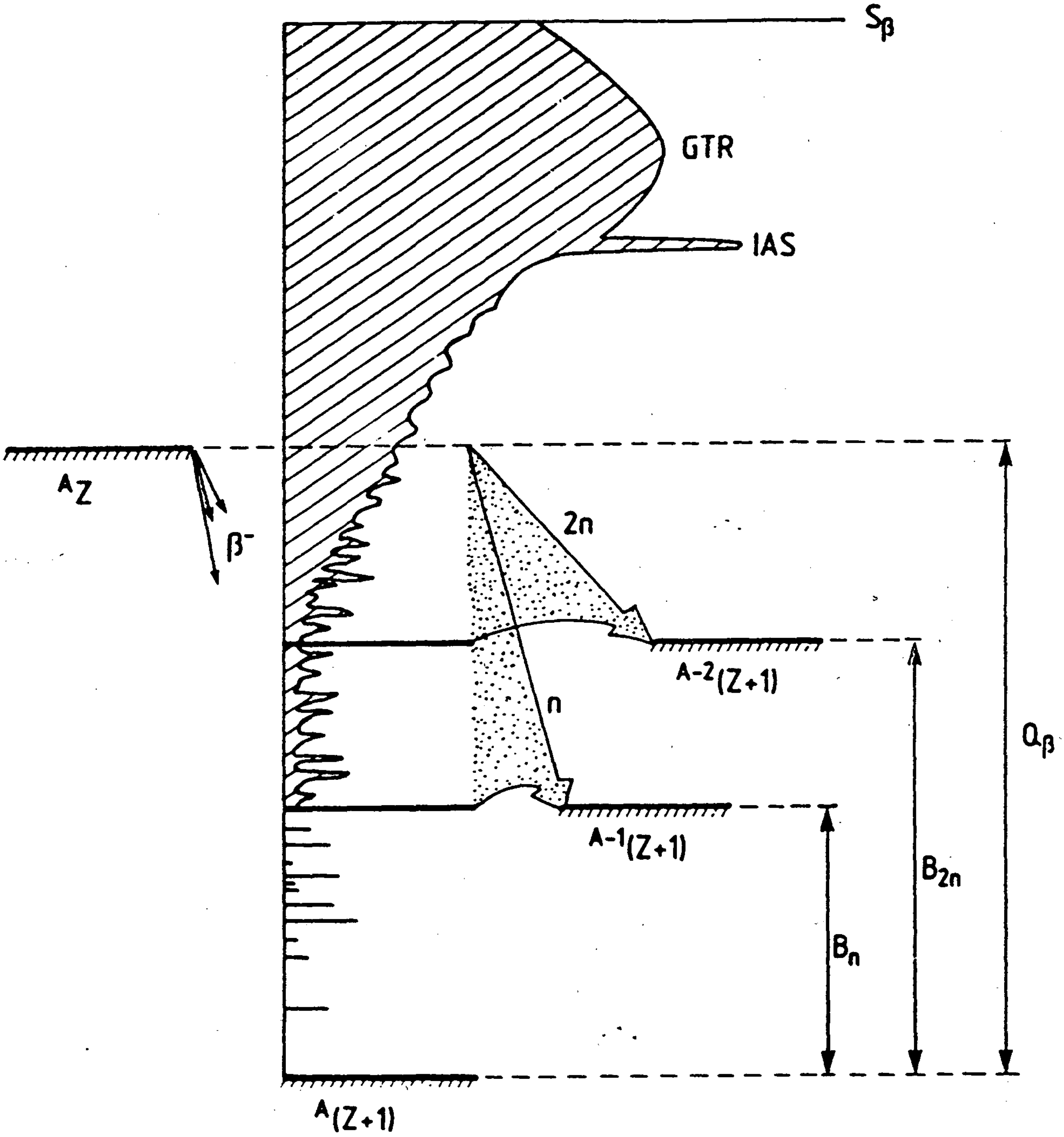

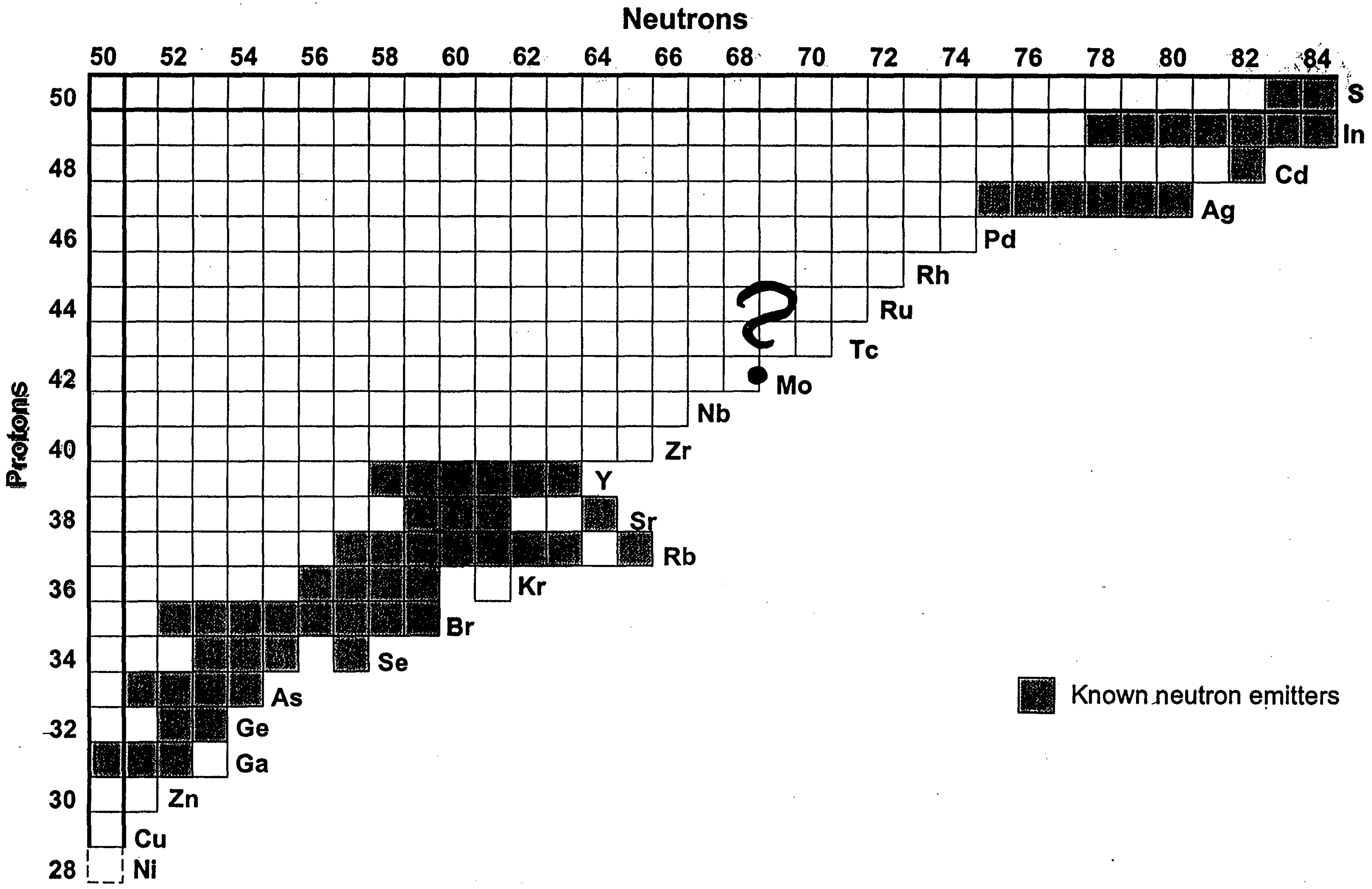

nem-old.ds4

IGISOL 6/95

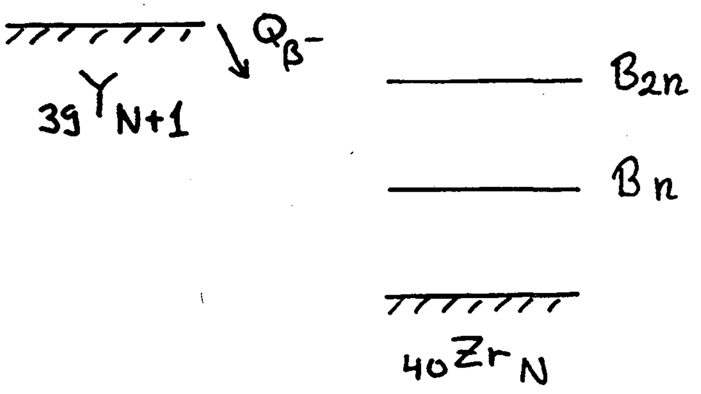
Q_{β^-}
$_{39}Y_{N+1}$
B_{2n}
B_n
$_{40}Zr_N$

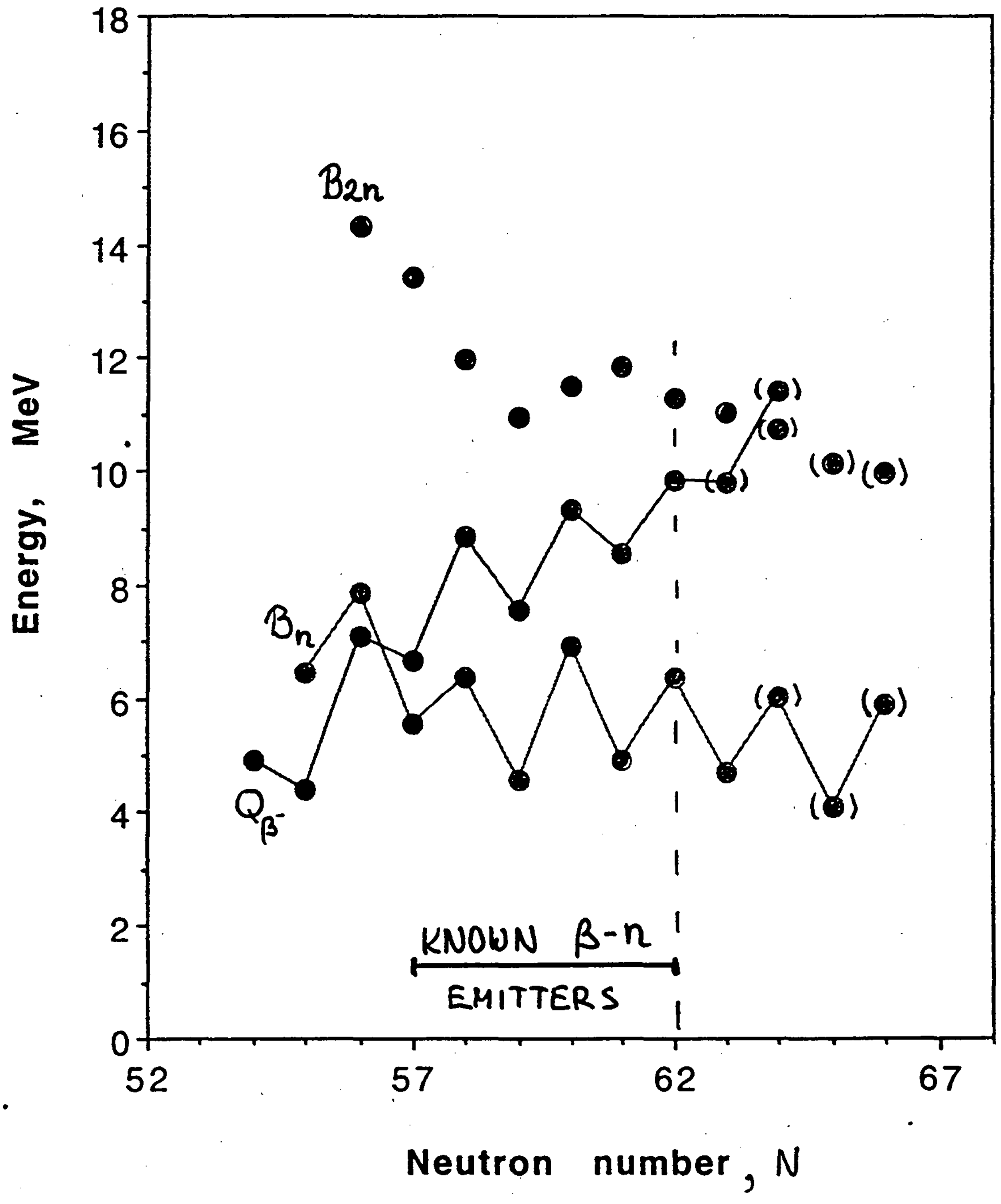
Energy, MeV
18
16
14
12
10
8
6
4
2
0
52
57
62
67
Neutron number, N
B_{2n}
B_n
Q_{β^-}
KNOWN β-n
EMITTERS

$${}_{41}Nb_{N+1} \xrightarrow{\beta^-} {}_{42}Mo_N$$

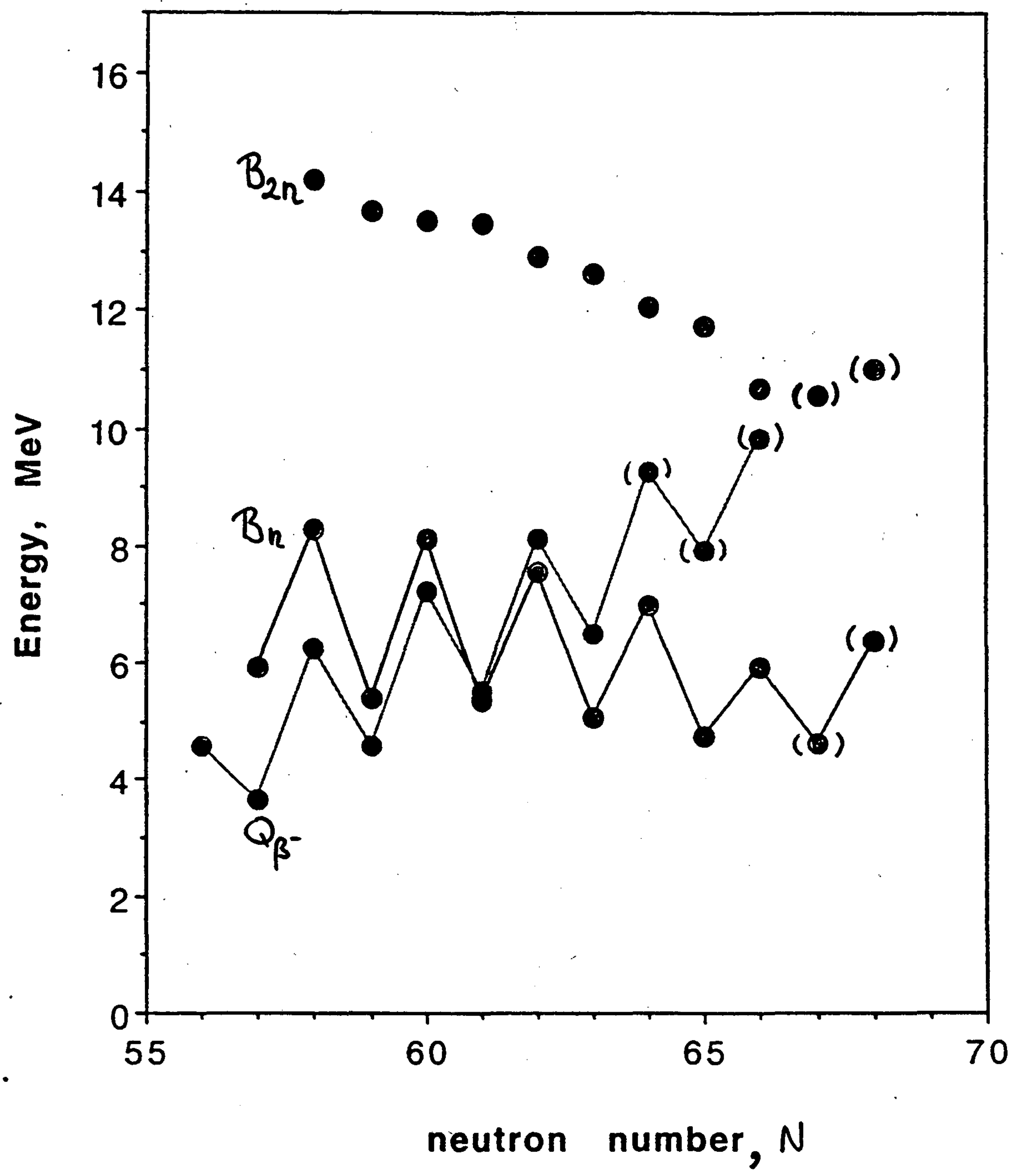

Reactions: (p,xnf), (d,xnf) & (d,pf)

$p + {}^{238}U$

$p + {}^{232}Th$

$E_p = 20 - 90$ MeV

$I_p = 40\ \mu A$ (up to 30 MeV)
$I_p = 10\ \mu A$ (above 30 MeV)

$d + {}^{238}U$

$d + {}^{232}Th$

$E_d = 15 - 65$ MeV
$I_d = 20\ \mu A$

Calculated Cross Sections / Phys. Rev. C49 (94) 2036

$^{238}U + ^{1}H$, E_p = 25 MeV

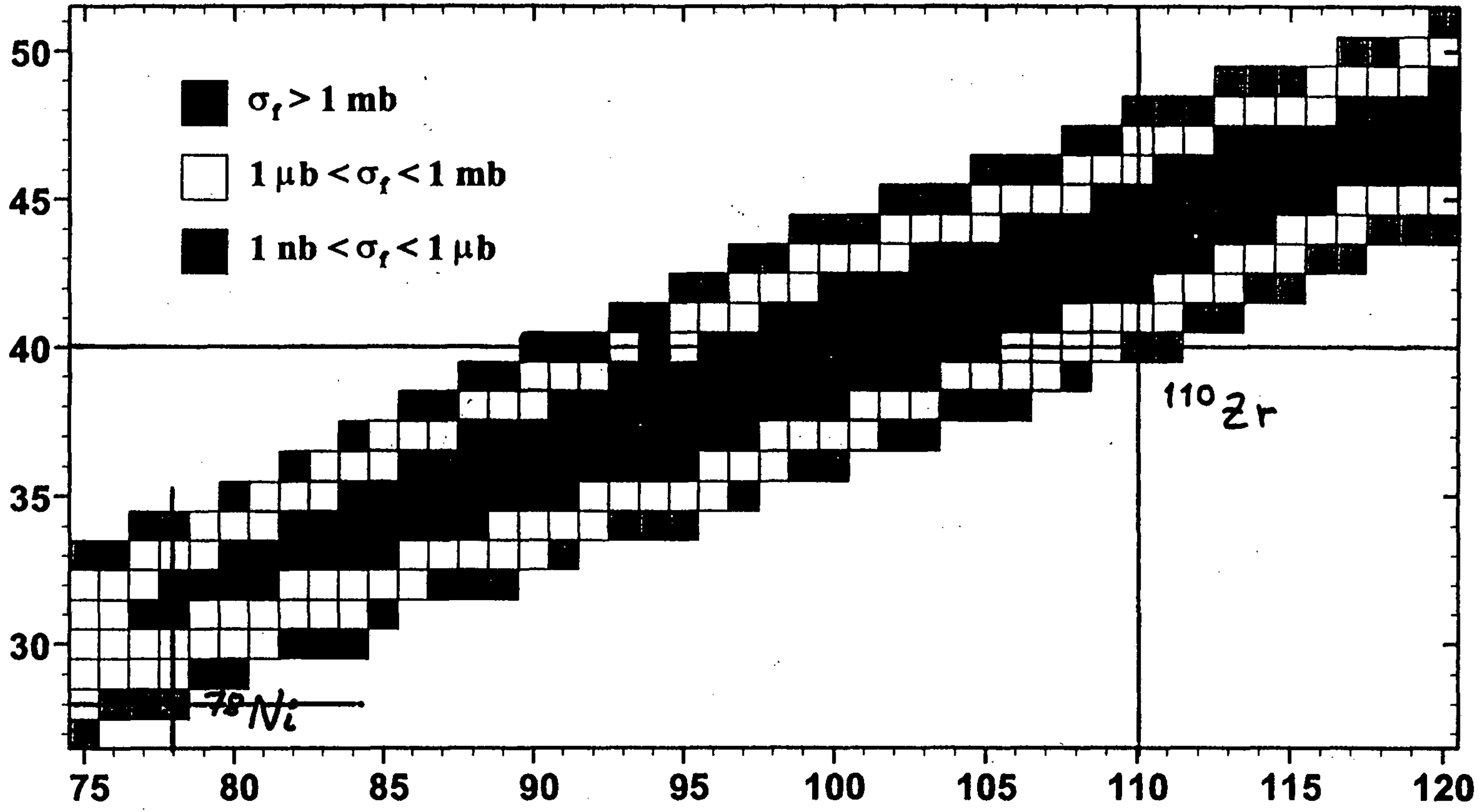

^{112}Rh:
$2 \cdot 10^4$ 1/s

XSect.ds4

Nalle 6/95

ION GUIDE TARGET CHAMBER

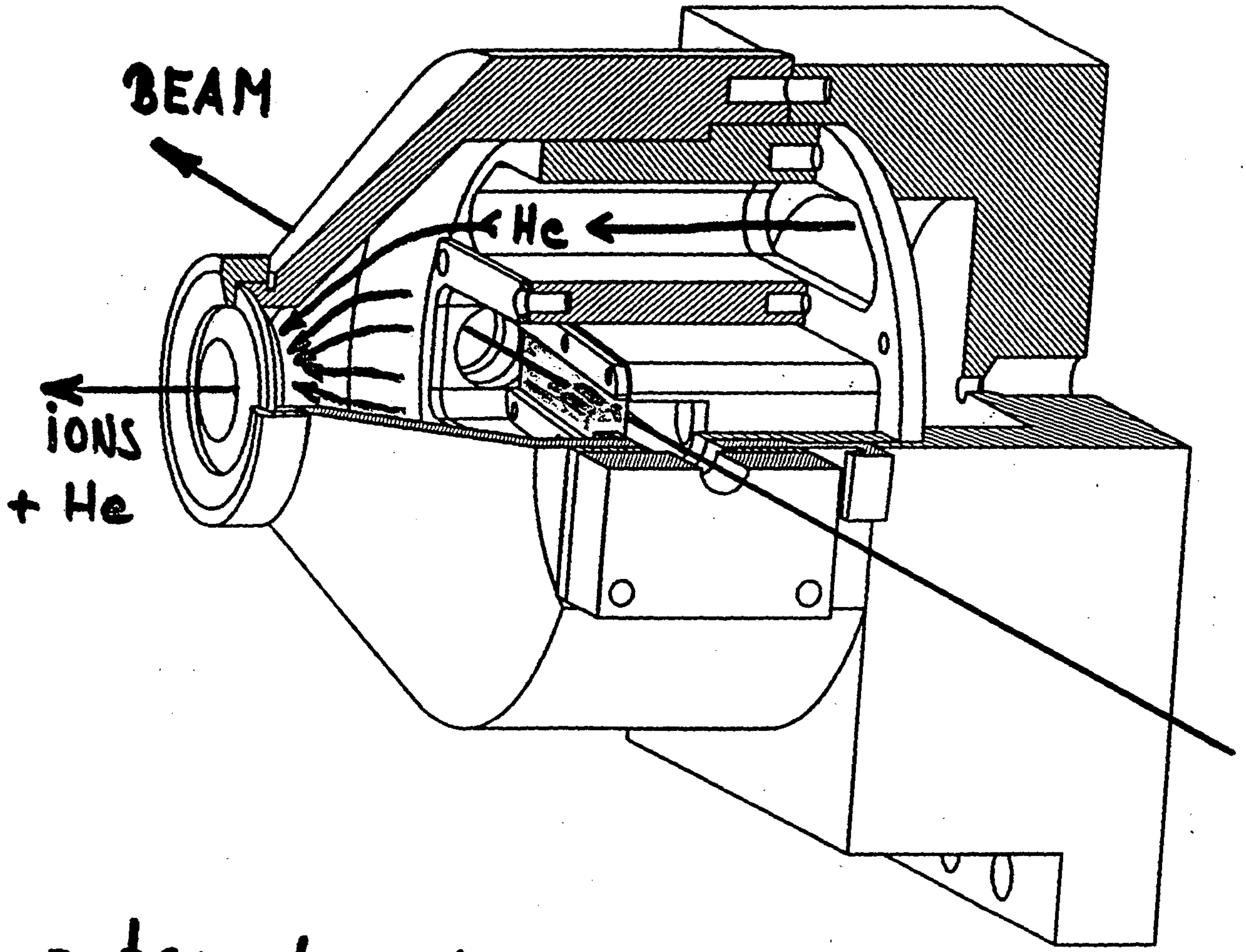

- target angle to the beam
  $\Theta \gtrsim 80°$
- extraction voltge
  V_{SK} : 0 – 1000 V

③ ISOTOPE PRODUCTION (MAP)

⑤ RECOIL SPECTROMETER (RITU)

④ ISOTOPE SEPARATOR (IGISOL)
+ LASER

⑥ ION BEAM APPLICATIONS

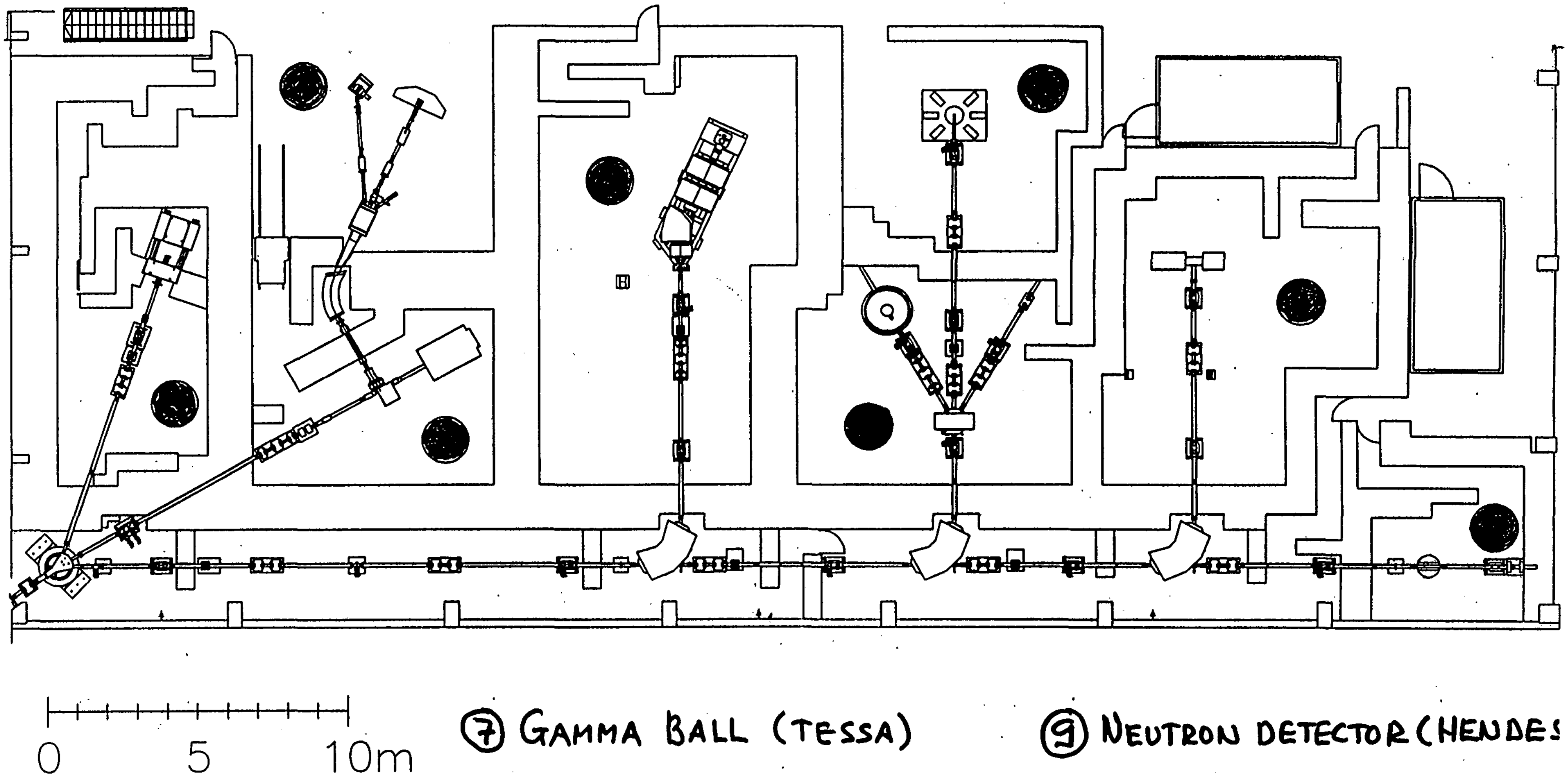

⑦ GAMMA BALL (TESSA)

⑨ NEUTRON DETECTOR (HENDES

⑧ ELECTRON SPECTROMETER

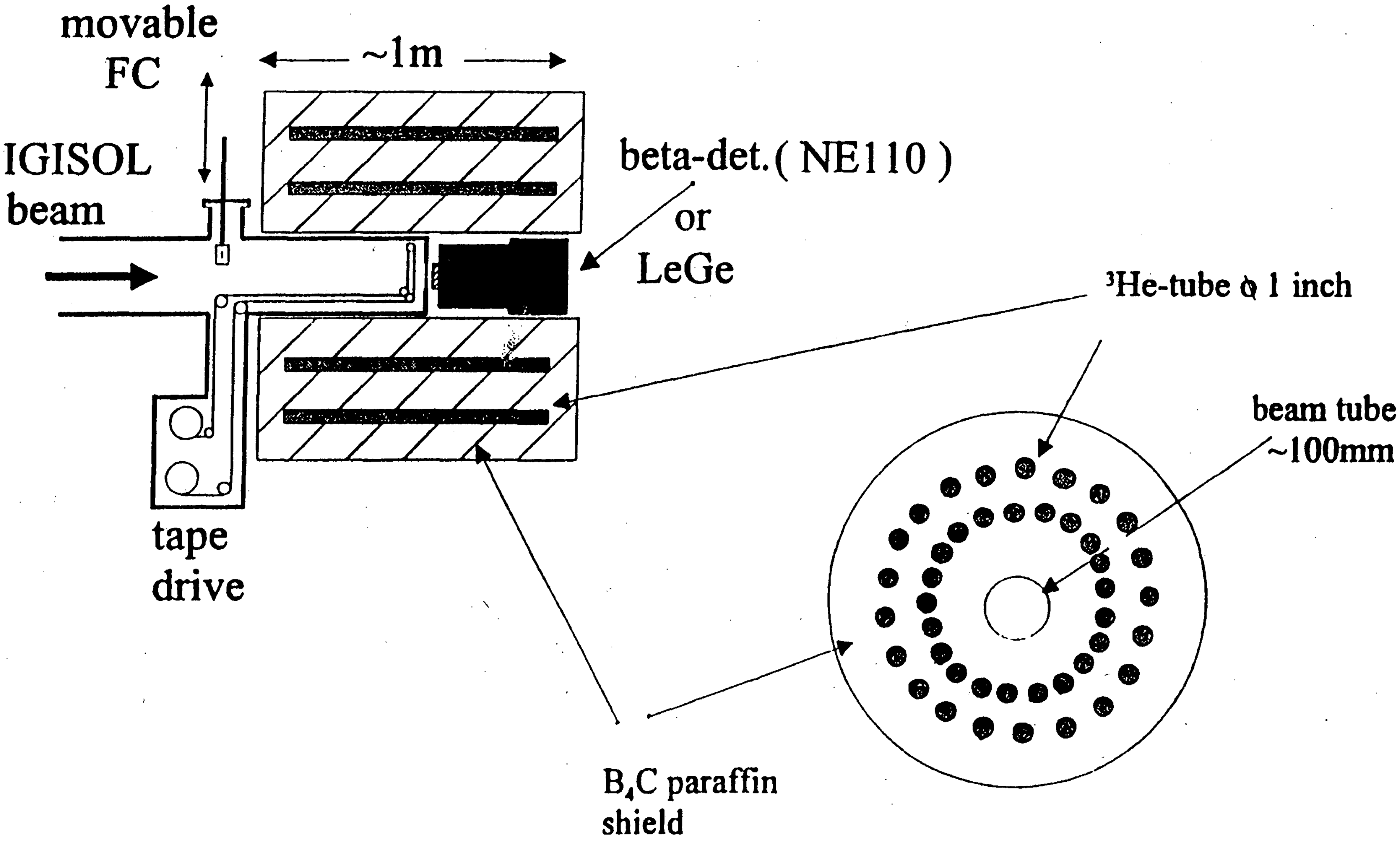
movable FC
~1m
IGISOL beam
beta-det. (NE110) or LeGe
³He-tube ϕ 1 inch
beam tube ~100mm
tape drive
B₄C paraffin shield

"NOT IN SCALE"

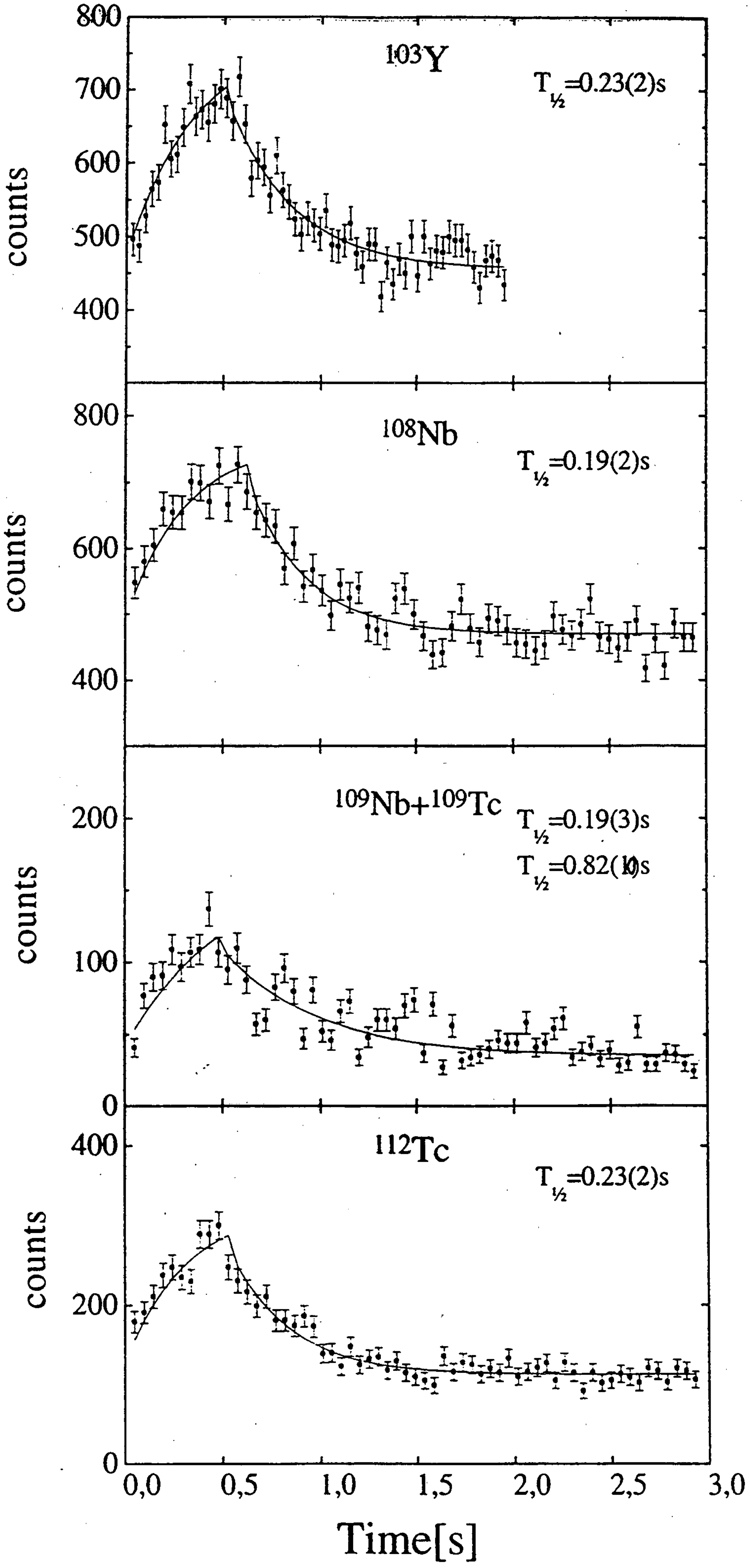
800
700
600
500
400
counts
^{103}Y
$T_{1/2}$=0.23(2)s
800
600
400
counts
^{108}Nb
$T_{1/2}$=0.19(2)s
200
100
0
counts
^{109}Nb+^{109}Tc
$T_{1/2}$=0.19(3)s
$T_{1/2}$=0.82(10)s
400
200
0
counts
^{112}Tc
$T_{1/2}$=0.23(2)s
0,0
0,5
1,0
1,5
2,0
2,5
3,0
Time[s]

New beta-delayed neutron-emitters observed at IGISOL

● Decay observed for the first time

	Nuclide	$T_{1/2}$ (s)	Pn-value (%)
●	103-Y	0.23	8
	104-Nb(gs)	5.0	0.06
	104-Nb(m)	1.0	0.05
	105-Nb	2.8	1.7
	106-Nb	0.90	4.5
	107-Nb	0.30	6.0
●	108-Nb	0.19	6.2
●	109-Nb	0.19	31
●	110-Nb	0.17	40
	109-Tc	0.82	0.08
	110-Tc	0.78	0.04
	111-Tc	0.29	0.85
	112-Tc	0.23	2.6

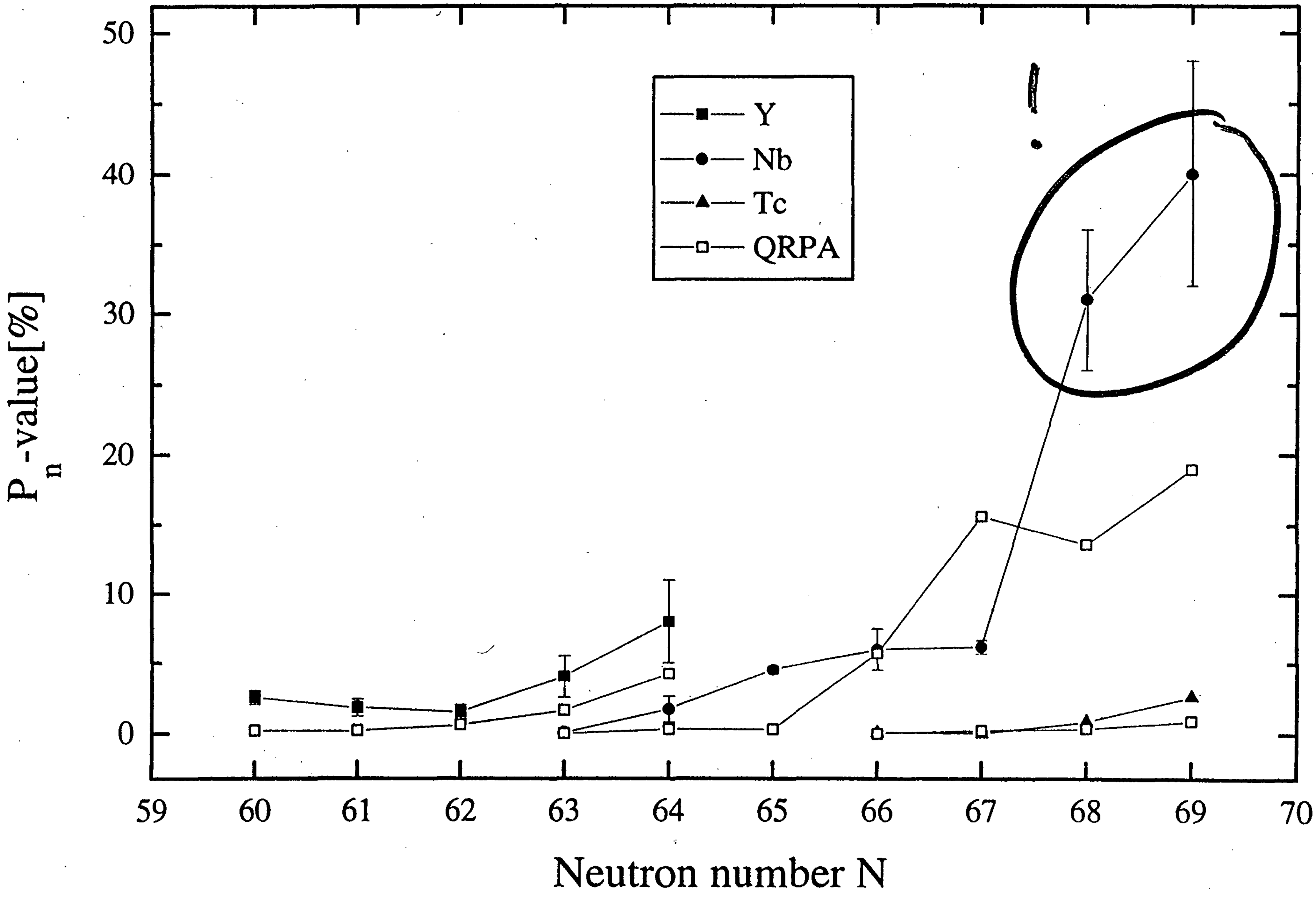
Y
Nb
Tc
QRPA
!
P$_n$-value[%]
0
10
20
30
40
50
59
60
61
62
63
64
65
66
67
68
69
70
Neutron number N

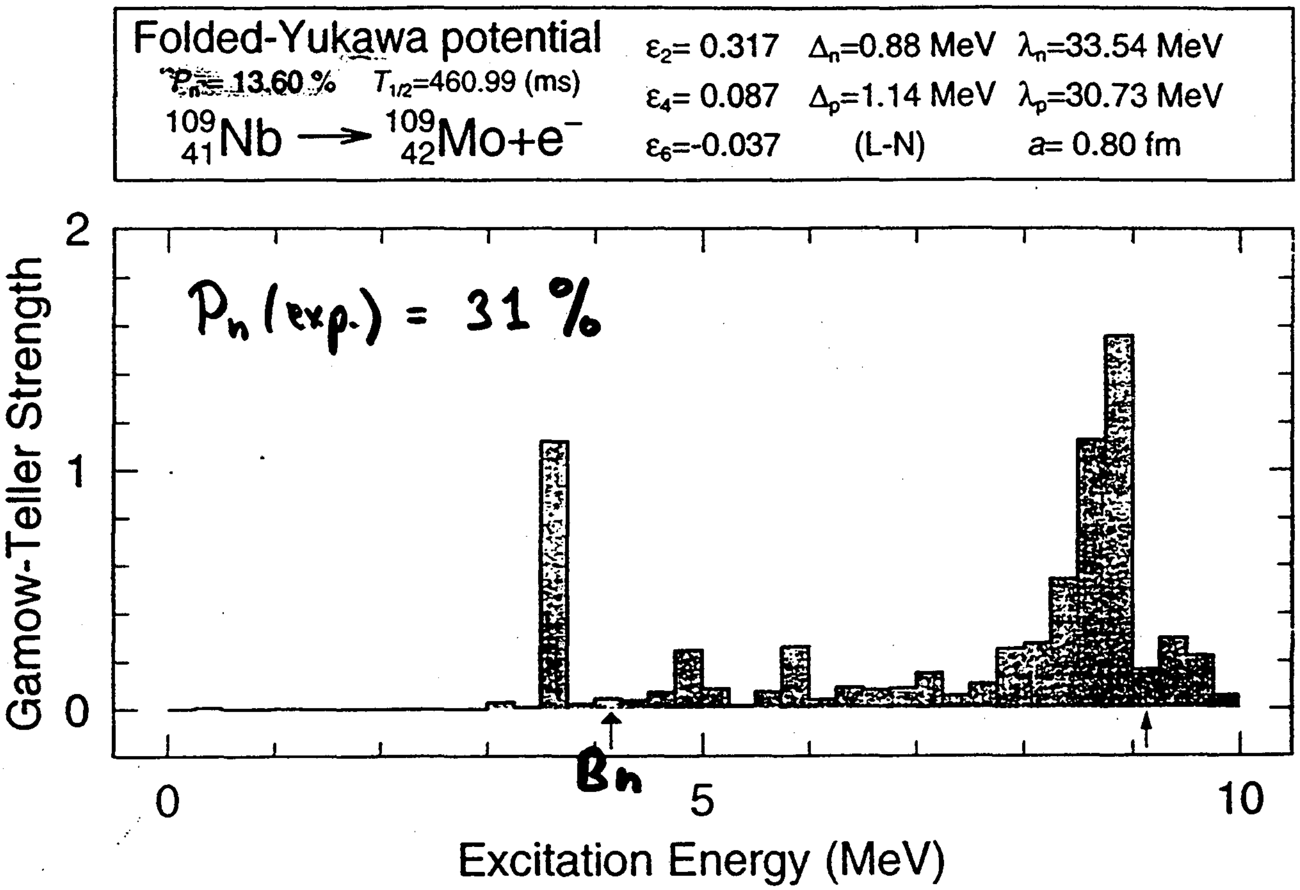

P_n (exp.) = 31 %

B_n

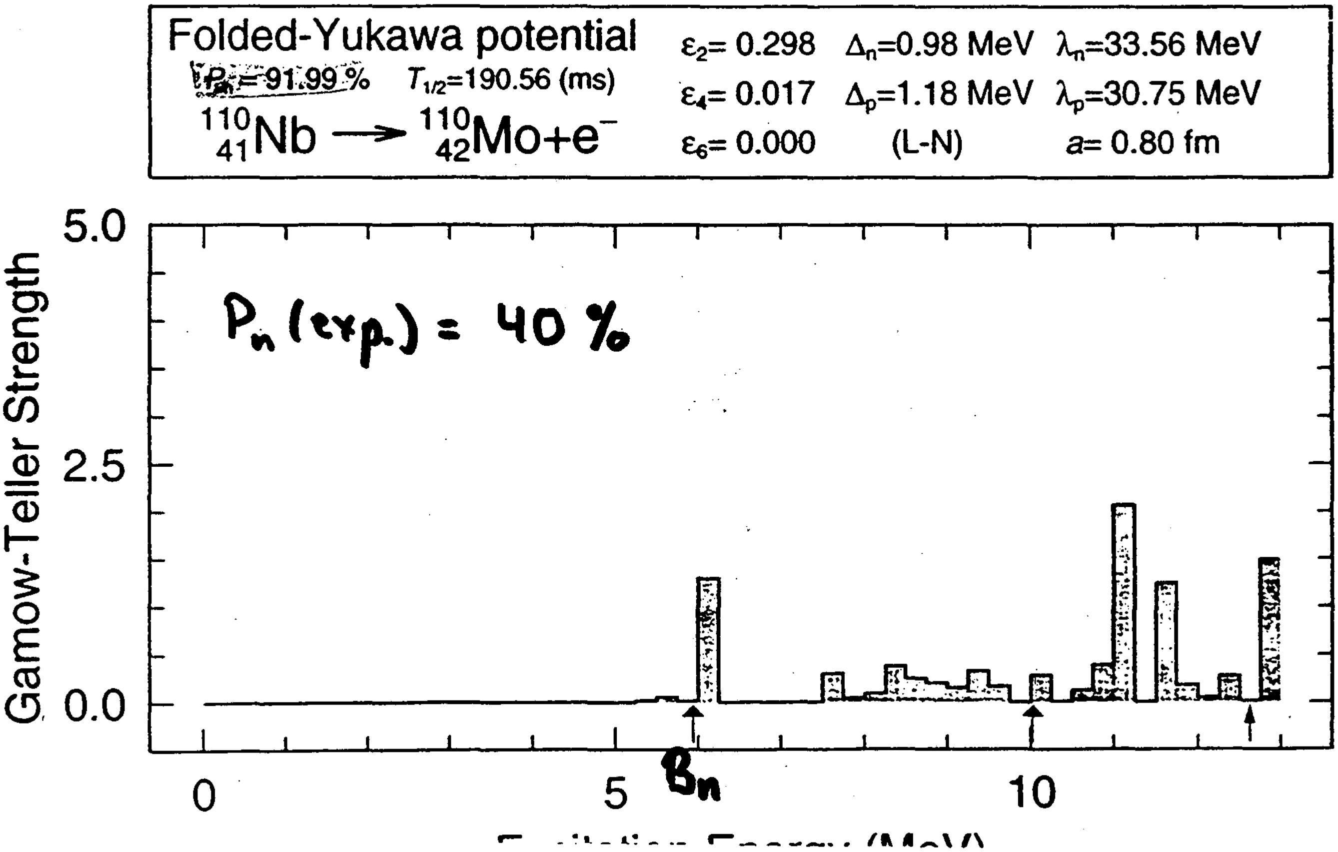

P_n (exp.) = 40 %

B_n

PROD. RATES IN βn-experiment

25 MeV p + uranium

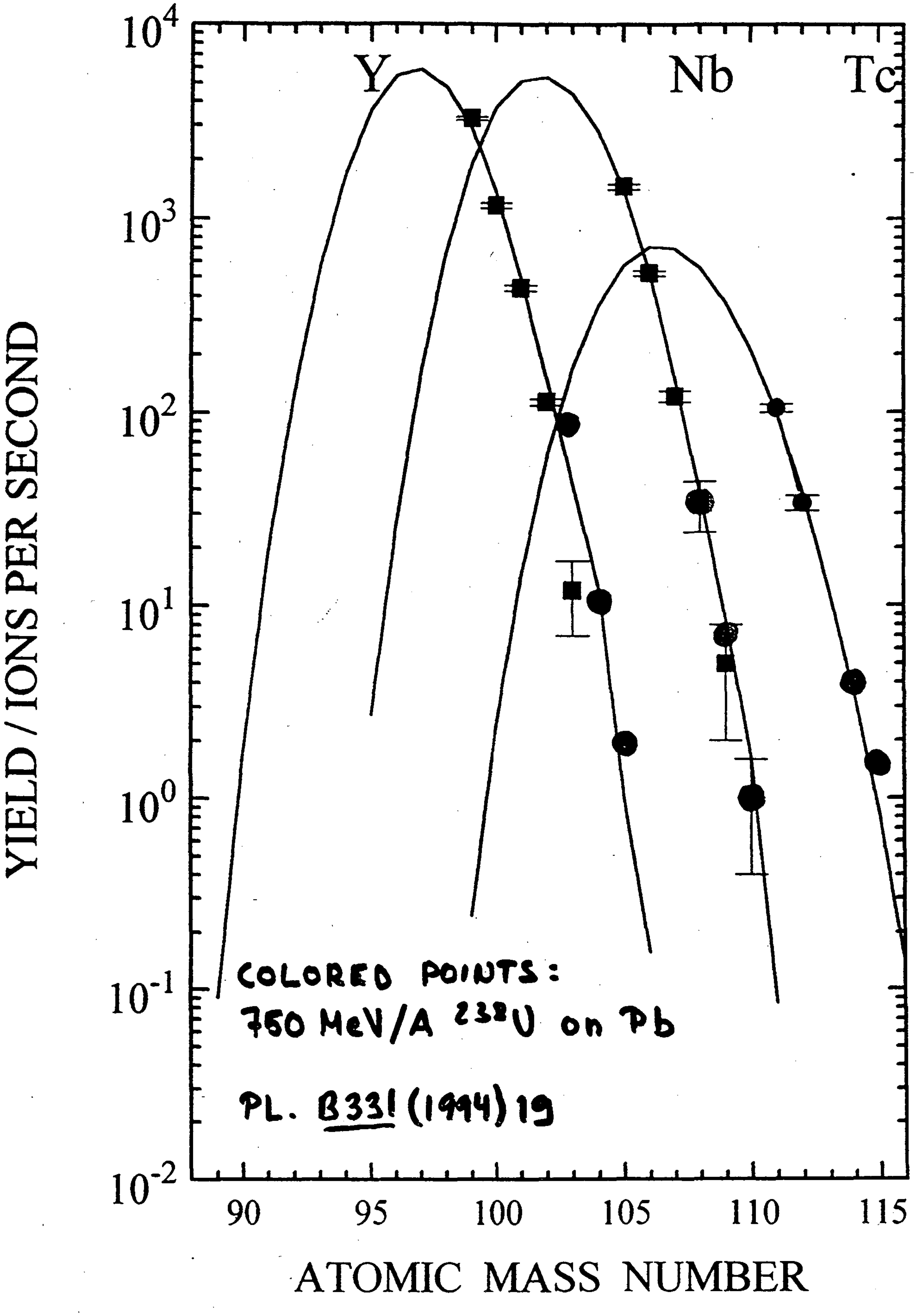

COLORED POINTS:
750 MeV/A ^{238}U on Pb

PL. B331 (1994) 19

UME 72, NUMBER 7 PHYSICAL REVIEW LETTERS 14 FEBRUARY 1994

Nuclear Shell Structure at Particle Drip Lines

J. Dobaczewski,[*] I. Hamamoto,[†] W. Nazarewicz,[*] and J. A. Sheikh[‡]
Joint Institute for Heavy-Ion Research, Physics Division, Oak Ridge National Laboratory,
P.O. Box 2008, Oak Ridge, Tennessee 37831
and Department of Physics, University of Tennessee, Knoxville, Tennessee 37996

(Received 1 September 1993)

The shell structure of exotic nuclei near proton and neutron drip lines is discussed in terms of the self-consistent mean-field theory. It is demonstrated that when approaching the neutron drip line, the neutron density becomes very diffused and the single-particle spectrum shows similarities to that of the harmonic oscillator with spin-orbit term. Interaction between bound orbitals and continuum is shown to result in quenching of shell effects in light and medium systems.

OLUME 72, NUMBER 10 PHYSICAL REVIEW LETTERS 7 MARCH 1994

Shell Effects in Nuclei near the Neutron-Drip Line

M. M. Sharma,[1] G. A. Lalazissis,[2] W. Hillebrandt,[1] and P. Ring[2]
[1]*Max Planck Institut für Astrophysik, Karl-Schwarzschildstrasse 1, D-85740 Garching, Germany*
[2]*Physik Department, Technische Universität München, D-85747 Garching, Germany*

(Received 20 October 1993)

Shell effects in nuclei close to the neutron-drip lines have been investigated. It has been demonstrated in the relativistic mean-field theory that nuclei very far from stability manifest the shell effects strongly. This behavior is in accord with the predictions of nuclear masses in the finite-range droplet model including shell corrections. The shell effects predicted in the existing Skyrme mean-field theory in comparison are significantly weaker than those of the other approaches.

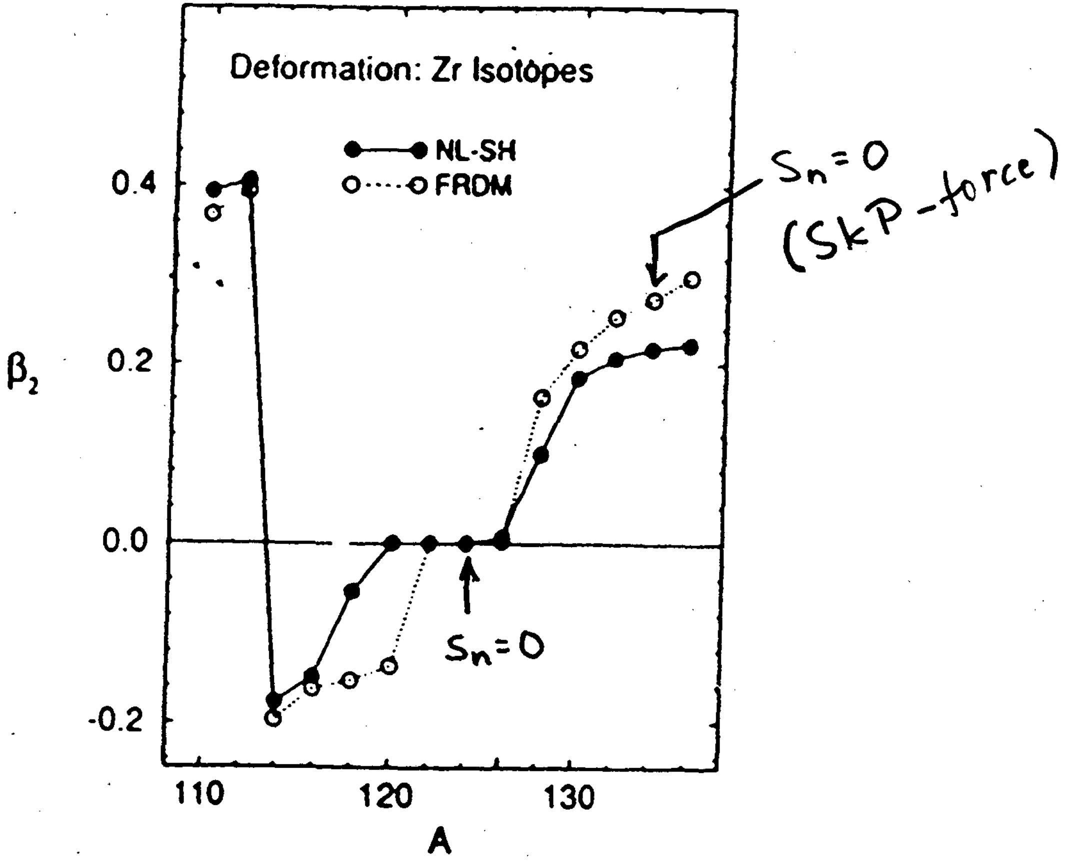

$S_n = 0$ (SkP-force)

$S_n = 0$

Gordon Wozniak

Lawrence Berkeley National Laboratory
Berkeley, CA

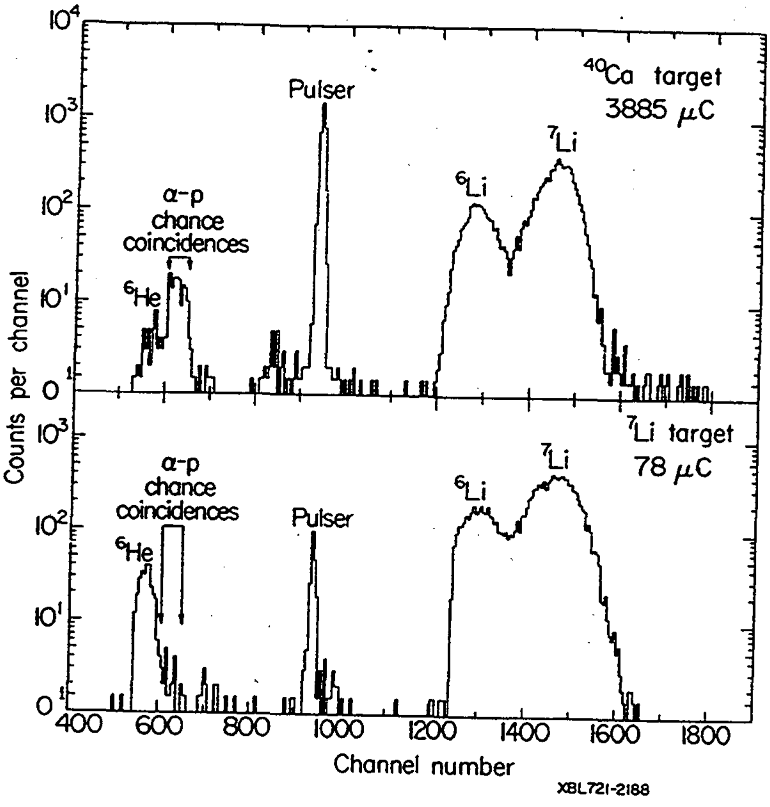

XBL721-2188

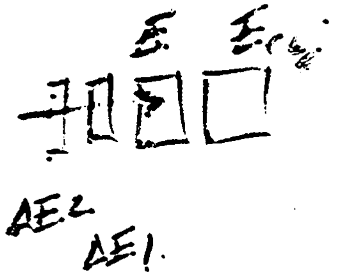

$^{40}Ca(^{12}C,^{7}Li)^{45}V$

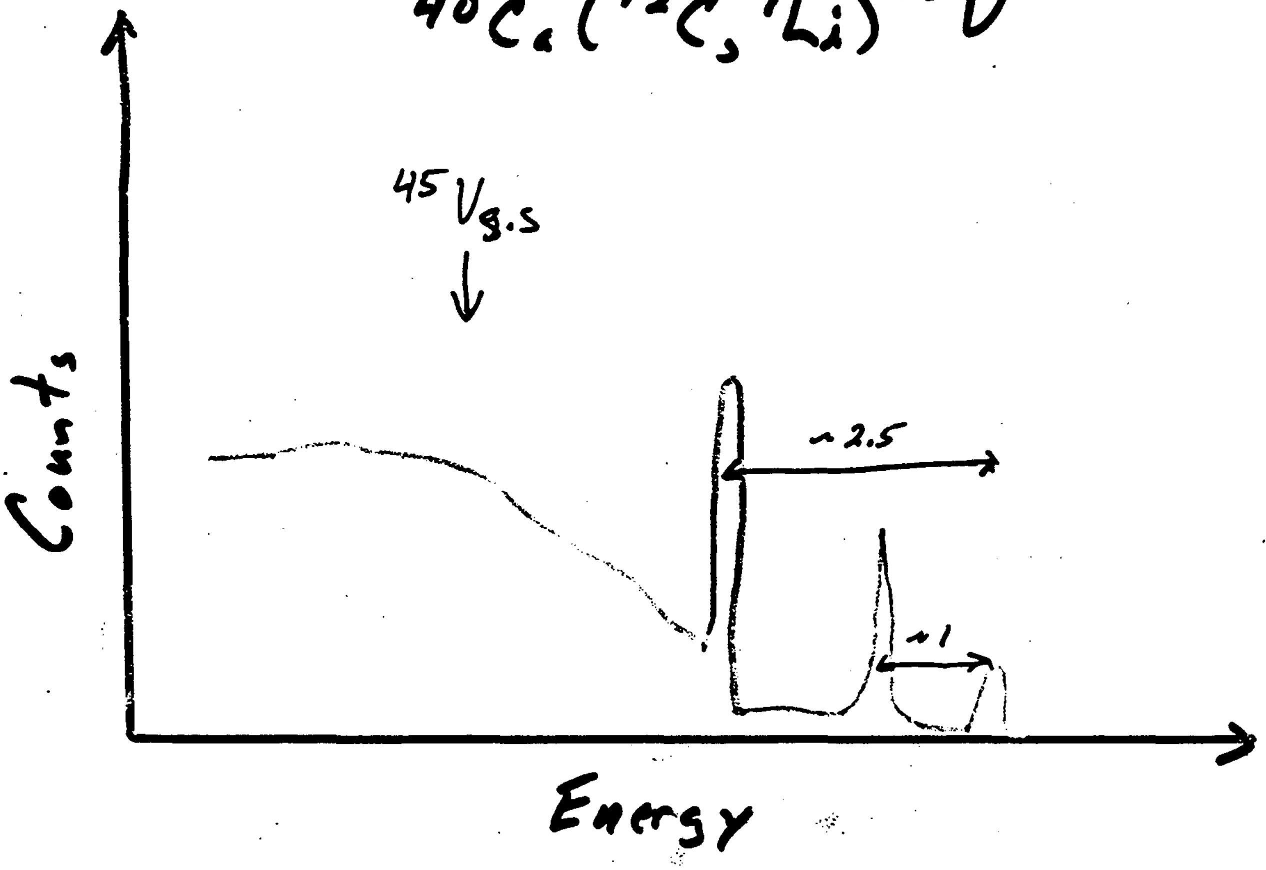

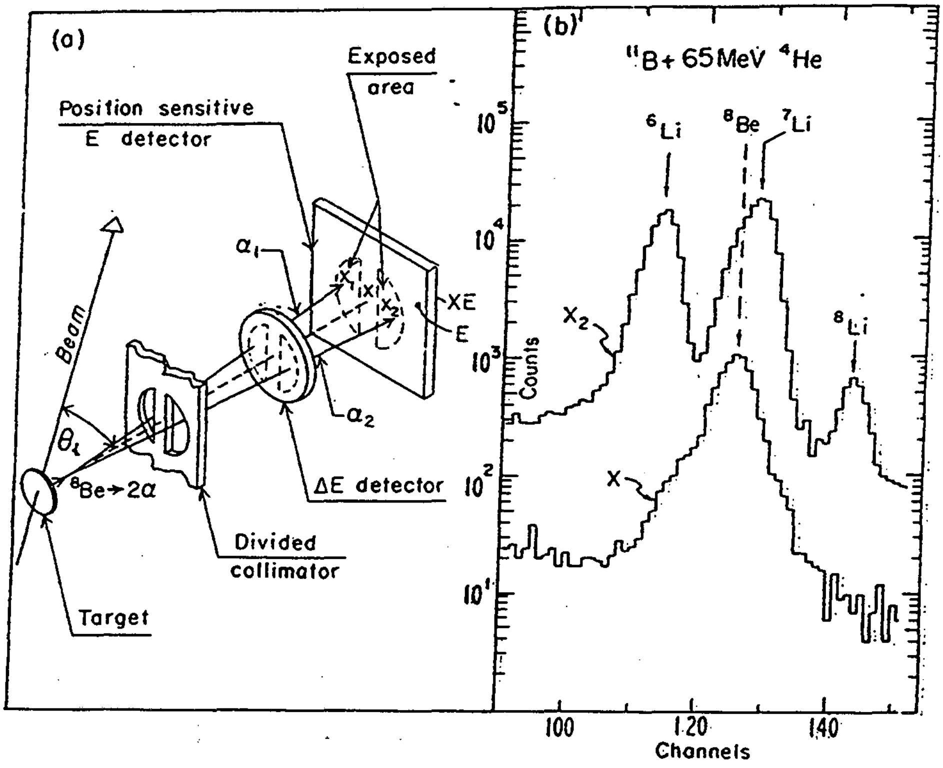

XBL735-2817

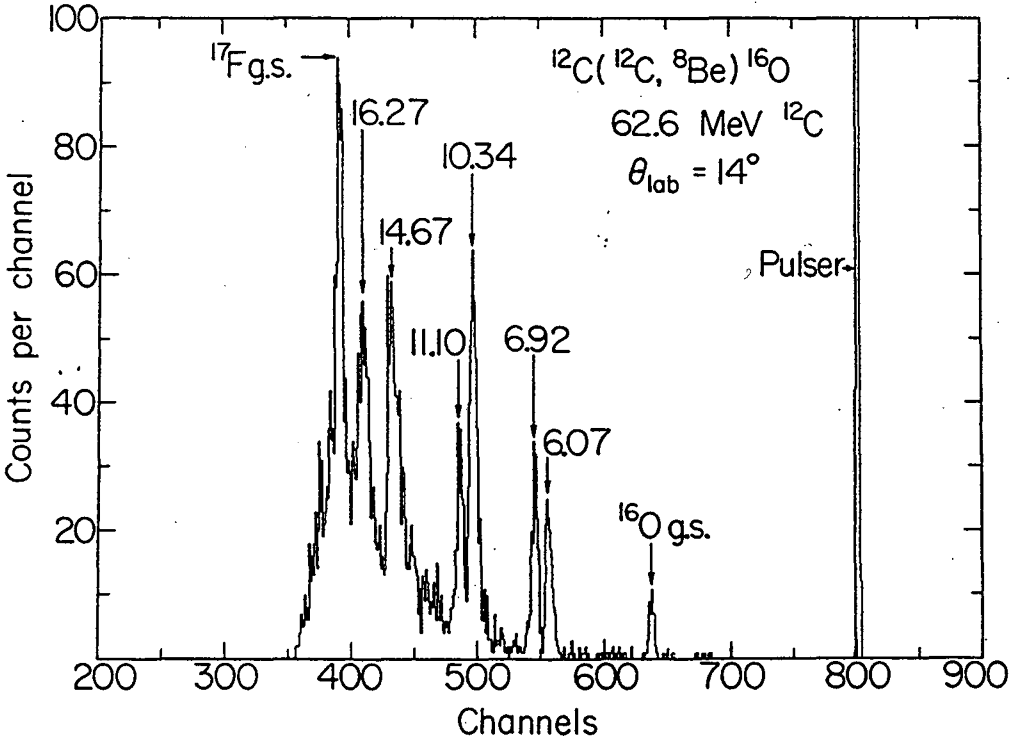

XBL721-2175

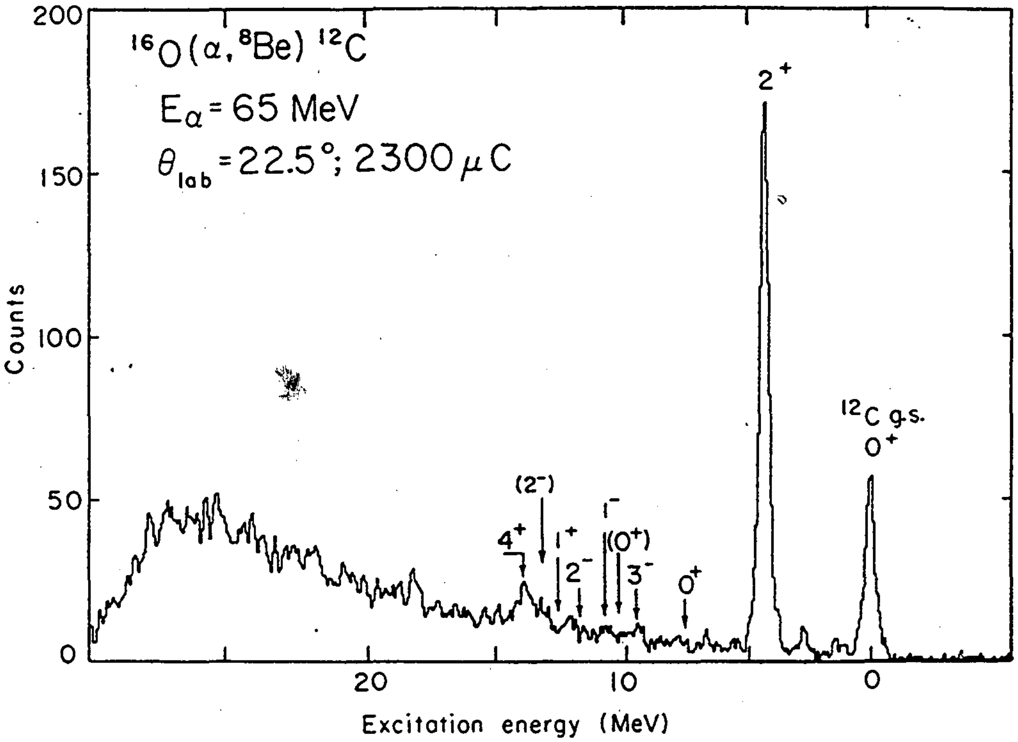

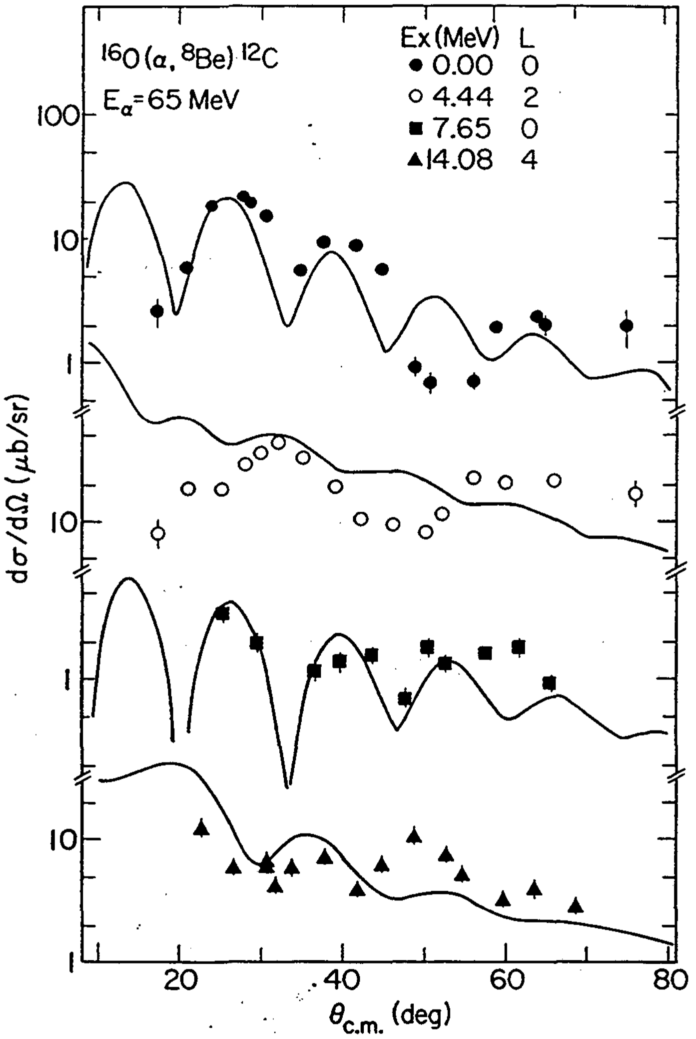

XBL 7512-9930

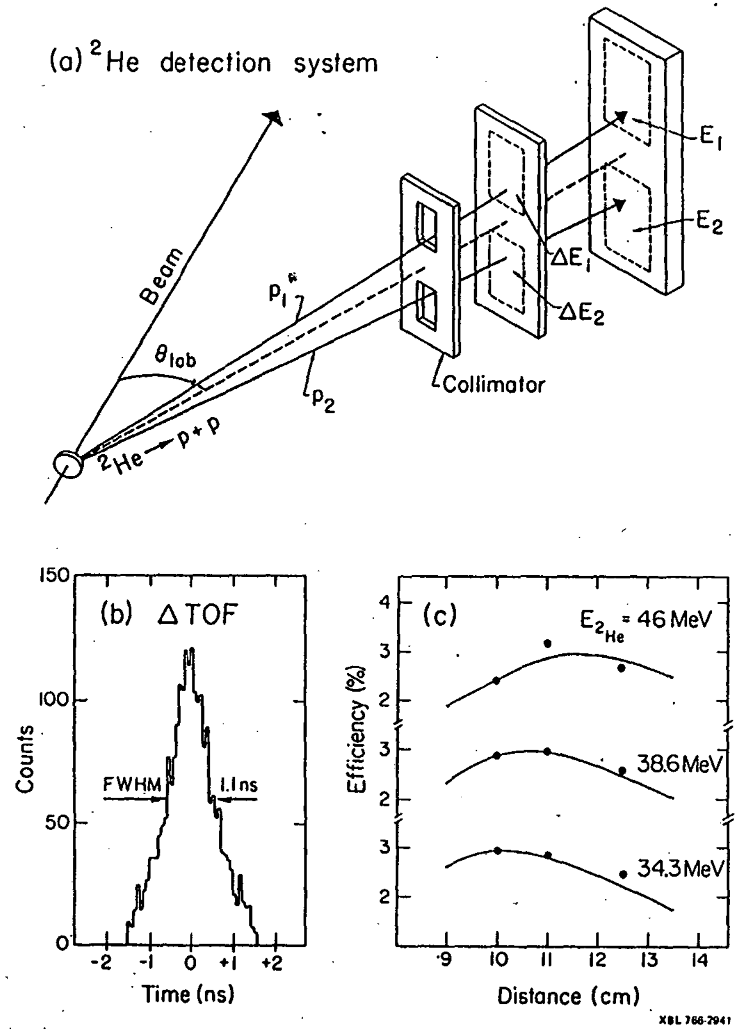
(a) ^{2}He detection system
Beam
θ_{lab}
^{2}He → p + p
p_1
p_2
Collimator
ΔE_1
ΔE_2
E_1
E_2
(b) ΔTOF
Counts
150
100
50
0
FWHM
1.1ns
-2
-1
0
+1
+2
Time (ns)
(c)
$E_{^2He}$ = 46 MeV
38.6 MeV
34.3 MeV
Efficiency (%)
4
3
2
9
10
11
12
13
14
Distance (cm)
XBL 766-2941

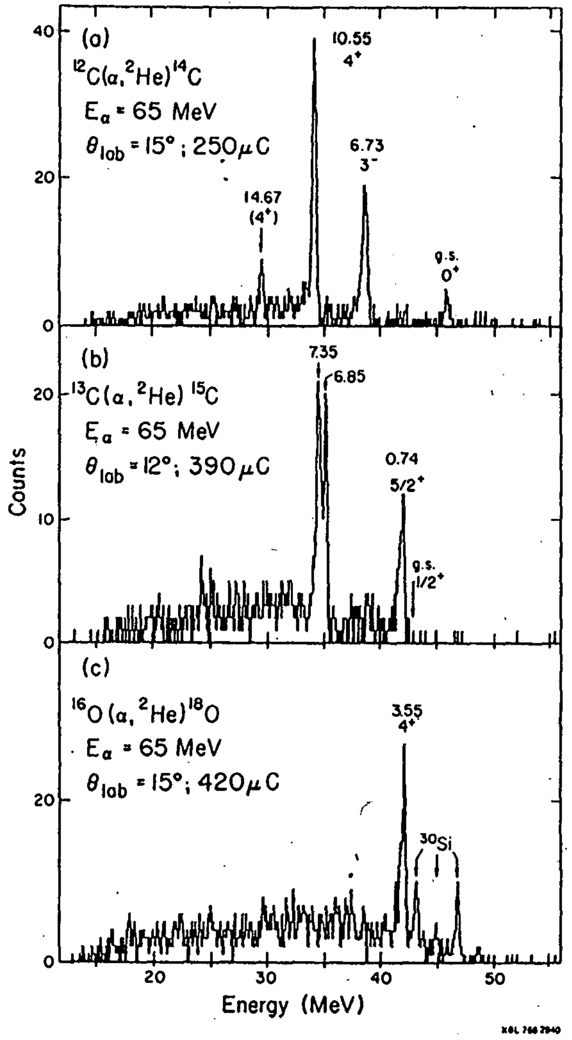
(a)
^{12}C(α, ^{2}He)^{14}C
E_α = 65 MeV
θ_{lab} = 15°; 250μC
10.55
4⁺
6.73
3⁻
14.67
(4⁺)
g.s.
0⁺
(b)
^{13}C(α, ^{2}He)^{15}C
E_α = 65 MeV
θ_{lab} = 12°; 390μC
7.35
6.85
0.74
5/2⁺
g.s.
1/2⁺
(c)
^{16}O(α, ^{2}He)^{18}O
E_α = 65 MeV
θ_{lab} = 15°; 420μC
3.55
4⁺
^{30}Si
Counts
40
20
10
0
20
30
40
50
Energy (MeV)
XBL 766-2940

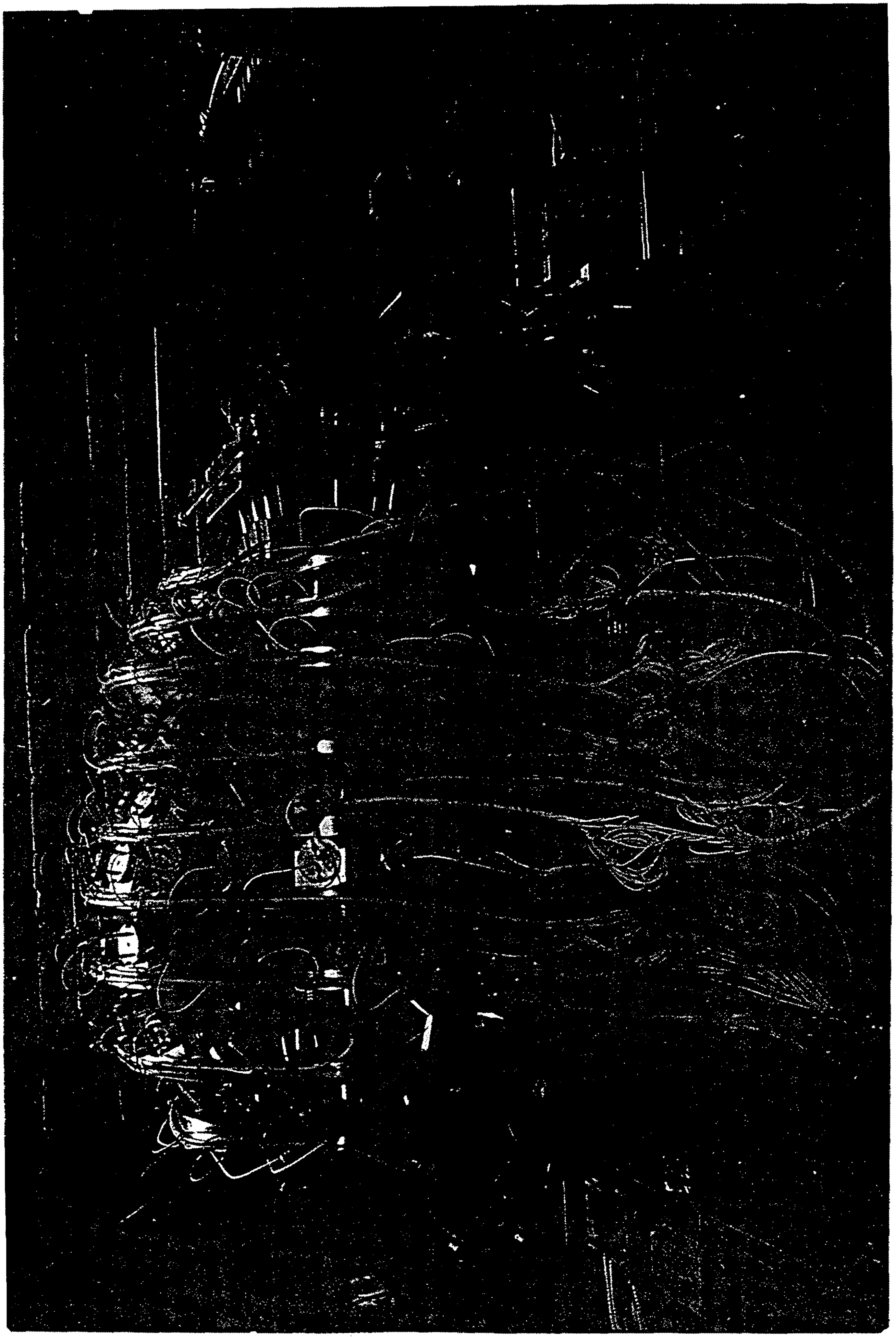

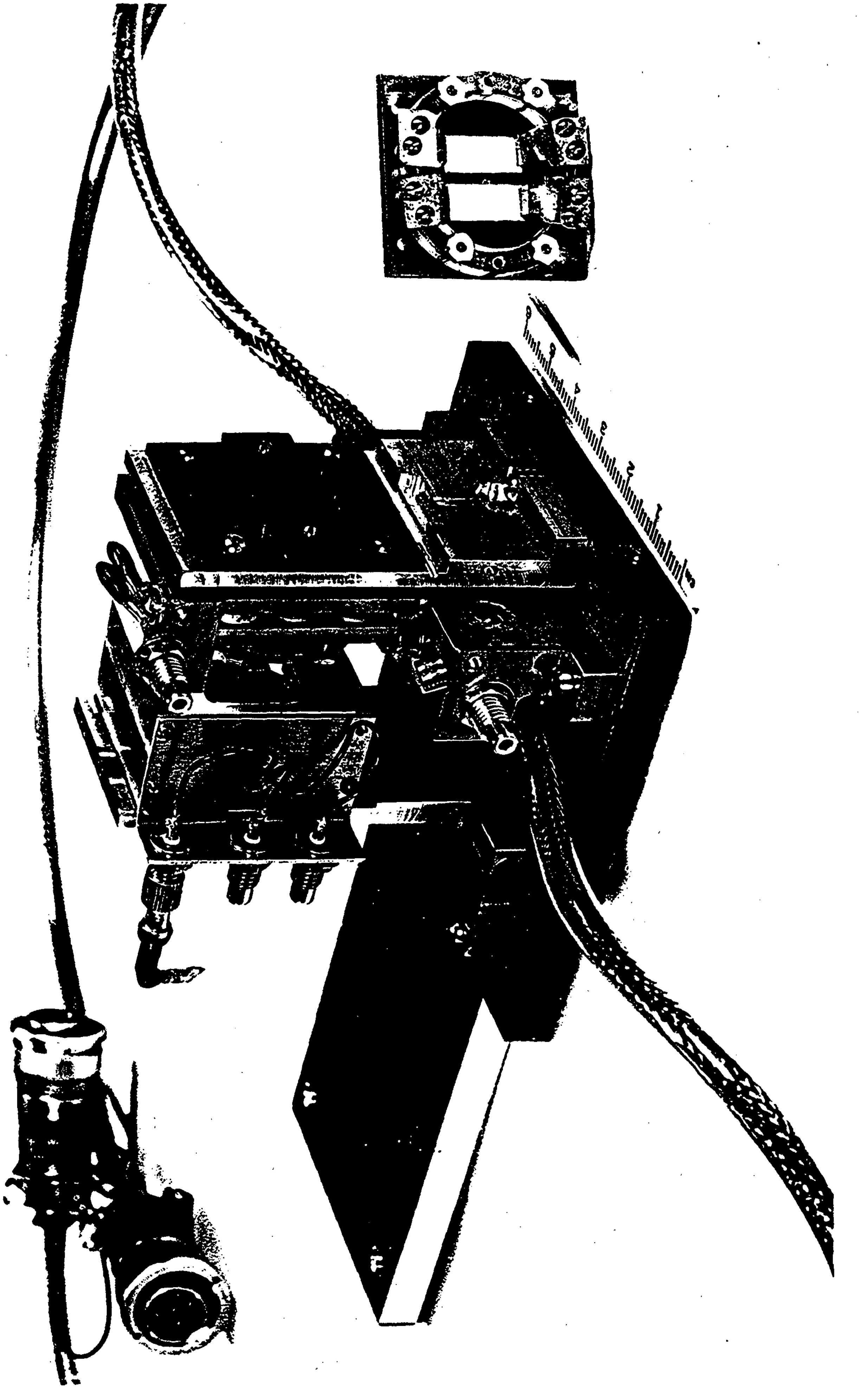

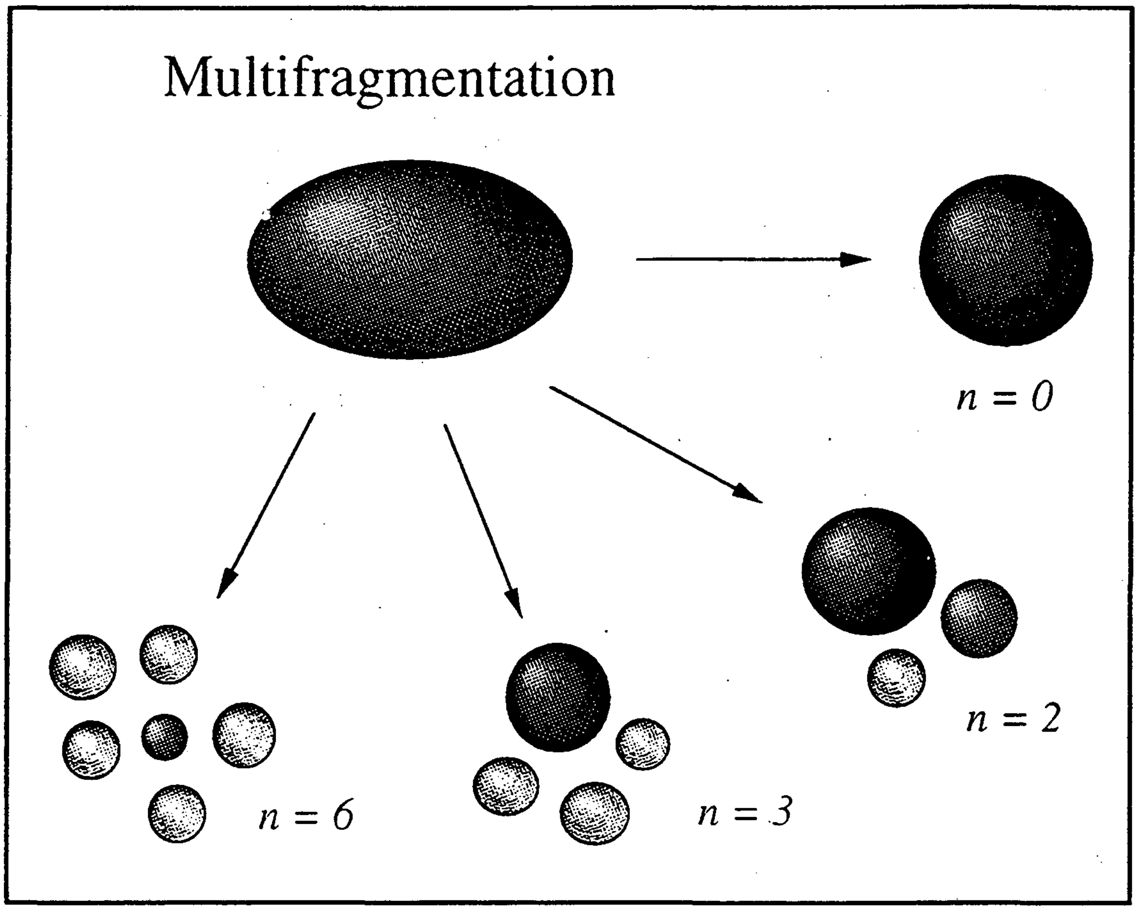

Binomial Reducibility

$$P_n^m = \frac{m!}{n!(m-n)!}p^n(1-p)^{m-n}$$

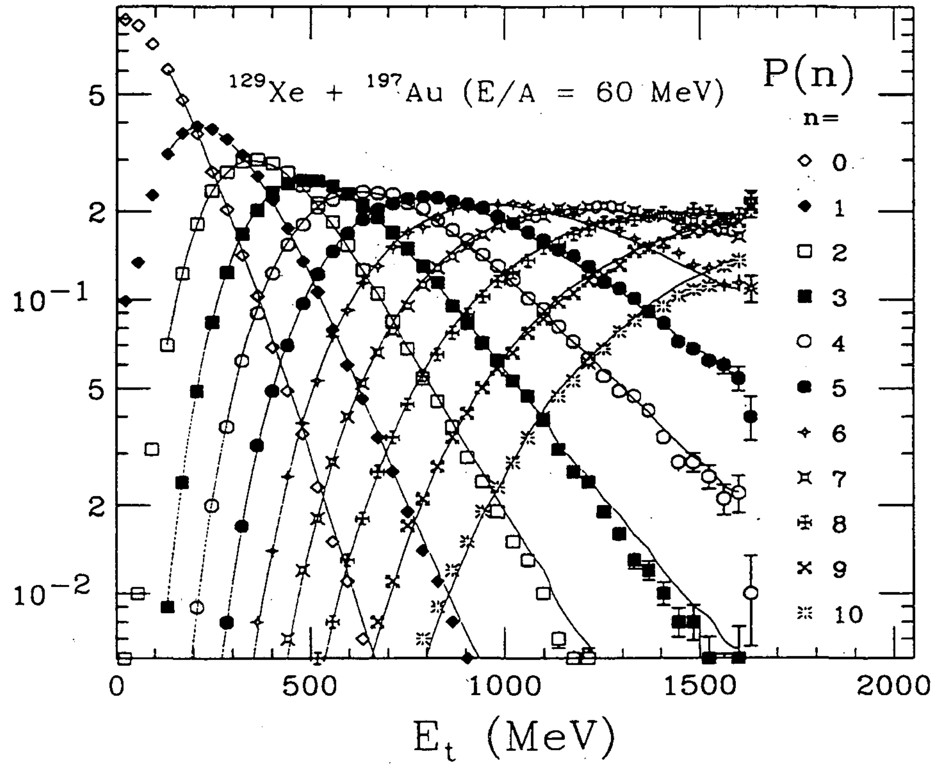

Thermal Scaling

$$p \propto e^{-B/T}$$

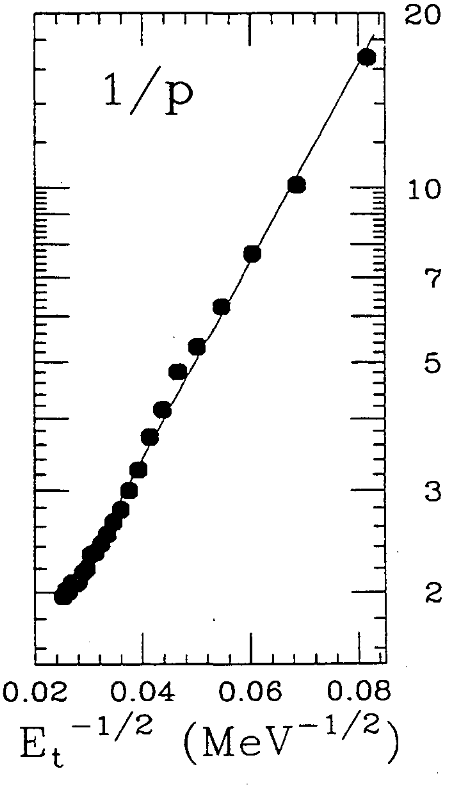

Reducible and Thermal Nature of the Charge Distributions

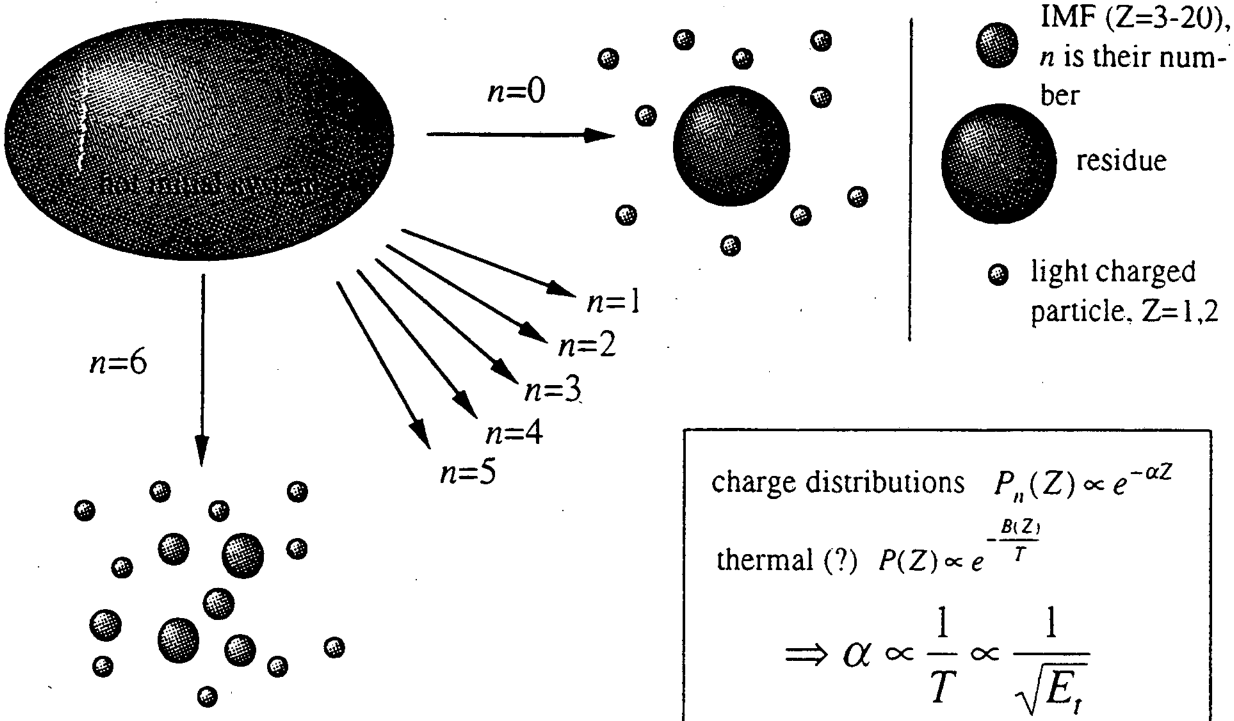

charge distributions $P_n(Z) \propto e^{-\alpha Z}$

thermal (?) $P(Z) \propto e^{-\frac{B(Z)}{T}}$

$$\Rightarrow \alpha \propto \frac{1}{T} \propto \frac{1}{\sqrt{E_t}}$$

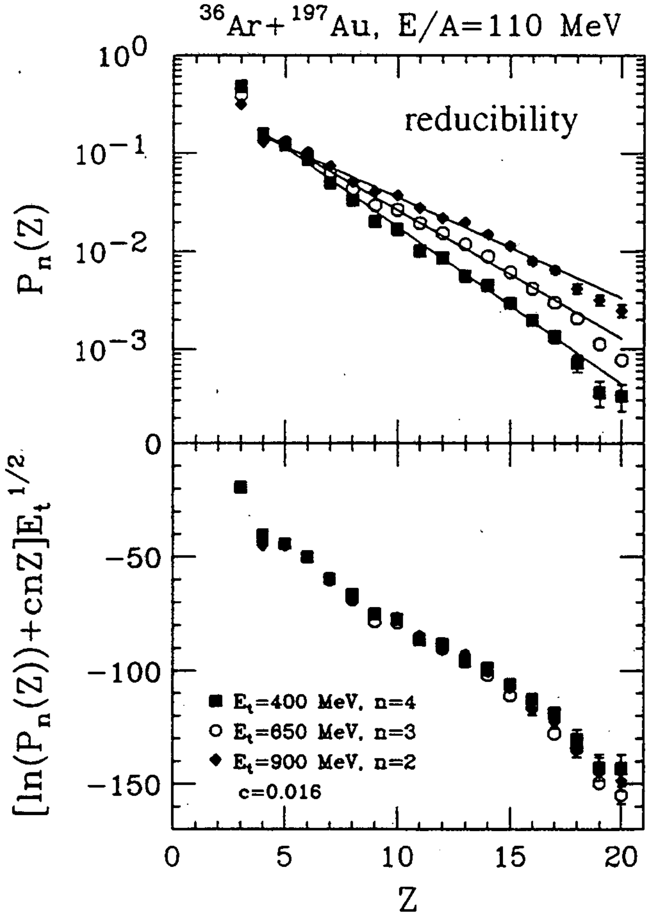

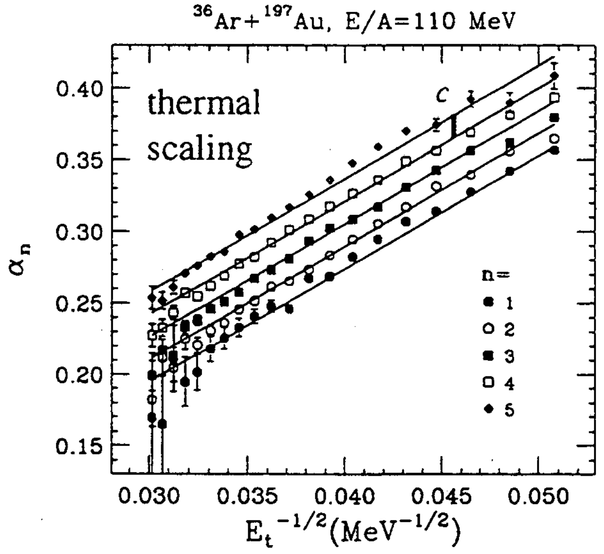

$$\alpha_n = \frac{K}{\sqrt{E_t}} + nc \Rightarrow P_n(Z) \propto \exp\left[-\frac{B(Z)}{T} - ncZ\right]$$

Euler's problem, break Z_0 into n smaller pieces

$$n_Z \approx \frac{n^2}{Z_0}\exp\left[-\frac{nZ}{Z_0}\right]$$

$$\boxed{c \propto \frac{1}{Z_0}}$$

Phase Coexistence in Multifragmentation?

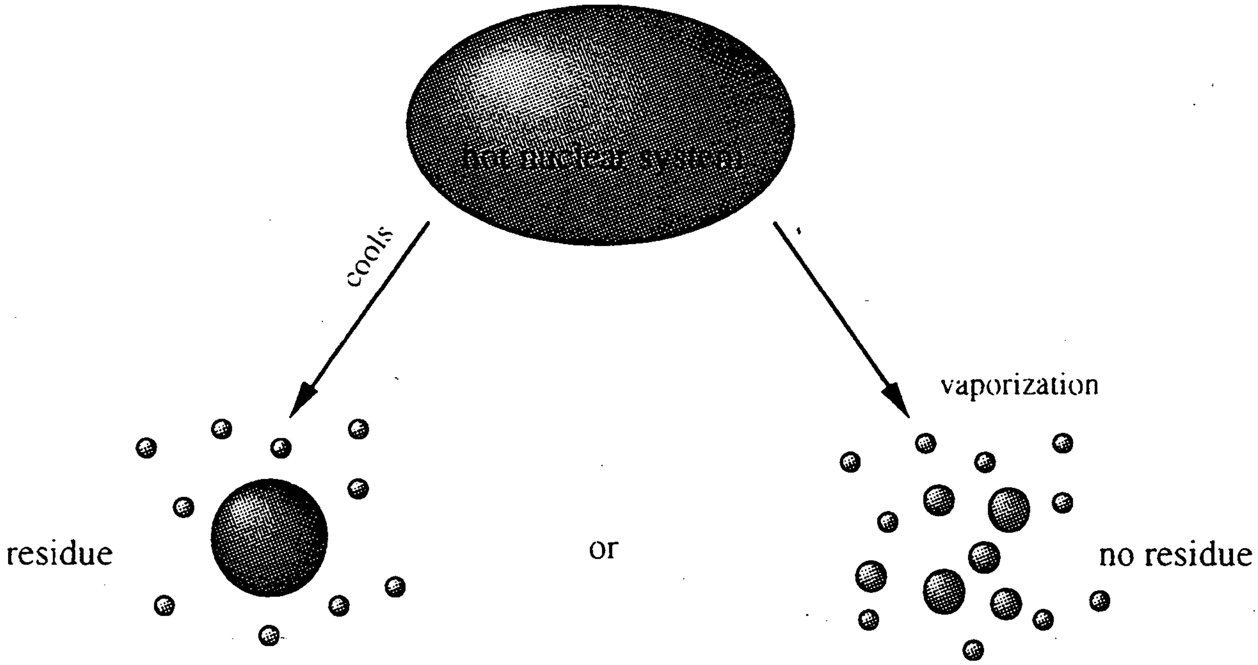

Charge distributions: $P_n(Z) \propto \exp\left[\underbrace{-\frac{B(Z)}{T}}_{\text{enthalpy}} - \underbrace{n\textcircled{c}Z}_{\text{entropy}}\right]$

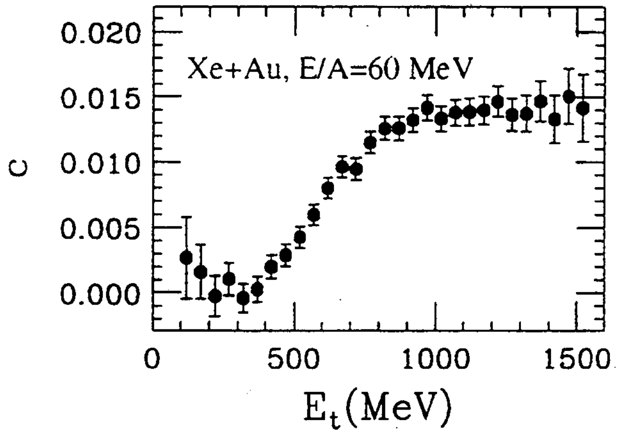

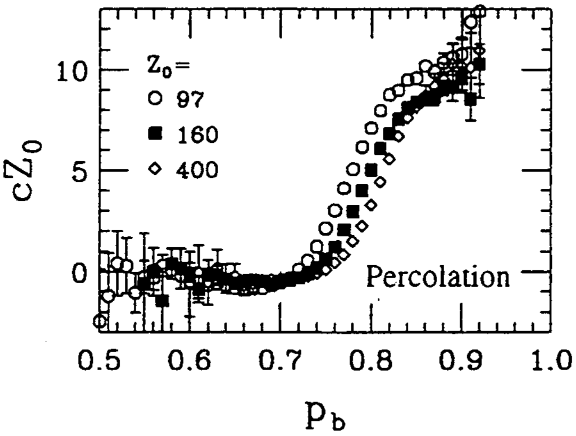

Classical Liquid-Gas
Phase Diagram

$$c \propto \mu_L - \mu_V$$

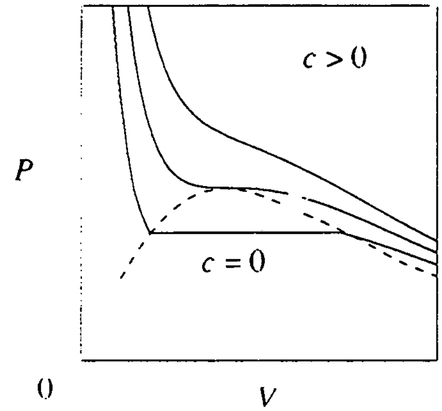

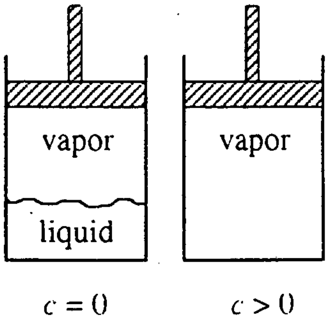

Mike Rowe

Lawrence Berkeley National Laboratory
Berkeley, CA

Beta-Delayed One- and Two- Proton Decay Studies of ^{23}Si and ^{22}Al

M. W. Rowe, T. J. Ognibene, J. Powell,
J. C. Batchelder, D. M. Moltz
and Joseph Cerny

88-Inch Cyclotron
Lawrence Berkeley National Laboratory

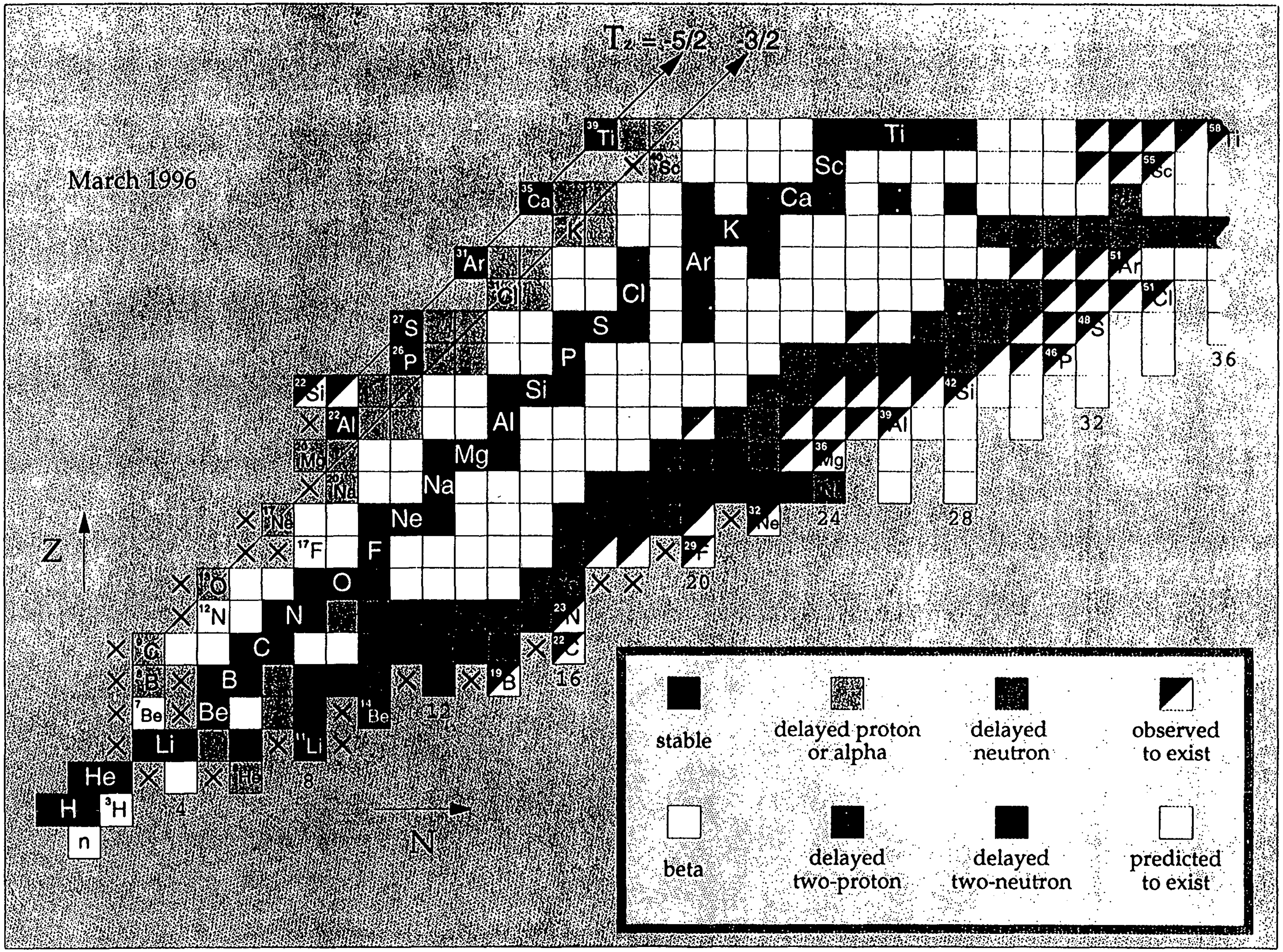

March 1996
T_z = -5/2
-3/2
Z
N
n
H
³H
He
⁶He
Li
¹¹Li
⁷Be
Be
¹⁴Be
⁸B
B
¹⁹B
⁹C
C
²²C
¹²N
N
²³N
¹³O
O
¹⁷F
F
²⁹F
¹⁷Ne
Ne
³²Ne
²⁰Na
Na
²⁰Mg
Mg
³⁶Mg
²²Al
Al
³⁹Al
²²Si
Si
⁴²Si
²⁶P
P
⁴⁶P
²⁷S
S
⁴⁸S
Cl
⁵¹Cl
³¹Ar
Ar
⁵¹Ar
K
³⁵Ca
Ca
⁴⁰Sc
Sc
⁵⁵Sc
³⁹Ti
Ti
⁵⁸Ti
4
8
12
16
20
24
28
32
36
stable
delayed proton or alpha
delayed neutron
observed to exist
beta
delayed two-proton
delayed two-neutron
predicted to exist

Si-23 Mass Predictions

Mass Model Authors	Method of Prediction	Mass Excess (MeV)	Lab. Proton Energy* (IAS-->g.s.; MeV)
Satpathy-Nayak	Infinite nuclear matter model	25.37	13.69
Tachibana et al.	Empirical liquid drop with odd/even and shell corrections	23.84	11.17
Moeller et al.	Finite-range droplet with shell/pairing corrections	24.39	12.22
Moeller-Nix	Yukawa+exponential model with shell/pairing corrections	23.86	12.52
Masson-Jaenecke	Imhomogeneous partial difference equation with isospin	23.94	11.74
Jaenecke-Masson	Transverse Garvey-Kelson mass relation	23.43	10.88
Comay-Kelson-Zidon	Transverse and longitudinal Garvey-Kelson relationships	23.51	10.76
Pape-Antony	Isobaric Mass Multiplet Equation (IMME)	23.44	10.95
Wapstra-Audi	Experimental data and systematic trends	23.77	11.33

* Proton energy calculated using Coulomb Displacement Energy of 5.03 MeV and predicted Mg-22 ground-state masses

All predictions taken from Atomic Data and Nuclear Data Tables, vol. 39, 186 (1988)
except for Wapstra-Audi, which is from Nuclear Physics A565, 1 (1993).

Predicted Decay Energetics for Silicon-23

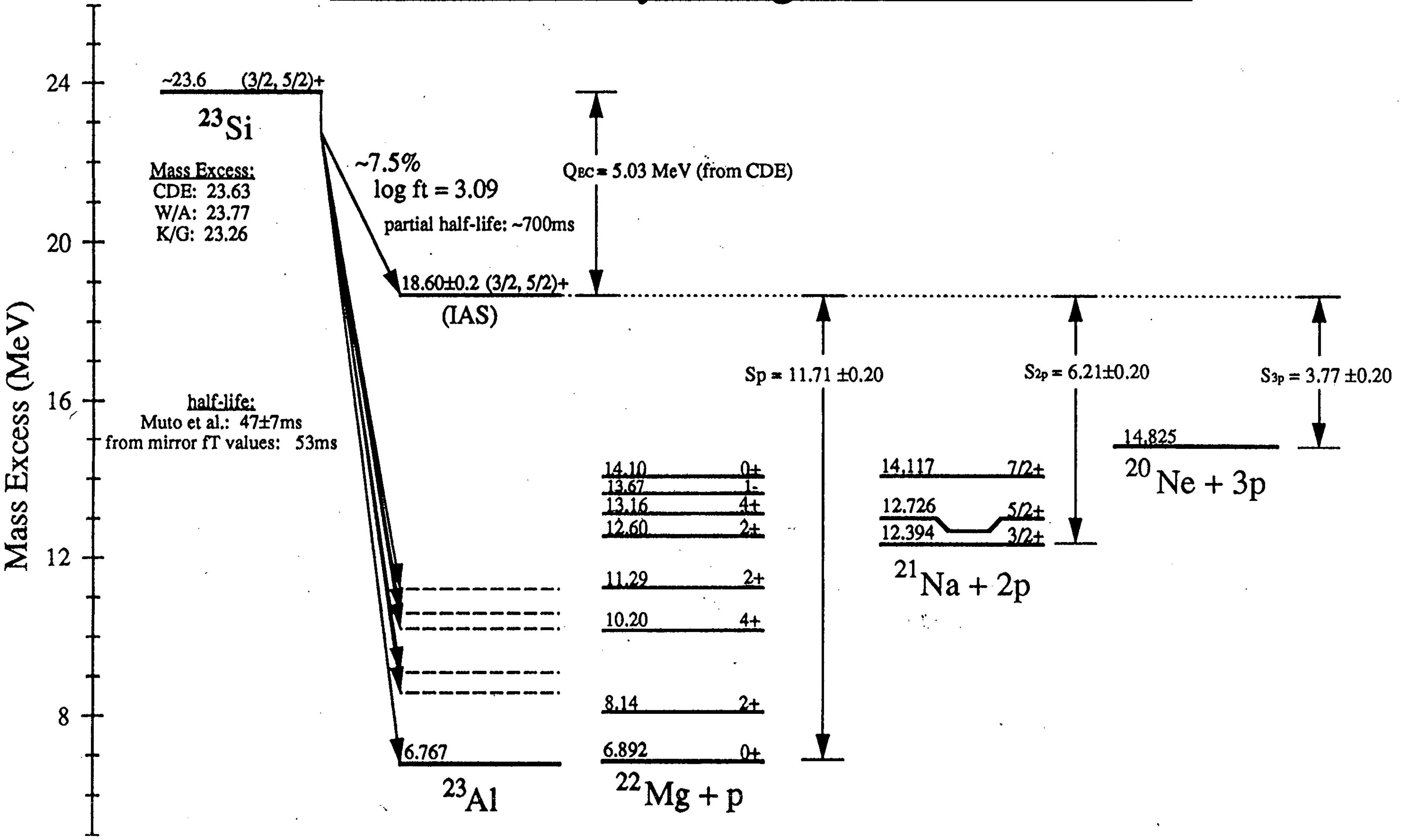

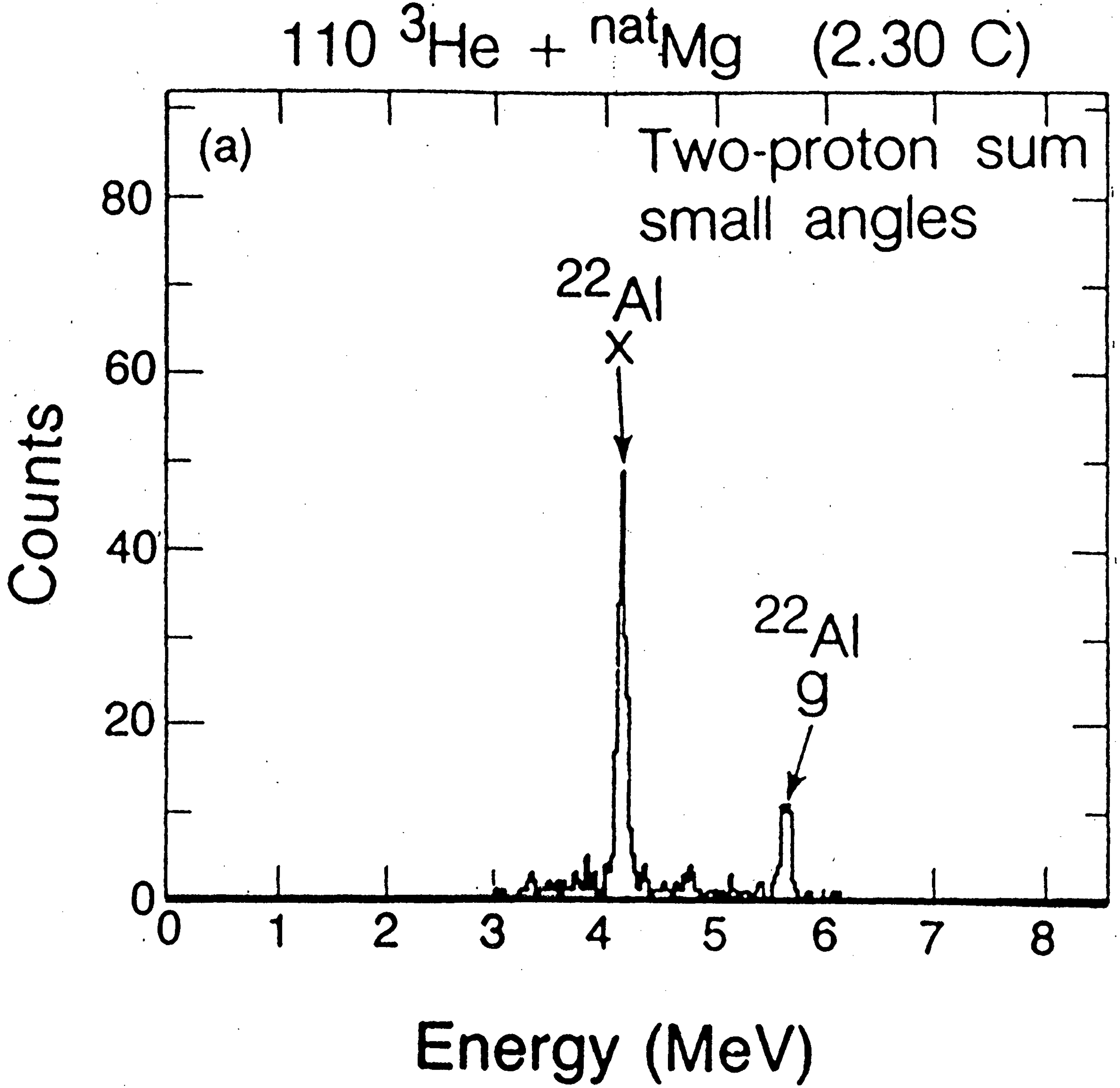

110 ^{3}He + ^{nat}Mg (2.30 C)
(a)
Two-proton sum
small angles
^{22}Al
x
^{22}Al
g
Counts
0
20
40
60
80
0
1
2
3
4
5
6
7
8
Energy (MeV)

Decay Energetics for Aluminum-22

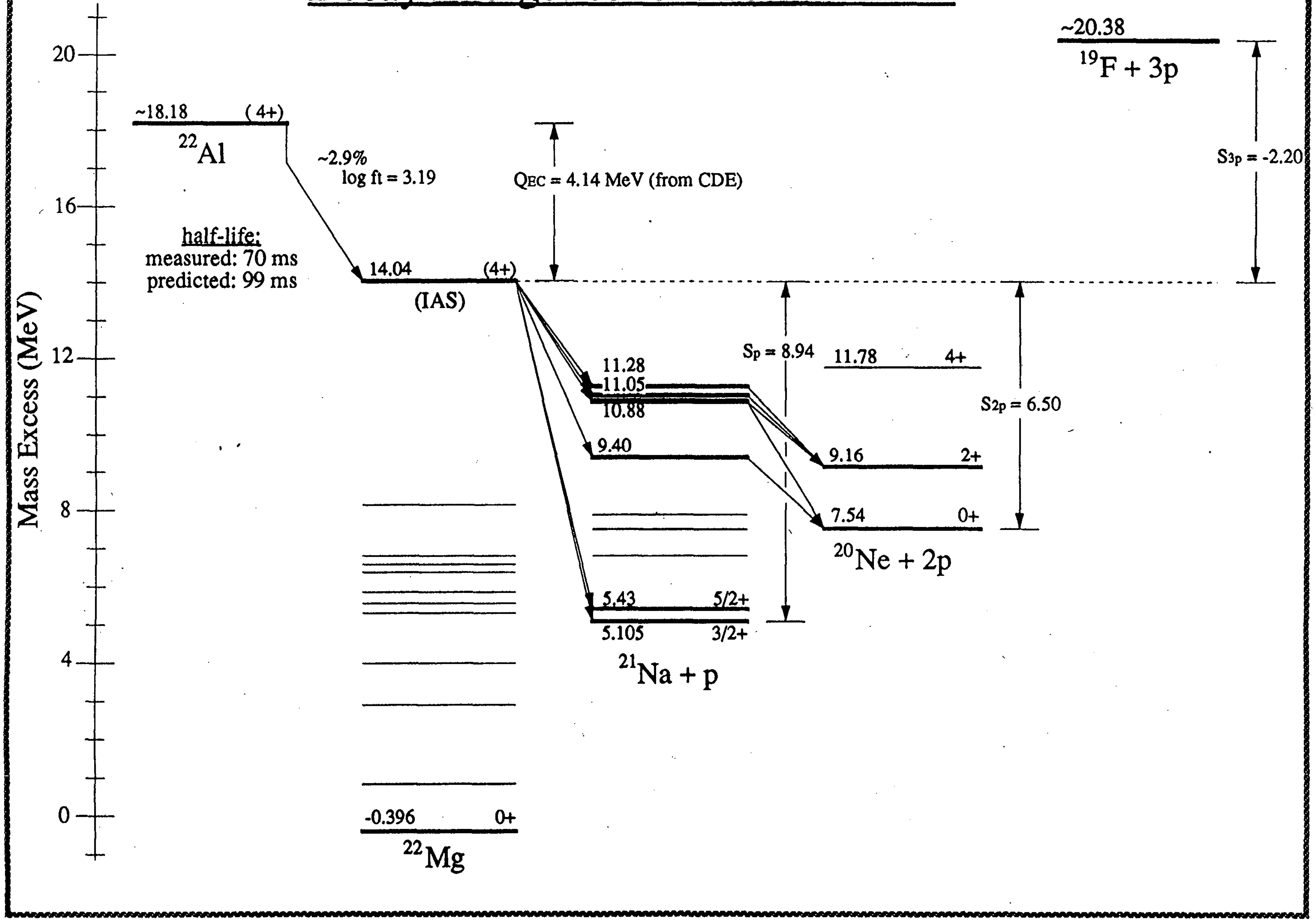

Shell Model Calculations of Isospin-Forbidden Beta-Delayed Proton Decays

B. A. Brown,
Phys. Rev. Lett. **65**, 2753 (1990)

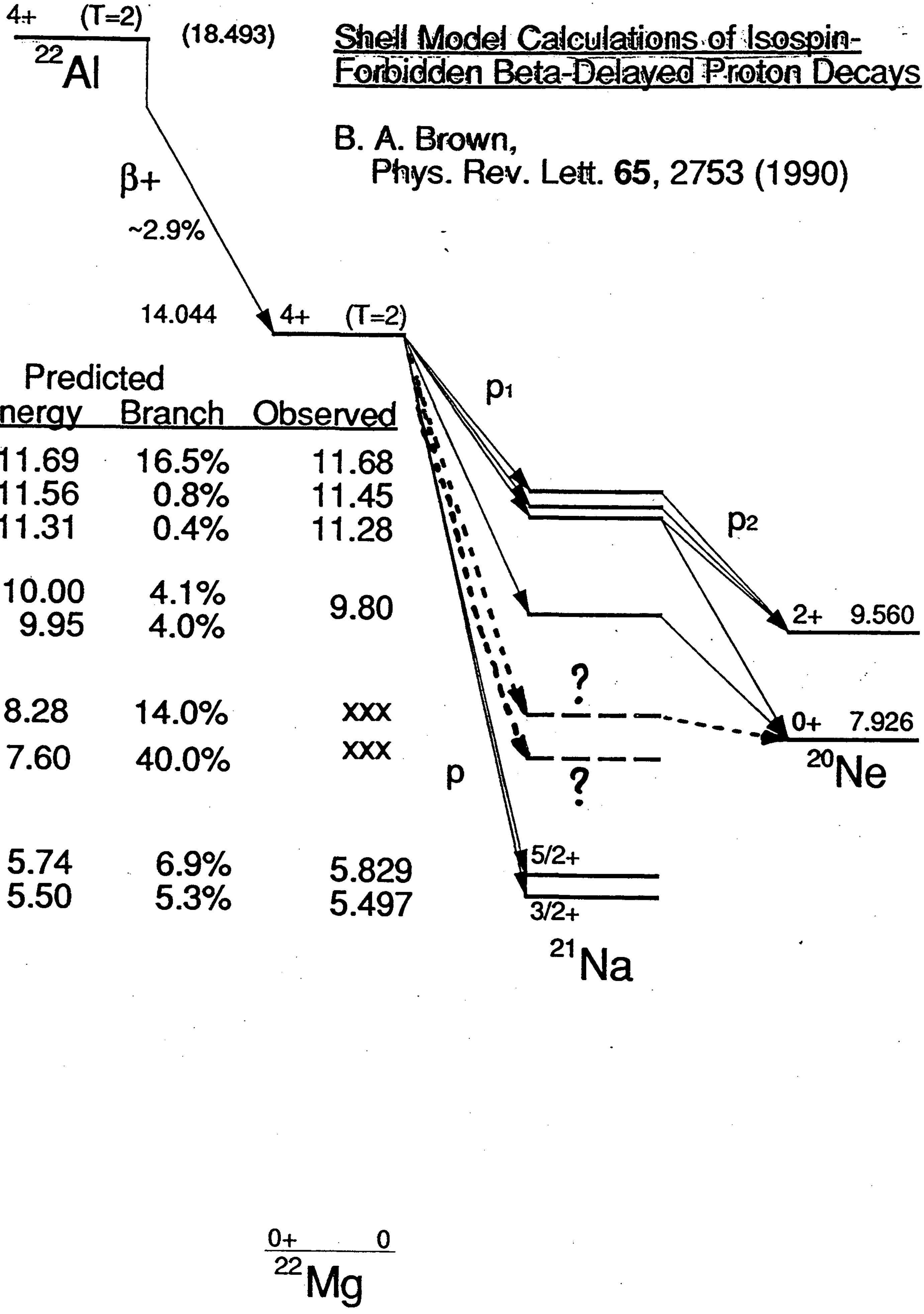

Predicted		
Energy	Branch	Observed
11.69	16.5%	11.68
11.56	0.8%	11.45
11.31	0.4%	11.28
10.00	4.1%	9.80
9.95	4.0%	
8.28	14.0%	xxx
7.60	40.0%	xxx
5.74	6.9%	5.829
5.50	5.3%	5.497

Experimental Goals

- Observe ^{23}Si beta-delayed proton decay
- Determine masses of ^{23}Si IAS and ^{23}Si
- Look for ^{23}Si beta-delayed two-proton decay
- Observe beta-delayed two-proton decay branch of ^{22}Al through predicted 2.78 MeV ^{21}Na state
- Measure ^{23}Si half-life

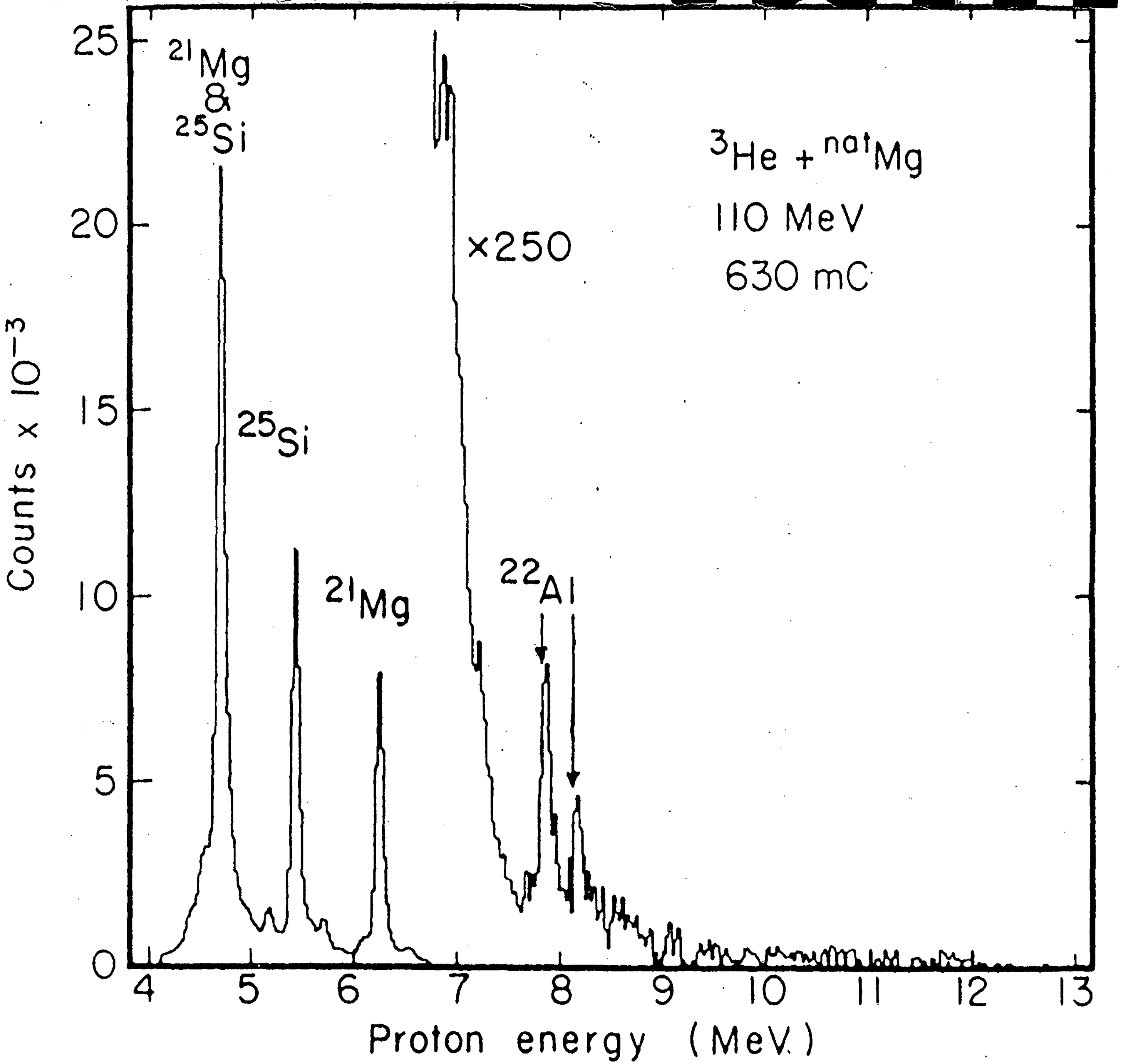

^{21}Mg & ^{25}Si
^{25}Si
^{21}Mg
×250
^{22}Al
^{3}He + ^{nat}Mg
110 MeV
630 mC
Counts × 10^{-3}
0
5
10
15
20
25
4
5
6
7
8
9
10
11
12
13
Proton energy (MeV)

Comparison of Experimental Parameters

	^{22}Al		^{23}Si
	Predicted	Observed (Cable et al.)	Predicted
Cross Section	6.75 µb (ALICE)	116-260 nb	450 nb (ALICE)
Half-Life	99±4 ms (Muto et al.)	70^{+50}_{-35} ms	47±7 ms (Muto et al.)
He-Jet Transport Time	~100 ms	N/A	~20 ms
IAS Feeding	4% (Muto et al.)	~2.9%	4.9% (Muto et al.)
Beta-Delayed p/2p Ratio	0.2 (Detraz)	0.52 - 0.18	1 (Detraz)
Proton Feeding to Ground and First-Excited Daughter States	21.6% (Brown)	N/A	36.4% (COCAGD3)

Experimental Requirements

- Large proton-energy range: ~300 - 13000 keV
- Ability to observe two-proton decay events
- Tolerate high beta-decay count rates (>30 kHz)
- Unambiguous identification of decay events
- Minimize background events
- Minimize transport time
- Reliable calibrations at both high and low energies

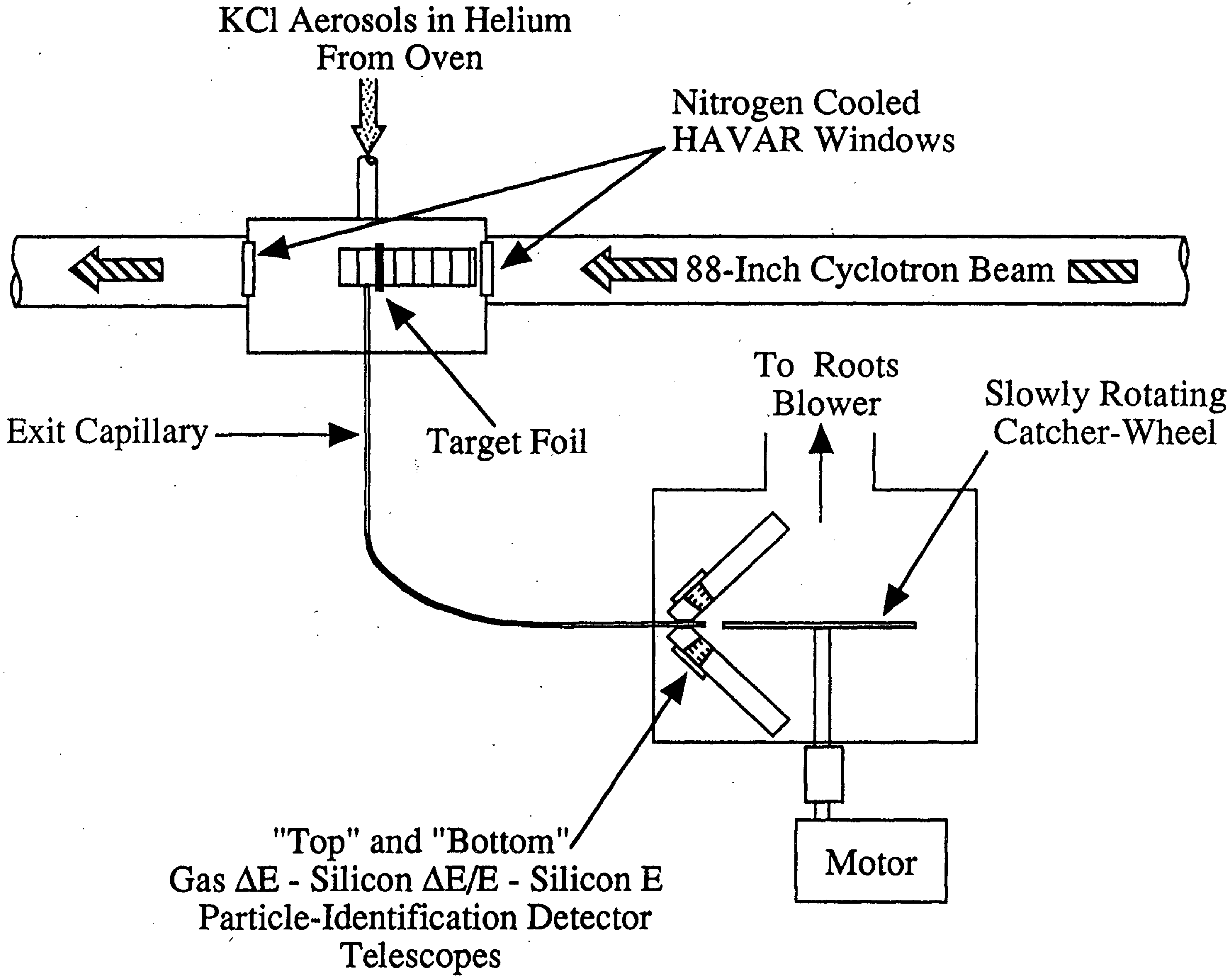
KCl Aerosols in Helium
From Oven
Nitrogen Cooled
HAVAR Windows
88-Inch Cyclotron Beam
To Roots
Blower
Slowly Rotating
Catcher-Wheel
Exit Capillary
Target Foil
"Top" and "Bottom"
Gas ΔE - Silicon ΔE/E - Silicon E
Particle-Identification Detector
Telescopes
Motor

Gas ΔE - Silicon ΔE/E - Silicon E

Large Energy-Range Particle Identification Telescope

Capable of detecting protons with energies from ~300 keV to ~14 MeV

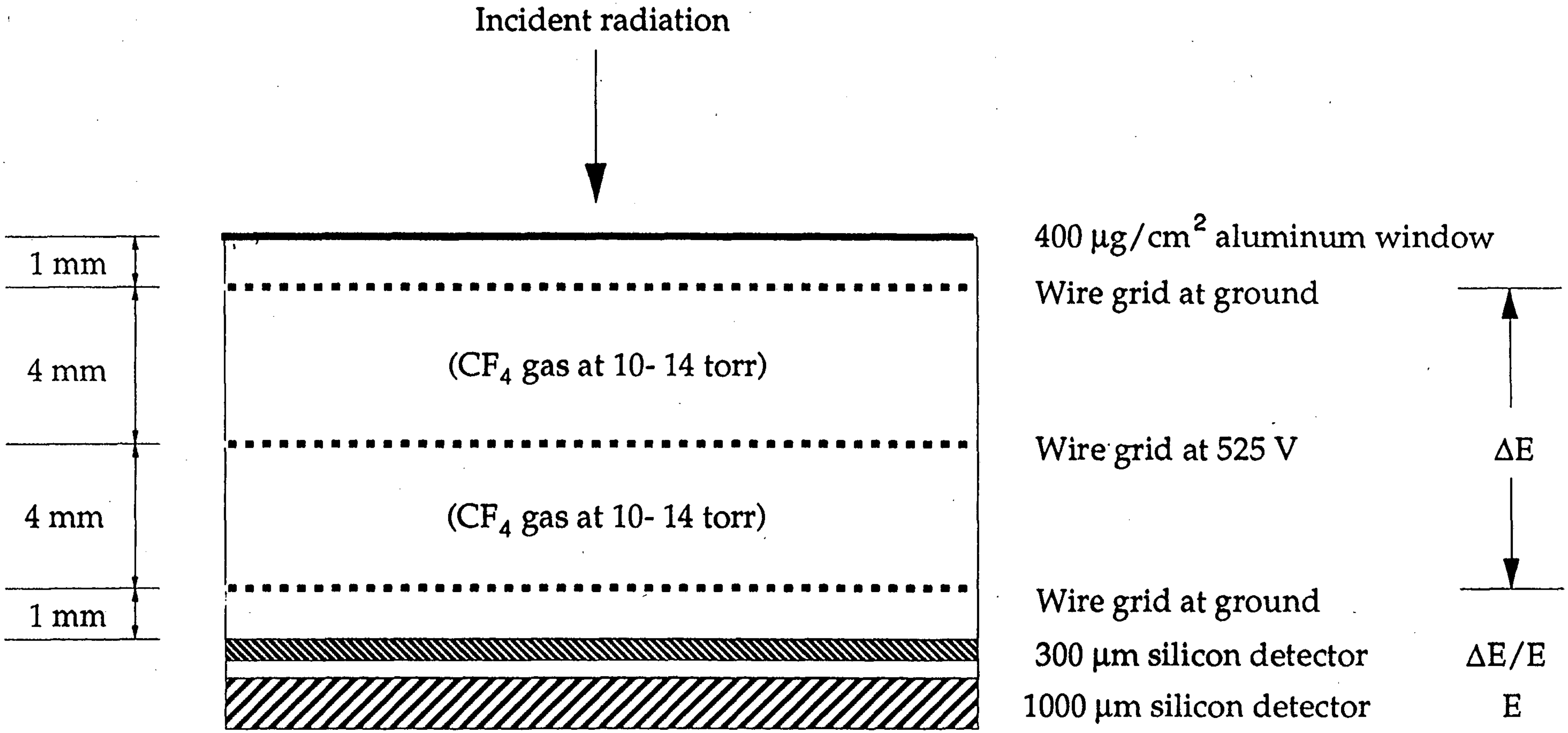

Incident radiation

1 mm

4 mm

4 mm

1 mm

(CF_4 gas at 10- 14 torr)

(CF_4 gas at 10- 14 torr)

400 μg/cm^2 aluminum window

Wire grid at ground

Wire grid at 525 V

Wire grid at ground

300 μm silicon detector

1000 μm silicon detector

ΔE

ΔE/E

E

Electronics Set-up for Large Energy-Range Telescopes

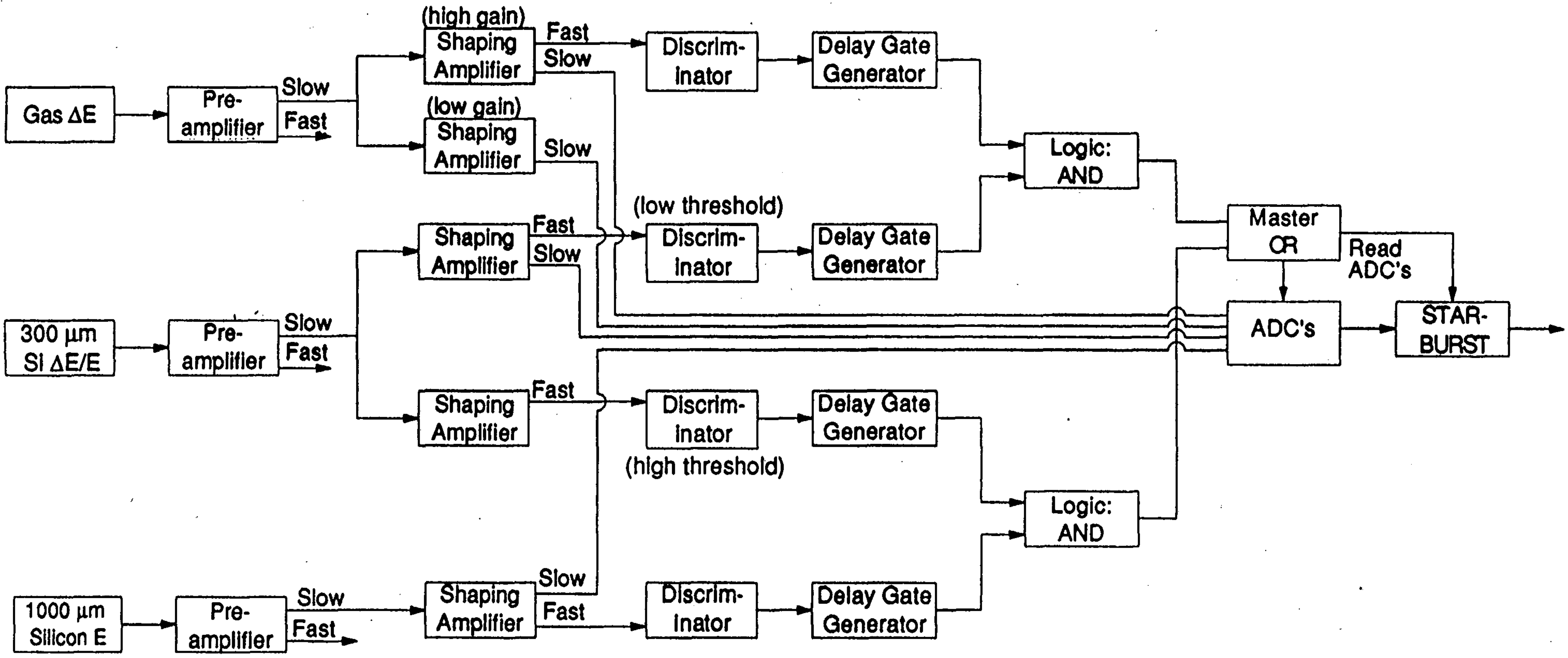

Pre-amplifier fast outputs are used for fast-timing measurements.
TAC signals are measured between gas-ΔE and Si-ΔE/E and between Si-ΔE/E and Si-E for each telescope and between the Top and Bottom Si-ΔE/E's

3/27/96

protons, run 3195–3199
300 μm $\Delta E/E$ detecto

^{21}Mg + ^{25}Si

~150 mC

110 MeV $^{3}He^{2+}$ + ^{NAT}Mg

beam on: 55 ms

beam off/counting: 70

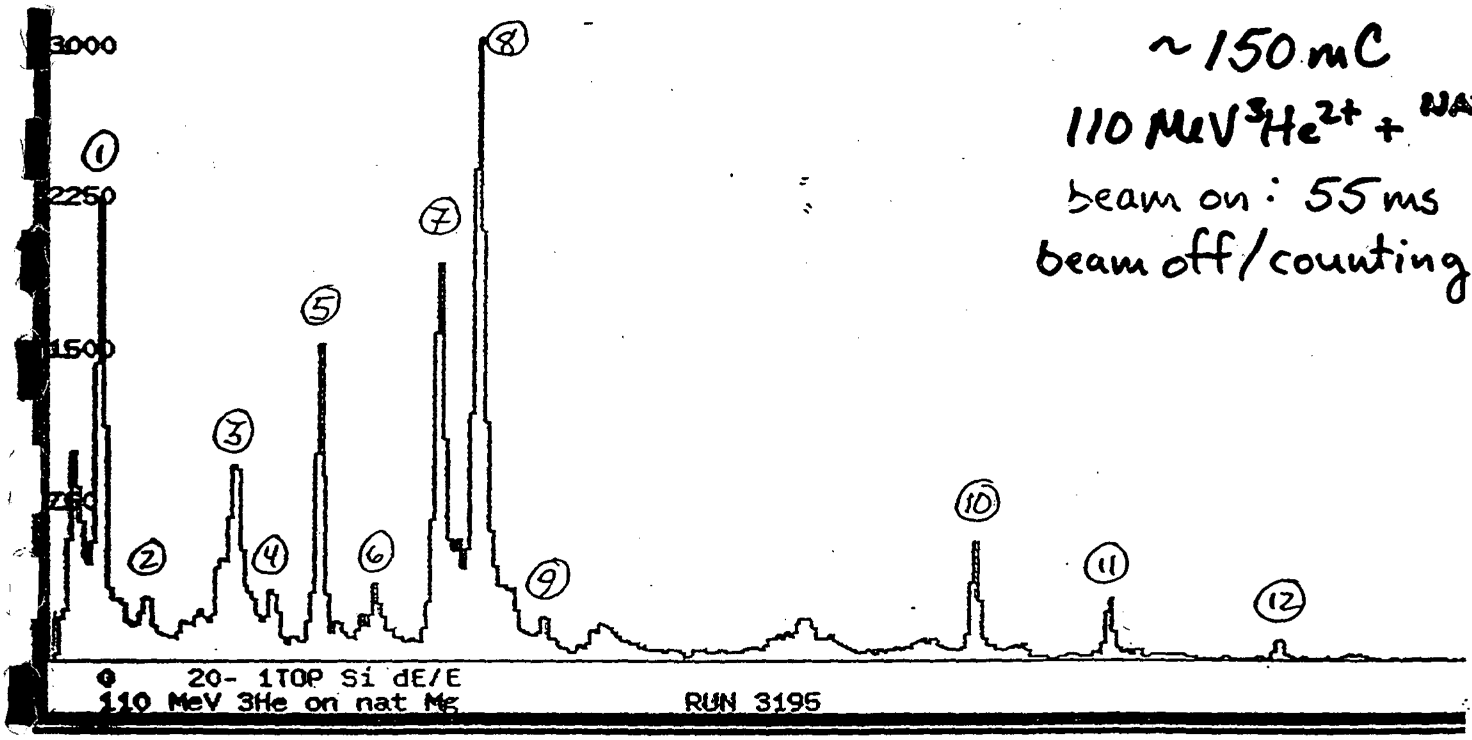

Peak #	E incident	Predicted E detected *
1	386	174
2	534	363
3	907	786
4	1060	951
5	1257	1160
6	1495	1409
7	1773	1697
8	1939	1867
9	2219	2154
10	4091	4049
11	4670	4632
12	5405	5371

* 85 μg/cm^2 deadlayer
66 μg/cm^2 gas
469 μg/cm^2 Al window

3/28/96

runs 3195 - 3199

^{23}Si β-p search test r

High Energy (>6 MeV) Proton Spectrum

Bottom Detector Telescope

gated on:

- PI
- TAC
- AND small gas-ΔE signal

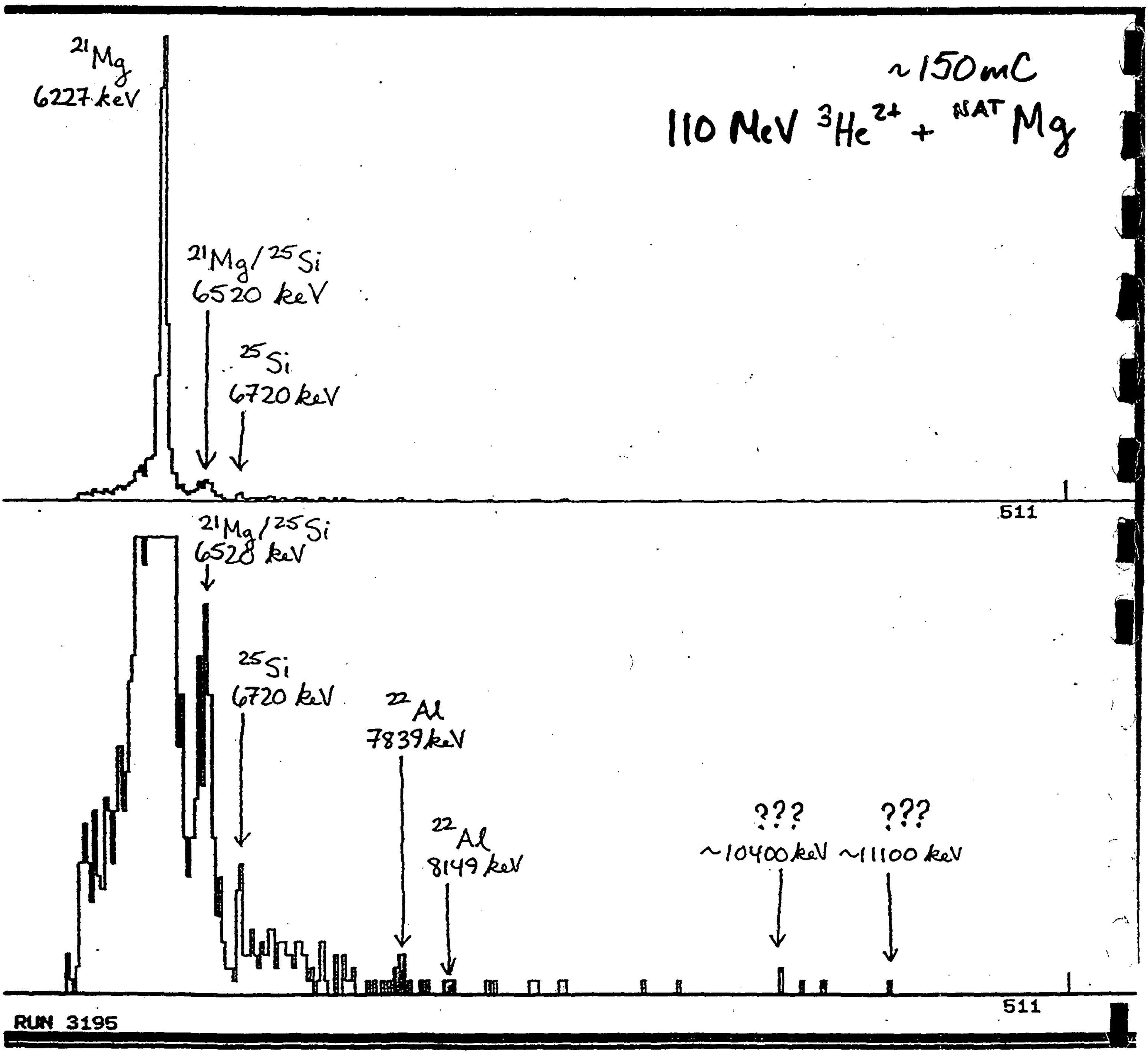

~150 mC

110 MeV $^3He^{2+}$ + ^{NAT}Mg

Modifications in the Experimental Set-up for the Main Run

- Fix the cyclotron!!!
- Switch to 1000 μm SiLi E detectors; negative detector biases on E detectors
- Increase solid angle by repositioning telescopes
- Improve activity catcher-wheel efficiency
- Change pulsing structure for faster transport
- Improve on-line analysis capabilities
- Use separated-isotope ^{24}Mg target

Dennis Moltz

Lawrence Berkeley National Laboratory
Berkeley, CA

1/96

Status of the Large-Scale Dark-Matter Axion Search

K. van Bibber, C. Hagmann, W. Stoeffl
LLNL

L. Rosenberg, E. Daw
MIT

P. Sikivie, N. Sullivan, D. Tanner
Univ. Florida

F. Nezrick, M. Turner
FNAL

D.M. Moltz, R. Tighe, J. Powell
LBNL

J. Clarke
U.C. Berkeley

N. Golubev, L Kravchuk
Moscow

Strong CP Problem.

$$\mathcal{L}_{QCD} = \begin{pmatrix} \text{Gluonic} \\ \text{Field} \\ \text{strength} \end{pmatrix} + \begin{pmatrix} \text{Quark} \\ \text{Fields} \end{pmatrix} + \underline{\underline{\underline{\text{4-Divergence}}}}$$

DOES NOT CONTRIBUTE IN PERTUBATION TH.

DOES CONTRIBUTE NON-PERTABABLE EFFECTS OR __ __ __ __ __

WHY IS THERE NO LIGHT PSEUDO-NAMBU-GOLDSTONE BOSON (Like the PIONS) PRODUCED IN SPONTANEOUS BREAKING OF the $U_A(1)$ QUARK FLAVOR SYMMETRY.

→ SOLVED ONLY FOR θ.

$$\bar{\theta} = \theta - \arg \det m_q = \theta - \arg(m_1 m_2 \dots m_n)$$

IF $\bar{\theta} \neq 0$, QCD Violates P and CP

Experimental Observation

$$d_n \simeq 10^{-16}\,\bar{\theta}$$

$$\leq 10^{-24}\ e\,cm$$

$$\Rightarrow\ \bar{\theta} \leq 10^{-8}$$

But P and CP Violation of the Weak Interaction Tends to Feed the Strong Interaction. (e.g. $K_L \to 2\pi$)

Why is $\bar{\theta}$ so small.

PECCEI & QUINN MAKE $\bar{\theta}$ a Dynamical Variable; Strong Interaction Will Align $\bar{\theta}$ $\ni$

$$\bar{\theta} = 0 \pmod{\pi}$$

$\Rightarrow$ Neutral Pseudoscalar or $\boxed{\text{AXION}}$

Where to look for Axions ?

ORIGINAL SUGGESTIONS BASED UPON

$f_a \gtrsim 250$ GeV

(From Weinberg & Wilczek)

① Axion exchange would give make the gyromagnetic ration of the muon of the order $G_F m_\mu^2 \pi^2 \simeq 10^{-8}$

② Axion exchange → Spin-Spin Interaction in Atoms & Molecules

3) Expect a spike in $K^+ \to \pi^+ \nu\bar{\nu}$ spectrum

④ Since a_0 is analogous to π_0 (Same quantum numbers)

$\bigcirc \to \pi^0 + \square$

$\bigcirc \to a_0 + \square$

⑤ Nuclear reactors

10^{-6} axion / prompt γ since 1 $\bar{\nu}_e$ / prompt γ

⑥ Any predominantly M1 Nuclear Transition.

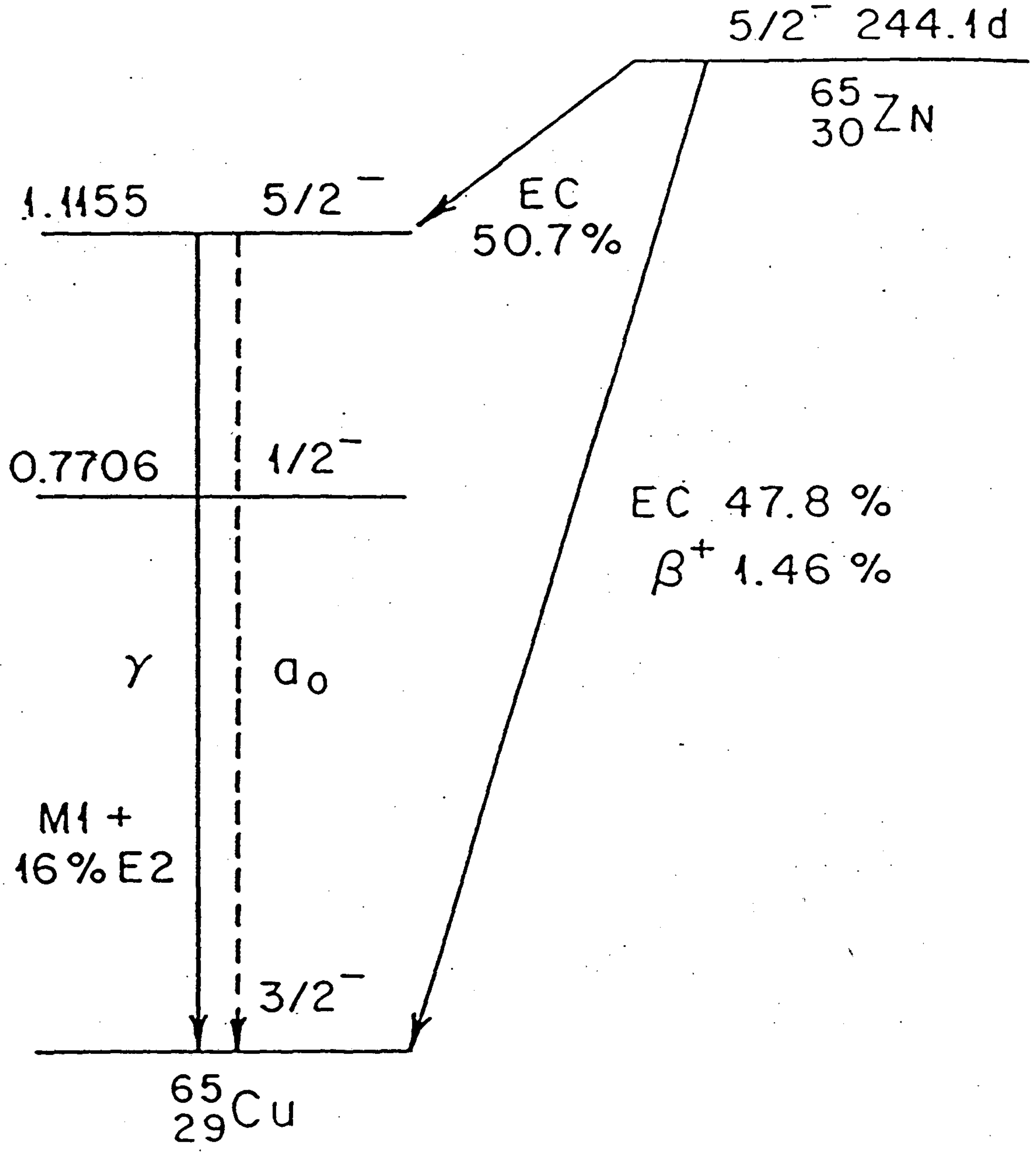
5/2⁻ 244.1d
65 30 ZN
1.1155
5/2⁻
EC 50.7%
0.7706
1/2⁻
EC 47.8 %
β⁺ 1.46 %
γ
a0
M1 + 16% E2
3/2⁻
65 29 Cu

Figure 1

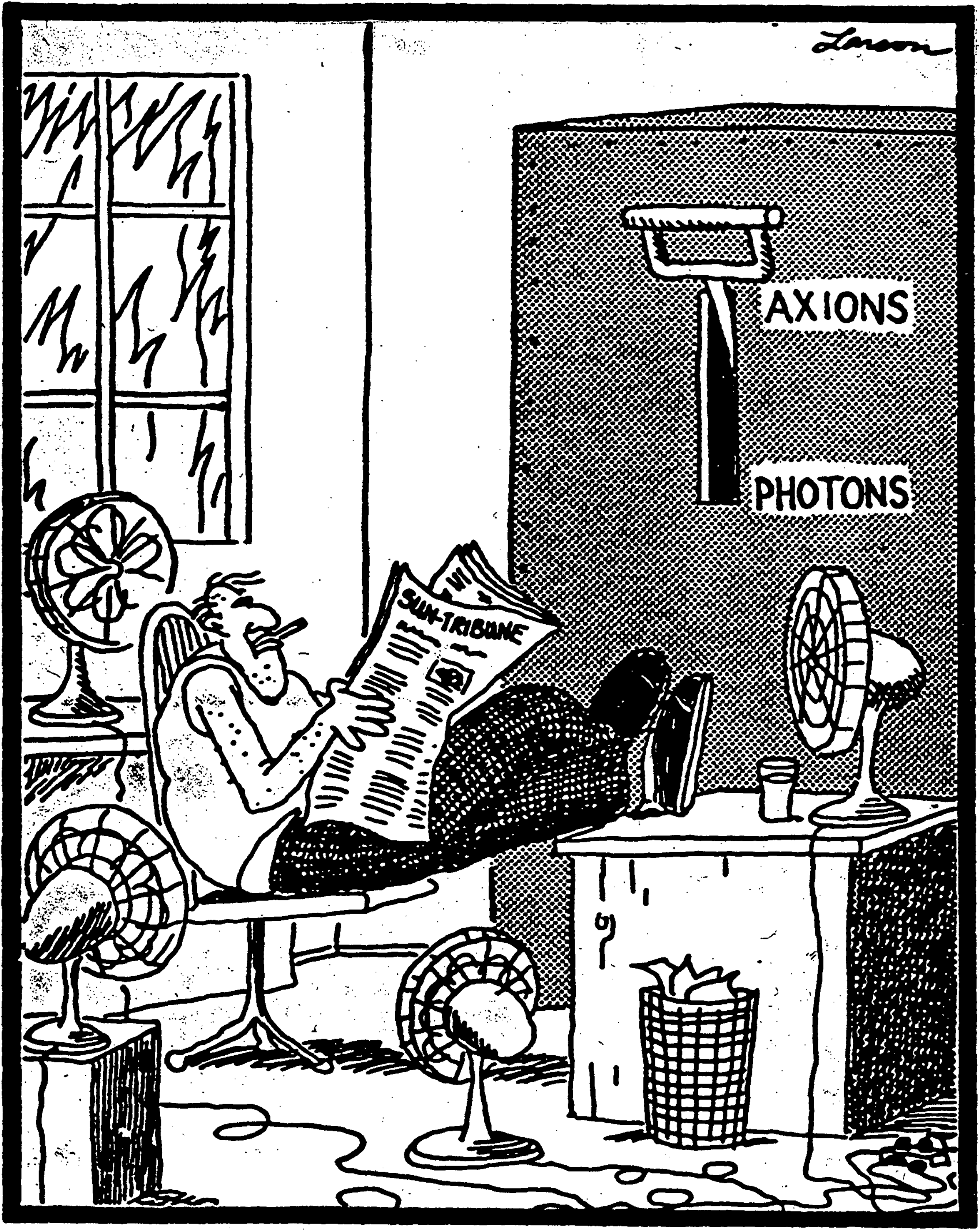

Inside the sun

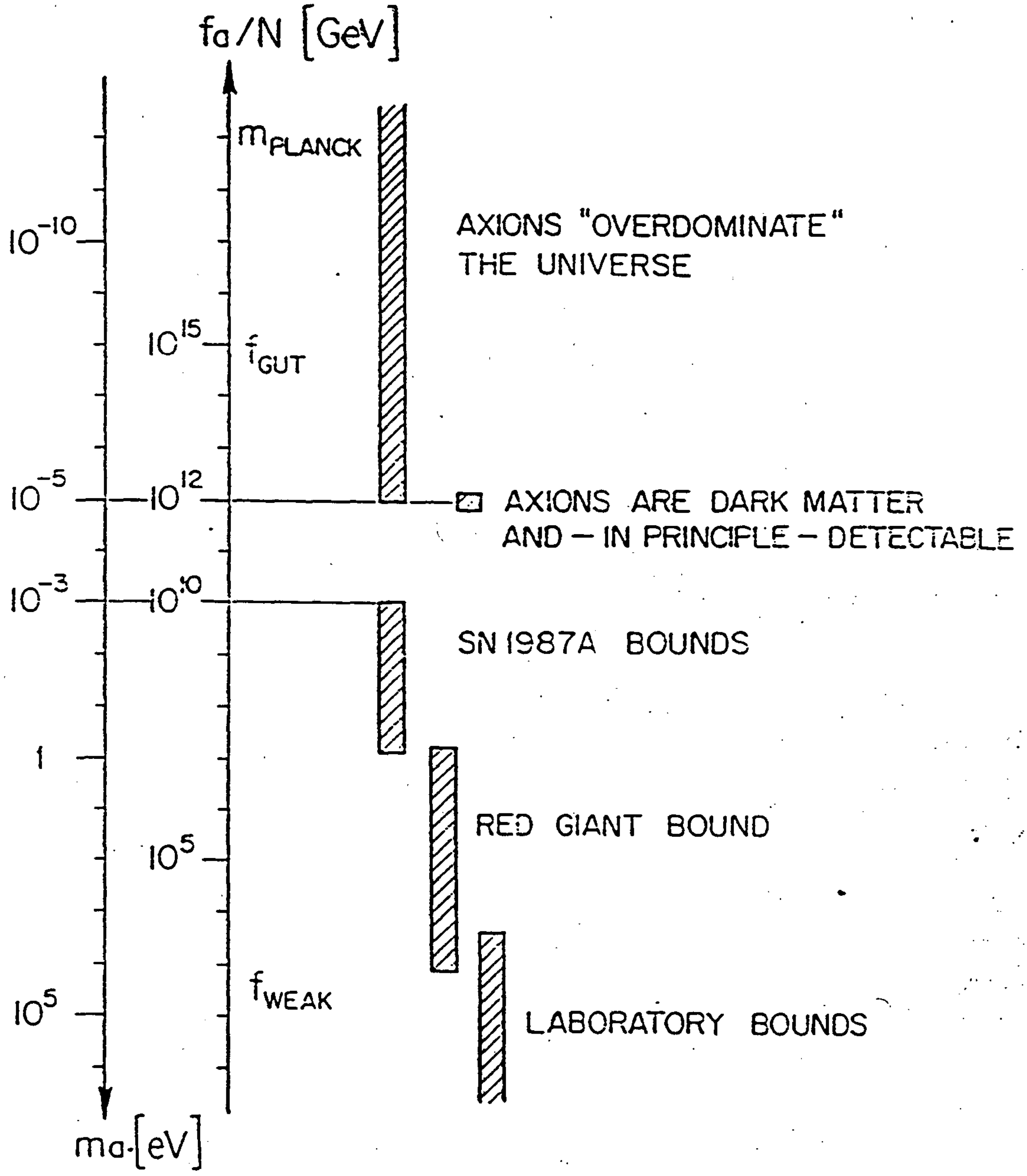

Figure 1
Axion parameters excluded by cosmological, astrophysical, and laboratory bounds. We only show results obtained from the generic axion couplings to nucleons and radiation.

nuclear bremsstrahlung, $N_1 + N_2 \rightarrow N_3 + N_4 + a$. This volume emission would compete

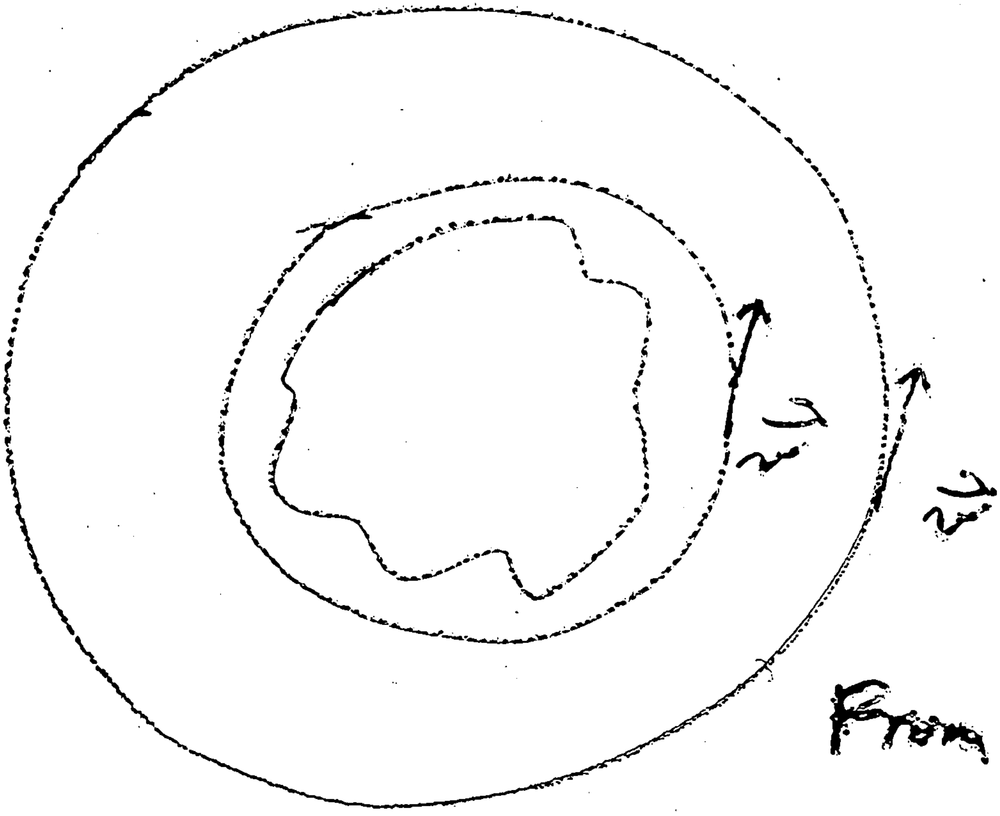

From Keplers
3rd Law

$$GM = v^2 \times r$$

$$v \propto r^{-\frac{1}{2}}$$

Found v = Constant

NOT ENOUGH PHOTONS
" " HADRONS

LOOK TO THE DARK SIDE

DARK MATTER

DARK/LUMINOUS ≥ 10

DARK/Baryonic ~ 10 ?

Velocities of Stars in Galaxies Not Consistent.

$$\langle \rho \rangle = \langle n_{GAL} \rangle \langle M_{GAL} \rangle$$

Need to find out how much matter in a galaxy.

WHO'S MINDING THE STORE?

Leading Dark-Matter Candidates:

• WIMP's : (Weakly Interacting Massive Particles)	NSF Science Center for Particle Astrophysics, Berkeley; Europe ...
• Massive Neutrinos :	SAGE, GALLEX, SNO, Homestake Mine, LLNL ...
• Axions :	? !

(Limits to the Baryonic Component in terms of Massive Compact Halo Objects – MACHO's—is being carried out by an IGPP/CfPA/Australia collaboration, and the French.)

Yet of the 3 leading candidates, Axions are:

- The only one for which we can achieve the required sensitivity today
- The only one for which the signal would be completely unambiguous
- At least as well motivated as m_ν, WIMP's.

COSMIC AXION PRODUCTION

① Thermal (Turner, Raffelt)

② Misalignment (Preskill, Wilczek, Wise
Abbot-Sikivie, Dine-Fischler)

③ Axionic String Decay (Davis)

1) thermal .

For $m_a \gtrsim 10^{-3}$ eV, axions in thermal equilibrium.

Relic Axions – $\rho_a \sim \rho_\gamma$

Many formation mechanisms

$$\gamma + q \rightarrow a + q$$

Phase Space Structure of Cold Dark Matter Halos
(Sikivie + Ipser)

$t_1 \simeq 10^{-6}$ s (Axion acquires mass)

For $m_a \gtrsim 10^{-5}$ eV , (a small initial velocity dispersion) due to (inhomogeneous axion field)

$d_{a_1 \to a_2}$ 10^{11} cm

whereas galactic scales $\sim 10^{23}$ cm

thus dark matter in a thin sheet spread uniformly over $\vec{r}$-space. As time increases, the energy momentum spectrum has a series of peaks (sheets wind up).

Detection of cold dark matter particles would form a record of our galaxy formation. Sheet Structure follows from Liouville's theorem and that trajectories cannot cross in phase space (and that dark matter is collisionless)

$N \equiv$ number of crossings

for neutrinos, N is very large

$\therefore$ peaks not distinguishable

$N \simeq 200$ for axions or WIMPS

Angular momentum changes the location, but not the number of folds!

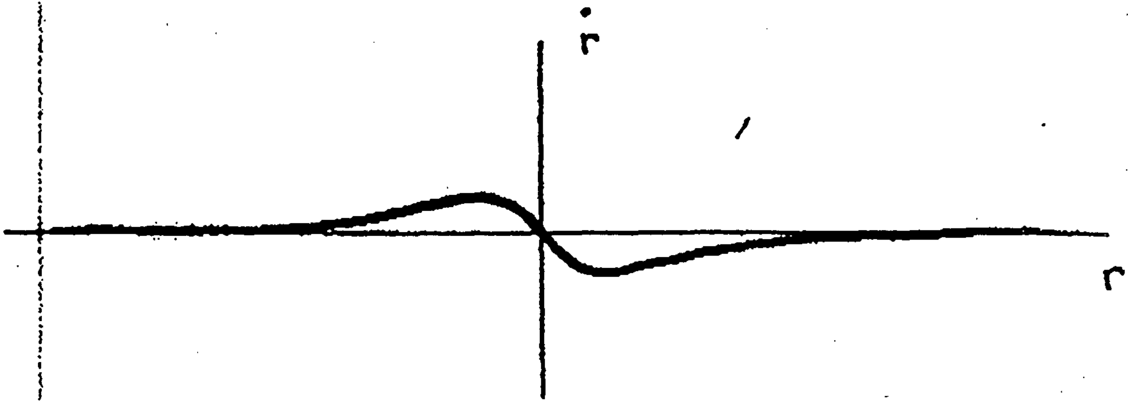
ṙ
r

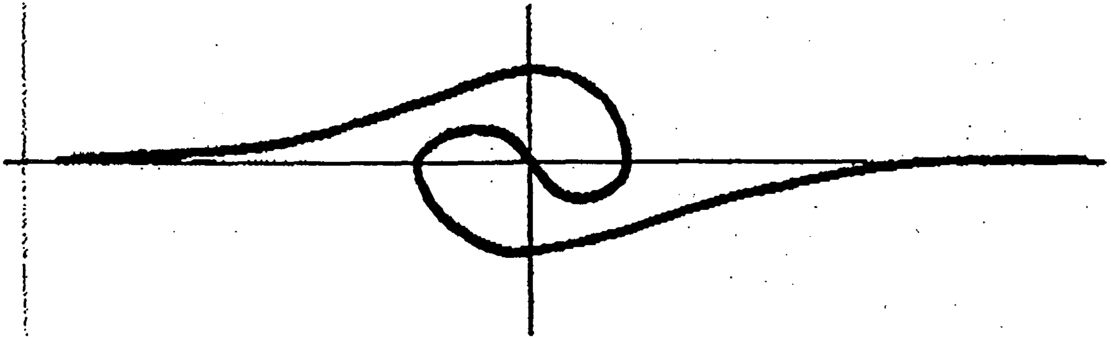

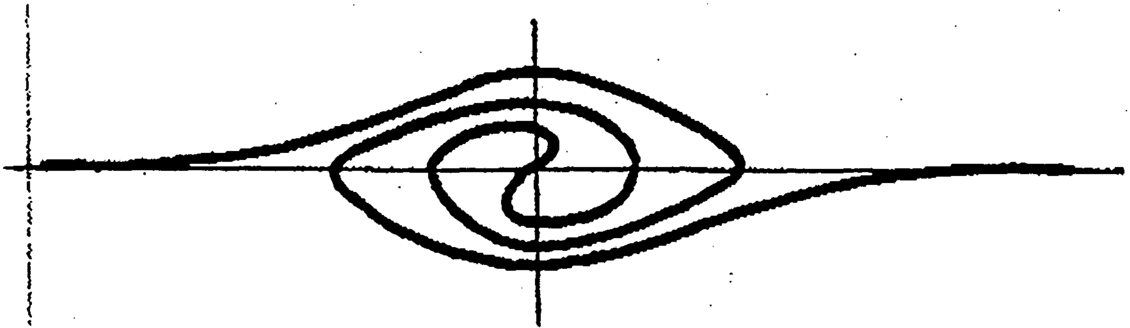

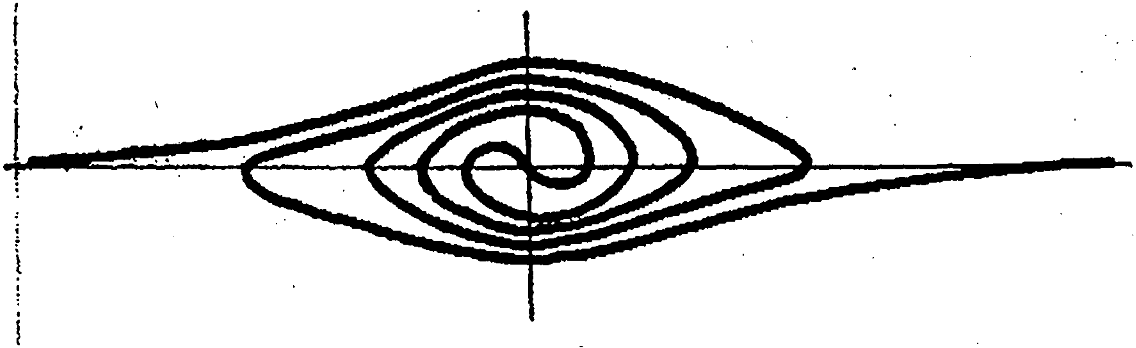

HOW TO SEARCH FOR DARK MATTER AXIONS

(Sikivie, 1983)

IMAKOFF
ROCESS:

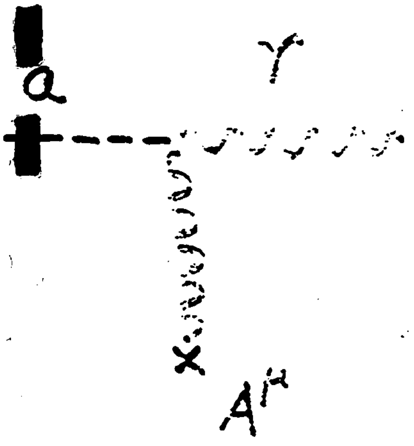

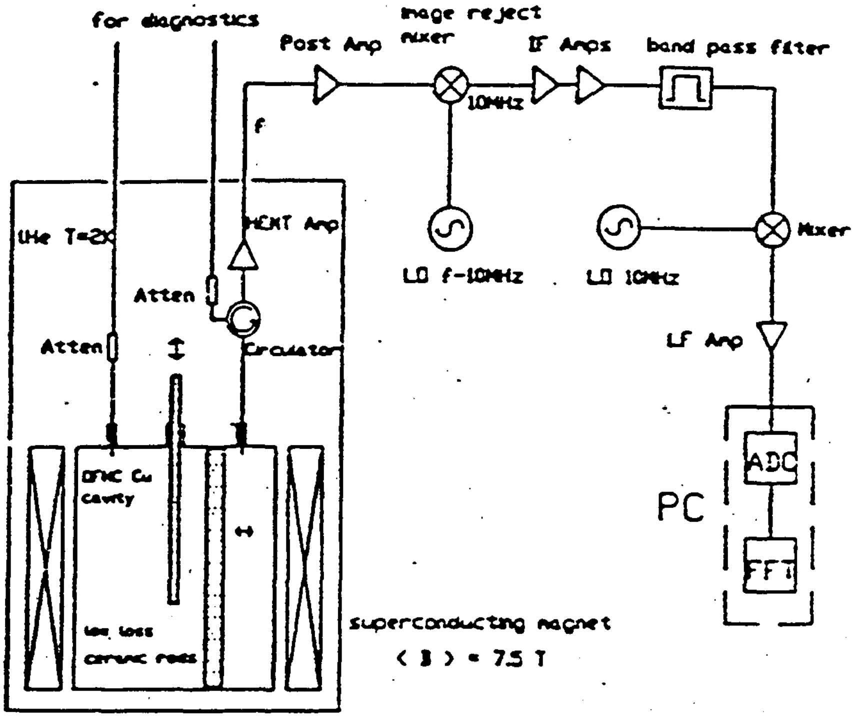

$$P_{n\ell} = \left(\frac{\alpha}{\pi} g_\gamma \frac{1}{f_a}\right)^2 V \; B_0^2 \rho_a C_{n\ell} \frac{1}{m_a} \mathrm{Min}(Q_L, Q_a)$$

$$= 3 \times 10^{-26} \mathrm{Watt} \left(\frac{V}{3\ \mathrm{m}^3}\right) \left(\frac{B_0}{7\ \mathrm{Tesla}}\right)^2 C_{n\ell} \left(\frac{g_\gamma}{0.36}\right)^2$$

$$\cdot \left(\frac{\rho_a}{\frac{1}{2} \times 10^{-24} \mathrm{gr/cm}^3}\right) \left(\frac{m_a}{2\pi (1 \mathrm{GHz})}\right) \mathrm{Min}(Q_L, Q_a)$$

- Q_L = LOADED Q OF TUNABLE MICROWAVE CAVITY ($\gtrsim 10^5$)

Q_a = "QUALITY FACTOR OF AXION ($> 10^5$)

[illegible]

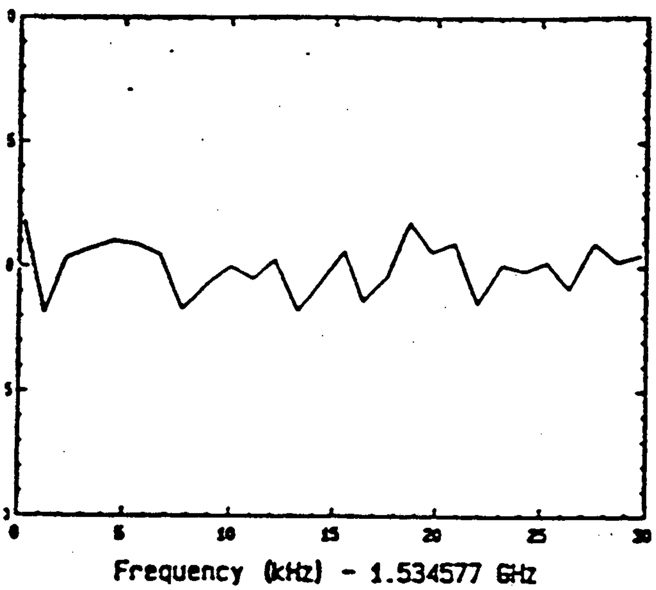

Typical power spectrum.

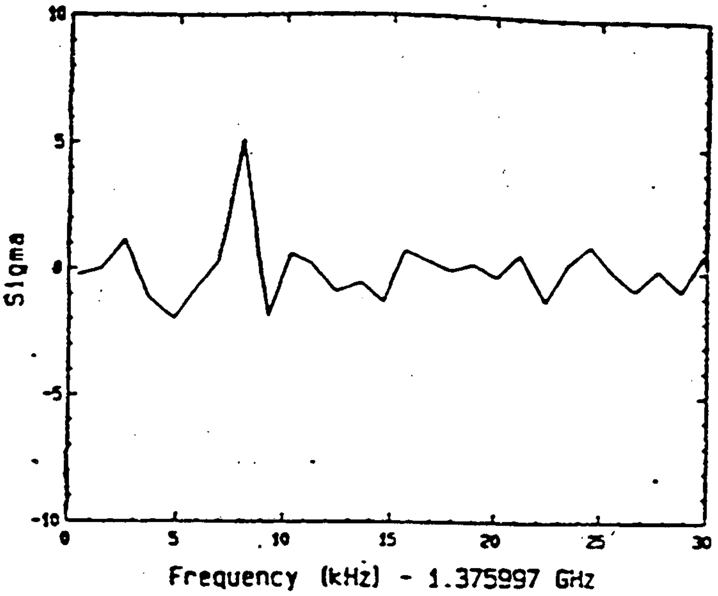

Power spectrum with candidate peak.

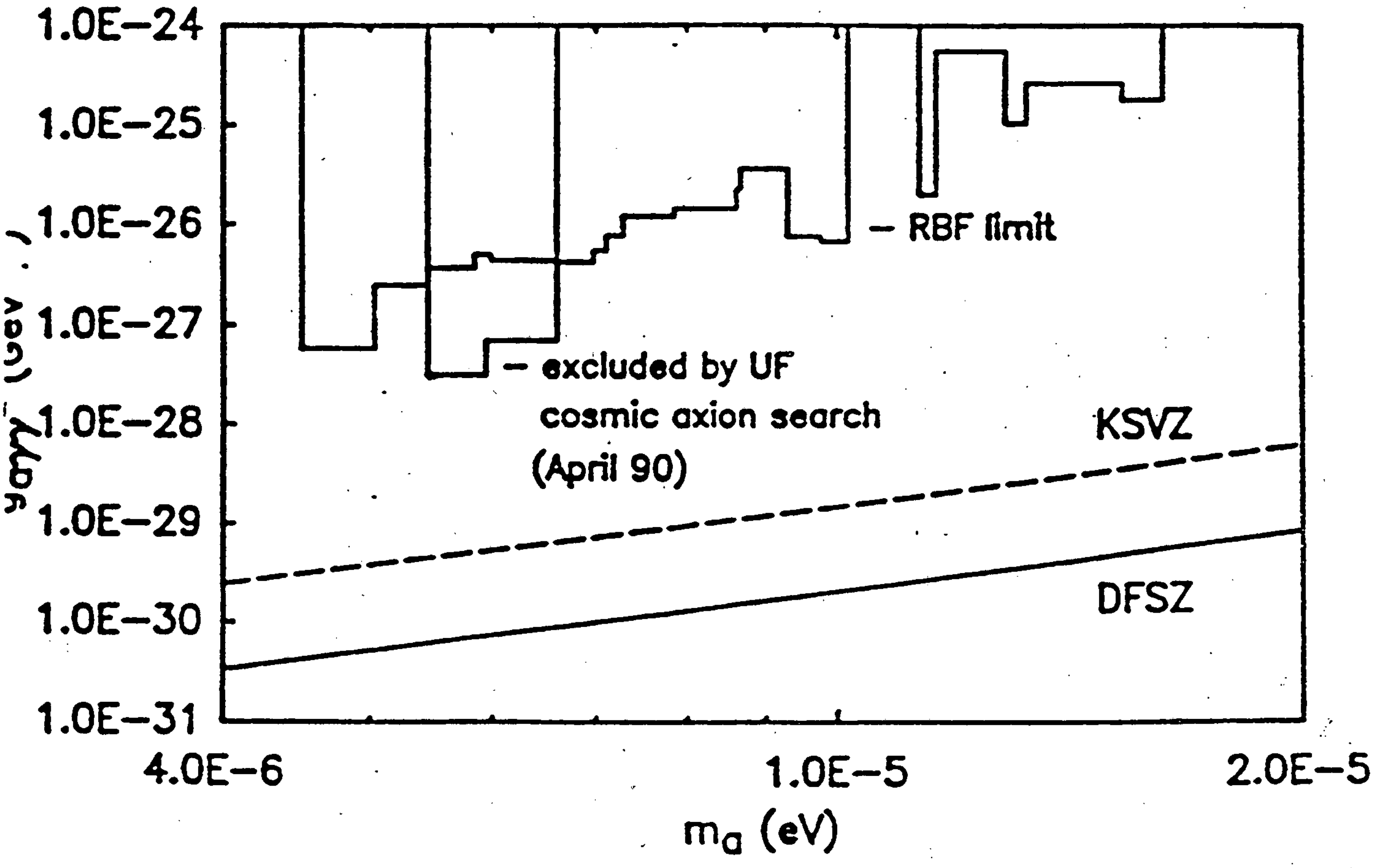

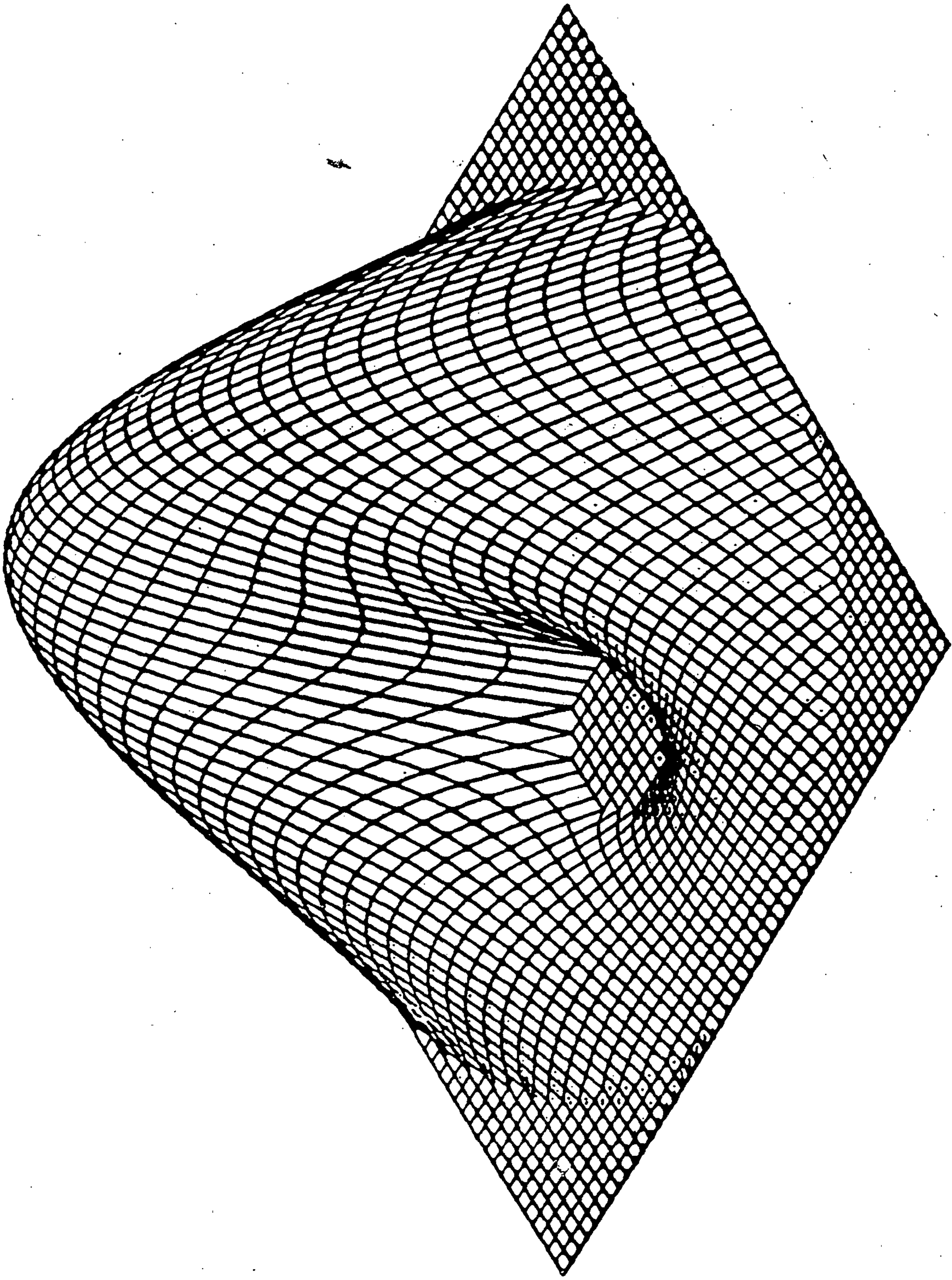

D

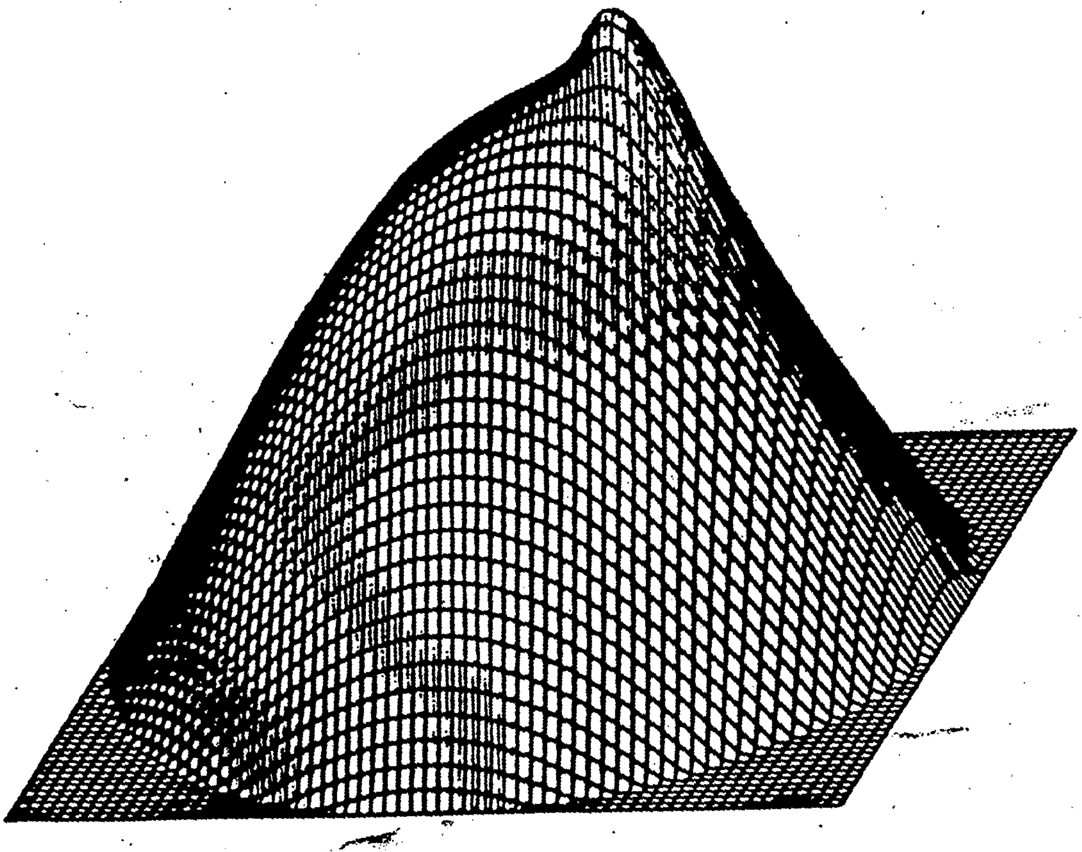

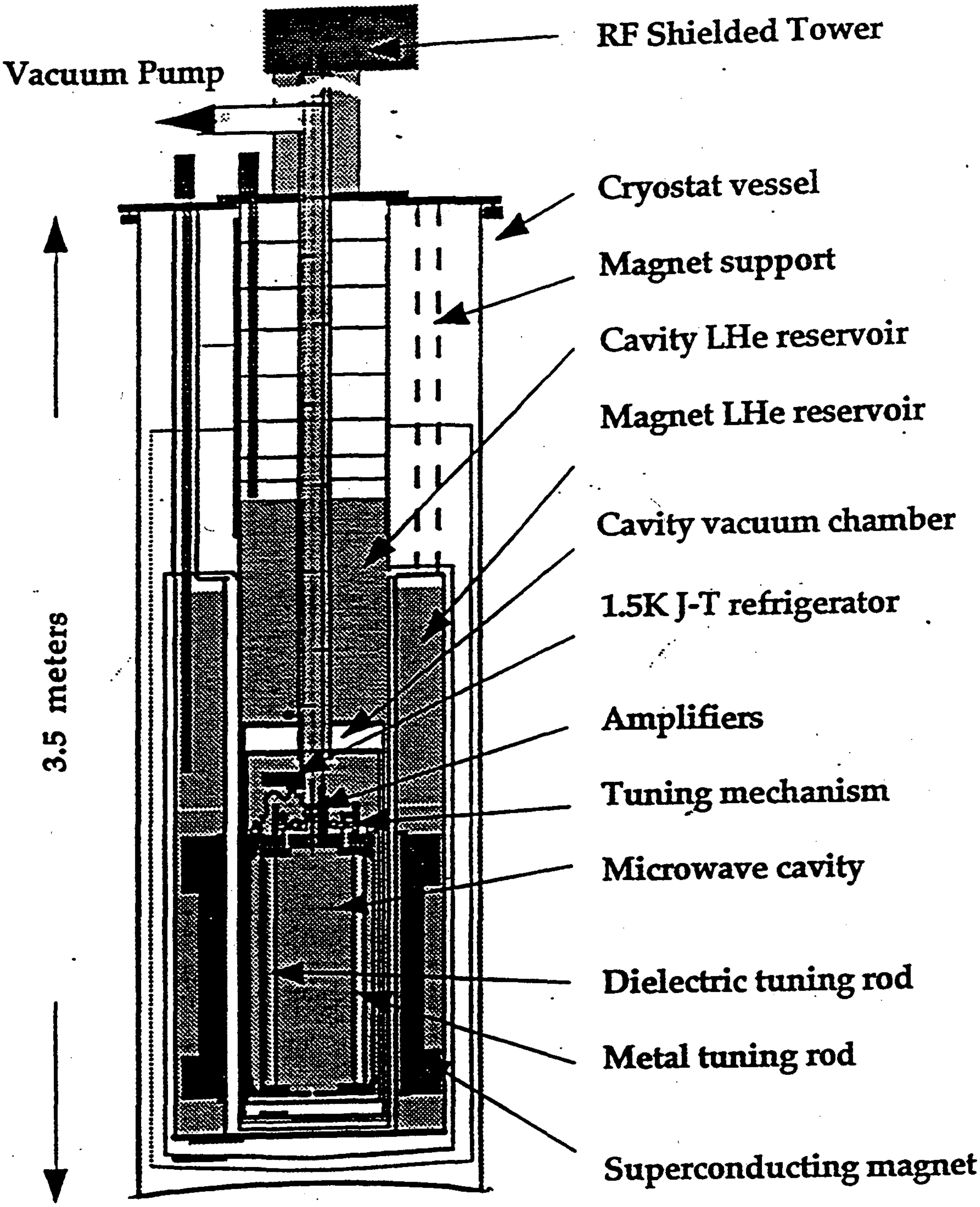

Figure 3. Schematic of the magnet and cryostat, with the physics package inserted.

Current Experiment

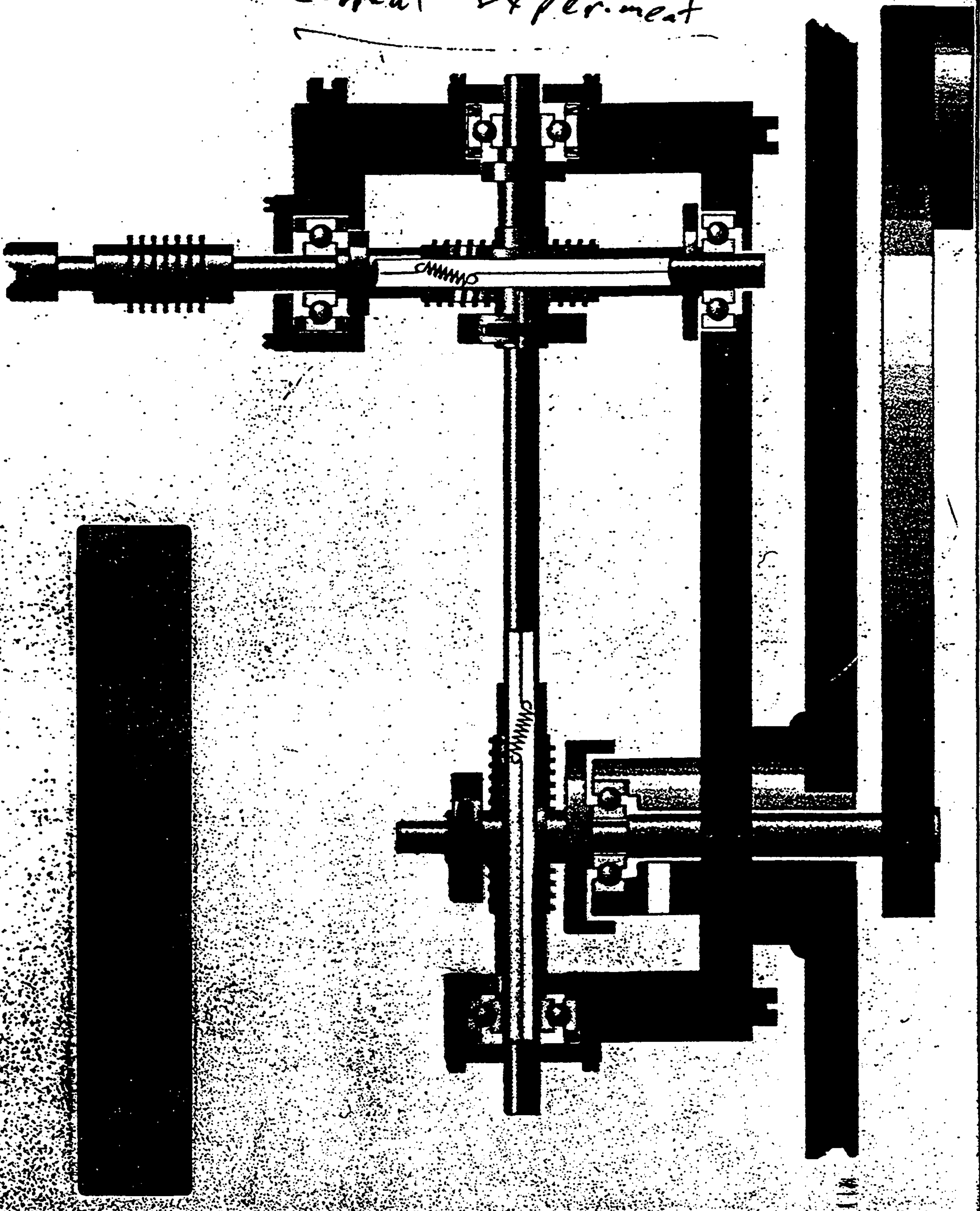

Parameter Space for Piezo Motion

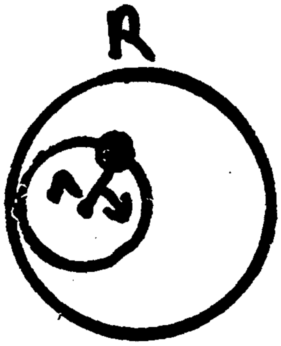

Motion must be consistent

X 4 or 16 or 64 ≡ N

1 Master Cavity
+ N-1 Slave Cavities

Goal: 0.1 μm / movement

Accept: 1.0 μm / movement

Must operate at 3°K in 8T Field!

134.5 kHz Driver

200 - 500 V.

Voltage
Breakdown in He at 1 Torr in 8T

Expansion / Contraction
from Warming / Cooling

Everything is elastic at 1 μm!

Gears have memory!

Piezos do not!

Micro Pulse Systems, Inc.

LINEAR MICROPOSITIONING
WITH
MICRO PULSE SYSTEMS' PIEZOELECTRIC ACTUATORS

FEATURES

- Direct microinch resolution
- Unlimited travel
- Power-off position locked without drift
- No lost motion — bearings and gears can be eliminated
- Simple drive circuitry with fast response
- High vacuum compatibility and non-magnetic options

The patented direct drive technology of MPS provides the advantages of piezoelectric actuators without the complexity and costly mechanics of conventional devices. MPS actuating drivers are simple and reliable; in most applications they are mounted kinematically, eliminating the need for critical tolerances and adjustment.

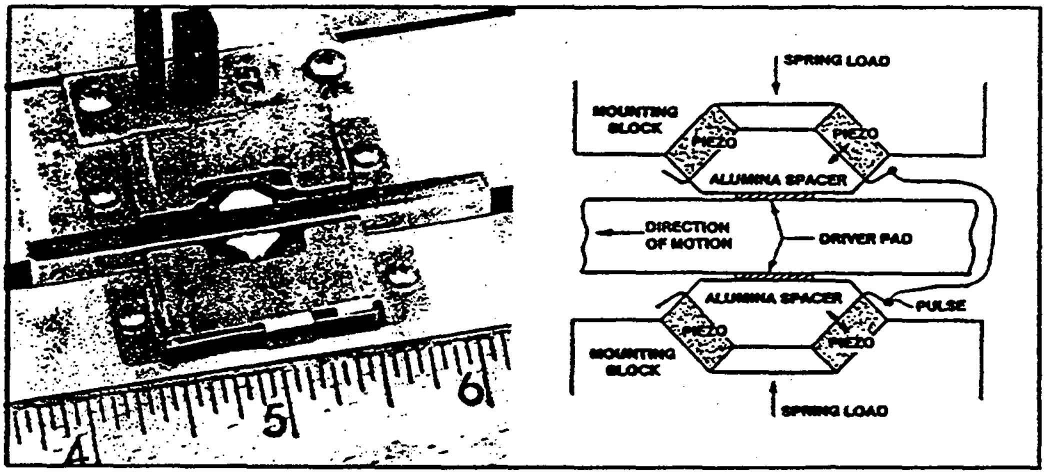

Figure 1

Figure 1 illustrates the direct drive principle in the linear mode using L-104 components. The actuator incorporates four piezoelectric elements which are excited in pairs to drive a hardened steel bar. When the thickness of the piezo element expands and contracts in response to pulses of the exitation voltage, the resultant motion has a component along the length of the bar, and the bar is moved in steps. By adjusting the width of the pulses the size of the steps can be varied. The bar can be driven in either direction with a minimum step of approximately 1 microinch.

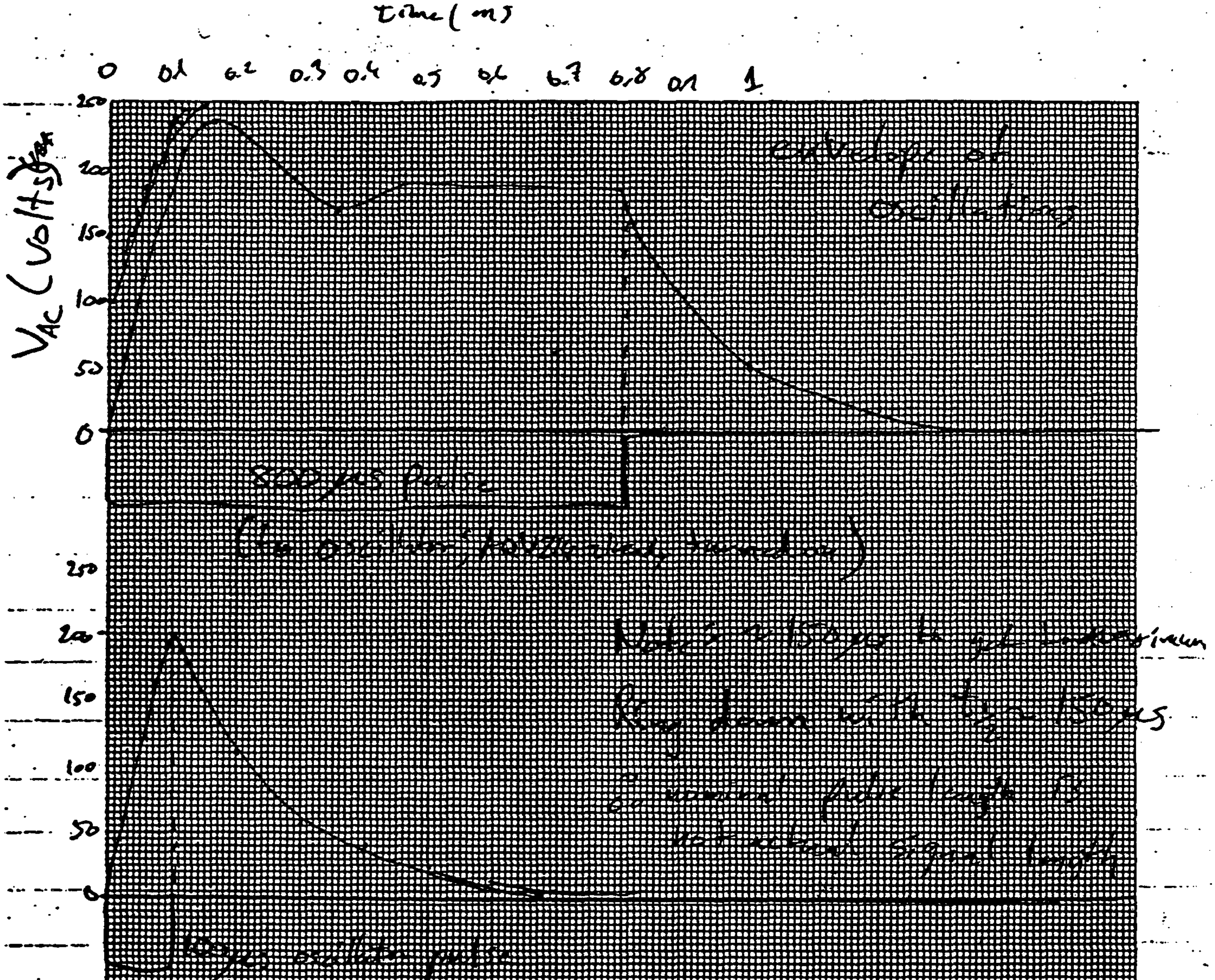

Note: ~150µs to get to maximum; Ring down with $t_{1/2}$ ~150µs. ∴ nominal pulse length ≠ actual signal length

[These drawings are with no piezo load (note [illegible]); signals differ ~20% with piezo motor connected]

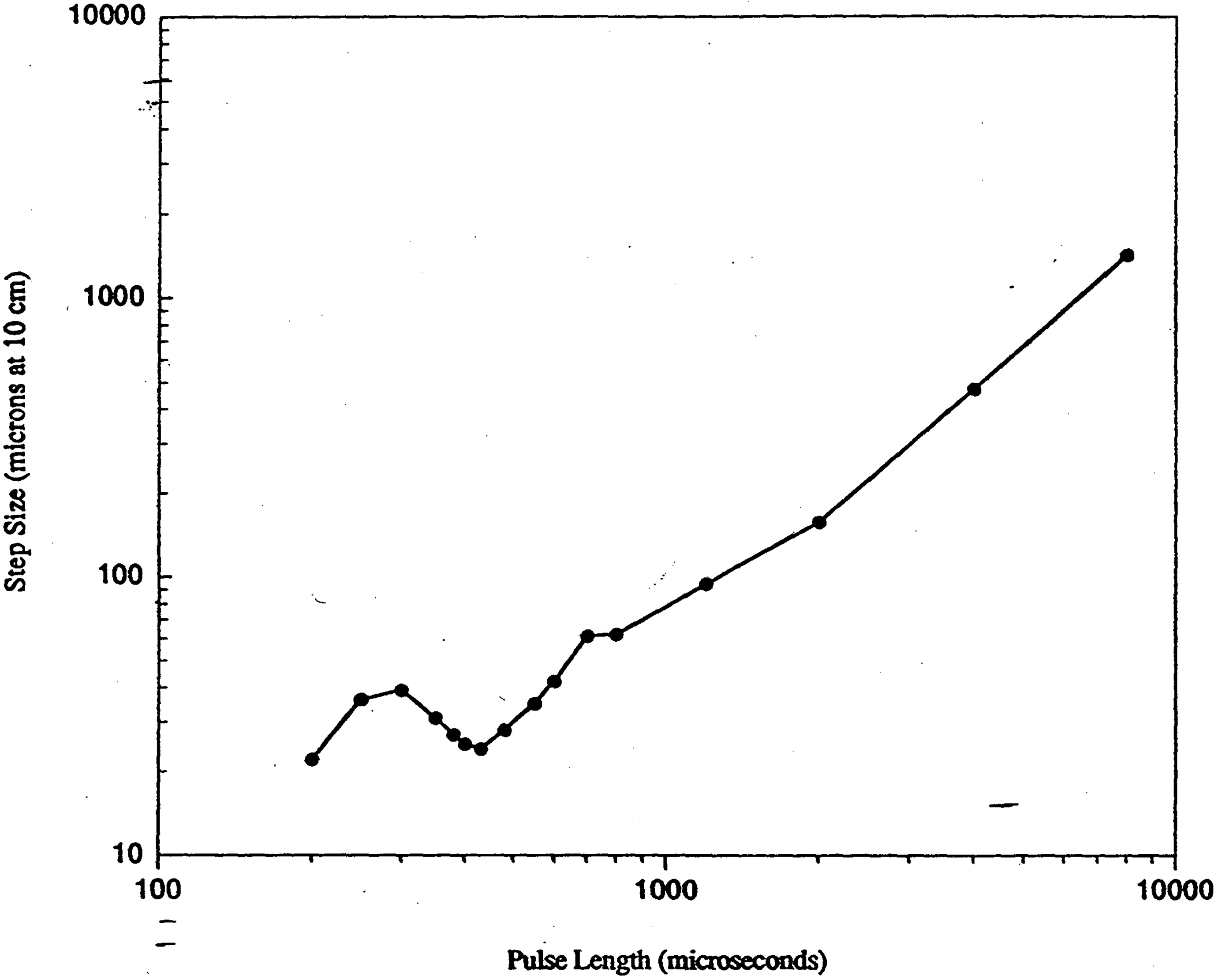

10000
1000
100
10
Step Size (microns at 10 cm)
100
1000
10000
Pulse Length (microseconds)

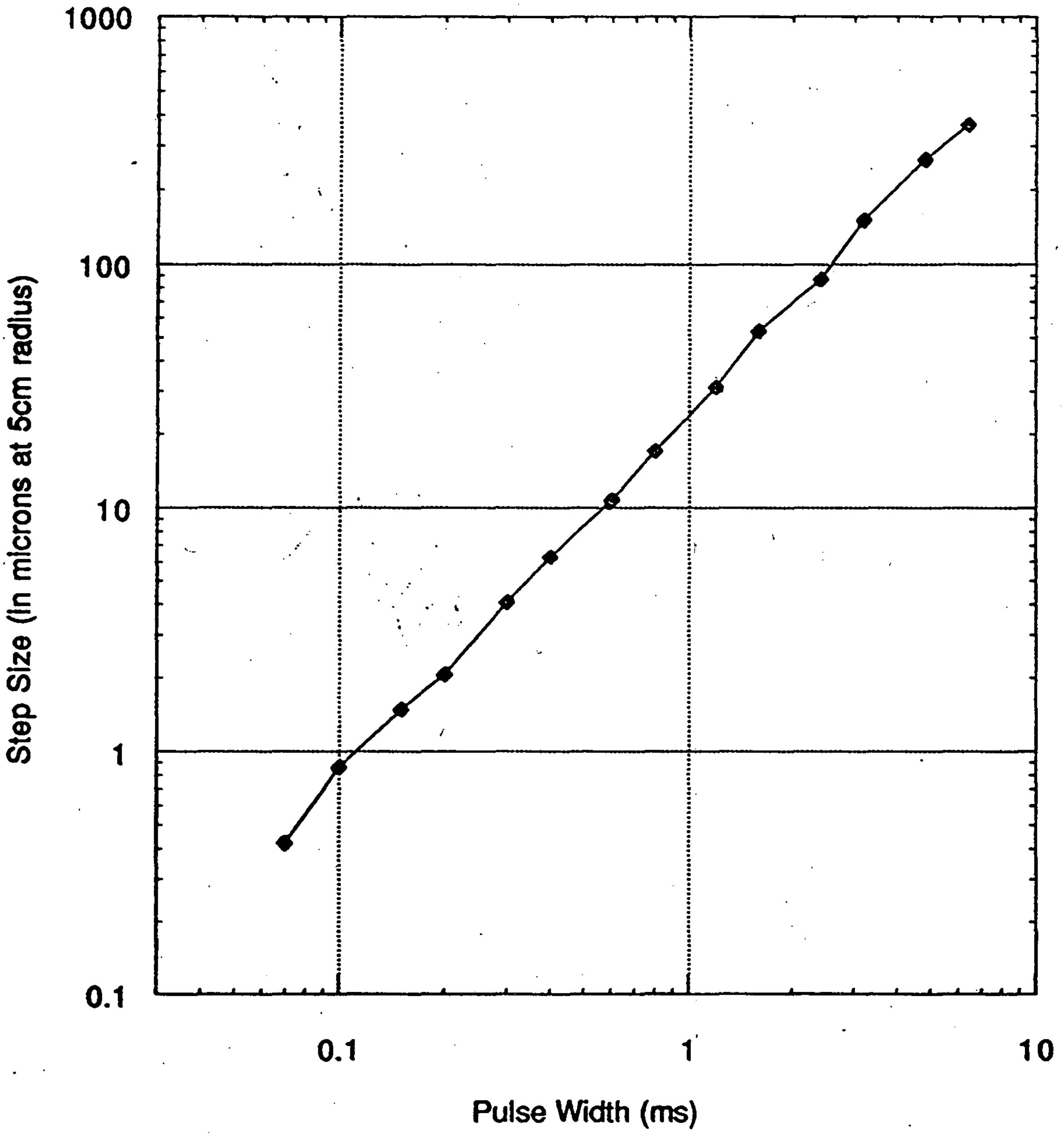
1000
100
10
1
0.1
Step Size (In microns at 5cm radius)
0.1
1
10
Pulse Width (ms)

THE REACH OF THE EXPERIMENT

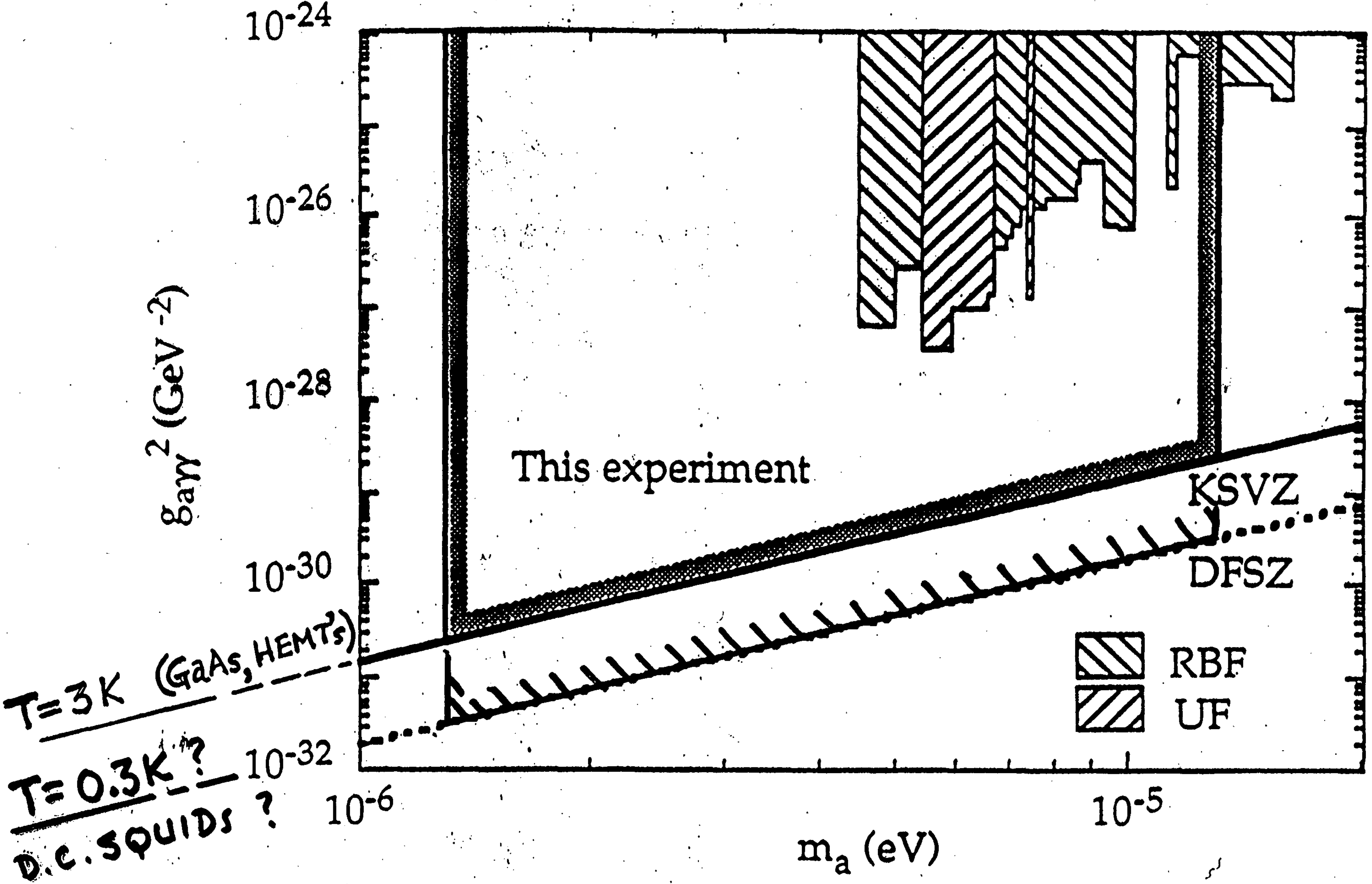

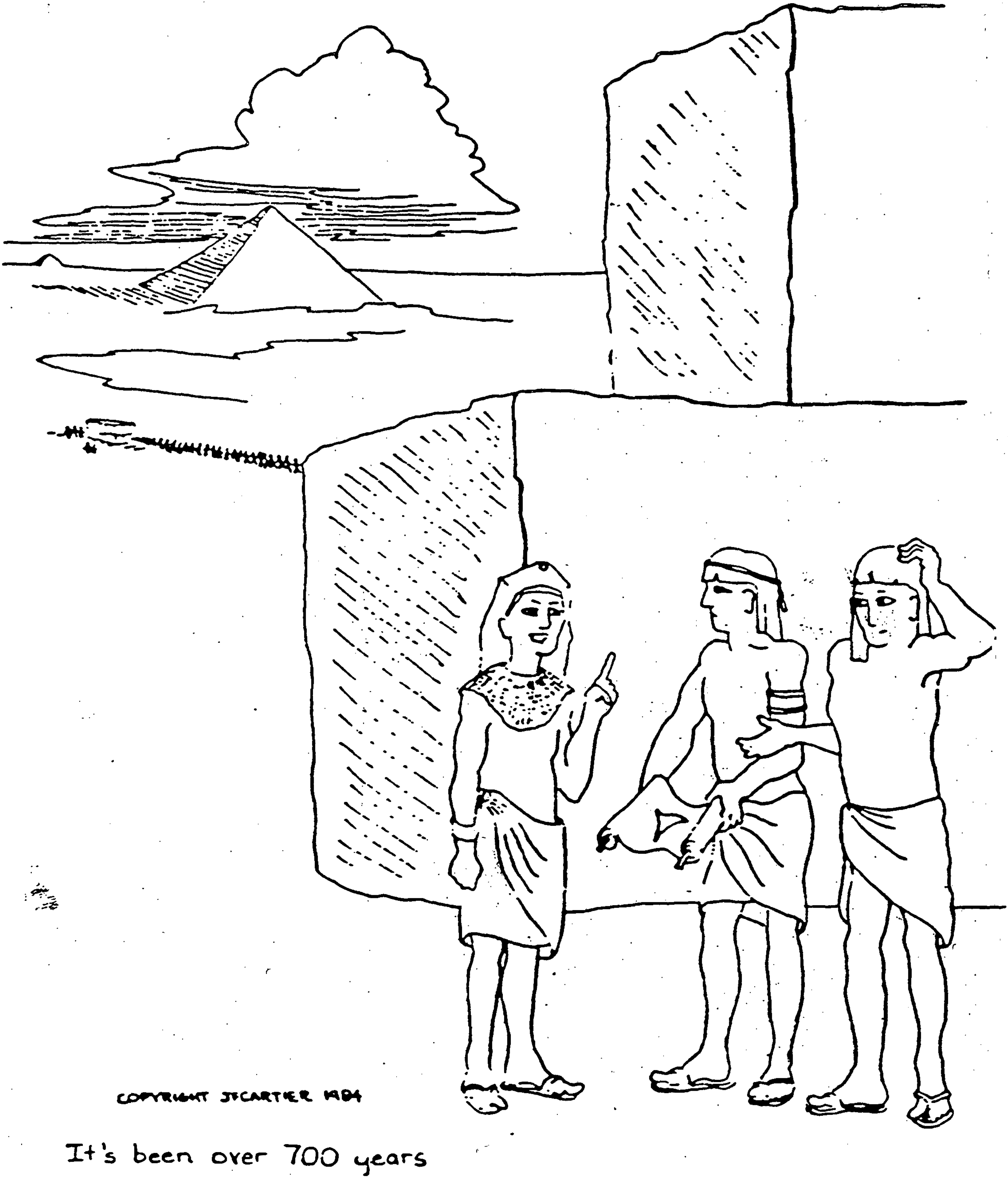

COPYRIGHT JTCARTIER 1984

It's been over 700 years

and we haven't observed a single  event.

We will have to make it BIGGER.

Claude Detraz

IN2P3
Paris, France

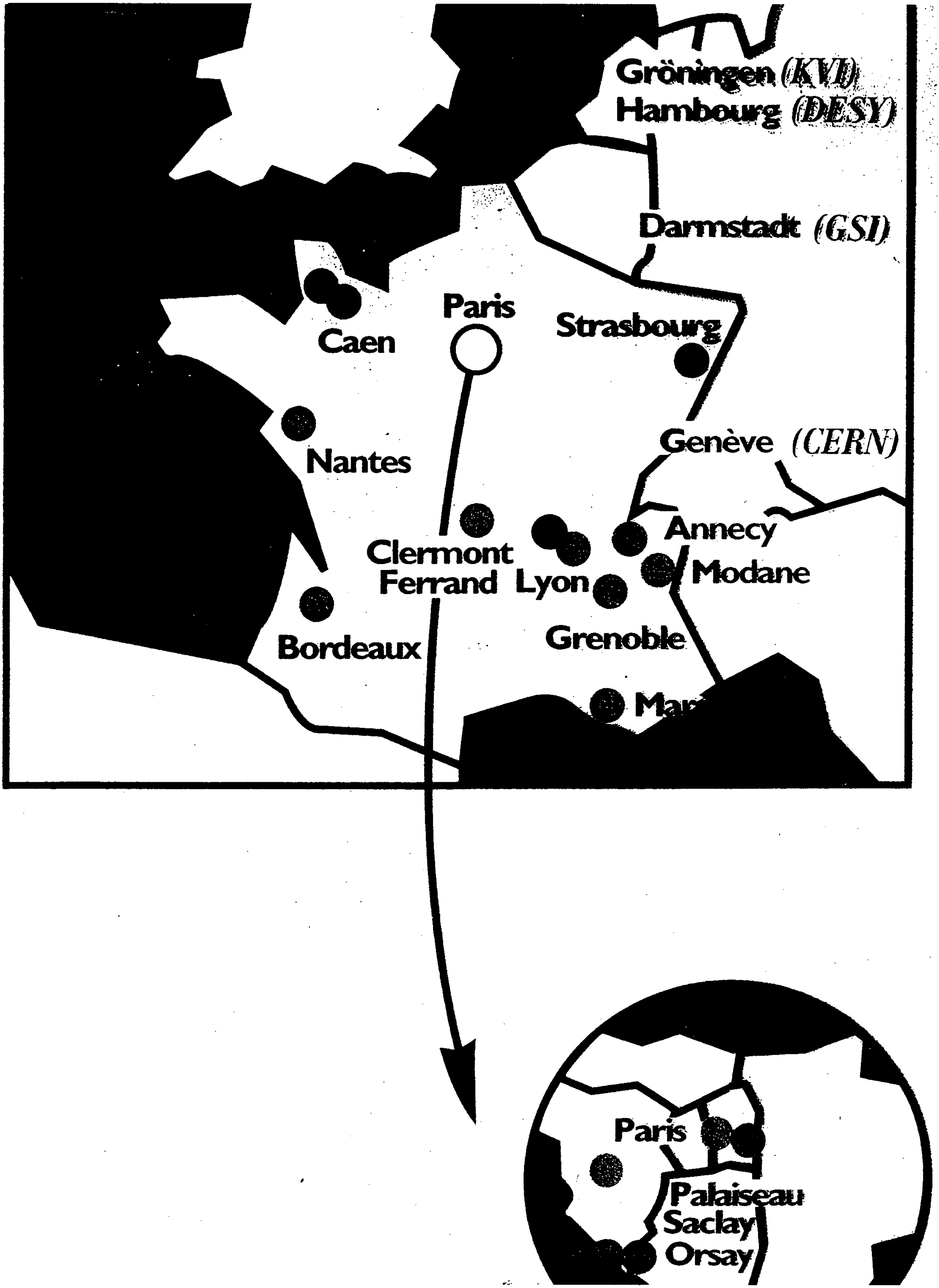
Gröningen (KVI)
Hambourg (DESY)
Darmstadt (GSI)
Paris
Strasbourg
Caen
Nantes
Genève (CERN)
Annecy
Clermont Ferrand
Lyon
Modane
Grenoble
Bordeaux
Mar
Paris
Palaiseau
Saclay
Orsay

IN2P3

BUDGET ET EFFECTIF (1994)

Budget total :
1 036 MF HT
Répartition

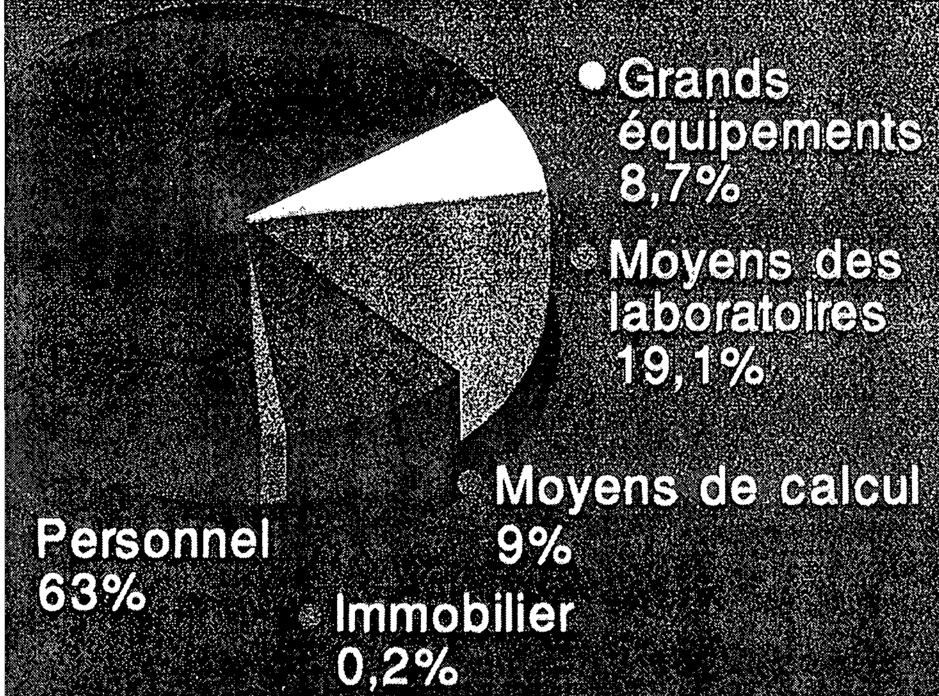

ce : SG/SBCG

Effectif total :
2 339 personnes *
Catégories

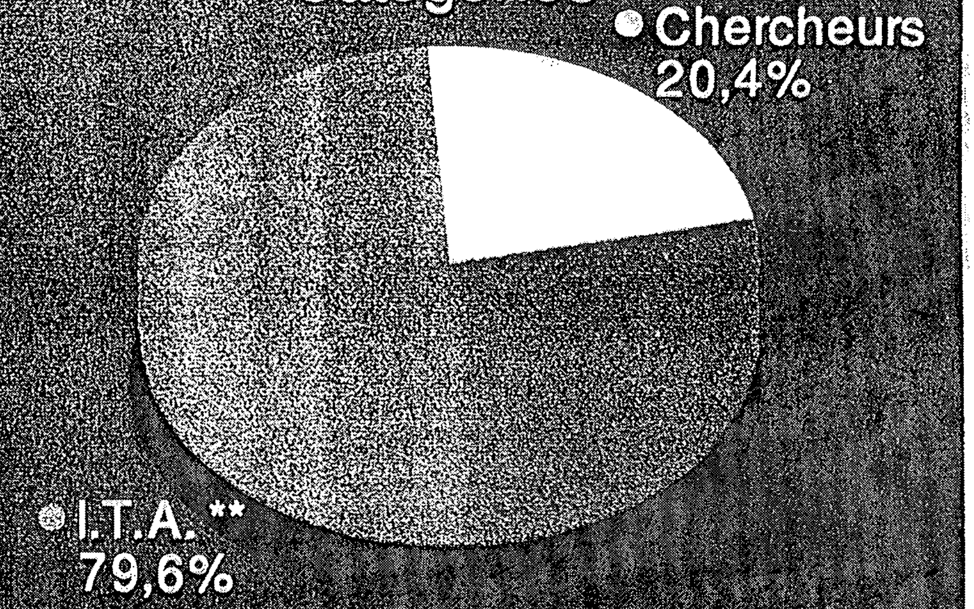

*Personnel permanent

**Ingénieurs Techniciens Administratifs : personnels d'appui à la recherche + TPN (Techniciens de Physique Nucléaire)

Source : SP

NUCLEAR MATTER

QUARKS AND LEPTONS

HADRONIC PHYSICS

FIELDS, PARTICLES, NUCLEI IN THE UNIVERSE

PERSPECTIVES

1. EVOLUTION

LEP (e^+e^-)

HERA (ep) ----------> LHC (pp)

SATURNE (hadrons) ----------> CEBAF, etc, ... ELFE (electrons)

2. NEW FIELDS

Neutrinos

Radioactive beams

Astro particles

B ou τc Factories

3. MAJOR PROGRAMS FOR THE DECADE

LEP 200

GANIL

SATURNE

HERA

VIVITRON

SHARED MULTI-DETECTORS

DETECTOR	PARTICIPATING COUNTRIES	PARTICIPATING LABORATORIES	SUCCESSIVE SITING
TAPS (Two arm Photon Spectometer)	France Germany Netherlands	GANIL Caen GSI Darmstadt Univ. Giessen KVI Groningen	GANIL Caen GSI Darmstadt KVI Groningen MAMI Mainz LEAR CERN
EDEN (Neutrons)	France Netherlands	IPN Orsay KVI Groningen	Tandem Orsay GANIL Caen KVI Groningen
DEMON (Neutrons)	France Belgium	LPC Caen; CRN Strasbourg U.L. Bruxelles, U.C. Louvain-la-Neuve	U.C. Louvain-la-Neuve GANIL Caen Vivitron Strasbourg
EUROGAM (Photons)	France	IPN Orsay CSNSM Orsay CEN Bordeaux GANIL CRN Strasbourg IPN Lyon ISN Grenoble	NSF Daresbury Vivitron Strasbourg (GANIL)
	United Kingdom	NSF Daresbury Univ. Manchester Univ. Liverpool Univ. Birmingham	
will evolve towards EUROBALL	+ Germany Italy Scandinavian Countries		

Creve Maples

Musetech
Albuquerque, NM

A New Dimension in Human-Computer Interaction

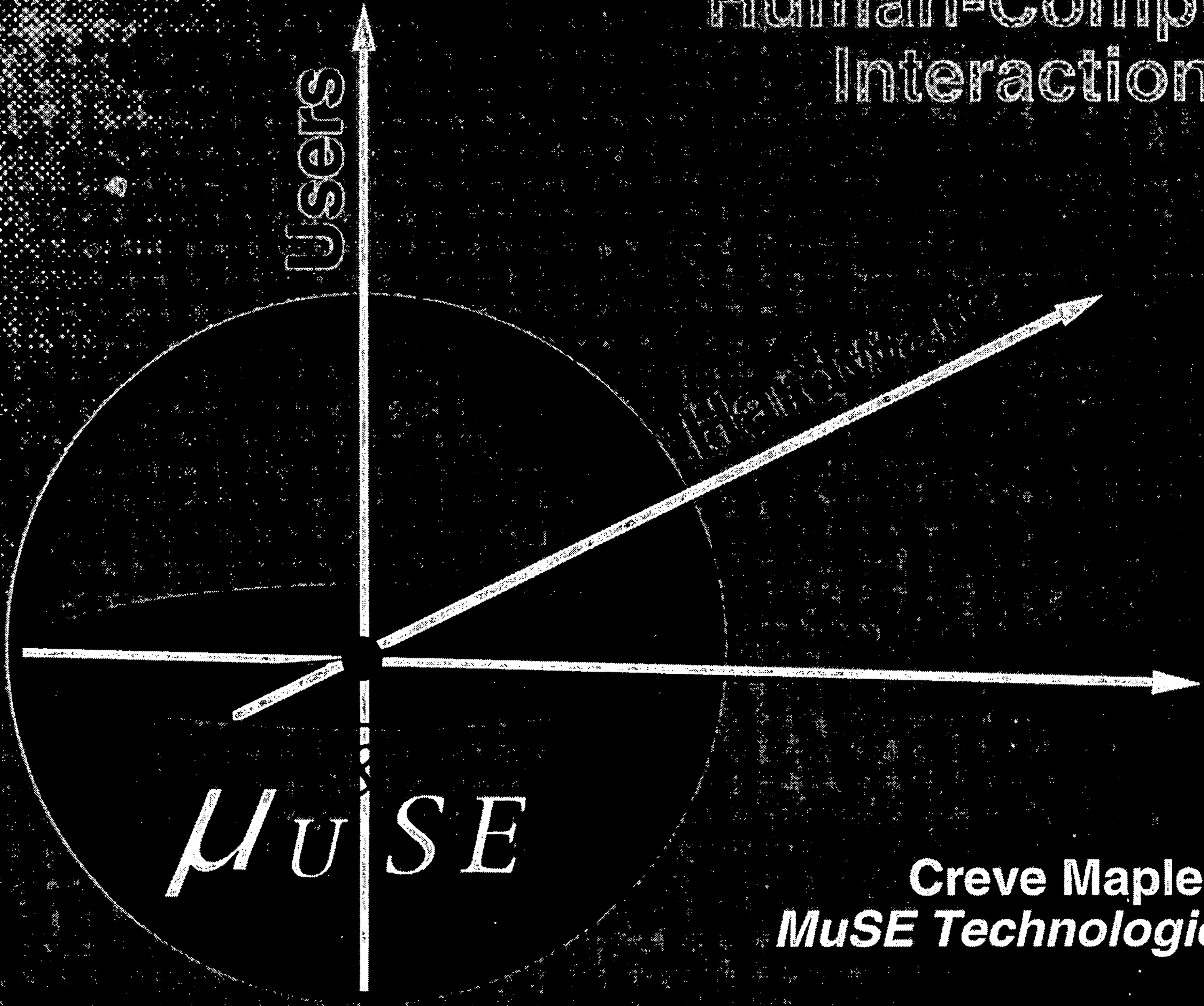

Creve Maples
MuSE Technologies, Inc.

1601 Ranpolph, Suite 210, Albuquerque, NM
(505) 843-6873 cmaples@musetech.com

"The purpose of computing is *insight*,

not *numbers*"

Richard Hamming

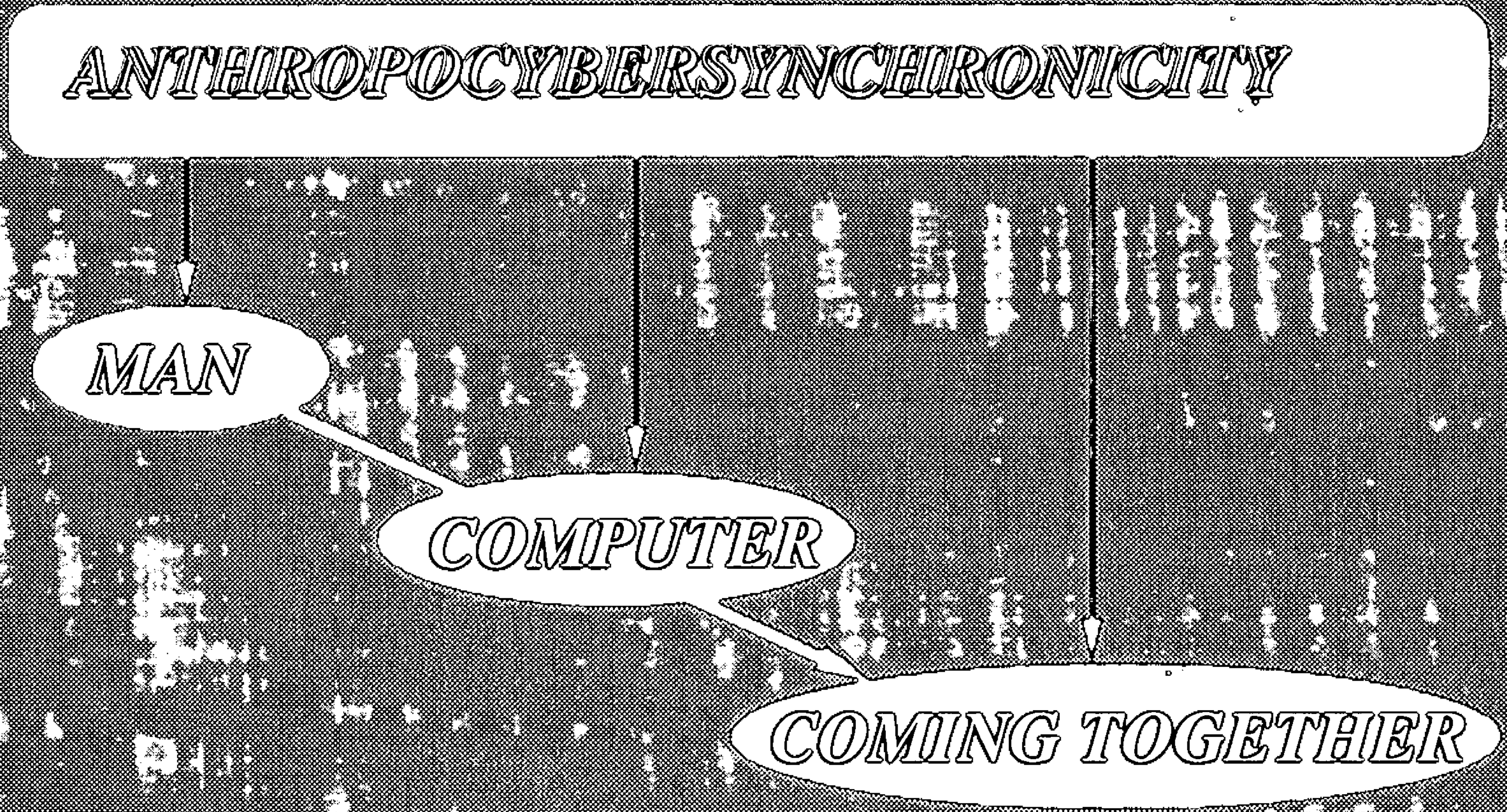

ANTHROPOCYBERSYNCHRONICITY

MAN

COMPUTER

COMING TOGETHER

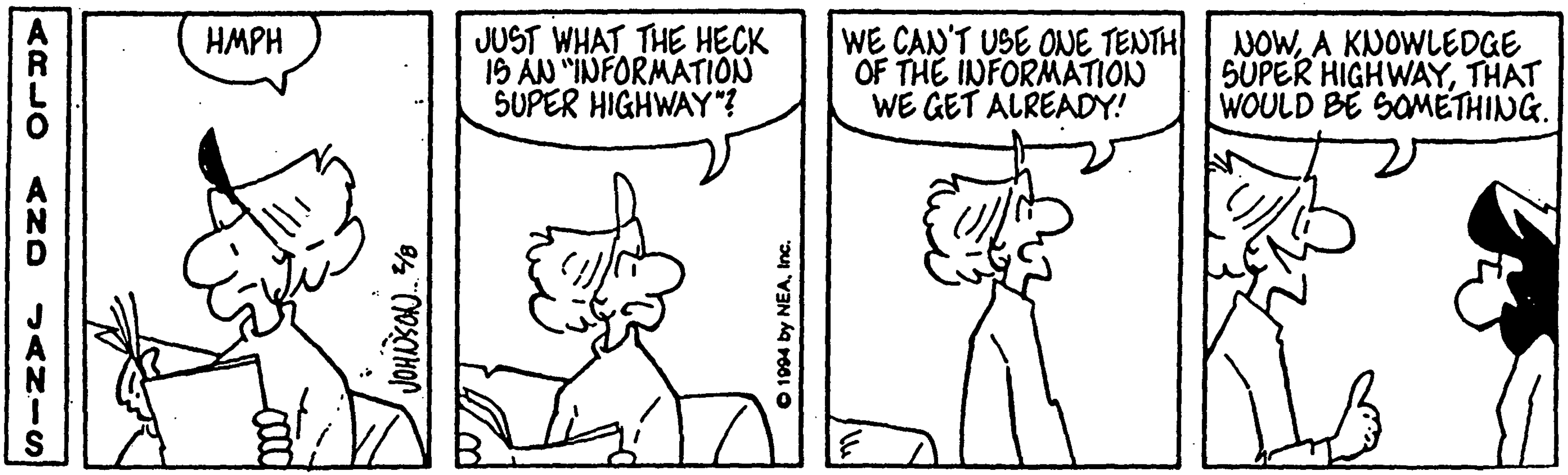

© 1994 by NEA, Inc.

The Dimension of HUMAN SENSES

SIGHT	length width height	color motion objects
SOUND	loudness pitch voice	location motion speech
TOUCH	texture pressure temperature	location motion
ODOR	type degree	direction
TASTE	type degree	

The Dimension of SOUND

SPEECH	*Voice recognition* *Synthetic speech*
DISCRETE DATA	*amplitude* *frequency* *voice*
LOCATION	*x, y, and z coordinates*
SENSORY QUEUES	*associated with events*
MOTION	*direction*

AREAS of HUMAN-COMPUTER INTERACTION

PRESENTATION

Approaches for representing complex, multi-dimensional information.

EXPLORATION

Techniques for moving within and between various representations and models.

NAVIGATION

Methods for maintaining location and reference within representations.

MANIPULATION

Control mechanisms for interacting with displays and information.

EXAMINATION

Control mechanisms for interacting with displays and information.

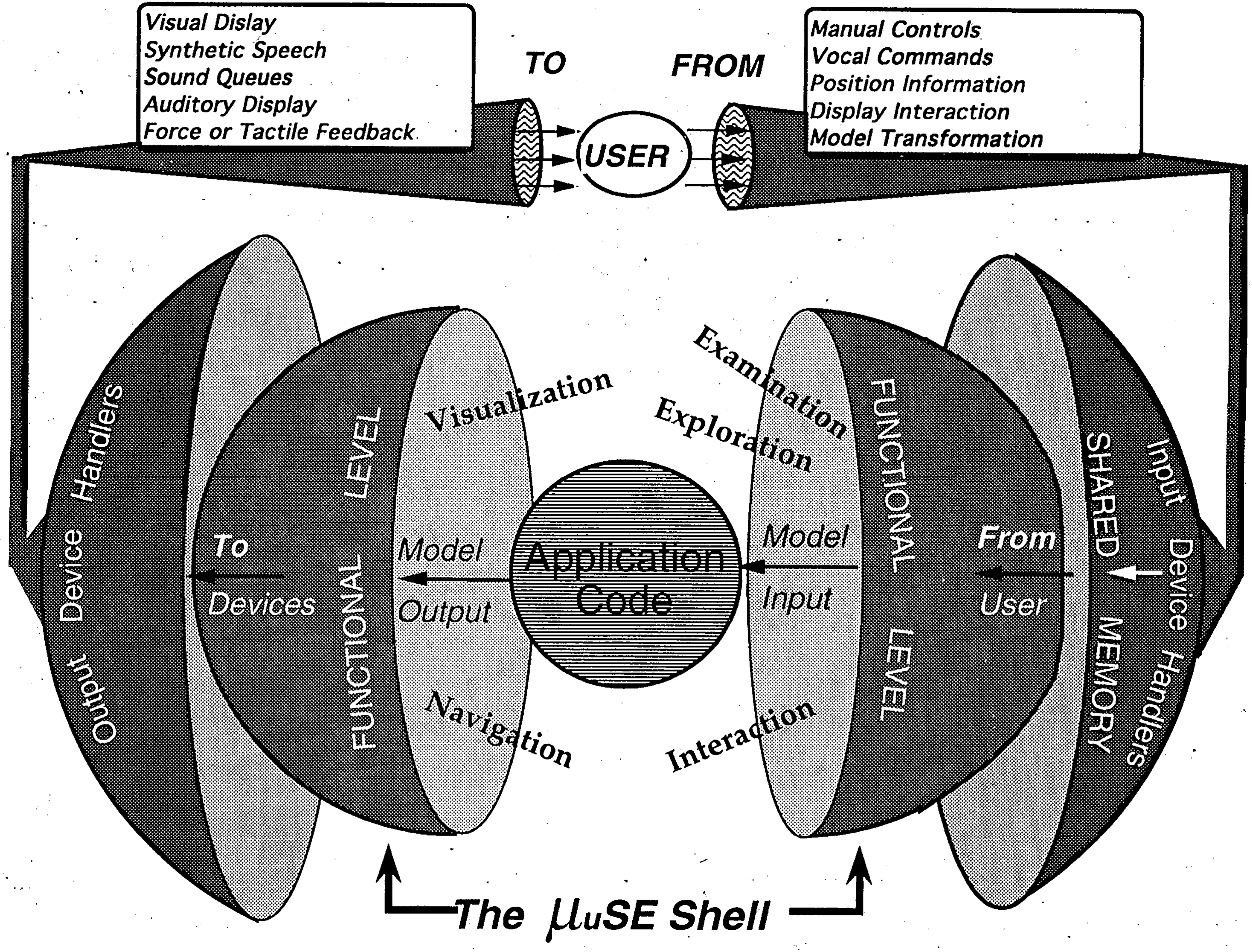
Visual Dislay
Synthetic Speech
Sound Queues
Auditory Display
Force or Tactile Feedback
TO
USER
FROM
Manual Controls
Vocal Commands
Position Information
Display Interaction
Model Transformation
Output Device Handlers
To Devices
FUNCTIONAL LEVEL
Model Output
Visualization
Navigation
Application Code
Examination
Exploration
Interaction
Model Input
FUNCTIONAL LEVEL
From User
SHARED MEMORY
Input Device Handlers
The μuSE Shell

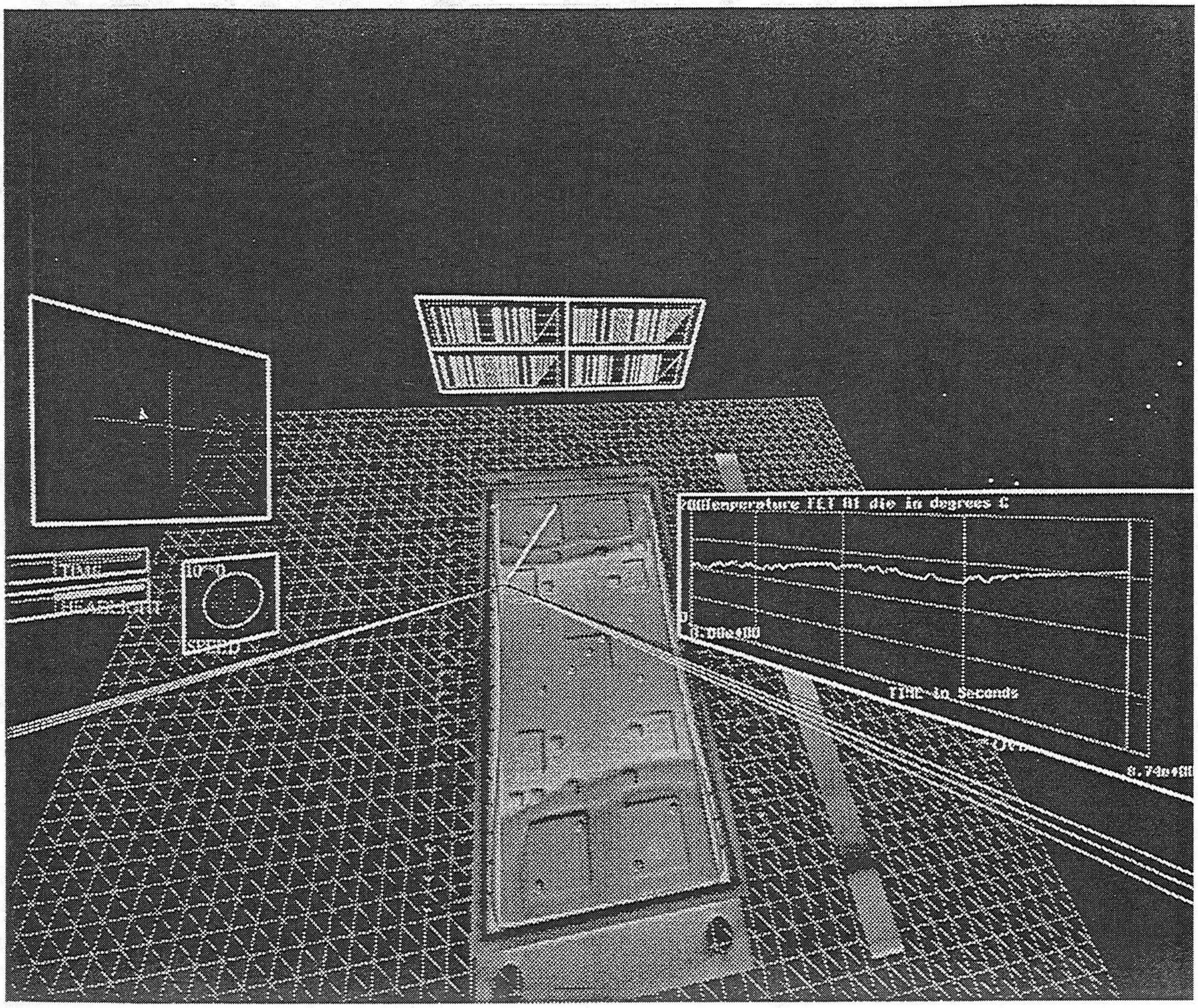

Operation of a Multichip Module

APPLICATIONS: Finite element analysis; Thermal conductivity; Circuit simulation; Stress analysis; CAD models; Data sonification.

DESCRIPTION: This model integrates diverse information associated with the electrical and thermal operation of a Modular Adaptable Controller. This multichip module contains various electrical components and controls the mechanical operation of a complex maze-wheel discriminator.

The system displays CAD and finite element models, and permits any of 25 points to be probed during the operation of the chip. Data from the probes may be displayed on the craft side wall, as spatial graphs, or transformed into sound output. Time-dependent thermal information is shown as color overlays to the finite element grid. Thermal conductivity of substrates may be altered, and electrical and thermal effects examined.

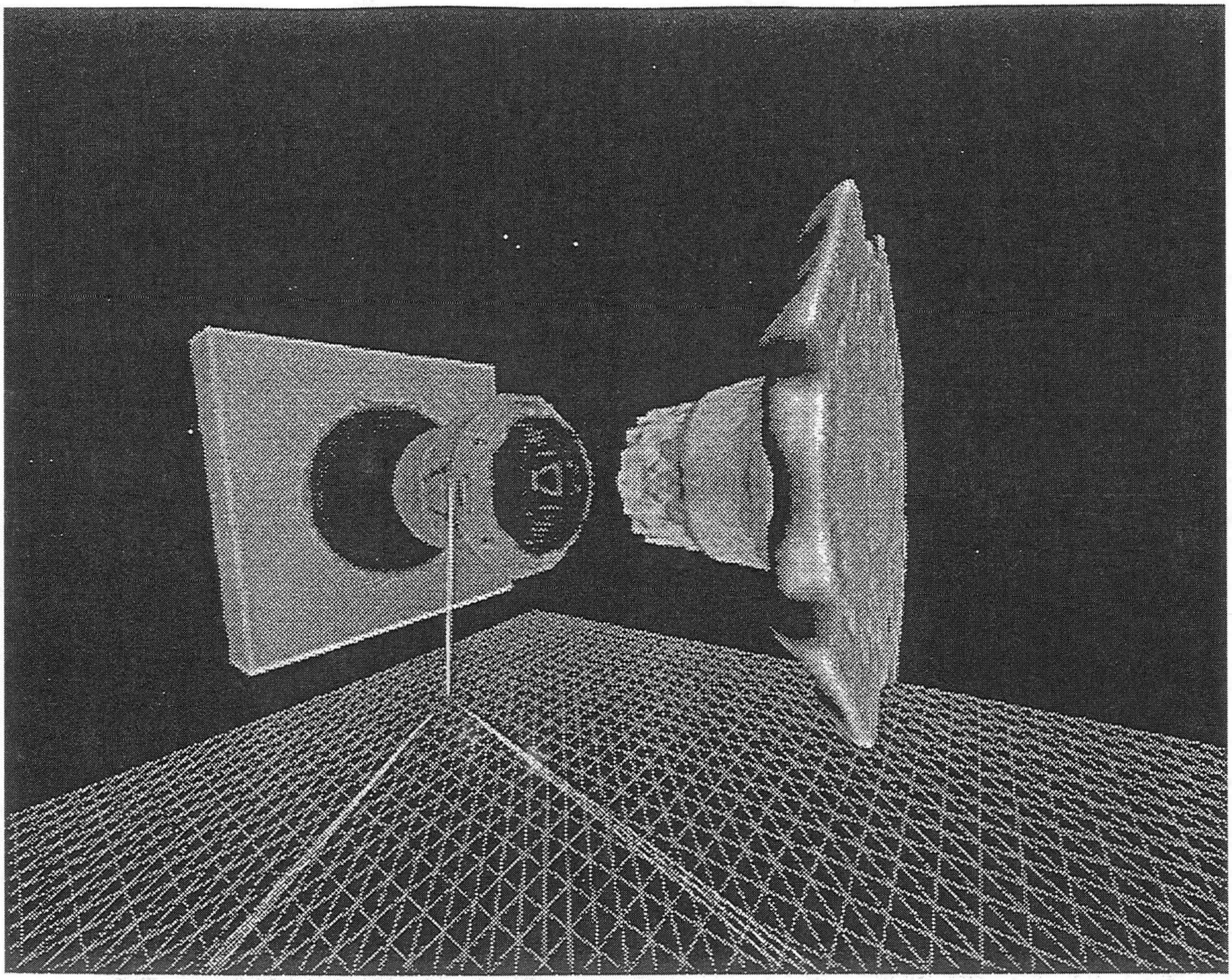

Explosive Welding

APPLICATIONS: Dynamic simulations (e.g.: stress, shock or impact analysis); Mass distribution analysis.

DESCRIPTION: The model represents a simulation of an attempt to simultaneously weld and force-fit a copper pipe to a beveled steel plate by setting off an explosive charge in the pipe. The simulation was run using the Parallel CTH code on the Paragon Super-computer in 95 time steps.

Spatial and temporal teleportation to specific marked locations, coupled with the ability to manipulate dynamically changing data sets, permits detailed examination of the welding process and its effect on materials.

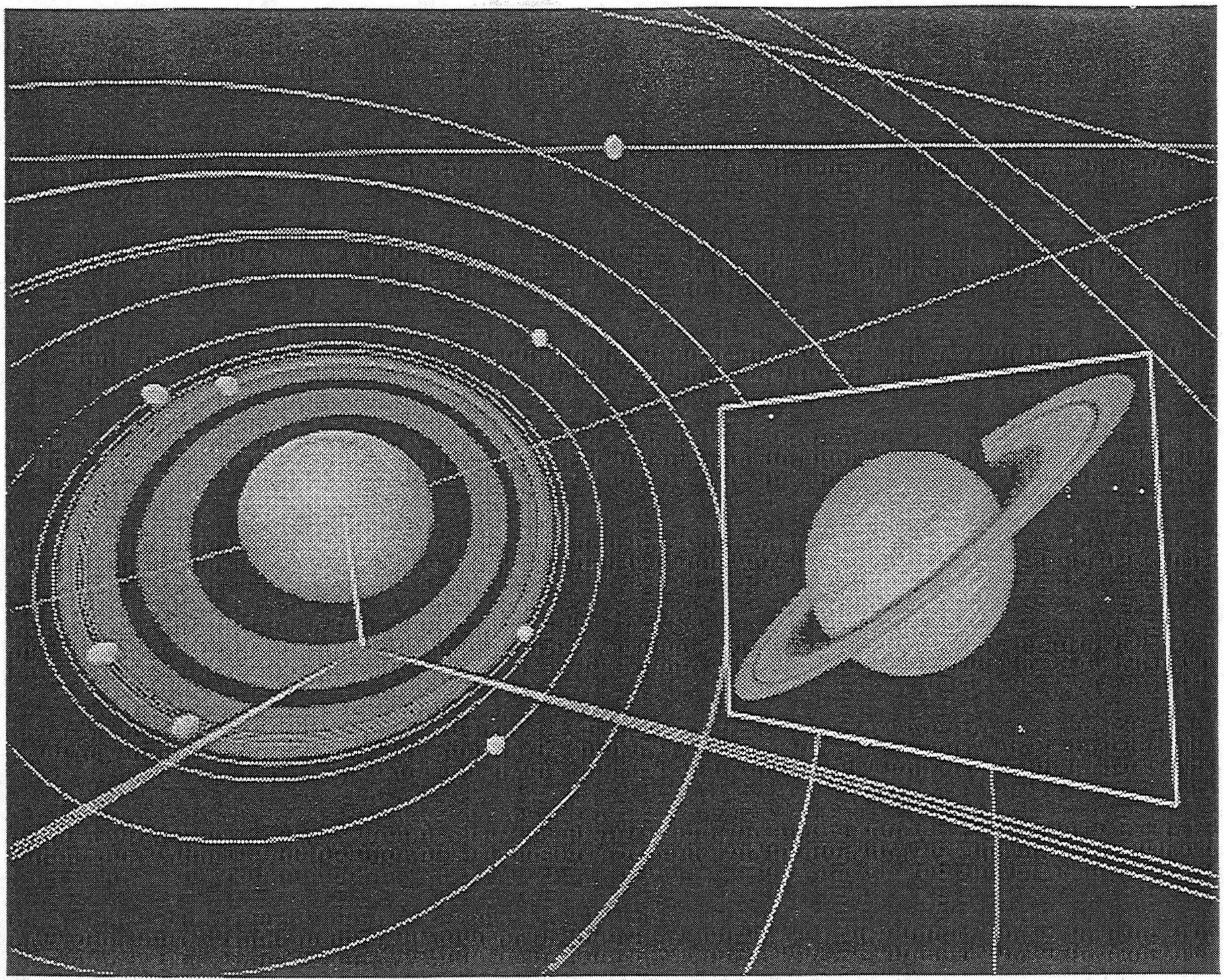

Dynamic Solar System

APPLICATIONS: Time-dependent models; Fusion of different types of correlated information (e.g., pictures, trajectories); Real-time interaction with dynamic models.

DESCRIPTION: The scale model of the solar system covers a spatial range of 1010 km with an individual positioning resolution of ~20km. It contains 73 objects, each with appropriate motion. Tethering or locking permits a viewer to attach to an object and travel with it, duplicating all or part (e.g., center of mass) of its inertial motion while retaining the ability to move independently. Here, tethering also triggers a search of available NASA data. Photographs and associated text information are displayed on the craft wall while tethered.

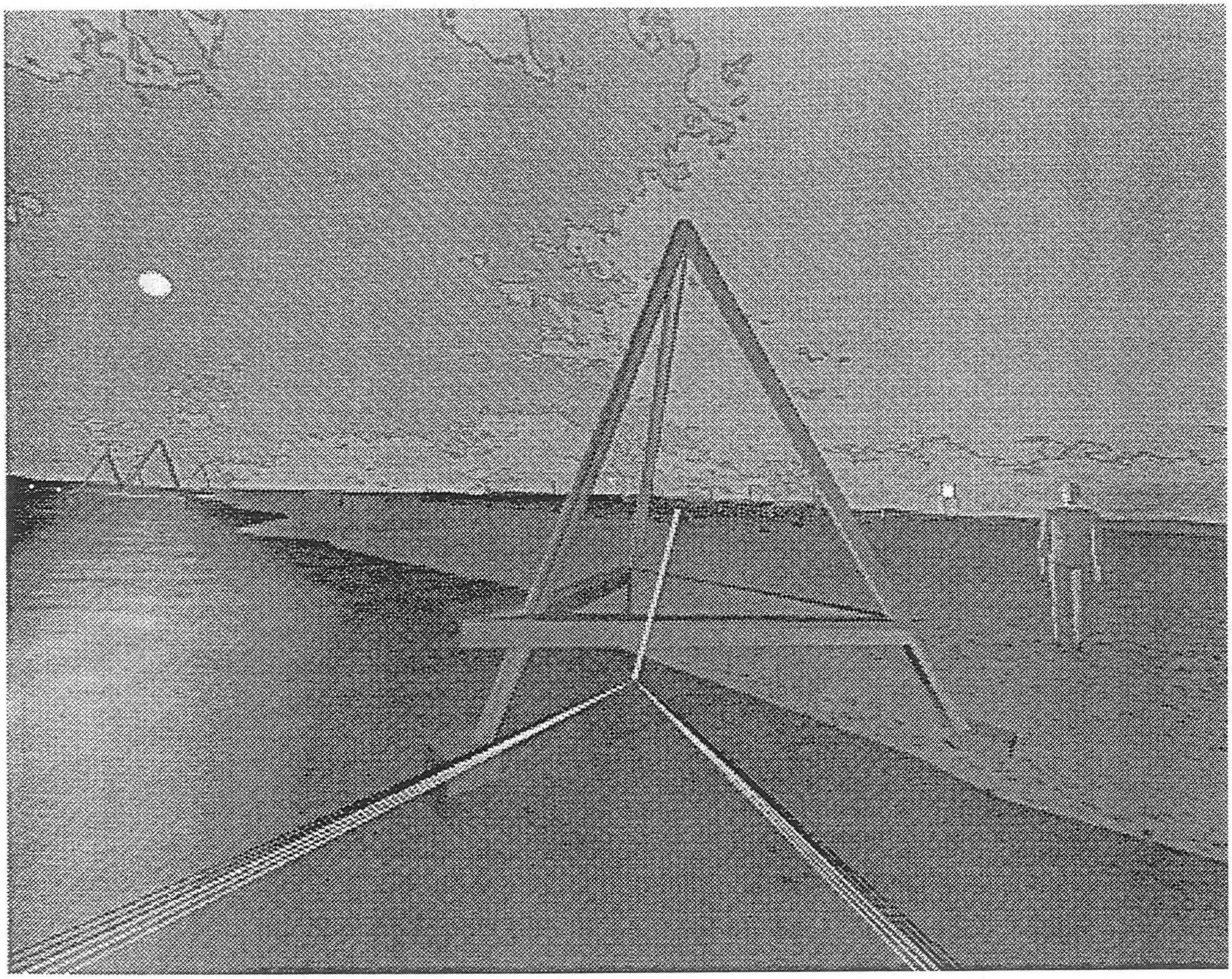

Environmental Evaluation

APPLICATIONS: Transportation, Construction, Planning, Architecture, Training, Environmental impact, Command and Control, Tactical and strategic analysis.

DESCRIPTION: Topographic, geometric, photographic, and observational information was combined to recreate a section of an actual beach over a three month period. The reconstruction included the dynamic lighting variation, actual weather and surf conditions, and changes in terrain and structures due to climate effects. The user has complete freedom of movement through both time and/or space, either by moving location and controlling the rate of time, or by teleporting to different spacial and temporal locations set by the viewer. A user can rapidly assess and evaluate the complete situation, and make informed decisions and plans that take all the various factors into account. The MuSE system was used both by the designers to actually construct this model, as well as by users to interact with it.

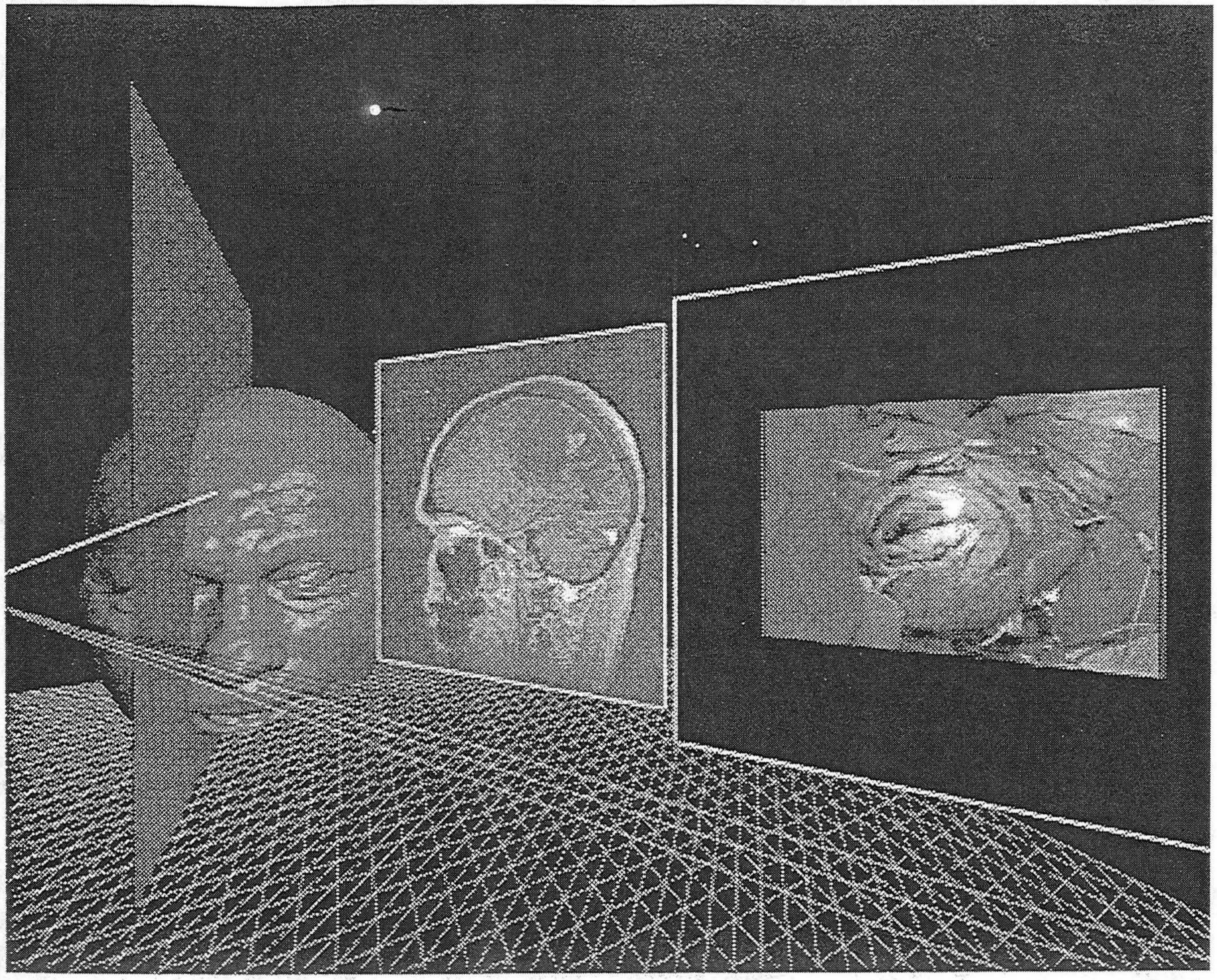

MRI Scan and Related Patient Data

APPLICATIONS: Medical imaging; Complex data evaluation; Analysis of 3-D volumetric data; Operation planning; Structural analysis

DESCRIPTION: Model is based on 128 MRI cranial scans. A dynamic cutting plane may be invoked to project cross sections on the wall of the craft. Additional patient information (e.g. actual photographs, test result) can be accessed as needed on the craft wall, or selectively mapped into sound (e.g. systolic pressure, heart rate, respiration rate, temperature).

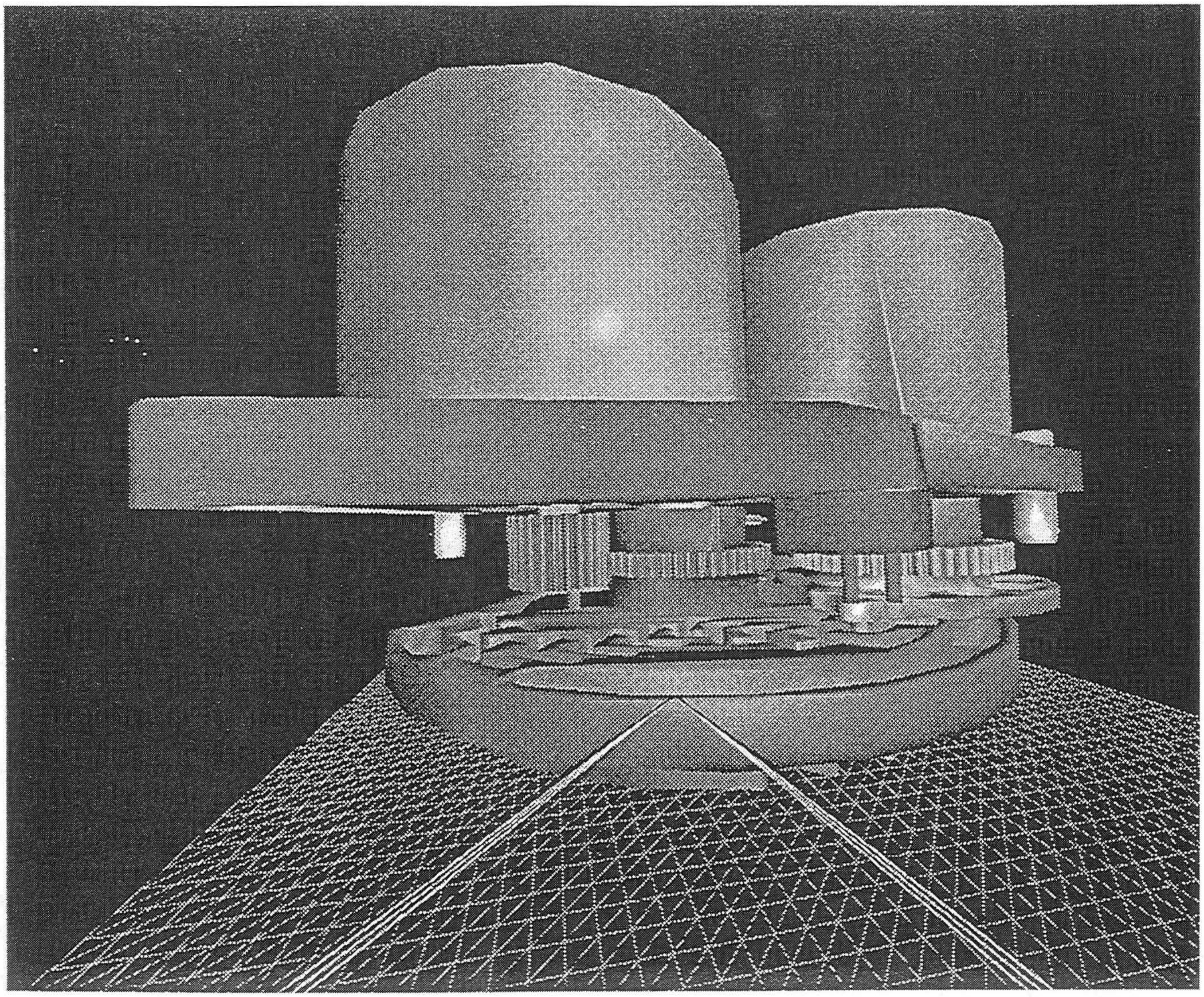

CAD Analysis and Operation

APPLICATIONS: Design analysis and verification; Component integration; Training.

DESCRIPTION: A synthetic working model of a complex electromechanical maze-wheel discriminator, designed and built at Sandia National Laboratories. MuSE integrates CAD information with functional kinematic calculations from commercial software. The actual device is approximately 2" x 1" x 2". MuSE permits the user to vary size ratios to explore the internal operation of the system. Users can control the speed and direction of time, manipulate components, examine subsystems, and disassemble the model, all while the motor is running. Cutting planes permit cross-sectional views during operation and side displays can access schematics or test result information.

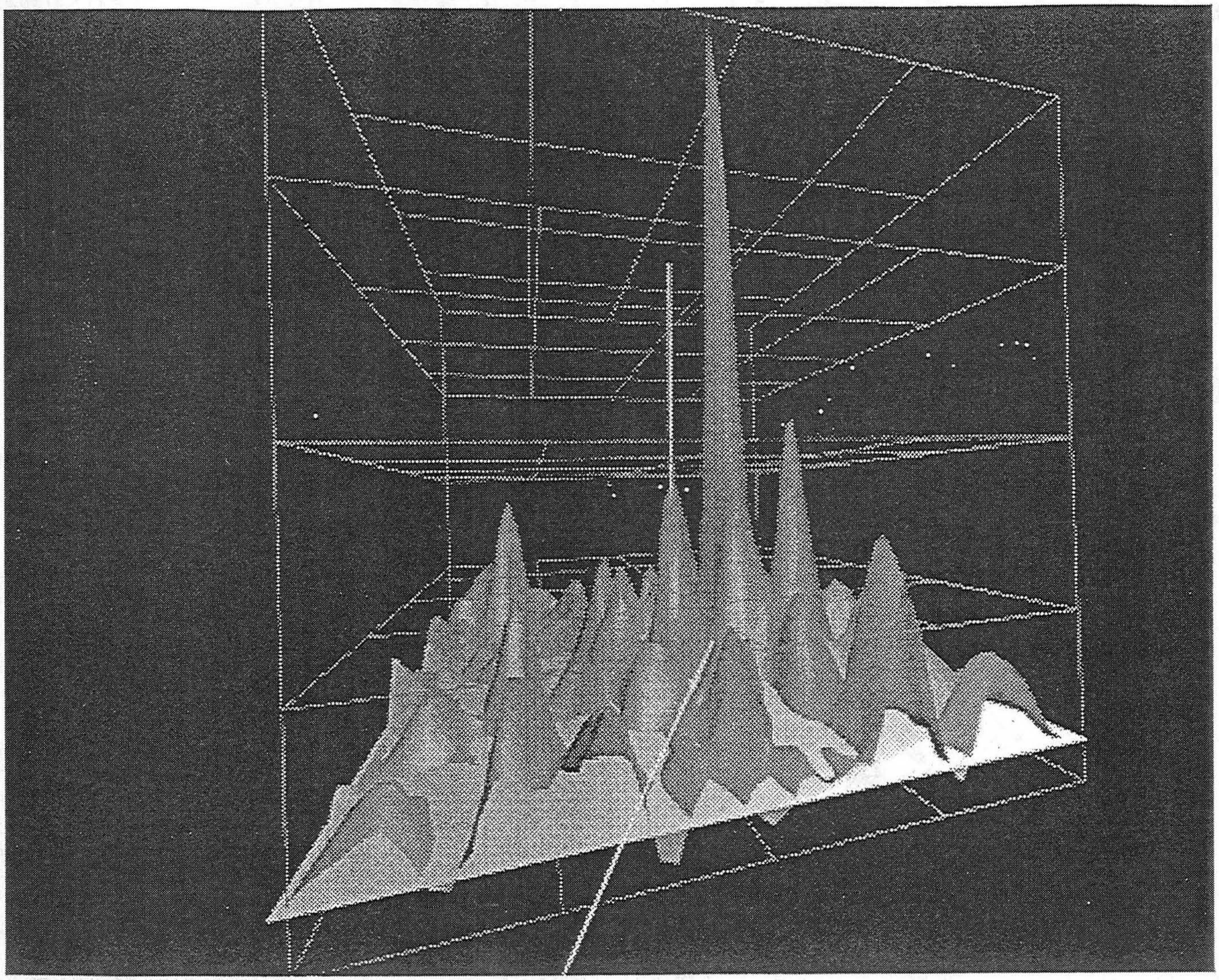

Seismic Information

APPLICATIONS: Investigation and evaluation of financial, economic, statistical or scientific data.

DESCRIPTION: Information was obtained from the ARCESS seismic detector array in Norway. The data is based on a fusion of individual detector information distributed over a roughly 1 km square area. The sensor information is transformed into time-dependent frequency wave number (F_k) data. The display shows the amplitude of seismic events. The location of a peak in this display is related to the direction and velocity of the approaching seismic wave. Interacting with this time-varying information in a synthetic environment enhances the ability to understand and separate independent seismic events which occur at different locations but are closely spaced in time.

The same technique can be applied to other numeric information, allowing a rapid evaluation of financial, economic, statistical, or scientific data.

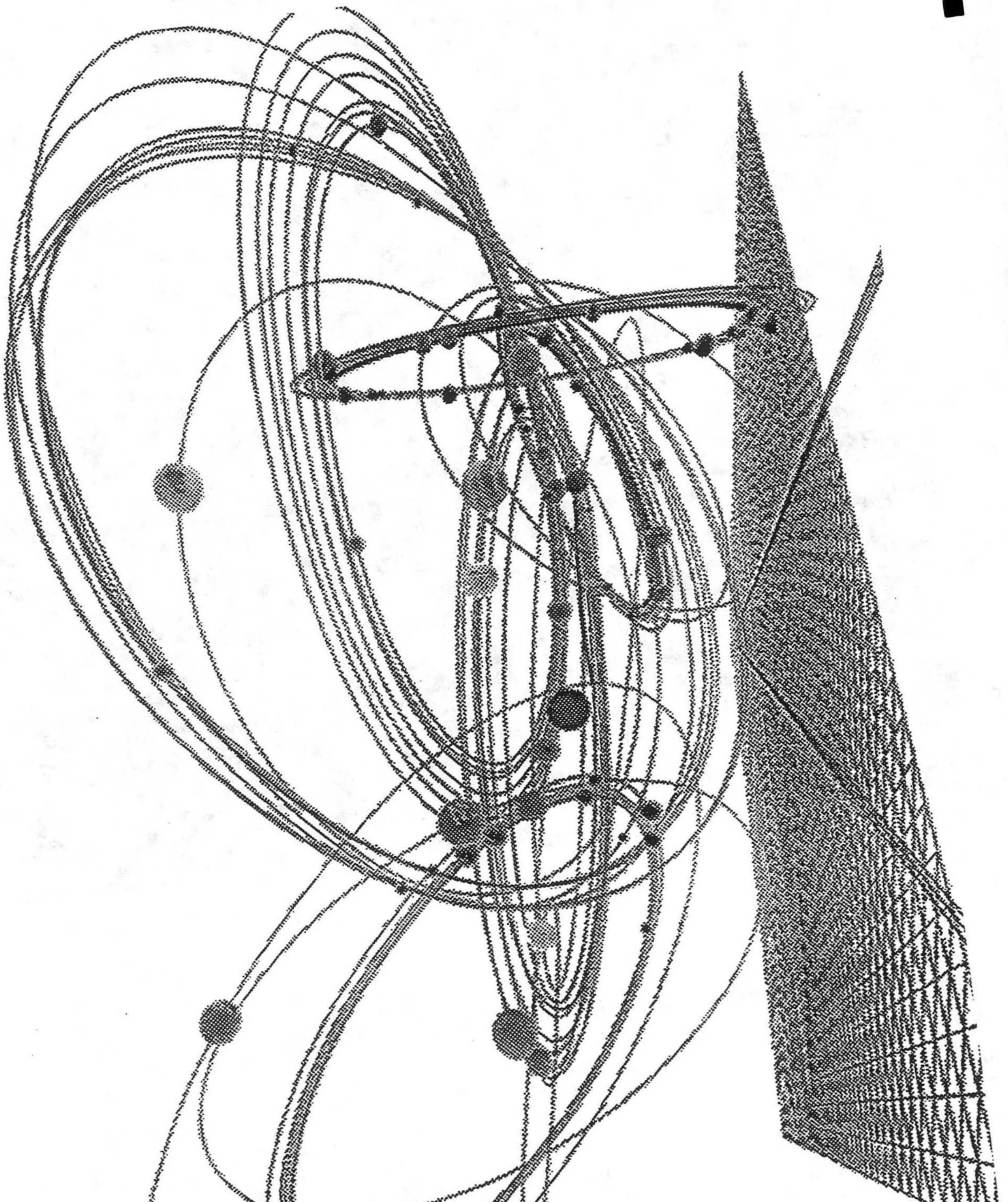

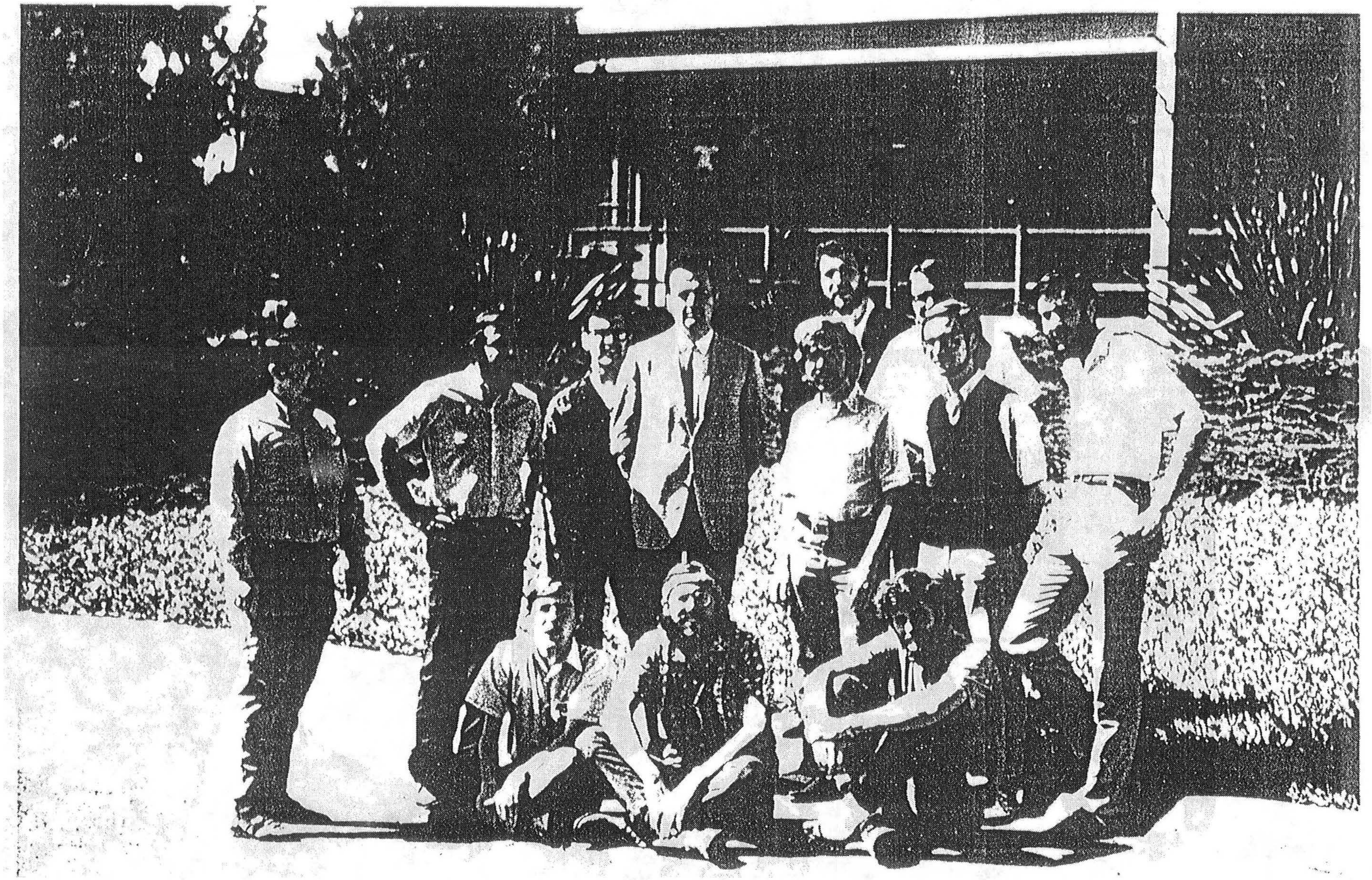

LESSON # 1

**TO BE SUCCESSFUL IN A FIELD
REQUIRES THAT 90%
of all waking efforts
BE DEVOTED to the PURSUIT
of that field!**

COROLLARY # 1

*It helps enormously, however,
if you can convince others to
buy-in to your potential success
and devote 90% of their time
to helping you achieve it !*

LESSON # 2

THE AMOUNT OF MONEY ONE
MAKES IS IMMATERIAL !
Since expenses increase
in proportion to income,
DISPOSABLE INCOME REMAINS
RELATIVELY CONSTANT.

COROLLARY # 2

Indentured servitude is viable,
if people can be convinced to
voluntarily accept it !

LESSON # 3

Devoting a portion of one's life to HELPING the LESS ADVANTAGED, is important to society, and is a WORTHWHILE UNDERTAKING!

COROLLARY # 3

This lesson may conflict with Lesson # 1. The conflict may be resolved, however, by convincing others to devote their time to bettering society under your sponsorship !

LESSON # 4

SUCCESS REQUIRES A CLEARLY DEFINED OBJECTIVE
and the
PATIENCE and PERSISTENCE TO STICK WITH IT !

COROLLARY # 4

IT IS NOT NECESSARY TO SHARE YOUR REAL OBJECTIVE WITH OTHERS,

They are free to draw their own conclusions !

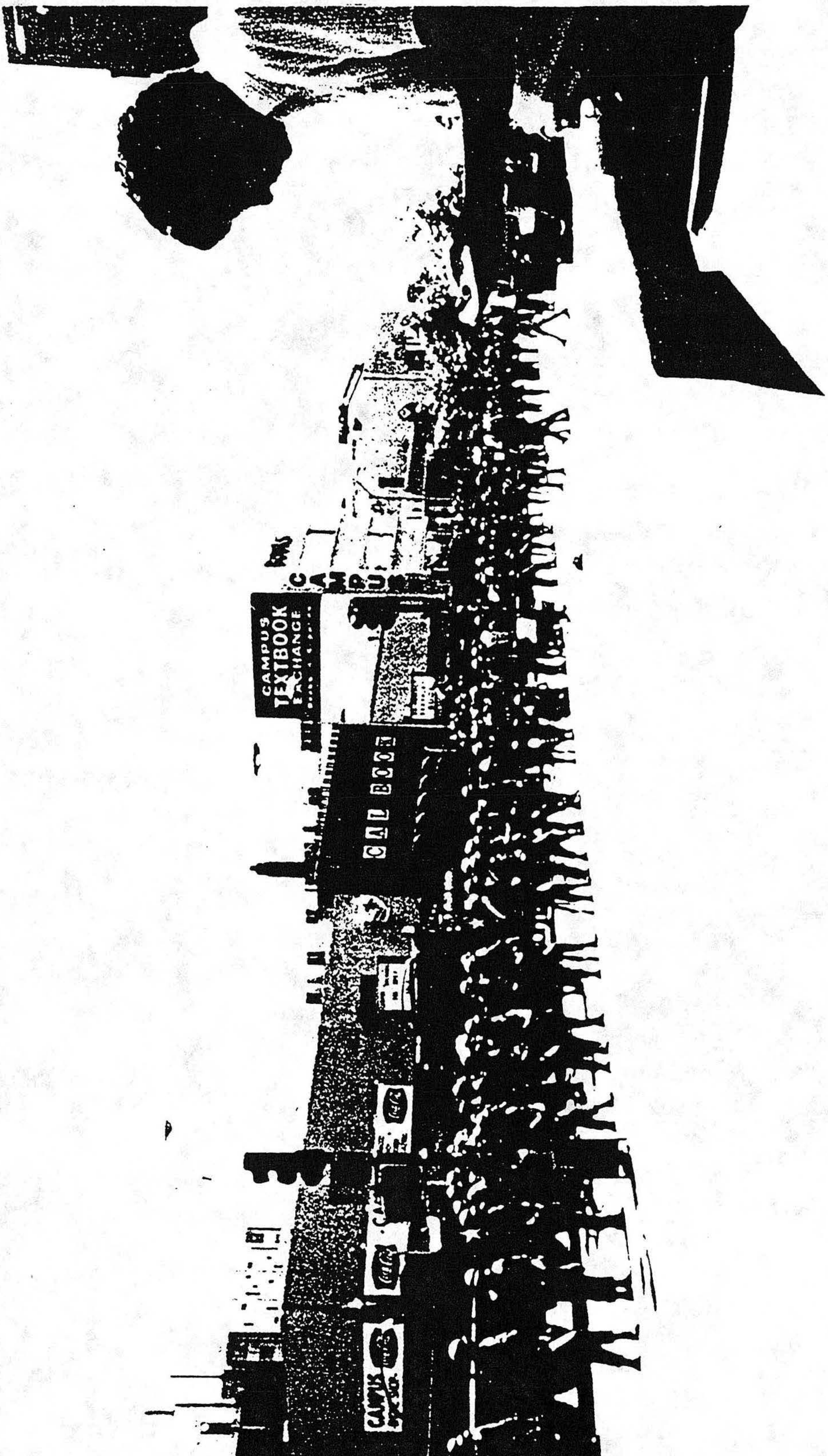
CAMPUS TEXTBOOK EXCHANGE
CAL BOOK
CAMPUS

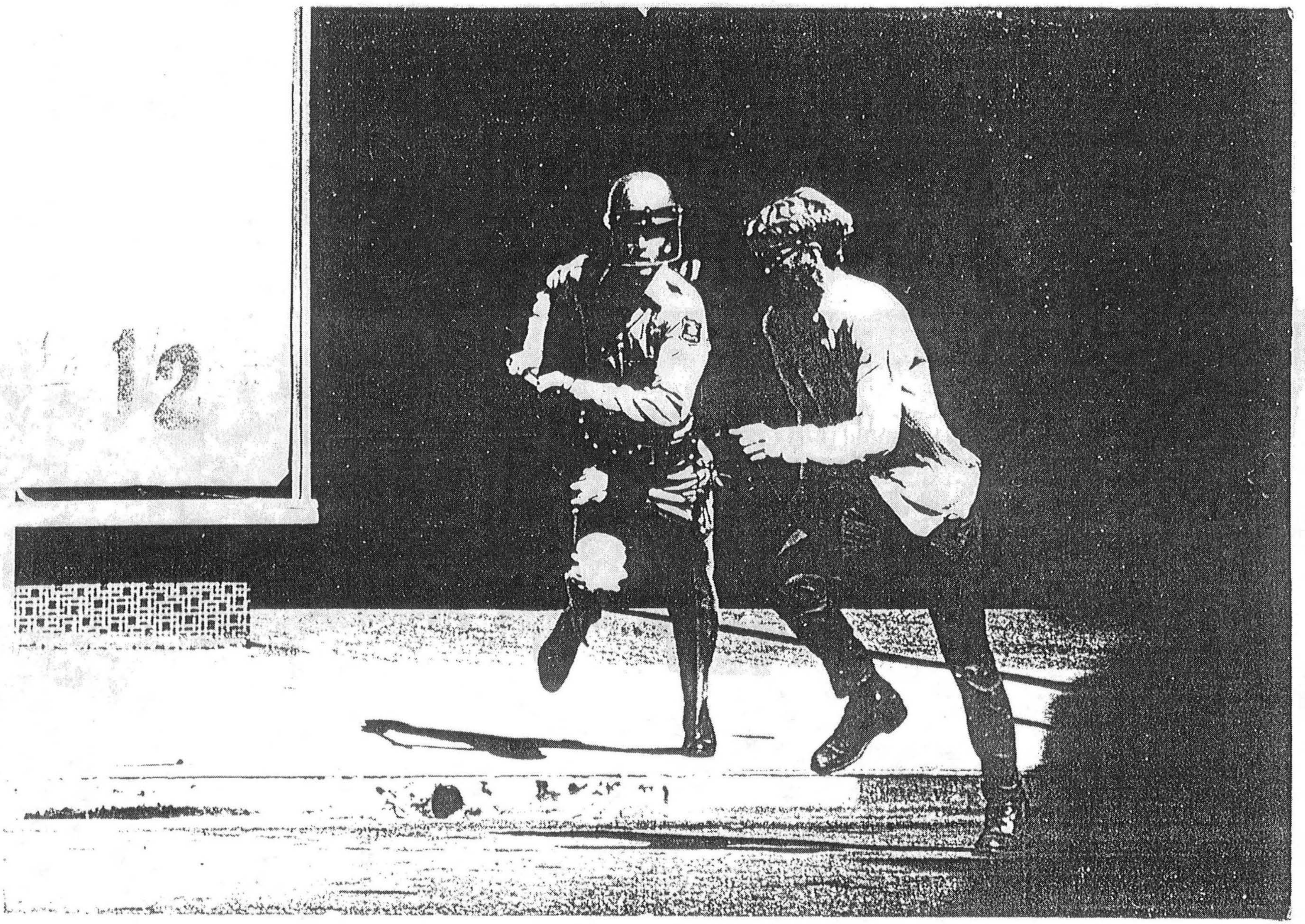
12

CHAOS – Where Brilliant Dreams are Born™ – *I CHING IMAGE*™, image #3

Before the beginning of great brilliance, there must be Chaos.
Before a brilliant person begins something great, s/he must look foolish to the crowd.

Mike Cable

Lawrence Livermore National Laboratory
Livermore, CA

Nuclear Measurement Techniques for Inertial Confinement Fusion*

Michael D. Cable
NIF Diagnostics Development Group

University of California
Lawrence Livermore National Laboratory

Exotic Nuclei Symposium

Bodega Bay, CA
April 14-16, 1996

---

*This work was performed under the auspices of the U.S. Department of Energy by Lawrence Livermore National Laboratory under contract No. W-7405-ENG-48.

Nova System

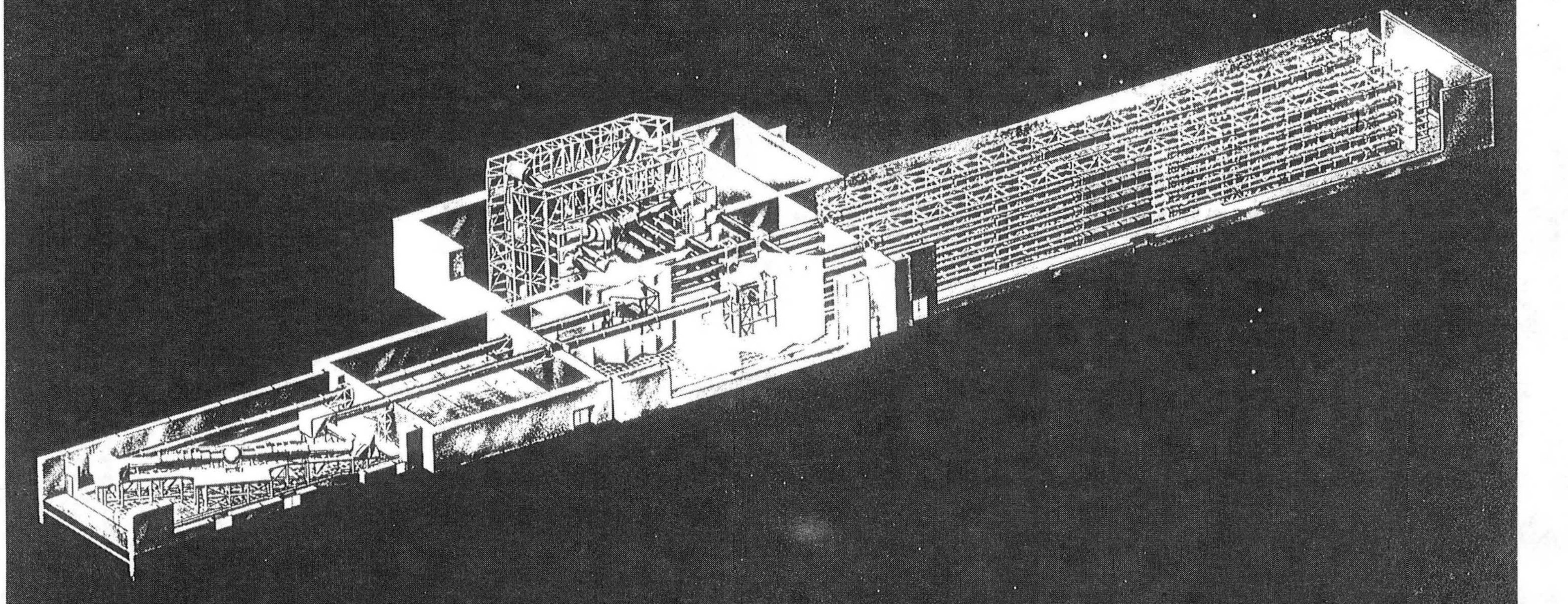

02-31-0385-1279

7/85

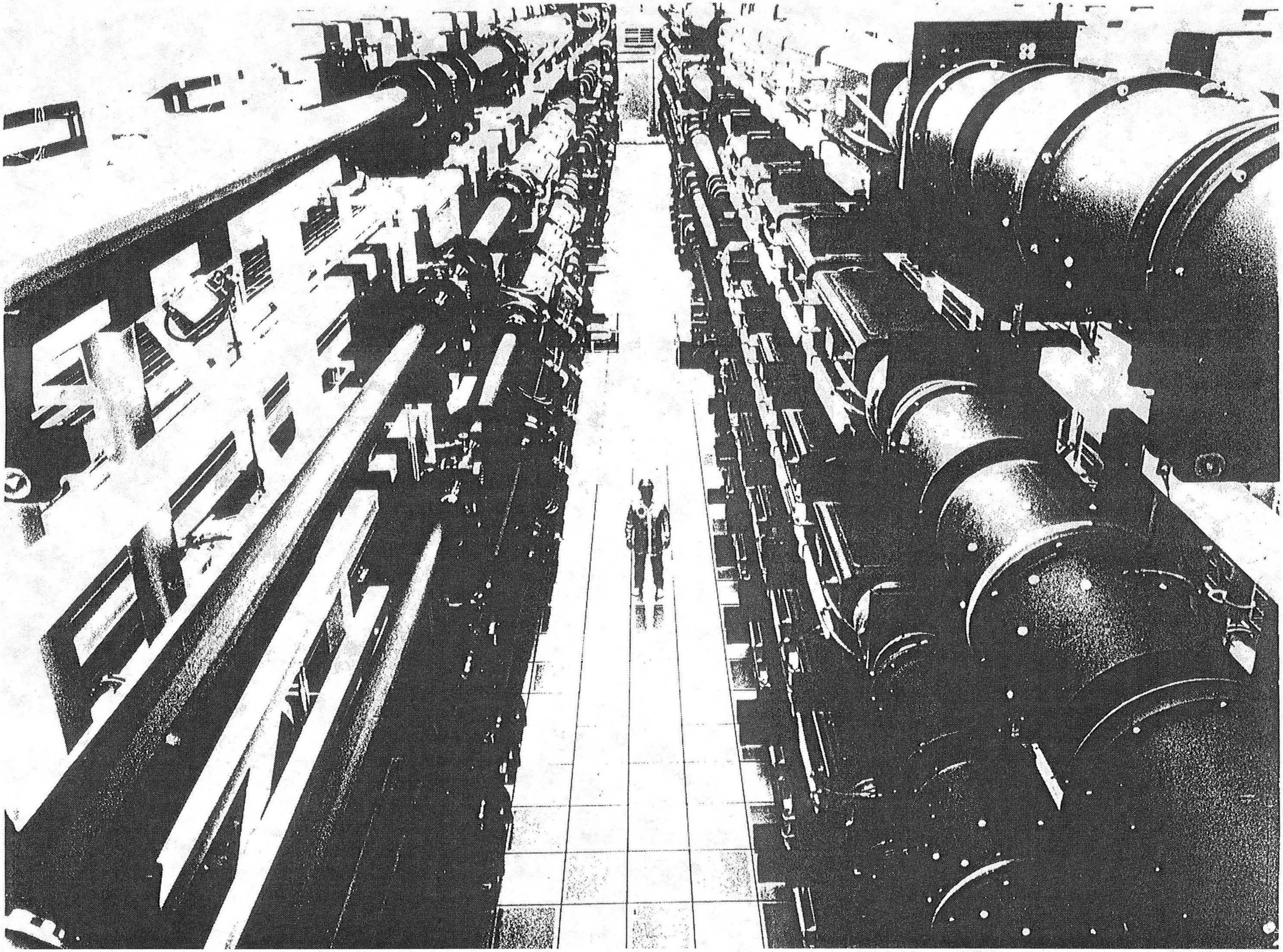

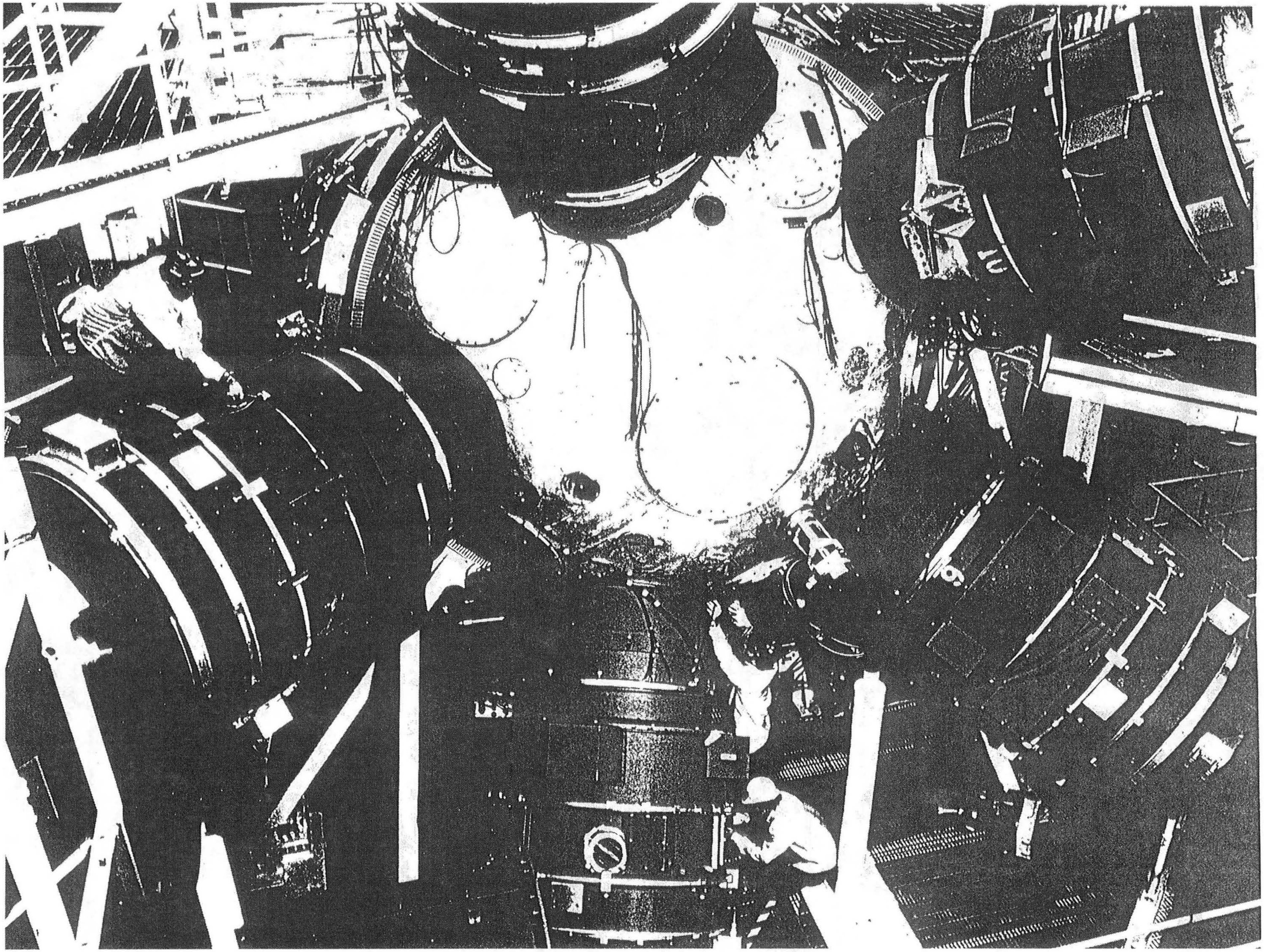
10
6

The National Ignition Facility—192 Beam

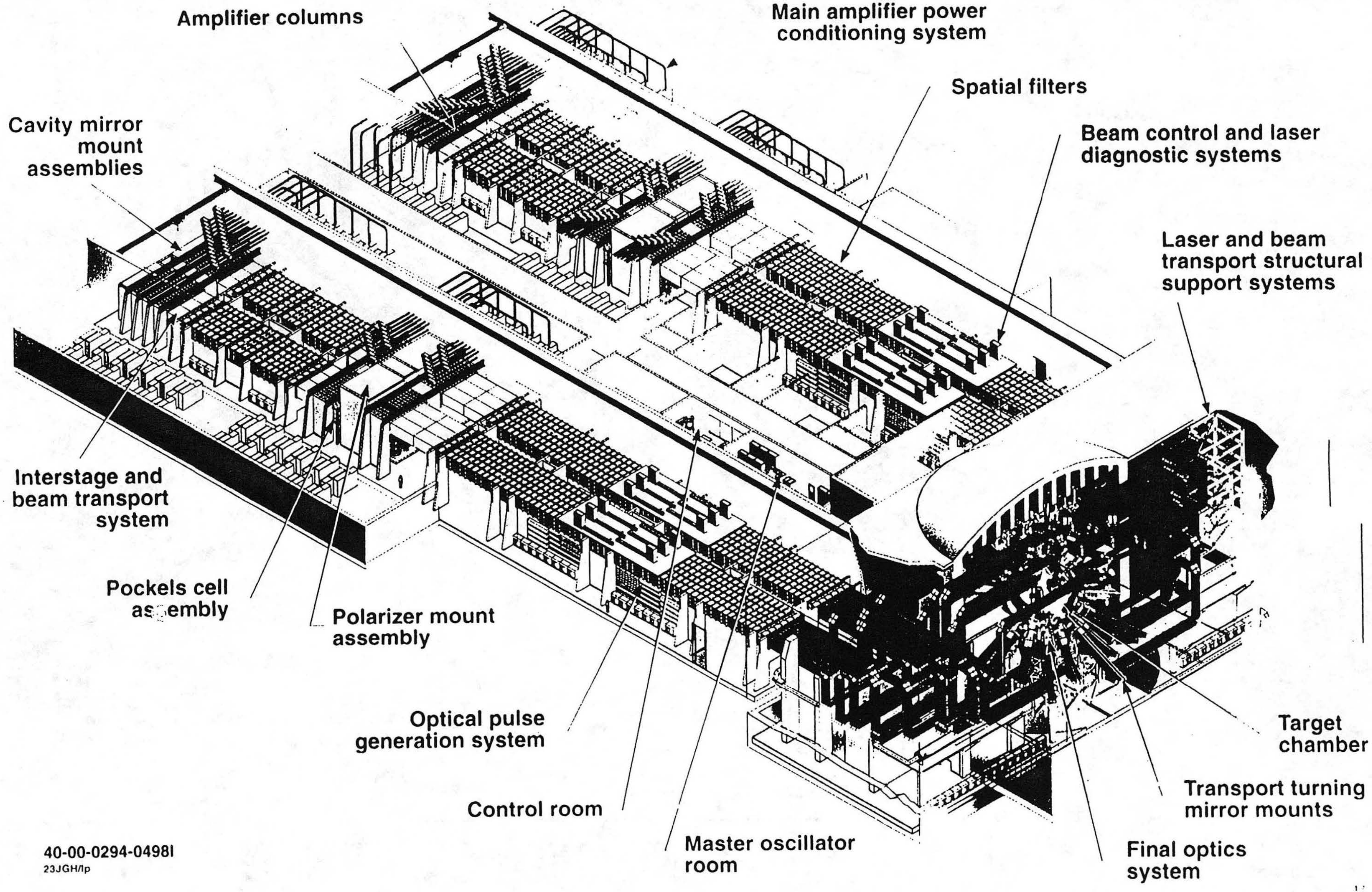

40-00-0294-0498I
23JGH/lp

The National Ignition Facility target area

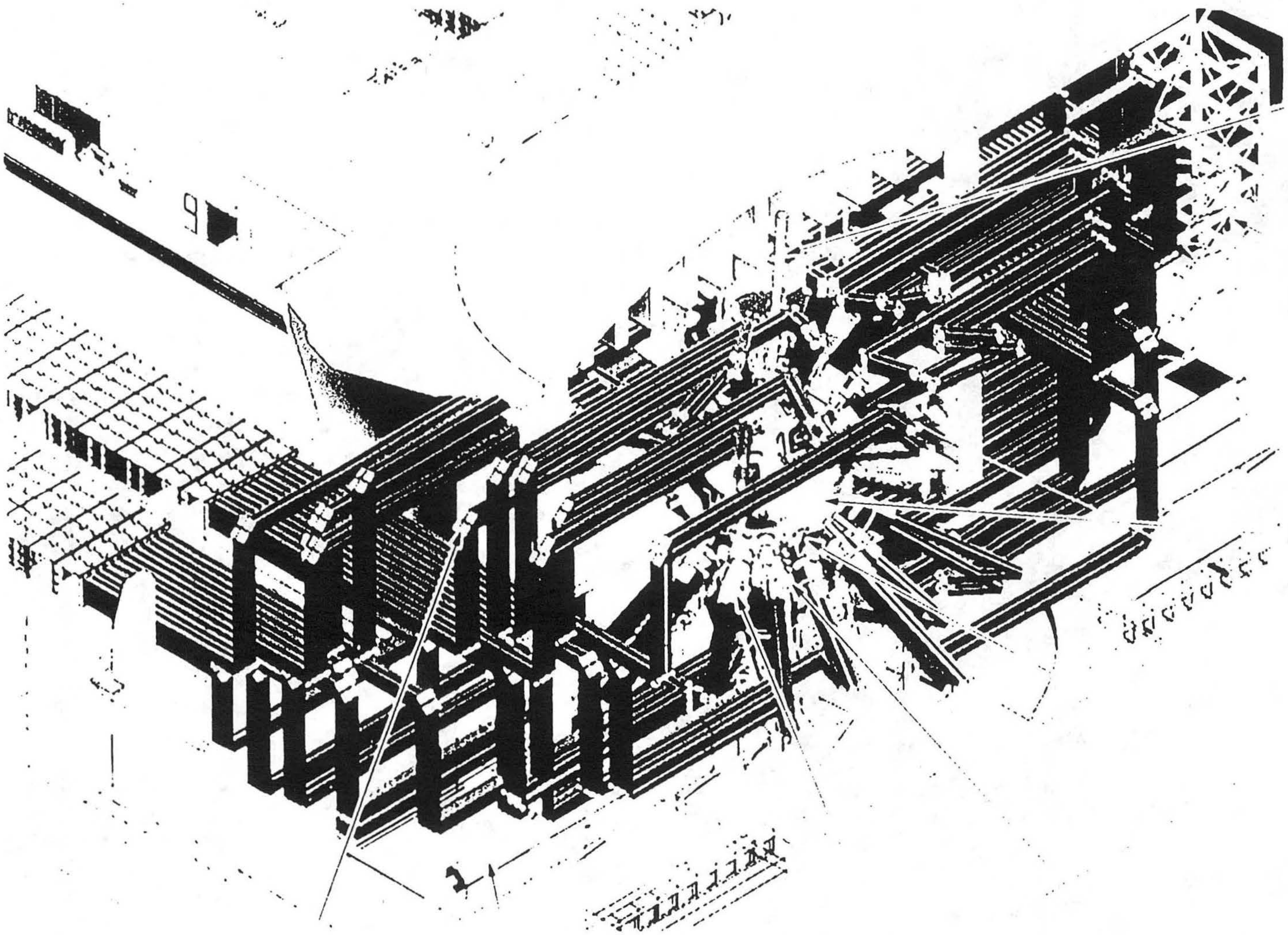

Static x-ray chamber

Mirror support structure

Target chamber

Vacuum pump

Turning mirror assembly

Target plane diagnostic station

Final optics assembly

Twelve-inch manipulator

NIF beam number and orientation (>192) meets implosion symmetry requirements for baseline target design

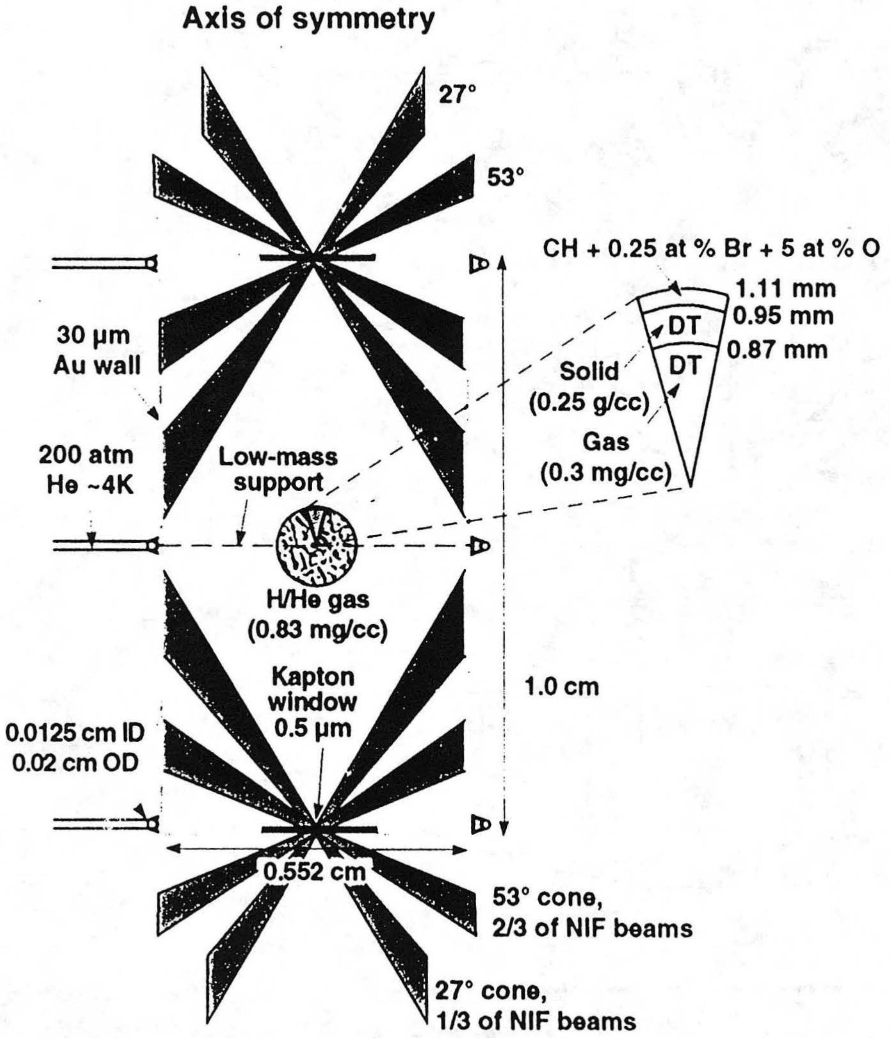

Representative NIF target

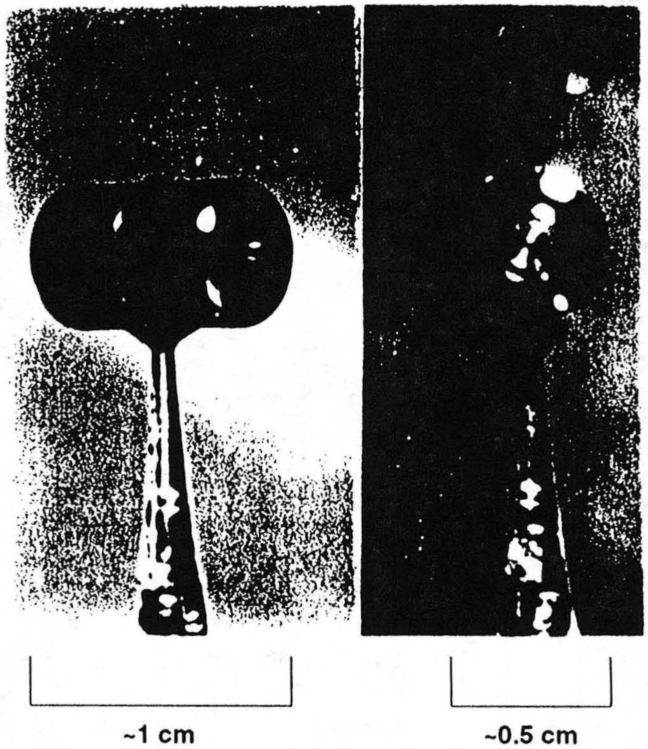

The target area is configured for accessibility and ease of maintenance

NIF
The National Ignition Facility

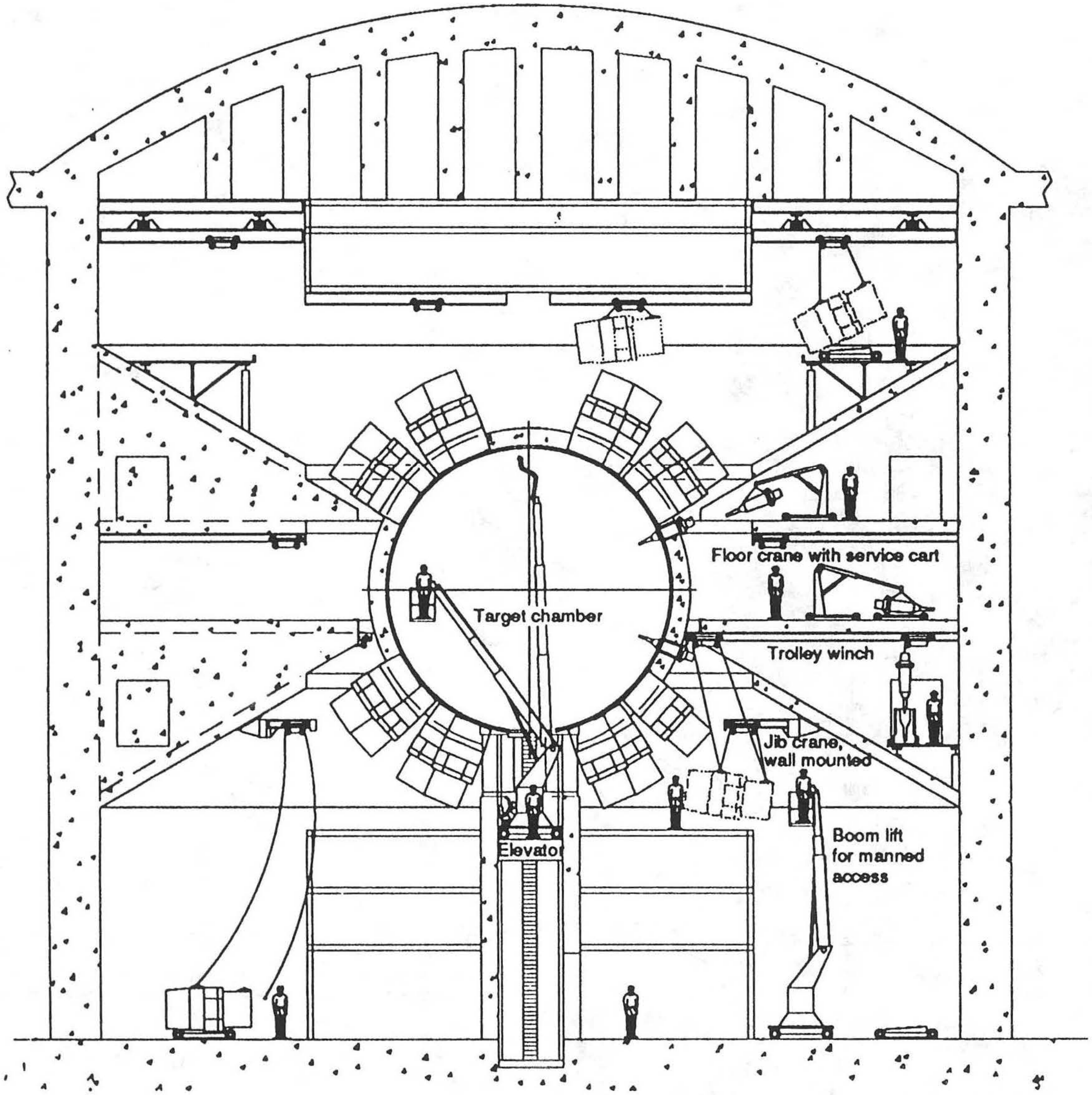

Nuclear reaction products can be used as penetrating "probes" for the central region of large ICF implosions.

Pros

Multi-MeV particles (particularly neutrons) can escape from the center of the implosion and carry out information about that region.

Nuclear reaction products are produced at burn time and are useful for probing the final fuel conditions - know when and where produced.

Cons

Early stages of implosion (pre-burn) can't be studied since no reactions occur during this time.

Failed implosions (no burn) provide little useful information.

Relatively small number of reactions historically has been technically limiting, but this situation has changed at Nova and is expected to change even more at NIF.

Comparison of NIF and Nova

Quantity	Nova	NIF
Laser energy on target	40 kJ	1.8 MJ
Capsule diameter	2.5 mm	9 mm
Hohlraum length	0.45 mm	1.1 mm
Implosion velocity	3.5×10^7 cm/s	4×10^7 cm/s
Convergence ratio	up to 24	25-35
Fuel areal density	20 mg/cm^2	1-2 g/cm^2
Fuel density	20 g/cm^3	800 g/cm^3
Fuel temperature	1-3 keV	5-20 keV
Confinement time	50 ps	100 ps
Neutron yield	10^{11}	10^{18}

High NIF neutron yields will make a variety of new nuclear diagnostic techniques possible.

A simple model for ICF shows some important properties to measure

$$Y_n = n_d n_t \langle \sigma v \rangle \tau V$$

This model of a spherical fuel with uniform density and temperature burning for time, τ, illustrates how the following quantities are fundamental to an ICF implosion.

Neutron yield	-	Gives the amount of fusion energy released.
Fuel density	-	Determined by the amount of fuel compression.
Fuel temperature	-	Determines the reaction rate (along with density).
Confinement time	-	Length of burn, the τ in $n\tau$.

More detailed simulations show other interesting properties that can be measured by nuclear techniques

NIF

The National Ignition Facility

Fuel areal density	-	Must be sufficient to stop alphas for ignition.
Pusher density	-	Useful for evaluating implosion dynamics.
"Bang" time	-	Can be compared to simulations with differing drive dynamics.
Neutron image	-	Directly shows distribution of burning fuel region.
Charged particle slowing	-	important for alpha heating.
Mix	-	Fuel and pusher mixing due to hydro dynamic instabilities.

Neutron energy spectra, measured with a time-of-flight technique, are used to determine fuel ion temperature

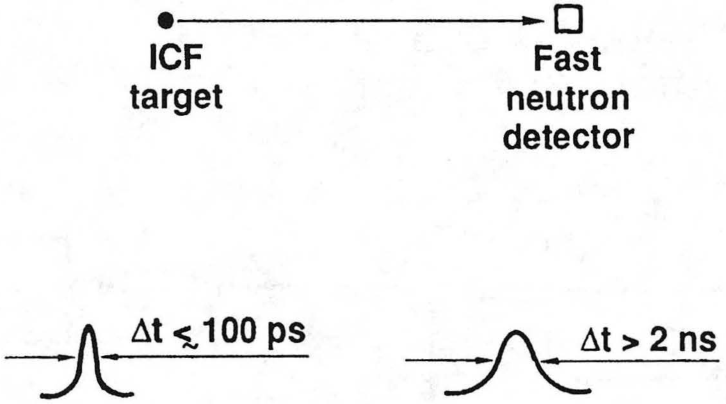

$\Delta E \propto \Delta t$

$\Delta E = 176 \sqrt{\theta_i}$ dt n

$\Delta E = 82.4 \sqrt{\theta_i}$ dd n

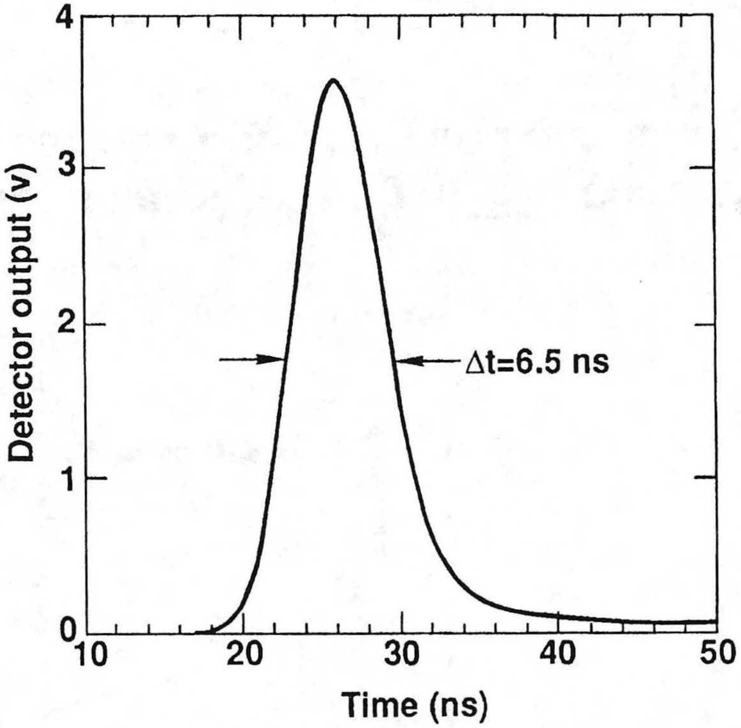

Shot # 17122303

$\theta_i = 8$ keV

Neutron energy spectra are measured using an array of single-particle time-of-flight detectors.

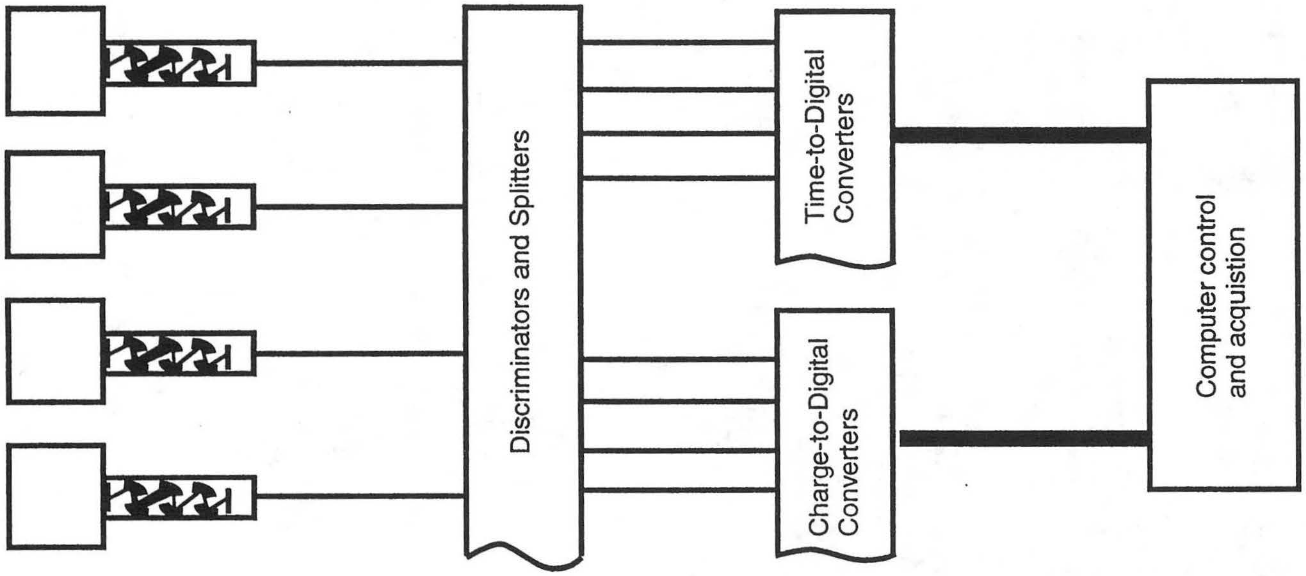

The Large Neutron Scintillator Array (LaNSA) consists of 960 scintillator-phototube detectors and associated electronics.

Each detector is capable of recording the arrival time (relative to the time at which the laser is fired) of at least one neutron. An energy spectrum is obtained by summing the results of all detectors.

Secondary neutron energy spectra are measured with an array of neutron time-of-flight detectors.

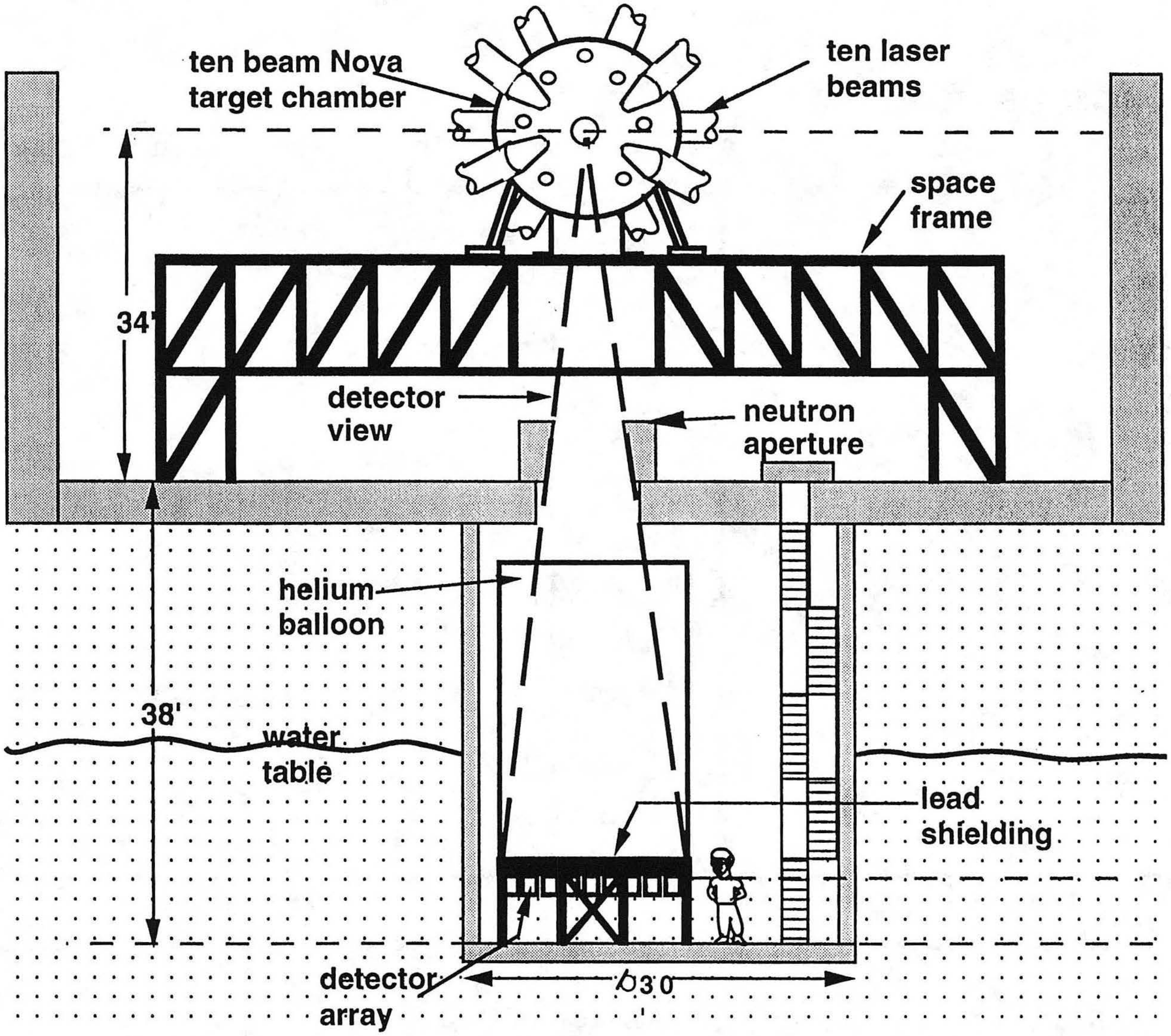

Cable/JC60/LanPit

A low yield calibration shot shows the 14.1 MeV dt neutron peak.

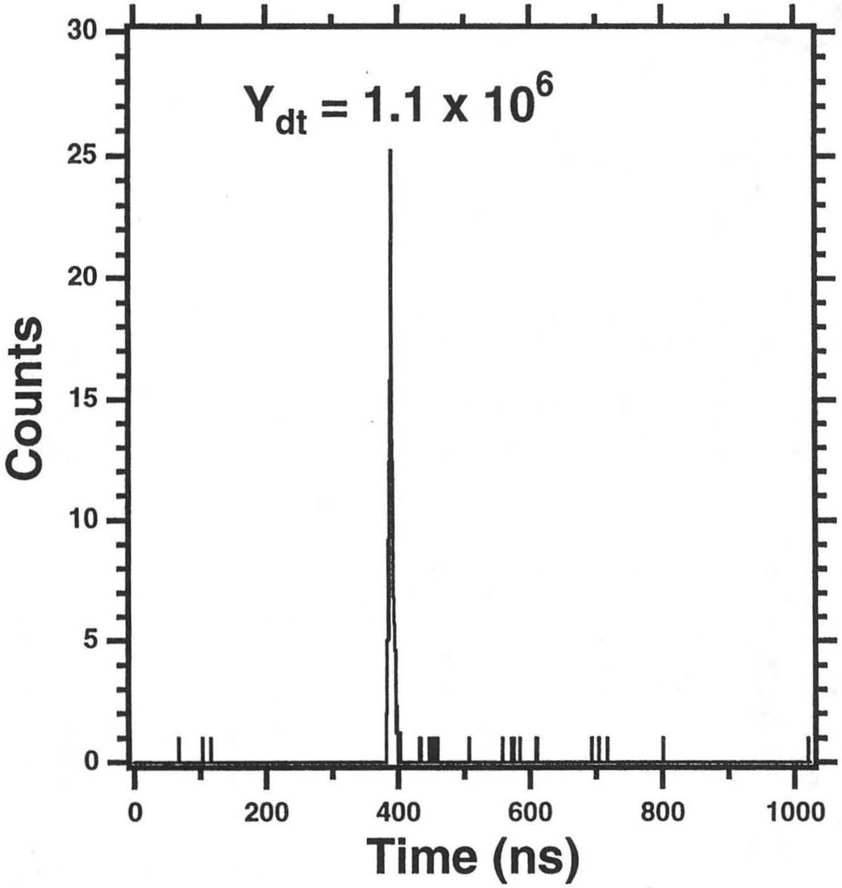

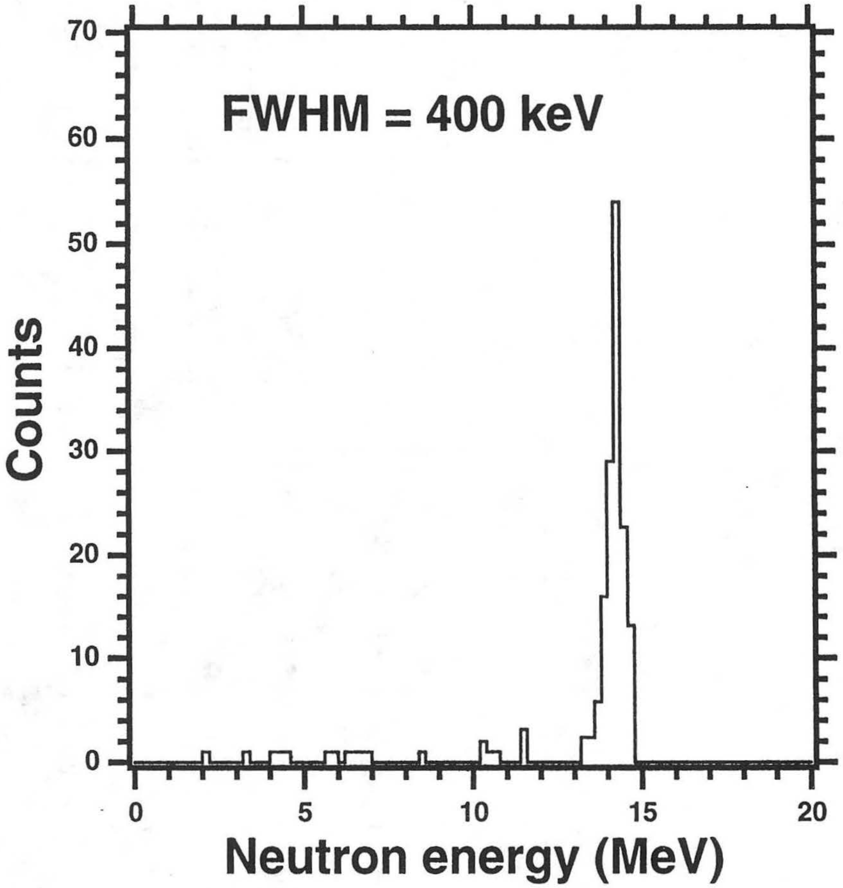

Cable/JC60/dtPeak

For low yield implosions, LaNSA can be used to determine ion temperatures in single particle mode.

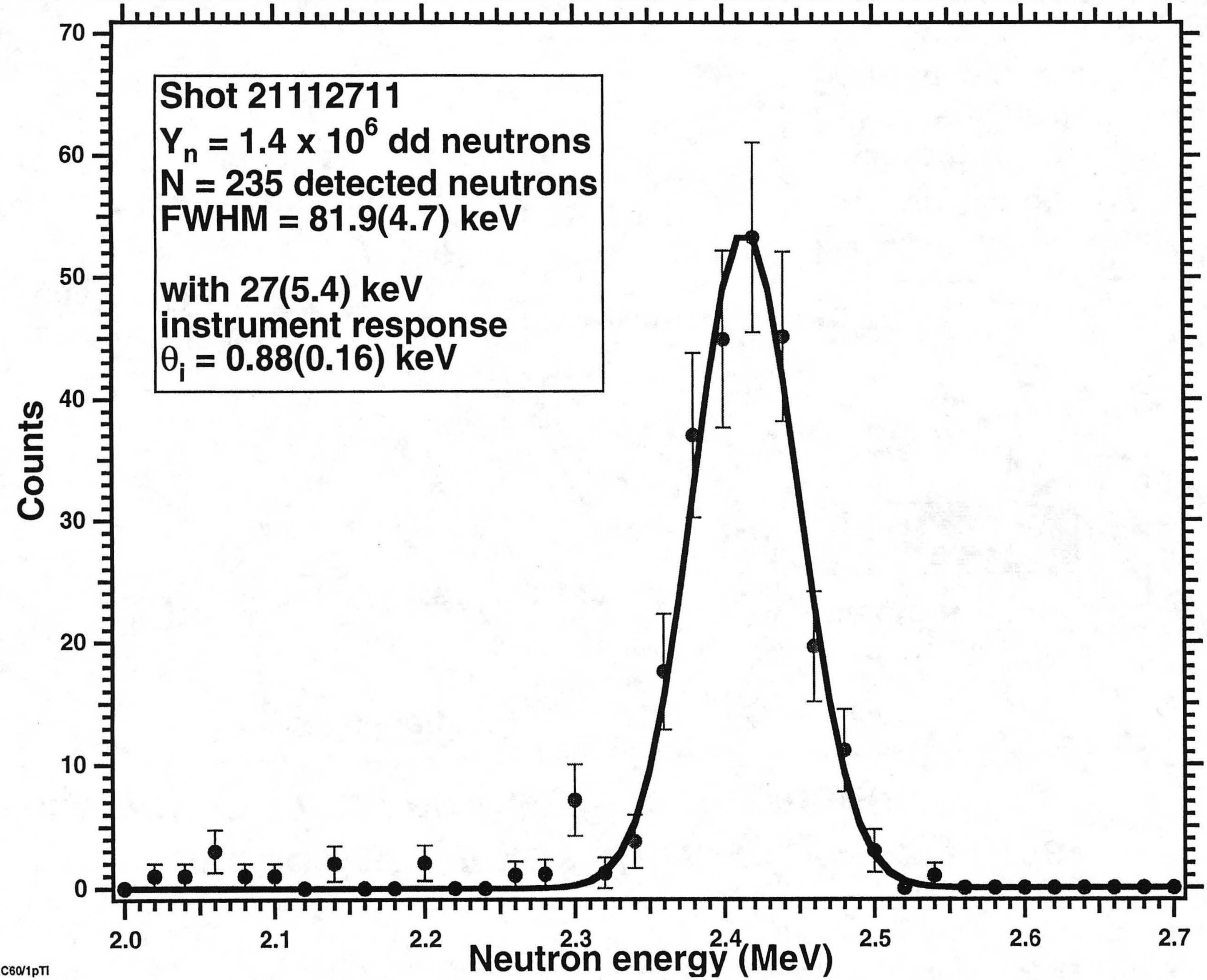

Cable/JC60/1pTI

The higher neutron yields at NIF may allow time-resolved ion temperature measurements.

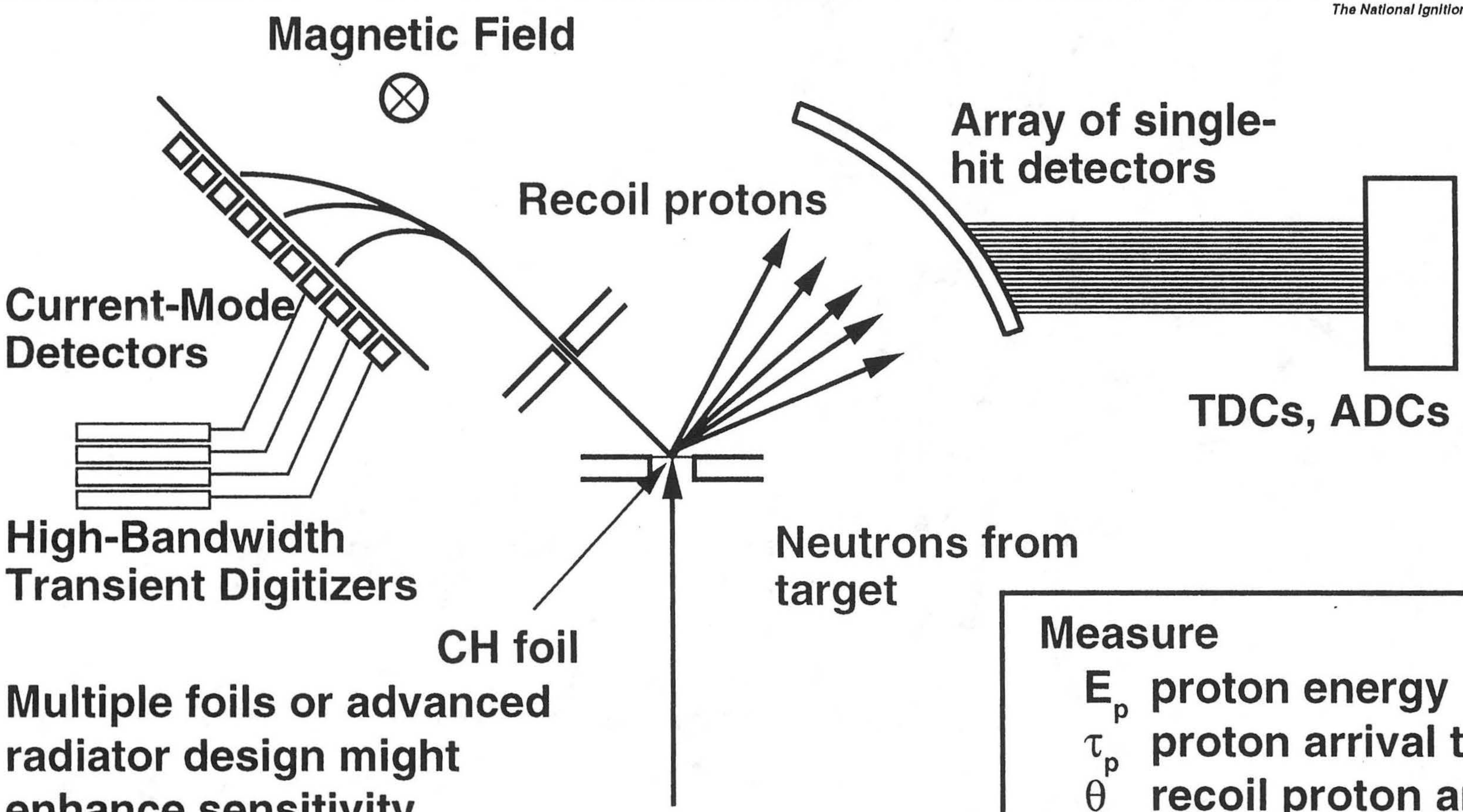

Multiple foils or advanced radiator design might enhance sensitivity

Measure

- E_p proton energy
- τ_p proton arrival time
- θ recoil proton angle

From these, calculate:

- E_n neutron energy
- τ_n neutron birth time

The measurement of fuel areal density can be illustrated with a simple example.

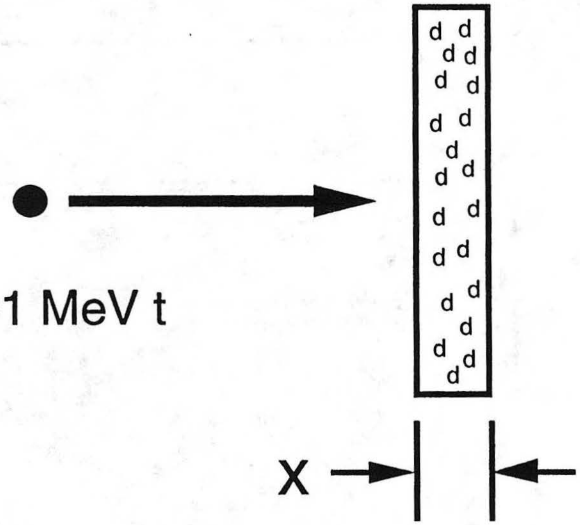

Probability of triton reaction in a thin slab of deuterium is $P = n_d \sigma x$. Since σ is known, ratio of reacting tritons to incident tritons gives $n_d x$.

$$\frac{\text{Number reacting tritons}}{\text{Number incident tritons}} = \sigma(E_t)\, n_d x$$

Secondary neutron measurements can be used to determine areal density for pure deuterium fuel.

$d + d \rightarrow {}^{3}He + n$ (2.45 MeV)

$\searrow p + t$ (1.01 MeV)

"in-flight"

$t + d \longrightarrow \alpha + n$ (11-17 MeV)

secondary neutrons

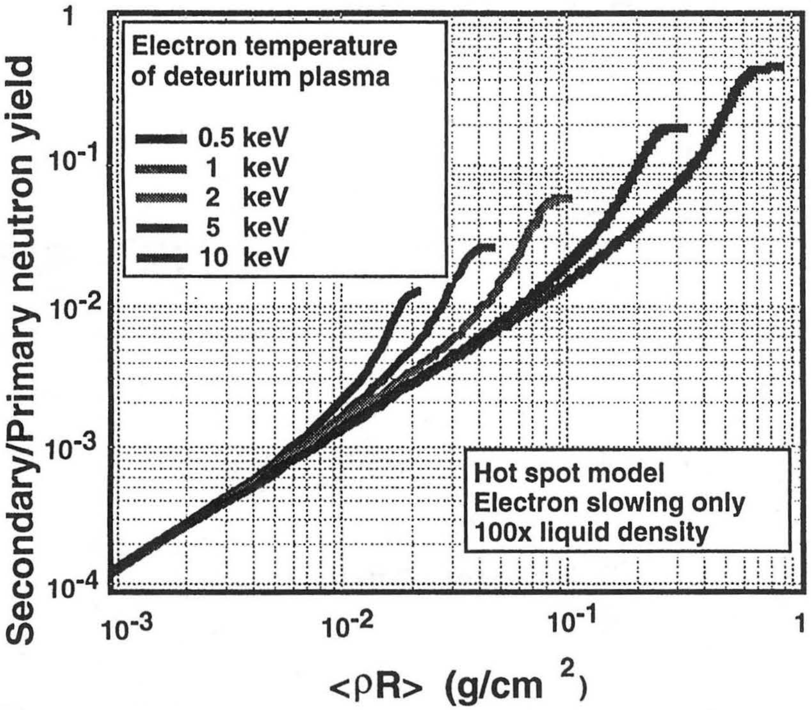

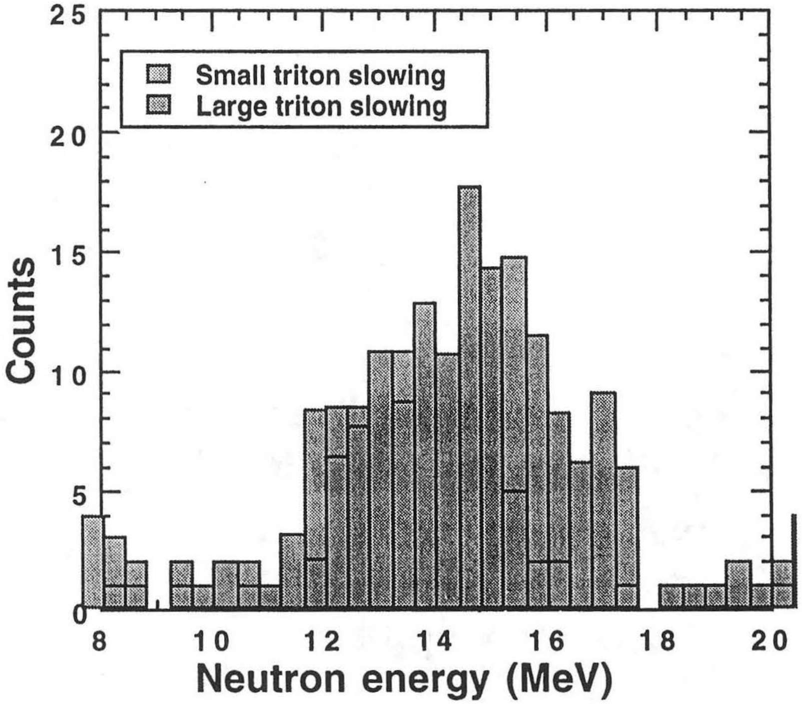

The spectrum width can be used to determine the amount of triton slowing. Triton slowing is sensitive to fuel/pusher mix.

Tertiary neutrons can be used to measure large fuel areal densities.

1) $d + t \longrightarrow \alpha + n$

2) $n + t \longrightarrow n' + t'$ (0-10.5 MeV)
$n + d \longrightarrow n' + d'$ (0-12.5 MeV)

3) $d' + t \longrightarrow \alpha + n$ (12 - 31.5 MeV)
$t' + d \longrightarrow \alpha + n$

For negligible ion slowing (no energy dependent cross-section effects) tertiary production is proportional to $<\rho R>^2$.

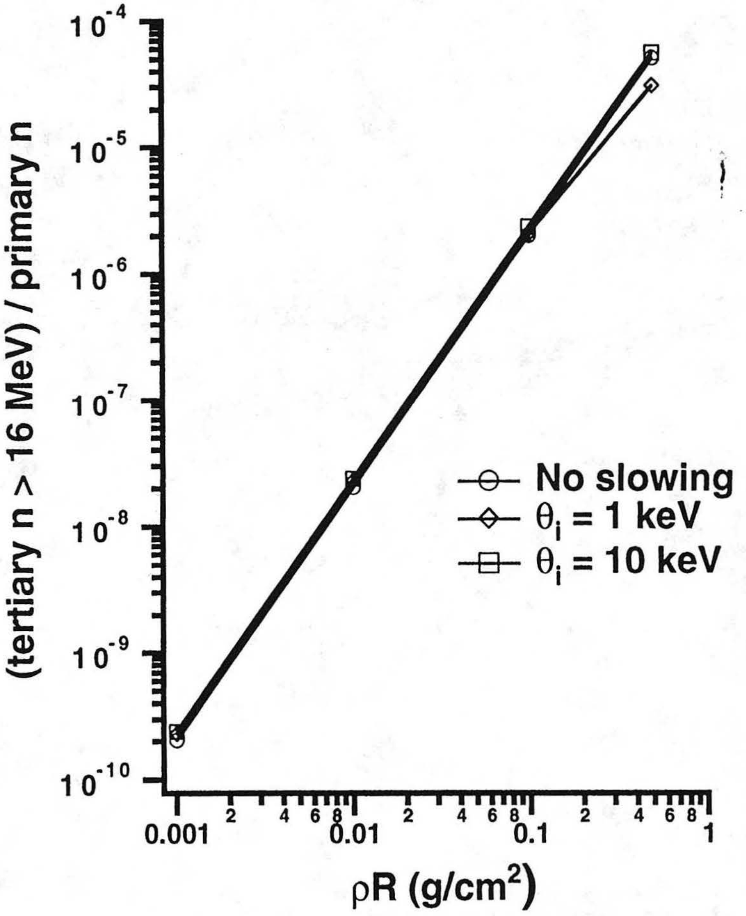

High energy tertiary neutrons or protons (>28 MeV) may be used to determine capsule symmetry at NIF.

1) $d + t \longrightarrow \alpha + n$ (14 MeV)

2) $n + d \longrightarrow n' + d'$ (0-12.5 MeV)

3) $d' + t \longrightarrow \alpha + n$ (12-31 MeV)
$d + {}^3He \longrightarrow \alpha + p$

Reaction sequence must be nearly collinear (momenta aligned) to reach high energies.

ρR measurements in different directions can be used to determine if the final fuel configuration is round.

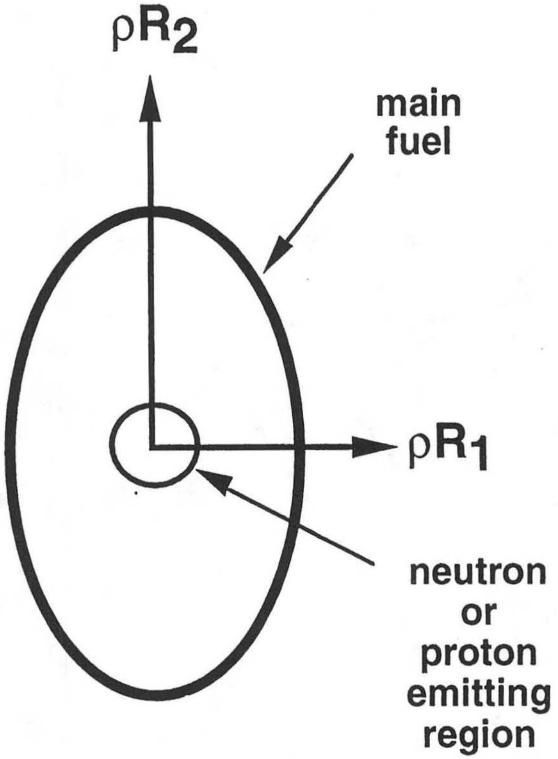

neutron version
Welch, Kislev and Miley, 1985

We use fusion neutrons to measure burn history for Nova ICF targets

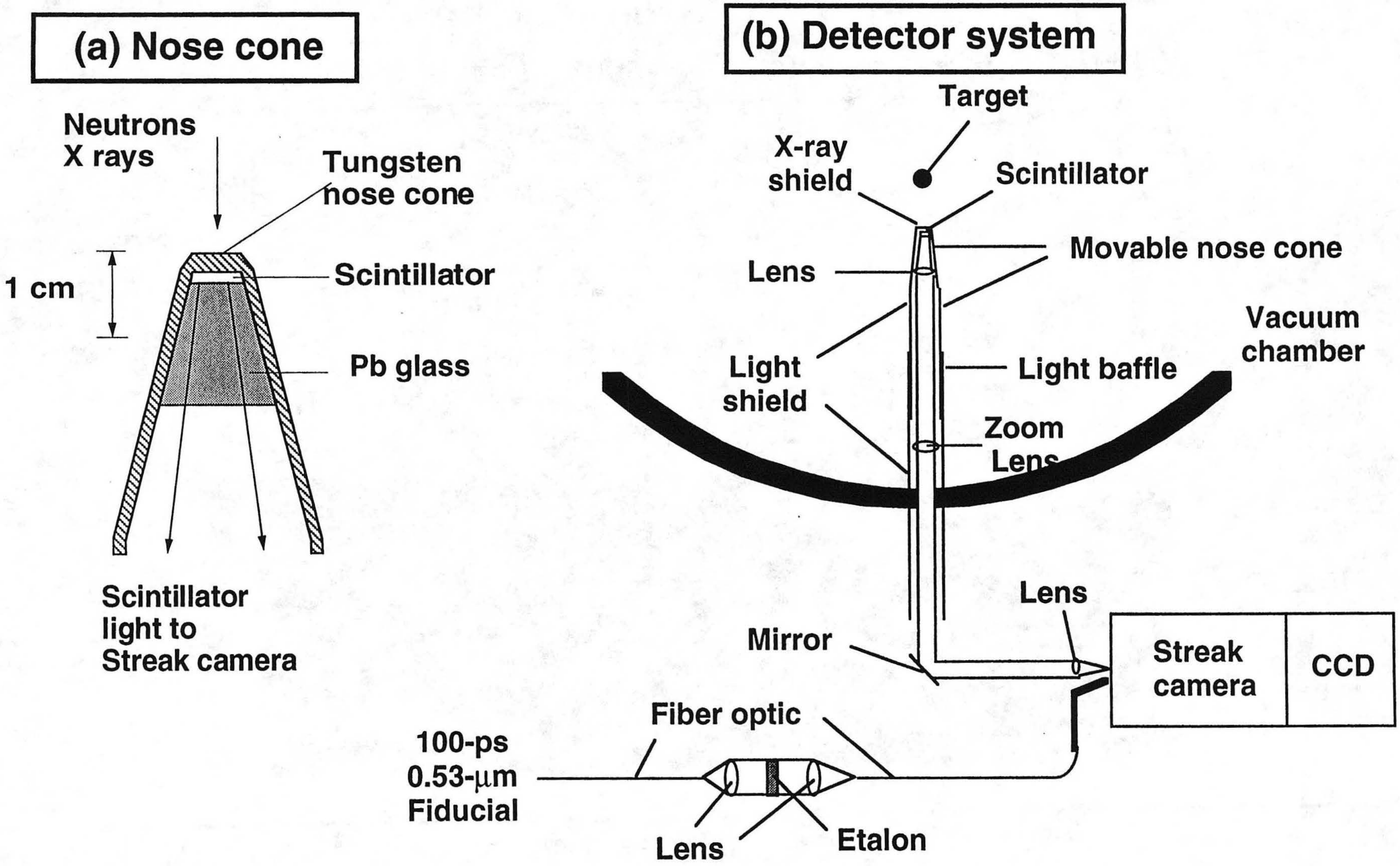

Excellent signals are recorded for targets producing only 5×10^8 DT neutrons

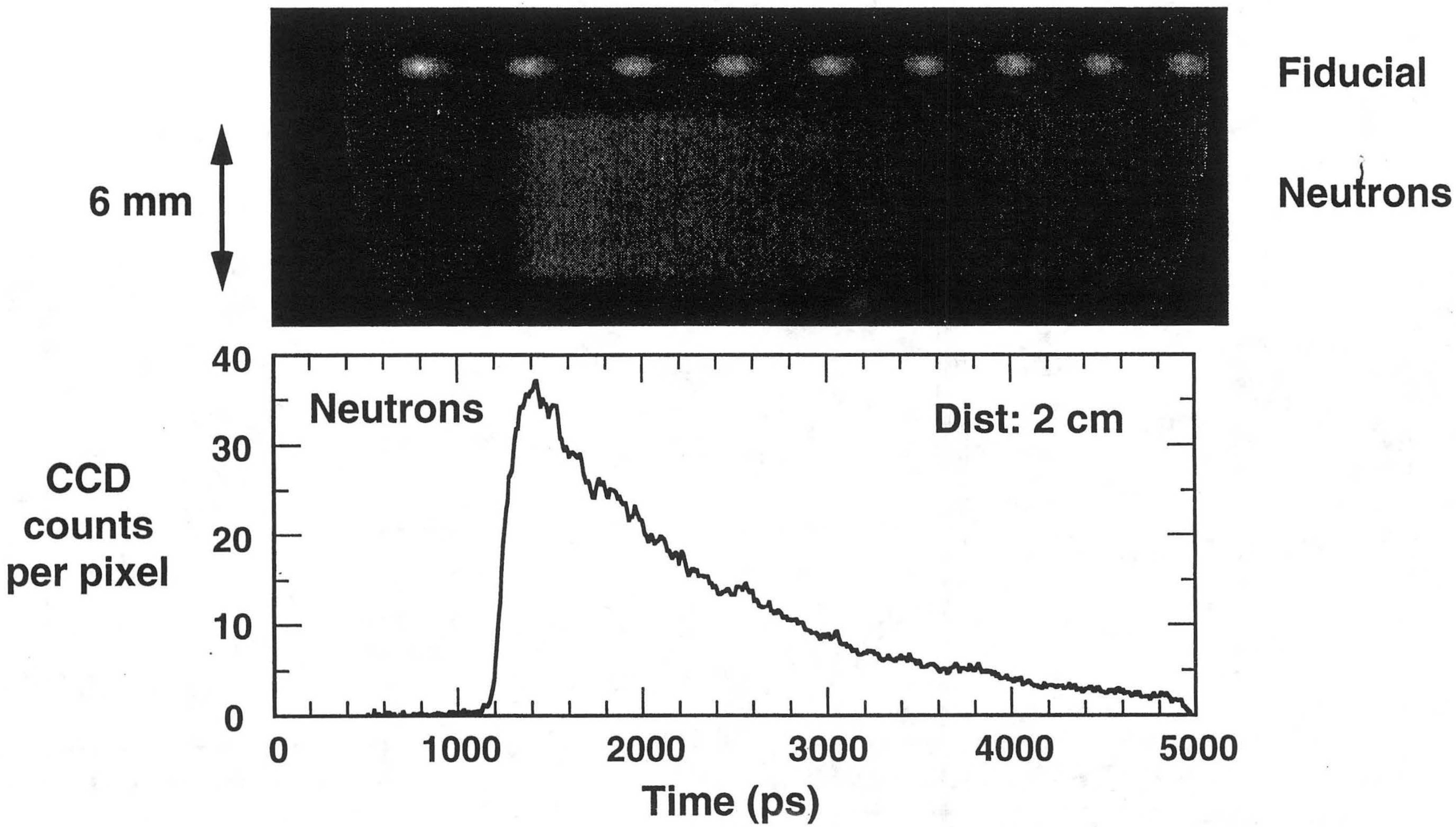

Cable/JC60/NTD rawData

[redacted]

Measured bang time and burn width agree with calculations.

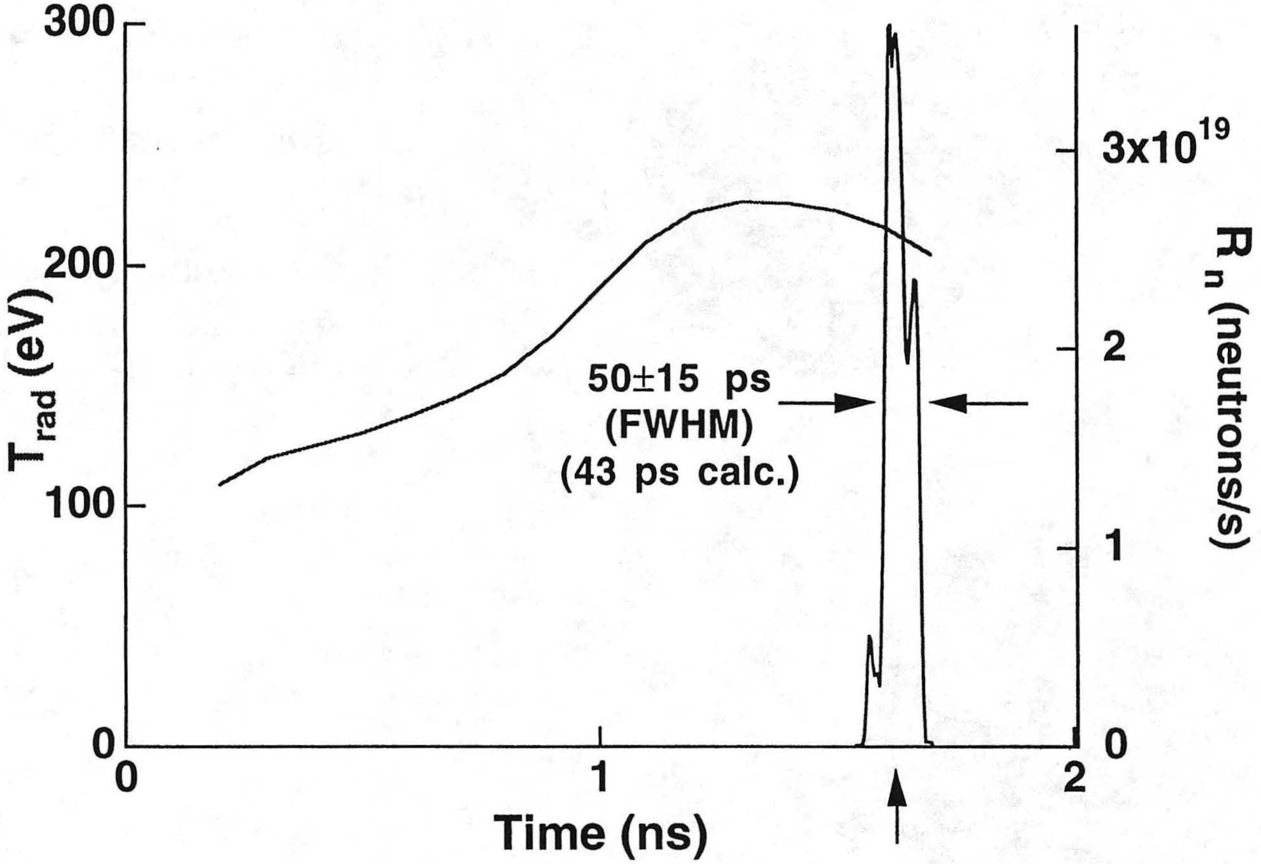

50±15 ps
(FWHM)
(43 ps calc.)

1.60 ± 0.10 ns
(1.60 calculated)

Bang time agreement supports implosion kinematics.
Burn width agreement supports mix sensitive cooling rate.

Laser-ablated ICF capsule: multimode surface

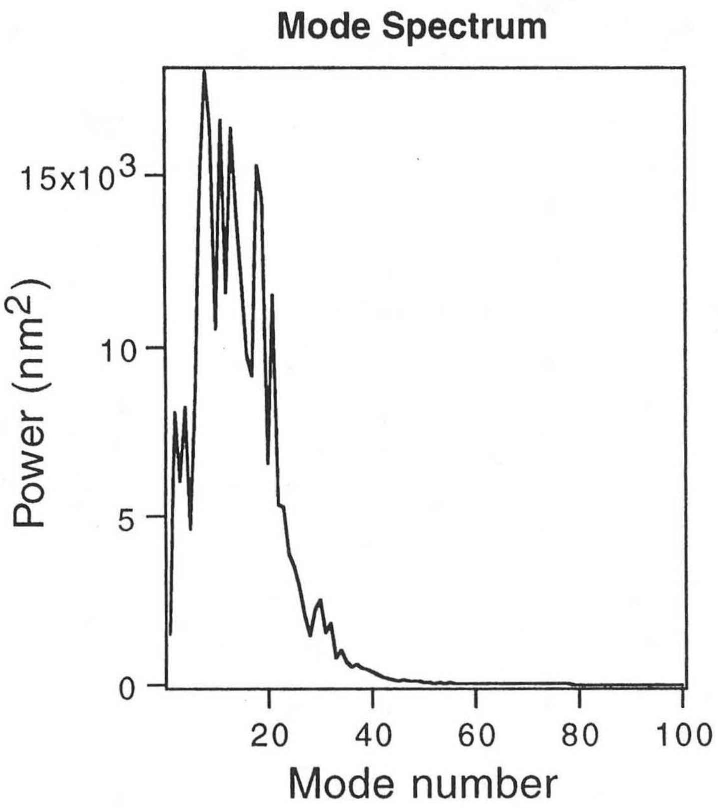
Mode Spectrum

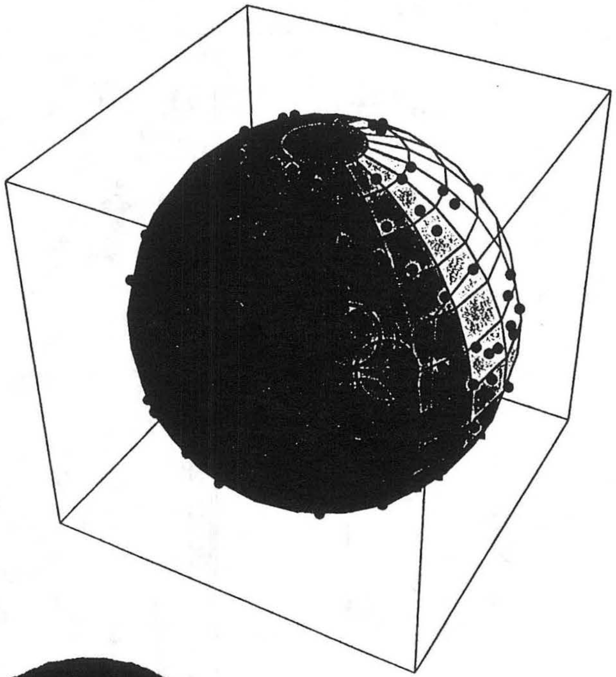

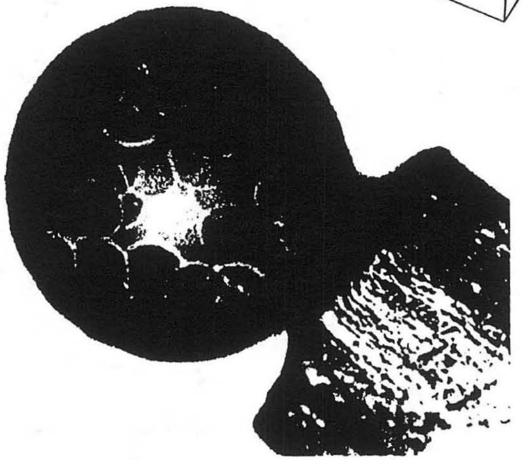

200 randomly-placed pits

75 μm diameter, gaussian profile

Laser-ablated ICF capsule: multimode surface

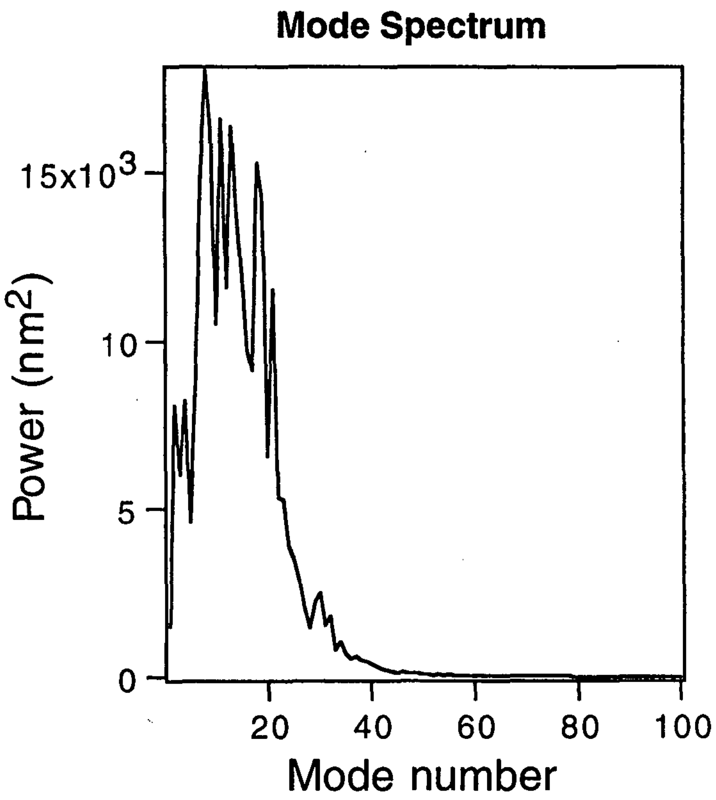
Mode Spectrum

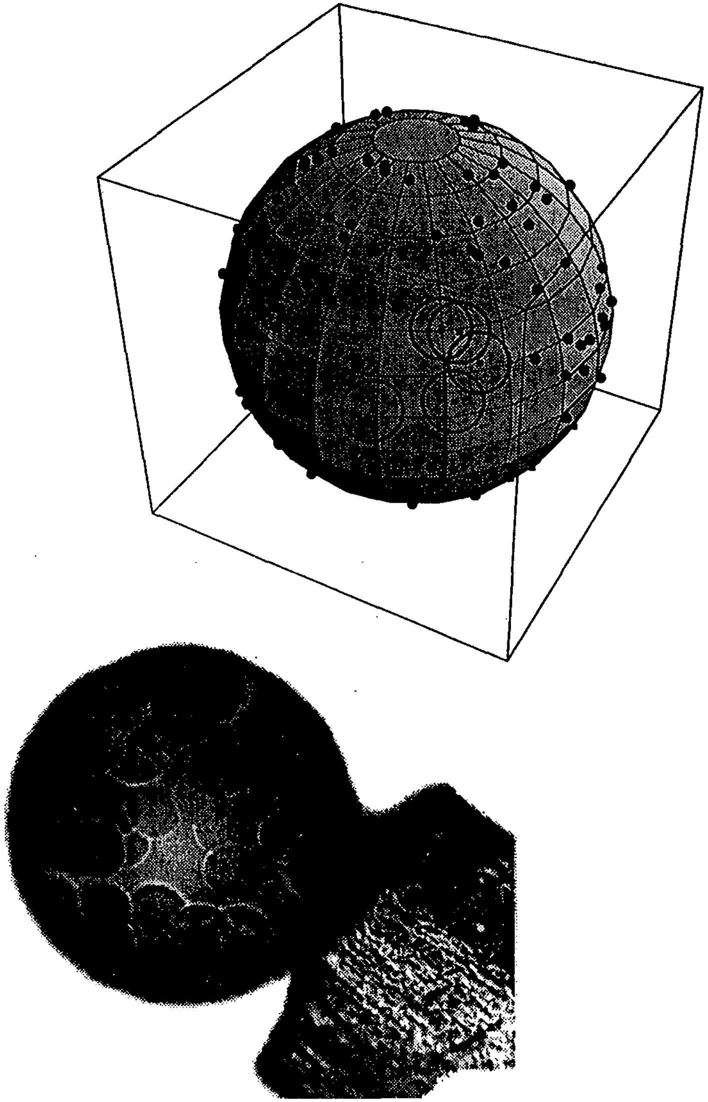

200 randomly-placed pits

75 μm diameter, gaussian profile

Neutron yield and final fuel areal density decrease with increasing surface roughness.

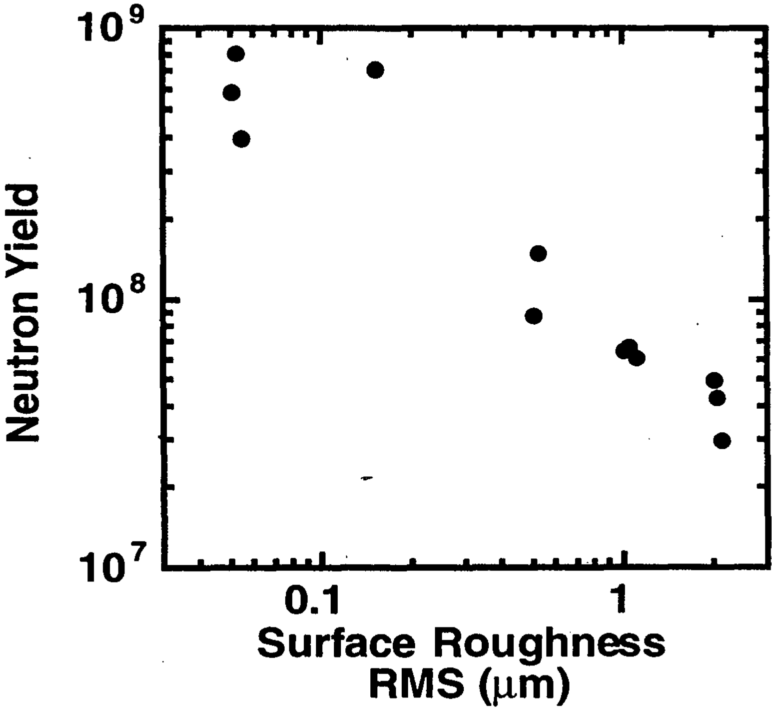

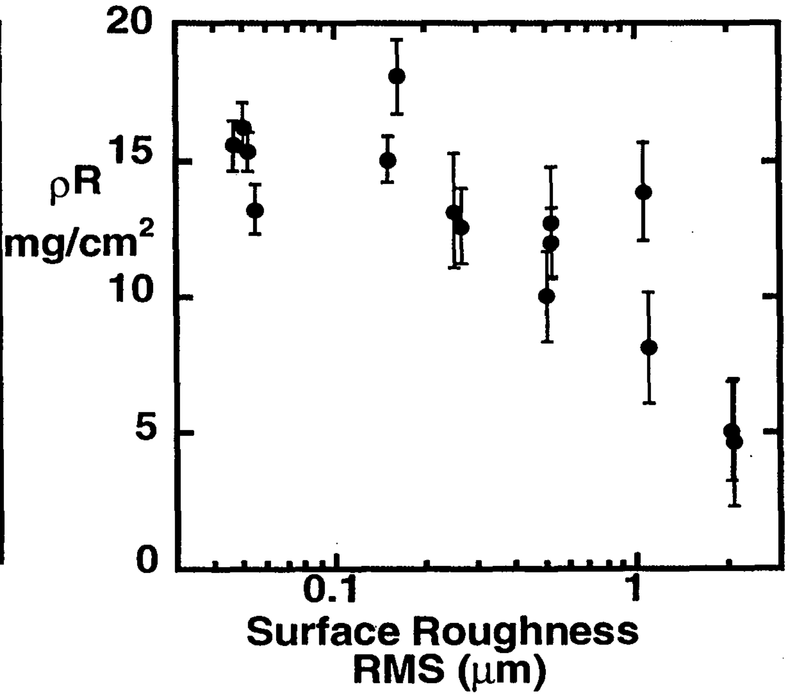

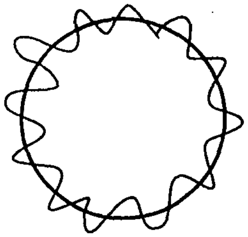

Cable/ JC60/ H4Yn&rR

Peter Haustein

Brookhaven National Laboratory
Upton, NY

Cerny Fest

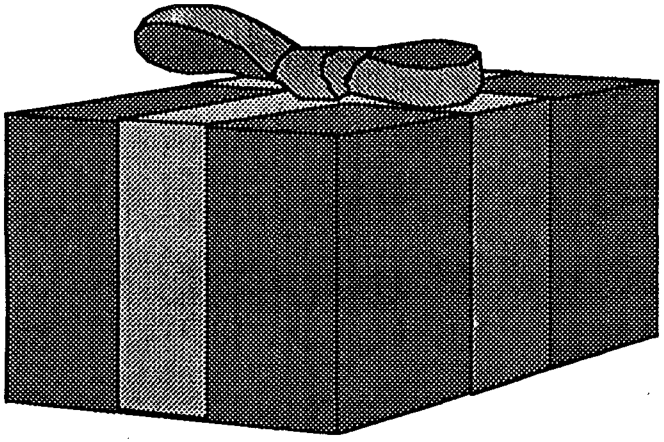

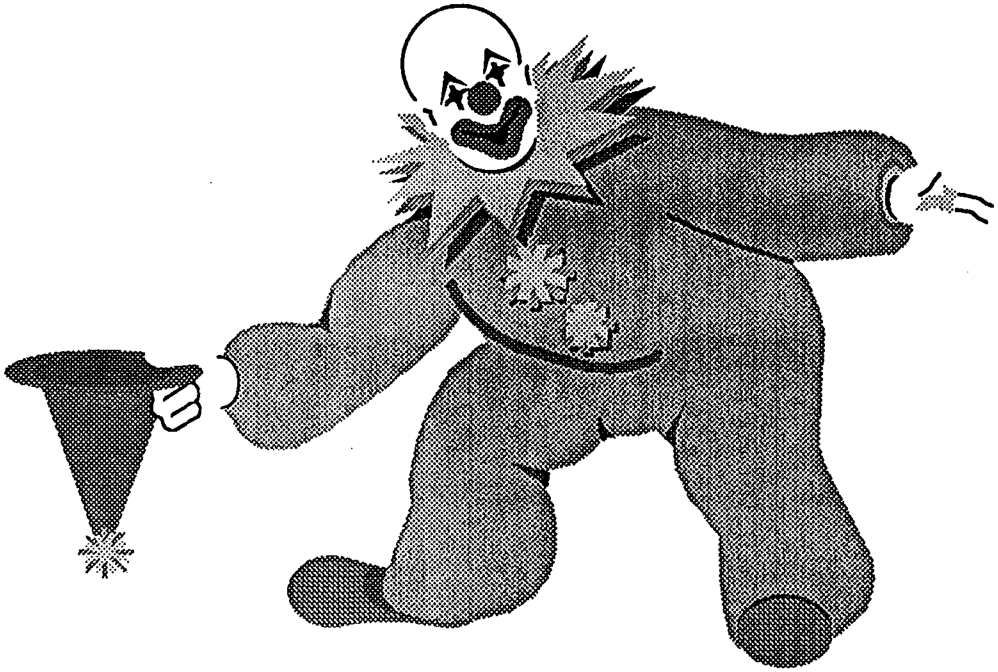

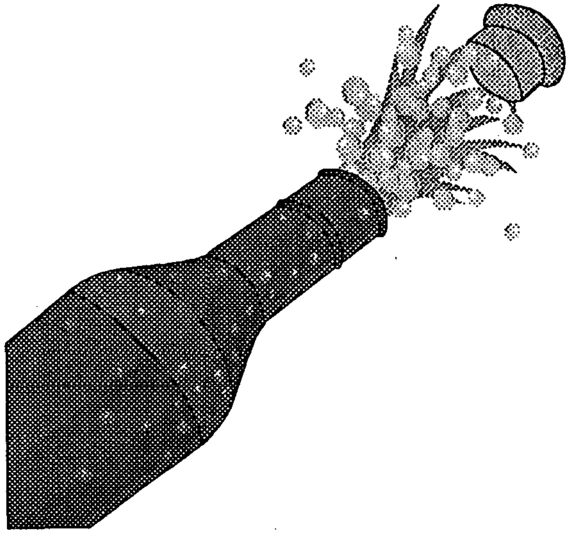

Happy Birthday
Joe!

April 14-16, 1996

Cerny Fest

My connections with Joe Cerny and his group

1965-66 UC Berkeley Undergraduate Days:
Maples, Fleming, Butler, Goth, Ball, McGrath, Cosper

1979 Sabbatical from BNL:
Aysto, Moltz, Wouters, Cable, Perry, Byce, Shotter

1989-90 Sabbatical from BNL:
Moltz, Lange, Ognibene, Batchelder (Stokstad for EB88)

April 14-16, 1996

Cerny Fest

NSD

Nuclear Stimulated Desorption

(Not the Nuclear Science Division of the Ernest Orlando Lawrence Berkeley National Laboratory)

Peter Haustein, Chemistry Dept., Brookhaven National Lab.

April 14-16, 1996

Cerny Fest

Nuclear Stimulated Desorption - -

A technique for studies of surfaces and thin films with relevance to the remediation of high level radioactive waste

April 14-16, 1996

Outline:

What is NSD? Why study it?

Consequences of nuclear recoil

Basic premise used in NSD interpretation

Typical events and experiments to study them

Relevance of NSD to remediation of High Level Radioactive Waste (HLW)

What is Nuclear Stimulated Desorption?

Nuclear decays or reactions generally impart some recoil energy to the heavy participant. This can range from eV (IT, low energy β) to keV (β, α or n-capture) to multi-Mev (fission).

This recoil energy is sufficient to promote the desorption of atoms from surfaces or thin films. It can also promote the desorption or dislocation of atoms near the NSD site.

Basic Premise of NSD and Goals in Studying NSD

Premise: The temporal, energetic and angular aspects of the process carry with them information about the desorbing species and its environment.

Goals: A basic quantitative understanding of the process for representative systems and, where possible, mathematical modeling of it. Application of this to development of remediation strategies for HLW.

Typical NSD Scenario:

Nuclear event occurs (n-capture, β-decay, etc.)

Recoil energy is imparted to nucleus, which starts to move in a random direction and eventually is stopped.

Nucleus motion is affected by surface binding and may be hindered by the presence of adjacent atoms or overlayers.

Besides the primary recoiling atom, other atoms may be dislodged and/or desorbed.

A Sampler of Typical NSD Events

1. Topmost atom on a surface
2. An atom just below the surface
3. An atom in the bulk
4. Primary and secondary events
5. Complicated cases with surface irregularities or dynamic surface conditions

Nuclear Techniques to Initiate NSD and Follow its Evolution

Initiate: Some type of nuclear tranformation, e.g. beta decay or neutron capture

Follow:

Primary desorbing species becomes (and remains) radioactive and can be followed (location, amount, etc.) with very high sensitivity.

Secondary stable atoms which also desorb can be assayed via neutron activation after the assay of primary species.

(n,γ) Events of ◇ atoms

1)

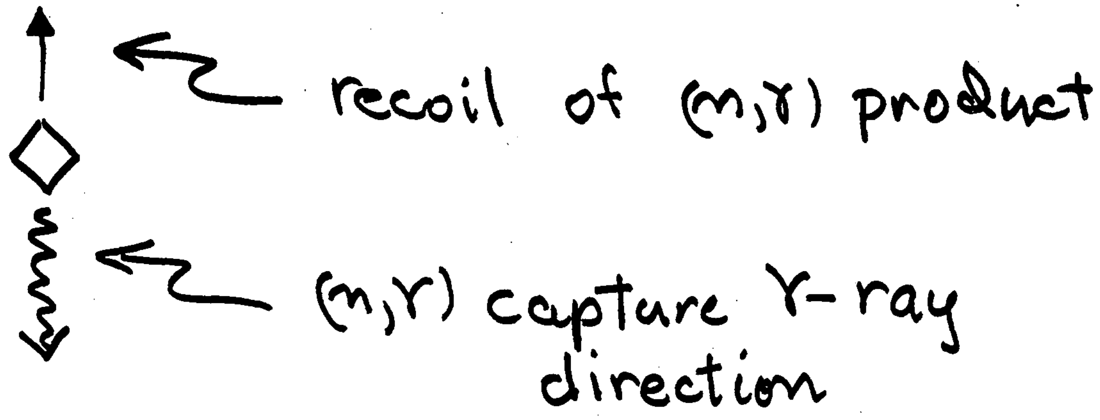

2)

3)

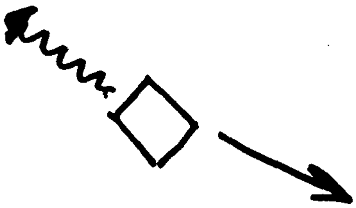

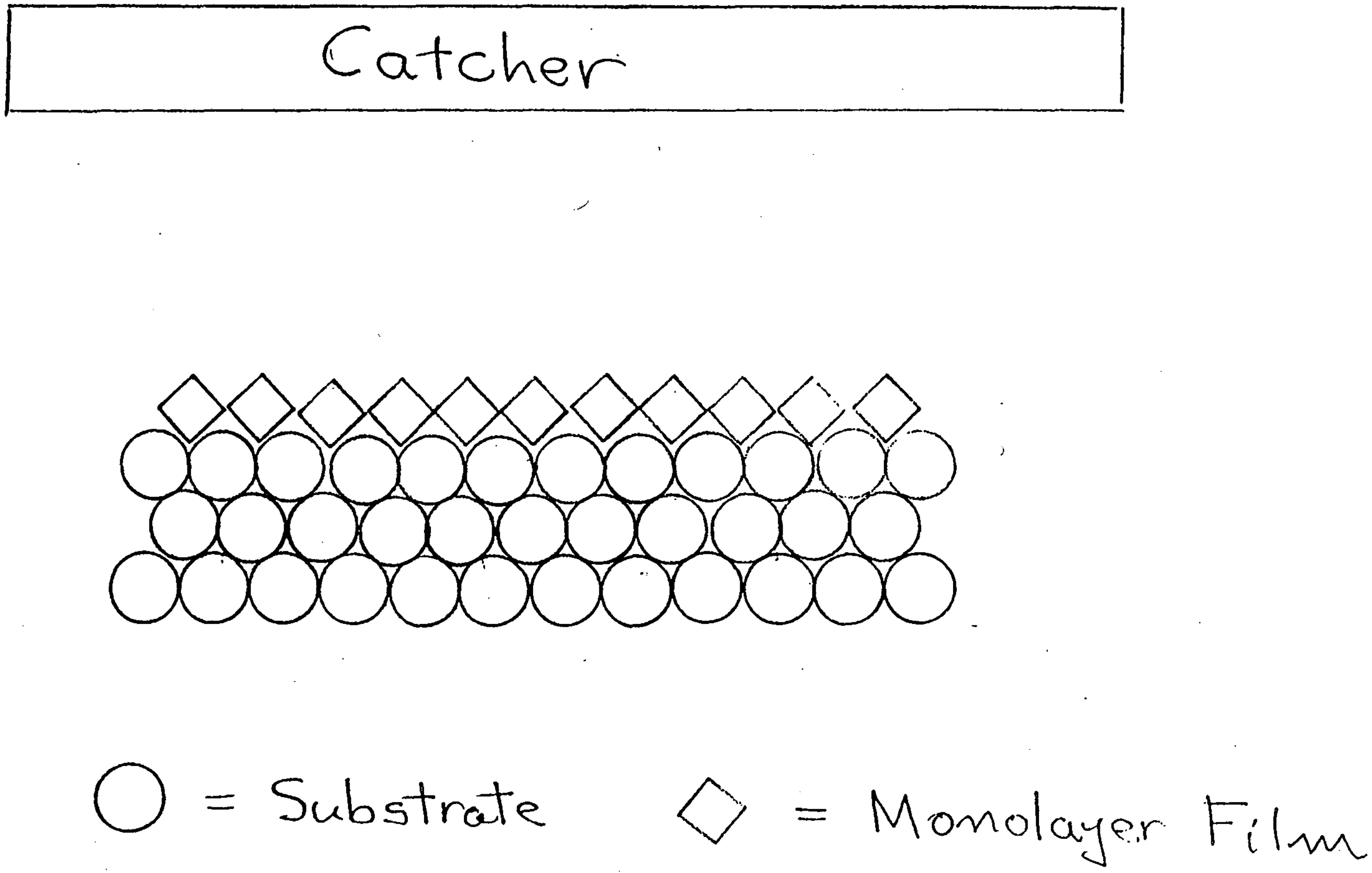
Catcher
= Substrate
= Monolayer Film

Event 1

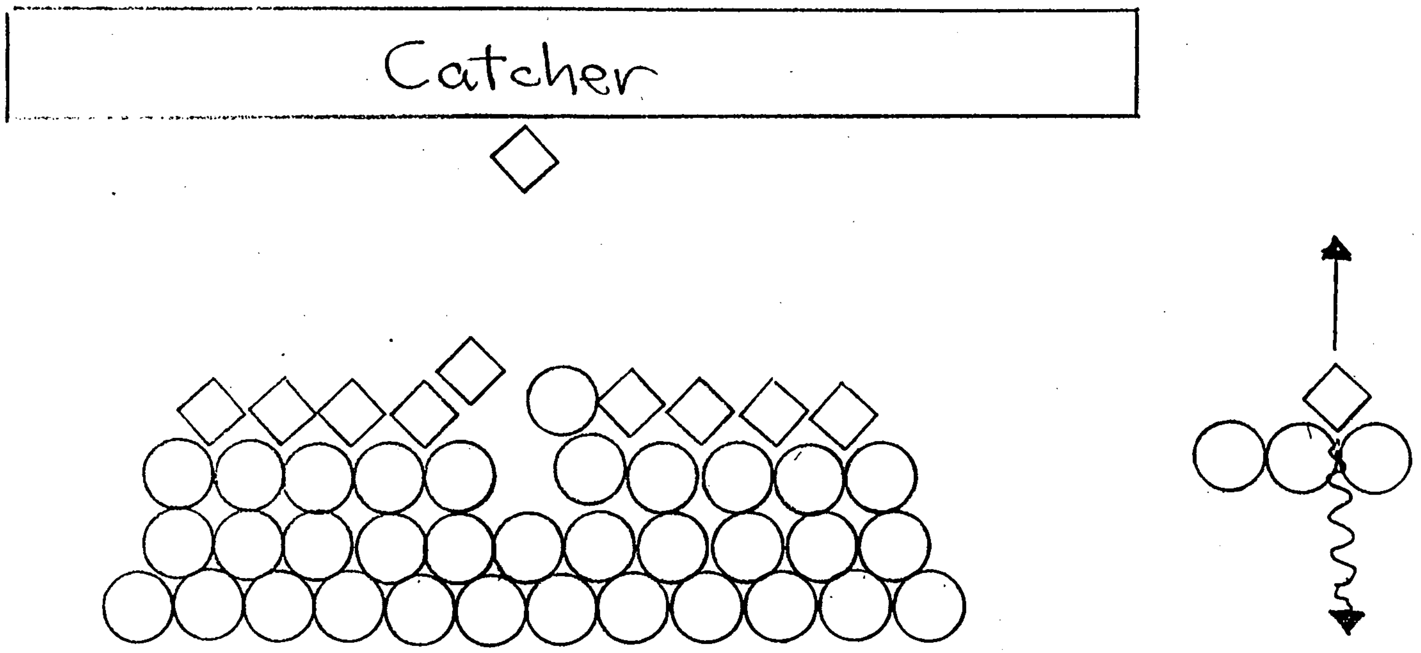

Event 2

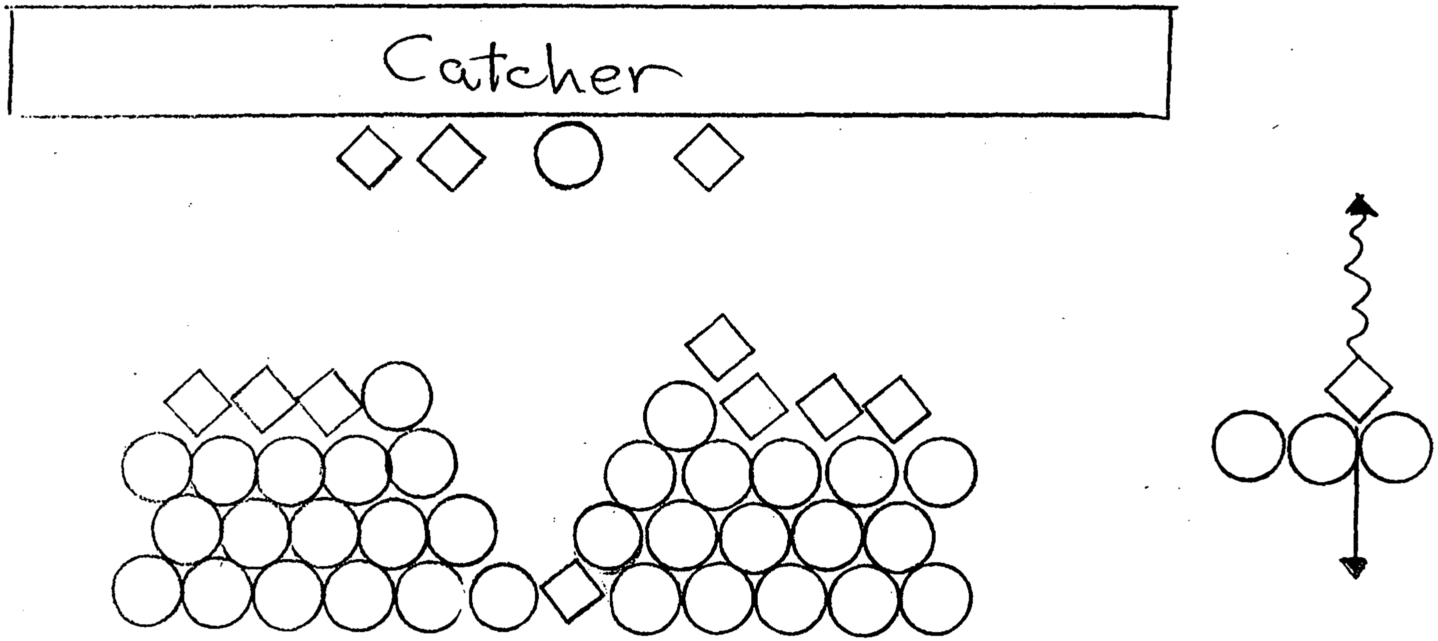

Event 3

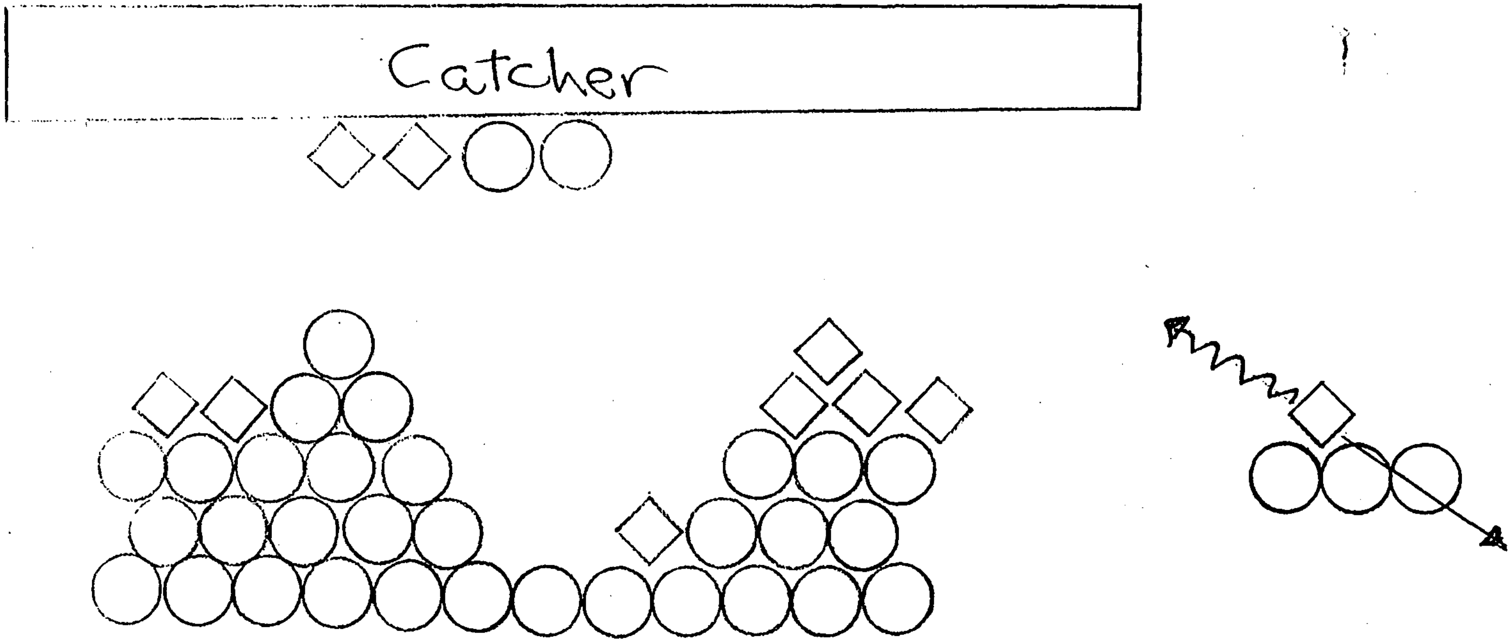

Activation of ◇ atom Causes NSD and allows one to follow where ◇ went.

Fate of dislodged (stable) atoms, ◇ or ○, can be followed by neutron activation analysis after the assay of the primary ◇ atoms from NSD

NSD and the Remediation of HighLevel Radioactive Waste (HLW)

HLW will contain high concentrations of many radionuclides (1.3 weight % ^{137}Cs for example), and will generate *intense* radiation fields, 20 watts/liter, 10^9 Rads/year self dose).

HLW surfaces and interfaces will contain high concentrations of radioactive species and NSD processes will be a major source of surface degradation and loss of interfacial integrity. At these NSD sites radiolysis promoted corrosion and unwanted chemical reactions, e.g. H_2 evolution are major problems.

H_2 Evolution from HLW and Spent Nuclear Fuel

"Wet option": Process with minimal removal of H_2O; essentially all waters of hydration remain.

"Dry option": Heat (to 50°C) and evacuate (to ~100 torr) to remove significant amounts of water; waters of hydration remain.

These options and H_2 evolution from radiolysis (promoted by NSD, photon stimulated desorption (PSD) and electron stimulated desorption (ESD)) dictate strategies for vented or non vented containers.

Cerny Fest

Long term collaborator: Prof. Itzhak Kelson, Physics Dept.,
Tel Aviv University, Israel

New collaborators (for the FY96 Environmental Management Sciences Program Initiative:

Prof. Ted Madey, Depts. of Chemistry & Physics, Rutgers University, Piscataway, NJ (Electron Stimulated Desorption)

Dr. Thomas Orlando, Environmental Molecular Sciences Laboratory, Pacific Northwest National Laboratory, Richland, WA (Photon Stimulated Desorption)

April 14-16, 1996

Title 1	First Name	Last Name	Address	Mailing City	Mailing State	Mailing Zip	Mailing Country	E-mail
Dr.	Bice	Alden	4549 East Mountain View Rd.	Phoenix	AZ	85028	USA	71233.2460@compuserve.com
Prof.	Juha	Äystö	University of Jyväskylä Accelerator Laboratory PO Box 35	Jyväskylä		FIN40351	FINLAND	
Dr.	Gordon	Ball	CRL	Chalk River	ONT	K0J 1J0	CANADA	ball@crl.aecl.ca
Dr.	Jon	Batchelder	ORNL Bldg. 6008, MS 6374	Oak Ridge	TN	37831	USA	batcheld@orph01.phy.ornl.gov
Dr.	Fred	Blönnigen	Ludwig Straβe 28	Freiburg		D-79104	GERMANY	

Title 1	First Name	Last Name	Address	Mailing City	Mailing State	Mailing Zip	Mailing Country	E-mail
Dr.	Hank	Brunnader	CFFTP 2700 Lakeshore Rd., West	Mississauga	ONT	L5J 1K3	CANADA	
Dr.	Gilbert	Butler	LANL MS J514	Los Alamos	NM	87545	USA	butler@lanl.gov
Dr.	Michael	Cable	LLNL MS-L473	Livermore	CA	94550	USA	cable@LLNL.gov
Dr.	Sam	Cosper	240 Thibodeaux	Lafayette	LA	70503	USA	
Dr.	Claude	Detraz	IN2P3 3 rue Michel Ange	Paris		F-75781	FRANCE	detraz@frcpn11.In2P3.fr

Title 1	First Name	Last Name	Address	Mailing City	Mailing State	Mailing Zip	Mailing Country	E-mail
Dr.	John	Esterl	216 Carmel Avenue	El Cerrito	CA	94530		
Prof.	Hugh	Evans	Queen's University Department of Physics	Kingston	ONT		CANADA	evans@midsz.phy.queensu.ca
Profes	Donald	Fleming	University of British Columbia Dept. of Chemistry 2036 Main Mall	Vancouver	BC	V6T 1Y6	CANADA	flem@triumf.ca
Dr.	George	Goth	1601 Kains Avenue	Berkeley	CA	94703	USA	goth@aol.com
Dr.	Richard	Gough	LBNL MS 71-259 1 Cyclotron Rd.	Berkeley	CA	94720	USA	ragough@lbl.gov

Title 1	First Name	Last Name	Address	Mailing City	Mailing State	Mailing Zip	Mailing Country	E-mail
Dr.	John	Hardy	CRL	Chalk River	ONT	K0J 1J0	CANADA	hardyj@crl.aecl.ca
Dr.	Hans	Harney	Max Planck-Institüt für Kernphysik Postfach 103980	Heidelberg 1		D-6900	GERMANY	harney@franny.mpi-hd.mpg.de
Dr.	Peter	Haustein	BNL Chemistry Department	Upton	NY	11973	USA	haustein@bnldag.ags.bnl.gov
Dr.	Jorma	Honkanen	Kulmakuja 3 A1	Varkaus			FINLAND	watol@pspt.fi
Dr.	Michael	Hotchkis	Australian National University	Canberra			AUSTRALIA	mach.2@anpnt22.anp.ansto.gov.au

Title 1	First Name	Last Name	Address	Mailing City	Mailing State	Mailing Zip	Mailing Country	E-mail
Dr.	Rainer	Jahn	Institut für Strahlen und Kernphysik Nuss Allee 14-16	Bonn		D-5300	Germany	jahn@iskp.uni-bonn.de
Dr.	Nick	Jelley	Oxford University Dept of Nuclear Physics	GB-Oxford		OX 1 3RH	UK	n.jelley1@physics.oxford.ac.uk
Dr.	Gary	Kekelis	133 Treasure Palm Drive	Panama City	FL	32408	USA	
Dr.	Thomas	Lang	UC San Francisco M-392, Dept. of Radiology 505 Parnassus Avenue	SanFrancisc	CA	94143	USA	
Dr.	J.M.	Loiseaux	Institut Max von Laue-Paul Langevin Avenue de Martyrs 156 X	Grenoble		38042	FRANCE	

Title 1	First Name	Last Name	Address	Mailing City	Mailing State	Mailing Zip	Mailing Country	E-mail
Dr.	John	MacDonald	TRIUMF 4004 Wesbrook Mall	Vancouver	BC	V6T 2A3	CANADA	jmacdonald@triumf.ca
Dr.	Creve	Maples	1401 Catron Avenue S.E.	Albuquerque	NM	87123		cmaples@musetech.com
Prof	Robert	McGrath	SUNY @ Stony Brook Dept. of Physics	Stony Brook	NY	11794	USA	mcgrath@nuclear.physics.sunysb.edu
Dr.	Robert	Mendelson	University of California, SF PO Box 0524	San	CA	94153	USA	mendel@musl.ucsf.edu
Dr.	Dennis	Moltz	LBNL 1 Cyclotron Rd. MS 88	Berkeley	CA	94720	USA	dmmoltz@lbl.gov

Title 1	First Name	Last Name	Address	Mailing City	Mailing State	Mailing Zip	Mailing Country	E-mail
Dr.	Ted	Ognibene	LLNL MS L-476	Livermore	CA	94550	USA	tjognibene@llnl.gov
Dr.	Roger	Parry	Dupont P.O. Box 800 Hyw. 11 North	Kingston	NC	28502	USA	
Dr.	James	Powell	LBNL MS 88	Berkeley	CA	94720	USA	jpowell@lbl.gov
Dr.	Jay	Reiff	Thomas Jefferson University Dept. of Radiation Oncology 111 S. 11th Street	Philadelphia	PA	19107	USA	
Dr.	Sextro	Richard	LBNL 1 Cyclotron Rd., MS 90-3058	Berkeley	CA	94720	USA	rsextro@lbl.gov

Title 1	First Name	Last Name	Address	Mailing City	Mailing State	Mailing Zip	Mailing Country	E-mail
Prof	J. David	Robertson	Department of Chemistry University of Kentucky	Lexington	KY	40506	USA	jdrobson@ukcc.uky.edu
	Mike	Rowe	LBNL 1 Cyclotron Rd. MS 88	Berkeley	CA	94720	USA	mwrowe@lbl.gov
Prof	Alan	Shotter	University of Edinburgh Department of Physics	Edinburgh		EH9 3JZ	UK	acs@np.ph.ed.ac.uk
Dr.	Dieter	Stahel	42 Muelheimer Strasse	Basel		CH 4057	Switzerland	wdst@chbs.ciba.com
Dr.	Richard	Tighe	8837 Country Vistas Way #103	Las Vegas	NV	89117		tighe-rj@egg.nv.doe.gov

Title 1	First Name	Last Name	Address	Mailing City	Mailing State	Mailing Zip	Mailing Country	E-mail
Dr.	David J.	Vieira	LANL INC-13, MS H824	Los Alamos	NM	87545	USA	vieira@lanl.gov
Dr.	Bob	Weisenmiller	2212 Roosevelt	Berkeley	CA	94703	USA	robertw768@aol.com
Dr.	Ken	Wilcox	1414 26th Street	Sacramento	CA	95816	USA	
Dr.	Jan	Wouters	LANL INC-13, MS H824	Los Alamos	NM	87545	USA	jwouters@lanl.gov
Dr.	Gordon	Wozniak	LBNL 1 Cyclotron Rd. MS 88	Berkeley	CA	94720	USA	gjwozniak@lbl.gov

Title 1	First Name	Last Name	Address	Mailing City	Mailing State	Mailing Zip	Mailing Country	E-mail
Dr.	X.J.	Xu	Institute of Modern Physics	Lanzhou	Ganso	730000	CHINA	
Dr.	Zong-yuan	Zhou	522 Poole Avenue	Pocatello	ID	83201	USA	
Dr.	Michael	Zisman	LBNL MS B71H 1 Cyclotron Rd.	Berkeley	CA	94720	USA	zisman@lbl.gov

ERNEST ORLANDO LAWRENCE BERKELEY NATIONAL LABORATORY
ONE CYCLOTRON ROAD | BERKELEY, CALIFORNIA 94720

Prepared for the U.S. Department of Energy under Contract No. DE-AC03-76SF00098